

5-2014

TOWARDS THE DEVELOPMENT OF PERFORMANCE BASED GUIDELINES FOR USING PHASE CHANGE MATERIALS IN LIGHTWEIGHT BUILDINGS

Niraj Poudel
Clemson University, npoudel@clemson.edu

Follow this and additional works at: https://tigerprints.clemson.edu/all_dissertations

Recommended Citation

Poudel, Niraj, "TOWARDS THE DEVELOPMENT OF PERFORMANCE BASED GUIDELINES FOR USING PHASE CHANGE MATERIALS IN LIGHTWEIGHT BUILDINGS" (2014). *All Dissertations*. 1360.
https://tigerprints.clemson.edu/all_dissertations/1360

This Dissertation is brought to you for free and open access by the Dissertations at TigerPrints. It has been accepted for inclusion in All Dissertations by an authorized administrator of TigerPrints. For more information, please contact kokeefe@clemson.edu.

TOWARDS THE DEVELOPMENT OF PERFORMANCE BASED GUIDELINES FOR
USING PHASE CHANGE MATERIALS IN LIGHTWEIGHT BUILDINGS

A Dissertation
Presented to
The Graduate School of
Clemson University

In Partial Fulfillment
of the Requirements for the Degree
Doctor of Philosophy
Planning, Design and the Built Environment

by
Niraj Poudel
May 2014

Accepted by:
Vincent Blouin, Committee Chair
Keith Green
Hoke Hill
Nigel Kaye

ABSTRACT

Incorporating Phase Change Materials (PCMs) in construction materials can increase the thermal mass of a building. With this increase in thermal mass, PCMs are known to reduce the heating and cooling loads of a building significantly. During the past 10 years, studies have estimated potential reduction of energy consumption of buildings between 10 and 30 percent. This wide range is due to the large number of parameters that effect energy consumption and make the process of selecting the optimal type and amount of PCM challenging. In fact, extensive engineering studies are generally necessary to determine the practicality of PCM in any specific case. As a result, architects and engineers are reluctant to use PCM because of the lack of such a comprehensive study.

In the United States, eight climate zones are identified on the basis of annual degree heating and degree cooling days. For a given building in a given climate, there exists an optimal melting temperature and enthalpy that can reduce the energy consumption and the payback period. In this research, the optimal properties of PCM boards are determined for all 15 representative cities. Additional topics discussed in this research are the sensitivity of the optimal properties of PCM and the effect of the average cost of energy on the selection of PCM. The effect of six independent variables on the performance of PCM boards is presented in detail and the climate types where PCM boards perform optimally are narrowed down. In addition, a new procedure is presented to study the temporal and directional melting and solidifying trend of the PCM placed in buildings.

The energy consumption and hourly data for the PCM enhanced buildings are determined numerically using the Department of Energy software EnergyPlus, which calculates the energy consumption for heating and cooling a building under any climate and operation schedule. The

software is run on a computer cluster for a wide range of properties from which the optimal values are extracted.

The findings from this research suggest that, there are only a few climate types within the United States where the use of PCM boards in lightweight buildings are viable. While the market potential for PCMs in building energy improvements can be significant, its acceptance is hindered by its extraordinary high cost. Analysis of the performance of PCM boards against six independent variables suggests that the internal load is a crucial factor in determining the optimal performance of PCM. Therefore any guideline on the selection of proper PCM should be formulated predominantly on the basis of internal load and the internal mean air temperature.

DEDICATION

This dissertation is dedicated to my late father Byas Jee Poudel and my mother Sharad Shashi Poudel. Their love and encouragement have made me into the person I am today and I am eternally grateful for their unconditional love and support.

ACKNOWLEDGMENTS

I would like to thank my committee members for their guidance and support during my time in the PDBE program. In particular, I would like to thank my advisor and committee chair Dr. Vincent Blouin for his support and encouragement throughout the program. Dr. Blouin has patiently guided me throughout this process and helped me stay focused within my research. I would like to sincerely thank Dr. Keith Green for introducing me to the PDBE program and believing in my ability to conduct independent research. Dr. Hoke Hill helped guide me, through his teaching and meetings with him, on the regression methods employed in this study. I would like to thank Dr. Nigel Kaye for agreeing to serve on my review committee and trusting in my ability to perform independent research. This research would not have been possible without the guidance of Dr. Edward Duffy who helped set up the thousands of simulations on the Palmetto Cluster at Clemson University. I am deeply grateful for his time and support. I would also like to thank Connie Robinson for helping me all the way throughout my registration woes.

My deepest gratitude goes to Anup Bhattarai and Elizabeth Brett who have provided me with unconditional love and support throughout my stay in Chicago and always. I would also like to thank Pallavi Sharma from the University of Illinois for taking the time out of her busy schedule to read this dissertation, provide me with invaluable advice and for helping me edit this dissertation. I appreciate the support provided by Shashwat Bee for helping me overcome my occasional writer's block. I would also like to thank all my friends at Clemson University and in particular Deborah Franqui, Noel Carpenter, John Lattimore and Jorge Mata Otero for making my stay at Clemson worthwhile.

Last but not least, I would like to thank my family members; my mother Sharad Shashi Poudel, my twin brother Suraj Poudel and my sister in law Mamta Kafle for all the love and encouragement that they constantly give me, even when they live oceans away.

TABLE OF CONTENTS

	Page
TITLE PAGE	i
ABSTRACT	ii
DEDICATION	iv
ACKNOWLEDGMENTS.....	v
LIST OF TABLES	ix
LIST OF FIGURES.....	xii
CHAPTER	
I. INTRODUCTION	1
Motivation	1
Objectives.....	5
Organization of the document	7
II. BACKGROUND AND LITERATURE REVIEW.....	9
Background	9
Benefits of TES	10
Methods of TES	12
Chemical heat storage	13
Sensible heat storage	13
Latent heat storage.....	14
Historical background	19
Chemical and thermo-physical properties of PCMs.....	21
Integration of PCMs in building materials	23
Experimental and numerical evaluation of PCM in buildings	25
Contribution towards literature	33
III. RESEARCH QUESTION AND DESIGN	37
Research method	37
Research design.....	38
Data collection method.....	47
Threats to validity.....	49
Pilot study.....	52
Development of the EnergyPlus model.....	52
Data collection.....	53

Table of Contents (Continued)

	Page
Data analysis and regression	54
Lessons learned	66
IV. CLIMATE MAPS.....	69
Payback period	70
Setup.....	72
Optimum melting temperature and enthalpy	74
Percent savings in energy	75
Pseudo payback period.....	78
Conclusion.....	80
V. PAYBACK PERIOD.....	82
Introduction	82
Energy saving and payback period constraint	84
PCM - R-value comparison.....	87
Payback period	90
VI. HVAC SETPOINT SCHEDULE AND LOCATION OF PCM.....	94
Setup.....	97
Results and discussion.....	103
HVAC A.....	104
HVAC B.....	110
HVAC C.....	114
Conclusion.....	116
VII. ALL CLIMATES AND ALL VARIABLES	119
Results and regression.....	124
People - internal loads	135
Volumetric heat capacity - enthalpy.....	141
R - value	145
Conclusion.....	149
VIII. PCM MELTING STUDY.....	154
Monthly indoor temperature and optimum PCM melting temperature	154
Monthly loads with different combinations of PCMs	160
Heating and cooling degree days (HDD & CDD).....	171
Performance of PCMs with different enthalpies	174
Hourly melting/solidifying of PCM	178
Results	182

Table of Contents (Continued)

	Page
Case 1: 0 people - 40 kJ/kg - 100 kJ/kg – WITH/WITHOUT HVAC	182
Case 2: 15 people - 40 kJ/kg - 100 kJ/kg – WITH/WITHOUT HVAC	197
Case 3: 24 people - 40 kJ/kg - 100 kJ/kg – WITH/WITHOUT HVAC	203
VI. CONCLUSION.....	208
Contribution and Discussion	208
Future Work	217
APPENDICES #	
A: PCM versus R-values and Payback period	221
B: PCM versus different insulation R-values	236
C: HVAC Study.....	251
D: Regression model plots for each climate	253
E: Magnitude of energy saved for individual internal load	264
F: Monetary savings for each additional enthalpy	279
G: Indoor Mean Air Temperature Plots for San Francisco.....	294
REFERENCES	296

LIST OF TABLES

Table	Page
3.1 List of independent variables, its number of levels, constant parameters and dependent variables.....	46
3.2 Regression details for the cooling load as dependent variable	57
3.3 Nested F-test for the surface coefficient terms - β_7 , β_8 , β_9 , β_{10} , β_{11}	58
3.4 Jackknifed prediction statistics for cooling as the dependent variable	58
3.5 Regression details for the heating load as dependent variable.....	59
3.6 Jackknifed prediction statistics for heating as the dependent variable	59
5.1 Construction details for the facade components.	84
5.2 An example of the equivalent latent heat storage (LHS).	86
6.1 Thermostat set-point temperatures and availability for HVAC A, B and C	98
6.2 PCM performance in a building with the HVAC A control schedule	100
6.3 HVAC A: Monthly heating load MJ for PCM melting at 24°C appended to the seven different scenarios	103
6.4 HVAC A: Monthly cooling load MJ for PCM melting at 24°C appended to the seven different scenarios	105
6.5 PCM performance in a building with the HVAC B control schedule.....	108
6.6 HVAC B: Monthly heating load MJ for PCM melting at 24°C appended to the seven different scenarios	109
6.7 HVAC B: Monthly cooling load MJ for PCM melting at 24°C appended to the seven different scenarios	111
6.8 HVAC C: Monthly cooling load MJ for PCM melting at 24°C appended to the seven different scenarios	113
6.9 The cost of electricity per kWh in each city.	113
6.10 The difference in annual load between the cases	115
7.1 List of independent variables, constant parameters and dependent variables.....	119

List of Tables (Continued)

Table	Page
7.2	Constants for the conversion of insulation R-values 123
7.3	The independent variables for the regression model 128
7.4	The regression models for the office HVAC schedule in all climates (Data: $19^{\circ}\text{C} \leq \text{Melting Temperature} < 25^{\circ}\text{C}$) 129
7.5	The regression models for the residential HVAC Schedule in all climates (Data: $19^{\circ}\text{C} \leq \text{Melting Temperature} < 25^{\circ}\text{C}$) 129
7.6	The regression models for the office HVAC schedule in all climates (Data: $\text{Melting Temperature} \geq 25^{\circ}\text{C}$) 130
7.7	The regression models for the office HVAC schedule in all climates (Data: $\text{Melting Temperature} \geq 25^{\circ}\text{C}$) 130
7.8	The regression models for the office HVAC schedule in all climates - Without PCM..... 131
7.9	The regression models for the residential HVAC schedule in all climates - Without PCM..... 131
8.1	The different scenarios simulated to make comparisons on how the two PCMs perform with and without the HVAC system 161
8.2	The optimum melting temperature of PCM and the corresponding energy saved - No internal loads. 173
8.3	The total heat storage offered by the PCM with different volumetric heat storage capacities..... 174
8.4	The energy dissipated indoors by the two levels of internal loads 177
8.5	Hourly reporting of the different variables from the simulations 178
8.6	The conditional statements that determine the physical state of the PCM 181
8.7	Conditional statements that determine the number of cycles the PCM goes through..... 182
8.8	Percentage of hours the PCM cycles through the different physical states..... 184

List of Tables (Continued)

Table	Page
8.9 Exact date and time observed for when the PCM fully melts and proceeds to fully solidify - 100 kJ/kg	185
8.10 Exact date and time observed for when the PCM fully melts and proceeds to fully solidify - 40 kJ/kg	186
8.11 Number of hours the PCM goes through each state during May. 40 kJ/kg & 100 kJ/kg	189
8.12 Number of hours the PCM goes through each state during October. 40 kJ/kg & 100 kJ/kg	189
8.13 Number of hours the PCM goes through each state during May. 0 people-23 melt-40 ent	192
8.14 Number of hours the PCM goes through each state during May. 0 people-23 melt-100 ent	192
8.15 Number of hours the PCM goes through each state during October. 0 people-23 melt-40 ent.....	193
8.16 Number of hours the PCM goes through each state during October. 0 people-23 melt-100 ent.....	193
8.17 Percentage of hours the PCM goes through each physical state 15 people-23 melt- 40 and 100 ent.....	198
8.18 Number of hours the PCM goes through each state during April. 40 kJ/kg & 100 kJ/kg - NO HVAC.....	201
8.19 Number of hours the PCM goes through each state during April. 40 kJ/kg & 100 kJ/kg - WITH HVAC.....	202
8.20 Number of hours the PCM goes through each state during April. 15 people-23 melt-40 ent	202
8.21 Number of hours the PCM goes through each state during April. 15 people-23 melt-100 ent	202
8.22 Percentage of hours the PCM goes through each physical state 24 people-23 melt- 40 ent.....	206
8.23 Percentage of hours the PCM goes through each physical state 24 people-23 melt- 100 ent.....	206

LIST OF FIGURES

Figure		Page
1.1	Buildings share of U.S. primary energy consumption.....	2
1.2	2008 U.S buildings energy end-use splits.....	3
2.1	a) Case with no TES system b) full TES system case.	11
2.2	Possible methods for reversible storage of thermal energy.....	12
2.3	Phase change diagram of water.....	16
2.4	Necessary layer thickness of different building materials to store as much heat as a 1 cm thick layer of PCM.....	17
2.5	Potential fields of application of PCM.....	18
2.6	Dover house (1949)	19
2.7	Comparison of organic, inorganic and eutectic PCMs..	22
2.8	Requirements for practical PCMs.....	23
2.9	a) SEM image of microcapsules b) Microcapsules in gypsum plaster.	24
2.10	a) shape-stabilized PCM plate b) SEM image of the microstructure.....	25
2.11	Maximum air temperature in the prototype room during July.....	30
2.12	Effect of phase change enthalpy, temperature and thickness.....	31
2.13	Energy consumption vs. insulation R-value..	32
2.14	Energy consumption vs. insulation R-value.....	32
3.1	Climate zones as defined by the US. DOE and its representative cities.	40
3.2	The wall, roof and floor construction as per the ASHRAE 90.1 standard.....	41
3.3	The three different length-to-width ratios: $\gg 1$, $=1$, $\ll 1$	41
3.4	The locations within the wall: exterior, interstitial, interior	42
3.5	The different surfaces to which PCM will be applied to..	43

List of Figures (Continued)

Figure	Page
3.6 Occupancy and internal loads within the building.....	44
3.7 Ventilation and infiltration in a building	45
3.8 Thermal property definition of a theoretical PCM melting at 23° C within EnergyPlus using the enthalpy-temperature function.....	48
3.9 South wall interior surface temperature comparison a) Chongqing Study b) EnergyPlus replication.....	50
3.10 South wall and roof - interior and exterior surface temperature comparison.	51
3.11 Building details for the pilot study.....	52
3.12 Heating load with respect to melting temperature and enthalpy.....	54
3.13 Cooling load with respect to melting temperature and enthalpy..	55
3.14 The heating and cooling load with PCM placed on different surfaces	55
3.15 a) The heating load versus enthalpy - PCM placed on the floor b) The cooling load versus enthalpy - PCM placed on the roof..	56
3.16 Scatter plot of the cooling and heating loads with PCM on the east wall.....	60
3.17 Regression statistics for the cooling and heating load - east wall.....	61
3.18 Scatter plot of the cooling and heating loads with PCM on the south wall	61
3.19 Regression statistics for the cooling and heating models - south wall.....	62
3.20 a) PCM placed inside of the insulation, b) PCM placed outside of the insulation..	63
3.21 Difference in heating load for when PCM is placed outside versus inside the insulation. Internal loads of zero people.....	63
3.22 Difference in cooling load for when PCM is placed outside versus inside the insulation. Internal loads of zero people.....	64
3.23 Difference in heating load for when PCM is placed outside versus inside the insulation. Internal loads of fifteen people..	65
3.24 Difference in cooling load for when PCM is placed outside versus inside the insulation. Internal loads of fifteen people	65

List of Figures (Continued)

Figure	Page
3.25	Difference in heating load for when PCM is placed outside versus inside the insulation. Internal loads of fifteen people 66
4.1	Thermal property definition of a theoretical PCM melting at 23° C within EnergyPlus using the enthalpy-temperature function..... 73
4.2	Analytical map for the annual load (magnitude) with the optimum PCM melting temperature for each climate..... 74
4.3	Analytical map of the energy savings in magnitude by using the optimum PCM in each climate zone.. 76
4.4	Energy saved as function of PCM’s melting temperature for the 15 climates (set point temperatures: 21°C and 25°C)..... 77
4.5	Analytical map of the pseudo payback period assuming a \$1/kg cost of PCM board & \$0.07/kWh cost of electricity..... 78
4.6	(a) Pseudo payback period (b) Cost of PCM and electricity needed to achieve a PPP of 10, 20 and 30 years in Albuquerque..... 79
5.1	The four cases simulated to assess the performance of PCM boards against different R-value of insulation..... 85
5.2	San Francisco - office HVAC - R-value, PCM comparison 87
5.3	San Francisco - residential HVAC - R-value, PCM comparison..... 88
5.4	Albuquerque - Office HVAC - R-value, PCM comparison..... 88
5.5	Seattle - office HVAC - R-value, PCM comparison..... 89
5.6	Seattle - residential HVAC - R-value, PCM comparison..... 89
5.7	San Francisco - office HVAC - money saved annually (Top) and payback period (bottom)..... 91
5.8	San Francisco - residential HVAC - money saved annually (top) and payback period (bottom)..... 91
5.9	Seattle - residential HVAC - money saved annually (top) and payback period (bottom)..... 92

List of Figures (Continued)

Figure	Page
5.10 Albuquerque - office HVAC - money saved annually (top) and payback period (bottom).....	93
6.1 Baseline building model and construction details.....	97
6.2 PCM properties appended to the gypsum board and the idealized enthalpy-temperature curve.....	99
6.3 The seven different cases where the PCM was cycled through the walls.....	99
6.4 Graphical representation of the thermostat set-point schedules for HVAC A, B and C.....	102
6.5 HVAC A: Total load chart for PCM with different melting temperatures placed on different surfaces.....	117
6.6 HVAC B: Total load chart for PCM with different melting temperatures placed on different surfaces.....	112
6.7 HVAC C: Total load chart for PCM with different melting temperatures placed on different surfaces.....	115
7.1 Aspect ratios for the three different buildings with the same floor area.....	121
7.2 Difference in actual and predicted values of a one regression model.....	125
7.3 Difference in actual and predicted values of a piecewise regression model.....	126
7.4 Difference in actual and predicted values of the data-split regression model.....	127
7.5 Difference in actual and predicted percent energy saved for the 25' X 49' building in Albuquerque with an Office HVAC schedule.....	132
7.6 Difference in actual and predicted percent energy saved for the 35' X 35' building in Albuquerque with an Office HVAC schedule.....	133
7.7 Difference in actual and predicted percent energy saved for the 49' X 25' building in Albuquerque with an Office HVAC schedule.....	134
7.8 Albuquerque - office - Percent energy saved for levels of internal loads.....	136
7.9 Albuquerque - office HVAC - Percent energy saved for additional levels of internal loads.....	137

List of Figures (Continued)

Figure	Page
7.10 Albuquerque - office HVAC – magnitude energy saved for additional levels of internal loads	138
7.11 San Francisco - office HVAC – magnitude energy saved for additional levels of internal loads.....	139
7.12 The percent energy saved for every 20 kJ/kg jump in enthalpy.	141
7.13 Albuquerque - Office HVAC - magnitude energy saved for additional PCM enthalpy.....	142
7.14 Albuquerque - Office HVAC - magnitude energy saved for additional PCM enthalpy.....	143
7.15 San Francisco - Office HVAC - money saved annually for additional PCM enthalpy.....	144
7.16 San Francisco - Residential HVAC - money saved annually for additional PCM enthalpy.....	145
7.17 Albuquerque - Office HVAC – percent Savings (top) and magnitude saved (bottom) for different R-value of insulation.....	146
7.18 Albuquerque - Office HVAC – percent Savings (top) and magnitude saved (bottom) for different internal loads in each column.....	148
7.19 San Francisco - Office HVAC – percent Savings (top) and magnitude saved (bottom) for different R-value of insulation.....	148
7.20 San Francisco - Office HVAC – percent Savings (top) and magnitude saved (bottom) for different internal loads in each column.....	149
8.1 Indoor mean air temperature with and without PCM, and monthly average without PCM. (0 people - Without HVAC).....	156
8.2 Indoor mean air temperature with and without PCM, and monthly average without PCM. (0 people - With HVAC).....	157
8.3 Indoor mean air temperature with and without PCM, and monthly average without PCM. (15 people - With HVAC).....	158
8.4 The indoor mean air temperature with and without PCM with different melting temperatures.	159

List of Figures (Continued)

Figure	Page
8.5 The indoor air temperature with and without PCM for three indoor loads, 0, 15 & 24 people.	160
8.6 Albuquerque - Office – 23-100-PCM - 0 people -monthly Loads. with PCM (top) without PCM (middle).....	162
8.7 Albuquerque - Office – 25-100-PCM - 0 people -monthly Loads. with PCM (top) without PCM (middle).....	163
8.8 Albuquerque - Office – 23-100-PCM - 24 people -monthly Loads. with PCM (top) without PCM (middle).....	164
8.9 Albuquerque - Office – 25-100-PCM - 24 people -monthly Loads. with PCM (top) without PCM (middle).....	165
8.10 Albuquerque - Office - 24 people. 23°C PCM (top) - 25°C PCM (bottom) - without HVAC - mean air temp - 24 people.....	166
8.11 Albuquerque - Office - 24 people. 23°C PCM (top) - 25°C PCM (bottom) - without HVAC - hourly Cooling Rate [W].....	167
8.12 Albuquerque - Office HVAC - 23 melt -100 enthalpy - energy saved - 0 people (top), 15 people (middle), 24 people (bottom)	168
8.13 San Francisco - Office HVAC - 24 melt -100 enthalpy - energy saved - 0 people (top), 15 people (middle), 24 people (bottom).....	169
8.14 San Francisco - Office - 24 People. 23°C PCM (top) - 24°C PCM (bottom) - without HVAC - Mean Air Temp - 15 people	170
8.15 San Francisco - Office - 24 People. 23°C PCM (top) - 24°C PCM (bottom) - without HVAC - Mean Air Temp - 24 people	171
8.16 Heating and cooling degree days for the different climates using a base of 65°F (18°C).....	172
8.17 Comparison of monthly energy saved by using 40 kJ/kg PCM (left) versus 100 kJ/kg PCM (right).....	175
8.18 Monthly difference in energy saved between the two volumetric heat capacities (40 & 100 kJ/kg).	176
8.19 Construction details and the nodal placements for the conduction finite difference algorithm.....	180

List of Figures (Continued)

Figure	Page
8.20 Hourly mean air temperature indoors for PCM melting at 23°C and 0 People. without HVAC (top) and with HVAC (bottom).....	183
8.21 Graphical representation of melting/solidifying of the PCM in table 7.10 (top) & 7.09 (bottom) without HVAC.....	187
8.22 Graphical representation of melting/solidifying of the PCM in table 7.10 (top) & 7.09 (bottom) with HVAC.....	187
8.23 Outside face solar radiation heat gain rate per area [W/m ²].....	191
8.24 Nodal temperatures compared against outdoor dry bulb temperature and radiation heat gain for the week in May.....	194
8.25 Nodal temperatures compared against indoor mean air temperature and radiation heat gain for the week in May.....	195
8.26 Nodal temperatures for the north wall (top) and roof (bottom) during the 2nd week in May.....	195
8.27 Nodal temperatures for the north wall (top) and roof (bottom) during the 2nd week in October.....	196
8.28 Hourly mean air temperature indoors for PCM melting at 23°C and 15 People. without HVAC (top) and with HVAC (bottom).....	197
8.29 Graphical representation of melting/solidifying of the PCM in table 7.10 & 7.11 with HVAC.....	200
8.30 Graphical representation of melting/solidifying of the PCM in table 7.10 & 7.11 without HVAC.....	200
8.31 Hourly mean air temperature indoors for PCM melting at 23°C and 24 People. without HVAC (top) and with HVAC (bottom).....	203
8.32 Melting/solidifying frequency shift - 23-100-PCM - 0 people (top) 15 people (middle) to 24 people (bottom) - without HVAC.....	204
8.33 Melting/solidifying frequency shift - 23-100-PCM - 0 people (top) 15 people (middle) to 24 people (bottom) - with HVAC.....	205

Chapter One

INTRODUCTION

Motivation

Sustainable energy has been a dominant theme in today's global lexicon. The search for efficient, economical and feasible sources of energy is a continual endeavor undertaken by researchers, practitioners and scientists alike. It is increasingly clear that our finite energy resources, namely coal, oil and natural gas, can by no means meet our needs of the future. Currently while the yearly global energy consumption rests at a staggering 513.2 Quadrillion British thermal units (Quads), it is projected to increase to 769.8 quads by the year 2035 (EIA, 2011). Yet we continue to meet these demands through use of non-renewable and dwindling resources. This problem is further exacerbated by the continual increase in global population, reduction of natural resources, the more populous countries trying to imitate the affluent lifestyle of the west and the political volatility that currently plagues some of the countries from the Organization of Petroleum Exporting Countries (OPEC) to name a few. As some scholars point out, this unprecedented rise in demand for energy not only leads to immeasurable ecological consequences but political consequences as well. They underscore that the fight for access and control over these energy resources will intensify more. Seen from this perspective, finding new ways to harness energy, using what we already have sparingly and simultaneously conserving it is not only a sensible environmental policy but is also a contribution towards peace (Schittich, 2003).

It is fairly evident that among the industrial nations the United States is one of the leading energy consumers and has been for quite some time. Take for example the energy consumption of

the United States as compared to that of the entire world in the year 2008. In 2008, while the global energy consumption totaled 505 Quadrillion British thermal units (BTU) (IEA, 2011), the United States consumed approximately 1/5th of that totaling 100.2 Quads (BEDB, 2010). Furthermore, of the 100.2 Quads of energy used within the United States, 39.9 percent is accounted for by buildings, both residential and commercial (BEDB, 2010). Similar statistics are available for Europe and Asia. Buildings account for roughly 40 percent of total energy consumption in Germany, higher than of transportation or industry (Schittich, 2003). Similar to Europe and America, yet less severe in 2007 was China's trend. As of 2007, China's buildings sector accounted for 23 percent of China's total energy use and this was projected to increase to one-third by 2010 (Liang, 2007).

1.1.3 Buildings Share of U.S. Primary Energy Consumption (Percent)							
	Buildings			Industry	Transportation	Total	Total Consumption (quads)
	Residential	Commercial	Total				
1980(1)	20.2%	13.6%	33.8%	41.1%	25.2%	100%	78.3
1985	21.0%	15.0%	36.0%	37.8%	26.2%	100%	76.7
1990	20.1%	15.8%	35.9%	37.7%	26.4%	100%	84.8
1995	20.3%	16.1%	36.4%	37.3%	26.2%	100%	91.5
2000	20.6%	17.4%	38.0%	35.0%	26.9%	100%	99.1
2005	21.5%	17.8%	39.3%	32.3%	28.4%	100%	100.8
2008	21.5%	18.4%	39.9%	32.1%	28.0%	100%	100.2
2010	22.5%	18.8%	41.3%	30.6%	28.1%	100%	97.8
2015	20.1%	18.6%	38.7%	33.3%	28.0%	100%	102.0
2020	20.0%	19.3%	39.3%	33.1%	27.7%	100%	104.9
2025	20.1%	19.9%	39.9%	32.6%	27.5%	100%	107.9
2030	20.1%	20.5%	40.6%	31.8%	27.6%	100%	111.1
2035	20.0%	21.0%	41.0%	31.0%	27.9%	100%	114.4

Note(s): 1) Renewables are not included in the 1980 data.
Source(s): EIA, State Energy Data 2008: Consumption, June 2010, Tables 8-11, p. 24-27 for 1980-2007; and EIA, Annual Energy Outlook 2011 Early Release, Dec. 2010, Summary Reference Case Tables, Table A2, p. 3-5 for 2008-2035 data and Table A17, p. 34-35 for non-marketed renewable energy.

Figure 1.1: Buildings share of U.S. primary energy consumption (Source: D&R International, 2010)

These statistics serve as a clear indicator that the building sector is where there is a lot of energy saving potential and possibly much room for improvement. After all, the residential and commercial buildings include all office buildings, hospitals, stores, restaurants and schools that together, combined, consume more energy than either of the other sectors, industry and transportation.

A closer look at the energy consumption within the buildings energy end-use splits in 2008 (Figure 1.2) tells us that, within the United States, approximately 46 percent of the energy went towards space heating and cooling (BEDB, 2010). That amounts to 18.4 Quadrillion British thermal units. This tremendous amount of energy is and has been traditionally provided by storage of fuel. In the case of wood, coal, petroleum and natural gas, fuel storage has been convenient and economical (Lane, 1983). However as the fallibility of our fossil fuel supplies becomes abundantly clear, it seems prudent to steer ourselves away from this dependency.

	Natural Gas	Fuel Oil (1)	LPG	Other Fuel(2)	Renw. En.(3)	Site Electric	Site	
							Total	Percent
Space Heating (5)	4.96	0.78	0.26	0.11	0.56	0.71	7.37	36.9%
Lighting						2.01	2.01	10.0%
Space Cooling	0.03					1.74	1.78	8.9%
Water Heating	1.77	0.13	0.09		0.03	0.57	2.58	12.9%
Refrigeration (6)						0.86	0.86	4.3%
Electronics (7)						0.78	0.78	3.9%
Ventilation (8)						0.53	0.53	2.7%
Computers						0.39	0.39	2.0%
Cooking	0.38		0.03			0.25	0.67	3.3%
Wet Cleaning (9)	0.05					0.31	0.37	1.8%
Other (10)	0.29	0.01	0.29	0.05	0.00	0.78	1.43	7.1%
Adjust to SEDS (11)	0.73	0.18				0.33	1.24	6.2%
Total	8.22	1.11	0.67	0.15	0.59	9.27	20.00	100%

Figure 1.2: 2008 U.S Buildings energy end-use splits (Source: BEDB, 2010)

One such way to steer ourselves clear from this predicament is to harness the abundant energy potential that the sun places at our disposal on a daily basis. The incident solar radiation on the earth surface alone is 3000 times greater than the worldwide demand (Schittich, 2003). Thus using solar energy as a means to heat buildings is an attractive alternative. Storing solar energy in order to heat homes, if done efficiently, has far reaching benefits. It is therefore incumbent on scientists, engineers, architects and scholars to find novel ways to heat and cool buildings using renewable resources thereby lowering our dependency on non-renewable sources of energy.

Over the last two decades ‘Smart materials’ such as phase change materials (PCMs), electro-chromic glass, light emitting diodes, shape memory alloys, etc. have sparked considerable interest within the building industry owing their intrinsic ability to respond quickly to any external stimulus. Defined as “highly engineered materials that respond intelligently to their environment” by (Addington, 2005), smart materials, today, are at the forefront of sustainable design. Although such materials offer the possibility of regulating the indoor environment to a certain extent, they cannot be considered to resolve all issues related to indoor temperature control without proper understanding of its thermal control features. For instance it would be wrong to merely design a curtain wall facade based on the expectation that the addition of electro-chromic windows will reduce the solar heat gain. The age old tussle between the form and material has been brought to the forefront once again. Thomas (2007) argues that within the practice of architectural design, the form is always privileged over the material and that the material merely acts as a servant to the form. Thomas argues that materials should matter and that it should influence the form and not always the other way around. Although the form/matter split has its proponents and detractors on both sides, this particular research will seek to emphasize the role of smart materials within the built environment, hopefully ‘revive’ materials from its perceived secondary status. As Thomas (2007) points out, “(Due to the ability of smart materials to respond to the immediate environment), form emerges out of a transaction with the material or the material demands/invites certain practices in terms of maintenance or behavior.” The material is thus no longer considered inert but rather a dynamic entity that inspires form. Rather than being chosen after the basic design is completed, materials and properties become the starting point of any architectural design (Addington, 2005). For example the knowledge of phase change materials and its ability to store large amounts of energy can become the ‘starting point’ for the designer. The designer can have more architectural freedom to consider using thinner partition

walls indoors that can provide the same thermal storage as that of thicker walls. Even though deemed ‘smart’ these materials still need to be strategically placed within the environment. It is unwise to indiscriminately apply such smart materials anywhere in the building and expect the material to perform in a desired manner so as to achieve certain energy related goals. It is therefore incumbent on the designers to possess a certain level of understanding of the material to successfully apply them within the context of the building.

Architecture has always sought to provide ‘service and delight’ as laid out in the Vitruvian Virtues of Architecture as *firmitas*, *utilitas* and *venustas* (Fernandez, 2006). *Firmitas* and *utilitas* define the service rendered by the buildings and *venustas* (also known as delight) defines the qualities of the building that are there to enhance our sensory experience. The idea of ‘delight’ or aesthetics of a building is continually evolving and has been, in part, fueled by the technological advances in the built environment. Such advances in technology have helped build monumental structures that were once thought inconceivable. We have also grown accustomed to greater comfort levels within our buildings due to such advances in technology. As a result designers and engineers alike are constantly searching for materials and methods to achieve an optimal mix of delight and service (Fernandez, 2006). When a new material is sought to achieve an optimal mix of delight and service it must be vetted and tested, its capabilities and limitations clearly delineated.

Objectives

This research seeks to develop guidelines for the use of phase change materials within the built environment from a service standpoint for architects and designers alike. Performance based guidelines will be developed in order to bridge the gap between the availability of new technology (i.e. phase change materials) and its use within the built environment. The increasing

influx of new materials and technology into the building industry is likely to cause confusion as to how such technology might be implemented intelligently. The application of new technology in buildings is often perceived as a new and risky field and it seems to generate conservatism among architects and stakeholders. This results in, either an extensive re-use of old and tested solutions for the fear of making mistakes resulting in litigation (Rygghaug, 2009) or the need for individuals with a propensity for risk taking (Bessant, 1995). If only architects and engineers had a set of guidelines on how or where to use the new technology, much of the strife about the use of such technology would dissipate. In (Cooke, 2007), a research conducted on 41 stakeholders (i.e. architect, building services engineer, client, consultant, planner, project manager, technology supplier, and contractor) and their perceptions on Alternative Energy Technologies (AET), the researchers found that across the participants there was strong support for the case that lack of education was the underlying problem and that that further education and presentation of experiences are required for them to be comfortable to adapt to new technology. The problem of lack of knowledge not only applies to the designers, contractors and workers, but also to the clients. Due to the lack of knowledge, clients also need to be convinced that these systems will work and will not have to be replaced with expensive traditional replacements post occupancy (Tsoutsos, 2005). Therefore the design methodology/guidelines presented in this document will serve to educate designers and engineers on the viability of using PCM in their designs. In addition, the guidelines will give the designer specific instructions on how much PCM to use, where to place it and what specific PCM to use in order to get the most energy savings in the building. The methodology presented in this document eliminates the guess-work pertaining to efficient energy usage and provides the designer with a set of guidelines to resolve energy related issues. Since the guidelines are developed by virtue of measuring the performance of PCMs in

buildings, the clients can also be informed so as to make a judicious choice on whether the application of PCMs will work for their particular project.

Organization of the document

The organization of this research is done in the following sequential order:

Literature Review: In chapter 2, the existing literature on the study of Phase Change Materials in buildings is surveyed. The characterization of and the different thermo-physical properties of PCM is studied. The metrics commonly associated with the use of PCM and the different methodologies used to determine and explain the potential benefits is surveyed.

Research question and design: In chapter 3, a research question is developed to address a specific field within the surveyed literature. A research methodology is also pursued in order to address and to best answer the research question. In this chapter, a pilot study is also performed in an attempt to improve the design of experiment, by identifying design issues and feasibility of data collection methods and tools, prior to the full scale experiment.

Climate map, PCM placement and HVAC schedules: Chapter 4 and 5, include the design and results of two studies performed on three different independent variables of the larger study. These two studies were conducted to improve on the design space of independent variables that would be used later during the larger study.

The larger study: Chapter 6 includes the analysis and results of the full factorial experiment. Regression models are developed in chapter 6, for each climate type in the US. The regression models allow a seamless integration of empirical data with the climate maps developed in Chapter 4. The influence of each independent variable (within the design space) on the energy performance of PCM in each climate is also analyzed and presented. In chapter 6, payback periods are calculated for each scenario and compared against the cases without the use of PCM.

The viability of the use of PCM boards in each climate is analyzed, questioned and results are explicated.

Hourly detailed analysis: In Chapter 7, the optimum scenarios of the use of PCM is selected. The annual, monthly, and hourly melting and solidifying of the PCMs are studied against the backdrop of exterior and interior environmental loads. The theory developed by Neeper (2000) about the maximum energy storage of PCM on the basis of the mean indoor temperature is tested for the average annual and monthly indoor mean air temperatures. A new methodology is applied to precisely identify the directional and temporal melting and solidifying of PCMs, which can be used for future study.

Conclusion, research limitations and future work: Chapter 8 includes the contributions made to literature by this research and also delineates the future work that can further enhance the knowledge on the appropriate use of Phase Change Materials in different contexts.

Chapter Two

BACKGROUND AND LITERATURE REVIEW

Background

It is worthwhile to note that fossil fuel has not always been the primary choice for regulating thermal condition of our living environment. It was not until the industrial revolution that we learned to harness energy stored within the depths of the earth. In the past however, we have employed various sustainable and innovative techniques, although not as efficient, to heat and cool our living spaces. About 2000 years ago, the Romans started to use thick stone walls and ceramic tiles on the floor to store heat in under floor heating systems (Mehling, 2008). This way the Romans exemplified how sunlight during the day could be captured and stored within the structural components of a building as heat; heat that could later be dissipated indoors. As a result, a comfortable indoor temperature was maintained even when there was no heat source in the form of fire. This example brings forth the idea of thermal energy storage (TES) by creating a ‘thermal mass’. The thermal mass in a building is created by exploiting inherent thermal properties, such as the thermal inertia, of one or many construction materials. Traditionally thick building walls and floors built out of masonry have served well as thermal masses, in regulating the indoor climate owing to their high thermal inertia. The working principle of a thermal mass is that during the summer days, the mass absorbs the heat (charging), keeping the internal space cooler than outside while during the night, when the outdoor temperature falls, the mass dissipates the heat indoors (discharging) to maintain the indoor temperatures at a comfortable level. In winter, the mass stores the heat from solar radiation, and releases it at night to help warm the internal space (Hyde, 2008). Thermal mass therefore allows the retention and release of solar

radiation within a building. However, energy can be stored not only as heat but as cold as well. Another form of using thermal mass is to store cold at a certain time and release it at some other later time when cooling is required. Traditionally blocks of ice, cut in the winter from frozen lakes or rivers were stored in “ice houses” to cool buildings during the summer season (Lane, 1983). The Hungarian parliament building in Budapest is still air-conditioned, with ice harvested from Lake Balaton in the winter (Dincer, 2011).

Thermal energy storage has been employed in buildings for a long time. The concept of harnessing renewable forms of energy to heat and cool buildings predates the use of air conditioners, space heaters and any form of mechanical equipment run on fossil fuels. While Europeans embraced the concept of building thick walls made of stone that helped regulate indoor temperatures, the Eskimos built igloos of compressed snow to trap indoor heat and shield them from harsh outdoor temperatures. Even today, due to some of the already mentioned contemporary global issues, thermal energy storage has garnered a lot of interest for space heating, hot water, cooling and air-conditioning.

Benefits of TES

There are three major benefits of using TES systems in buildings. According to (Dincer, 2011), “the increasing societal energy demands, shortages of fossil fuels, and concerns over environmental impact are providing impetus to the development of renewable energy sources such as solar, biomass, and wind energies. Because of their intermittent nature, effective utilization of these and other energy sources are, in part, dependent on the availability of efficient and effective energy storage systems.” Thus, one of the first benefits of TES systems is to help store renewable energy that is inherently intermittent in nature. This allows for TES systems to provide energy to meet instantaneous demands. For instance the thermal energy stored in hot

water during the day can be used instantaneously in the morning when the sun is not out yet. Another benefit of using TES systems is that it can manage the electrical load in buildings (Dincer, 2011; Mehling, 2008). The need for cooling and air-conditioning during the day often causes a peak demand in electricity. Because of this high demand, electricity prices are high during the day. A thermal storage system stores excess indoor heat during the day thereby reducing the indoor temperature for some time.

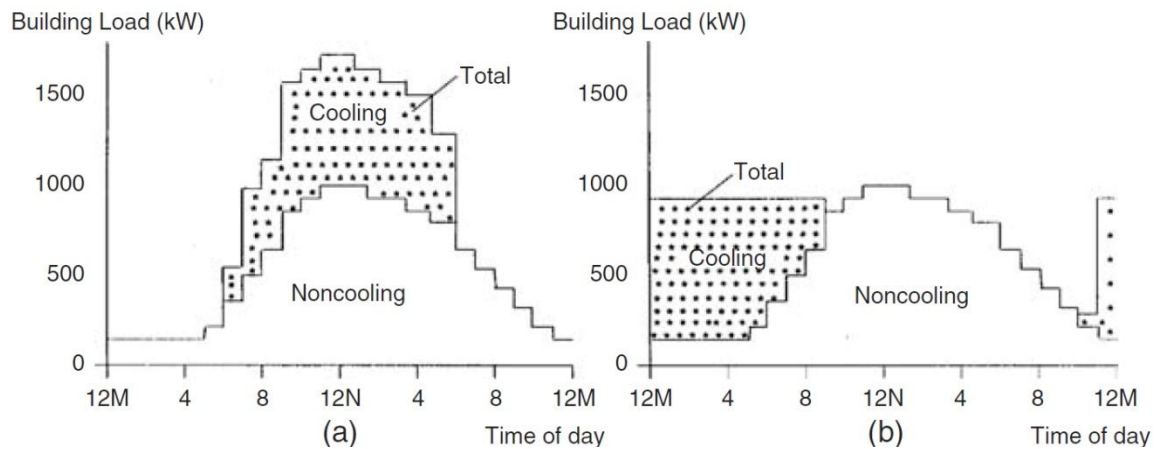


Figure 2.1:a) Case with no TES system b) full TES system case. (Source: Dincer, 1997b)

Figure 2.1 shows an example of daily load profiles for a building with and without TES technology (Dincer, 1997b). It can be seen from Figure 2.1b) that TES provides enough storage capacity to meet the peak (i.e. 9:00 a.m. to 9:00 p.m.) cooling load, shifting the entire electrical demand for cooling to off-peak hours when there is little cooling load. TES systems therefore shift the heating and cooling demands to later time periods when electricity prices are lower. Load shifting can also reduce demand charges, which can represent a significant proportion of total electricity costs for commercial buildings. Consider an office building where on a typical summer day the peak cooling demand is at around 3 P.M. A TES system, in principle, can absorb the excess heat until it can no longer store more energy thereby postponing the time when peak cooling demand occurs. As a result the peak cooling demand is shifted to 5 P.M as opposed to 3

P.M. Since the employees leave for the day at 5 P.M, there is no need to cool a building at a time when no one occupies it. The third benefit is very closely related to the benefits of shifting the heating and cooling demands. Because of the capability of TES systems to shift the load, dampen and temper the diurnal temperature fluctuations within the building, TES systems allow for the downsizing of the Heating, Ventilating and Air-Conditioning (HVAC) systems as well. This translates directly to initial cost savings by having to use smaller air-handling units, smaller ducts and smaller variable air volume (VAV boxes) within the system (Dincer, 2011; Mehling, 2008). The downsizing of mechanical equipment not only means initial cost savings but also means that more space is created within the building. This newly freed up space provides architectural freedom for the designers of the building as well. From a systems thinking approach, it is a win-win situation for all parties (i.e. occupants, architects, engineers etc).

Methods of TES

There are two possible methods for reversible storage of heat and cold as shown in Figure 2.2 namely physical and chemical (Dincer, 2011; Mehling, 2008; Lane, 1983). In order for a system to retrieve the stored energy and use it for many continuous cycles (charging and discharging), these methods need to be reversible.

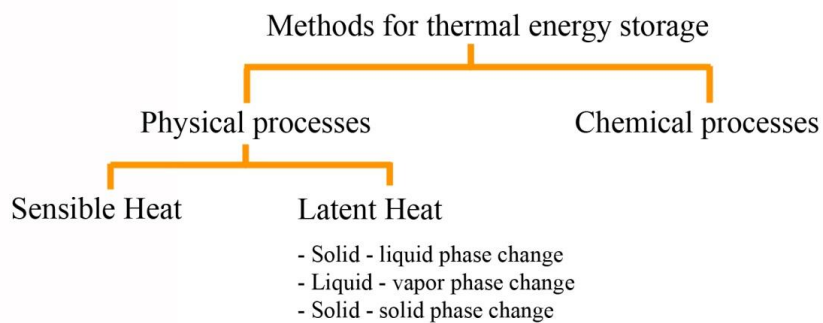


Figure 2.2: Possible methods for reversible storage of thermal energy.

Chemical heat storage

The storage of thermal energy when chemicals either form bonds or break bonds during a chemical reaction is essentially the theory behind chemical storage. When a chemical reaction takes place, the total energy of the system either increases by absorbing energy (endothermic reaction) or decreases by dissipating energy (exothermic reaction) (Lane, 1983; Mehling, 2008). Only chemicals whose reactions are reversible and that possess a high heat of reaction (i.e. high amount of energy absorbed or desorbed during a reaction) are suitable for thermal storage applications in buildings. This type of storage is unfamiliar in ordinary human experience especially since thermo-chemical storage technology has not been widely used within building applications.

Sensible heat storage

Sensible heat storage is the most common form of thermal energy storage. This type of storage is the most familiar form as our senses gauge the heat content of a material by how hot or cold it may feel (Lane, 1983). In sensible heat storage, energy is stored while temperature of the material rises. Rock beds and masonry walls are familiar and pervasive technologies that store thermal energy in the form of sensible heat. Similarly in the liquid medium, we are aware of hot water heat storages used for domestic hot water in households. Although we are most familiar with this form of heat storage, we cannot for certain quantify the amount of thermal energy stored in a medium only by touch. The actual heat content stored within the material is a function of its heat capacity. Two materials could, in essence, feel the same to touch but contain different amounts of thermal energy. Mathematically, the amount of thermal energy stored in a medium can be defined as:

$$Q = \int_{T_1}^{T_2} m \cdot C_p \cdot dT = m \cdot C_p (T_2 - T_1)$$

Where,

Q = Quantity of heat stored

T_1 = Initial temperature

T_2 = Final temperature

m = Mass of heat storage medium \newline

C_p = Specific heat capacity of storage medium.

Latent heat storage

Latent heat storage shows the most promise in thermal energy storage systems. This is because latent heat thermal energy storage (LHTES) systems are capable of storing large amounts of energy with little to no temperature change of the medium. In addition, Mehling and Cabeza (2008) state that, “people like to have room temperatures in a very narrow temperature range and a narrow temperature range is exactly the situation where latent heat thermal energy storage systems can be used for temperature regulation and for heat or cold storage with high storage density.” The majority of energy is stored when the medium changes phase (i.e. solid to liquid, liquid to gas etc). In general, the term “latent heat” describes the heat of solid-solid, solid-liquid, and liquid-vapor phase changes. However, for building applications the most feasible materials that change phase are the ones that change from solid to solid or from solid to liquid. Any phase change to gas is not deemed practical because of the high volumetric expansion associated with gas and the resulting difficulty in confining it properly. Therefore the solid-solid and solid-liquid latent heat storage materials that are used in building applications are called phase change materials (PCMs) (Mehling, 2008). In addition, PCMs not only store latent energy but also the

sensible heat energy gained from its increase in temperature before and after the phase change.

This additional contribution can be seen in the mathematical expression below (Lane, 1983):

$$Q = m \cdot a_m \cdot \Delta h_m + \int_{T_1}^{T_m} m \cdot C_{p_s} dT + \int_{T_m}^{T_2} m \cdot C_{p_l} dT = m [a_m \cdot \Delta h_m + C_{p_s} (T_m - T_1) + C_{p_l} (T_2 - T_m)]$$

Where,

a_m = Fraction melted

Δh_m = Heat of fusion per unit mass or specific enthalpy

T_m = Melting temperature

C_{p_s} = Specific heat capacity during solid phase

C_{p_l} = Specific heat capacity during liquid phase.

The first term on the right hand side of equation pertains to the energy stored by the material in the form of latent heat. The fraction melted (a_m), ranging from zero to one, takes into account the amount of material melted. The two other terms and account for the sensible heat gained by the material. The term $\int_{T_1}^{T_m} m \cdot C_{p_s} dT$ represents the amount of sensible heat gained while its initial temperature is raised to the melting temperature (denoted by the subscript 's') and the second term $\int_{T_m}^{T_2} m \cdot C_{p_l} dT$ denotes the amount of sensible heat gained when the temperature continues to increase after the material is completely melted (denoted by the subscript 'l'). The equations only depict a solid-liquid phase change and additional terms would be necessary to include the liquid-gas phase change. Phase change is also more conveniently shown in phase diagrams.

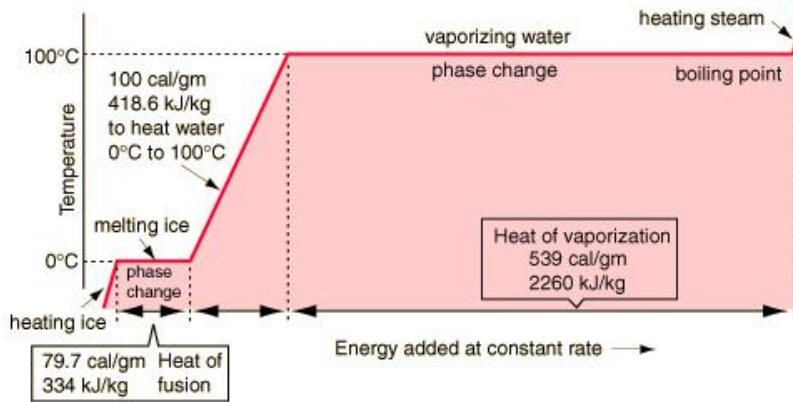


Figure 2.3: Phase change diagram of water. (Source: Nave, 2010)

Figure 2.3 shows the phase diagram of water and the associated energy absorbed and released during the change of phase. Water during its change of phase from liquid to gas absorbs 2260 kJ/kg of latent energy. This is approximately five times the amount of sensible energy absorbed when raising the temperature of water from 0°C to 100°C. Added to that, while the 2260 kJ/kg of energy is absorbed, the temperature of water does not change; it stays constant at 100°C. Hence, water absorbs a lot of energy (i.e. 2260 kJ/kg) without the change in temperature; it only changed in phase from liquid to gas. The same principle is used in solid-liquid phase change materials (PCMs) which absorb energy during the phase change from solid to liquid. The process is the same with solid-solid PCM as well, except that the melting temperature is replaced by a phase transition temperature since there is no melting but a change of micro-structure, which requires energy (i.e. latent heat). The PCM remains solid during the absorption of energy. While water is considered to be the best known and most widely used phase change material, around 200 phase change materials with varying thermo-physical properties have been identified as candidates for use in building applications (Lane, 1983).

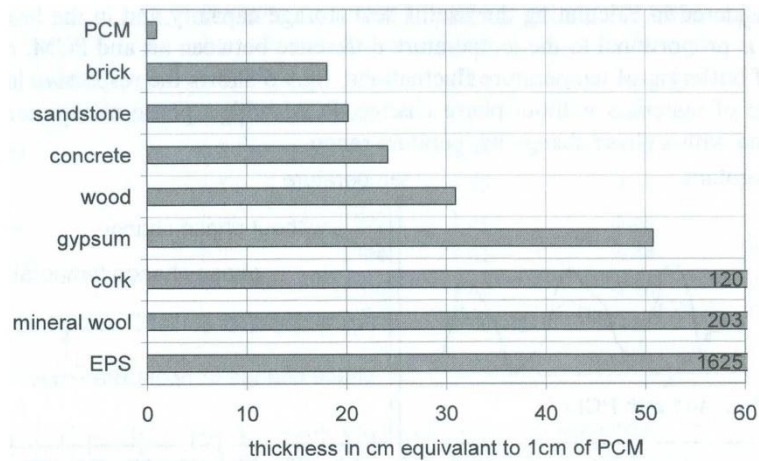


Figure 2.4: Necessary layer thickness of different building materials to store as much heat as a 1 cm thick layer of PCM. (Source: Mehling, 2008)

In comparison to other construction materials, PCMs are capable of storing tremendous amounts of heat. Figure 2.4 shows the required thickness of other construction materials to store an equivalent amount of thermal energy that a 1 cm thick layer of PCM is able to absorb. The PCM in this particular comparison is capable of storing 130 MJ/m^3 at a temperature difference of 4 Kelvin (Mehling, 2008). It takes approximately 18 cm of brick or 24 cm of concrete to store an equivalent amount of energy. This comparison further underscores the benefit of latent heat thermal energy storage (LHTES) over sensible heat storage, since brick and concrete are only capable of storing energy in the form of sensible heat. Due to this ability of PCMs, immediate benefits can be envisioned about their use in buildings. The two most promising applications of PCM in buildings can be found directly from the basic difference between sensible and latent heat storage (Lane, 1983; Mehling, 2008).

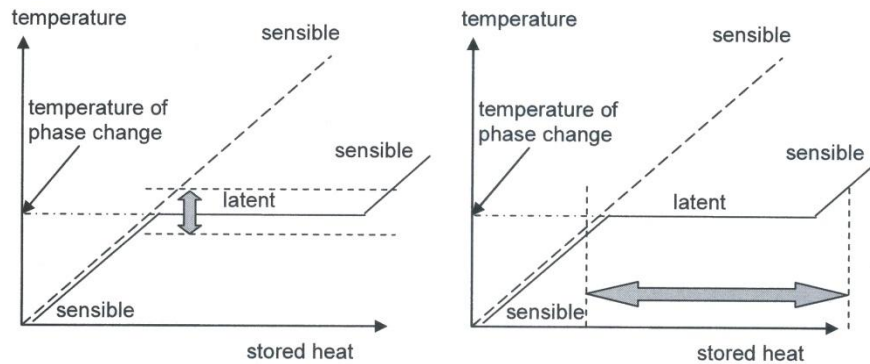


Figure 2.5: Potential fields of application of PCM: a) Temperature control b) storage and supply of heat or cold with little to no temperature change. (Source: Mehling, 2008)

In Figure 2.5a and 2.5b the heat is stored and released from PCMs without a significant change in temperature. Owing to the very high specific heat capacity of PCMs during melting, ambient temperature is maintained without drastic fluctuations. Analytically, it can be deduced that the use of PCMs can therefore stabilize the indoor temperature. The benefits of using PCM can be understood better using the analogy of a tent and a cave. Mehling (2008) state, “tents have extremely low heat storage capacity; caves are the opposite. In a tent, the temperature can be unbearably high on a summer afternoon and freezing cold during the night on the same day. In caves, the large heat capacity of the cave walls regulates the temperature and fluctuations are often less than 1 K between day and night; in deep caves even between summer and winter.” Buildings lie somewhere between a tent and a cave when it comes to heat exchange with the exterior environment. Thus in older buildings, the regulation of temperature were accomplished by using thick walls made of concrete or brick. The thickness of these walls in tandem with the heat capacity of the materials provided enough thermal lag during the day and night so as to reduce uncomfortable temperature fluctuation indoors. However today, most buildings, especially in the western world are made of lightweight walls. This is partly due to architectural and cost reasons. Lightweight construction has long been considered to have low thermal mass owing to the low mass of building materials compared to the concrete or masonry buildings. The use of

PCMs can add to the thermal mass and therefore seems like a viable option for use in such buildings.

Historical background

Although the use of ice as phase change material is quite old, research and development of PCMs for use in buildings is known to have started during late 1940s. Dr. Maria Telkes is considered to be one of the pioneers in the field of LHTES using PCMs. The first documented use of PCMs in a building was ‘the Dover House’ in Boston in 1948 (Lane, 1983).



Figure 2.6: In the Dover house the solar panels with Glauber's salt sat directly behind a bank of eighteen windows that lined the second story of the south-facing wall. (Source: Sherburne, 2009)

Dr. Maria Telkes, with the help of a grant provided by wealthy sculptress Miss Amelia Peabody, constructed the first passive solar house that employed Glauber's salt (Sodium sulfate decahydrate – $\text{Na}_2\text{SO}_4 \cdot 10\text{H}_2\text{O}$) as the Phase Change Material. During the same time Dr. Telkes's brother and his family were looking for a house to relocate in. Her brother's family moved in and the 'solar house' performed well for two winters in Boston “without a fuel bill” until the

Glauber's salt started to separate into layers, losing most of its storage capacity (Lane, 1983). It was evident from this full scale experiment that something needed to be done to prevent the phase segregation of Glauber's salt. However, since the price of petroleum was low enough to relinquish any need for new technology, less attention was given to phase change storage research until the early 1970s (Agyenim, 2010).

A few sporadic experimental investigations were conducted during the time between the 50's and the 70's on the performance of PCMs on its own, and the identification of new PCM candidates for the use in buildings. Later, the study of latent thermal storage systems gained particular interest and considerable impetus only after the oil crisis in 1973 (Lane, 1983; Pasupathy. 2008; Zhu. 2009). In 1974 NSF awarded a contract to the Dow Chemical Company, to identify materials that could be used as PCMs in buildings. (Lane, 1983) writes, "A prodigious number of materials were considered (Dr. Glew estimates nearly 20,000) by examining secondary literature sources. About one percent of those were selected for further examination." Because of the fact that there are many types of PCMs available, the available literature on PCMs is quantitatively enormous. This immense variability in the types of PCMs available for use in buildings has led the information to be scattered and hard to organize. However this variability can be seen as both a threat and an opportunity. On one hand due to the fact that there is an enormous amount of materials to choose from, it seems difficult to summarize the thermo-physical behavior of each PCM in a uniform manner and on the other hand this variability gives designers the freedom to choose the best possible PCM for the job. Despite much interest in the technology of PCM, indicated by the large number of publications, there is no single source that serves as a compendium on all the work that has been done on PCMs. While (Lane, 1983) provided an in depth review and detailed information on phase change materials and its applications many advances have been made in the thermal performance, storage concepts and

applications of PCMs and technology has advanced considerably since then. More recently, (Mehling, 2008) have reviewed the basics and the applications of PCMs and the information is not only limited to building applications. (Dincer, 2011) focused solely on thermal energy storage and have thus devoted a few chapters on phase change materials and the numerical simulation techniques to date. (Lane, 1983) and (Mehling, 2008) have also delved into the different methodologies developed for the numerical simulations of PCMs. Since the field of latent thermal storage today stands on firm scientific and engineering foundations, there are many books available that explain in detail the advances in the theory of computational fluid dynamics and its accompanying numerical simulations in order to numerically evaluate the behavior of thermal energy storage systems.

Existing literature on PCMs can roughly be divided in three categories. The majority of literature on PCMs has dealt primarily on:

1. The chemical makeup and thermo-physical properties of existing PCMs.
2. Methods of encapsulation and incorporation of PCMs into regular construction materials.
3. Experimental and numerical studies on the performance of PCMs within the building environment.

Chemical and thermo-physical properties of PCMs

The vast spectrum of PCMs available makes it necessary to classify them in an orderly fashion. Because the two most important criteria of phase change materials, the melting temperature and energy absorbed, depends on molecular bonds, they have been classified primarily based on their chemical makeup (Mehling, 2008). A complete list of PCMs, including

commercially available ones, can be found in (Zalba, 2003; Sharma, 2004; Sharma, 2009; Farid, 2004). PCMs have been classified into three distinct categories owing to their chemical makeup.

1. Organic PCMs - These PCMs are then classified as paraffin (alkanes) and non-paraffins (non-alkanes).
2. Inorganic PCMs - These PCMs are grouped as salt hydrates and metallics.
3. Eutectics - Eutectics are proportional mixtures of organic-organic, inorganic-inorganic or inorganic-organic PCMs.

Organics	Inorganics	Eutectics
Advantages No corrosives Low or none undercooling Chemical and thermal stability	Advantages Greater phase change enthalpy	Advantages No phase separation
Disadvantages Lower phase change enthalpy Low thermal conductivity Inflammability	Disadvantages Undercooling Corrosion Phase separation Phase segregation, lack of thermal stability	Disadvantages Lack of test data of thermophysical properties

Figure 2.7: Comparison of organic, inorganic and eutectic PCMs. (Adapted from: Zalba, 2003)

Each category of PCMs has desirable and undesirable properties when it comes to their applicability in buildings. The authors (Zalba, 2003; Farid, 2004; Sharma, 2004; Tyagi, 2007; Mehling, 2008; Pasupathy, 2008; Sharma, 2009; Kuznik, 2011) have listed them in literature. The choices of PCMs for latent heat thermal energy storage systems need to fulfill certain requirements and exhibit various beneficial thermo-physical properties as well. These requirements and selection criteria for the practical use of PCMs have been listed in literature by (Lane, 1983) in 1983 and later by (Zalba, 2003; Sharma, 2004; Tyagi, 2007; Pasupathy, 2008; Mehling, 2008; Agyenim, 2010; Zhou, 2011) as depicted in Figure 2.8:

Thermal properties	Physical properties	Chemical properties	Economic properties
Phase change temperature fitted to application	Low density variation	Stability	Cheap and abundant
High change of enthalpy near temperature of use	High density	No phase separation Compatibility with container materials	
High thermal conductivity in both liquid and solid phases (although not always)	Small or no undercooling Low vapor pressure	Non-toxic, non-flammable, non-polluting No nuisance factor	

Figure 2.8: Requirements for practical PCMs. (Adapted from: Zalba, 2003)

No material fulfills each and every requirement and various techniques have been developed to offset any undesirable quality. The undercooling or subcooling of various PCMs have been minimized by the use of nucleating agents (Lane, 1983; Farid, 2004; Mehling, 2008). Similarly incongruent melting can be inhibited by the use of artificial mixing (Mehling, 2008), by gelling or thickening (Pasupathy, 2008; Mehling, 2008) or by limiting the distance of phase separation by using shallow containers (Mehling, 2008; Tyagi, 2010).

Integration of PCM in building materials

PCMs are capable of storing and releasing large amounts of heat by melting and solidifying at a given temperature. When the PCM melts it needs proper containment so that it does not leak or evaporate. In addition the PCM should be compatible with the building material that it is in contact with. (Kuznik, 2011) classified the containment of PCMs in four categories namely, a) direct impregnation of building materials, b) micro-encapsulation, c) macro encapsulation and d) Shape-stabilized PCM.

1. Direct impregnation - Direct impregnation of PCM into materials is done by either mixing PCM with the host material during the production stage (direct immersion) or by immersion which is imbibing the material into PCM once already produced. Direct immersion is the simplest method in which liquid or powdered PCMs are directly

added to building materials such as gypsum, concrete or plaster during production (Zhou, 2011). (Khudhair, 2004) have explained the different impregnation techniques into gypsum and concrete. Other materials used for impregnation are vermiculite, wood, cement and various other compounds (Kuznik, 2011).

2. Micro-encapsulation - Micro-encapsulation of PCMs consists of enclosing the PCM in a microscopic polymer capsule. (Tyagi, 2010) mention the various physical and chemical methods for the preparation of microcapsules with PCM. The major benefit of micro-encapsulation is that it provides a larger surface area for heat transfer and that it can be mixed with a variety of construction materials such as plaster, gypsum, cement and insulation. Figure 2.9 shows the microcapsules and the mixture of microcapsules when mixed in gypsum plaster.

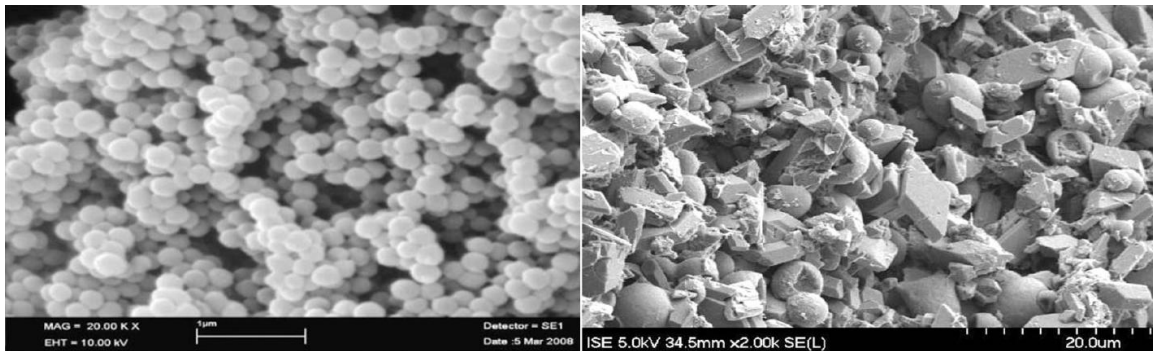


Figure 2.9: SEM Image of microcapsules. a) Microcapsules. b) Microcapsules in gypsum plaster. (Source: Tyagi, 2010)

3. Macro-encapsulation - Macro-encapsulation is the technology where the PCMs are encapsulated in a container. Macro-encapsulation of PCM is placed in long thin heat pipes, cylindrical containers or rectangular containers. (Agyenim, 2010) state that the most intensely analyzed LHTES unit is the shell and tube system, accounting for more than seventy percent. Examples of macro-encapsulation of PCMs used in PVC panels, rigid plastic containers, tested aluminum foils and steel containers can be found in literature.

4. Shape-stabilized PCM - Shape-stabilized PCMs are prepared from a liquid mixture of PCM and a supporting material. The most common supporting material found in literature is high density polyethylene (HDPE). The distinct benefit of shape-stabilized PCM is that it can contain up to 80 percent PCM and still maintain structural integrity. While shape-stabilized PCMs are relatively new compared to other forms of encapsulation, and more conclusive research on its thermo-physical properties are yet to be performed. (Zhang2006a) prepared their in-house shape-stabilized PCM and performed experimental as well as numerical analysis with it. They show that the melting temperature of the shape-stabilized PCM can be adjusted by using different types of paraffin and that the optimum composition of paraffin in shape-stabilized PCM is 80 percent.

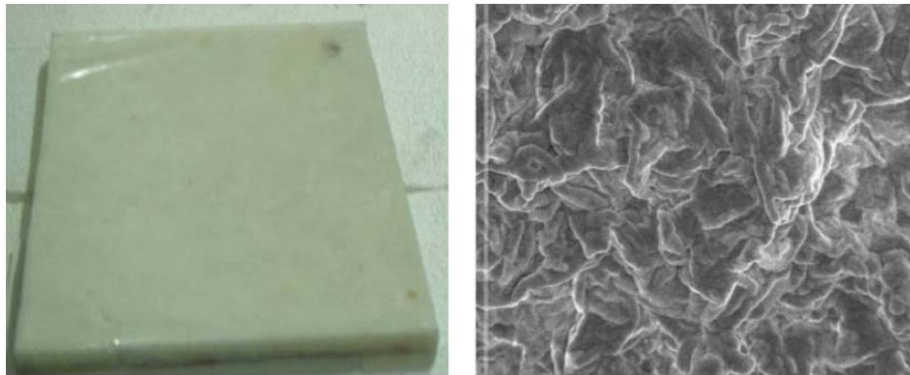


Figure 2.10: a) shape-stabilized PCM plate b) Scanning Electron Microscopy (SEM) image of the microstructure. (Source: Zhang, 2006)

Experimental and numerical evaluation of PCMs in buildings

Numerous evaluations have been performed on the performance of PCM in buildings. These evaluations, both experimental and numerical, can be further divided into two categories.

1. Active incorporation - the use of PCMs working in conjunction with air conditioning systems.

2. Passive incorporation - the use of PCMs in buildings without resorting to the utilization of additional air-conditioning to heat or cool the PCM.

The objectives for conducting these evaluations have been varying throughout literature. While few such as (Peippo, 1991; Stetiu, 1997; Neeper, 2000; Heim, 2004; Kuznik, 2008; Alawadhi, 2008; Zhang, 2008; Heim, 2010) have performed such evaluations to develop design guidelines (i.e. how much PCM to use? what is the optimum thickness of the PCM-gypsum board? etc). (Stovall, 1995; Athienitis, 1997; Huang, 2006a), have performed the evaluations to study the energy saving and temperature reduction potential of particular PCM technologies. (Ahmad, 2006; Carbonari, 2006; Pasupathy, 2008a; Kuznik, 2010; Borreguero, 2011) carried out experimental evaluations and validated numerical models. Also some have evaluated the peak shifting potential of a PCM technology (Halford, 2007; Khudair, 2007; Mettawee, 2013). All these evaluations have carried out either experimentally or numerically.

In the numerical simulation front, (Peippo, 1991) developed an in-house code to numerically investigate the thermal performance of placing PCM panels on the south facing room. They have used fatty acids as the PCM and placed the PCM panels on the inside surfaces of the south facing room except for the floor. By performing simulations for two different climates (i.e. Helsinki, Finland and Madison, Wisconsin), they have concluded that optimum diurnal storage can be achieved when the PCM has a phase change temperature of 1-3 degrees above the average room temperature.

Numerical simulations on an office space can be found in (Stetiu, 1997). They have modeled the thermal performance of an office space equipped with phase change wallboard, where they have used phase-change wallboard containing 20% paraffin by mass on the interior face of all vertical walls. A facade window area (vision glazing of the curtain-wall construction) equal to 20% of the floor area of the space was chosen. Since their study had been on an office

space, a daily occupancy range of 1 to 2 persons with a weekday schedule from 8 to 5 pm was chosen to simulate internal loads. The simulation was performed for two climates, namely, Sunnyvale, CA and Red Bluff, CA. As a guideline, the authors have concluded by saying that the use of their particular wallboard performs well even without chiller assisted pre-cooling, but only in locations in California where the outdoor night temperature drops below 18° Celsius. If the outdoor night temperature exceeds 18°C, then a chiller assisted space pre-cooling is necessary to discharge the heat that is stored in the boards.

(Athienitis, 1997) performed both an experimental and a numerical evaluation of a passive solar house in Montreal. They used a gypsum board for this study that was made in-house in an earlier study at Concordia University by (Banu, 1998). A conventional gypsum board was soaked in liquid butyl stearate (BS) to create this PCM-gypsum board. The PCM in the study had a melt range of 16-20.8 degree Celsius and the PCM-gypsum board contained 25% by weight proportion of butyl stearate. The boards were placed on all the vertical walls. Simultaneously (Athienitis, 1997) also performed a numerical simulation that was based on the Enthalpy model. The experimental results showed that on a sunny day in Montreal the internal temperature of the PCM board rose to 21°C and the ordinary gypsum board rose to 27°C. Concurrently, the indoor room temperature was reduced by 4 degrees when the PCM boards were used. The experimental measurements were in good agreement with the numerical simulation results they performed. While, the potential benefits of the use of PCMs were clearly evident in the study, design guidelines could not be obtained from this study alone.

(Neeper, 2000) created two hypothetical wall boards where the first wallboard with 10% PCM and a latent heat capacity of 19.2 kJ/kg and the second wallboard with 20% PCM and a Latent Heat Capacity of 38.4 kJ/kg for his numerical simulation and placed them in two different locations. Situations with the wallboard on an interior partition and on the building envelope were

investigated separately. The numerical simulation was performed using the effective heat capacity method and custom time varying temperature functions for the indoors and outdoors. (Neeper, 2000) provided three design guidelines: a) the maximum diurnal energy storage occurs with a PCM melting temperature that is close to the average room temperature when the PCM board is placed on an interior partition, which is similar to the design guideline proposed by (Peippo, 1991) ,b) the maximum diurnal storage for the PCM board placed on the exterior surface, on the other hand, occurs at a melting temperature 1 degree below the average room temperature and finally c) the storage capacity of the PCM board decreases if the PCM transition range is greater than 1°C.

(Heim, 2004) also performed a numerical simulation using a hypothetical wall board but with varying melting temperatures. They chose to use the weather file of Warsaw, Poland. The PCM board embodied a latent heat of 45 kJ/kg and was placed on the inner linings of all the vertical walls. The results of their numerical analysis on the PCM-gypsum composites during the heating season showed that the optimal PCM melting temperature was 22°C, which is 2 degrees higher than the heating set point for the room. In another numerical investigation (Heim, 2010) investigated two different cases (direct radiation and indirect radiation) in a room and suggested other guidelines specific to Warsaw climate. Heim (2010) states that Thermal zones with rapidly changing internal conditions (direct gains room) the thin layer with a high latent capacity is preferred against a thick layer with a relatively lower latent capacity. On the other hand, for indirect gains zone (a solar wall) thick elements provided a process continuing over time and allowed the energy stored to be used at night.

(Zhou, 2007) worked with shape-stabilized phase change material (SSPCM and performed a numerical investigation to evaluate the characteristics of the SSPCM wallboard versus a mixed type PCM-gypsum board. The numerical simulation employed the Enthalpy

method in the Beijing climate. The effects of different thermo-physical properties, the melting temperature and phase transition zone of the PCM were analyzed. Zhou2007 concluded that the optimal melting temperature of the SSPCM is 21°C and that PCM composites with a narrow phase transition zone provide better thermal performance.

(Kuznik, 2008) has performed experimental and numerical analysis for the optimization of a phase change material wallboard applied to lightweight buildings. In their evaluation they used a commercially available PCM board composed of 60% micro-encapsulated paraffin that had a melting temperature of 22°C. (Kuznik, 2008) first validated their numerical model using experimental results from a study using two test cells of cubical enclosure of 0.5 m. Then, for the numerical simulation they created a time varying temperature function to simulate the weather of Paris in July. They used the Enthalpy method for their numerical approach. As a guideline they concluded that the optimum thickness for the PCM board 10 was mm.

(Ibanez, 2005) performed a parametric study based on the Lleida, Spain climate using numerical simulations. In their numerical evaluations they placed PCMs in the ceiling, and compared the performance of the room with two phase change temperatures 25°C and 30°C, simultaneously while comparing the performance of PCMs with two thermal storage densities 15,000 kJ/m³ and 60,000 kJ/m³. Although they mention that close to 200 simulations were run to study the influence of other variables and their different combinations, the other simulation results cannot be found in literature yet. Nevertheless, the authors have specified various guidelines through the study. They have said: a) The PCM should be included in the ceiling and west wall of the prototype room b) The needed storage capacity of the panels for the maximum air temperature to be reduced to a significant level is around 15,000 kJ/m³ and 37,500 kJ/m³ and c) The PCMs used for that particular climatic conditions and that particular application needs to have a phase change temperature between 25°C and 27.5°C. As can be seen in Figure 2.11 the

dependent variable of their study is the maximum air temperature in the room. The maximum air temperature and the performance of PCM will change in the case of HVAC use depending on the heating and cooling set-point. (Ibanez, 2005) have underscored that the combination of the considered variables need to be compared by performing more numerical simulations.

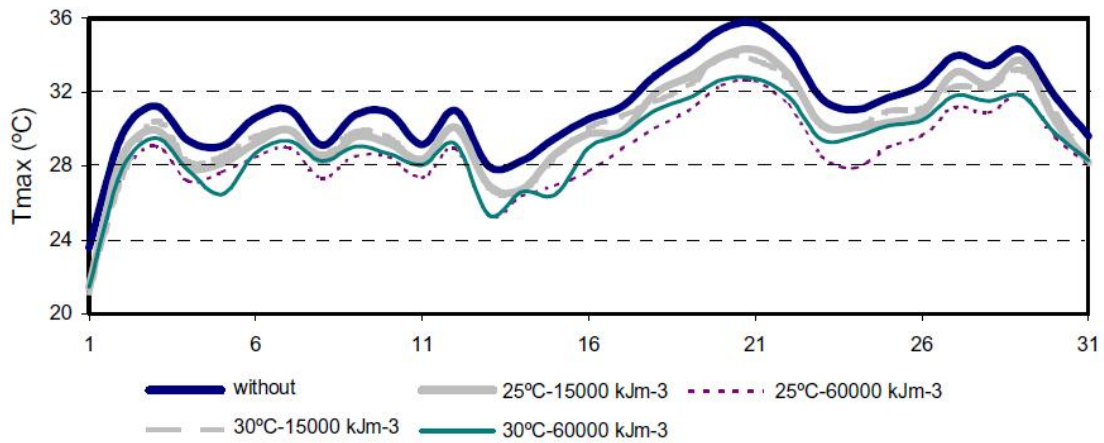


Figure 2.11: Maximum air temperature in the prototype room during July. (Source: Ibanez, 2005)

(Chen, 2008) have performed numerical simulations for a single room located in Beijing, China. Paraffin based PCM gypsum board was modeled and simulated for the heating season using the effective heat capacity method. The PCM boards were placed on the inner surfaces of the North Wall. By varying the melting temperature, the thickness and melting enthalpy of the PCM a parametric study was performed. The simulations were only performed for the heating season in Beijing. From the plots in Figure 2.12 it can be seen that the relationship of thickness and enthalpy to the energy saving rate or phase change temperature and enthalpy to the energy saving rate is not linear but quadratic.

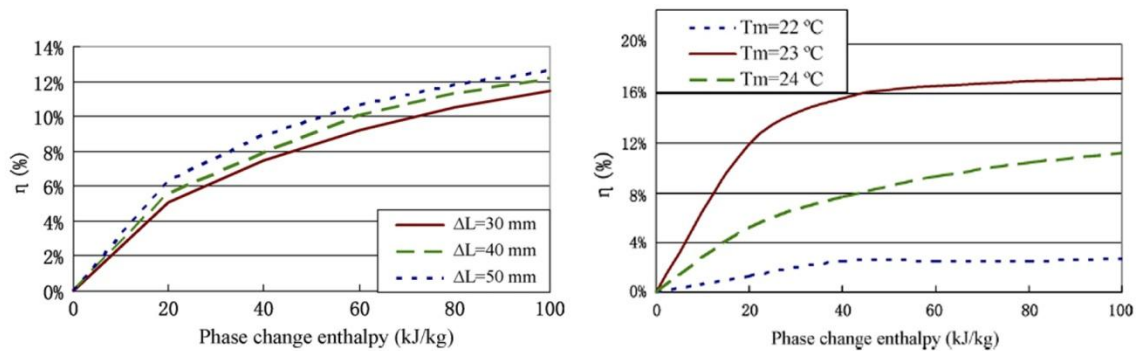


Figure 2.12: a) Effect of phase change enthalpy and the thickness of the board on the percent energy savings (η), b) Effect of phase change temperature and phase change enthalpy on the percent energy savings (η). (Source: Chen, 2008)

(Chen, 2008) have given guidelines for the Beijing climate as: the phase change temperature and the phase change enthalpy are the main influential factors to the energy-saving rate of heating season in the PCM room, and the influence of PCM thickness is relatively small. The phase change temperature should be chosen reasonably based on the indoor air heating set-point temperature.

A similar parametric study has been performed by (Alawadhi, 2008). Numerical simulations were performed in this study to assess the thermal performance of PCM cylinders placed inside hollow bricks. The objective of the brick PCM system was to reduce the heat flow from outdoor space by absorbing the heat gain in the brick before it reached the indoor space during daytime. This parametric study was conducted to assess the effects of different design parameters, including the quantity and type of PCMs used, and the location of PCMs inside the brick. Three different PCMs with various melting temperatures 27° , 37° , 47°C were tested. (Alawadhi, 2008) created a time varying temperature function to simulate the weather for a hot climate. The results indicate that when PCM is incorporated in the brick: a) Increasing the quantity of the PCM has a positive effect, b) The PCM with a melting temperature of 37°C shows the best performance among the examined PCMs and c) The centerline of the brick is the best

location to place the PCM cylinders inside the hollow brick. Even though the study developed these guidelines, it does not consider the interaction effects of these various parameters. Each parameter is studied independently of the other.

(Kim, 2009) conducted a study to quantify the impact of insulation on building energy consumption. In the insulation study the authors ran a parametric study in Miami, Florida (Warm) and Detroit, Michigan (Cold) with insulation of different R-values, and have concluded that the overall home energy consumption as a function of R-value shows diminishing returns. They have also concluded that since the majority of heat loss and gain are through the windows, there exists an optimum R-value of insulation in the walls after which any increase in insulation capability does not contribute much towards the energy savings of the building. The following Figure 2.13 and Figure 2.14 of energy consumption versus R-value depict this phenomenon.

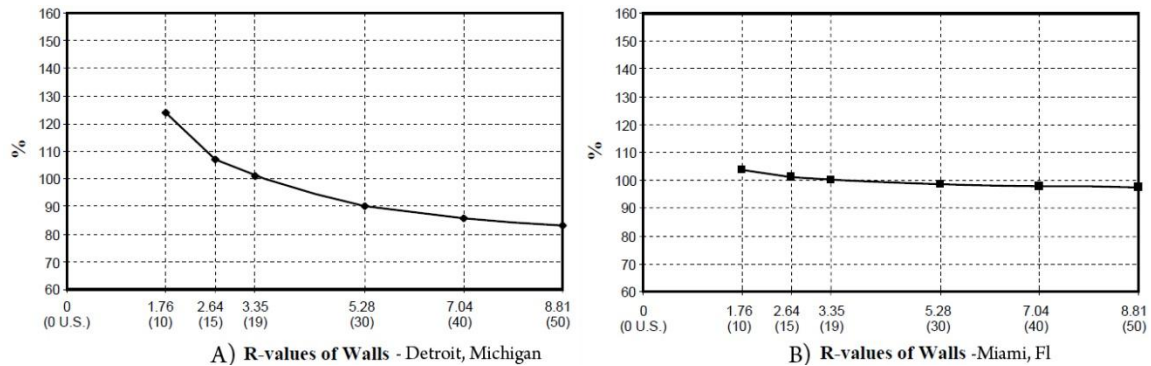


Figure 2.13: Energy consumption vs. insulation R-value. (Source: Kim, 2009)

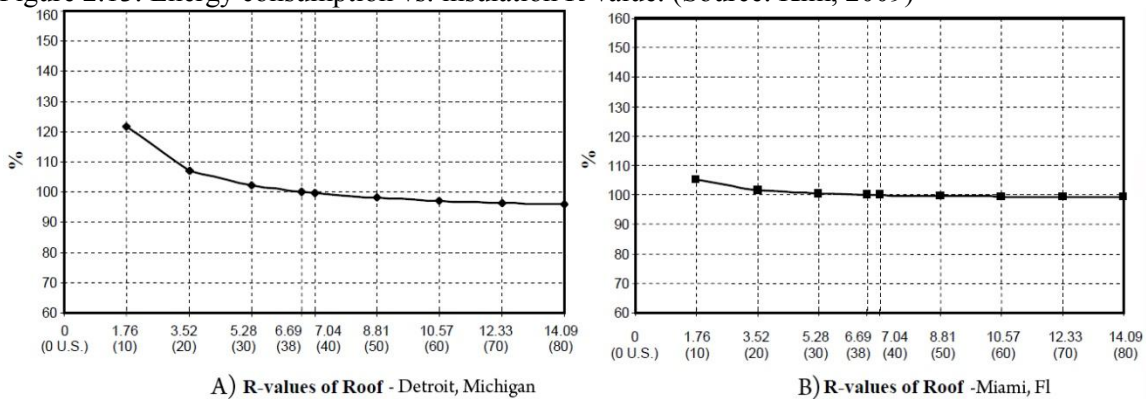


Figure 2.14: Energy consumption vs. insulation R-value. (Source: Kim, 2009)

The plots show that any further addition of insulation capability compared to the baseline provides only marginal energy savings. However it is important to study how the increase in time lag of heat or cold from entering the building through the walls, due to the increase in R-value, affects the performance of PCMs.

Contribution of this research towards literature

From the preceding discussion it can be concluded that there are numerous benefits of using PCM technology in buildings. Theoretically the benefits of using PCM-based TES systems in buildings is that it helps; a) maintain constant temperature indoors and b) shift energy consumption from periods of peak electricity rates to periods of lower rates accompanied by the additional advantage of lower demand charges. Considering theoretical properties alone, due to the very thermo-physical nature of PCMs, they work very well in absorbing tremendous amounts of energy. But how well do PCMs work within the context of a building? In spite of the well understood benefits, due to some existing challenges, the widespread use of PCM-based LHTES technologies in building applications is yet to take full effect. Harland (2011) argue that the momentum for the widespread use of PCMs has stalled and accessible information has been limited and scattered. Despite decades of development of phase change materials (PCMs) for building purposes they have not yet made it into mainstream interior architecture. One of the reasons is also because the successful use of PCMs in buildings is highly contextual and case specific. The selection of PCM, based on phase transition temperature for one climatic region will not be appropriate for another (Pasupathy, 2008). A building's energy consumption and indoor temperature fluctuation is obviously influenced by, and a direct result of, the climate it is built in. The total energy balance of a building is a complex process since the building as a system is continuously exposed to varying degrees of environmental factors, as well as internally generated

loads. At the most fundamental of levels, these thermal forces then interact with the building fabric in three modes, namely, conduction, convection and radiation. Each of these dynamic forces acting on a building fabric is both, climate specific and temporal. As a result, the use of PCM in a building and the methodological guidelines to employ the PCM technology cannot be the same for every climate. For instance colder climates may require PCMs melting at different temperatures as opposed to in warmer climates. A “one size fits all” design methodology therefore cannot work.

Dincer (2011) state that independent technical criteria for such thermal storage systems are difficult to establish due to the fact that they are usually always case specific. The scholars further suggest that before proceeding with a project, a designer should possess or obtain technical information such as the types of storage appropriate for the application, the amount of storage required, the effect of storage on system performance, reliability and cost, and the storage systems or designs available. Mehling and Cabeza (2008) underscore the need for a better understanding of the thermo-physical interactions of the PCM with the building. They state that it is necessary to know the main heat fluxes and heat storage mechanisms in order to understand how PCM technology can be applied to fulfill human comfort requirements in buildings. To properly use PCMs in buildings, a good knowledge of the dynamic characteristics of buildings using PCMs is essential. The dynamic characteristics of buildings with PCMs add complexity and variation to the heating and cooling load, which influences the design and selection process of LHTES systems. Roth (2007) therefore state that there have been limited evaluations and more comprehensive analyses are needed to better understand the energy-saving potential of building materials with PCMs. A thorough understanding of the parameters that affect the thermal performance of a PCM within the context of a building is necessary. Furthermore, the optimization of these parameters is fundamental towards achieving successful PCM application in

buildings (Zhang, 2007). This knowledge will; a) help building practitioners, in an already risk averse industry, fully understand building temperature response characteristics and the potential energy savings due to the application of PCMs, b) help building designers adopt proper design options and concepts that will guide the decision making process during the initial planning stages, c) and help operators utilize advanced control to maximize system operating efficiency and provide better indoor environmental quality (Zhu, 2009).

It is also clear that although there have been many investigations, they have been sporadic, spread all over the globe and have mostly focused on many different variables making it difficult to extend the knowledge to other applications beyond the original source. As highlighted in the preceding section, each study has been performed under different environmental conditions. Each study has used different amounts of Phase Change Materials in the buildings that are studied. Most studies have used PCM in a passive setting while others have combined the charging and discharging of PCM to an external air conditioning system. Agyenim (2010) express this concern and state that, "individual authors used different phase change materials with different heat transfer characteristics. In the case where the same PCM has been used, the researchers employed different parameter ranges and presentations making it difficult to cross correlate between the characteristics influencing the heat transfer in specific PCMs." Even though the experimental and numerical simulations have been accurate in predicting the behavior of the specific PCMs used in the experiments, the literature clearly lacks a more unified study on the effects of each variable and its relationship to the indoor environment. As highlighted by Kuznik (2011), from a practical point of view, a more systematic evaluation of the various PCM integrated in the building structure is needed, in particular in real use condition.

Based on the existing literature survey and an understanding of on the complex and time variant nature of energy exchange indoors, a preliminary set of questions is formulated as follows:

1. Does the application of any arbitrary PCM in a building achieve the same energy performance?
2. What is the optimum amount of PCM required to maintain a constant ambient temperature?
3. What should be the optimum melting temperature of the PCM to achieve maximum energy savings?
4. Does the location of PCM inside the building make a significant difference in the energy performance of the building?

There is a lack of clear indicator to effectively assess the phase change materials in building walls. It is also evident that a study needs to be performed where major variables are identified for specific climate types and optimized based on performance. The variables need to be studied within the whole building system and an empirical model that defines the relationships of each variable to the system needs to be developed.

A complete understanding of the impacts, benefits and limitations of the application of phase change materials in buildings is necessary for its successful use within the building industry. Therefore this research will seek to contribute towards filling this gap in literature. A uniform study will be performed for all the climates throughout the United States, in order to better understand the energy saving potential of PCM boards placed in a lightweight building. The performance of the PCM boards will be studied against the independent variables within a whole building system and the results analyzed.

Chapter Three

RESEARCH QUESTION AND DESIGN

The research question is formulated to address the specific gaps in literature. In addition, the long term objective of this project is to develop performance based guidelines based on the complete understanding of the impacts, benefits, and limitations of integration of phase change materials in buildings. This research will be guided by the following question:

Where and what PCM should be incorporated in lightweight buildings for a given climate?

The outcome of this research is to develop climate specific empirical models that will explain the behavior of PCMs when integrated inside buildings. In addition, climate specific response surfaces need to be developed to understand the confounding effects, if there are any, of the different variables (i.e. melting temperature, latent heat of fusion, proportion of PCM, location within the building etc) in the total thermal performance of a building. Finally, a cost benefit optimization study needs to be performed to develop concrete guidelines that can assist designers and engineers, as well as manufacturers make performance based decisions when implementing or manufacturing PCM technology.

Research method

Since this research involves the study of the effects of multiple input variables on the response variable Design of Experiment (DOE) methodology will be used. The goal of this experimental design is:

1. Variable screening - the ultimate goal of variable screening is to identify the variables that have the most influence on the response variable (energy consumption of the

building) when PCMs are used. Variable screening will also help minimize the number of experiments while maximize retrievable information from the data.

2. Response surface and Empirical model development - the goal is to develop response surfaces to pinpoint interaction effects of the variables on the response variable. Apart from the response surfaces, climate specific empirical models will also be developed that will provide a complete description of the process behavior, the interaction effects (i.e. two way, three way etc.) based on the significance of each variable. The empirical models will serve as a tool to help develop performance based design guidelines when using PCM in buildings.

Research design

The experimental design requires a control group and an experimental group. The control group will serve as the baseline against which PCM technology and its combinations will be measured and compared against. The baseline building will be developed in accordance with the ASHRAE 90.1 standard (ASHRAE, 2010) which specifies mandatory requirements that need to be met when building in different locations within the United States. The experimental group, on the other hand, will employ different PCM combinations to measure the dependent variable which is the annual energy consumption of the building. Multiple factors have been identified in literature that affect the thermal performance and energy consumption of buildings and are listed as independent variables for this research as follows:

1. PCM Enthalpy or Volumetric Heat Storage Capacity - The amount of energy the PCM can absorb per kilogram during phase transition is an important variable for this study. From the Beijing based study by (Chen, 2008), it is evident that there is an optimum PCM enthalpy for a particular climate. The study shows that there exists an optimum

PCM enthalpy after which any more increase in energy storing capability does not affect the total energy consumption of the building. Seven different levels of PCM enthalpy will be tested. The enthalpy will range from 50 kJ/kg up to 230 kJ/kg that increases in steps of 30 kJ/kg. The PCM enthalpy along with the PCM melting temperature plays a vital role in the thermal performance of PCMs.

2. PCM melting temperature - One of the requirements of choosing the proper PCM for a building application is the selection of its phase change temperature. In addition, the selection of PCM based on phase transition temperature for one climatic region may not be appropriate for another. It is imperative therefore to identify the optimum melting temperature of PCM for a specific climate. In literature, PCMs melting from 19°C to 28°C are recommended for passive building applications where a PCM is applied to the interior surfaces. However, since the PCM will also be applied within the wall compositions, 20 levels of PCM melting temperatures will be defined in this study and the impact of each will be measured against the control group.
3. Climate - The United States Department of Energy (DOE) has classified the United States into 8 standardized climate zones. The eight U.S. climate regions are based on the climate designations used by the International Energy Conservation Code (IECC) and the American Society of Heating, Refrigerating and Air-Conditioning Engineers (ASHRAE). Each climate zone is determined on the basis of annual degree heating and degree cooling days. Climate zones are categorized from 1 to 8 and are further divided into moist, dry and coastal regions. These climate zones can also be mapped to other climate locations for international use. The DOE has also specified representative cities within the United States which represent each of the climate

zones and its 3 subdivisions. This study will perform experiments on 15 of the cities as depicted in the climate map seen in Figure 3.1.

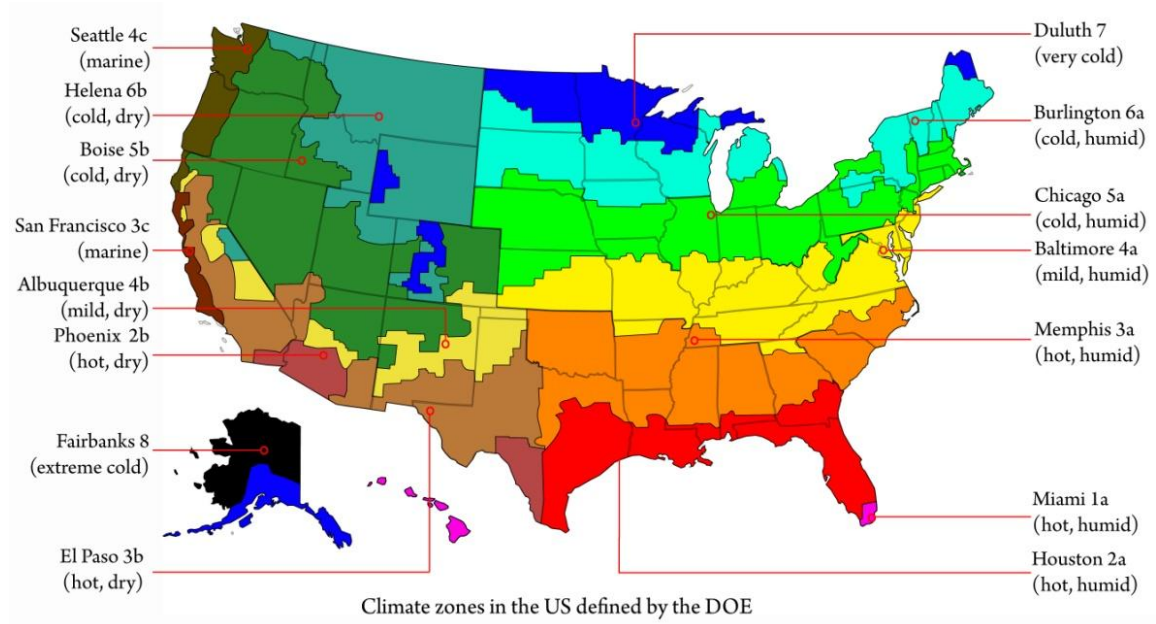


Figure 3.1: Climate Zones as defined by the US. DOE and its representative cities.

4. Construction - Construction plays a vital part in the energy consumption of a building. A heavy weight building performs differently when compared to a light weight construction. Even within each construction type there are many different combinations of wall compositions that perform differently thermally. A heavy weight concrete construction could provide more thermal inertia as opposed to a light weight concrete construction. In order to understand the behavior of PCM within a building, and to pick a starting point, a lightweight construction is chosen, as shown in Figure 3.2, in accordance with the ASHRAE 90.1 mandatory guidelines. Furthermore, the ASHRAE 90.1 standard recommends minimum requirements that need to be met for each climate zone. Therefore, every building will be customized for each climate as recommended by the standard.

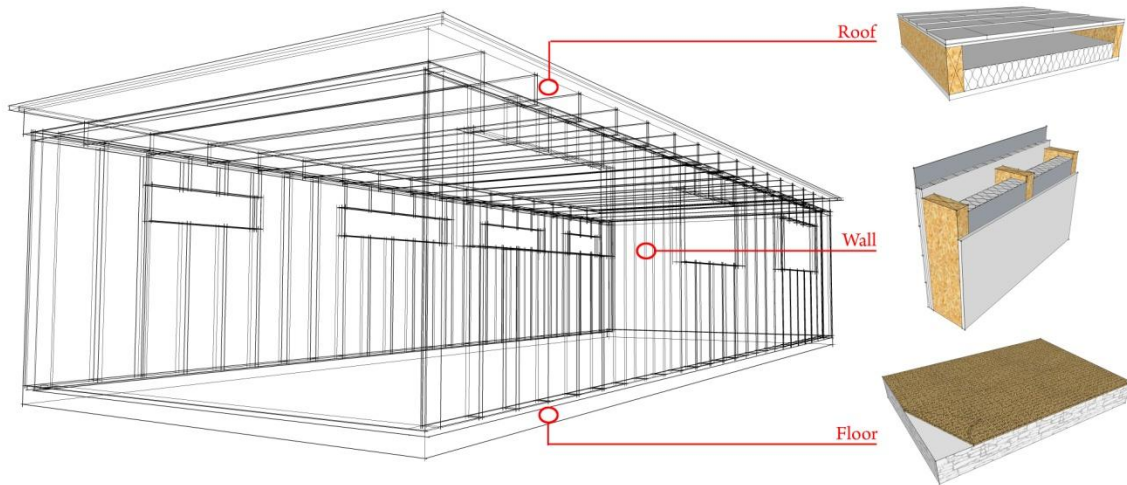


Figure 3.2: The wall, roof and floor construction as per the ASHRAE 90.1 standard.

5. Building length-to-width ratio - The building orientation determines the amount of solar radiation each surface receives thereby affecting the total heat gain to the indoors. In addition, the ratio of the length to the width of the building also plays a significant role in the annual energy consumption of the building.

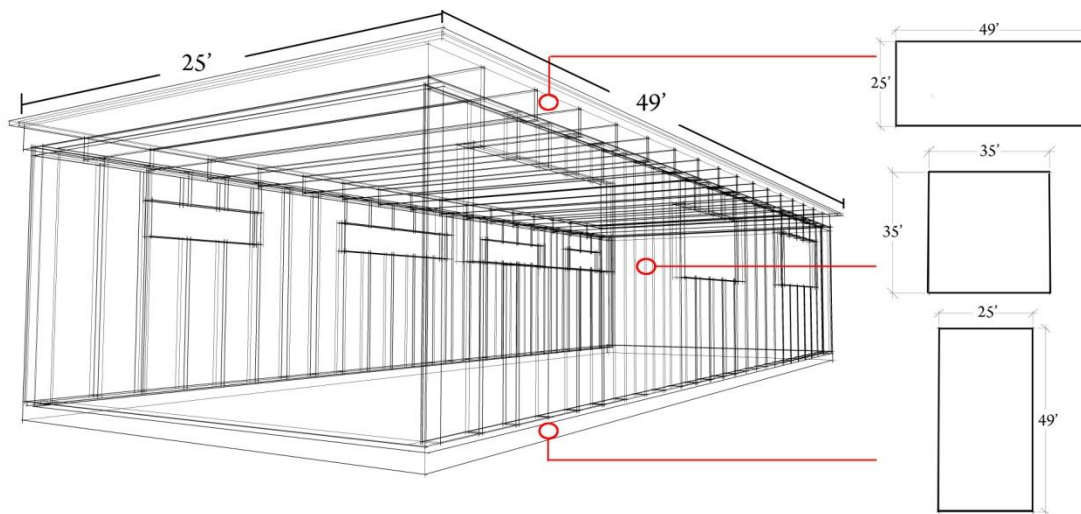


Figure 3.3: The three different length-to-width ratios: $\gg 1$, $= 1$, $\ll 1$.

These two variables, length and width, when combined together form one independent variable 'length-to-width' ratio that can measure whether the performance of PCM

depends on the orientation and the building's proportions while the floor area remains the same. For this very reason, each of the 'length-to-width' ratios the gross floor area stays the same at 1225 sq ft and takes 3 levels as shown in Figure 3.3.

6. PCM location within the wall - As evidenced in the literature from the Kuwait study (Alawadhi, 2008), there seems to be an optimum location within the wall where the inclusion of PCM works best. It is the objective of this research to pinpoint that location within the wall as well. The study of this variable will also help clarify how the behavior of PCM within a wall behaves in different climates within the United States. The variable is therefore divided into three levels: the exterior, interstitial and interior as shown in Figure 3.4. This is done in order to ascertain the effect of position of PCM within each surface.

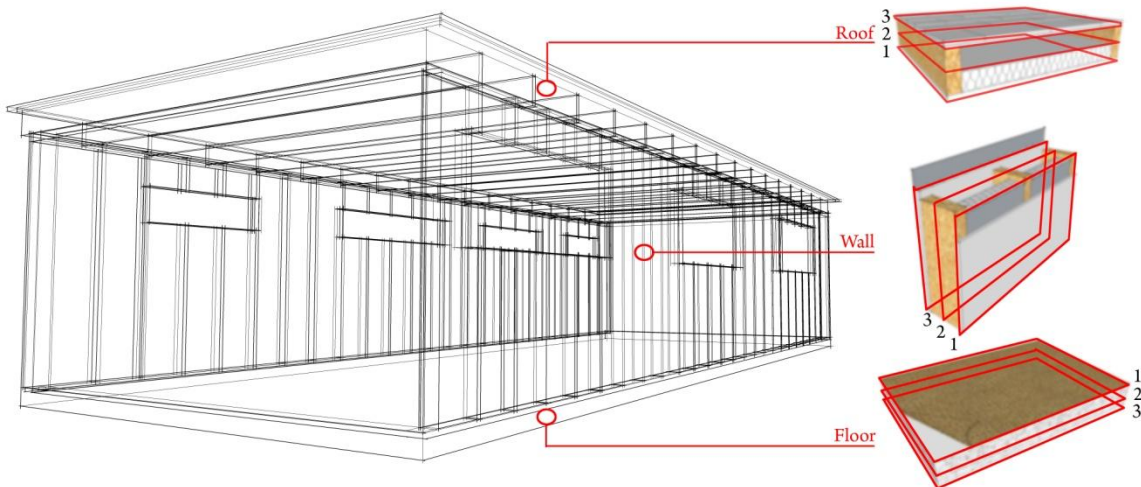


Figure 3.4: The locations within the wall: exterior, interstitial, interior.

7. PCM location within the building - As evidenced in the literature review, it is unclear as to which surface when treated with PCM provides the optimum savings in energy. If there is an optimum surface to which the implementation of PCM would bring about the most energy savings, the inclusion of this variable will make it possible to pinpoint

that surface within the building. The PCM location variable will have 6 levels representing the 6 surfaces of the building as shown in Figure 3.5. However careful consideration needs to be taken while defining the amount of PCM in each wall, especially since the building with either length-to-width ratio $\gg 1$ or $\ll 1$ will most likely have the PCM on longer surfaces performing better than the shorter surfaces. The inclusion of the variable 'length-to-width ratio' of 1 will ensure that all the wall surfaces will have the same amount of PCM on it.

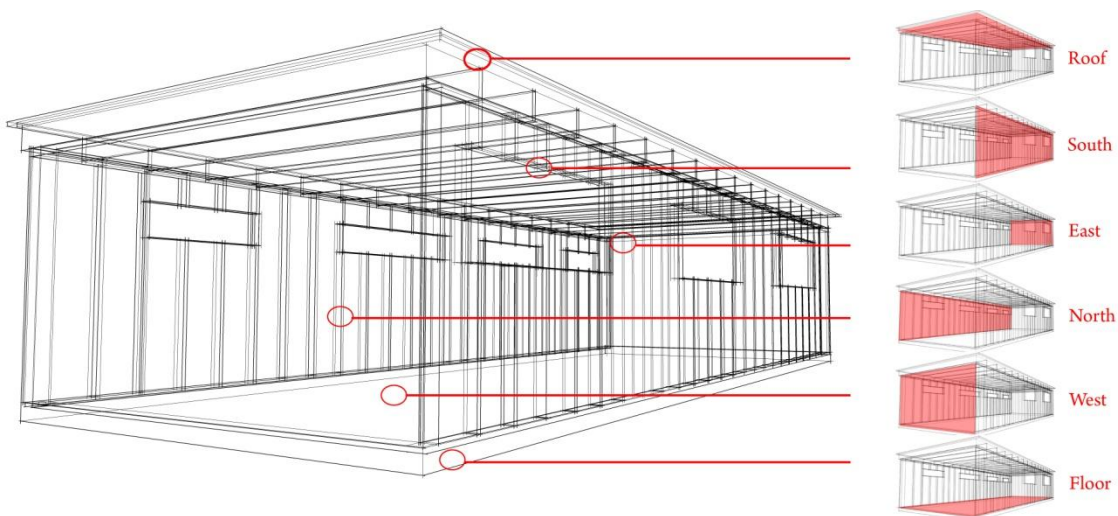


Figure 3.5: The different surfaces to which PCM will be applied to.

8. Occupancy schedule/internal loads - Buildings are meant to be occupied, and the majority of internal gains are from the heat dissipated by the people indoors, electric equipment and lights within the thermal space. The occupancy schedule for an office is vastly different from a residential space. While many standards prescribe a minimum 'people per area' requirement for an office space, the occupancy of a building whether it be residential or commercial cannot be defined by one 'standard' occupancy schedule because it can take any arbitrary form.

In order to understand how PCM behaves in the presence of internal loads and internal heat gains three different combinations (Low, Medium and Maximum) internal loads will applied to measure the performance of PCMs in the building as figuratively shown in Figure 3.6.

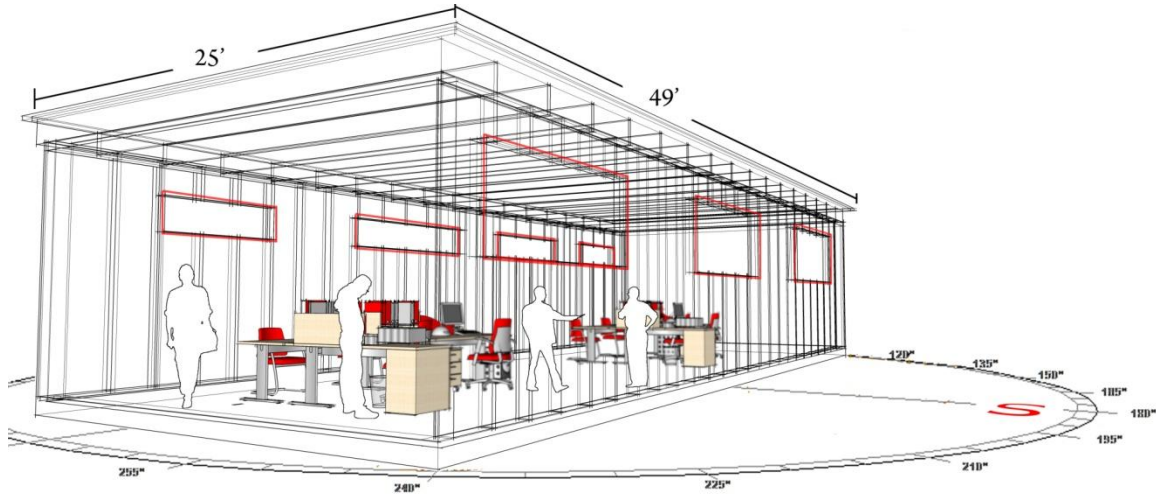


Figure 3.6: Occupancy and internal loads within the building.

9. Air change per hour - The ASHRAE 62 standard (ASHRAE, 2007) specifically requires for buildings to take into account the amount of fresh air brought in from outdoors for optimum indoor air quality. In addition the ASHRAE 90.1 standard specifies a lower limit on the infiltration per fenestration surface. When forced ventilation is coupled with infiltration of outdoor air, this changes the internal load of the building as shown in Figure 3.7.

Depending on the temperature of the outdoor air that is coming in, it either adds to the heating load or the cooling load. But how does this affect the performance of PCMs within the building at the different climate locations? Since the HVAC heating and cooling set-points are set to 25°C and 21°C respectively for the whole year, the incoming air is always conditioned to fall within the 21-25 bandwidth. Furthermore, it

is practically impossible to take into account for all possible combinations of infiltration. The infiltration variable will therefore be defined as a constant since this variable can take any arbitrary value and will always be conditioned by the HVAC.

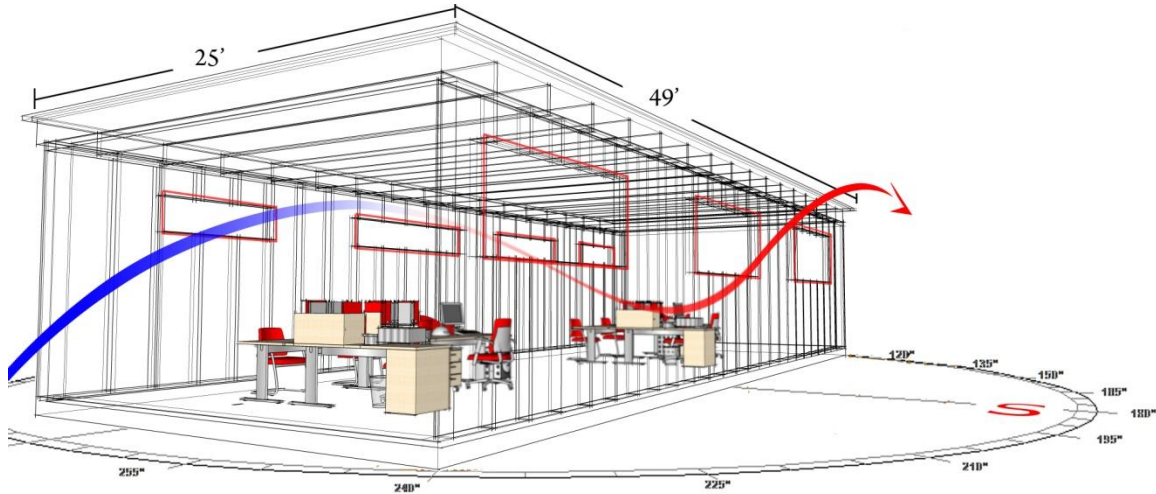


Figure 3.7: Ventilation and infiltration in a building.

10. R-value: The R-value of the insulation changes the U-value of the construction. There is no question that insulation is better for preventing heat loss from the walls during the winter and slowing the heat gain during summer. Although the (Kim, 2009) study shows that the increase in R-value after a certain point does not contribute much to the energy saving potential, this study will test to see if the increase in R-value of insulation has a significant effect on the performance of PCM.

Some of the variables that shall be kept constant throughout the study are listed in Table 3.1, which depicts the categorization of variables into independent variables and constant variables that shall be held constant throughout the study.

Independent variables	Number of Levels	Constant Parameters	Dependent Variable
Melting Temperature	20 [19-38]	Building type	Annual Energy load
PCM Enthalpy	7 [50:230]	Infiltration schedule	Annual Heating Load
Length to Width Ratio	3 [$\gg 1, 1, \ll 1$]	Ventilation schedule	Annual Cooling Load
Climate/Cities	15	Internal load schedule	

PCM Location	6 [N,S,E,W,R,F]	HVAC schedule	
PCM Position	3 [In, Middle, Out]	Shading schedule	
Internal Loads	3 [low, med, high]	Window-to-Wall ratio	
Insulation R-Value	3 [low, med, high]		

Table 3.1: List of independent variables, its number of levels, constant parameters and dependent variables.

The levels of the independent variables that are listed in the table pertain to the number of different values or 'states' a variable can represent. For example the melting temperature which is a quantitative variable has 20 levels. This means that the melting temperature can take any value ranging from 19°C to 38°C in increments of one degree. Similarly, PCM position which is a qualitative variable can assume three different states namely interior, exterior and interstitial. To test the effect of each variable at each level requires a full factorial experimental design. The full factorial design is an experimental design where all the possible combinations of all the levels are tested. The full factorial design for this particular case therefore requires 68040 experiments (i.e. $20 * 7 * 3 * 6 * 3 * 3 * 3$) for each representative city. Due to the sheer number of experiments required for this asymmetric full factorial design, initially a 3 level variable screening (i.e. $3^7 = 2187$ experiments) will be performed so the important variables are identified and the unimportant variables removed. Once the important variables are identified, assuming that some variables prove unimportant, a full factorial design will be performed on the remaining variables. However, if all the identified variables seem to contribute significantly to the dependent variable then a fractional factorial design will be performed. Subsets of all level-combinations of the factors are considered in the form of a fractional factorial design. After the experiments are run on this sample and results obtained, regression analysis will be performed to develop climate specific empirical models for each representative city. A linear regression model is as follows:

$$Y(x) = \beta_0 + \underbrace{\beta_1 \cdot x_1 + \beta_2 \cdot x_2 + \beta_3 \cdot x_3}_{\text{Quantitative}} + \underbrace{\beta_4 \cdot x_4 + \beta_5 \cdot x_5 + \beta_6 \cdot x_6 + \beta_7 \cdot x_7 + \beta_8 \cdot x_8}_{\text{PCM Location}} + \underbrace{\beta_9 \cdot x_9 + \beta_{10} \cdot x_{10}}_{\text{PCM Position}} + \underbrace{\beta_{11} \cdot x_{11} + \beta_{12} \cdot x_{12}}_{\text{L/W Ratio}} + \underbrace{\beta_{13} \cdot x_1 \cdot x_2 + \beta_{14} \cdot x_1 \cdot x_3 + \beta_{15} \cdot x_2 \cdot x_3}_{\text{Interaction Terms}}$$

Where, x_1 = melting temperature, x_2 = PCM Enthalpy, x_3 = Internal Loads, x_4 =

$$\begin{aligned} & \begin{cases} 1 \text{ if East} \\ 0 \text{ if otherwise} \end{cases}, & x_5 = \begin{cases} 1 \text{ if West} \\ 0 \text{ if otherwise} \end{cases}, & x_6 = \begin{cases} 1 \text{ if South} \\ 0 \text{ if otherwise} \end{cases}, & x_7 = \\ & \begin{cases} 1 \text{ if North} \\ 0 \text{ if otherwise} \end{cases}, & x_8 = \begin{cases} 1 \text{ if Floor} \\ 0 \text{ if otherwise} \end{cases}, & x_9 = \begin{cases} 1 \text{ if Interior} \\ 0 \text{ if otherwise} \end{cases}, & x_{10} = \begin{cases} 1 \text{ if Middle} \\ 0 \text{ if otherwise} \end{cases}, \\ & x_{11} = \begin{cases} 1 \text{ if } \gg 1 \\ 0 \text{ if otherwise} \end{cases}, & x_{12} = \begin{cases} 1 \text{ if } 1 \\ 0 \text{ if otherwise} \end{cases} \end{aligned}$$

In the regression model, the variables x_4 through x_{12} define the qualitative variables in the research (i.e. PCM location, PCM position, and Length-to-Width ratio). If a qualitative variable has n number of levels then it is defined in the regression model by using $n-1$ indicators. For example the PCM location variable has 6 levels (i.e. East, West, South, North, Roof, and Floor) therefore the regression model uses 5 indicator variables to measure the contribution of each level. If the PCM is placed on the east wall, x_4 assumes a value of 1 while all the other 'PCM location' variables (i.e. x_5 , x_6 , x_7 , and x_8) are zero. The same principle applies to the other qualitative variables when trying to explain the contribution of all levels in one regression model. The linear regression model mentioned is generally appropriate for simple linearly proportional behaviors. In this study various nonlinear regression models with coupling terms will be considered.

Data collection method

The experiments will be performed by running numerical simulations. The numerical simulation route is chosen especially since experimental assessment of each of the numerous experiments on every city is not feasible. Physical experimentation is impossible since it is economically prohibitive to run many experiments on physical buildings to be able to gather sufficient information to answer the research question. Therefore the simulation program EnergyPlus will be used for running the whole building energy simulations.

EnergyPlus is a simulation program developed by the U.S. Department of Energy and is capable of modeling PCM behavior accurately within any building type (Kosny, 2009; Energy, 2010; Zhuang, 2010; Shrestha, 2010; Shrestha, 2011; Velasco, 2012). For each climate type, the representative weather file will be obtained from the U.S. Department of Energy website. The database for all these weather files is managed by the U.S. Department of Energy (DOE) and can be accessed on the internet for free. The weather files are created from 30 years of meteorological and weather station data as recommended in the standard (ASHRAE, 2009) developed by the American Society of Heating, Refrigeration, and Air-Conditioning Engineers.

Within the EnergyPlus modeling environment a simple light weight building based on the ASHRAE 90.1 standard will be designed. The different combinations of variables will be modeled in the EnergyPlus model. It is not feasible to run numerous simulations for this parametric analysis by manually changing one variable at a time. Matlab will be used to generate the numerous input files for use in EnergyPlus.

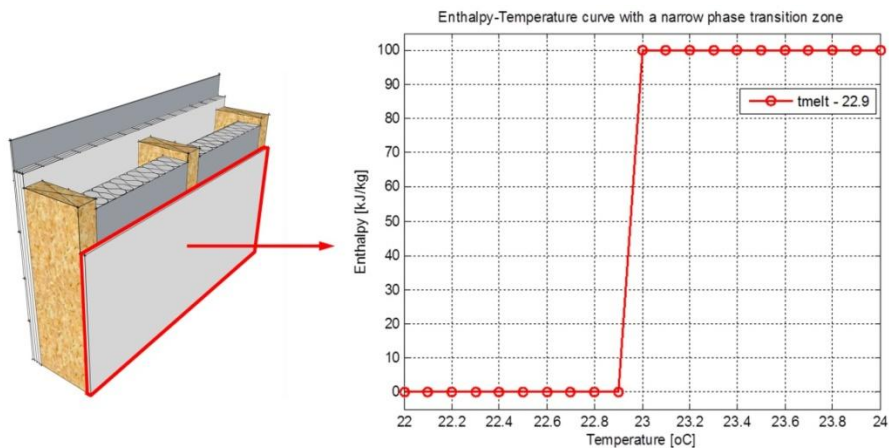


Figure 3.8: Thermal property definition of a theoretical PCM melting at 23°C within EnergyPlus using the enthalpy-temperature function.

The thermal storage properties of the PCMs will be defined within EnergyPlus using the enthalpy-temperature input. EnergyPlus uses the conduction finite difference algorithm and uses

an implicit finite difference scheme coupled with an enthalpy-temperature function to account for phase change energy accurately (Energy, 2010) an example of which is shown in Figure 3.8.

Annual simulations of the treatment will be run for each city and the results will be compared to the control variable, which is the annual energy consumption of the building without PCM treatment. The vast number of data obtained from each simulation needs to be analyzed properly. The hourly temperature fluctuation within the wall layers and the indoors, incoming heat flux through each wall, energy consumption for the cooling load during summer, energy consumption for heating load during the winter and the annual energy consumption are a few output parameters that need to be properly analyzed. The analysis and post processing of the data will be performed using statistical analysis software (SAS) and Matlab.

Threats to validity

Internal Validity: The threat to internal validity comes from instrumentation. Validation studies have been done in order to validate EnergyPlus as a building energy simulation tool and in particular the numerical modeling of phase change materials using EnergyPlus has been validated by (Pedersen, 2007; Kosny, 2010; Zhuang, 2010; Shrestha, 2010; Shrestha, 2011) and (Campbell, 2011). Although EnergyPlus as a building energy simulation tool has been validated, the particular model developed for this research needs to be validated. In order to check the validity of the model designed in EnergyPlus, a quasi-empirical validation study is performed (Underwood, 2004). In the process of finding published journals on the experimental evaluation of PCM in buildings, it was evident that most studies did not provide enough information on the building and its material properties to accurately model in EnergyPlus. Pertinent information on the properties of the building can be found in (Zhuang, 2010) in Chongqing, China. The building model is replicated in EnergyPlus in order to validate the experimental results obtained in the

Chongqing study. The Chongqing study was performed on a $1.5m \times 1.5m \times 2m$ test hut using EnergyPlus version 2.1 while the current version of EnergyPlus is 8.1.

The building facade was replicated as in the study and as was the run period for the simulation. Since the Chongqing study did not provide the ground surface temperatures in their study, a monthly average temperature for august was assumed to be 40°C . A 40°C ground temperature was assumed to be reasonable since the Chongqing test hut was built on the roof of a building and tested during the summer month of august. The material properties were defined in accordance to chapter 33 of the ASHRAE fundamentals handbook (ASHRAE, 2009).

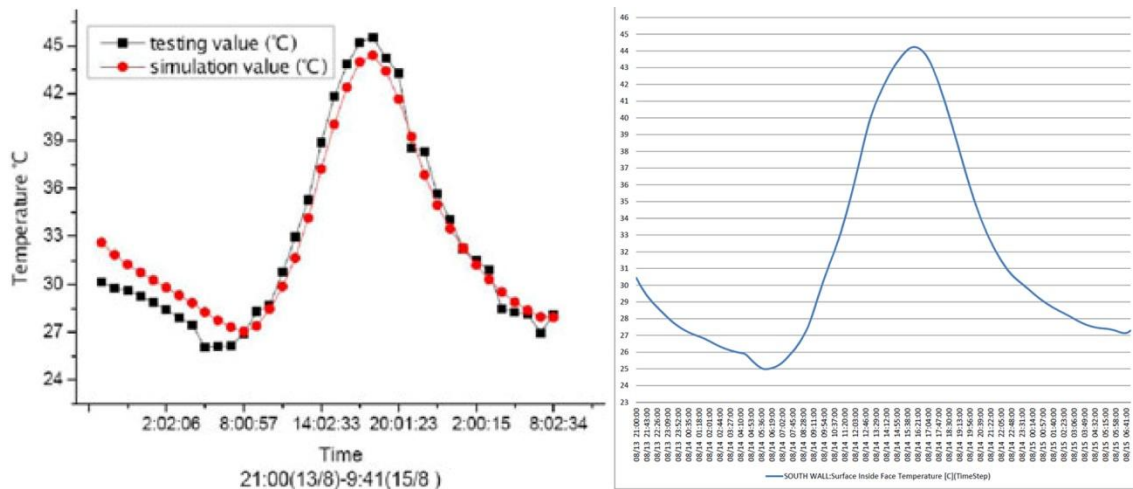


Figure 3.9: South wall interior surface temperature comparison a) Chongqing Study b) EnergyPlus replication.

The results of the paper are shown on the left plot in Figure 3.9. The plot shows the temperature of the wall that contained PCM with melting temperature at 33 degrees and latent heat of fusion of 70 kJ/kg. It can be seen that the south surface interior temperature modeled in EnergyPlus version 8.1, the plot on the right, very closely matches the testing value of the Chongqing.

In addition to this quasi-empirical comparison an inter-modal comparison was also performed to test for any bugs or problems that need further fixing. The inter-modal comparison

of the EnergyPlus model was performed with the software ABAQUS, a finite element modeling software. A 3ft X 3ft X 3ft test hut was modeled in both EnergyPlus and ABAQUS. In addition, a custom weather file was created for uniformity in the results. The boundary conditions in ABAQUS were set according to the custom weather file developed. In both the models, the roof and the south surface construction had PCM melting at 25 degrees and a heat of fusion of 50 kJ/kg.

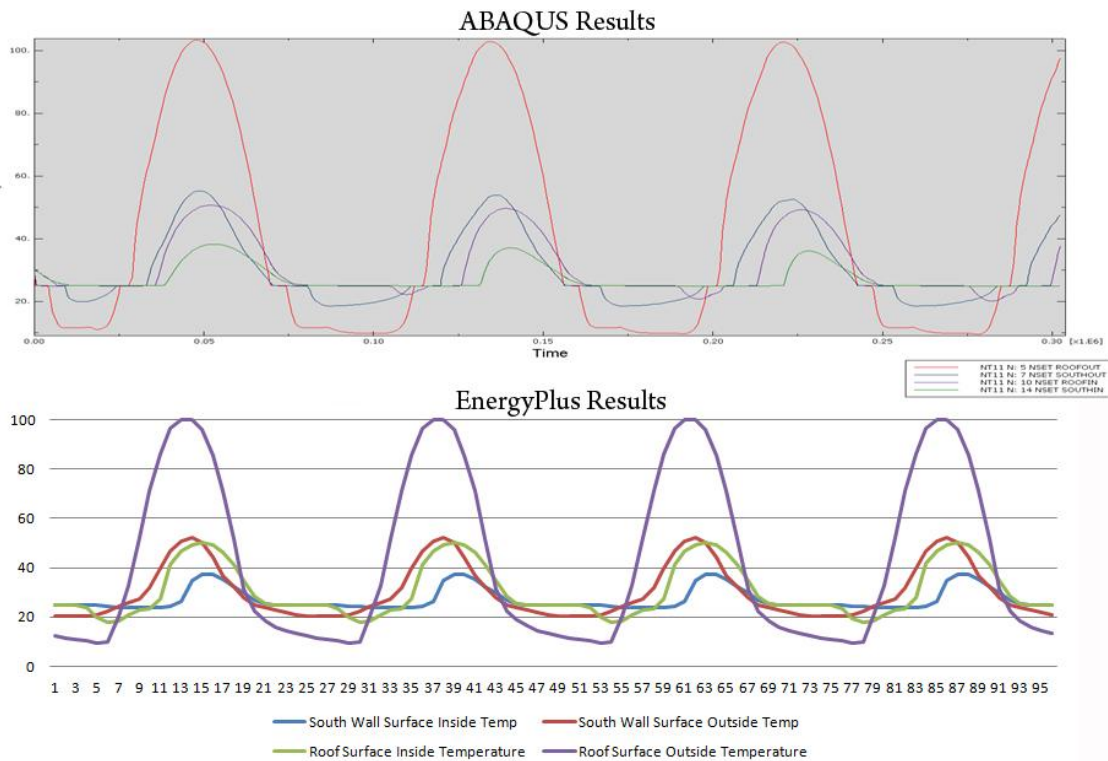


Figure 3.10: South wall and roof - interior and exterior surface temperature comparison.

The plots in Figure 3.10 show that the results from both the models in ABAQUS and EnergyPlus are in agreement with each other. In addition to these validation studies, the expertise and feedback of seasoned numerical simulation professionals will be sought throughout the research to counter the threats to internal validity

External Validity: Since the simulations are climate specific, the results obtained for one climate zone cannot be generalized to other climate zones within the U.S. However, the results obtained for one city will be generalized over the climate zone that the city represents.

Pilot study

The pilot study was performed in three steps:

- a) The development of the climate specific EnergyPlus model
- b) Data collection using the parametric analysis tool jEPlus and
- c) The regression analysis of the data.

Development of the EnergyPlus model

The control building was set in Greenville, South Carolina and was designed to meet the mandatory requirements as stated in the ASHRAE 90.1 Standard as shown in Figure 3.11

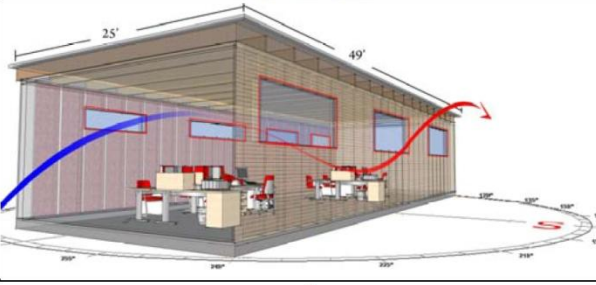
Item	Descriptions	Additional Info
Location	Zone 3 A: Greenville, SC	
Total Floor Area (sq feet)	1225 (25 ft x 49 ft)	Pilot Study Details
Building shape		Construction: Roof: Attic and Other Wall: Wood-framed & other Floor: Slab-on-grade Constants: Internal Load: 5 People Ventilation: None Lighting: None Shading Schedule: None Electric Equipment: None Orientation: 0 Degree North
Length to Width Ratio	2	>>1
Window Fraction (Window-to-Wall Ratio)	14.19% for total window to wall ratio 15% wwr - South & North 12% wwr - East & West	SHGC: 0.25 U-Value: 3.97
HVAC		
Thermostat Setpoint	25°C Cooling/21°C Heating	Available: 24/7

Figure 3.11: Building details for the pilot study.

In order to simplify the pilot study compared to the actual research, a number of factors were left constant as seen in Figure 3.12. The whole model was greatly simplified in that all the internal loads (i.e. lights, electric equipment) were accounted for by people, each of whom emits 120 Watts. The occupancy schedule of 5 people was left constant throughout the year. The infiltration, ventilation and shading objects were removed for simplicity. The orientation of the building and the length-to-width ratio was kept constant throughout the pilot study as well. The only variables that were tested for and varied was the PCM melting temperature, PCM enthalpy and the location of PCM in the building.

Data collection

For the pilot study, the actual research design was simplified by only testing a subset of the variables. The variables tested for the study were:

1. PCM melting temperature - The PCM melting temperature was defined to encompass 20 levels. The PCM was allowed to melt from 19°C to 38°C in increments of 1 degree.
2. PCM enthalpy - The PCM enthalpy was defined to hold 7 levels. Enthalpy ranging from 50 kJ/kg to 230 kJ/kg was defined in increments of 30 kJ/kg. In total $20 \times 7 = 140$ different PCMs were defined as separate input files that would later be called in by jEPlus, a parametric simulation engine developed for EnergyPlus.
3. The 140 different PCMs were then one by one, automatically placed on the 6 different surfaces. Separate input files were created for each surface so that each surface simulation could be run on separate computers.

Once the PCMs were defined and separate input files were created for each surface simulation, jEPlus was allowed to run the parametric study. A total of $140 \times 6 = 840$ jobs were

run on 3 computers. 140 jobs required 5 hours of computing time. Since the simulations were performed on 3 different computers the results for the 840 jobs were obtained in approximately 11 hours. For every combination of PCM melting temperature, PCM enthalpy and surface an output of annual heating load and cooling load was obtained.

Data analysis and regression

The data was collected and then a regression analysis was performed using the statistical analysis software, SAS. The regression model based on the variables in the pilot study is as follows:

$$Y(x) = \beta_0 + \overbrace{\beta_1 \cdot x_1 + \beta_2 \cdot x_2}^{\text{Quantitative}} + \overbrace{\beta_3 \cdot x_3 + \beta_4 \cdot x_4 + \beta_5 \cdot x_5 + \beta_6 \cdot x_6 + \beta_7 \cdot x_7}^{\text{PCM Location}} + \overbrace{\beta_8 \cdot x_1 \cdot x_2}^{\text{Interaction Term}}$$

Where,

$$x_1 = \text{melting temperature}, x_2 = \text{PCM Enthalpy}, x_3 = \begin{cases} 1 & \text{if East} \\ 0 & \text{if otherwise} \end{cases}, x_4 = \begin{cases} 1 & \text{if West} \\ 0 & \text{if otherwise} \end{cases},$$

$$x_5 = \begin{cases} 1 & \text{if South} \\ 0 & \text{if otherwise} \end{cases}, x_6 = \begin{cases} 1 & \text{if North} \\ 0 & \text{if otherwise} \end{cases}, x_7 = \begin{cases} 1 & \text{if Floor} \\ 0 & \text{if otherwise} \end{cases}.$$

The results from the parametric analysis were obtained in two categories, the annual heating and cooling loads.

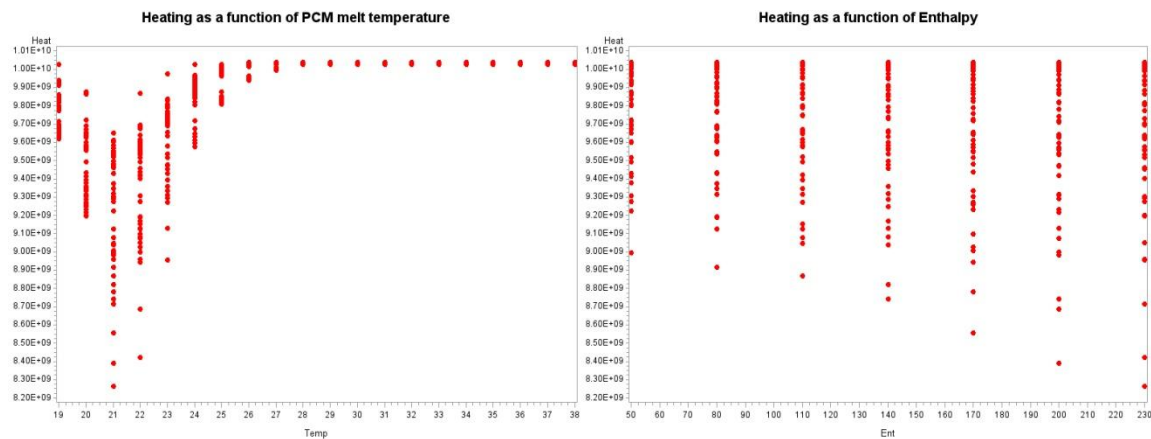


Figure 3.12: Heating load with respect to melting temperature and enthalpy.

The scatter plots in Figure 3.12 show the annual heating load changes with respect to the melting temperature and enthalpy. It is evident from the scatter plots that melting temperature of PCMs seems to have a larger impact in lowering the heating load as opposed to the enthalpy of the PCMs. The PCM that melts at 21°C seems to work best for the months that require heating.

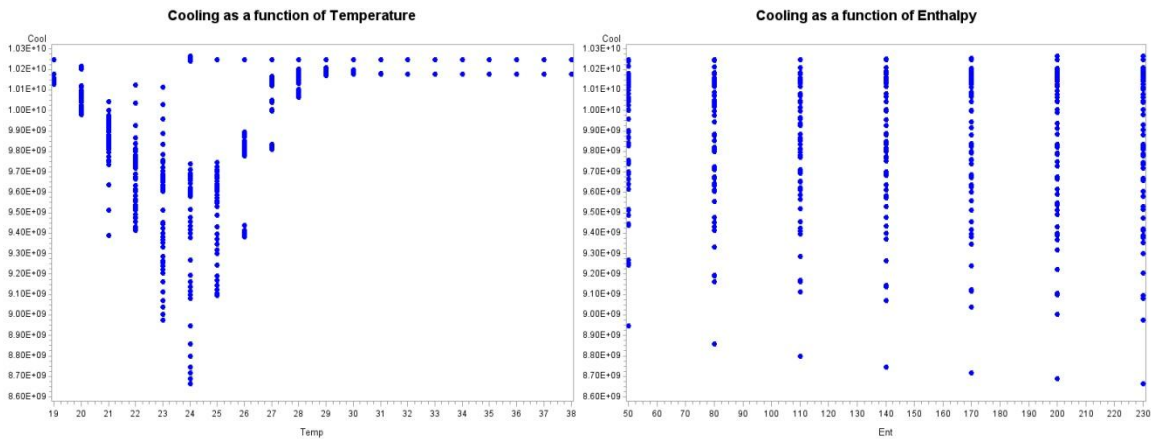


Figure 3.13: Cooling load with respect to melting temperature and enthalpy.

Similarly the PCM that melts at 24°C seems to perform best during the months that require cooling as evidenced by Figure 3.13. On the other hand the increase in PCM enthalpy seems to show diminishing returns for both the heating and cooling months. The scatter plot includes results from all surfaces and the charts in Figure 3.14 depict the optimum surfaces where PCM works best in this scenario.

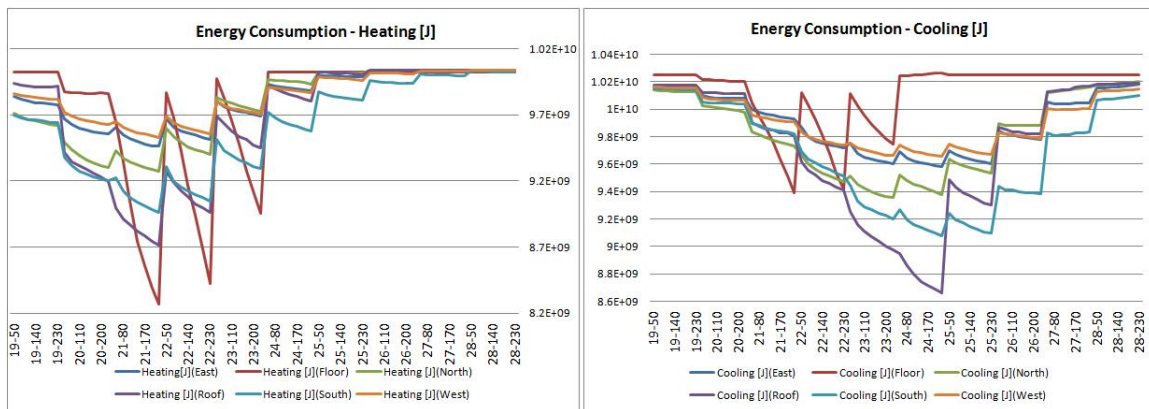


Figure 3.14: The heating and cooling load with PCM placed on different surfaces.

In Figure 3.14, the '20-200' on the horizontal axis represents the results for the PCM with a melting temperature of 20°C and enthalpy of 200 kJ/kg. PCM applied to the floor shows the most energy savings during the months that require heating and PCM applied to the roof shows the most energy savings during the months that require cooling.

The percent energy savings for the floor during heating months and the roof during cooling months depicts how the increase in enthalpy, especially during the cooling months, has diminishing returns. This is evidenced in the bar chart in Figure 3.15.

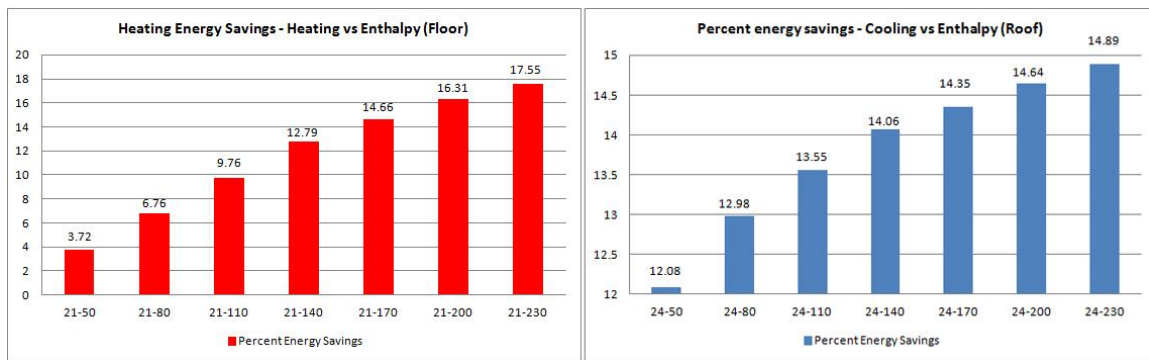


Figure 3.15: a) The heating load versus enthalpy - PCM placed on the floor b) The cooling load versus enthalpy - PCM placed on the roof.

Even though the stepwise increase in PCM enthalpy only shows diminishing increase in energy savings, the PCM energy storage capacity needs to be compared against the price of PCM to be able to make the decision as to what heat storage capacity is optimal. A cost-benefit analysis on the basis of PCM cost and electric energy cost will be devised that will allow for the development of design guidelines based on the price and energy saving capacity of PCMs.

After the plots were analyzed the data for cooling was truncated past 29 degrees and the data for heating was truncated past 28 degrees since it was evident from the scatter plots in Figure 3.12 and Figure 3.13 that the PCM did not work past these melting temperatures. The fitted regression models on the truncated data are as follows:

Cooling Load [J]

$$= 2.0886 * 10^{12} - 1.1885 * 10^{13}/x_1 - 1.3468 * 10^{11} \cdot (x_1) + 3.8310 * 10^9 \cdot (x_{12}) - 4.0377 * 10^7 \cdot (x_{13}) - 4.7779 * 10^5 \cdot (x_2) + 1.8439 * 10^8 \cdot (x_3) + 1.9123 * 10^8 \cdot (x_4) - 5.1722 * 10^7 \cdot (x_5) + 1.0607 * 10^8 \cdot (x_6) + 4.0843 * 10^8 \cdot (x_7)$$

Analysis of Variance					
Source	DF	Sum of Squares	Mean Square	F Value	Pr > F
Model	10	4.076233E19	4.076233E18	134.54	<.0001
Error	451	1.366412E19	3.029739E16		
Corrected Total	461	5.442646E19			

Root MSE	174061457	R-Square	0.7489
Dependent Mean	9876807346	Adj R-Sq	0.7434
Coeff Var	1.76233		

Table 3.2: Regression details for the cooling load as dependent variable.

SST = the variability of the sample measurements about the overall mean.

SSE = the sum of squared deviations of actual values from predicted values.

SSR = the sum of squared deviations of predicted values from the mean value.

MSE = the estimated variance determines to what extent the model does not fit the data.

RMSE= measures the spread of the distribution of y values about the regression line.

R^2 = explains what percentage of the variation in the dependent variable can be explained by the regression model.

As shown in Table 3.2, the global test for the fitted model at a significance level of α (Alpha) = 0.05 seems significant in predicting the annual cooling load. The R^2 and adjusted R^2_{Adj} tell us that the model explains approximately 74% of the variability in the data in this particular example. A hypothesis test for the surface coefficient terms (i.e. $\beta_7, \beta_8, \beta_9, \beta_{10}, \beta_{11}$) is performed

using the F-test for comparing the nested model as shown in Table 3.3. As can be seen the surface coefficient terms contribute significantly to the model as well.

Test 1 Results for Dependent Variable Cool				
Source	DF	Mean Square	F Value	Pr > F
Numerator	5	1.751161E18	57.80	<.0001
Denominator	451	3.029739E16		

Table 3.3: Nested F-test for the surface coefficient terms - $\beta_7, \beta_8, \beta_9, \beta_{10}, \beta_{11}$.

Once the fitted model was defined, the predictive validity of the model was assessed using the Jackknife validation technique (Mendenhall, 2003).

Jackknifed Prediction Statistics-Cooling

Obs	_RSQ_	RsqrJack	MSE	MSEJack
1	0.74894	0.73731	3.0297E16	3.1701E16

Table 3.4: Jackknifed prediction statistics for cooling as the dependent variable.

As can be seen from the jackknife predictive assessment in 3.xxTable 3.4 the $R^2_{Jack} \ll R^2$ and similarly $MSE_{Jack} \gg MSE$. In order to reject the validity of the fitted model the MSE needs to be at least a multiple of 2 or 3 of the MSE_{Jack} . Since that is not the case, it can be concluded that the fitted model has predictive validity.

Similar statistical tests were performed on the annual heating load as well. The fitted model that explains the annual heating load with respect to the PCM melting temperature, PCM enthalpy and the surface treatment of PCM is as follows:

$$\begin{aligned}
 \text{Heating Load} = & 1.5191 * 10^{12} - 7.2523 * 10^{12}/x1 - 1.1457 * 10^{11}.x1 + 3.7744 \\
 & * 10^9.(x12) - 4.5684 * 10^7.(x13) - 9.3728 * 10^5.(x2) + 1.9192 \\
 & * 10^8.(x3) + 2.1295 * 10^8.(x4) - 8.4888 * 10^7.(x5) + 1.2809 \\
 & * 10^8.(x6) + 1.0710 * 10^8.(x7)
 \end{aligned}$$

Analysis of Variance					
Source	DF	Sum of Squares	Mean Square	F Value	Pr > F
Model	10	3.46461E19	3.46461E18	107.31	<.0001
Error	367	1.184868E19	3.228524E16		
Corrected Total	377	4.649478E19			

Root MSE	179680947	R-Square	0.7452
Dependent Mean	9708702975	Adj R-Sq	0.7382
Coeff Var	1.85072		

Table 3.5: Regression details for the heating load as dependent variable.

Based on Table 3.5, the global test for the fitted model for the heating load at a significance level of α (Alpha) = 0.05 seems significant. The model is also statistically useful for predicting the annual heating load. The R^2 and adjusted R^2_{Adj} tells us that the fitted model explains approximately 73% of the variation in the dependent variable. A hypothesis test for the surface coefficient terms (i.e. $\beta_7, \beta_8, \beta_9, \beta_{10}, \beta_{11}$) was performed again using the nested F-test and it was found that the surface coefficient terms contributed significantly to the model predicting the heating load. Similarly the predictive validity of the model was once again assessed using the jackknife validation technique.

Jackknifed Prediction Statistics-Heating

Obs	_RSQ_	RsqJack	MSE	MSEJack
1	0.74516	0.73006	3.2285E16	3.4199E16

Table 3.6: Jackknifed prediction statistics for heating as the dependent variable.

The jackknife predictive assessment of Table 3.6 shows that the $R^2_{Jack} \ll R^2$ and similarly $MSE_{Jack} \gg MSE$. In order to reject the validity of the fitted model the MSE needs to be at least a multiple of 2 or 3 of the MSE_{Jack} . Since that is not the case, the fitted model for the annual heating load was shown to have predictive validity. Although the statistical test results showed that the

regression models for both heating and cooling exhibited predictive validity, a closer examination showed that the models were producing negative values of the dependent variable. For every temperature and enthalpy combination, the heating and cooling loads were negative, when in fact the loads could never take values less than zero. When trying to overlay the regression model on top of the data set it was clear that the regression model was not nearly as close to defining the behavior of the different PCMs on the walls. The qualitative terms that represented the surfaces seemed to be causing this error. In order to test to see whether the inclusion of all the qualitative variables in one regression model was the cause for the negative results, regressions were run on each surface one at a time. This way the regression analysis was simplified considerably and as a result the method was also adopted for the actual research. The east wall cooling and heating plots with respect to temperature and enthalpy respectively is shown in Figure 3.16:

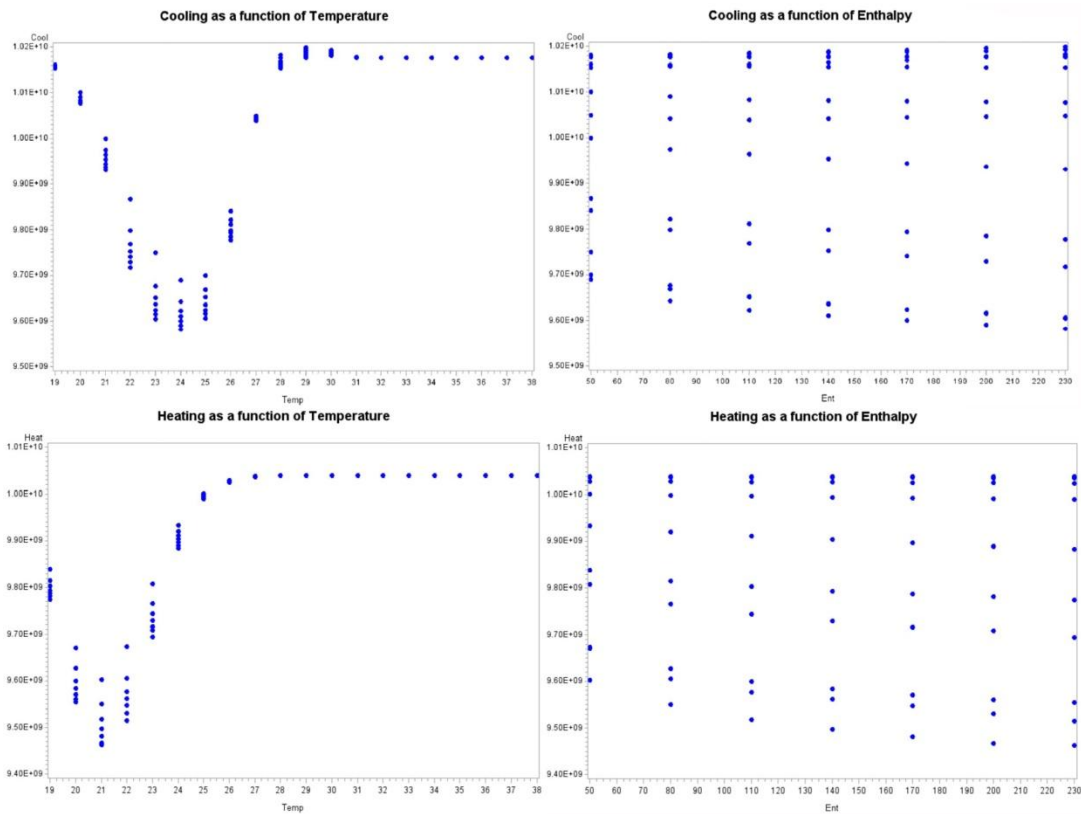


Figure 3.16: Scatter plot of the cooling and heating loads with PCM on the east wall.

Regression - East Wall (Cooling)

Analysis of Variance					
Source	DF	Sum of Squares	Mean Square	F Value	Pr > F
Model	5	3.545151E18	7.090302E17	766.83	<.0001
Error	71	6.564868E16	9.246292E14		
Corrected Total	76	3.6108E18			

Root MSE	30407717	R-Square	0.9818
Dependent Mean	9916792947	Adj R-Sq	0.9805
Coeff Var	0.30663		

Parameter Estimates					
Variable	DF	Parameter Estimate	Standard Error	t Value	Pr > t
Intercept	1	1.521213E12	71740408336	21.20	<.0001
Temp_Rec	1	-8.73548E12	4.195684E11	-20.82	<.0001
Temp	1	-9.67788E10	4568947897	-21.18	<.0001
Temp_sq	1	2718408270	128461023	21.16	<.0001
Temp_cube	1	-28267621	1345509	-21.01	<.0001
Ent_Rec	1	3443592321	676009786	5.09	<.0001

Regression - East Wall (Heating)

Analysis of Variance					
Source	DF	Sum of Squares	Mean Square	F Value	Pr > F
Model	5	2.728012E18	5.456023E17	602.20	<.0001
Error	64	5.798481E16	9.060126E14		
Corrected Total	69	2.785996E18			

Root MSE	30100044	R-Square	0.9792
Dependent Mean	9822114631	Adj R-Sq	0.9776
Coeff Var	0.30645		

Parameter Estimates					
Variable	DF	Parameter Estimate	Standard Error	t Value	Pr > t
Intercept	1	-7.73833E11	1.040102E11	-7.44	<.0001
Temp_Rec	1	4.928654E12	5.979242E11	8.24	<.0001
Temp	1	46004209183	6745741411	6.82	<.0001
Temp_sq	1	-1183307989	193336064	-6.12	<.0001
Temp_cube	1	11269895	2066194	5.45	<.0001
Ent_Rec	1	4088787299	701831145	5.83	<.0001

Figure 3.17: Regression statistics for the cooling and heating load - east wall.

Similarly the regression for when the PCM is placed on the south wall is:

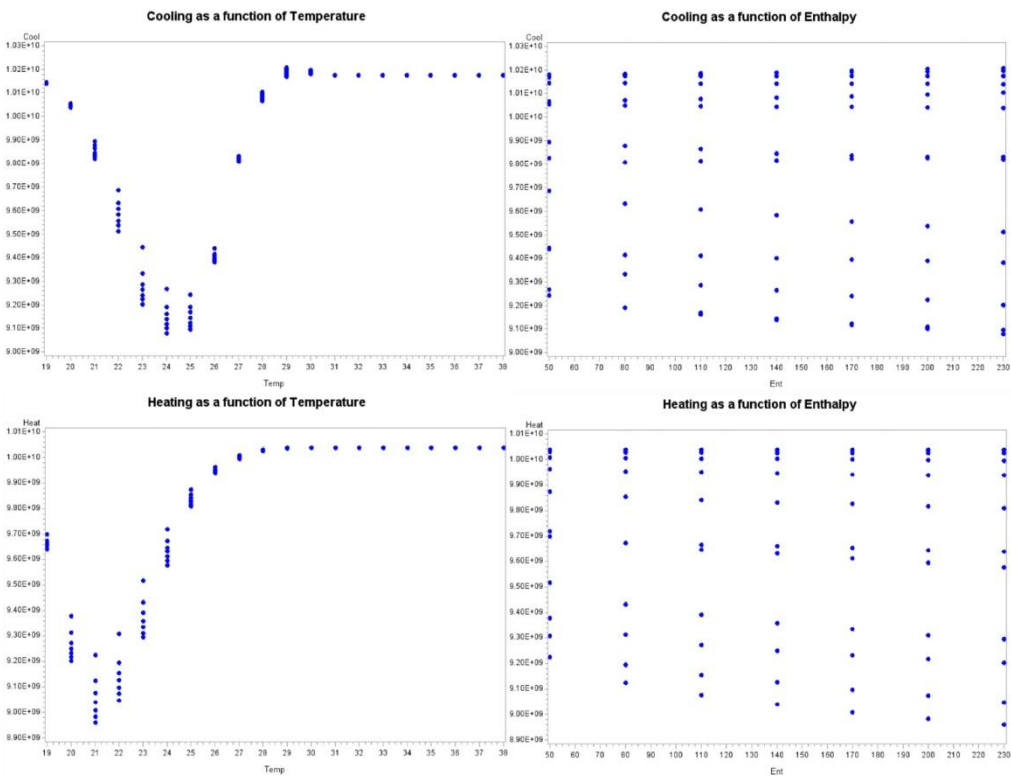


Figure 3.18: Scatter plot of the cooling and heating loads with PCM on the south wall.

Regression - South Wall (Cooling)

Analysis of Variance					
Source	DF	Sum of Squares	Mean Square	F Value	Pr > F
Model	5	1.114439E19	2.228879E18	581.93	<.0001
Error	71	2.719413E17	3.830159E15		
Corrected Total	76	1.141634E19			

Root MSE	61888280	R-Square	0.9762
Dependent Mean	9702378602	Adj R-Sq	0.9745
Coeff Var	0.63787		

Parameter Estimates					
Variable	DF	Parameter Estimate	Standard Error	t Value	Pr > t
Intercept	1	2.563254E12	1.46012E11	17.56	<.0001
Temp_Rec	1	-1.49276E13	8.5394E11	-17.48	<.0001
Temp	1	-1.61599E11	9299097640	-17.38	<.0001
Temp_sq	1	4483707150	261454414	17.15	<.0001
Temp_cube	1	-46034959	2738490	-16.81	<.0001
Ent_Rec	1	4530884036	1375870582	3.29	0.0015

Regression - South Wall (Heating)

Analysis of Variance					
Source	DF	Sum of Squares	Mean Square	F Value	Pr > F
Model	5	8.358891E18	1.671778E18	830.48	<.0001
Error	64	1.288336E17	2.013026E15		
Corrected Total	69	8.487725E18			

Root MSE	44866754	R-Square	0.9848
Dependent Mean	9595986988	Adj R-Sq	0.9836
Coeff Var	0.46756		

Parameter Estimates					
Variable	DF	Parameter Estimate	Standard Error	t Value	Pr > t
Intercept	1	-9.14504E11	1.550363E11	-5.90	<.0001
Temp_Rec	1	6.071191E12	8.912584E11	6.81	<.0001
Temp	1	51517210786	10055118917	5.12	<.0001
Temp_sq	1	-1246466825	288184352	-4.33	<.0001
Temp_cube	1	11040749	3079844	3.58	0.0007
Ent_Rec	1	7552846319	1046140845	7.22	<.0001

Figure 3.19: Regression statistics for the cooling and heating models - south wall.

For both the surfaces the global test for the fitted models for the heating and cooling at significance level of $\alpha = 0.05$ were highly significant. The R^2 and adjusted R^2_{Adj} turned out to be approximately 98% which was very encouraging. The R^2 and adjusted R^2_{Adj} of approximately 98% meant that the regression models explained at least 98 percent of the variability in the data. Upon plotting the regression models over the actual data it was evident that running the regression analysis on one surface at a time was a viable option. The results and regression models were more comprehensible when the analysis was performed on one surface at a time.

A separate pilot study was also performed for a 35' by 35' building located in Albuquerque, NM and Fairbanks, AK. The buildings were designed in accordance to the ASHRAE 90.1 standard. The window to wall ratio was set to 15% across all the other simulations in this study. Two different cases of internal loads were tested, 0 people and 15 people. Each person was set to dissipate 120 Watts and constantly occupied the space. The HVAC set-point schedule was set to mimic an office set-point schedule. The primary reason for the separate pilot

study was to ensure whether the interstitial placement of PCM towards the outer layer of the insulation was a sensible variable to study since it seemed very counterintuitive that the PCM placed towards the outside of the insulation would mitigate any substantial amount of heat or cold penetrating or leaving the building. Any heat trying to penetrate the building would, at an instant, melt the PCM without the insulation as a buffer mechanism. The results showed the placing the PCM anywhere, for example in Figure 3.20, other than the inside of the insulation was counterproductive.

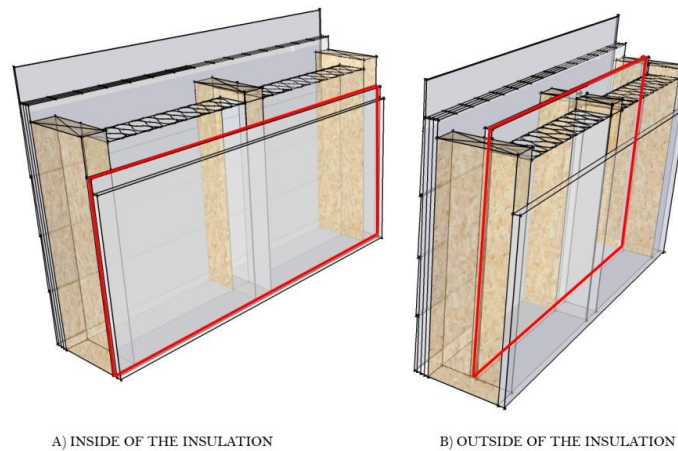


Figure 3.20: a) PCM placed inside of the insulation, b) PCM placed outside of the insulation.

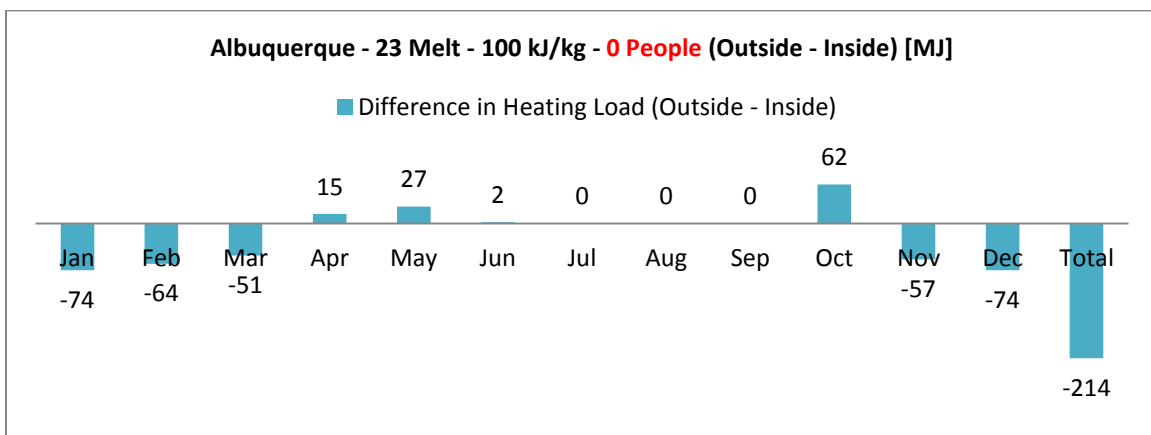


Figure 3.21: Difference in heating load for when PCM is placed outside versus inside the insulation. Internal Loads of Zero people.

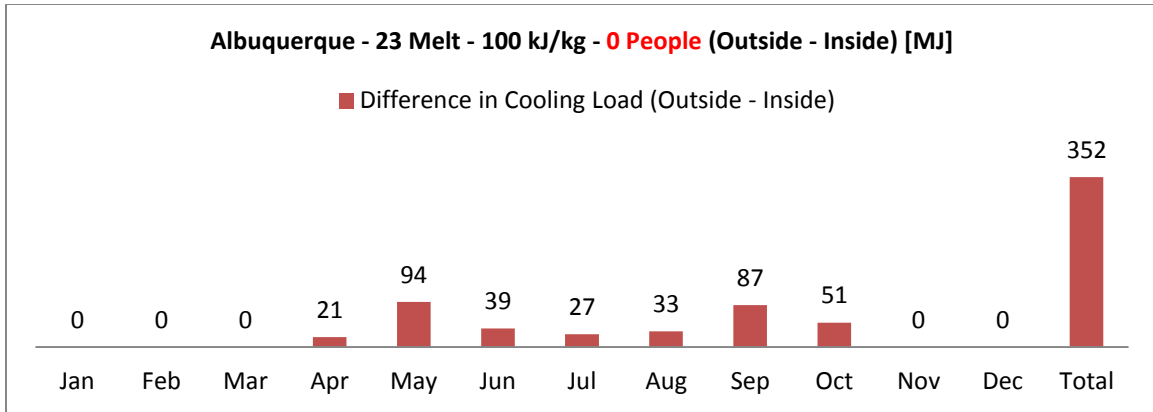


Figure 3.22: Difference in cooling load for when PCM is placed outside versus inside the insulation. Internal loads of zero people.

The Figure 3.21 and Figure 3.22 depict the difference in heating and cooling load for the cases where the PCM board is placed outside of the insulation and the PCM board is placed closer to the indoors. The building in Albuquerque, NM with 0 people exhibited a lower annual heating load (i.e. -214 Mega Joules less) with the PCM placed outside of insulation as opposed to when the PCM was placed closer to the indoors, inside of the insulation. The annual cooling load on the other hand, evident in Figure 3.28, was much higher (i.e., 352 Mega Joules) than when the PCM was placed closer to the inside. The aforementioned results were for the building with zero internal loads (i.e. no people occupying the building) where only the heating and cooling loads as a result of the exterior environment were mitigated by the PCM and met by the HVAC. The same sets of simulations were then performed for an internal load of 15 people (i.e., 15×120 watts = 1800 watts all year round) and the results can be seen in Figure 3.23 and Figure 3.24.

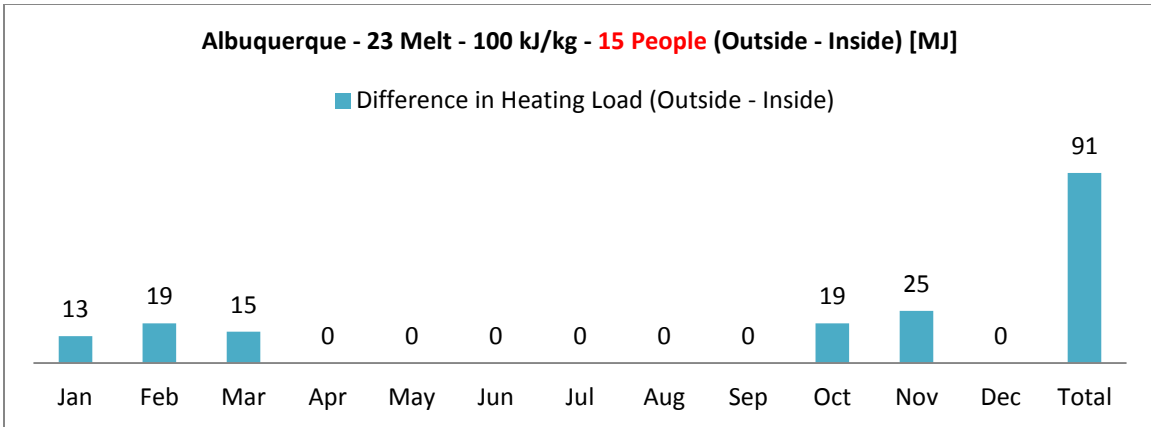


Figure 3.23: Difference in heating load for when PCM is placed outside versus inside the insulation. Internal loads of fifteen people.

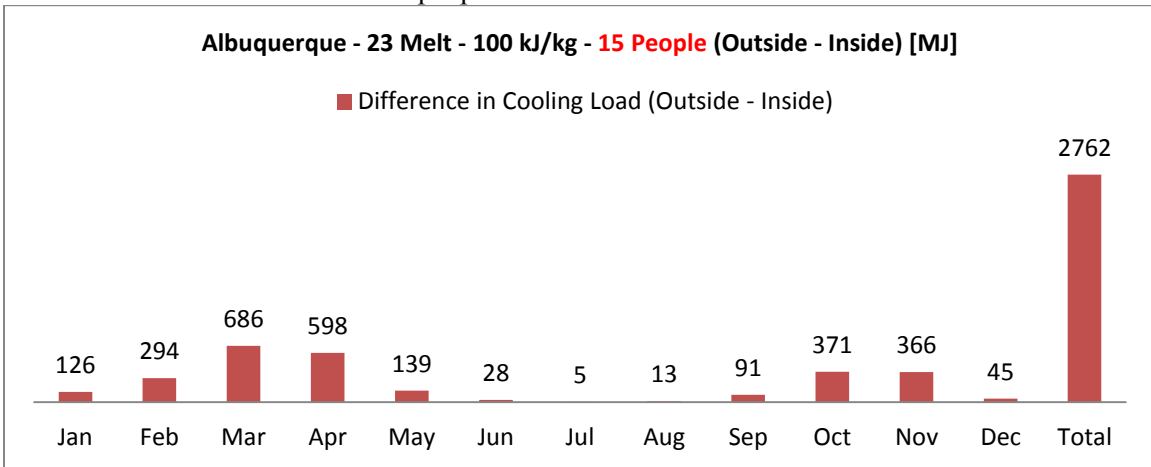


Figure 3.24: Difference in cooling load for when PCM is placed outside versus inside the insulation. Internal loads of fifteen people.

As the internal load was increased to 15 people (1800 watts), the placement of PCM toward the inside performed better than placing it outside of the insulation. Placing PCM boards on the outside of the insulation required more annual heating energy to maintain the set-point temperature indoors than when PCM was placed closer to the inside, therefore less efficient. The cooling load exhibited similar attributes. In this particular case, placing PCM boards closer to the indoors was 2762 mega joules more efficient than when placing it outside of the insulation.

Albuquerque is considered to fall in climate region 4, and it was necessary to check to see if

placing the PCM boards closer to the interior was true for the more extreme climates. Miami is more cooling dominated with cooling degree days (CDD/65) of 4458 and heating degree days (HDD/65) of 130. On the other hand, Fairbanks is very heating dominated with cooling degree days (CDD/65) of 71 and heating degree days (HDD/65) of 13528 (ASHRAE, 2009).

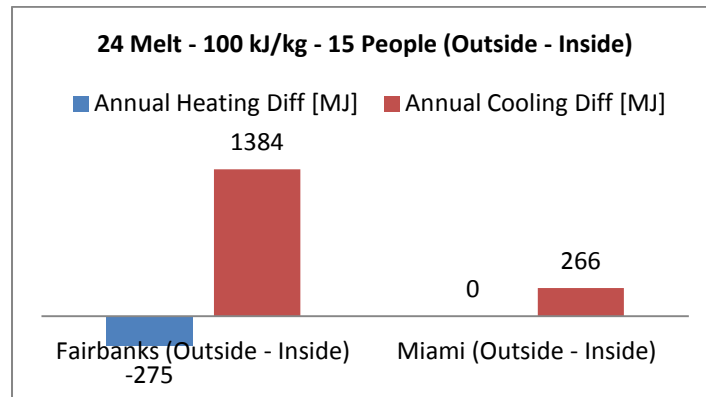


Figure 3.25: Difference in heating load for when PCM is placed outside versus inside the insulation. Internal loads of fifteen people.

For the building located in Fairbanks, 275 mega joules of heating energy was reduced by placing the PCM boards outside of the insulation. The annual cooling load however was saved only when the PCM boards were placed closer to the indoors (i.e., inside of the insulation). The placement of PCM boards closer to the indoors saved 1384 mega joules more of cooling energy compared to when the boards were placed outside. Similar conclusions could be drawn from the results from Miami, evident in Figure 3.25.

Lessons Learned

Some preliminary design guidelines could be drawn from the pilot study. In addition the pilot study was invaluable in identifying the areas of improvement in the research. The main lessons learned from the pilot study are listed as follows:

1. Simulation run times: While running the parametric analysis on one computer during the pilot study it was found that the baseline model required approximately 36 hours to run 1000 simulations. A computer equipped with a quad core processor and 8 gigabytes of RAM required approximately 7 to 8 minutes per simulation. The Palmetto Cluster (HPC) was sought for the running of the simulations.
2. Window-to-wall ratio: The windows cannot be defined in terms of window-to-wall ratio but should be defined in terms of each window area and should always be kept constant on all walls regardless of the length-to-width ratio of the building. This way the solar radiation entering the building is uniform for all buildings with different length-to-width ratios.
3. Rotation of the building: When setting up the parametric study to rotate the building from 0° relative to north to 90° relative to north a problem occurs. The wall facing east, defined as 'east wall' in EnergyPlus, when rotated 90 degrees is now facing south but still retains the name 'east wall'. This poses a big problem when trying to analyze the results. So three different .idf files (i.e. EnergyPlus input files) will be developed for the different orientations or length-to-width ratio variables and will be called upon by jEPlus separately to work around this issue.
4. PCMs on the slab: The slab pre-processor calculates the building ground surface temperature. This calculation is performed assuming a 3-dimensional heat flow and the values are fed into EnergyPlus. EnergyPlus on the other hand assumes a 1-dimensional heat flow when performing heat transfer calculations through the building envelope. When coupling latent heat thermal storage with the slab pre-processor program EnergyPlus crashes. So as a practical work around, a 0.1 mm thin layer of concrete with very low thermal resistance and without PCM was defined that would

stay in contact with the ground. This way the program would not crash and the slab above it would still retain the latent thermal storage with the PCM properties assigned to it. In addition, since this study focuses primarily on PCM boards the viability of using PCM boards on the floor seems against the norm of building construction. PCM boards on the floor as a variable will be removed altogether.

5. Regression analysis of one surface at a time: The complexity and number of variables involved in trying to encompass all the variables into one regression model is daunting and fraught with uncertainty. It is also very difficult to draw any meaningful conclusions when all the variables are present in the single regression model. Especially the addition of categorical variables with many levels can complicate the model beyond the scope of understanding the contribution that each variable makes. This was particularly true when all the surface variables were included in the regression during the pilot study. Due to this reason, the actual research will include regression analysis on the effect of placing PCM on each surface individually.
6. Since the 'interstitial' placement of PCM boards was not a viable variable to study, apparent from the second pilot. It was removed from the study.

Throughout the pilot study the developers of both jEPlus and EnergyPlus were contacted in order to clarify any issues that came up that were specific to those softwares.

Chapter Four

CLIMATE MAPS

Introduction

There are a large number of parameters that affect energy consumption in buildings and make the process of selecting the type and amount of PCM challenging. The thermal performance of a building is dependent on many factors. The envelope characteristics such as the building geometry, orientation, construction type, placement and size of windows, the thermo-physical properties of the construction materials, their interaction with outdoor conditions, plus indoor control strategies such as the HVAC schedules and set-point temperatures are a few parameters that, in tandem, determine the amount of heat or cool required to maintain comfortable indoor living conditions. The large number of factors that affect the heating and cooling loads and the complex nature of energy flows in buildings make it extremely difficult to study the effect of all factors at the same time. In fact, extensive engineering studies are generally necessary to determine the practicality of PCMs in any specific case. As a result, architects and engineers are reluctant to use PCM because of the lack of design guidelines and/or the lack of intuitive ways to visualize the potential of energy savings. While PCM gypsum boards are becoming commercially available in the construction industry in the US, designers and engineers are still unsure as to the guidelines for selecting the proper PCM (i.e. Melting temperature, heat storage capacity) specific to particular climatic conditions.

Assuming that for a building in a given climate, there exists an optimal melting temperature and enthalpy that can minimize the energy consumption as well as the payback period, how can this information be disseminated to designers in a concise way? This issue is

addressed first by developing climate maps in this chapter. Additional topics discussed in this chapter are the sensitivity of the optimal properties of PCM and the effect of the average cost of energy on the selection of PCM.

While the main study of the different independent variables was being setup to run on the computer cluster, a small subset of the simulations was performed using JEplus and EnergyPlus. The energy consumption was determined numerically using the Department of Energy software EnergyPlus, which calculates the energy consumption for heating and cooling a building under any climate and operation schedule.

Payback period

Some of the common criteria used by builders and designers to determine successful design can include: cost, energy performance, thermal comfort, aesthetics, environmental impact etc. Due to the relative high levels of subjective judgment that goes into decision making about aesthetics and proper design, only the cost is taken as criteria for the decision making for this study. The high capital cost and subsequently long payback period of new technologies is seen as one of the most significant barriers in implementing it in buildings (Cooke, 2007). Three cash-flow analysis tools – payback period, return on investment and present worth analysis – are commonly used to evaluate investments that improve energy performance. While the latter two analyses are predicated on the notion of setting a time frame of useful life, the payback period analysis is the most basic financial gauge to obtain the time (usually in number of years) for an investment cumulative cash flow to reach zero. Assuming that energy prices rise to keep up with inflation the change in time value of money is ignored in this analysis. In addition, the availability of tax benefits and subsidies for energy efficient homes provided by the federal government adds significant complexity to the payback period analysis. The effect on the payback period by the

inclusion of the time value of money, the savings accrued from the downsizing of HVAC equipment, reduction in construction costs, the lower interest rates provided by the energy efficient mortgage (EEM) again is not considered for this particular study. By relegating the 'systems' thinking approach for a later study, this chapter therefore considers 'pseudo' payback periods (PPP) based solely on the initial capital investment for the PCM boards and the money saved due to the savings in energy.

In the existing literature, research on payback periods for the use of PCMs is predominantly assessed on the basis of its environmental impacts. In a rudimentary sense such payback period analysis seeks to answer questions such as, how long does it take for the use of PCMs in buildings to surpass its embodied energy to mitigate greenhouse gases. Chan (2011) studied the environmental and economic impact of PCM impregnated walls in subtropical Hong Kong. Based on the embodied energy of the particular PCM in question, the study concluded with an energy payback period of 23.4 years. On the other hand the economic payback period, disregarding the time value of money, was concluded to be 91 years. Gracia et al. (2010) and Castell et al (2012) performed LCA analysis on five different test huts with and without PCM in Puigverd de Lleida, Spain. They concluded that the energy payback period can be reduced by lowering the embodied energy of PCM since it was too large to counteract the benefits during its operation. Stovall and Tomlinson (1995), through better management of the thermostat set point temperature schedules during the winter months and also by taking into account the differential tariff systems, found an economic payback of using PCM boards in a small house in Boston to be 5 years. Moheisen et al (2011) conducted a study on a test hut equipped with bio-PCM on the walls and/or ceiling by subjecting the test hut to a constant heat source. Under the assumption that the bio-PCM with 220 kJ/kg of enthalpy under-went a complete cycle for 100 days out of the year, Moheisen et al. (2011) have analytically concluded that the economic payback period of

bio-PCM to 5 years. As such the economic payback period of using PCM in buildings depends on a number of factors (i.e., the cost of PCM and the cost of energy etc.). In this chapter the cost of PCM is set to an arbitrary yet reasonable number and the cost of energy is based on the cost per kilo-watt-hour of electricity according to the average state electricity rates.

Setup

The aim and scope of this initial study is to identify the optimum melting temperature and enthalpy of PCM for each given climate type and also quantify the ‘pseudo’ payback period (PPP) associated with the use each optimum PCM board. The energy analysis was performed using EnergyPlus, a whole building energy simulation software developed by the US Department of Energy. The objective is also to perform a sensitivity analysis as to understand the magnitude of difference in savings if a less than optimum melting temperature or enthalpy is chosen. To that end different theoretical gypsum boards-PCM mixture (PCM boards) were defined using the Enthalpy-Temperature function in EnergyPlus. The PCM property was thus appended to the Gypsum board which lined the interior surface for all walls and the roof. A total of 60 different PCMs were defined to test the optimum PCM for each specific climate. The PCM’s melting temperature ranged from 16°C to 30°C in increments of 1 degree. Each PCM was defined to have a sharp melting range of 0.1 degree as seen in Figure 4.1. Similarly, for each PCM board the enthalpy ranged from 20kJ/kg to 80 kJ/kg in increments of 20 kJ/kg.

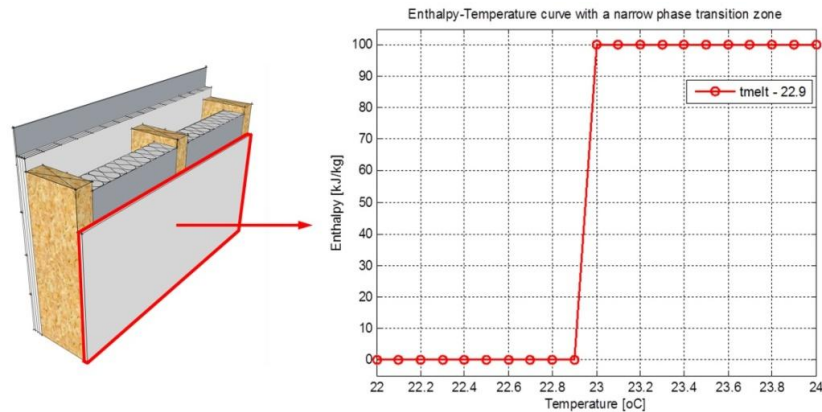


Figure 4.1: Thermal property definition of a theoretical PCM melting at 23° C within EnergyPlus using the enthalpy-temperature function.

A baseline building was developed for each representative city following the guidelines recommended in the ASHRAE 90.1 - 2010 standard. The 15 different climate specific buildings were created to match the specific recommendations on the insulation R-value, window SHGC and U-value in the standard. The construction specifics recommended in the standard were adopted for the building surface as well as the fenestration components. In terms of the internal loads, the building was set to be occupied by five people throughout the 24 hours of the day and every day through the year. Each person was set to dissipate 120 watts of energy into the interior environment. The heating and cooling thermostat set-point temperatures were set at 21° and 25° Celsius respectively throughout the year and the building was set to be conditioned by the Ideal Air Loads System. The energy performance of each specific building was simulated for the 15 different cities using the typical meteorological data (TMY3) weather data available from the EnergyPlus weather repository. The output variables, annual cooling and heating energy were requested as the dependent variables. Due to the high number of simulations required for each climate the software JEplus (Zhang, 2009) was used to setup and perform parametric runs for each PCM board. The data was then compared to the control or baseline building without PCM

properties appended to the gypsum board in order to quantify the magnitude of savings offered by the inclusion of PCM.

Optimum melting temperature and enthalpy

The results for each climate was obtained and analysed separately. It is clear from Figure 4.2 that the climate zone 8 (Fairbanks, AK) has the highest magnitude in annual load predominantly due to its high number of heating degree days (HDD) that requires a significant heating load throughout the winter. On the other end of the spectrum climate zone 3c (San Francisco, CA) has the lowest annual loads predominantly owing to its all year round mild temperature that requires neither too much heating nor cooling.

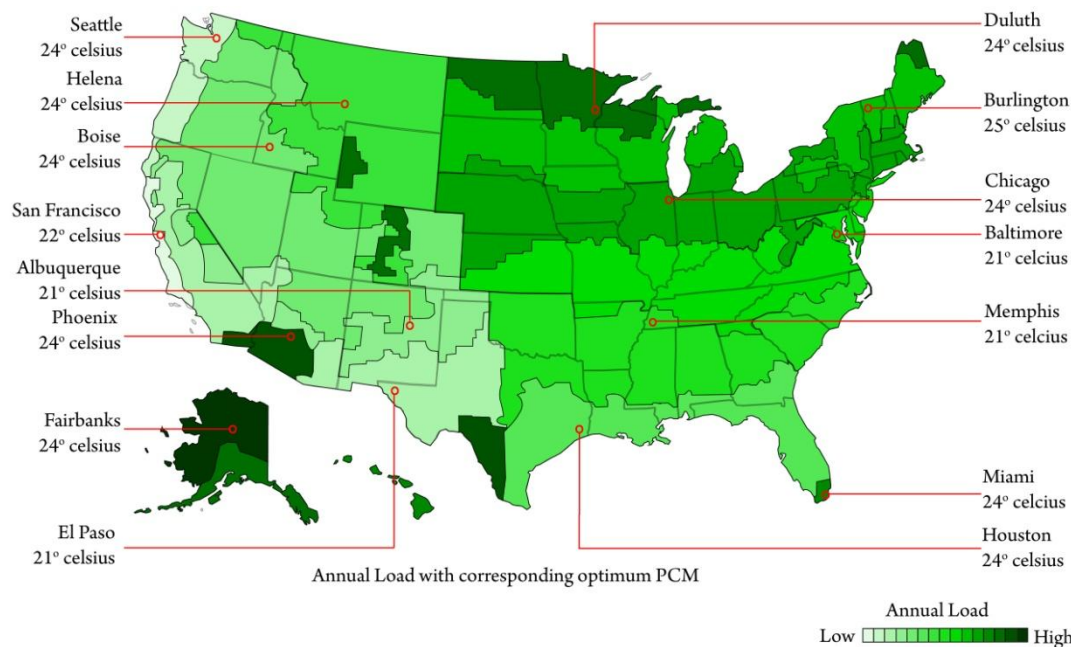


Figure 4.2: Analytical map for the annual load (magnitude) with the optimum PCM melting temperature for each climate.

The optimum melting temperature and enthalpy were determined for each climate by selecting the corresponding lowest annual load. The results show that the annual load for every climate was the smallest for when the PCM board possessed the largest storage capacity. The

PCM boards in this particular study were set to take four different heat storage capacity values (i.e. 20, 40, 60, 80 kJ/kg) and the optimum energy savings was obtained by the PCM board with 80 kJ/kg enthalpy for all the climates. The gradual increase in energy saved every increase in enthalpy is analyzed later in the main study.

In terms of the optimum melting temperature, it can be seen in Figure 4.2 that the melting temperatures vary by climate. Due to this variability in optimum melting temperature a causal relationship between the heating degree days (HDD) and cooling degree days (CDD) and the optimum PCM melting temperature cannot be conclusively drawn. The heating and cooling set-point temperatures along with the HVAC schedule can be an important determining factor for the selection of the optimum melting temperature of the PCM. The HVAC system in this particular research was set to be available 24 hours a day and all year round. The heating and cooling set-point temperatures were set to 21°C and 25°C respectively. The principle of free-cooling of PCM that can provide cold storage and also naturally ‘charge’ PCM through night ventilation was not applied for this study. The application of the PCM free-cooling principle can further help alleviate the stress on the HVAC systems by providing cold storage through night ventilation, as well as help ‘discharge’ the PCM for use the next day. Similarly different HVAC schedules can also provide for energy efficient management of indoor thermal conditions. The effect of these parameters on the optimum melting temperature will be presented and discussed in the main study.

Percent savings in energy

The magnitude in savings in energy was determined once the optimum melting temperature and enthalpy for each climate zone was obtained. It can be seen in Figure 4.3 that the maximum percent in savings was obtained for climate zone 4c (San Francisco, California). It

should also be noted that the percent savings in energy (51.91%) for San Francisco is very high due to the fact that the annual load without PCM is very low compared to other climate zones to begin with. Since PCM was applied, the percent decrease in annual load came to be 51.91% compared to an already relatively low annual load compared to the other climates.

It is also clear that the highest percent savings occurs in the dry and marine climates. Within the subset of dry and marine climates, the PCM technology performs better in the warmer climates. The diurnal temperature fluctuates to a greater extent in the dry climates than in similar humid climates. It is not uncommon for the ambient air to cool significantly during the night in the dry climates and thereby cooling (discharging) the PCM boards for use the next day. Since the PCM is cooled by this drop in ambient temperature there is no need for the HVAC to expend extra energy in these dry climates to ‘discharge’ the PCM. It is possible that the effect of free-cooling and cold storage will improve the percent energy savings in the colder climates.

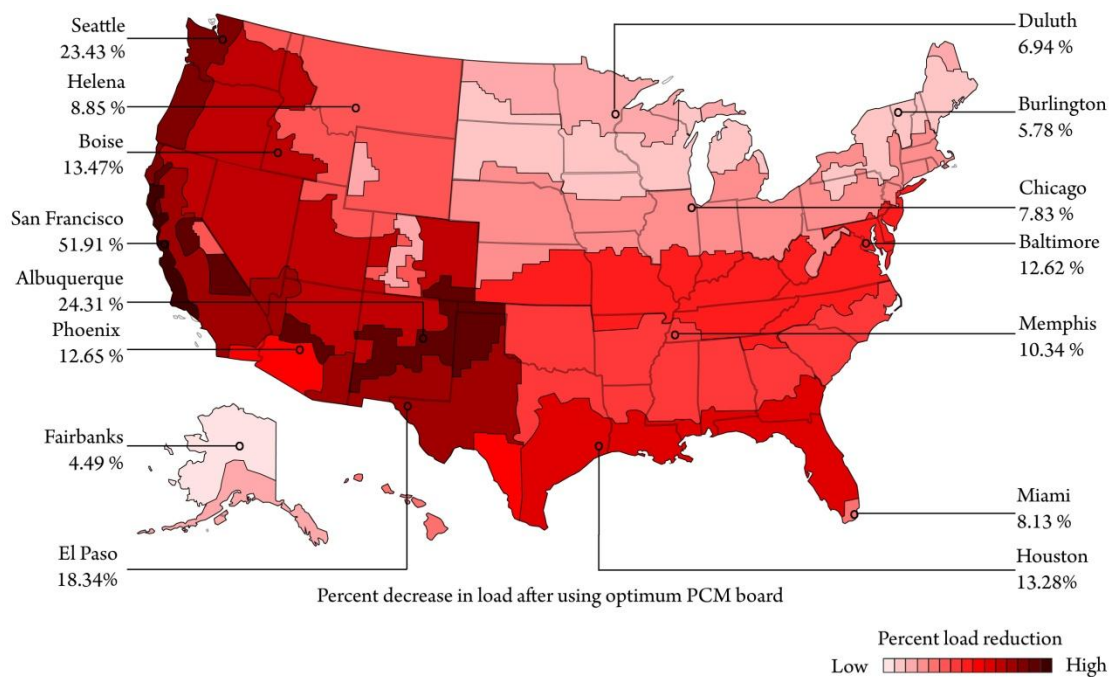


Figure 4.3: Analytical map of the energy savings in magnitude by using the optimum PCM in each climate zone.

A sensitivity analysis on the optimum temperature was also performed in order to provide an understanding of the magnitude of loss in percent savings if optimum temperatures of 1 degree higher or 1 degree lower is to be chosen.

In Figure 4.4 **Error! Reference source not found.**, PCM boards melting at 21°C offers the most in energy savings for Albuquerque. If however the designer chooses to select a PCM melting temperature of 20°C then there is a loss of 20% in energy savings. A similar trend can be seen for the other climates as well. It is crucial to choose the optimum melting temperature to obtain the maximum benefits of using PCM boards.

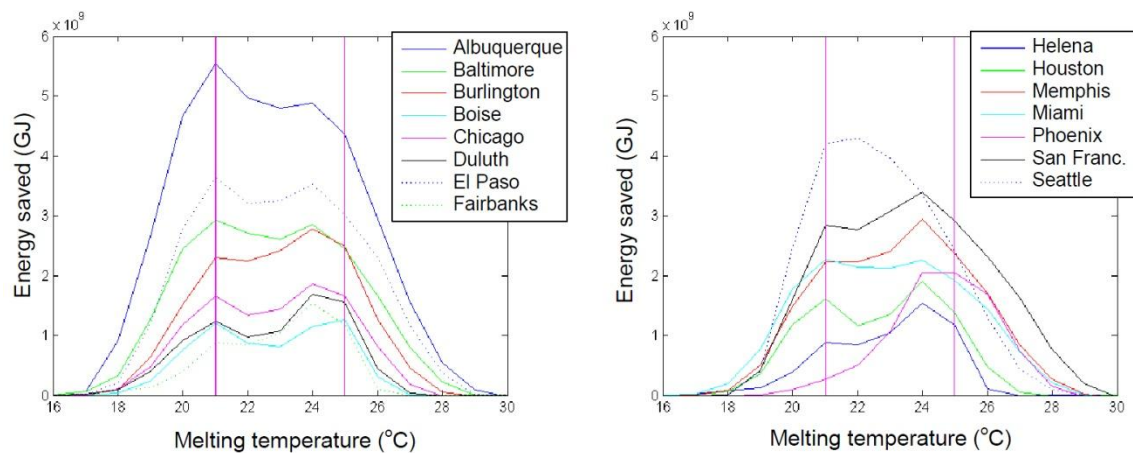


Figure 4.4: Energy saved as function of PCM’s melting temperature for the 15 climates (setpoint temperatures: 21°C and 25°C)

Additionally it can also be seen that the optimum melting temperature hovers in and around the heating and cooling set-point temperatures, hence the double peaks. There is no distinct pattern in the results to suggest a direct correlation between the set-point temperatures and the optimum melting temperature. Clear guidelines for the selection of optimum melting temperature based solely on the set-point temperatures are not feasible. Therefore for the main study, two common set-point schedules will be chosen to address this issue.

Pseudo payback period

A 'pseudo' payback period (PPP) is determined for the use of the PCM boards for each climate. The cost of commercially available PCM boards varies on the basis of melting temperature, heat storage capacity from each manufacturer. In order to evaluate the PPP of the optimum PCM boards for every climate type, a wider range of costs were incorporated into the calculation. The cost of PCM board was therefore set to vary from \$1/kg to \$3/kg. Similarly every state has a different electricity tariff. In order to encompass a wider range of tariffs the cost of electricity was also set to vary from \$0.07/kWh to \$0.18/kWh. In the PPP calculations the time value of money, the savings accrued due to the downsizing of HVAC equipment, reduction in construction costs, and the lower interest rates provided by the energy efficient mortgage (EEM) and other federal subsidies for the investment in energy efficient homes are ignored.

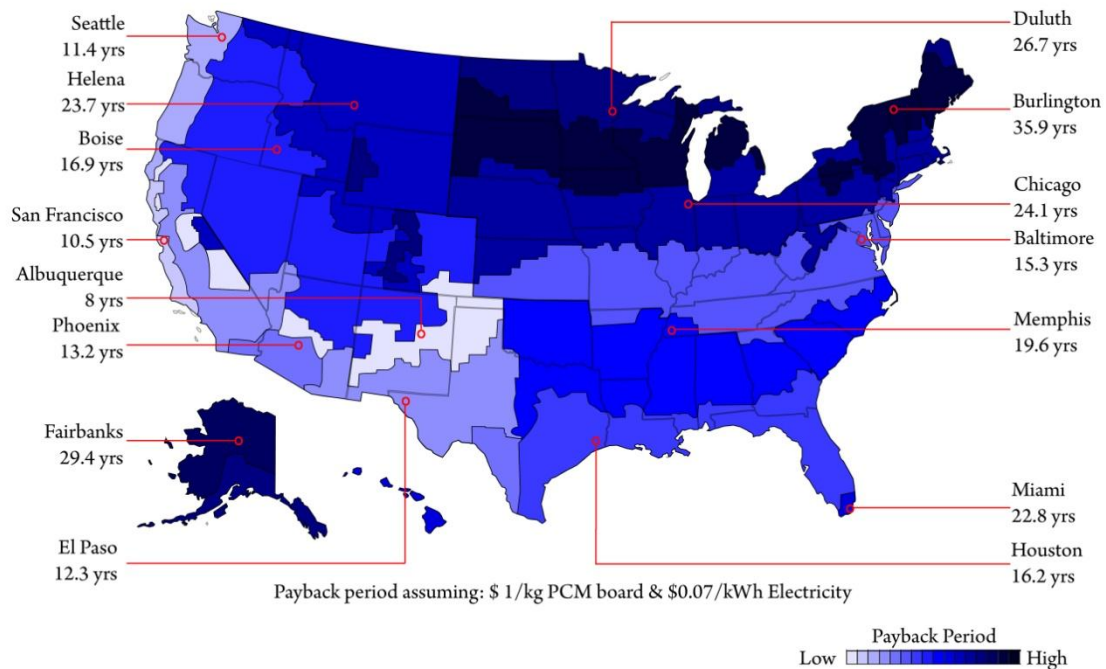


Figure 4.5: Analytical map of the pseudo payback period assuming a \$1/kg cost of PCM board & \$0.07/kWh cost of electricity.

It is evident from Figure 4.5 that the lowest PPP is for the climate zone 3b represented by Albuquerque, which is a mild and dry climate. Even though the highest percentage savings in energy was seen for climate zone 4c represented by San Francisco, climate zone 3b fares better in terms of the economic payback period. Similarly while climate zone 2a represented by Houston, exhibited a slightly higher percentage savings in energy than climate zone 2b represented by Phoenix, zone 2b is better in terms of the number of years to payback the initial investment in PCM boards. Again it can be seen that PCM boards perform best in the warm, dry and marine climates as opposed to cold and humid climates.

The PPPs were plotted against the cost of PCM and electricity (Figure 4.6(a)). In addition, the required costs of PCM and electricity to achieve a PPP period of 10, 20 and 30 years were obtained for each climate (Figure 4.6(b) shows the case of Albuquerque).

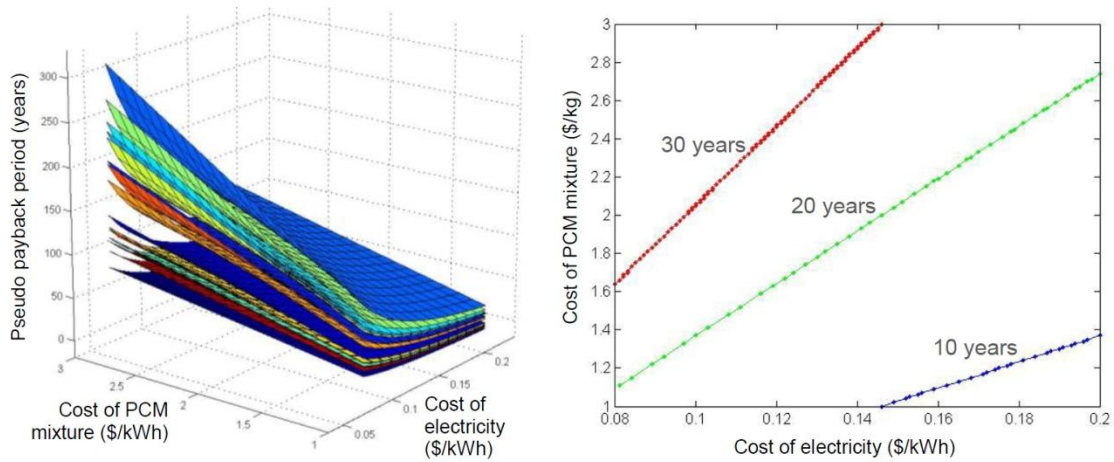


Figure 4.6: (a) Pseudo payback period as function of cost of PCM mixture and cost of electricity for all 15 climates and (b) Cost of PCM and electricity needed to achieve a PPP of 10, 20 and 30 years in Albuquerque.

The PPP of all the 15 climates can be visualized in Figure 4.6 (a). The PPP is influenced by a greater degree by the cost of PCM due to the greater slope. The cold and humid climates exhibited a PPP far greater than the warm and dry climates. The plot in Figure 4.6 (b) shows the optimum cost of PCM and electricity for Albuquerque. If a PPP of 10 years is desired for

Albuquerque then any combination of cost of PCM and cost of electricity on the blue line will achieve that.

Conclusion

In this particular study, building energy performance simulations were performed for a simple building fitted with PCM boards on all interior surfaces except the floor. The simulations were carried out for the 15 different climate types as defined by the U.S. Department of Energy. The application of PCM wallboards in those buildings shows significant benefits in terms of annual energy savings.

1. The PCM boards seemed to perform best in hot, dry and marine climates. The diurnal fluctuation of ambient temperature in the hot and dry climates as well as the mild marine climates can be attributed to the better performance of PCMs. The dry and marine climates exhibit a larger diurnal temperature fluctuation that helps facilitate the night-time purging of heat from the PCM boards. In addition, the PCM boards perform worse in humid than dry climates because of the added requirement of the HVAC and PCM boards to dehumidify the indoor environment as well.
2. The PCM boards did not perform well in the cold and humid climates. This can probably be improved by allowing free-cooling during the night. In addition, different set point schedules for the HVAC, different occupancy schedules as well as different night ventilation schemes should be included in the main study in order to optimize the performance of PCM boards in such climates.
3. The 'pseudo' payback period of the use of PCM boards were comparatively very high. For the PCM boards to be economically viable, the cost needs to be close to \$1/kg and have a higher heat storage capacity. The effect of the time value of money, the savings

accrued due to the downsizing of HVAC equipment, reduction in construction costs, and the lower interest rates provided by the energy efficient mortgage (EEM) and other federal subsidies for the investment in energy efficient homes need to be applied as well in order to conclusively determine the economic viability of PCM wall boards in the US climates.

4. The sensitivity study shows that the optimum temperature is an important factor in determining the energy saving potential of the PCM board. A slight divergence from the optimum temperatures for each climate can reduce the energy saving potential by 5-10 percent.

The present study is an attempt to assess theoretically the energy performance of PCM boards on all climates in the United States and represent the information in a visual manner. The climate maps allow for any designer to quickly gauge, in terms of return on investment, the different PCMs viable for each climate. The climate maps are more illustrative rather than exhaustive, given the infinite different possibilities of how buildings are made. To address this issue, starting with a simple building model the main study will gradually add more variables to the simulations and register the changes assessed. Later, regression models will be developed and can be linked to the climate map allowing for designers to only insert the values of different input variables of which the results can then be instantaneously represented in the climate maps.

Chapter Five

PAYBACK PERIOD

Introduction

The economic analysis presented in this report is exclusively for PCM enhanced gypsum boards. In order to compute a simple payback period when using PCM boards, it was necessary to first find the cost of either the types of PCM or the cost of the PCM boards itself. During this search process it was found that the cost of PCM boards and the cost of PCMs were very disparate and hard to locate. Of the handful of manufacturers in the US, none had any pricing listed on their websites. They only provided technical specifications of the PCM boards. Even if the cost of pure PCM could be obtained from chemical companies, the costs of encapsulating them along with the cost of production of PCM boards were not readily available. This lack of a uniform cost standard of PCMs was further exacerbated by the fact that the PCMs considered for building applications differed in price on whether they were organic or inorganic PCMs. Furthermore, the disparate units used to explain the cost and thermal performance of PCM products made it impossible to make a sound comparison of products. For example, according to Kosny et al. (2013), the current cost of paraffin wax is \$0.85–\$0.91/lb (\$1.88–\$2.00/kg) and another low-cost paraffin alternative available is Baker Petrolite's POLYWAX, which costs \$ 2.00/gal (\$ 0.53/Liter). Here, one of the costs of paraffin is listed in terms of weight while the other is listed in terms of its volume without any information on the density of each product. Similarly, National Gypsum sells PCM boards by the name of Thermalcore PCM panel¹ which

¹ See <http://www.thermalcore.info/product-info.htm> for more information.

melts at 23°C and exhibits a latent heat storage capacity of 22Btu/ft² (250 kJ/m²). Eco building boards on the other hand sells PCM clay boards² that have a phase transition temperatures of 23°C and 25°C and exhibit a latent heat storage capacity of 110 Wh/m² (396 kJ/m²). Both of which express heat storage capacity in different units for power and for the cross sectional area.

A quick literature review suggested that the cost of PCMs depend on three key parameters. The first of which is that the cost depends on the classification of PCMs i.e., Organic, Inorganic, or Eutectic. The second parameter is the cost of encapsulation of the PCM. The two main approaches, whether it is macro-encapsulation or micro-encapsulation, can add to the cost of the PCM (Mehling, 2008). The cost to macro-encapsulate a PCM is nearly 20% of the total cost. The micro-encapsulation process is even more expensive at around 50% of the final product cost (Kosny et. al, 2013). The third parameter is the market demand and supply relationships that drive the cost of the PCM products. According to Kosny et al. (2013), today's U.S market for PCMs is not fully developed which results in their relatively higher prices. The market potential for building energy efficiency is significant and because manufacturers base their prices on future market expectations, prices are likely to drop in the future. There is a possibility of a fourth parameter, which is the volumetric latent heat storage capacity of the PCM itself, which in turn may also decide the market adoption of PCMs as a building energy efficiency material. However, no information was found on whether there was a price increase or decrease for PCM products on the basis of how high or low of a volumetric latent heat storage capacity i.e. enthalpy possessed by the PCM. The cost of a Thermalcore Panel is \$288 for a 4' by 12' sheet³. The cost of a 4' by 12' regular gypsum board panel on the other hand is \$13.44. While the PCM board sells for \$6/ft²,

² See <http://ecobuildingboards.weebly.com/pcm-board.html> for more information.

³ Private communication with Todd Brawley, National Gypsum.

the regular gypsum board panel in comparison costs a mere \$0.28/ft². The question still persists as to whether the difference in cost (i.e., \$6/ft² versus \$0.28/ft²) is due to the cost of PCM in the Thermalcore panel or is it the cost added by the manufacturing process. For this study, the cost of PCM boards is assumed to be \$0.50/ft² in order to identify the climates where PCM boards will be a viable option if it were to cost that much. The payback period is then calculated for all the climates based on their average retail price of electricity based on the end use sector, commercial or residential denoted by C* and R* in Table 5.1.

CLIMATE	CITY	HDD/65	CDD/65	Cents/Kwh_C*	Cents/Kwh_R*
1a	Miami, FL	130	4458	9.48	11.65
2a	Houston, TX	1414	3001	7.83	11.33
2b	Phoenix, AZ	941	4557	10.48	12.22
3a	Memphis, TN	2935	2214	9.98	9.89
3b	El Paso, TX	2466	2314	7.83	11.33
3c	San Fran, CA	2708	142	16.14	17.09
4a	Baltimore, MD	4567	1228	11.1	13.92
4b	Albu, NM	4069	1348	9.86	11.99
4c	Seattle, WA	4729	177	7.71	8.97
5a	Chicago, IL	6311	842	7.72	9.74
5b	Boise, ID	5658	890	7.6	9.52
6a	Burl, VT	7406	496	14.64	17.29
6b	Helena, MT	8031	386	9.71	11.07
7a	Duluth, MN	9425	209	10.02	12.59
8a	Fairbanks, AK	13528	71	15.58	18.49

Table 5.1: The cost of electricity per kWh in each city. (U.S. EIA, 2013).

Energy saving and payback period constraint

The performances of PCM boards were also compared to the thermal performance of increasing the R-value of the thermal insulation alone. Conventional thermal insulations are the most popular and widely accepted means to improve the thermal performance of building envelopes. Each building model for the simulations is fitted with insulation levels recommended

in the ASHRAE 90.1 standard. So how does the energy performance of PCM board fare against only increasing the R-value of the insulation of the roof and walls by multiples of 1.25 (Medium) and 1.5 (High)? Or in other words, would it be prudent to just increase the R-value of insulation by a factor of 1.25 or 1.5 instead of making a separate investment in PCM boards in the beginning? In order to better answer this question, four different envelopes were simulated for all the combinations of individual variables for all the climates.

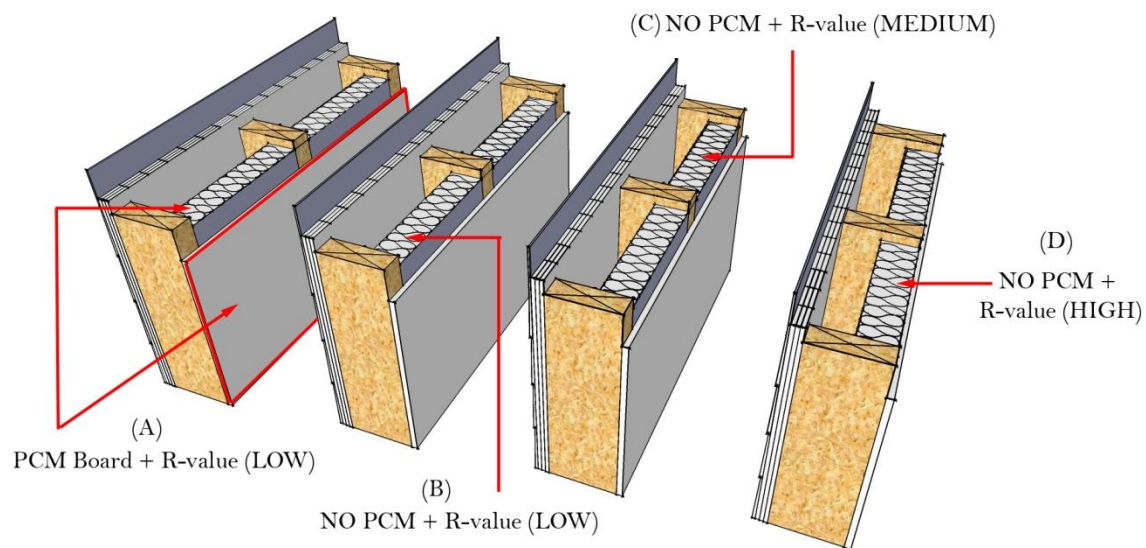


Figure 5.1: The four cases simulated to assess the performance of PCM boards against different R-value of insulation.

Figure 5.1 shows the four cases simulated where case A is the wall and roof equipped with PCM boards with a latent heat storage capacity of 100 kJ/kg and also with the minimum, climate specific, prescribed insulation as recommended in the ASHRAE standard. Case B is the situation where there still is the minimum prescribed R-value for the insulation but no PCM board. Case C is the situation where the R-value of the insulation is increased to 1.25 times the prescribed value. Case D is the situation where the R-value of the insulation is increased to 1.5 times the prescribed value. Case C and D both do not have any PCM boards. The annual loads for each of the cases were obtained from each simulation. The annual loads for the cases A, C and D

were compared against case B in order to gauge the amount of energy saved by employing each technology.

Case B - Case A	Energy saved by the use of PCM boards.
Case B - Case C	Energy saved by increasing the R-value from Low to Medium.
Case B - Case D	Energy saved by increasing the R-value from Low to High.

Table 5.2: The difference in annual load between the cases.

Based on the results, two constraints were applied to justify the use of PCM boards in each climate. The first constraint being that the application of PCM should at least perform better than, in terms of magnitude of energy saved, when the R-value is increased to a multiple of 1.25 i.e. medium. The magnitude of energy saved is chosen as opposed to the percent energy saved for the reason that the magnitude of energy saved translates directly to money saved while the percent energy saved does not. When this first criterion is satisfied then the energy saved by each case is converted to a dollar value on the basis of the cost of electricity for each location as listed in Table 5.1. Then the second constraint was introduced to filter the results further. The second constraint for the PCM boards to pass was for the payback period to fall below 75 years. The current price of PCM boards is around \$6/ft² and the payback period is calculated on the assumption that the initial investment for the PCM boards is made at a cost of \$6/ft². Once the climates are filtered on the basis of the two constraints, the initial cost of the PCM boards is allowed to further decrease to a value of \$0.5/ft², \$0.20 more per square foot than a conventional gypsum board. This was done to understand how feasible PCM boards would be if the cost were to drop substantially to a cost of \$0.50/ft². If the PCM board payback period does not fall below 15 years even for this 'reduced' price it would seem highly unlikely for the PCM boards to be economically viable for these climates. The results for the case when PCM boards cost \$0.5/ft² can be found in Appendix A.

PCM - R-value comparison

Firstly the results for the office HVAC schedule were analyzed. It was found that for all the climates except for climate 1 (Miami) and climate 8 (Fairbanks) the magnitude of energy saved was greater with the PCM (Case A) as opposed to using an insulation R-value 1.25 times that of the prescribed value (Case C). In terms of the magnitude of energy saved alone, it seems beneficial to apply PCM boards in all the climates except for Miami and Fairbanks for an office HVAC schedule. All the corresponding plots can be found in appendix B. Similarly the results for the residential HVAC schedule were analyzed. It was found that the only climates where Case A saved more energy than Case C was for climate 3c (San Francisco) and climate 4c (Seattle). PCM boards were working very well in the marine climates, including climate 4b (Albuquerque) but only for the office HVAC schedule. The Figures 5.2 and 5.3 depict the energy saving potential of PCM boards in San Francisco. For the San Francisco office schedule, it can be seen in Figure 5.2, that using PCM that melts at a temperature of 24°C saved approximately 7.5 gigajoules of energy (67% of 11.49 gigajoules) for when the building had an internal load of 1800 watts i.e. 15 people * 120 watts/person = 1800 watts.

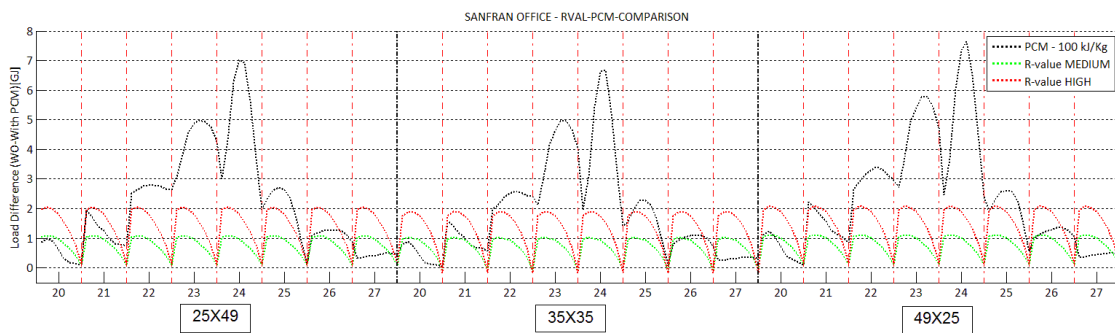


Figure 5.2: San Francisco - office HVAC - R-value, PCM comparison.

This can be seen in the plot, in the column labeled '24' for 24°C. The curve for the PCM board reaches peak (changes slope) approximately at the center of this column. The independent

variable hidden in this column is that of the number of people which increases from 5 till 24 along the width of the column. There is a sharp drop in energy savings as the number of people is increased for the PCM melting at 24°C. On the other hand in the column for melting temperature 23°C the energy savings does not drop as fast as for the case when PCM melted at 24°C. Even though the magnitude of energy saved is not as high (approximately 5 gigajoules) as when the PCM melted at 24°C, it does not seem to drop in magnitude with the increase in internal loads. The same trend was found for many of the other plots except for Albuquerque where the greatest amount of energy is saved when the internal load increases. This is evident in Figure 5.4 for the PCM phase transition temperature of 23°C.

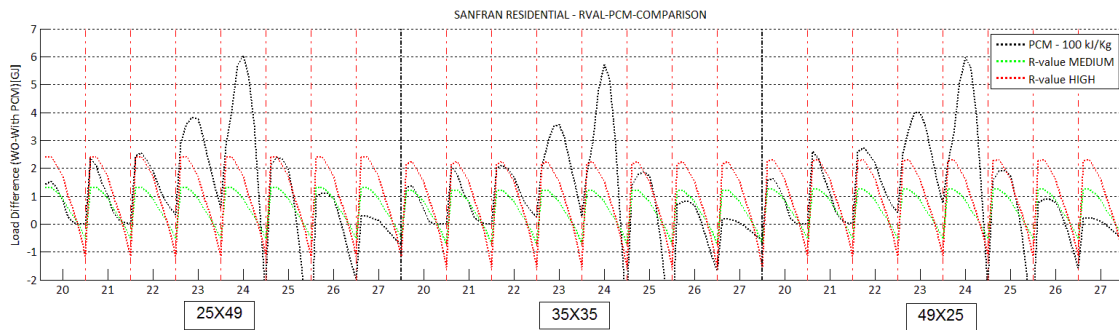


Figure 5.3: San Francisco - residential HVAC - R-value, PCM comparison.

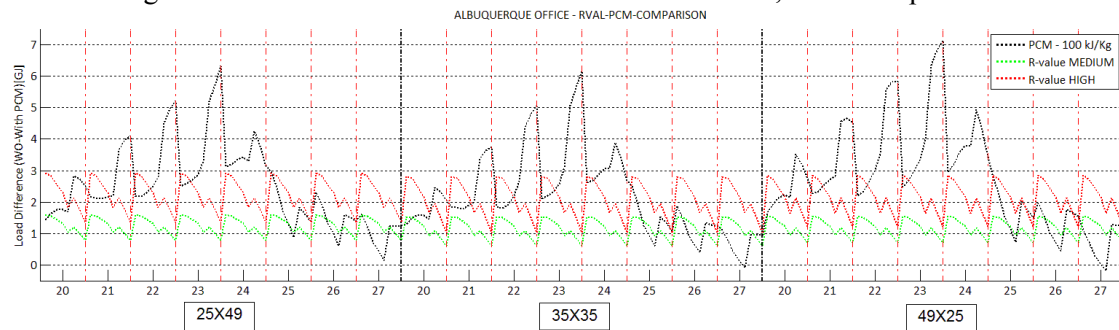


Figure 5.4: Albuquerque - office HVAC - R-value, PCM comparison.

A closer inspection of Figure 5.4 reveals that when the internal loads it at its least, at 600 watts (5 people); PCM melting at 24°C seems to work better. As soon as the internal load is increased the magnitude of energy saved by employing PCM melting at 23°C increases

dramatically. In the case of Seattle, the maximum amount of energy saved is around 4 gigajoules at the 24°C melting point. The optimum melting temperature changes to 23°C as soon as the internal load increases.

The increase in internal loads seems to determine the optimum melting temperature of the PCM for a specific climate, also evident for both the Seattle plots in Figure 5.5 and 5.6. At first glance it seems like the PCM melting at 24°C offers the best energy management. Upon closer look it is clear that the energy mitigating potential of PCM melting at 24°C decreases significantly with the increase in internal loads. The PCM melting at 23°C, in this case, performs much better. The effect of people along with the other independent variables on the performance of PCM boards is discussed later in this chapter.

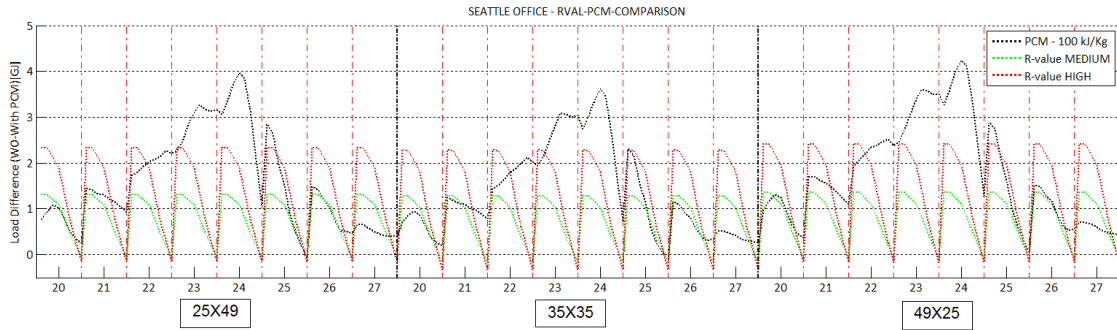


Figure 5.5: Seattle - office HVAC - R-value, PCM Comparison.

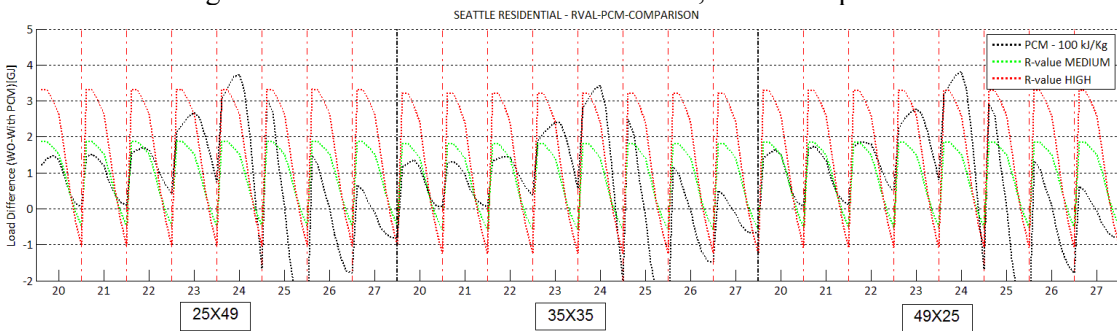


Figure 5.6: Seattle - residential HVAC - R-value, PCM comparison.

Once the difference in magnitude for each case of PCM was observed the second set of constraints were applied to the results. The payback period for all the climates using the fee

structure for one kWh of energy (table 5.1) was computed. There were only a handful of situations where the payback period fell below 75 years.

Payback period

Only a handful of scenarios passed the second constraint where the payback period would fall below the 75 year mark. One of the scenario was that of the San Francisco Office and Residential HVAC schedule. In Figure 5.7, in the top plot, the magnitude of energy saved in the particular cases (Case A, B and C) is converted to a monetary value on the basis of the cost per kWh of electricity. The initial investment cost for PCM boards is obtained by multiplying the cost of PCM boards (i.e., \$6/ft²) with the total surface area of PCM boards in the building. The cost of PCM as the initial investment is then divided by the money saved annually, case by case, to obtain the payback period in the bar plot (below). In the bar plot in Figure 5.7 and 5.8, there are bars missing. Any payback period over 200 years was automatically assigned a value of 0 which denotes the empty bars. The individual bars within each column of melting temperature correspond to the number of people ranging from 5 (all the way in the left) to 24 (all the way to the right). For the office HVAC schedule, both PCMs melting at 23°C and 24°C in climate 4C (San Francisco) exhibit a payback period less than 50 years. The case with the residential HVAC is a little different in the sense that for the maximum internal load of 2880 watts (i.e., 24 people X 120 watts/person = 2880 watts) the payback period bar for melting temperature 24°C is missing on all three building aspect ratios. In addition, the two other aspect ratios of 25'X49' and 35'X35' has a payback period greater than 50 years for the internal load of 2520 watts (i.e., 21 people X 120 watts/person = 2520 watts) as well. For these cases, the PCM melting temperature of 23°C performs better.

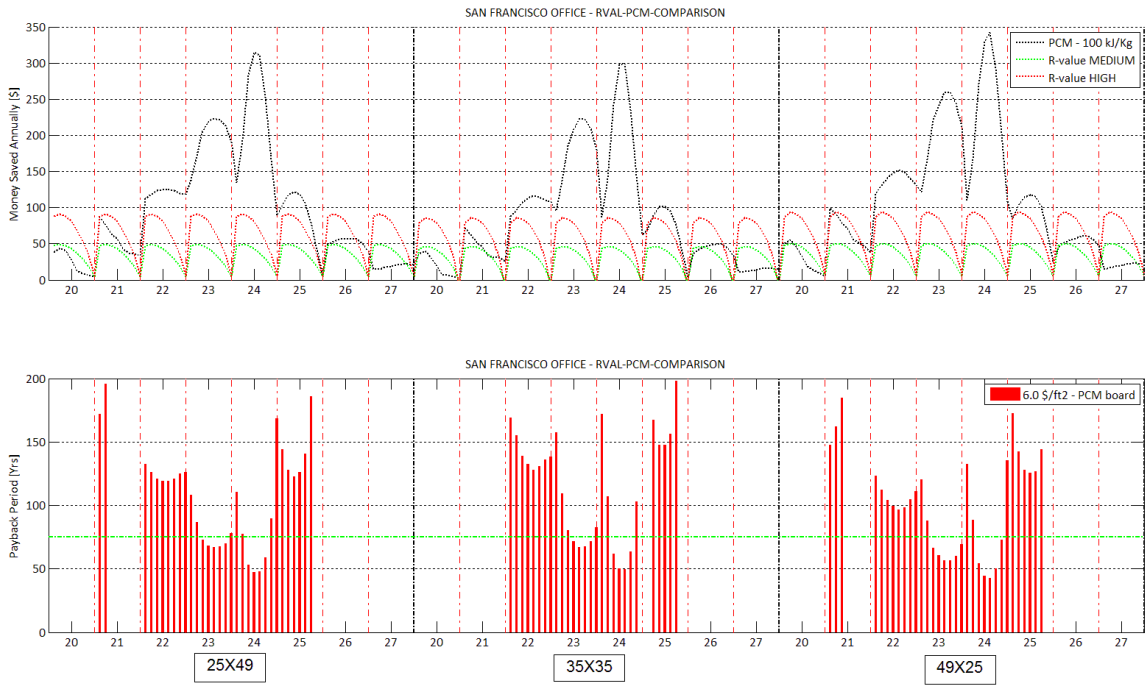


Figure 5.7: San Francisco - office HVAC - money saved annually (Top) and payback period (bottom).

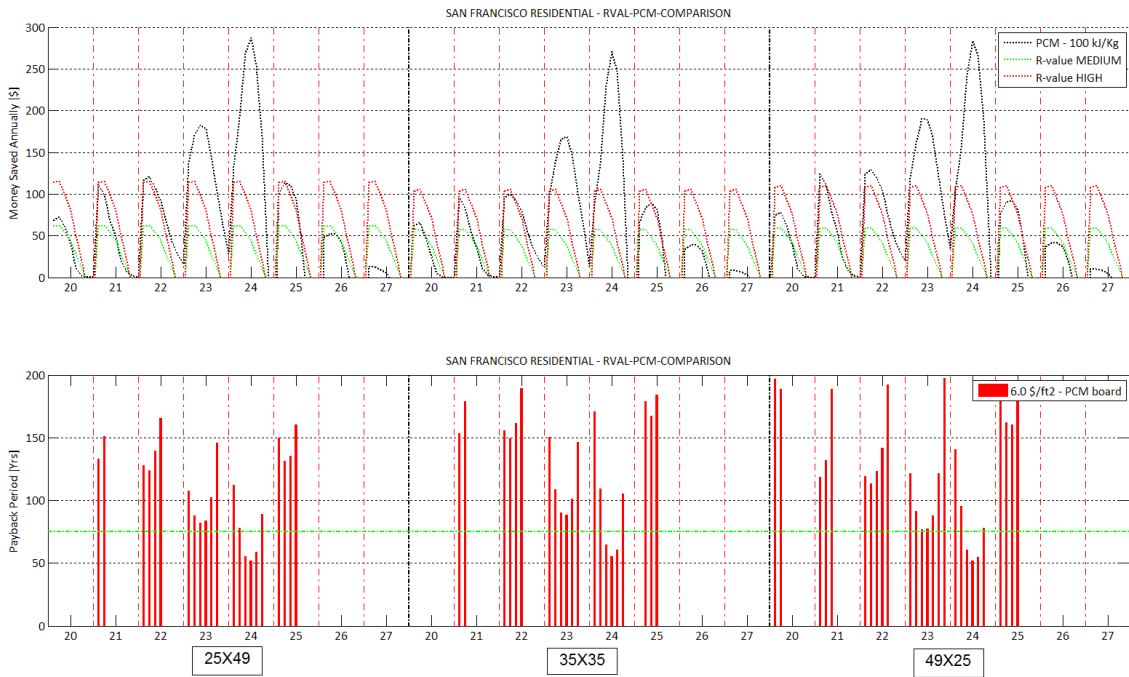


Figure 5.8: San Francisco - residential HVAC - money saved annually (Top) and payback period (bottom).

Seattle on the other hand, as seen in figure 5.9, does not meet the second criteria of having a payback period less than 75 years, owing to the fact that one kWh of electricity costs \$0.077 for commercial end use and \$0.089 for residential end use cases in Seattle. The payback period would gradually shift below 75 years if the cost of energy would be higher than what it is today.

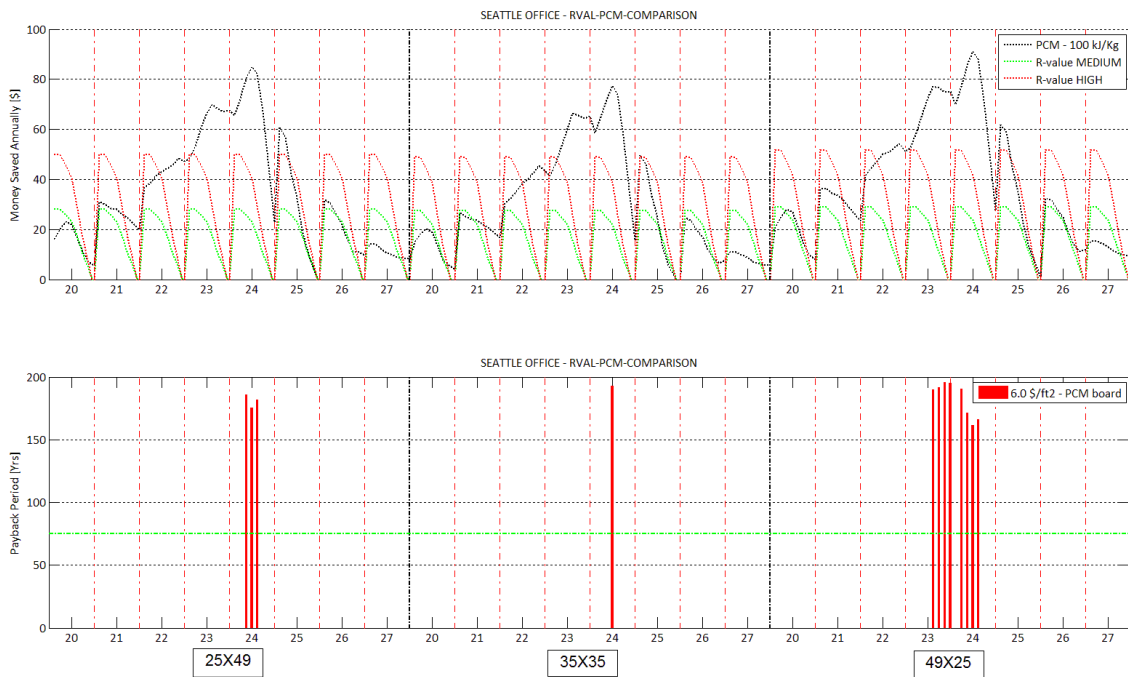


Figure 5.9: Seattle - office HVAC - money saved annually (Top) and payback period (bottom).

Obviously a decrease in the cost of PCM boards, lower than \$6/ft² would also decrease the payback period to less than the 75 year mark. Albuquerque, residential HVAC schedules does not meet the second criteria but the office HVAC does meet the 75 year payback period for medium to high internal loads, evident in Figure 5.10. San Francisco Office and Residential HVAC as well as Albuquerque Office HVAC were the only scenarios that successfully passed the two initial criteria (i.e., greater savings in energy as compared to an increased insulation R-value and the payback period to fall below 75 years).

At the 23°C melting temperature, the payback period for Albuquerque - Office decreases as the internal load increases as shown in Figure 5.10.

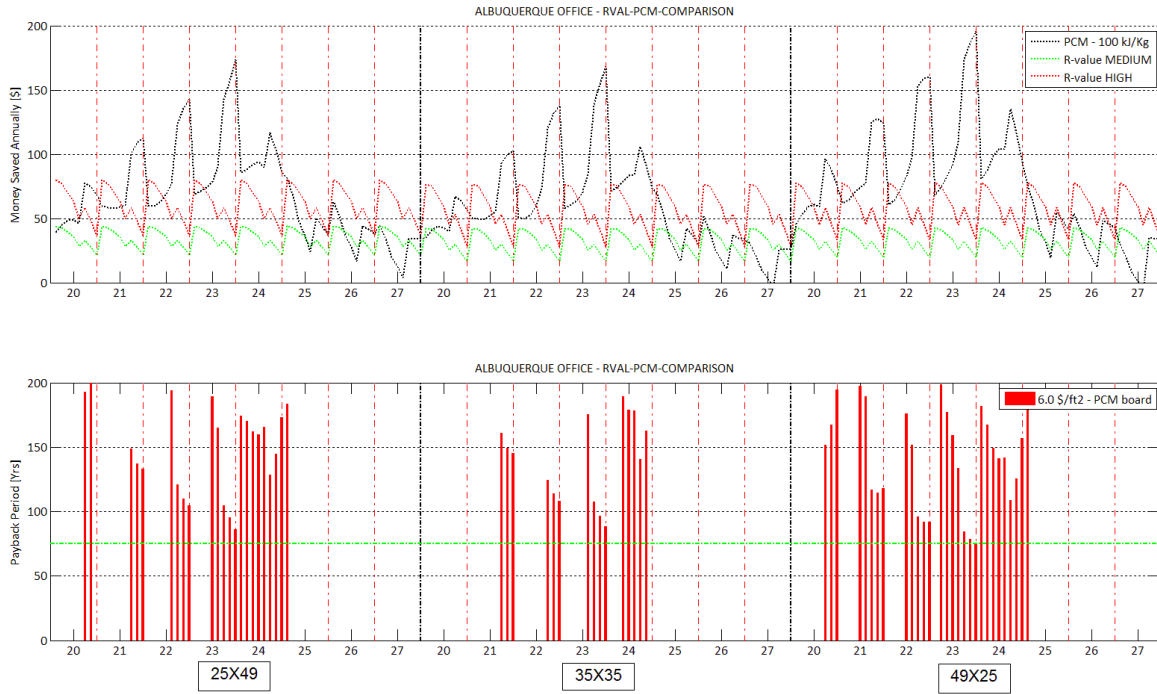


Figure 5.10: Albuquerque - office HVAC - money saved annually (Top) and payback period (bottom).

When the PCM boards were assumed to cost \$ 6.0/ft², only three scenarios (i.e., San Francisco Office + Residential HVAC, Albuquerque Office HVAC) passed the imposed payback period limit of 75 years. The question that immediately followed was that, what if the price of PCM boards were to be comparable yet not quite as cheap as regular gypsum boards? The results for when the PCM boards took an assumed cost of \$ 0.5/ft² are available in Appendix A.

Chapter Six

HVAC SETPOINT SCHEDULE AND LOCATION OF PCM

One of the parameters such as the set-point temperature, set-back temperature and schedules for the HVAC system can be an important factor in obtaining the most energy savings in buildings with PCMs. As the building absorbs ambient energy and begins to heat or cool, the time when the HVAC starts operating and the moment when the PCM starts to absorb the energy can play a crucial role in the amount of energy saved versus the amount of energy used in buildings. So far the only HVAC set-point schedule studied in this report has been the one where heating and cooling is provided all year round to maintain 21°C and 25°C respectively. In this chapter, the effect of three different HVAC schedules and set-point temperatures are tested against the placement of PCM on different surfaces on the building. In addition the application of three different HVAC schedules and the application of PCM with 5 different phase change temperatures (i.e., melting temperatures) were also tested parametrically for the climate zone 4B as defined by the U.S Department of Energy. In particular the annual energy consumption is determined for Albuquerque, New Mexico which was the climate that exhibited the largest magnitude in energy savings from last chapter.

As evident from the literature review, over the years studies have been conducted, especially for passive solar designs, to determine the energy saving potential in buildings by manipulating a few parameters at time. One such parameter is the HVAC set-point temperature schedule. The heating or cooling demand needing to be met by the HVAC system is conveyed by a thermostat present in the space to be conditioned. The thermostat as a primary control strategy signals the HVAC system to condition the space to a prescribed set-point temperature or a schedule of set-point temperatures in order to improve occupant thermal comfort and through the

process save energy as well. Similarly thermal storage technologies such as Phase Change Materials seek to achieve occupant thermal comfort and savings in energy by storing and releasing thermal energy at a predefined prescribed temperature. While both the HVAC system and PCM's end goal is one and the same, they need to be properly coupled so one does not impede the optimum performance of the other. For example consider the indoor placement of a PCM that melts at 27°C in a room set to be cooled to 25°C. The PCM will rarely or never get a chance to 'activate' for the sole reason that the HVAC system will 'kick-in' as soon as the thermostat reads the room temperature to be above 25°C thereby never reaching an indoor temperature to allow for the PCM to absorb thermal energy. In addition, for every case, the thermostat control strategy must focus on providing a fully 'charged' PCM for energy storage during the beginning of each new day. This complexity is further exacerbated when the HVAC set-point temperatures are programmed to fluctuate based on the time of the day or the month of the year when the PCM melting temperature is constant. In the past, researchers have provided guidelines on the proper selection of the phase change temperatures of PCMs (Pieppo, 1991; Neeper, 2000; Ibanez, 2005). Some have recommended guidelines and/or shown the indoor temperature mitigating capability of PCMs in buildings equipped with and without active HVAC systems. Peippo et al. (1991) has recommended that the optimum diurnal storage can be achieved when the PCM has a phase change temperature of 1-3 degrees above the average room temperature. Similarly, Neeper (2000) performed an analytical and experimental study on selecting optimum PCM properties for a passive building. The author's recommendations for selecting a proper PCM was to select a melting temperature close to the average room temperature if the PCM is to be placed on the interior partition and a melting temperature close to 1°C below the average of the room temperature if the PCM is to be selected for the exterior wall. The author further suggested that 1°C maladjustment of the transition temperature of optimum

PCM exacts about the same storage penalty as increasing the transition width to 2°C. In a separate study, Stovall (1995) examined the possibility of improved occupant comfort and utility management by using PCM wallboards and different thermostat control strategies. Their study was based only on the combination of convective and conductive heat transfer, with no solar radiant energy to warm the surface of the storage wall since the window and door area was assumed to be opaque in their numerical simulations. They conclude that the PCM boards, under their reasonable engineering assumptions, with the proper selection of thermostat control strategies show a good return on investment for the Boston winter months (i.e., 3 yrs) but a poor performance for the Miami and Nashville summer months (i.e., 20 yrs). Chen et al. (2008) performed numerical simulations for a unit room located in Beijing, China and recommend that, for the heating season, the phase change temperature should be reasonably chosen based on the indoor air heating set-point temperature. In their study a phase transition temperature of 23°C (when the heating set-point temperature is set to 20°C) is recommended.

Similar studies can be found in literature that demonstrates the benefits of the use of PCMs in buildings. Due to the very sporadic and varying nature of such studies it is very hard to draw conclusive guidelines on the optimum selection of PCMs in buildings with different shapes and sizes, different climatic loads and different thermostat control strategies. Although the studies do depict the energy saving potential of PCMs in buildings, the varied nature of the studies makes it difficult to cross-correlate between the independent variables that affect the annual load and the energy performance of the building as well. Since the combinations of all the possible parameters that affect the energy performance of buildings with PCM are endless, this chapter seeks to study how the thermostat control strategies play a role in the selection of PCMs and the effect of placing PCMs on different surfaces of the building.

Setup

For the purpose of simulating the thermal performance of buildings with PCM placed on individual walls and different thermostat control strategies, the building energy simulation program EnergyPlus developed by the US Department of Energy (DOE) was adopted. The conduction finite difference algorithm with a time-step of 1 minute allowed for the simulation of the thermal behavior of latent heat storage technology in this study. Figure 6.1 depicts the baseline model input in EnergyPlus for the simulation of the thermal behavior of the different PCM under different thermostat set-point combinations. The building model used in this study followed the mandatory and prescriptive guidelines for the construction set by the ASHRAE 90.1 standard. The energy performance of the baseline building was simulated for the Albuquerque, New Mexico climate because of the apparent savings seen, in chapter 4, for the climate type 4b (mild, dry) in the US-DOE climate map for the United States (PNNL 2011).

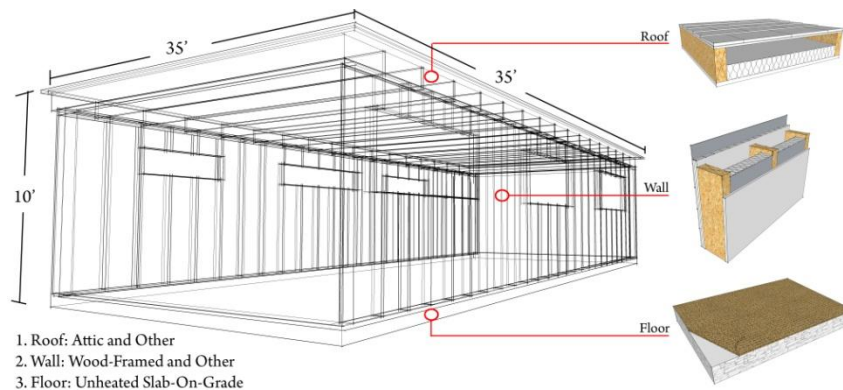


Figure 6.1: Baseline building model and construction details.

The baseline building input in EnergyPlus followed the exact prescriptive R-values, U-values and SHGC coefficients as recommended by ASHRAE 90.1 for construction in Albuquerque, NM. The construction specifics recommended in the standard were adopted for the building surface as well as the fenestration components. Each facade was modeled with three

windows with a total fenestration area per facade of 45 ft². The length to width ratio of the building was set to a ratio of 1:1 with the volumetric dimension set to 35' * 35' * 10'.

Construction	Materials [Out-In]	U-value [W/m ² -k]
Roof (R-38)	Wood Shingles Wood Decking Insulation Gypsum Board	0.055
Wall (R-13)	Wood Siding Fiberboard Sheathing Wall Insulation Gypsum Board	0.182
Floor	Concrete Slab Carpet Pad	1.082

Table 6.1: Construction details for the facade components.

The latent thermal storage properties were appended to the gypsum board by idealizing a PCM enthalpy-temperature curve for the input in EnergyPlus, as seen in Figure 6.2. Even though most PCMs follow their own specific thermal behavior defined by a more or less smooth transition region, an idealized enthalpy-temperature curve with a short transition or narrow-phase change zone was used in this study. The reason for idealizing the PCM curve was to see the behavior of buildings with latent thermal storage as opposed to a particular individual PCM. Enthalpy temperature curves obtained from manufacturers were therefore not used. In accordance with the studies performed by Darkwa (2006) and Neeper (2000), the idealized PCM with a narrow phase change zone was selected for its better performance over PCMs with wide phase change zones. The enthalpy-temperature curve in Figure 6.2 depicts the PCM that starts melting at 22.9°C and gradually absorbs 100 kJ/kg of energy at a narrow phase change zone of 0.1 degree until being fully saturated or completely melted at 23°C.

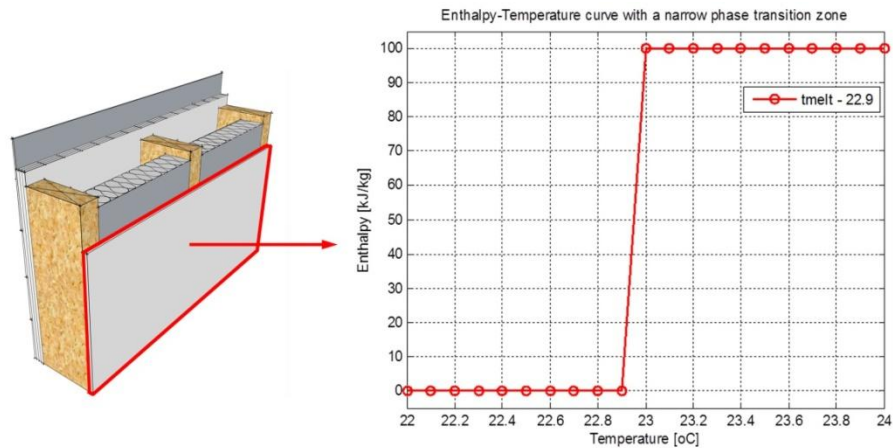


Figure 6.2: PCM properties appended to the gypsum board and the idealized enthalpy-temperature curve.

The PCM properties were then appended to the gypsum board of each wall individually. First each of the six different PCMs (i.e., 21°, 22°, 23°, 24°, 25°, 26°) were individually placed only on the interior face of the east facade and monthly heating and cooling load was collected for all the different HVAC set-point schedules. The PCM was then cycled throughout the remaining six different placement cases as seen in Figure 6.3, and the annual energy consumption was obtained for the three different HVAC set-point schedules.

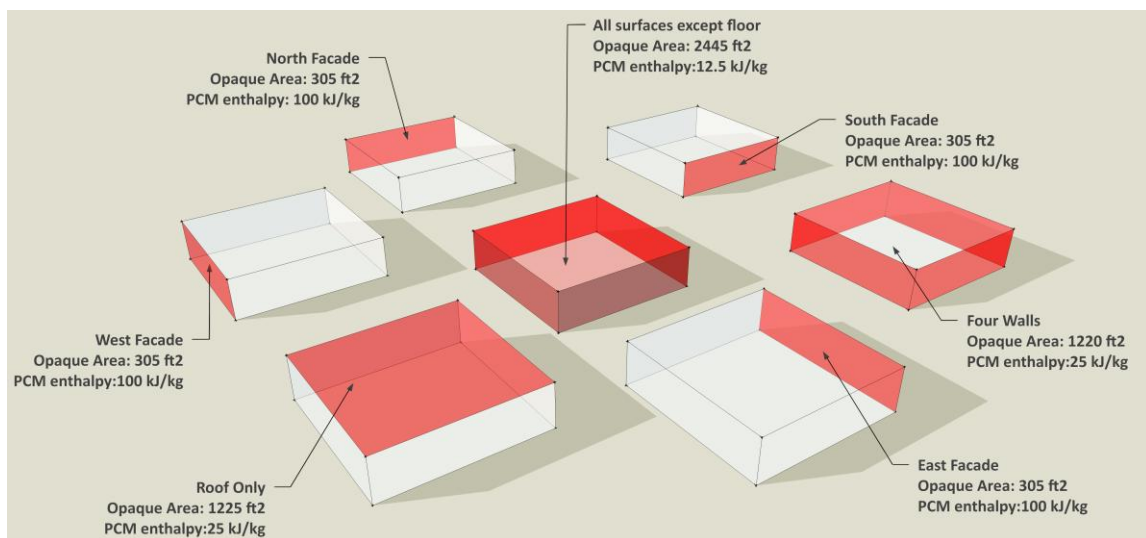


Figure 6.3: The seven different cases where the PCM was cycled through the walls.

An equivalent latent heat storage (LHS) was developed so the energy saving potential after placing PCM on different surfaces could be quantified. The latent heat storage capacity of PCM was normalized based on the opaque area of the surface to which the PCM properties were appended to in order to compensate for the difference in heat storage capacities for the different areas of opaque walls. For example, an equivalent Latent heat storage is computed for the case when PCM is placed on more than one surface due to the fact that a larger wall can place more PCM on it and thus have a higher latent heat storage capacity, and therefore the amount of PCM is normalized for specific cases so that each will have the same magnitude of latent heat storage capacity regardless of its area. The equation below shows the methodology in computing the normalized or equivalent latent heat storage capacity for the different surfaces.

$$LHS_{EQ} = \frac{\{(A_1 - F_1)\} * LHS_{REF}}{(A_2 - F_2)}$$

where,

A_1 & A_2 = Area of surface 1 and surface 2,

F_1 & F_2 = Area of fenestration on surface 1 and on surface 2,

LHS_{REF} = Latent Heat Storage of surface A_1 [kJ/kg],

LHS_{EQ} = Normalized Latent Heat Storage of surface A_2 [kJ/kg] based on its surface area.

South Wall	LHS_{EQ} $= \frac{(305) * 100}{(2445)}$	All surfaces except floor
$A_1 = 350 \text{ ft}^2, F_1 = 45 \text{ ft}^2$		$A_2 = 2625 \text{ ft}^2, F_2 = 180 \text{ ft}^2$
$(A_1 - F_1) = 305 \text{ ft}^2$		$(A_2 - F_2) = 2445 \text{ ft}^2$
$LHS_{REF} = 100 \text{ kJ/kg}$		$LHS_{EQ} = 12.5 \text{ kJ/kg}$

Table 6.2: An example of the equivalent latent heat storage (LHS).

Since the five surfaces (all surfaces except floor) exhibit a combined opaque area of 2445 ft^2 , a PCM of only 12.5 kJ/kg enthalpy is appended to the gypsum board for the total area. Both

cases (i.e., South Wall and All surfaces except floor) now exhibit the same magnitude of total latent heat storage capacity. The same procedure was repeated for any surface that was different in area from the other surfaces. The equivalent PCM enthalpy for each corresponding surface is depicted in Figure 6.3 as well as in Table 6.2.

The HVAC set-point schedules were defined in the whole building energy simulation program, EnergyPlus. Three sets of HVAC set-point schedules were defined for the ideal loads HVAC system. The ideal loads system air system was chosen because it is the simplest piece of zone equipment in EnergyPlus which is used in situations where the performance of the building can be studied without modeling a full HVAC system. This system within EnergyPlus can add and remove heat and moisture at 100% efficiency in order to produce a supply air stream at the specified conditions (US. DOE, 2013). Figure 6.4 and Table 6.3 show the different set-point temperatures and the availability of the three different HVAC schedules selected for this study. HVAC A was set to be available every hour throughout the year in case the room required either heating or cooling based on the set-point temperatures. HVAC B was available for heating and cooling throughout the year but the heating and cooling temperatures were set-back to outside comfort levels (i.e., 15°C heating and 30°C cooling) after 6 PM till 6 AM. This mimics the set-point schedule of an office setting. Finally HVAC C was set to available throughout the year but while heating was available for the spring and winter seasons, there was no cooling. Similarly cooling was available for the summer and fall seasons but not the heating. HVAC C was set under the assumption of a residential home where individuals set their thermostats for heating during the colder months and cooling during the warmer months.

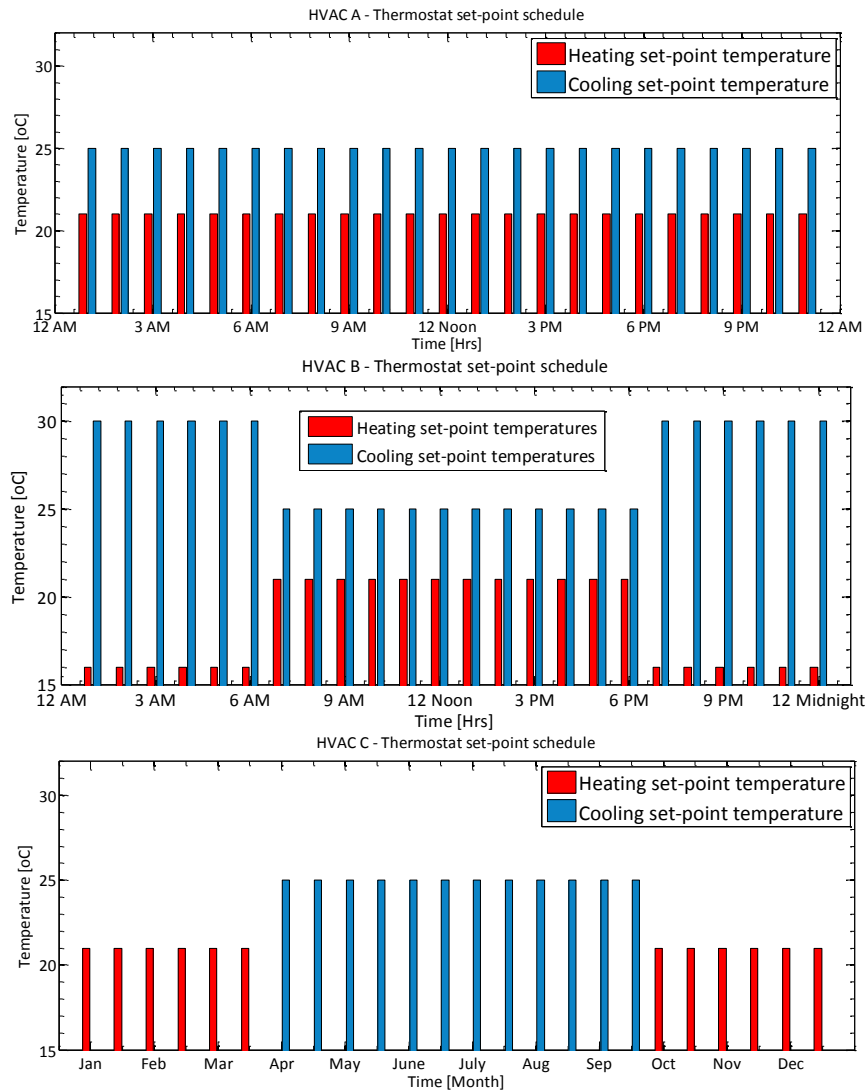


Figure 6.4: Graphical representation of the thermostat set-point schedules for HVAC A, B and C.

In terms of the internal loads, the building was set to be occupied by seven people throughout the 24 hours of the day and every day throughout the year and not in any particular predetermined schedule especially since the idea was to disassociate the analysis from any assumptions of occupant behavior. Nevertheless each person was set to dissipate 120 watts of energy (a total of 840 watts all year) into the interior environment so as to contribute towards the internal loads. The energy performance of each specific building was simulated for Albuquerque using the typical meteorological data (TMY3) weather data available from the EnergyPlus

weather repository. The requested output variables were annual cooling and heating energy as well as the nodal temperatures for each surface in order to get an understanding of the thermodynamic behavior through the wall thickness. Due to the high number of simulations required for each climate the software jEplus (Zhang 2009) was used to setup and perform multiple runs.

Results and Discussion

The results of each simulation were collected and arranged so as to capture the effects, first of the placement of PCMs on each wall surface, and then the effects of PCM melting temperature on the heating and cooling load. The heating and cooling loads for individual PCM placed on individual wall were collected for the different HVAC schedules.

Seasons	HVAC A (No setback)	HVAC B (Nighttime setback)	HVAC C
Spring	Heating – 21°C (24/7) Cooling – 25°C (24/7)	Heating – 21°C (6 AM – 6 PM) setback – 15°C Cooling – 25°C (6 AM – 6 PM) setback – 30°C	Only Heating - 21°C (24/7) No Cooling
Summer	Heating – 21°C (24/7) Cooling – 25°C (24/7)	Heating – 21°C (6 AM – 6 PM) setback – 15°C Cooling – 25°C (6 AM – 6 PM) setback – 30°C	No Heating Only Cooling - 25°C (24/7)
Fall	Heating – 21°C (24/7) Cooling – 25°C (24/7)	Heating – 21°C (6 AM – 6 PM) setback – 15°C Cooling – 25°C (6 AM – 6 PM) setback – 30°C	No Heating Only Cooling - 25°C (24/7)
Winter	Heating – 21°C (24/7) Cooling – 25°C (24/7)	Heating – 21°C (6 AM – 6 PM) setback – 15°C Cooling – 25°C (6 AM – 6 PM) setback – 30°C	Only Heating - 21°C (24/7) No Cooling

Table 6.3: Thermostat set-point temperatures and availability for HVAC A, B and C.

The reason was to see if the optimum melting temperature of PCM for this particular building was the same for all the different HVAC schedules. Once the data was collected the mean and standard deviation was obtained in two directions: one along the PCM melting temperatures and the other along the different surfaces the PCM was appended to. For example,

in the case of HVAC A, the heating and cooling loads for each month, for each melting temperature and for each surface placement were obtained. Then the mean and standard deviation of the heating, cooling and total load, along the six different melting temperatures for each month was obtained. This was done in order to understand the variability in the performance of PCM along the PCM melting temperatures. The second direction was along the different surfaces the PCM was appended to. This was done in order to understand the variability in the performance of PCM when it was placed on one surface over the other.

HVAC A

Firstly the variability of placing a PCM working under the HVAC A schedule on different surfaces was analyzed. The variability in the direction of 'placement' of PCMs, as can be seen from Table 6.4, is considerably smaller than the variability in the direction of 'PCM melt temperature' as denoted by the standard deviation in both directions. It must be noted that the variability in the direction of the 'placement' of PCMs were only analyzed for the placement of PCM on the four individual walls (East, West, North, and South). The reason for only placing PCM on individual surfaces first was because it was initially hypothesized that placing PCM on individual surfaces would help in determining the surface the PCM could be appended to in order to obtain the most savings in energy. It was later seen that lowering the enthalpy (i.e., kJ/kg) of a PCM and appending it to a larger surface area performed better than placing concentrated amounts of PCM with a higher enthalpy on smaller surface areas of the building. However, of the initial four surfaces compared, before the normalizing of PCM enthalpy on other surfaces, it was found that the placement of PCM on either surface does not make a big difference in the variability in energy savings. The standard deviation shows that, even though placing PCM on individual surfaces is about 7 percent efficient in reducing the annual load than without PCMs,

there is very less variability in the annual load among the placement of PCM in the separate individual surfaces. On the other hand when attention is focused on the variability in the direction of PCM melting temperatures, it seems that the optimum selection of PCM melting temperatures is a much more important variable to consider than on which surface the PCM is placed. There exists a bigger variability in total load due to the effect of the PCM melting temperatures and this is true even when the PCM is spread over a larger surface area as can be seen in columns 8, 9 and 10 in Table 6.4.

1	2	3	4	5	6	7	8	9	10	11	12
Surface	East:	West:	North:	South:	Mean (East, West, North, South)	Std Dev (East, West, North, South)	Roof	4 walls	Except Floor	NO PCM: Total Load	% Saved
PCM Enthalpy	100 kJ/kg	100 kJ/kg	100 kJ/kg	100 kJ/kg			25 kJ/kg	25 kJ/kg	12.5 kJ/kg		
Melt Temp [°C]	Total Load [GJ]	Total Load [GJ]	Total Load [GJ]	Total Load [GJ]	[GJ]	[GJ]	Total Load [GJ]	Total Load [GJ]	Total Load [GJ]	[GJ]	
21	17.84	17.95	17.86	17.90	17.89	0.05	17.29	17.12	17.11	18.88	9.38
22	17.40	17.57	17.46	17.41	17.46	0.08	17.25	17.07	17.16	18.88	9.58
23	17.43	17.76	17.57	17.47	17.56	0.14	17.12	16.88	16.97	18.88	10.61
24	17.83	18.21	17.98	17.93	17.99	0.16	16.87	16.76	16.57	18.88	12.25
25	18.22	18.57	18.41	18.36	18.39	0.14	18.25	17.69	17.82	18.88	6.30
26	18.66	18.84	18.83	18.75	18.77	0.09	18.81	18.52	18.52	18.88	1.89
Mean	17.90	18.15	18.02	17.97			17.60	17.34	17.36		
Std Dev	0.48	0.48	0.52	0.51			0.76	0.66	0.70		

Table 6.4: PCM performance in a building with the HVAC A control schedule.

The columns 8, 9 and 10 in Table 6.4 represent the annual load of the building once PCM is appended to the roof, 4 walls or all surfaces (except the floor) respectively. The PCM enthalpy on each corresponding case is normalized based on the surface area on which the PCM properties are appended to. It is evident, through comparison with cases in columns 2, 3, 4 and 5, that applying PCM to a larger surface provides better energy savings in the building. The surfaces that do not have PCM act as a thermal bridge to the building as a whole. Because of the one surface with concentrated PCM with high enthalpy the other surfaces without PCM allow for heat or cold

to flow freely in and out of the building. The smallest total is obtained for the case '*Except Floor*', column 10, with a melting temperature of 24°C. Upon closer inspection the annual load for the case '4 walls' with a PCM of the same melting temperature is very close, with a difference of only 194.4 mega joules which corresponds to a difference of 54 kWh annually. Assuming that the air is conditioned by electric heating and cooling systems and that the cost of 1 kWh of electricity is \$0.1, the difference in the two cases would amount to only \$5.4 annually. Therefore the decision to optimize the annual load is based on whether the cost of PCM boards vary on the basis of per kilogram of enthalpy i.e., the cost of PCM boards increase or decrease on the basis of its heat storage capacity or if the cost depends on the simple fact that PCM boards are expensive than regular gypsum boards and that there is not much variability in price on the basis of the heat storage capacity. Similarly placing PCM only on the east facade with a melting temperature of 22°C results in a storage penalty of 832.4 mega joules of annual energy; resulting in a drop of only 4.41% in energy savings from the optimum value (from 12.25% to 7.84%). Nevertheless, if we are to follow our earlier assumptions, the loss in 832.4 mega joules in energy amounts to a difference in 231 kWh which only amounts to a loss of 23 dollars annually. Regarding the assumptions above, it should be pointed out that the aforementioned data is obtained for the building with minimal internal load i.e., only 7 people occupying the space throughout the year with no electric equipment or lighting etc. The main study later will delve into the behavioral response of these buildings with different internal loads.

Figure 6.5 shows a graphical representation of how the annual loads change for each of the seven cases for the different PCM melting temperatures. It can be seen from the Figure that all cases provide considerable savings i.e., at the very least approximately 7% in energy when compared to the case without PCM. The annual load of the building without the use of PCM rests at 18.88 GJ annually, which translates to 5245 kWh annually. The case where PCM is placed on

all walls except for the floor performs best at a PCM melting temperature of 24°C. There is a 12.25% savings in energy with this case. A total of 2.313 GJ of energy is saved which translates to a savings of 642.5 kWh annually which is highlighted in Table 6.4, column 12. As a general trend PCMs melting at 21, 22, 23 and 24 seem to perform better than PCM melting at 25 and 26 under the HVAC A schedule. Since 25°C is the cooling set-point temperature throughout the day, it seems logical that the HVAC system would start without the opportunity for the PCMs melting at 25°C and 26°C to be fully 'charged'. Albuquerque falls in region 4b of the US.DOE climate map and from the simulation results PCM melting at 24 degrees, 1°C below the cooling set-point temperature performs best when the building envelope, except the floor, is appended with this PCM. This seems like this building is cooling dominated and therefore the PCM melting at 24°C is performing best because it absorbs a significant amount of indoor energy before the HVAC system is called upon.

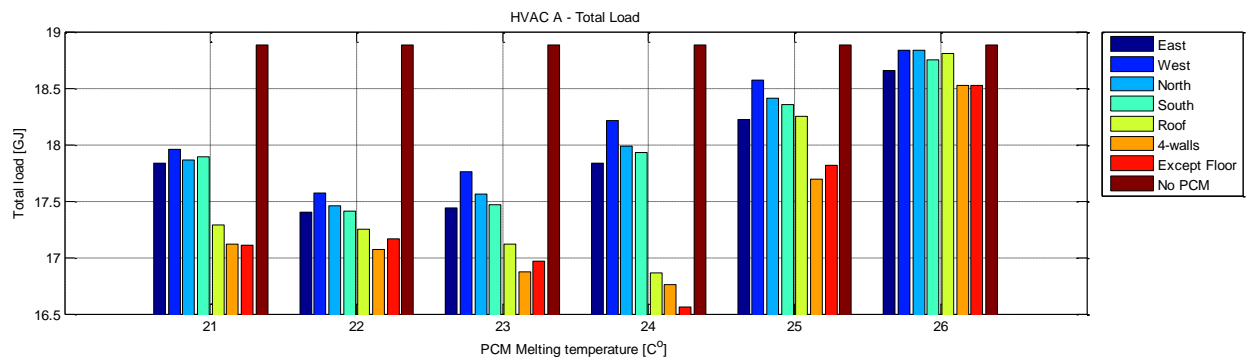


Figure 6.5: HVAC A: Total load chart for PCM with different melting temperatures placed on different surfaces.

The data was further analyzed to identify the particular months of the year where the PCM performed optimally and which ones did not. The heating load and cooling load for each month were recorded for each of the seven cases, but only the PCM melting at 24°C, and analyzed separately in order to identify the months when the PCM worked best and where it did

not perform as well. Table 6.5 and Table 6.6 represent the heating and cooling load for the building conditioned by the HVAC A scenario.

Months	Jan	Feb	Mar	Apr	May	Jun	Jul	Aug	Sep	Oct	Nov	Dec
Surface	MJ	MJ	MJ	MJ	MJ	MJ	MJ	MJ	MJ	MJ	MJ	MJ
East	611	366	95	1	0	0	0	0	0	39	170	646
West	623	378	104	1	0	0	0	0	0	40	183	656
North	615	373	105	2	0	0	0	0	0	40	176	651
South	605	362	96	1	0	0	0	0	0	38	166	639
Roof	612	363	89	0	0	0	0	0	0	38	168	651
4 Walls	596	349	84	0	0	0	0	0	0	38	155	639
Except Floor	600	352	85	0	0	0	0	0	0	38	158	643
Mean	609	363	94	1	0	0	0	0	0	39	168	646
Std Dev	9	10	9	1	0	0	0	0	0	1	10	6
NO PCM	633	394	126	7	0	0	0	0	0	46	196	660

Table 6.5: HVAC A: Monthly heating load MJ for PCM melting at 24°C appended to the seven different scenarios.

From Table 6.5, it is evident that the PCM melting at 24°C does not perform optimally for the months when heating is required. The mean of all the cases is not very different (i.e., at most a difference of 30 MJ) from the case when no PCM is used for any month. In addition the standard deviation, that gives us a measure of how the heating load is different from case to case, too is very small for each month i.e., at most a standard deviation of 10 MJ. On the other end, the results for PCM melting at 21°C (see Appendix table C1) shows much variability from case to case i.e., at most a standard deviation of 80 MJ. Also larger difference between the mean and the case without PCM (at most a difference of 200 MJ can be observed. Even though the PCM melting at 21°C performs better over the PCM melting at 24°C for the months that require heating, this offset in heating load is not enough to make a large contribution in the annual load to catapult it to the optimum PCM for this case. The cooling load is the dominant factor in determining the optimum PCM under this HVAC schedule and at this Albuquerque climate.

Months	Jan	Feb	Mar	Apr	May	Jun	Jul	Aug	Sep	Oct	Nov	Dec
Surface	MJ	MJ	MJ	MJ	MJ	MJ	MJ	MJ	MJ	MJ	MJ	MJ
East	47	143	357	967	1663	2721	3211	3159	2419	1043	165	9
West	95	193	416	999	1670	2721	3211	3159	2419	1075	232	33
North	55	155	403	990	1667	2720	3211	3159	2418	1049	179	12
South	59	158	385	983	1667	2721	3211	3159	2418	1061	186	15
Roof	2	40	137	770	1579	2710	3212	3160	2414	878	42	0
4 Walls	0	27	120	772	1579	2710	3212	3159	2411	881	29	0
Except Floor	0	12	68	719	1558	2708	3212	3160	2411	827	16	0
Mean	37	104	269	886	1626	2716	3212	3159	2416	974	121	10
Std Dev	37	75	153	125	51	6	0	0	4	106	89	12
NO PCM	130	255	526	1137	1722	2729	3211	3160	2426	1164	306	51

Table 6.6: HVAC A: Monthly cooling load MJ for PCM melting at 24°C appended to the seven different scenarios.

Table 6.6 depicts the monthly cooling load in mega joules. It can be seen that the PCM does not perform well for the months June, July, August, and September. In fact there is almost no variability in the seven cases and additionally every case exhibits the same annual load as the case when no PCM is used. This goes to show that the PCM does not perform optimally for the summer months in Albuquerque under the HVAC A schedule. The assumption is that during the summer months, any given PCM melts instantly and never gets the opportunity to discharge the energy for the next daily cycle which seems at direct odds with the conventional understanding that a PCM that absorbs indoor heat during the summer months is the one that performs best. It is in fact, evident from Table 6.6, that the indoor heat the PCM absorbs during the spring and fall months is a necessary condition to determine the optimality of PCM. The PCM that melts at 24°C therefore is the most effective during the months of February, March, April, May and also during the month of October. A closer look at the cooling load and the heating load for all the different melting temperatures shows that the optimization of total load i.e., the lowest total load is a balancing act between the heating and cooling load after the application of PCMs on different walls. It is evident from the data that the PCM with melting temperature of 21 degrees that works

well to curb the heating load during the winter months falls short of PCM melting at 24°C in performance when it comes to maintaining the cooling load during the hot months.

HVAC B

HVAC B schedule was set to operate under a night time setback schedule so the HVAC was not required to condition the indoors for occupant comfort during the night time. The guiding assumption was that the building being conditioned was an office building and therefore the need for air conditioning during the night time was redundant.

Similar to the analysis for HVAC A, the variability of placing a PCM working under the HVAC B schedule on different surfaces was calculated. Table 6.7 depicts the annual load for all the seven building cases analyzed for the six different PCM melting temperatures. The annual load is expressed in gigajoules and when compared to the annual loads of HVAC A it is considerably smaller due to the night time setback. The night time setback of 5 degrees from both the heating and cooling set points allowed for the HVAC to 'not-expend' the additional 3.18 GJ ($18.8 \text{ GJ} - 15.7 \text{ GJ} = 3.18 \text{ GJ}$) of energy annually.

The general trend on the variability from the results of HVAC A hold true for the case in HVAC B as well. The variability in the direction of *placement* of PCMs is considerably smaller than the variability in the direction of PCM melt temperature thereby placing more importance in the melting temperature of PCM as selection criteria. The variability in the direction of PCM melt temperature for the 3 cases in columns 8, 9 and 10 of Table 6.7 are more pronounced than when PCM is placed on individual surfaces.

1	2	3	4	5	6	7	8	9	10	11	12
Surface	East:	West:	North:	South:	Mean (East, West, North, South)	Std Dev (East, West, North, South)	Roof	4 walls	Except Floor	NO PCM:	% Saved
PCM Enthalpy	100 kJ/kg	100 kJ/kg	100 kJ/kg	100 kJ/kg			25 kJ/kg	25 kJ/kg	12.5 kJ/kg		
Melt Temp [°C]	Total Load [GJ]	Total Load [GJ]	Total Load [GJ]	Total Load [GJ]	[GJ]	[GJ]	Total Load [GJ]	Total Load [GJ]	Total Load [GJ]	Total Load [GJ]	
21	14.90	14.99	14.93	14.90	14.93	0.04	14.74	14.60	14.65	15.70	6.98
22	14.62	14.76	14.68	14.62	14.67	0.07	14.57	14.42	14.50	15.70	8.17
23	14.55	14.80	14.65	14.60	14.65	0.11	14.23	14.04	14.12	15.70	10.54
24	14.82	15.13	14.94	14.93	14.95	0.13	13.89	13.83	13.62	15.70	13.21
25	15.16	15.46	15.30	15.29	15.30	0.12	14.98	14.61	14.51	15.70	7.60
26	15.43	15.63	15.56	15.53	15.54	0.08	15.34	15.17	15.04	15.70	4.20
Mean	14.91	15.13	15.01	14.98			14.63	14.44	14.41		
Std dev	0.33	0.35	0.36	0.37			0.52	0.47	0.48		

Table 6.7: PCM performance in a building with the HVAC B control schedule.

Similar to the results observed for HVAC A, lowering the enthalpy of a PCM and appending it to a larger surface area performs better than placing concentrated amounts of PCM with a higher enthalpy on smaller surface areas of the building under a HVAC B schedule. The lowest annual load is obtained for the case '*Except Floor*', column 10, with a melting temperature of 24°C. The next best option is the case '*4 walls*' with PCM of the same melting temperature. The case '*4 walls*' is very close to the optimum, with a difference of only 202.6 mega joules which corresponds to a difference of 56 kWh annually. Operating under the same assumptions for the air conditioning and the cost of energy in the previous section, the difference in the two cases would amount to only \$5.6 annually. Nevertheless, the aforementioned data is obtained for the building with minimal internal load i.e., only 7 people occupying the space throughout the year with no electric equipment or lighting etc. and if the internal load is increased, the difference in the two loads could be compounded.

Figure 6.6 shows a graphical representation of how the annual loads change for each of the seven cases for the different PCM melting temperatures. It can be seen from the Figure that all cases provide considerable savings i.e. at the very least approximately 7% in energy when compared to the case without PCM. The annual load of the building without the use of PCM is 15.70 GJ annually, which translates to 4361 kWh annually. The case where PCM is placed on all walls except for the floor performs best at a PCM melting temperature of 24°C. There is a 13.21% savings in energy with this case. A total of 2.07 GJ of energy is saved when this PCM is used, and that translates to an annual saving of 575 kWh (Table 6.7column 12).

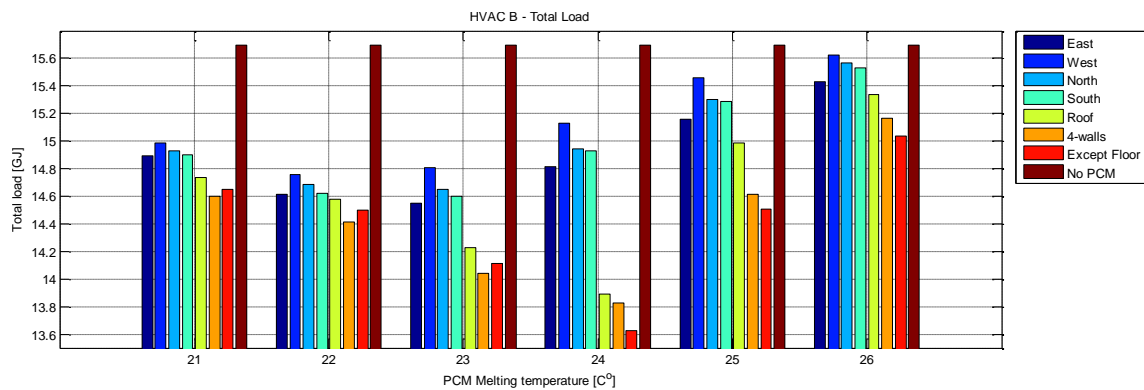


Figure 6.6: HVAC B: Total load chart for PCM with different melting temperatures placed on different surfaces.

The scenario for the monthly heating loads follows a similar trend as to the results from HVAC A as can be seen in Table 6.8. The magnitude of the monthly heating loads however is half of what was seen for each corresponding month in HVAC A. While there is no heating required for the months April, May, June, July, August and September, the heating loads for the remaining months do not vary among the seven different cases either when PCM melting at 24°C is used.

Months	Jan	Feb	Mar	Apr	May	Jun	Jul	Aug	Sep	Oct	Nov	Dec
Surface/Heating	MJ	MJ	MJ	MJ	MJ	MJ	MJ	MJ	MJ	MJ	MJ	MJ
East	332	200	57	1	0	0	0	0	0	22	92	344
West	335	204	61	1	0	0	0	0	0	23	97	346
North	333	202	62	1	0	0	0	0	0	23	94	344
South	330	198	57	1	0	0	0	0	0	22	91	342
Roof	332	196	53	0	0	0	0	0	0	22	90	345
4 Walls	328	191	50	0	0	0	0	0	0	22	85	342
Except Floor	329	192	50	0	0	0	0	0	0	22	86	343
Mean	331	197	56	1	0	0	0	0	0	22	91	344
Std Dev	2	5	5	1	0	0	0	0	0	1	4	1
No PCM	338	210	74	5	0	0	0	0	0	28	101	347

Table 6.8: HVAC B: Monthly heating load MJ for PCM melting at 24°C appended to the seven different scenarios.

Months	Jan	Feb	Mar	Apr	May	Jun	Jul	Aug	Sep	Oct	Nov	Dec
Surface	MJ	MJ	MJ	MJ	MJ	MJ	MJ	MJ	MJ	MJ	MJ	MJ
East	33	134	351	922	1463	2281	2677	2650	2098	999	156	6
West	75	178	408	953	1473	2280	2677	2650	2097	1031	221	22
North	40	144	395	946	1470	2281	2677	2650	2097	1005	170	8
South	44	148	378	938	1470	2280	2677	2650	2098	1016	177	10
Roof	1	38	133	720	1390	2272	2677	2650	2095	834	41	0
4 Walls	0	25	117	723	1386	2271	2677	2650	2093	838	28	0
Except floor	0	11	68	664	1369	2269	2677	2650	2093	785	16	0
Mean	28	97	264	838	1432	2276	2677	2650	2096	930	116	7
Std Dev	29	69	150	129	47	5	0	0	2	105	84	8
No PCM	104	231	512	1074	1519	2287	2677	2650	2104	1113	290	35

Table 6.9: HVAC B: Monthly cooling load MJ for PCM melting at 24°C appended to the seven different scenarios.

Table 6.9 depicts the monthly cooling load in mega joules. PCM does not perform well for the months June, July, August, and September. In fact there is almost no variability in the seven cases and additionally every case exhibits the same annual load as the case when no PCM is used. Once again it can be seen that the PCM does not perform optimally during the summer months in Albuquerque under the HVAC B schedule. In terms of the monthly loads, the PCM

was found to perform optimally during the month of March, April and October providing the largest magnitude of savings in energy for cooling. The temperature profile for these three months therefore opens the possibility of using the PCM in other climates that exhibit relative similarity in weather as these three months in Albuquerque.

The performance of PCMs under the conditions of HVAC B is very similar, yet better in magnitude, to the performance of PCMs in the buildings with HVAC A.

HVAC C

HVAC C was defined to operate such that it would provide only heating during the six months of the year and only cooling during the other six months of the year as depicted in Figure 6.4. The guiding assumption was that the building being conditioned by HVAC C was a residential space and therefore only one thermostat set-point temperature for each season.

While the general trend in variability, along the two directions, remained similar to what was observed in the results from HVAC A and HVAC B, the magnitude of the annual load was found to lie in between the results observed from HVAC A and HVAC B. So, the HVAC C schedule performed better than the HVAC A schedule but poorer than the HVAC B schedule. The annual load, without PCM, was 16.39 GJ as can be seen in column number 11 in Table 6.10. Another distinction from the performance of PCMs under HVAC A and HVAC B was that the optimum PCM however changed from the one melting at 24°C to 21°C. Nevertheless, the percent savings decreased considerably from what was found in HVAC B. The optimum case for HVAC C, i.e. PCM melting at 21°C and the case '*Except floor*' only saved 6.78% of energy annually in comparison to the optimum PCM in HVAC B that provided a saving of 13.21% in annual energy consumption with its use. The PCM melting at 21°C, in the HVAC C scenario, offered a total of 1117 MJ in savings that translates to 310 kWh annually. The corresponding annual load for the

building with different PCMs placed on the 7 different scenarios for the building is shown in

Table 6.10.

1	2	3	4	5	6	7	8	9	10	11	12
Surface	East:	West:	North:	South:	Mean (East, West, North, South)	Std Dev (East, West, North, South)	Roof	4 walls	Except Floor	NO PCM: Total Load	% Saved
PCM Enthalpy	kJ/kg	kJ/kg	kJ/kg	kJ/kg			kJ/kg	kJ/kg	kJ/kg		
Melt Temp [oC]	Total Load [GJ]	Total Load [GJ]	Total Load [GJ]	Total Load [GJ]	[GJ]	[GJ]	Total Load [GJ]	Total Load [GJ]	Total Load [GJ]	[GJ]	
21	15.86	15.91	15.85	15.89	15.88	0.02	15.36	15.32	15.28	16.39	6.78
22	15.79	15.85	15.80	15.77	15.80	0.03	15.67	15.61	15.65	16.39	4.77
23	15.93	16.02	15.97	15.90	15.96	0.05	15.91	15.74	15.80	16.39	3.95
24	16.04	16.11	16.09	16.02	16.07	0.04	15.76	15.70	15.64	16.39	4.59
25	16.12	16.19	16.20	16.14	16.16	0.04	16.12	16.00	16.10	16.39	2.41
26	16.29	16.35	16.38	16.32	16.33	0.04	16.30	16.22	16.20	16.39	1.15
Mean	16.01	16.07	16.05	16.01			15.86	15.76	15.78		
Std dev	0.19	0.18	0.22	0.20			0.33	0.31	0.34		

Table 6.10: HVAC C: Monthly cooling load MJ for PCM melting at 24oC appended to the seven different scenarios.

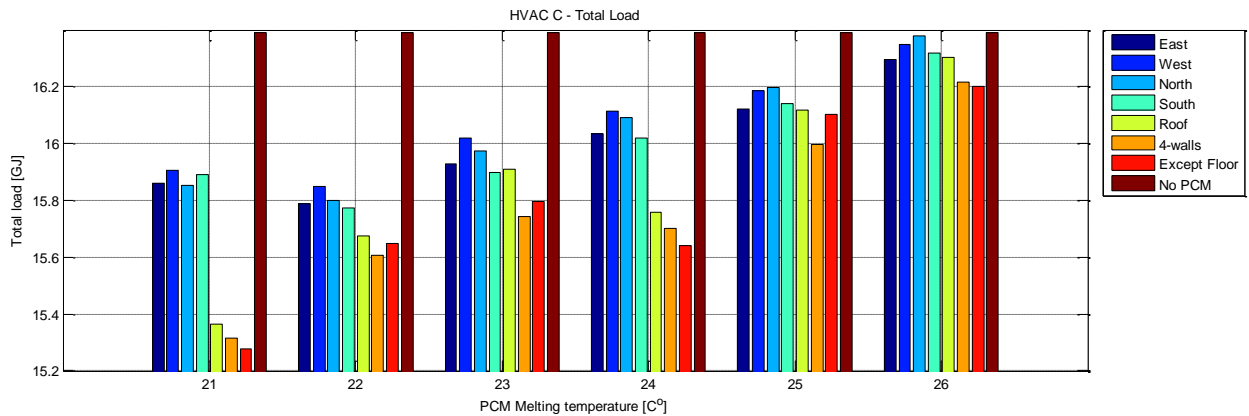


Figure 6.7: HVAC C: Total load chart for PCM with different melting temperatures placed on different surfaces.

Since there is no heating required/available during the six months of the year through the HVAC C set-point schedule, the PCM melting at 21°C performs best in curbing the monthly heating load and conversely performs inadequately in curbing the monthly cooling loads.

However, while the cooling load is reduced considerably for the months of April and May by the PCM melting at 24°C, that decrease in cooling load is not enough to offset the magnitude of energy saved by using PCM melting at 21°C during the months that require heating. Therefore it is a balancing act in which selecting the optimum PCM is a matter of selecting one that reduces the total load.

Conclusion

In this chapter various variables that affect the total annual energy consumption of the buildings with PCM are analyzed. The influence of the HVAC schedule in building, the placement of PCM in different walls and the different PCM melting temperatures were studied. The studies were chosen for a particular building construction recommended in the ASHRAE 90.1-2010 standard and was simulated only for Albuquerque, New Mexico which falls under zone 4b in the U.S. Department of Energy climate map. The building energy performance simulations were performed for a simple 35' X 35' building fitted with PCM boards on combinations of the interior surfaces of the walls. The application of PCM wallboards was studied for buildings with three different thermostat set-point schedules. It was found that the PCM offered savings in annual energy for all cases.

1. For the seven cases with a particular building type, internal loads and HVAC schedules it was observed that the placement of optimum PCM on the larger surface area was invariably better than placing it on a smaller area, even though the surfaces exhibited the same amount of latent heat storage capacity. It was found that the surface area of the placement of PCM dictated the magnitude in energy savings. It was best to cover more surface area with latent heat storage than to concentrate it in one surface area of the building. If the cost of PCM boards are inherently more expensive

than regular gypsum boards, solely due to the fact that it is a PCM board and regardless of its heat storage capacity, it is probably more economical for the consumer to consider placing PCM with higher concentration on only one facade and place regular gypsum boards on the remaining surfaces. However, if the cost of PCM boards increase with respect to its heat storage capacity then spreading the PCM throughout the surfaces seems viable in terms of initial investment. Nevertheless, an optimization study with respect to two criterions i.e., willingness to spend a certain cost per unit energy storage and willingness to tolerate a certain cost of annual heating and cooling load), the process can help determine the optimum placement and selection of PCM.

2. All the applications of PCM showed to curb the annual energy consumption. The optimum performance of PCM was seen in the building that employed an HVAC thermostat schedule with night-time setback. The difference in annual load however from the optimum PCM with the other scenarios was not too far off. Nevertheless, the increase in internal loads of the buildings can compound this difference in annual loads therefore a determination cannot be made about the relative importance of the optimum PCM unless a study is performed to assess the behaviour of PCMs in buildings with different yet increasing internal loads.
3. The performance of PCMs under HVAC A and HVAC B followed a similar trend in results. The optimum PCM was found to be the one melting at 24°C for both the cases. It was found that none of the PCMs performed well during the summer months of Albuquerque. Therefore it was evident from the data for all the cases, including the ones in literature, that recommended the selection of an optimum PCM by taking the summer months as a representative climate was an erroneous assumption (for the

Albuquerque climate type). The PCM melting at 24°C was efficient in reducing the cooling load but only during the spring and fall climates. This reduction in load was much greater than the reduction in heating load provided by PCM melting at 21°C for both the HVAC A and HVAC B schedules. The finding that the optimum PCM worked best during the spring and fall months opens the possibility of using this PCM in other climates that exhibit relative similarity in weather as these two seasons in Albuquerque. In the case of HVAC C, since no cooling was provided for particular 6 months, it was seen that PCM melting at 21°C offered the most savings in annual load by curbing the heating load for the other 6 months. Considering a scenario when the internal loads are increased, this increase in internal load in turn will reduce the heating load, thereby could render the use of PCM useless under the HVAC C set-point schedule.

4. Overall, the proper selection of melting temperature was found to be an important variable than compared to the placement of PCM in the building. The annual load was found to vary more in the direction of the PCM melting temperature than the placement of PCM. Therefore the melting temperature of PCM is an important variable when considering its use in buildings. A slight divergence from the optimum temperature can reduce the energy saving potential by 5-10 percent.

In order to understand the behavior of PCM within the buildings the variable change in internal loads along with different HVAC schedules are a few of the variables that need to be included in the main study. A detailed, time dependent temperature profile of the walls and when the PCM melts and solidifies are few outputs that will be analyzed in detail to pinpoint the major factor that promotes efficient use of PCMs in buildings in the following chapters.

Chapter Seven

ALL CLIMATES AND ALL VARIABLES

The previous two chapters focused primarily on the Albuquerque climate after following the results in chapter 4 (climate maps). It was found that PCM boards performed best in terms of magnitude of energy saved in climate 4b, that of Albuquerque, NM. However, the study included only a subset of the full factorial design. For instance the internal load was set to a constant 600 watts. Any additional number of people would add to the internal loads to be serviced.

Furthermore, the HVAC set-point schedule was set to 21°C for heating and 25°C for cooling available year round. It is still unsure how PCM boards would perform in Albuquerque, along with other climates, with the other variables included in the study. A full factorial design was therefore used to study the effect of all the variables in the study. The full factorial study was setup to run on the Clemson University's Palmetto cluster.

The design is as follows:

Independent Variables	Number of Levels & [values]	Constant Parameters	Dependent Variable
Melting Temperature	9 [19:27]	Building Type	Annual Energy Load
PCM Enthalpy	5 [20:100]	Infiltration Schedule	Annual Heating Load
Length-to-Width ratio	3 [2,10,0.5]	Ventilation Schedule	Annual Cooling Load
Climate/Cities	15	Internal load schedule	
HVAC Schedule	2 [Office, Residential]	PCM Location	
Internal Loads	6 [5,7,10,12,15]	Shading Schedule	
R-Value	3 [low, medium, high]	WWR	
		PCM Position	

Table 7.1: List of independent variables, constant parameters and the dependent variables. (The number of levels of each independent variable is given in brackets.)

1. PCM Melting Temperature [9]: The PCM melting temperature was set to hold 9 values as shown in Table 7.1 after realizing from the pilot study that the PCM melting temperatures lower than the heating set-point temperature or higher than cooling set-

point temperature respectively would never get the chance to actively participate in the absorption and desorption of energy. For instance the PCM will never get the opportunity to absorb energy at 28°C if the cooling set-point temperature is set at 25°C. In short, the indoor temperature will reach the set-point temperature before reaching the PCM melting temperature thereby requiring the HVAC system to cool the indoors to a comfortable 25°C before even allowing for the PCM to absorb the excess energy. Now consider the situation where the PCM melt temperature is 16°C and heating is required to maintain the indoor temperature at 21°C. The first loss is experienced when the heat provided by the HVAC to heat the indoors to gradually increase up to 21°C is absorbed by the PCM at 16°C. Then, after the indoors is sufficiently conditioned, even if the indoors could use that excess heat stored by the PCM at 16°C, the HVAC kicks in as soon as the indoor temperature drops below the heating set-point temperature of 21°C. The energy stored at 16°C therefore never gets the opportunity to be used.

2. PCM enthalpy-[5 levels]: For this study the PCM enthalpy was set to take on five values as shown in Table 7.1 to represent the heat storage capacities of a PCM gypsum board. The PCM boards were selected for this study as opposed to other stand-alone PCM technologies due to the lack of data on such new technologies. According to Kosny et al. (2013) most experiments show that the thermal performance of advanced integrated PCM technologies can be significantly higher than the simpler dispersed PCM applications such as PCM boards. However, these systems are complex and are difficult to analyze using existing whole-building energy simulation tools. As a result, field test results are particularly valuable for energy performance and cost analyses before sufficient computer tools are developed and validated for these technologies.

Dispersed PCM systems, i.e. PCM boards, are less complex, easier to analyze, and more forgiving from the perspective of potential errors in numerical analysis. Usually, a wide selection of PCMs with slightly different PCM functional temperatures can be used for the same climatic conditions and for the same location within the building envelope. At the same time, concentrated PCM applications require more precise selection of the PCM's functional temperature range, location, and heat storage density. There is a wide variety of PCMs having different temperature profiles, hysteresis, and heat storage capacities available today for building envelope applications. In order to analyze the thermal performance of specific PCMs, computer models need to use detailed enthalpy/temperature profiles that are developed using dynamic testing methods (eg. Differential Scanning Calorimetry). Since dynamic testing is not an objective of this project, ideal PCM enthalpy-temperature curves were defined in EnergyPlus to represent the thermal characteristics of the PCM boards for the parametric thermal simulations.

3. Aspect ratio [3-levels]: As mentioned in chapter 3 and depicted in Figure 7.1, the buildings designed for this study will take three different aspect ratios while maintaining the same floor area.

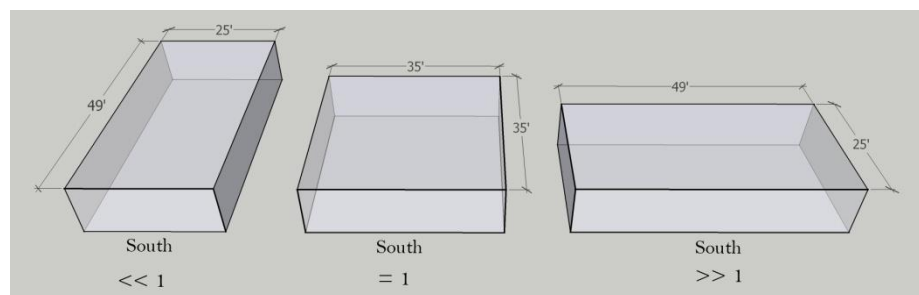


Figure 7.1: Aspect ratios for the three different buildings with the same floor area.

Each facade will have a constant window to wall ratio of 15%. The solar heat gain coefficients of the glazing surfaces take the prescriptive values recommended in the ASHRAE 90.1 standard, section 5.5. The window to wall ratio as an independent variable is not included in this study and therefore left constant at 15%.

4. HVAC schedules [2-levels]: From Chapter 5 it was seen that the performance of PCMs differs with the selection of specific HVAC set-point schedules. Therefore the main study will include the '*office*' and '*residential*' set-point schedules as independent variables.
5. Internal loads [6-levels]: The internal loads for this study will be expressed in totality by the number of people indoors. Every person is set to dissipate 120 watts individually. The internal loads therefore increase with each increase in the number of people. According to the ASHRAE 62.1 standard (2007), table 6.1 defines the default occupancy of 5 people every 1000 ft² in offices. Likewise the default occupancy for dwelling units (i.e., residential) is 2 people for studio and one bedroom units, with one additional person for each additional bedroom. For the 1225 ft² building in this study, any additional wattage beyond 6 people (i.e., $6 \times 120 = 720$ watts) can be considered additional load from lights and plug loads such as computers, printers, monitors, etc. The 6 levels considered for the independent variable, internal loads, is 0, 5, 7, 10, 12 and 15 people to occupy the space all year round.
6. R-Value [3-levels] - Each of the climate zones have a corresponding mandatory R-value assigned to walls and roofs as per ASHRAE 90.1, section 5.5. This is the minimum R-value for the insulation that must be met for the building to achieve the baseline standard. For this study, each of the prescriptive R-values takes 3 values. The

minimum recommended by the standard, 1.25 times the standard and 1.5 times the standard. For instance,

$$R - value = \frac{Thickness(m)}{Conductivity (K * m/W)}$$

The R-value is inversely proportional to conductivity, multiplying the conductivity by a certain constant will allow the conversion of R-value into 1.25*R-value and 1.5* R-value. The conductivity of each insulation was therefore multiplied with the specified constants in Table 7.2 in order to express the change in R-values. The assumption here was that even though the conductivity is altered to express the change in R-value of the insulation, the density, mass and volume of the insulation stays the same.

R-value	Thickness (T)	Conductivity (K)
1.25 (medium)	T*(5/4)	K*(4/5)
1.5 (High)	T*(3/2)	K*(2/3)

Table 7.2: The constants that when multiplied to the thickness or conductivity allows the conversion of R-values.

All the individual buildings per climate were designed and the variables were automated and assigned using Matlab. A total of 9 (Melting temp) * 5 (Enthalpy) * 3 (Length-to-width ratio) * 2 (HVAC schedules) * 6 (Internal loads) * 3 (R-values) = 4860 input files per city were generated for EnergyPlus as per the full factorial design. A total of 15 cities required 4860*15 = 72900 .idf files that were run on the computer cluster at Clemson University.

Nevertheless, a few challenges were experienced while setting up the full factorial of experiments on the computer cluster (palmetto cluster). The two main challenges were as follows:

1. JEplus, an EnergyPlus batch shell for parametric studies was used earlier for the required simulations on a windows based platform. However it was incompatible with

the linux based platform when trying to replicate its use on the Clemson University Palmetto Cluster. One of the developers of JEplus was contacted to sort the issue. The developer assured that the parametric modeling tool had to be modified at the coding level to be compatible with the particular distribution of linux at Clemson University, therefore not immediately possible. Without the parametric modeling tool, in house shell scripts were written to accept all the input files for EnergyPlus in the computer cluster.

2. The second challenge was that the Linux version of EnergyPlus 8.1 was compiled on a different Linux distribution and hence incompatible to run on the cluster at Clemson University. However after communicating with the developers of EnergyPlus, a newly compiled EnergyPlus was provided that worked seamlessly on the cluster here.

Results and regression

All the results for the simulations were collected and post processed using Matlab to obtain the magnitude of energy saved when a PCM board was used versus when it was not. In addition, the percent energy saved was also computed for each different scenario. First and foremost the data was arranged so the independent variables could be regressed against the dependent variable, annual load.

The regression model developed for the cases with PCM boards is as follows:

$$Y(x) = \beta_0 + \overbrace{\beta_1 \cdot x_1 + \beta_2 \cdot x_2 + \beta_3 \cdot x_3 + \beta_4 \cdot x_4}^{\text{Quantitative}} + \overbrace{\beta_5 \cdot x_5 + \beta_6 \cdot x_6}^{\text{Aspect Ratio}} + \overbrace{\beta_7 \cdot x_1 \cdot x_2}^{\text{Interaction Term}}$$

Where, $Y(x)$ = Annual Load, x_1 = melting temperature, x_2 = PCM Enthalpy, x_3 = People,

$$x_4 = \text{R-value}, \quad x_5 = \begin{cases} 1 & \text{if aspect ratio} < 1 \\ 0 & \text{otherwise} \end{cases}, \quad x_6 = \begin{cases} 1 & \text{if aspect ratio} = 1 \\ 0 & \text{otherwise} \end{cases}.$$

The first set of regressions was run for the annual loads using PCM boards. For all the different scenarios it was found that the regression results were best when the data was split at 25°C for the melting temperature and separate regressions were run for the set of data below 25°C and another set above 25°C.

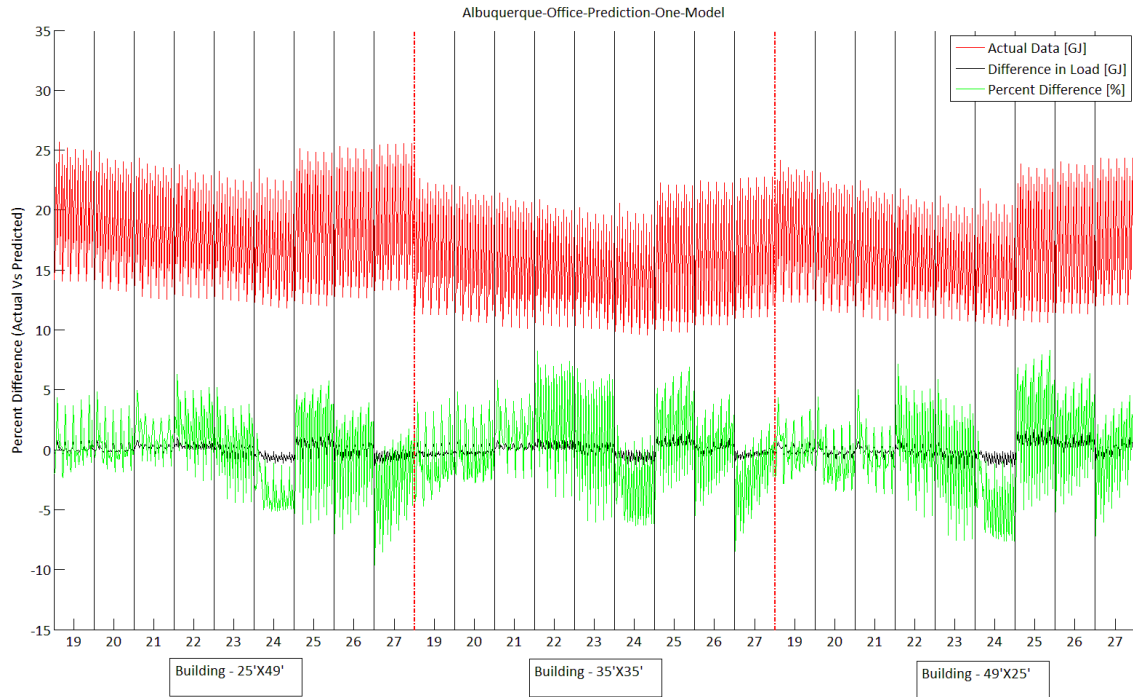


Figure 7.2: Difference in actual and predicted values of a one regression model.

In Figure 7.2, for the three office buildings in Albuquerque, the difference between the values obtained from the simulations and the predicted values of the regression model is plotted. This difference is expressed as a percent in green. The one model regression approach explained close to 96% of the variability in the data. However, it can be seen that for melting temperatures 24°C, 25°C, 26°C and 27°C the difference in actual data versus the predicted data is approximately 10%. Other approaches were sought to improve the regression model's predictive ability around those melting temperatures. It can also be seen from the plot that the slope changes in the actual data at the 25°C melting temperature point. The annual load seems to increase

beginning at the 25°C point. Since it looks like the relationship between the dependent variable (annual load) and the independent variables differs for different intervals over the range of melting temperature, two piecewise regression approaches were employed. First the continuous piecewise regression model, as seen in Figure 7.3, was used where the assumption was made that the data, although changing directions in the plot, is a continuous change i.e. there is no break in data.

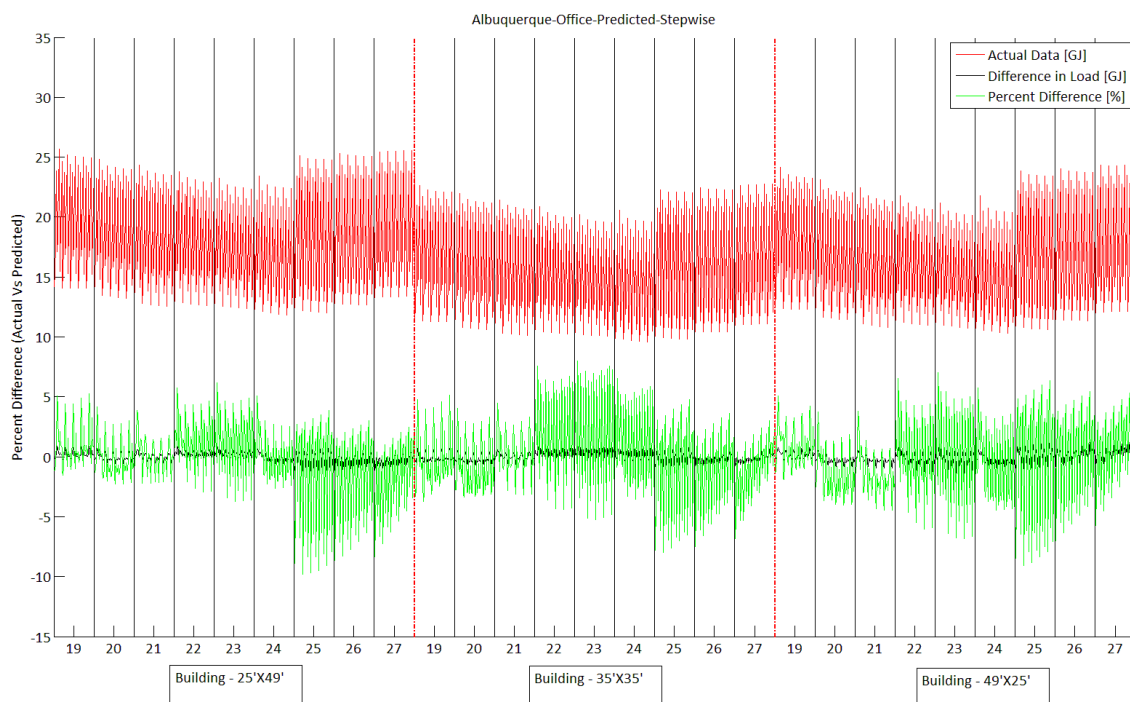


Figure 7.3: Difference in actual and predicted values of a piecewise regression model.

For instance the regression model used for the assumption of continuity was,

$$E(y) = \beta_0 + \beta_1 \cdot x_1 + \beta_2 \cdot (x_1 - k)x_2$$

where,

k = knot value (i.e., the value of the independent variable x_1 at which the slope changes)

$$x_2 = \begin{cases} 1 & \text{if } x_1 > k \\ 0 & \text{if not} \end{cases}, \text{ k in this case took the value of } 25^\circ\text{C}.$$

The assumption of discontinuity was also tested. While the assumption of continuity, yet stepwise, regression explained close to 96% of variability in the data, the assumption of discontinuity fared worse by only explaining close to 92% of the variability. While the continuous piecewise regression model too explained approximately 96% of the data denoted by the R^2_{adj} , the model did not seem to fare any better than the one model regression approach since the difference in predicted and actual values were observed to be close to 10% around the 24°C, 25°C, 26°C, and 27°C. The data was therefore split in two at the 25°C point and two separate regressions were run. The actual versus predicted data can be viewed in Figure 7.4.

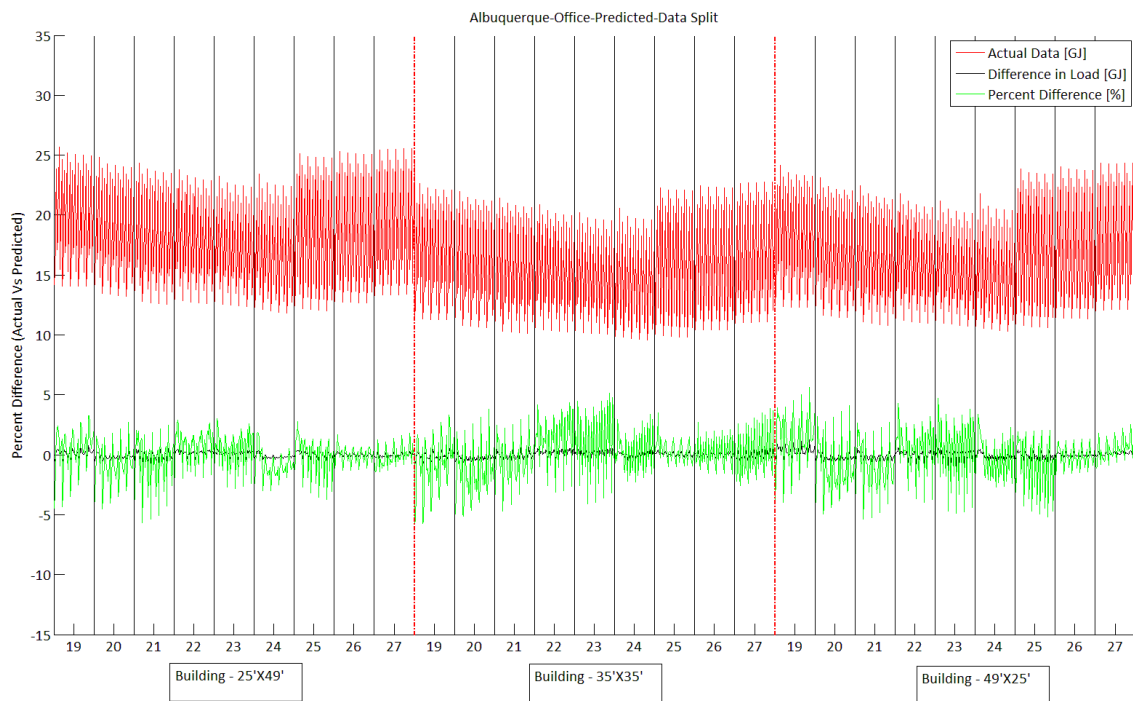


Figure 7.4: Difference in actual and predicted values of the data-split regression model.

The first set of regression was run on the data for melting temperatures from 19°C to 24°C, and then the second set of regression was run on the remainder of the data. The two regression models were both combined and plotted in Figure 7.4. Each model explained close to 98% of the variability in data. The percent difference between the actual and predicted data was

observed to fall below 5% for all the cases. The rest of the regression models were therefore performed by splitting the data into two groups at the 25°C point. The regression models for each of the climates and the corresponding plots are listed in appendix D. The independent variables were assigned values to place hold for the regression and they are as follows:

x ₁	Melting Temperature	19,20,21,22,23,24,25,26,27
x ₂	Enthalpy	20,40,60,80,100
x ₃	People	5,7,10,12,15
x ₄	R-value ⁴	Low = 1, Med = 1.5, High = 2.
x ₅	Aspect <<1	
x ₆	Aspect =1	

Table 7.3: The independent variables for the regression model.

The regression equations for the first set of data i.e. melting temperatures below 25°C have been listed in table 7.4, 7.5. The regression models for the second set of data (i.e., melting temperatures over 25°C) are listed in tables 7.6 and 7.7. The regression models for the buildings without PCM are listed in tables 7.8 and 7.9. Regression models for the annual load for the building without PCM were also developed so that the percent energy saved could be obtained from the regression models alone. Without the data on the cases without PCM, computing the percent energy saved would not have been possible. For all cases, the regression models for the climates 3c (San Francisco) and 4c (Seattle) are not listed because of the fact that there exists a sharp drop in annual load for PCMs melting at 24°C which could not be captured in the regression models. The difference in actual data and predicted data was found to be more than 2 gigajoules for the two climates. The actual data plots for these climates can be found in appendix B.

⁴ While 'medium' corresponds to 1.25 times the actual R-value of the insulation prescribed for the particular climate and 'high' corresponds to 1.5 times the actual R-value, the regression model was developed by assigning 1.5 to the 'medium' R-value and 2 to the 'high' R-value.

OFFICE																				R2Adj					
Albuquerque	25.29	-0.20	.x1	-0.007	.x2	-0.004	.x3	+	1.49	.x4	-0.004	.x1^2	+	0.043	.x3^2	-8.10	.x4^(1/2)	+	1.88	.x5	-0.80	.x6	0.993		
Baltimore	8.85	+	1.56	.x1	-0.005	.x2	-0.161	.x3	+	1.83	.x4	-0.043	.x1^2	+	0.040	.x3^2	-9.41	.x4^(1/2)	+	1.12	.x5	-1.06	.x6	0.992	
Boise	-7.93	+	3.05	.x1	-0.004	.x2	-0.482	.x3	+	2.80	.x4	-0.078	.x1^2	+	0.046	.x3^2	-10.28	.x4^(1/2)	+	1.32	.x5	-1.04	.x6	0.981	
Burlington	-3.80	+	2.86	.x1	-0.003	.x2	-0.663	.x3	+	3.00	.x4	-0.071	.x1^2	+	0.043	.x3^2	-11.55	.x4^(1/2)	+	0.95	.x5	-1.22	.x6	0.963	
Chicago	9.32	+	1.84	.x1	-0.004	.x2	-0.480	.x3	+	3.32	.x4	-0.048	.x1^2	+	0.041	.x3^2	-13.11	.x4^(1/2)	+	1.08	.x5	-1.23	.x6	0.980	
Duluth	-13.88	+	4.42	.x1	-0.003	.x2	-1.046	.x3	+	4.08	.x4	-0.110	.x1^2	+	0.053	.x3^2	-15.46	.x4^(1/2)	+	1.18	.x5	-1.26	.x6	0.953	
ElPaso	11.72	+	0.86	.x1	-0.005	.x2	+	0.229	.x3	+	1.24	.x4	-0.027	.x1^2	+	0.040	.x3^2	-8.14	.x4^(1/2)	+	1.40	.x5	-0.67	.x6	0.996
Fairbanks	-7.53	+	5.20	.x1	-0.003	.x2	-1.420	.x3	+	5.02	.x4	-0.127	.x1^2	+	0.053	.x3^2	-20.62	.x4^(1/2)	+	0.73	.x5	-2.56	.x6	0.985	
Helena	-8.87	+	3.34	.x1	-0.004	.x2	-0.844	.x3	+	3.01	.x4	-0.082	.x1^2	+	0.048	.x3^2	-11.46	.x4^(1/2)	+	1.18	.x5	-1.05	.x6	0.950	
Houston	-4.58	+	2.32	.x1	-0.005	.x2	+	0.678	.x3	+	1.09	.x4	-0.062	.x1^2	+	0.035	.x3^2	-7.38	.x4^(1/2)	+	0.88	.x5	-0.81	.x6	0.999
Memphis	1.63	+	2.07	.x1	-0.004	.x2	+	0.118	.x3	+	1.50	.x4	-0.054	.x1^2	+	0.038	.x3^2	-9.02	.x4^(1/2)	+	0.96	.x5	-0.93	.x6	0.997
Miami	-24.72	+	3.92	.x1	-0.001	.x2	+	1.740	.x3	+	0.03	.x4	-0.095	.x1^2	+	0.012	.x3^2	-4.98	.x4^(1/2)	+	0.87	.x5	-0.96	.x6	1.000
Phoenix	15.45	+	1.36	.x1	-0.004	.x2	+	0.740	.x3	+	2.51	.x4	-0.041	.x1^2	+	0.035	.x3^2	-13.78	.x4^(1/2)	+	1.36	.x5	-1.39	.x6	0.998

Table 7.4: The regression models for the office HVAC schedule in all climates (Data: 19°C ≤ Melting Temperature < 25°C)

RESIDENTIAL																								R2Adj	
Albuquerque	0.24	+	2.29	.x1	-0.007	.x2	-0.230	.x3	+	2.67	.x4	-0.049	.x1^2	+	0.056	.x3^2	-12.48	.x4^(1/2)	+	2.44	.x5	-0.61	.x6	0.986	
Baltimore	-18.68	+	4.54	.x1	-0.005	.x2	-0.249	.x3	+	2.87	.x4	-0.103	.x1^2	+	0.050	.x3^2	-14.08	.x4^(1/2)	+	1.57	.x5	-1.14	.x6	0.989	
Boise	-41.81	+	6.89	.x1	-0.005	.x2	-0.722	.x3	+	3.49	.x4	-0.162	.x1^2	+	0.059	.x3^2	-14.92	.x4^(1/2)	+	1.86	.x5	-1.20	.x6	0.982	
Burlington	-15.41	+	4.82	.x1	-0.003	.x2	-0.923	.x3	+	3.95	.x4	-0.114	.x1^2	+	0.058	.x3^2	-16.52	.x4^(1/2)	+	1.20	.x5	-1.63	.x6	0.985	
Chicago	-10.00	+	4.25	.x1	-0.005	.x2	-0.502	.x3	+	3.86	.x4	-0.099	.x1^2	+	0.049	.x3^2	-16.99	.x4^(1/2)	+	1.38	.x5	-1.52	.x6	0.990	
Duluth	-43.07	+	8.05	.x1	-0.004	.x2	-1.235	.x3	+	5.10	.x4	-0.190	.x1^2	+	0.059	.x3^2	-20.88	.x4^(1/2)	+	1.50	.x5	-1.68	.x6	0.983	
ElPaso	6.28	+	1.37	.x1	-0.004	.x2	+	0.163	.x3	+	2.16	.x4	-0.029	.x1^2	+	0.052	.x3^2	-10.98	.x4^(1/2)	+	1.83	.x5	-0.56	.x6	0.994
Fairbanks	-24.12	+	7.51	.x1	-0.003	.x2	-1.241	.x3	+	5.33	.x4	-0.179	.x1^2	+	0.044	.x3^2	-23.47	.x4^(1/2)	+	0.97	.x5	-3.09	.x6	0.994	
Helena	-29.75	+	6.59	.x1	-0.005	.x2	-1.044	.x3	+	3.92	.x4	-0.154	.x1^2	+	0.055	.x3^2	-17.40	.x4^(1/2)	+	-2.06	.x5	-5.04	.x6	0.966	
Houston	15.57	+	0.12	.x1	-0.003	.x2	+	0.928	.x3	+	1.66	.x4	-0.001	.x1^2	+	0.029	.x3^2	-8.67	.x4^(1/2)	+	1.19	.x5	-0.65	.x6	0.999
Memphis	-9.56	+	3.26	.x1	-0.004	.x2	+	0.265	.x3	+	2.46	.x4	-0.072	.x1^2	+	0.041	.x3^2	-12.62	.x4^(1/2)	+	1.29	.x5	-1.02	.x6	0.995
Miami	13.44	-0.03	.x1	0.000	.x2	+	1.685	.x3	+	1.38	.x4	+	0.001	.x1^2	+	0.003	.x3^2	-7.38	.x4^(1/2)	+	1.15	.x5	-0.49	.x6	0.999
Phoenix	40.67	-1.39	.x1	-0.002	.x2	+	1.035	.x3	+	2.50	.x4	+	0.033	.x1^2	+	0.025	.x3^2	-13.49	.x4^(1/2)	+	1.82	.x5	-1.11	.x6	0.999

Table 7.5: The regression models for the residential HVAC Schedule in all climates (Data: 19°C ≤ Melting Temperature < 25°C)

OFFICE																								R2Adj		
Albuquerque	51.12	-3.15	.x1	-0.001	.x2	+	0.32	.x3	+	0.35	.x4	0.07	.x1 ²	+	0.04	.x3 ²	-5.34	.x4 ^(1/2)	+	1.32	.x5	-1.27	.x6	0.998		
Baltimore	60.86	-3.33	.x1	-0.001	.x2	+	0.02	.x3	+	1.48	.x4	0.07	.x1 ²	+	0.04	.x3 ²	-8.43	.x4 ^(1/2)	+	0.94	.x5	-1.20	.x6	0.997		
Boise	-0.38	+	1.24	.x1	+	0.000	.x2	-0.30	.x3	+	2.52	.x4	-0.02	.x1 ²	+	0.04	.x3 ²	-10.12	.x4 ^(1/2)	+	1.13	.x5	-1.16	.x6	0.988	
Burlington	70.05	-3.71	.x1	+	0.000	.x2	-0.52	.x3	+	3.27	.x4	+	0.08	.x1 ²	+	0.04	.x3 ²	-12.43	.x4 ^(1/2)	+	0.84	.x5	-1.29	.x6	0.976	
Chicago	112.91	-6.91	.x1	-0.001	.x2	-0.38	.x3	+	3.02	.x4	+	0.14	.x1 ²	+	0.04	.x3 ²	-12.47	.x4 ^(1/2)	+	0.95	.x5	-1.29	.x6	0.989		
Duluth	-8.62	+	2.70	.x1	+	0.000	.x2	-0.91	.x3	+	4.44	.x4	-0.05	.x1 ²	+	0.05	.x3 ²	-16.67	.x4 ^(1/2)	+	1.03	.x5	-1.35	.x6	0.952	
ElPaso	95.33	-6.55	.x1	0.000	.x2	0.48	.x3	+	0.32	.x4	+	0.13	.x1 ²	+	0.03	.x3 ²	-5.76	.x4 ^(1/2)	+	1.19	.x5	-0.87	.x6	0.999		
Fairbanks	-66.00	+	8.20	.x1	+	0.000	.x2	-1.32	.x3	+	5.14	.x4	-0.15	.x1 ²	+	0.05	.x3 ²	-20.93	.x4 ^(1/2)	+	0.63	.x5	-2.58	.x6	0.985	
Helena	19.47	+	0.20	.x1	+	0.000	.x2	-0.73	.x3	+	3.51	.x4	+	0.00	.x1 ²	+	0.05	.x3 ²	-13.03	.x4 ^(1/2)	+	1.03	.x5	-1.17	.x6	0.967
Houston	178.79	-12.38	.x1	-0.001	.x2	+	1.06	.x3	+	1.58	.x4	+	0.24	.x1 ²	+	0.02	.x3 ²	-8.81	.x4 ^(1/2)	+	1.12	.x5	-0.74	.x6	0.999	
Memphis	89.40	-5.59	.x1	-0.001	.x2	+	0.28	.x3	+	1.15	.x4	+	0.11	.x1 ²	+	0.03	.x3 ²	-7.95	.x4 ^(1/2)	+	0.87	.x5	-1.02	.x6	0.999	
Miami	214.03	-15.55	.x1	-0.001	.x2	+	1.87	.x3	+	0.36	.x4	+	0.30	.x1 ²	+	0.01	.x3 ²	-4.95	.x4 ^(1/2)	+	0.89	.x5	-0.82	.x6	0.999	
Phoenix	34.08	-1.09	.x1	-0.001	.x2	+	0.88	.x3	+	2.10	.x4	+	0.03	.x1 ²	+	0.03	.x3 ²	-12.45	.x4 ^(1/2)	+	1.28	.x5	-1.48	.x6	1.000	

Table 7.6: The regression models for the office HVAC schedule in all climates (Data: Melting Temperature $\geq 25^{\circ}\text{C}$)

RESIDENTIAL																									R2Adj	
Albuquerque	78.80	-4.33	.x1	-0.002	.x2	+	0.34	.x3	+	1.84	.x4	+	0.09	.x1 ²	+	0.03	.x3 ²	-11.52	.x4 ^(1/2)	+	2.09	.x5	-0.96	.x6	0.993	
Baltimore	108.79	-6.14	.x1	+	0.000	.x2	+	0.10	.x3	+	2.51	.x4	+	0.12	.x1 ²	+	0.04	.x3 ²	-13.72	.x4 ^(1/2)	+	1.37	.x5	-1.34	.x6	0.994
Boise	-29.76	4.49	.x1	+	0.000	.x2	-0.39	.x3	+	3.66	.x4	-0.08	.x1 ²	+	0.05	.x3 ²	-15.77	.x4 ^(1/2)	+	1.69	.x5	-1.38	.x6	0.98		
Burlington	16.44	+	1.47	.x1	+	0.000	.x2	-0.58	.x3	+	4.43	.x4	-0.03	.x1 ²	+	0.05	.x3 ²	-17.76	.x4 ^(1/2)	+	1.13	.x5	-1.76	.x6	0.974	
Chicago	24.06	+	0.83	.x1	+	0.000	.x2	-0.21	.x3	+	4.06	.x4	-0.02	.x1 ²	+	0.04	.x3 ²	-17.81	.x4 ^(1/2)	+	1.28	.x5	-1.63	.x6	0.988	
Duluth	-14.91	+	4.33	.x1	+	0.000	.x2	-0.97	.x3	+	5.54	.x4	-0.08	.x1 ²	+	0.05	.x3 ²	-22.00	.x4 ^(1/2)	+	1.39	.x5	-1.87	.x6	0.945	
ElPaso	128.23	-8.33	.x1	-0.001	.x2	+	0.56	.x3	+	1.63	.x4	0.16	.x1 ²	+	0.03	.x3 ²	-10.47	.x4 ^(1/2)	+	1.62	.x5	-0.78	.x6	0.998		
Fairbanks	-43.20	+	7.37	.x1	+	0.000	.x2	-1.11	.x3	+	5.30	.x4	-0.14	.x1 ²	+	0.04	.x3 ²	-23.18	.x4 ^(1/2)	+	0.86	.x5	-3.21	.x6	0.975	
Helena	6.24	+	2.43	.x1	+	0.000	.x2	-0.74	.x3	+	4.09	.x4	-0.04	.x1 ²	+	0.05	.x3 ²	-18.01	.x4 ^(1/2)	-2.63	.x5	-5.65	.x6	0.969		
Houston	178.79	-12.38	.x1	-0.001	.x2	+	1.06	.x3	+	1.58	.x4	+	0.24	.x1 ²	+	0.02	.x3 ²	-8.81	.x4 ^(1/2)	+	1.12	.x5	-0.74	.x6	0.999	
Memphis	127.21	-7.76	.x1	-0.001	.x2	+	0.49	.x3	+	2.22	.x4	+	0.15	.x1 ²	+	0.03	.x3 ²	-12.41	.x4 ^(1/2)	+	1.19	.x5	-1.14	.x6	0.998	
Miami	208.15	-15.01	.x1	-0.001	.x2	+	1.71	.x3	+	1.37	.x4	+	0.29	.x1 ²	+	0.00	.x3 ²	-7.20	.x4 ^(1/2)	+	1.13	.x5	-0.49	.x6	1	
Phoenix	82.53	-4.21	.x1	-0.002	.x2	+	1.13	.x3	+	2.62	.x4	+	0.08	.x1 ²	+	0.02	.x3 ²	-14.10	.x4 ^(1/2)	+	1.76	.x5	-1.19	.x6	0.999	

Table 7.7: The regression models for the office HVAC schedule in all climates (Data: Melting Temperature $\geq 25^{\circ}\text{C}$)

OFFICE - NO PCM													R2 Adj	
Albuquerque	18.17	-0.18	.x3	-3.52	.x4 +	0.05	.x3^2	1.61	.x5	-1.34	.x6 +	0.11	.x3.x4	0.997
Baltimore	19.22	-0.18	.x3	-3.55	.x4 +	0.04	.x3^2	0.91	.x5	-1.45	.x6 +	0.10	.x3.x4	0.998
Boise	17.89	-0.55	.x3	-3.13	.x4 +	0.04	.x3^2	1.16	.x5	-1.38	.x6 +	0.12	.x3.x4	0.994
Burlington	20.05	-0.81	.x3	-3.25	.x4 +	0.04	.x3^2	0.90	.x5	-1.40	.x6 +	0.14	.x3.x4	0.991
Chicago	21.52	-0.65	.x3	-3.62	.x4 +	0.04	.x3^2	1.00	.x5	-1.44	.x6 +	0.13	.x3.x4	0.992
Duluth	24.46	-1.27	.x3	-4.48	.x4 +	0.05	.x3^2	1.10	.x5	-1.51	.x6 +	0.20	.x3.x4	0.993
ElPaso	14.52	0.35	.x3	-3.07	.x4 +	0.04	.x3^2	1.14	.x5	-1.12	.x6 +	0.01	.x3.x4	0.991
Fairbanks	35.35	-1.58	.x3	-5.11	.x4 +	0.05	.x3^2	0.63	.x5	-2.73	.x6 +	0.17	.x3.x4	0.999
Helena	20.65	-1.03	.x3	-3.48	.x4 +	0.05	.x3^2	1.08	.x5	-1.31	.x6 +	0.16	.x3.x4	0.991
Houston	14.05	+ 0.73	.x3	-2.97	.x4 +	0.03	.x3^2	0.76	.x5	-1.08	.x6 +	0.05	.x3.x4	0.990
Memphis	17.16	+ 0.17	.x3	-3.19	.x4 +	0.03	.x3^2	0.84	.x5	-1.18	.x6 +	0.05	.x3.x4	0.999
Miami	13.74	+ 1.69	.x3	-2.63	.x4 +	0.01	.x3^2	0.86	.x5	-1.05	.x6 +	0.04	.x3.x4	0.999
Phoenix	19.08	+ 0.84	.x3	-3.74	.x4 +	0.03	.x3^2	1.01	.x5	-1.76	.x6	-0.01	.x3.x4	0.999
San Fran	8.28	-0.69	.x3	-1.70	.x4 +	0.07	.x3^2	0.50	.x5	-0.66	.x6 +	0.00	.x3.x4	0.991
Seattle	14.09	-0.53	.x3	-2.04	.x4 +	0.04	.x3^2	0.50	.x5	-1.19	.x6 +	0.00	.x3.x4	0.984

Table 7.8: The regression models for the office HVAC schedule in all climates - Without PCM.

RESIDENTIAL - NO PCM													R2 Adj	
Albuquerque	22.58	-0.35	.x3	-4.20	.x4 +	0.05	.x3^2	2.21	.x5	-0.97	.x6 +	0.16	.x3.x4	0.997
Baltimore	26.03	-0.33	.x3	-4.75	.x4 +	0.04	.x3^2	1.42	.x5	-1.43	.x6 +	0.14	.x3.x4	0.997
Boise	25.19	-0.75	.x3	-4.32	.x4 +	0.05	.x3^2	1.74	.x5	-1.48	.x6 +	0.12	.x3.x4	0.989
Burlington	27.00	-0.95	.x3	-3.86	.x4 +	0.05	.x3^2	1.17	.x5	-1.79	.x6 +	0.09	.x3.x4	0.988
Chicago	27.93	-0.63	.x3	-4.59	.x4 +	0.05	.x3^2	1.33	.x5	-1.69	.x6 +	0.12	.x3.x4	0.993
Duluth	31.25	-1.27	.x3	-4.71	.x4 +	0.05	.x3^2	1.44	.x5	-1.92	.x6 +	0.11	.x3.x4	0.983
ElPaso	19.66	+ 0.06	.x3	-4.15	.x4 +	0.04	.x3^2	1.69	.x5	-0.84	.x6 +	0.12	.x3.x4	0.998
Fairbanks	40.77	-1.22	.x3	-4.87	.x4 +	0.04	.x3^2	0.89	.x5	-3.27	.x6 +	0.06	.x3.x4	0.993
Helena	32.35	-1.02	.x3	-4.43	.x4 +	0.05	.x3^2	-2.97	.x5	-6.11	.x6 +	0.09	.x3.x4	0.974
Houston	15.01	+ 0.77	.x3	-3.09	.x4 +	0.03	.x3^2	1.15	.x5	-0.78	.x6 +	0.09	.x3.x4	0.999
Memphis	22.24	+ 0.15	.x3	-4.12	.x4 +	0.04	.x3^2	1.21	.x5	-1.19	.x6 +	0.11	.x3.x4	0.998
Miami	8.97	+ 1.65	.x3	-1.80	.x4 +	0.00	.x3^2	1.15	.x5	-0.50	.x6 +	0.01	.x3.x4	0.998
Phoenix	20.73	+ 0.87	.x3	-4.11	.x4 +	0.02	.x3^2	1.77	.x5	-1.26	.x6 +	0.07	.x3.x4	0.998
San Fran	10.96	-0.94	.x3	-2.12	.x4 +	0.06	.x3^2	0.88	.x5	-0.49	.x6 +	0.04	.x3.x4	0.981
Seattle	20.44	-0.83	.x3	-3.51	.x4 +	0.04	.x3^2	0.94	.x5	-1.26	.x6 +	0.09	.x3.x4	0.973

Table 7.9: The regression models for the residential HVAC schedule in all climates - Without PCM.

The regression models for the cases of using and when not using PCM boards were used in conjunction to see how closely the predicted data matched the actual data. The percentage energy saved were plotted for each building in all the climates and a few representative examples can be seen in Figures 7.5, 7.6 and 7.7.

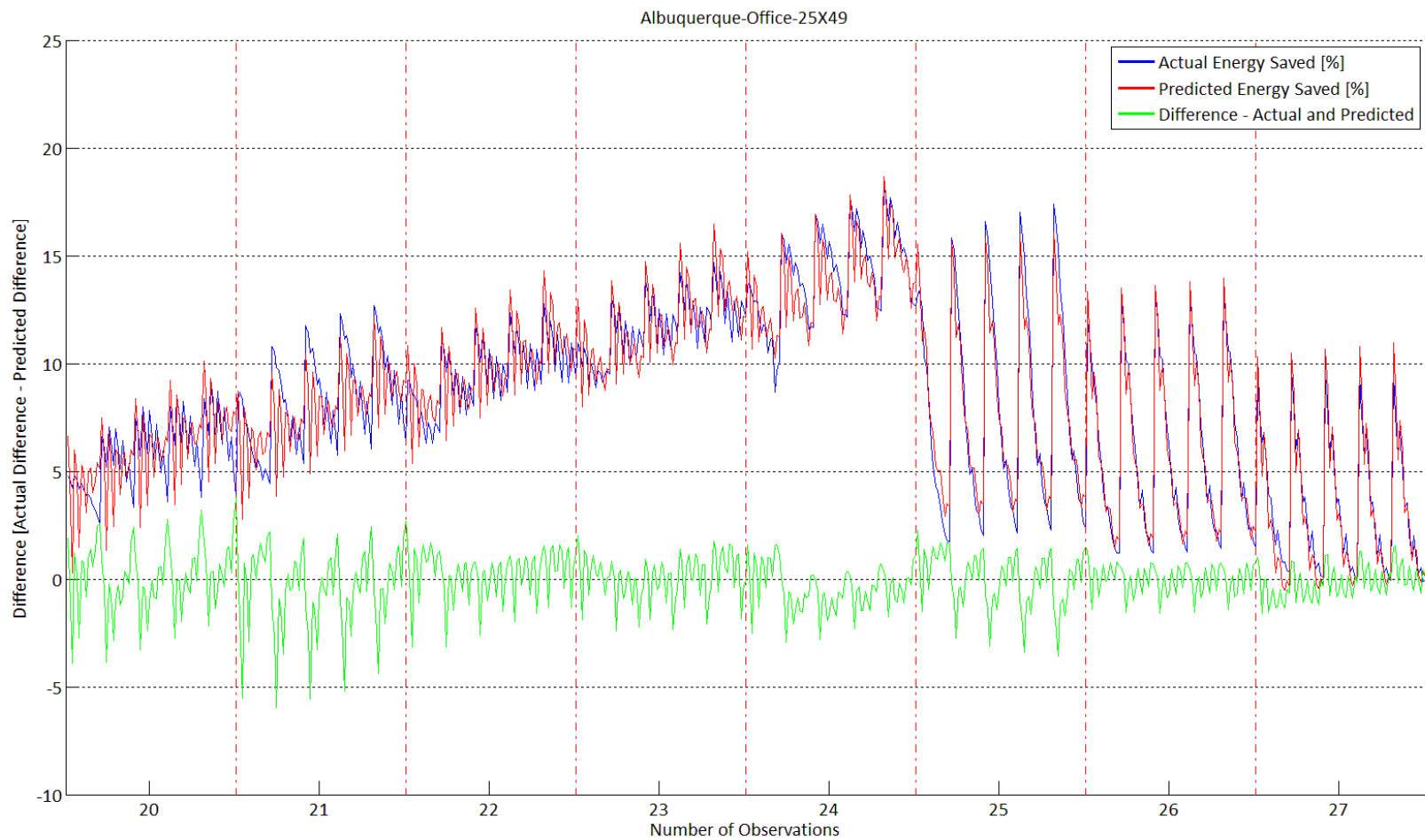


Figure 7.5: Difference in actual and predicted percent energy saved for the 25' X 49' building in Albuquerque with an office HVAC set-point schedule.

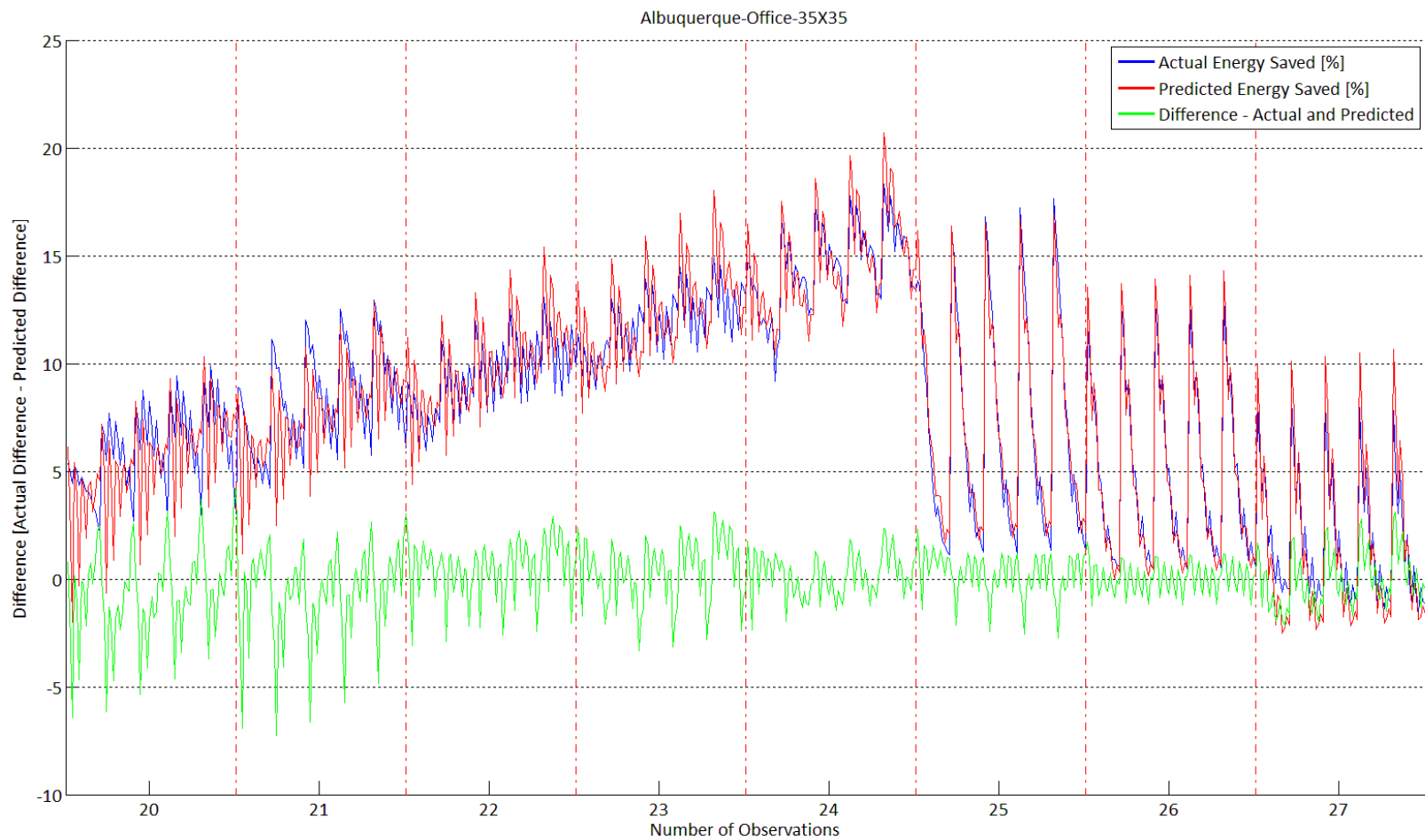


Figure 7.6: Difference in actual and predicted percent energy saved for the 35' X 35' building in Albuquerque with an office HVAC set-point schedule.

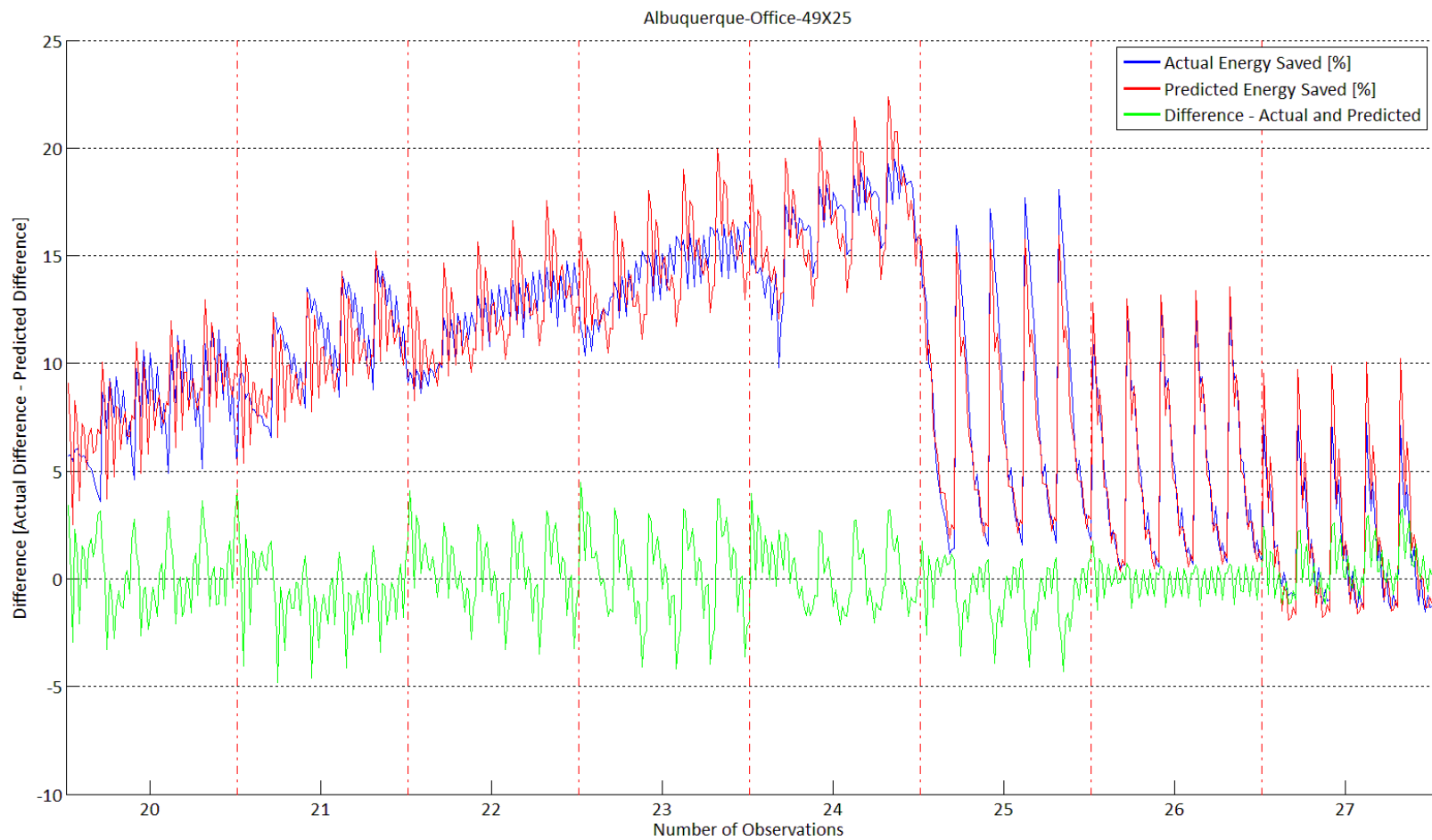


Figure 7.7: Difference in actual and predicted percent energy saved for the 49' X 25' building in Albuquerque with an office HVAC set-point schedule

Similar to Figures 7.5, 7.6 and 7.7 all the regression models were plotted against the actual data to see how closely the predicted values matched the actual ones. For the sake of brevity, the plots for the other climates and buildings are not included here, however it was found that the difference between the predicted and actual data in terms of percent energy saved was always in between $\pm 5\%$ for all the climates. The regression models can therefore be connected to the concept of climate maps as developed in chapter 4, thereby allowing engineers and architects to quickly visualize what type of percent energy savings they can expect if they so choose to employ PCM boards in their buildings; staying within the constraints imposed by the independent variables.

While the development of regression models could serve as a tool to quickly compute or visualize the percent energy saving potential with the application of PCM boards, not all climates offered the opportunity of substantial savings. It can be seen from the regression models in table 7.8 and 7.9 i.e., the β_0 terms in the regression models that the buildings with the residential HVAC set-point schedules generally require more annual energy to meet the set-point temperatures as opposed to the office HVAC set-point schedules. The regression models that were developed for each city will help predict the percent energy savings for similar climate types for the levels of independent variables defined within the scope of this study. This unique study therefore helps predict energy savings in buildings based on independent variables such as PCM melting temperature, PCM heat storage capacity etc. In order to better understand and filter the optimum climate, a payback period analysis would help narrow down the climates where the application of PCM boards would work best for this particular type of building.

People - internal loads

From the results obtained the preceding section, it was found that the optimum melting temperature for the PCM board changed with the increase or decrease in internal loads. In this

section the effect of internal loads is analyzed. Initially the experimental design only included 6 levels of the internal load (0, 5, 7, 10, 12 and 15 people), each dissipating 120 Joules of energy every second. With the data at hand, plots were generated for the percent energy saved for each level of internal loads. For the sake of brevity, only the plot for Albuquerque - Office HVAC schedule is included here. Figure 7.8 shows the change in percent energy saved across the melting temperatures for individual level of internal loads.

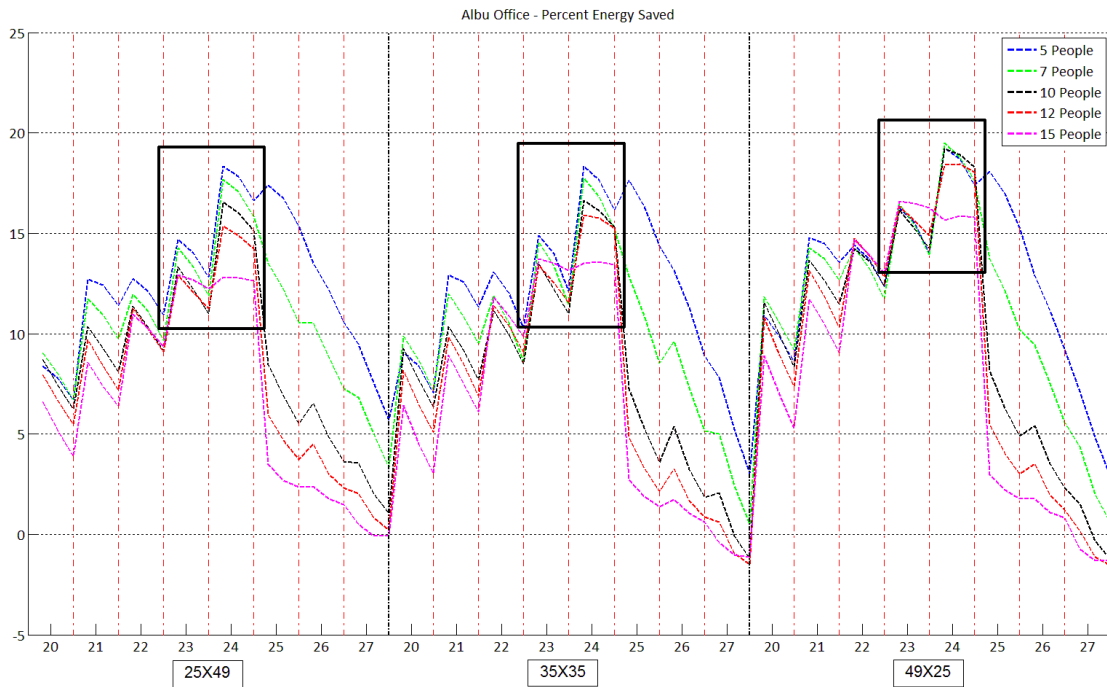


Figure 7.8: Albuquerque - office HVAC - percent energy saved for levels of internal loads.

In Figure 7.8 the percent energy saved for all three aspect ratios seems to be highest when the PCM melting temperature of PCM is 24°C. However for the case when there are 15 people indoors, the PCM melting at 23°C seems to perform better than with PCM melting at 24°C. The hidden variable in each column for the melting temperature is the R-value of insulation. The plot includes information on the three levels of R-value (i.e., Low, Medium and High). It is also evident from the columns in Figure 7.8 that increasing the R-value on the surfaces with PCM

boards does not automatically translate to an increase in percent energy saved. In fact, a higher percent energy is saved when the R-value of the insulation is kept at its prescribed level.

Since it seemed like the assumption of 24°C being the optimum PCM melting temperature was incorrect for increased internal loads, three more levels of people were added to the study. The 3 additional levels (i.e., 18, 21 and 24 people) were added to see how this would affect the optimum PCM melting temperature in each climate.

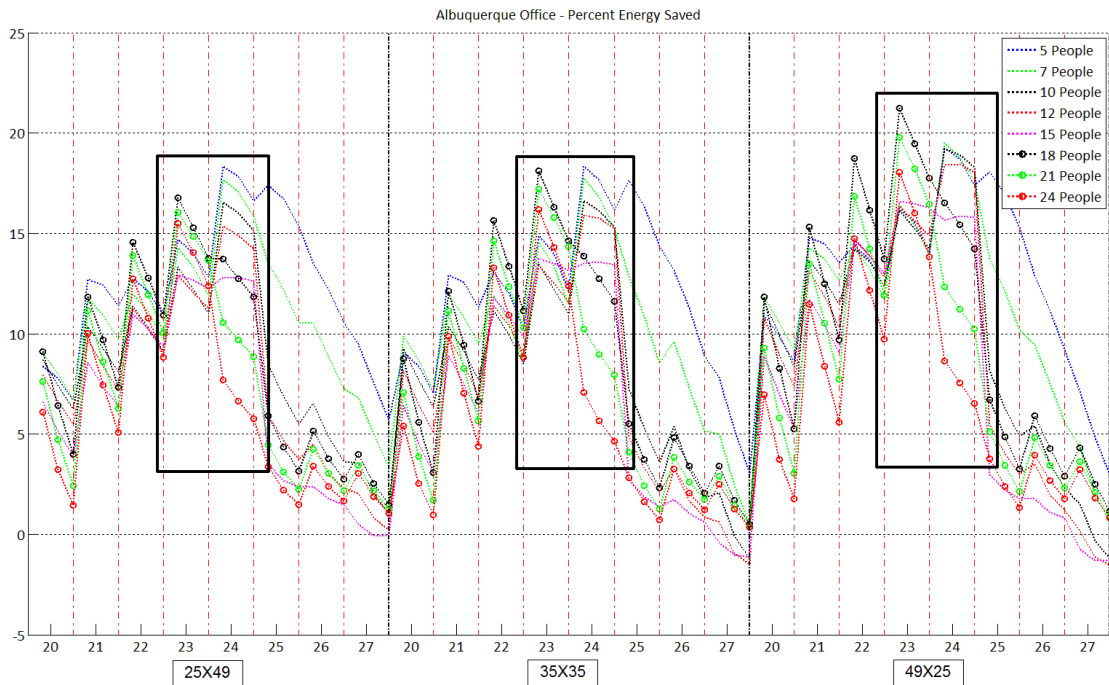


Figure 7.9: Albuquerque - office HVAC - percent energy saved for additional levels of internal loads.

Evident in Figure 7.9 is the results obtained from adding three more levels to the internal load was then added to the plot of the original levels (Figure 7.8). The black box that encompasses the data points was placed there to emphasize the two melting temperatures where the most energy savings was recorded. As soon as the internal loads increased from 12 to 15 people and above, 23°C overtook 24°C as the new optimum melting temperature. In order to get a better picture of the changes in optimum melting temperature, the magnitude of energy saved is also taken into consideration and not just the percent saved.

In Figure 7.10 each bar plot represents the magnitude of energy saved for different internal loads for climate 4b (Albuquerque). From top to bottom, the sub-plots are for, 0 people, 10 people, 15 people, 18 people, 21 people and 24 people. The upper limit for the y-axis is 7 gigajoules and the three bars inside of each column for the melting temperature represent the magnitude of energy saved for the three different R-values. When the internal load is zero, the optimum melting temperature is 25°C, saving approximately 3 gigajoules (approximately 23% of 12.14 gigajoules) for the when the R-value for each building aspect ratio is *low*. At 10 people indoors the optimum melting temperature suddenly jumps to 24°C. As internal load is increased in the subsequent sub-plots the magnitude of energy saved keep increasing and the optimum melting temperature starts shifting to 23°C. The maximum load saved is approximately 7 gigajoules (18% of 39.5 gigajoules) and the optimum melting temperature remains 23°C as evident in the final subplot.

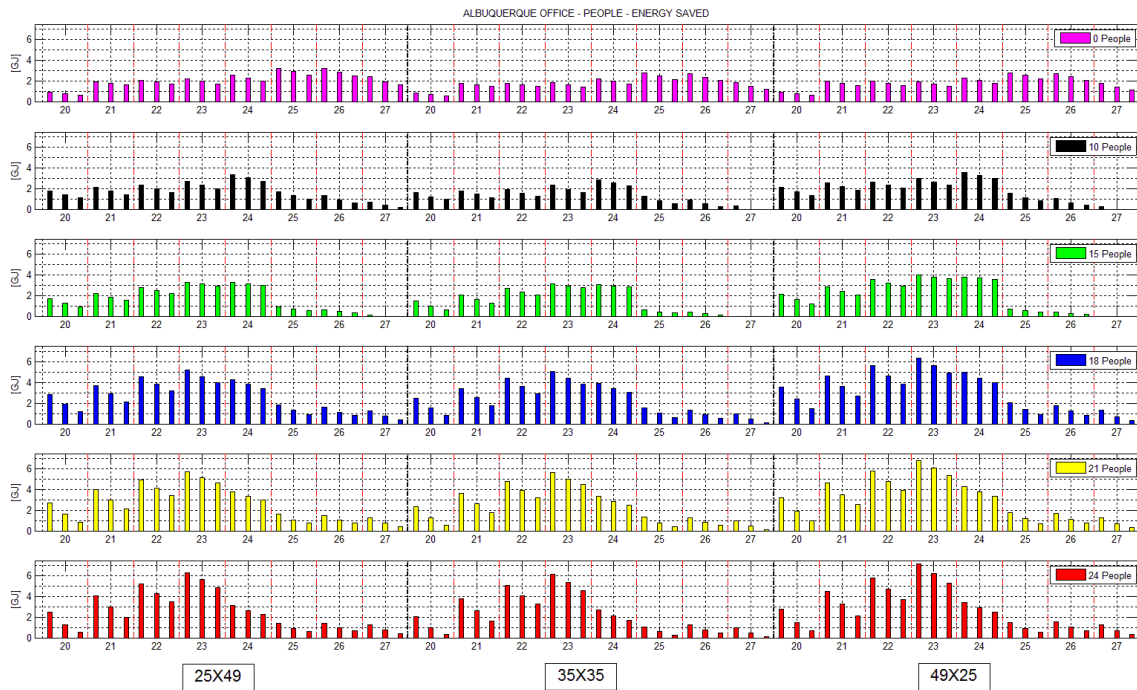


Figure 7.10: Albuquerque - office HVAC – magnitude energy saved for additional levels of internal loads.

Similar trend is witnessed for climate 3c (San Francisco) evident in Figure 7.11. The plots for all the other cases can be found in appendix E.

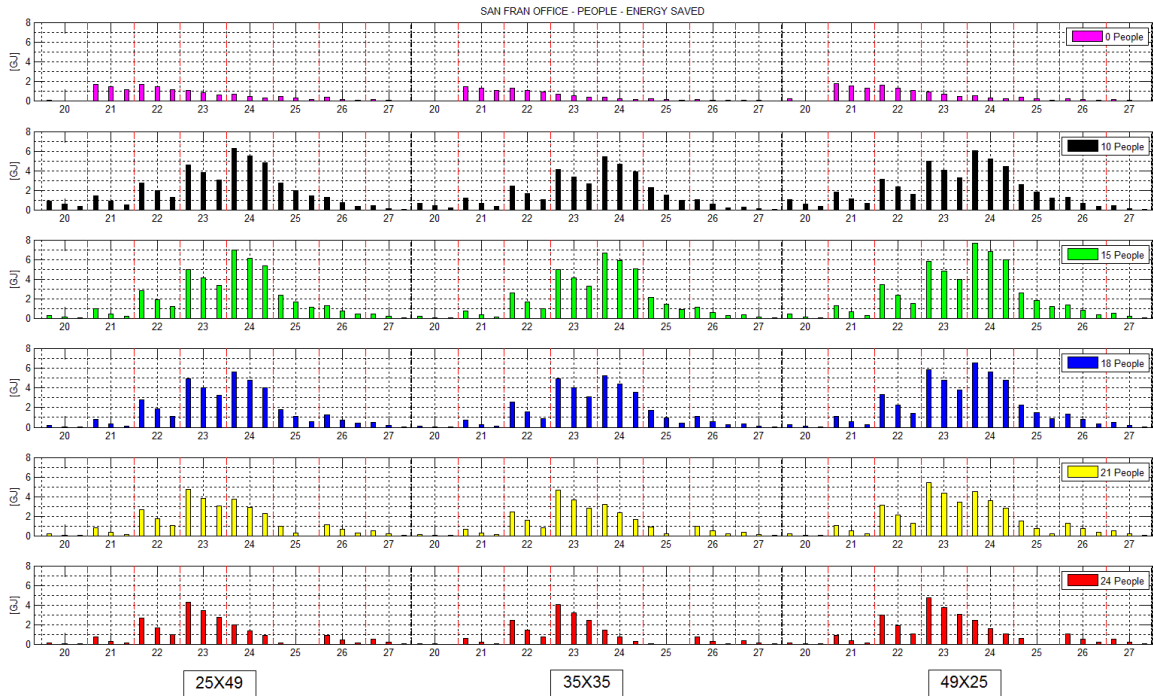


Figure 7.11: San Francisco - office HVAC – magnitude energy saved for additional levels of internal loads.

As shown in Figure 7.11, for the San Francisco office HVAC schedule, when there is no internal loads, the optimum melting temperature for the PCM is 21°C. When the internal load is increased to 10 and 15 people indoors, the optimum melting temperature then changes to 24°C. At 24°C, where the building is equipped with the minimum prescribed insulation, and when the internal load is 15 people, there is a savings of 8 gigajoules (67% of 11.49 gigajoules) of energy.

The ASHRAE 62.1 standard (2007) defines the default occupancy of 5 people every 1000 ft² in offices. For the 1225 ft² building in this study, any additional wattage beyond 6 people (i.e., 6 X 120 = 720 watts) can be considered additional load from lights and plug loads (i.e., Computers, Printers, Monitors etc). ASHRAE (2009) have developed representative rates at which heat and moisture are given off by human beings during different states of activity. Often these sensible and latent heat gains constitute a large fraction of the total load. For people

performing seated office work the adjusted total heat gain is 115 watts of which 70 watts is assigned for sensible heat gain and 45 watts for latent heat gain. The conversion of sensible heat gain from people to space cooling load is affected by the thermal storage characteristics of that space, latent heat gains are considered instantaneous (ASHRAE, 2009). The addition of people above 6 people can be considered lighting and plug loads.

The recommended maximum lighting power density (LPD) (Lighting heat gain per square foot) for an enclosed or open plan office is 1.1 W/ft² (Table 2, Chapter 18 ASHRAE Handbook of Fundamentals). For a 1225 ft² space the lighting power required is 1348 watts. Added to the wattage dissipated by the 6 people i.e., 720 + 1348 = 2068 watts the total wattage still is not equivalent to the wattage dissipated by 24 people (2880 watts). Approximately 800 watts is still unaccounted for.

For office equipment the actual power consumption is assumed to equal total (radiant and convective) heat gain. The actual power consumption was measured for desktop computers⁵ and by averaging all of all the desktops measured, each computer can be assumed to dissipate 100 watts of heat during moderate use. The remainder of the 800 watts that was unaccounted for can be taken up by the office electronic equipment. The 24 people can therefore take on the value of representative internal load for an office of size 1225 ft². For future studies the plug load schedule, lighting schedule and people occupancy schedule should take on a more representative profile to test how the optimum PCM changes with the change in each variable. In this study the internal loads generated in the conditioned space was left constant throughout the year.

For all the cases (seen in appendix E) it was evident that the optimum PCM melting temperature changed with the increase or decrease in internal loads. It is also necessary to analyze

⁵ For more information on the actual measurements please visit:

www.upenn.edu/computing/resources/category/hardware/article/computer-power-usage

how often the PCM melts and solidifies, when gradually increasing the internal load to the upper limit of 24 people, to better understand why the optimum melting changes with respect to continuous internal loads. The next chapter will focus on the frequency of melting and solidifying of PCM for the different cases.

Volumetric Heat Capacity - Enthalpy

From all the results it was evident that the higher the volumetric heat storage capacity the more the energy saved. However from Chen's (2008) study on the energy reduction potential of PCMs with respect to enthalpy, there seems to be an 'optimum' PCM enthalpy where any more addition of heat storage capacity shows diminishing returns. This trend is evident in Figure 7.12.

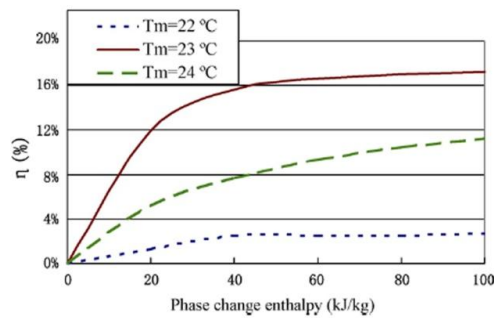


Figure 7.12: The percent energy saved for every 20 kJ/kg jump in enthalpy. (Chen, 2008)

It can be seen from in Figure 7.12 that the percent energy saved (denoted by η) starts to increase at a slower rate as soon as PCM enthalpy of 40 kJ/kg is used. Since it could not be verified whether the cost of PCM also depends on its volumetric heat capacity, it was assumed that there was a need to identify the maximum heat storage for these buildings per kJ/kg of heat storage capacity of PCM used. Apart from the San Francisco and Albuquerque office plots, all the remaining of the corresponding plots to this section can be found in Appendix F.

In order to grasp the amount of energy saved for every additional 20 kJ/kg of enthalpy the results from the building 49'X25' were used. From all previous plots, it was evident that there was not much difference in percentage of energy saved among the buildings with different aspect

ratios. This decision to only plot the results for the building 49'X25' was made to be able to see the differences clearly with less data on the plots. In addition the three bars in each temperature column correspond to only 5, 10 and 15 people as internal loads as seen in Figure 7.13. The R-value in the plots is for the building equipped with the minimum recommended R-value for the insulation. The first in the set of subplots (top subplot) is the corresponding energy saved for when using 20 kJ/kg of enthalpy. The subplot right below is a stacked subplot where the stacked portion in red corresponds to the additional amount of energy saved just by increasing the heat storage capacity of the PCM from 20kJ/kg to 40 kJ/kg. The stack in blue is the initial energy saved by using 20 kJ/kg. The addition of the red and the blue therefore makes up the total amount of energy saved by using the 40 kJ/kg PCM. Similarly the second subplot is the addition of energy saved by jumping from 40 kJ/kg to 60 kJ/kg and so forth.

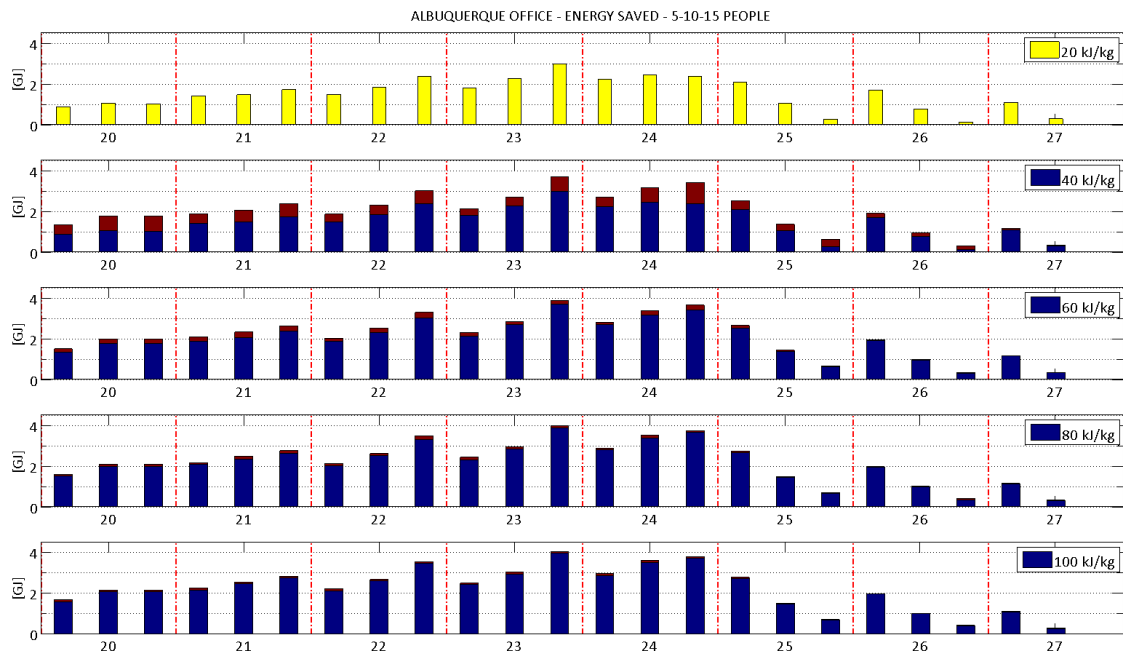


Figure 7.13: Albuquerque - office HVAC - magnitude energy saved for additional PCM enthalpy.

It can be seen in Figure 7.13 that any addition of volumetric heat storage capacity after 40 kJ/kg results in diminishing returns. When the PCM enthalpy is 20 kJ/kg and the number of people indoors is 15, there is a saving of 3 gigajoules of energy. When the PCM enthalpy is

increased to 40 kJ/kg, the same bar increases by approximately 0.8 gigajoules, as seen in red. However if the PCM enthalpy is further increased to 60 kJ/kg the increase in energy saved is hardly 0.1 gigajoules. By the time the enthalpy is increased to 80 kJ/kg and to then to 100 kJ/kg, any additional energy saved is barely visible in the plot. Similar situations were observed for all the other cases in the other climates. The results in Figure 7.13 were then converted from the magnitude of energy saved to dollars saved for every addition of volumetric heat storage capacity. The dollar value was again obtained by multiplying every unit of energy saved in kilowatt-hours by the cost of electricity for that particular city as listed in Table 5.1.

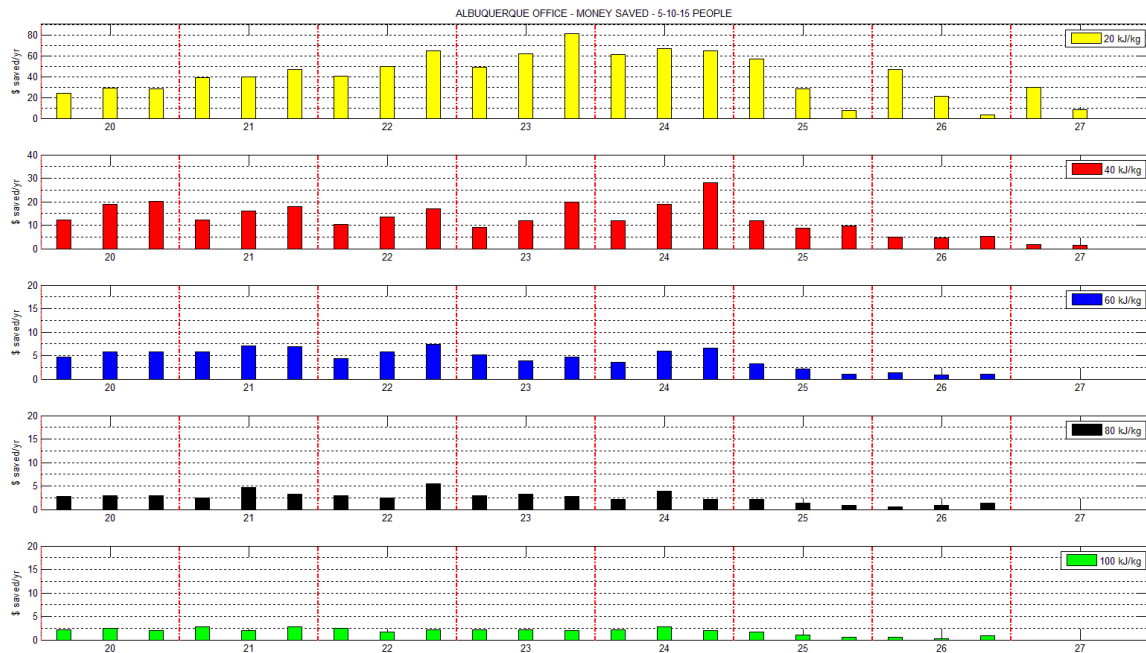


Figure 7.14: Albuquerque - Office HVAC - magnitude energy saved for additional PCM enthalpy.

In Figure 7.14 each subplot shows the money saved annually for the corresponding heat storage capacities of the PCM boards. The only difference from Figure 7.13 in this Figure is that each subplot (i.e., 20 kJ/kg, 40 kJ/kg etc) has no connection to each other. The money saved is the additional money saved from the previous subplot. For instance, the subplot for 20 kJ/kg (in yellow) shows the annual monetary savings for the various cases and the y-axis ranges from 0-80

dollars. The second subplot (in red), on the other hand, is for the PCM with 40 kJ/kg enthalpy. The y-axis only ranges from 0-40 dollars. The reason is because this subplot only shows the additional amount of money saved, from the previous subplot (in red), if the PCM with heat storage capacity is increased to 40 kJ/kg. In other words, if the volumetric heat storage capacity is increased from 20 kJ/kg to 40 kJ/kg, this is the amount of additional money that would be saved, the same goes for the third subplot (in blue). This is the amount of money that can be saved through energy consumption reduction if the heat storage capacity is increased from 40 kJ/kg to 60 kJ/kg. It can be seen that the y-axis range decreases to 0-20 dollars. By the time the 100 kJ/kg subplot is reached (in green), it is evident that there is at most 3 dollars of annual savings. The same trend can be found for the San Francisco office and residential HVAC schedules.

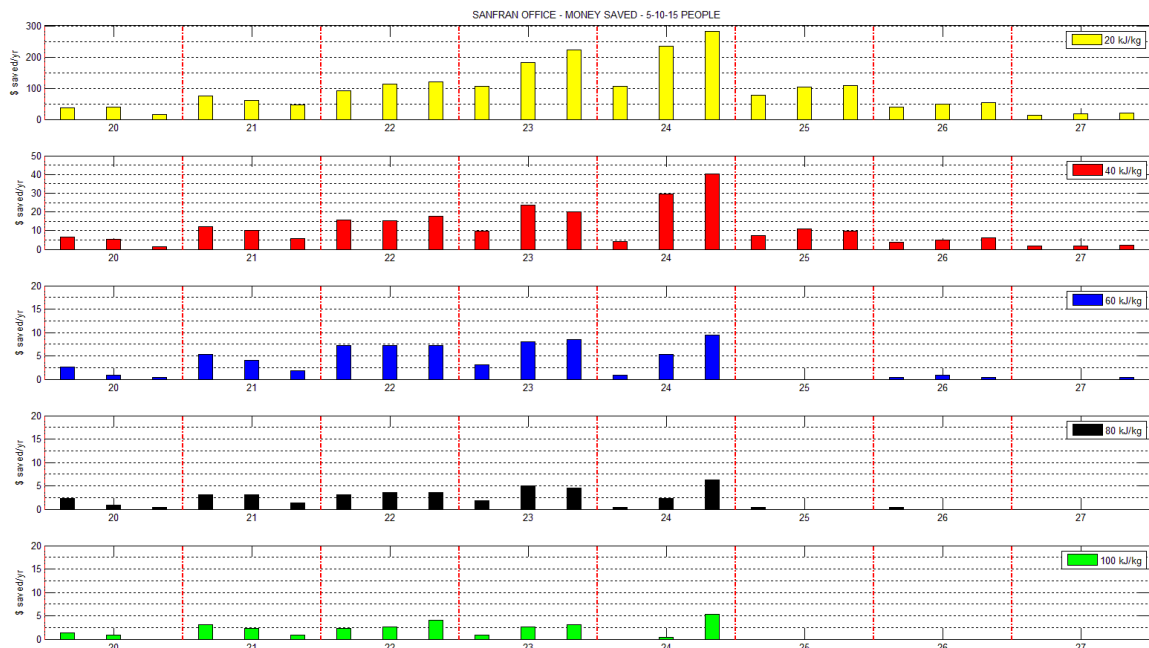


Figure 7.15: San Francisco - Office HVAC - money saved annually for additional PCM enthalpy.

In Figure 7.15 the y-axis ranges from 0-300 dollars for the first subplot (in yellow); the second subplot (in red) ranges from 0-50 dollars. And the rest range from 0-20 dollars. Similarly in Figure 7.16, for the San Francisco residential HVAC, the first subplot ranges from 0-250

dollars. The second subplot ranges from 0-40 dollars and the rest range from 0-20 dollars. The trend of diminishing returns is the same for these cases as well. The only difference is that the office HVAC schedule saves more energy, therefore more money, as opposed to the residential HVAC schedule (Figure 7.16), all the while everything else is kept constant. This is true even though the cost of electricity for commercial end use is cheaper than the residential end use categories for San Francisco.

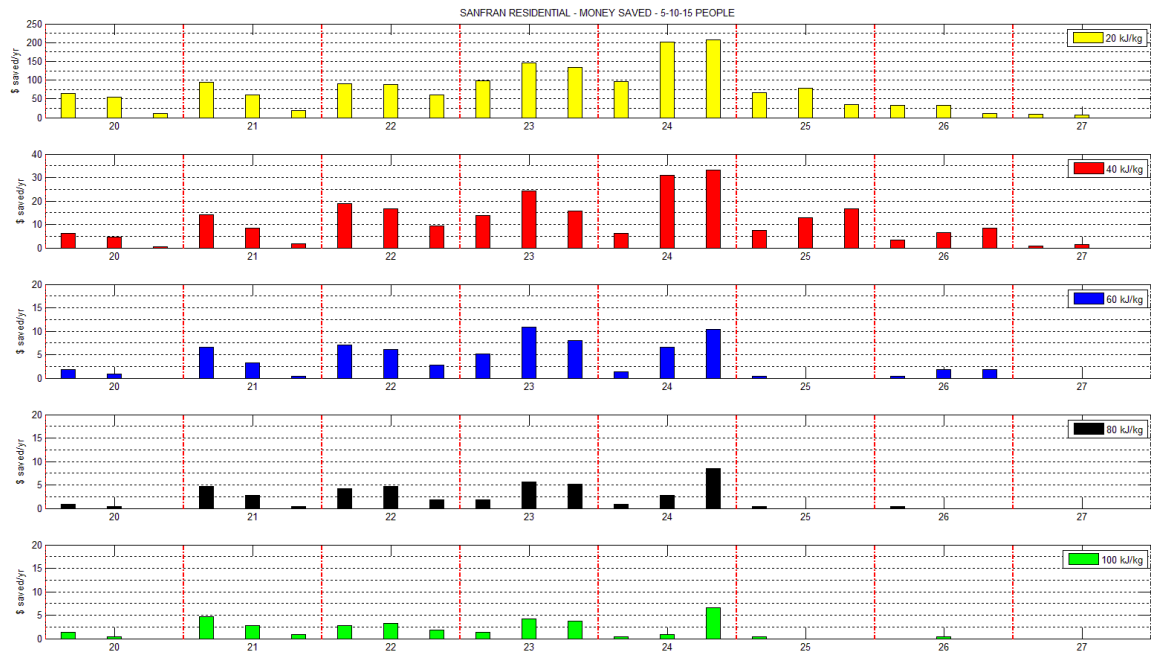


Figure 7.16: San Francisco - Residential HVAC - money saved annually for additional PCM enthalpy.

R-Value

The results obtained from the preceding sections show that increasing the R-value of insulation when PCM boards line the inside of the building is counterproductive. The magnitude of energy saved decreases with every addition of insulation capability. In other words, when the R-value of insulation is increased while PCM boards line the inside of the walls, there is a loss in savings with every addition in R-value. On the other hand, when there are no PCM boards lining the interior surface of the walls, an increase in R-value, for most climates, tends to increase the

magnitude in savings, nonetheless with diminishing returns. In order to be certain of this observation, plots were generated for the magnitude and percent energy saved when fitting the building with insulation of varying R-values.

In Figure 7.17 the top sub-plot corresponds to the percent energy saved corresponding to the different levels of R-value. The percent saved for the low R-value is always greater than the other two R-values. Similarly the lower subplot corresponds to the magnitude of energy saved corresponding to the different levels of R-value. The magnitude saved, too, is always greater for when the low R-valued insulation is used. Nonetheless, the percent energy saved and magnitude saved does not capture the whole picture. The increase in R-value could very well have reduced the total annual load for both, when PCM is used and when it is not. This reduction in total annual load for both cases could therefore lead to the low percent energy saved and low magnitude saved.

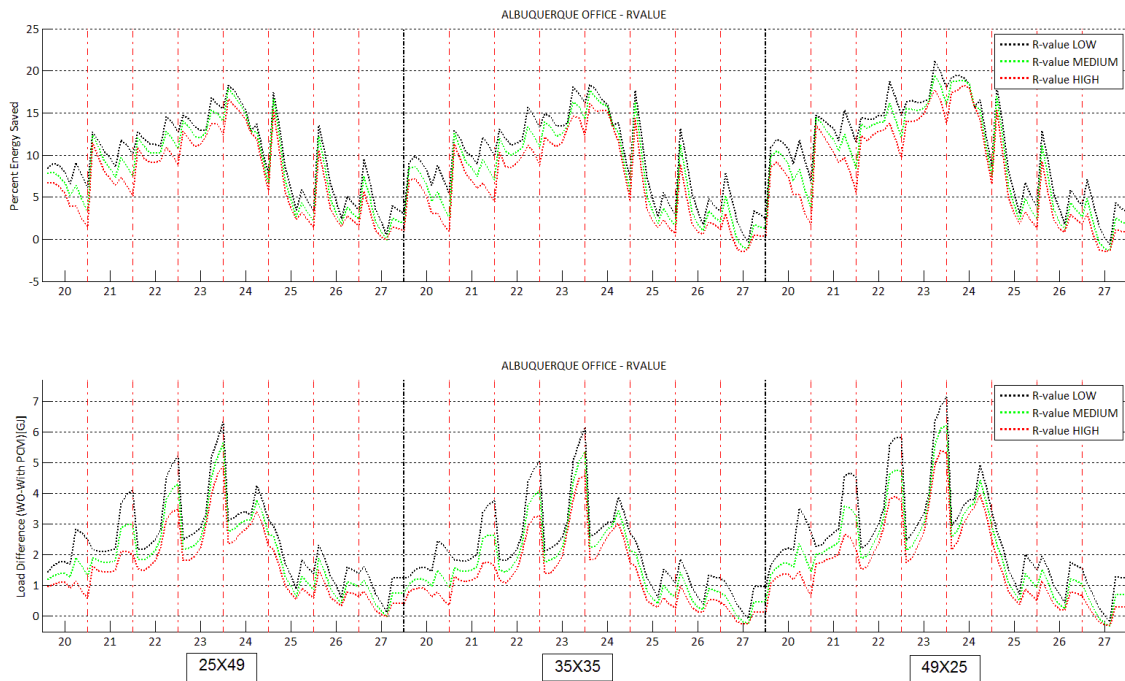


Figure 7.17: Albuquerque - office HVAC – percent Savings (Top) and magnitude Saved (bottom) for different PCM enhanced buildings with different R-value of insulation.

To verify that this was true for the case of Albuquerque – office HVAC, only the annual loads, with and without PCM, were plotted against each other as can be seen in Figure 7.18. As the number of people was increased, the PCM boards performed best when the R-value was at its prescribed minimum. This can be seen by focusing on the column for the 23°C melting temperature. The bar representing 24 people is emphasized by the green arrow. The annual load without PCM (top subplot) is highest when the minimum R-value is used. As the insulation R-value is increased from low (red), to medium (green) to high (blue), the annual load with PCM subsequently decreases for all the different cases of internal loads. An increase in R-value of insulation that resulted in a decrease in annual load is what was expected. Now, as soon as PCM boards were introduced inside the building, the case with the minimum R-value outperformed the other cases with higher insulation R-values. Similar conclusions could be drawn from the San Francisco cases. The performance of PCM was best when the R-value was at its minimum prescribed value stipulated in the ASHRAE 90.1 standard. The increase in R-value resulted in a decrease in the PCM performance.

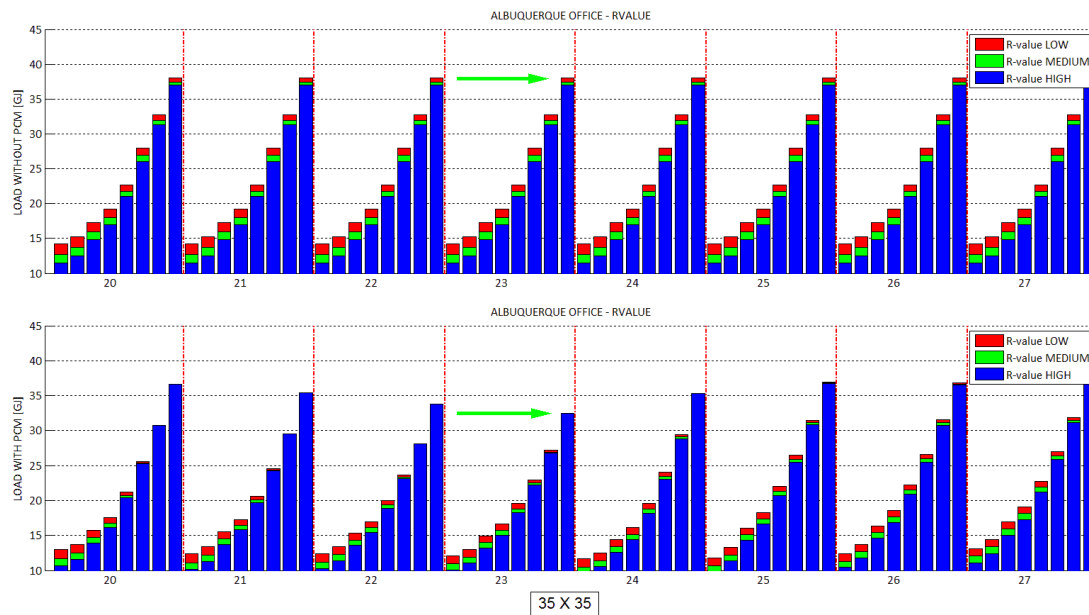


Figure 7.18: Albuquerque - office HVAC – annual Load without PCM (Top) and annual load with PCM (bottom) for different internal loads (5,7,10,12,15,18,21,24 people) in each column.

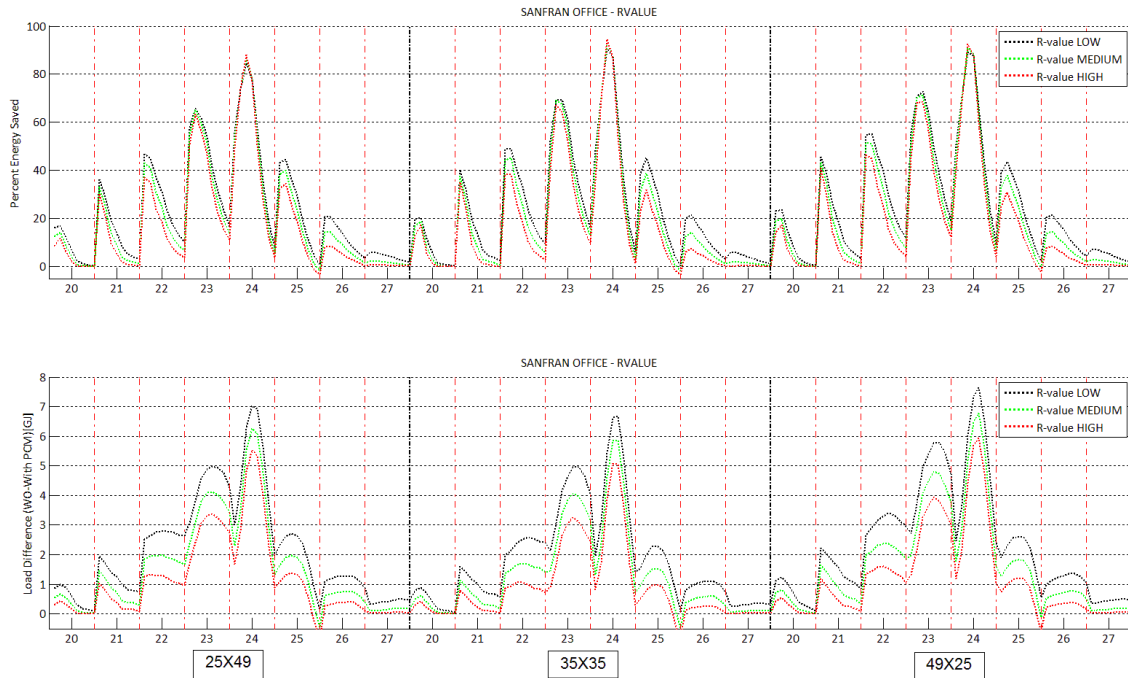


Figure 7.19: San Francisco - office HVAC – percent Savings (Top) and magnitude saved (bottom) for different PCM enhanced buildings with different R-value of insulation.

An inversely proportional relationship seemed to exist between the insulation R-value and PCM performance. Similar conclusions can be drawn when focusing on the case of 15 people occupying the office building in San Francisco. The highest savings in energy can be found for an internal load of 15 people and for the PCM melting at 24°C. As the internal loads are increased, however, the PCM melting at 23°C performs better (Already seen in section - 'People - Internal Loads'). In Figure 7.20 the increase in R-value results in a decrease in annual load (top subplot). However, for the cases where PCM boards are used (bottom subplot) the increase in R-value does not mean an automatic reduction in annual load when compared to cases where the R-value is at its prescribed minimum. In other words, any increase in R-value of the insulation seemed counterproductive in a room with PCM boards lining the inside of all walls and roof. A conclusion was developed to say that an increase in R-value does not lead to an increase in PCM performance, but rather a loss in energy saving potential.

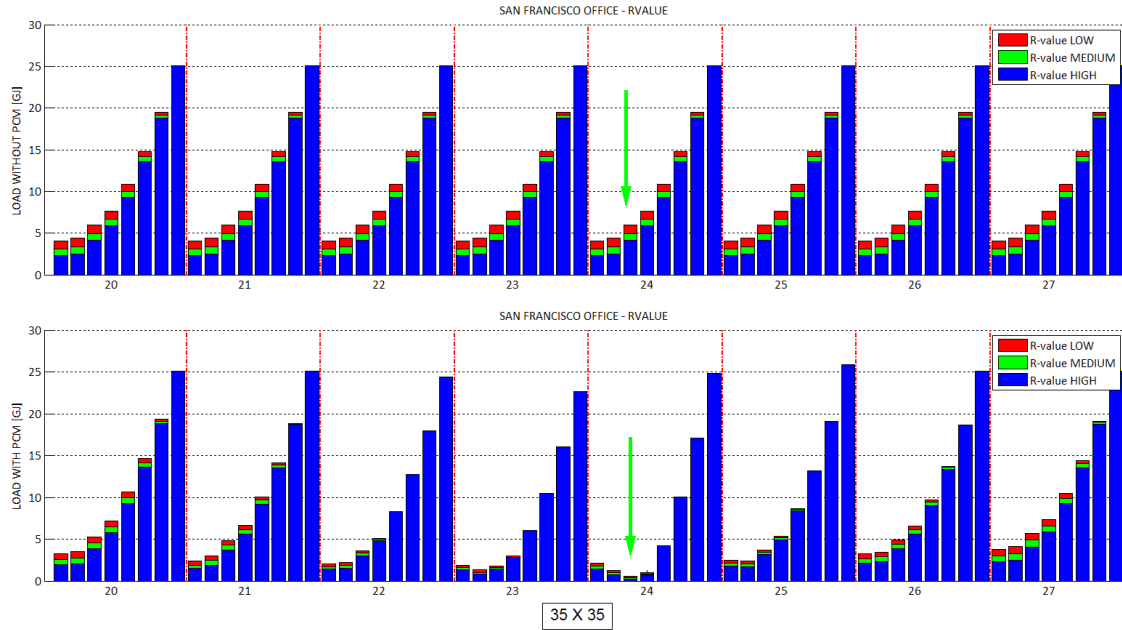


Figure 7.20: San Francisco - office HVAC – annual load without PCM (Top) and annual load with PCM (bottom) for different internal loads (5,7,10,12,15,18,21,24 people) in each column.

Conclusion

This chapter examined the actual data obtained from the full factorial design simulations, developed regression models for each climate that could, in a future study, be linked to the climate maps developed in Chapter 4. In addition this chapter also presented a simple pay-back period analysis to filter the optimum climates where PCM boards would perform best and then each independent variable and its effect on the PCM performance was studied individually.

- Regression Models: The data obtained from the full factorial design simulations were arranged on a climatological basis. The data was then split according to the *office* or *residential* HVAC setting. Another set of simulations were performed for the control group i.e., building without PCM. Regression models were then developed for the cases with PCM in each climate location for each HVAC type. The *data-split* at the 25°C melting temperature mark was optimal in defining the behaviour of PCM boards in the lightweight building with the different levels of independent variables. Similarly

regression models were developed for the control group. Once the models for the two cases (i.e., with PCM and without PCM) was developed, they were combined in order to predict the magnitude and percent energy savings in each climate.

The global test for the regression models (except for San Francisco and Seattle) at a significance level of α (Alpha) = 0.05 was found significant in predicting the annual load with and without PCM. The predicted values were within 5% of the actual data for all the models developed. Therefore the regression models when connected with the climate maps developed in Chapter 4, as well as the cost of energy in each city, can assist architects, engineers and researchers to quickly visualize the benefits and payback period of using PCM boards in the specific climates.

- Payback period: A simple payback period analysis was performed on each climate for the actual data obtained from the full factorial design simulations. The payback period was calculated for all the climates using the average retail price of electricity that is based on the end use sector, commercial or residential. Similarly, for the payback period analysis, the cost of PCM boards was allowed to take on a price much cheaper than what was communicated by a manufacturer here in the U.S (\$6/ft²). The PCMs boards were allowed to take on a price of \$0.50/ft², which is \$0.20/ft² more expensive than ordinary gypsum boards (\$0.30/ft²).

It was found that, for the assumed cost of PCM boards (which is still many folds cheaper than the actual cost of PCM boards), only the PCM boards placed in buildings with the office HVAC settings for the climate types represented by Albuquerque and San Francisco was below the 15 year payback period mark. While placing PCM boards in the same building located in Seattle showed considerable savings in energy, (approximately 36% of 11.92 gigajoules or 4.25 gigajoules saved by using 24-100-PCM (i.e., 24°C melting temperature and 100 kJ/kg enthalpy PCM) for 15 people occupying indoors and

the prescribed minimum R-value of insulation) the cheap cost of electricity for Seattle pushed the payback period over the 15 year mark. Therefore it was concluded that, until and unless the cost of energy increases or the cost of PCM boards decreases from the current levels, the viability of PCM boards in other climates besides the ones represented by Albuquerque and San Francisco seems unpromising.

- Internal Loads: Occupant behaviour is arguably the single greatest challenge to building energy researchers and analysts (O'Brien, 2011). While mathematical and physical models continue to increase to high levels of accuracy, there is still a lot of uncertainty on how building occupants behave to affect building energy use. Additionally, lighting and plug loads are beginning to dominate over envelope based loads. This chapter clearly identified the importance of occupant based loads on the proper selection of PCM melting temperature.

Different levels of internal loads were setup in order to understand the behavior of PCM boards in each climate. It was found that the optimum melting temperature of PCM boards changed with the increase or decrease in internal loads. This chapter concluded that while the external environment does play a role in determining the viability of Phase Change Materials, the optimal melting temperature of PCM boards is determined by the change in internal loads in the building. When the office building in San Francisco was occupied by 15 people indoors, the 24-100-PCM saved 8 gigajoules (67% of 11.49 gigajoules) of energy annually. As soon as the internal load is increased to 24 people occupying the indoors, the optimum PCM melting temperature switches to 23°C and saves only 4.8 gigajoules (19% of 25 gigajoules) annually. Similar results were observed for all the climates. The optimum melting temperature changed with the change in internal loads.

- R-value of insulation: It was found that for lightweight buildings lined with PCM boards on all walls and roof, the increase in R-value of the insulation was counter-productive and therefore not suitable for simultaneous operation with PCM boards. For most climates it was evident that increasing the insulation R-value by a factor of 1.25 could perform just as well, if not better than, placing PCM boards in the building. This was evident for most of the cases except for PCM boards placed in Albuquerque, El Paso, San Francisco and Seattle where the PCM boards performed better than when R-value of the insulation was increased by a factor of 1.5. On the other hand for the residential buildings, increasing the R-value of the insulation performed better than placing PCM boards in the building in all climates except for climate 3c represented by San Francisco.

The energy absorbed by the PCM boards' needs to be released for the PCM board to absorb energy on its next cycle. Ideally, in situation where the indoors needs to be cooled, the energy absorbed by the PCM is to be released outdoors. The greater the indoors is insulated from the outside, the PCM will therefore not get the proper opportunity to release the absorbed energy to the outdoors. For this very reason any increase in R-value after the prescriptive minimum prohibits the optimal functioning of PCM boards.

- Volumetric heat storage capacity (Enthalpy): The PCM boards were appended with 5 different levels of heat storage capacity. It was found from literature (Neeper, 2000; Chen, 2008) that the increase in volumetric heat storage capacity does not necessarily translate to a one-to-one increase in energy savings. From the study in this chapter it was found that, for all the cases, the energy savings increased at a decreasing rate after any increase in PCM heat storage capacity of 40 kJ/kg. Every 20 kJ/kg increase in heat storage capacity for the PCM yielded fewer and fewer monetary savings annually. Would an increase in heat transfer to and from the PCM boards alleviate this issue? This opened

up the possibility to test, but beyond the current scope, whether a decrease in surface thermal resistance of the PCM wallboard would facilitate a greater ability to exchange energy for the PCM boards with higher volumetric heat storage capacities.

Chapter Eight

PCM MELTING STUDY

In the previous chapter, it was found that climate 3c (San Francisco) and climate 4b (Albuquerque) exhibited the most energy savings with PCM boards lining the interior of lightweight buildings. Various other phenomena were observed as well. For instance, it was found that for all cases the optimum melting temperature of PCM varied with the change in internal loads. It was also evident that every addition of volumetric heat storage capacity (enthalpy) of PCM past the 40 kJ/kg mark resulted in diminishing returns. In addition, the PCM boards were most conducive when placed in buildings with an office thermostat schedule as opposed to a residential one.

In this chapter, in order to understand the major causes for the performance of PCMs, the melting and solidifying of PCM is studied against the increase or decrease in internal loads, exterior solar radiation and the times which HVAC system is called forth to service the indoor environment. This chapter therefore delves into how often the PCM melts throughout the year and also the months where the PCM boards absorb and release most energy. The loads are also analyzed to understand the behavior of PCM boards on a month by month basis. First the monthly loads are analyzed and then an hourly profile of the PCM board surface temperatures, on each facade, is looked into.

Monthly average indoor temperature and optimum PCM melting temperature

Neeper (2000) had analytically examined the thermal dynamics of a PCM wallboard that was subjected to the diurnal variation of the indoor room temperature. The PCM boards were not directly illuminated by the sun in that the PCM board did not experience direct beam solar radiation. Neeper developed a thermal resistance circuit, an analog of an external wall equipped

with PCM boards. The board was then coupled by radiation and convection to room temperature on one side, and by conduction through insulation to the outdoor temperature on the other side. Neeper theorized that for PCM placed on the exterior walls and roof/ceiling, the PCM melting temperature that provides the optimal storage of energy is 1°C below the average room temperature for that day. The average of the diurnal temperature fluctuation for one day cannot represent the climate type for a season or even a whole year and therefore cannot be extrapolated throughout the year. The optimum melting temperature of PCM obtained from the simulation results is compared against the monthly average indoor temperature to see if a correlation exists between the optimum PCM melting temperature and the average monthly temperature. On the basis of the guideline developed by Neeper, plots were generated for the optimum PCM melting temperature in the Albuquerque and San Francisco buildings in a passive design (NO HVAC) setting against the average indoor monthly temperatures.

Figure 8.1 depicts the indoor mean air temperature for a 35'X35' building in Albuquerque without any internal loads and without any HVAC. The optimum melting temperature of PCM for this building with no internal loads in Albuquerque was found to be 25°C . The line running across the plots depicts the 25°C mark. It can be seen from the top subplot in Figure 8.1 that the majority of temperature reduction indoors takes place in the months of May, June, August and September. However, extending Neeper's theory that is based on average indoor diurnal fluctuations to average indoor monthly temperatures does not work here. The average indoor temperatures for the month of October for instance is exactly 25°C without the PCM and in this case the 25°C PCM seems to absorb the most magnitude of energy. Another problem that arises when extending Neeper's theory based on diurnal temperature fluctuation to a monthly basis is that there is no uniform way to propose a guideline. Especially since the selection of the optimum melting temperature of the PCM cannot be done in a month by month basis.

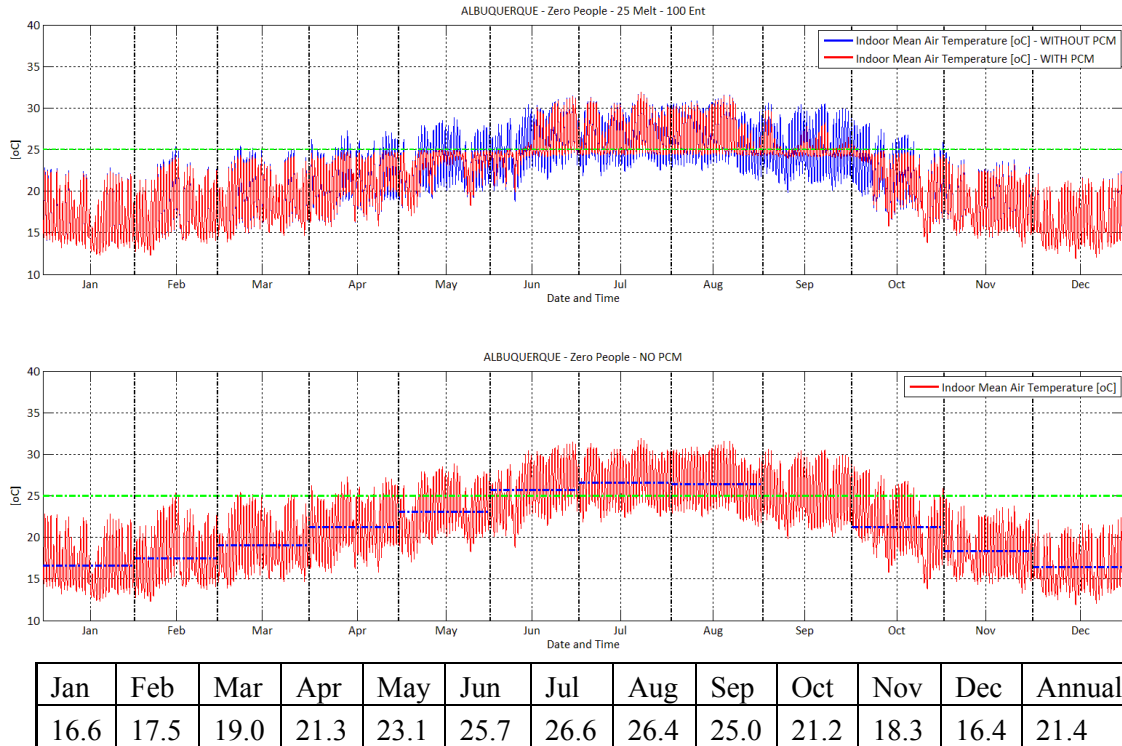


Figure 8.1: The indoor mean air temperature with and without PCM, and monthly average without PCM. (0 People - Without HVAC)

A second approach that was tested was to see if there would be any correlation between the optimum melting temperature of PCM and the average indoor monthly load with the HVAC present. The same scenario as in Figure 8.1 was tested, only this time the HVAC servicing the indoors was present. The results are shown in Figure 8.2. In this case as well, it was found that the optimum melting temperature of PCM was higher than the average indoor temperatures for each month. Similarly, even though the optimum melting temperature was to align itself very well to each of the monthly averages, with every increase in internal load the months where PCMs work best change. It is not possible to state for certain as to what months out of the year the PCM would work best.

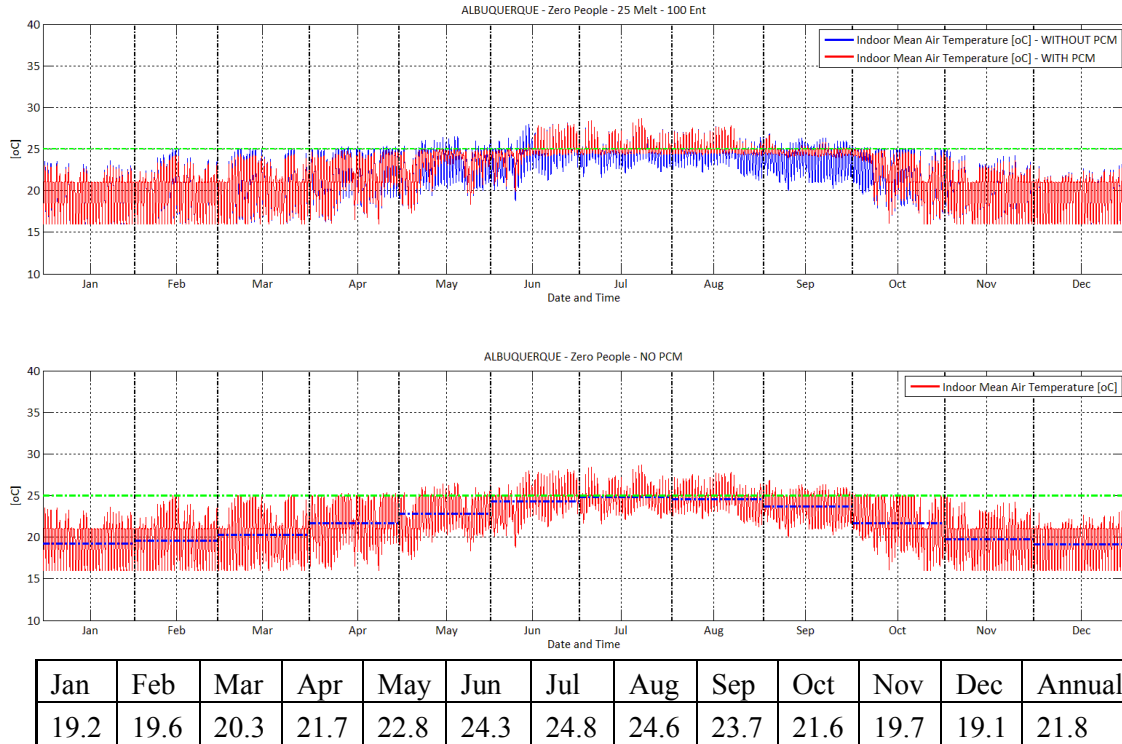


Figure 8.2: The indoor mean air temperature with and without PCM, and monthly average without PCM. (0 People - With HVAC)

In Figure 8.3 however, for the case of 24 people dissipating energy indoors, the optimum melting temperature of the PCM is either close to or just less than the average indoor temperature for the months of January, February, November and December. These are the months where the PCM is shown to absorb the most energy due to the high level of internal load. Nevertheless, the theory of selecting a PCM melting temperature that is only 1°C below the average indoor temperature cannot be extended to monthly variations, seasonal variations or yearly variations. Even the average annual indoor air temperature cannot be used to correlate the optimum melting temperature of the PCM with the average temperature indoors. This in part is also due to the fact that one cannot tell for certain what month of the year the PCM will work best.

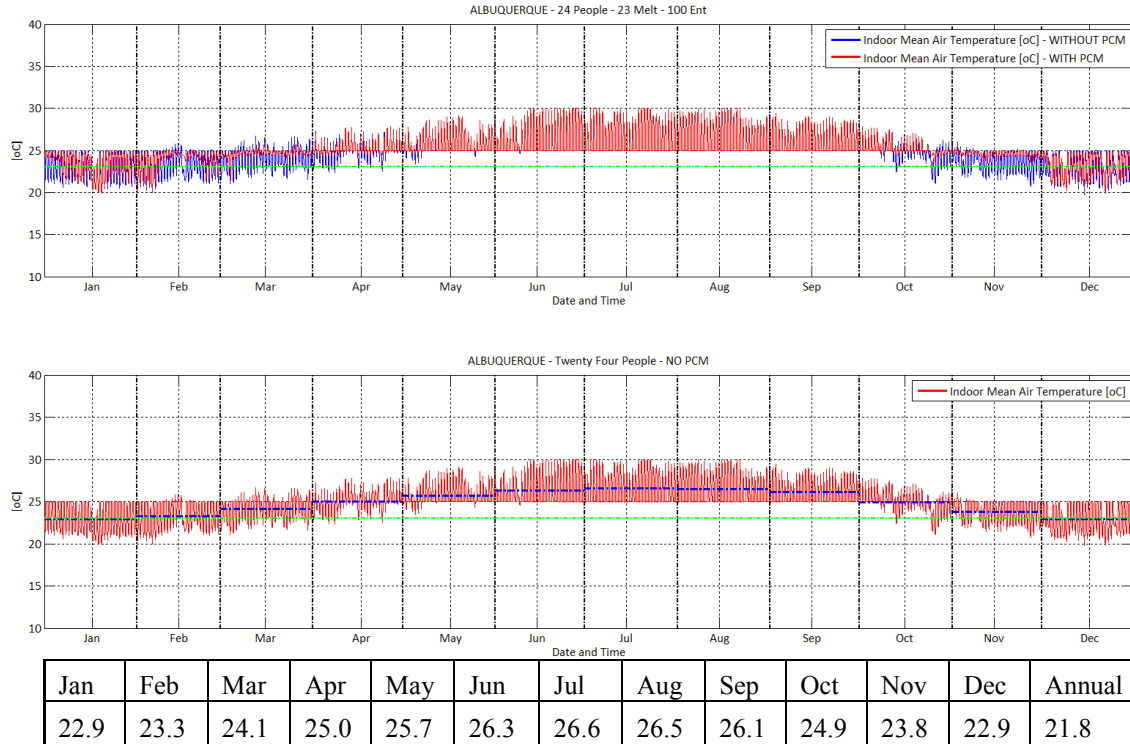


Figure 8.3: The indoor mean air temperature with and without PCM, and monthly average without PCM. (24 People - With HVAC)

The optimum months for the application of PCM not only change with every addition in internal loads but also with every change in PCM melting temperature. The increase in melting temperature and increase in internal loads tend to shift the optimum months in two opposite directions.

In Figure 8.4, in the building without indoor loads, the difference in mean air temperature indoors due to the placement of PCMs and without PCMs is plotted for the different melting temperatures of PCM. In Figure 8.4, the PCM melting temperature increases from 21°C till 25°C from the top subplot till the bottom subplot. It is evident that as the melting temperature of PCM is increased the optimum months for when PCM works best moves closer and closer to the summer. This is expected in the sense that the larger the melting temperature, as long as within the acceptable limits, will absorb more energy during the warmer months. Similarly, as the internal load increases, the PCM with a certain melting temperature will absorb the most energy

when there is a balance between the internal mean air temperature and the internal loads. While the increase in internal loads is forcing the optimum months towards the colder extreme, evidenced in Figure 8.5, the increase in PCM melting temperature is forcing the optimum months towards the warmer extreme. It seems like there exists a point for each PCM where the balance between internal loads and optimum melting temperature exist. From plots generated for the variable 'people' in chapter 6 it was evident that this balance, as the internal load is increases, occurred at 23°C for a majority of the climates.

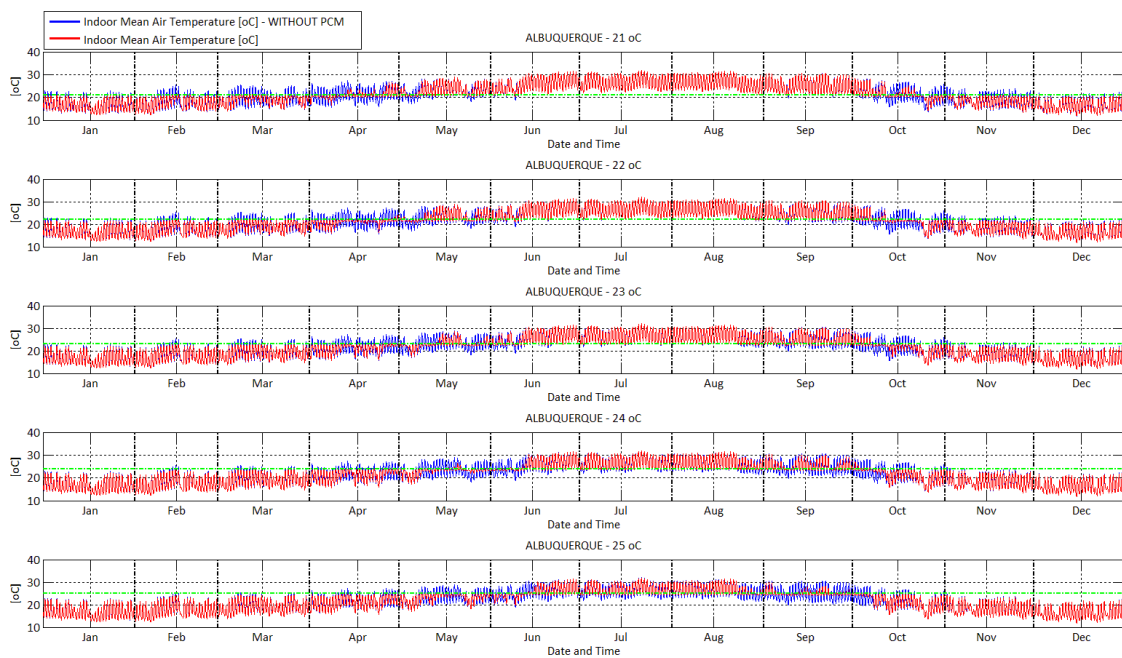


Figure 8.4: The indoor mean air temperature with and without PCM with different melting temperatures.

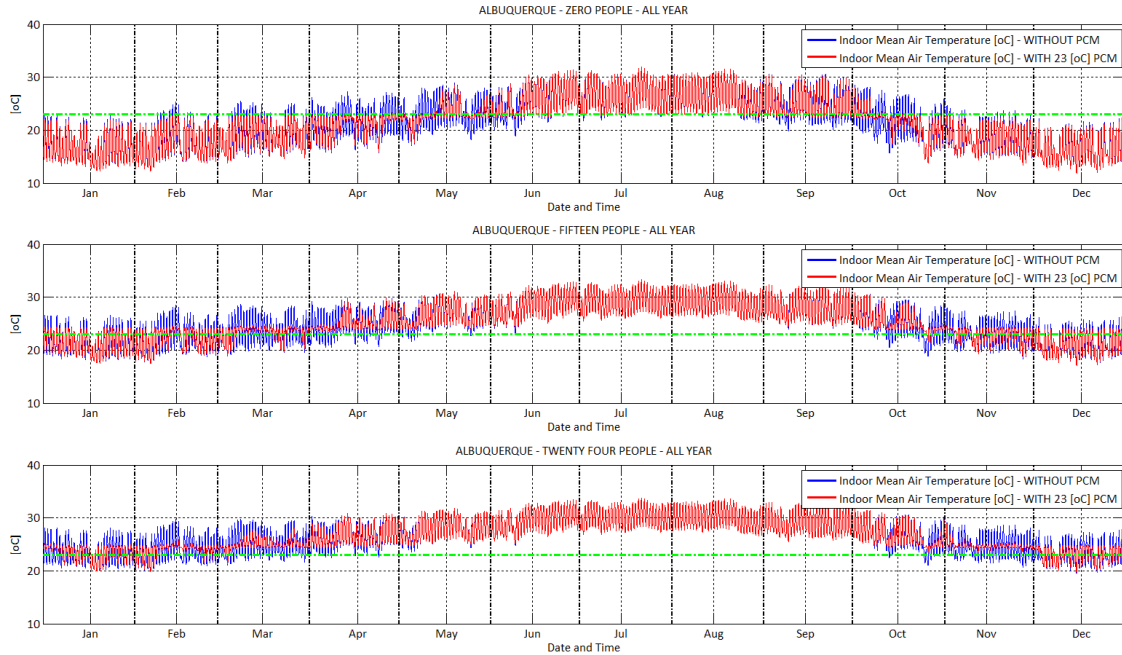


Figure 8.5: The indoor air temperature with and without PCM for three indoor loads, 0, 15 & 24 people.

The plots analogous to Figure 8.4 and 8.5 for the case of San Francisco are listed in Appendix G.

Monthly loads with different combinations of PCMs

As seen in Figure 7.10, for the case of Albuquerque office HVAC schedule, it was found that the optimum PCM melting temperature changed with the increase or decrease in internal loads. While the optimum melting temperature changed, the magnitude of energy saved also either increased or decreased along with it. As a case in point, the final subplot in Figure 7.10 corresponds to the internal load of 24 people. The largest magnitude of energy was saved, approximately 7 gigajoules (18% of 39.5 gigajoules), for the 49'X25' building, with the minimum prescribed r-value and for a 23-100-PCM. In the same Figure, the first subplot representing zero people, the optimum melting temperature of PCM was 25°C. However, the magnitude of energy saved was not nearly as much as when compared to the situation where 24 people inhabited the

indoors. With no internal load indoors, the magnitude of energy saved was approximately 3 gigajoules (approximately 23% of 12.14 gigajoules). It was therefore evident that while the internal loads were increased or decreased, the magnitude of energy saved changed along with the optimum melting temperature.

The cases listed in the table 8.1 were simulated for the Albuquerque Office HVAC building.

1. PCM melting at 23°C & 25°C, WITH HVAC	1a) Zero People 1b) Fifteen People 1c) Twenty-four People	1-abc-a) 40 kJ/kg Enthalpy 1-abc-b) 100 kJ/kg Enthalpy
2. PCM melting at 23°C & 25°C, NO HVAC	2a) Zero People 2b) Fifteen People 2c) Twenty-four People	2-abc-a) 40 kJ/kg Enthalpy 2-abc-b) 100 kJ/kg Enthalpy
3. NO PCM, WITH HVAC	3a) Zero People 3b) Fifteen People 3c) Twenty-four People	
4. NO PCM + NO HVAC	4a) Zero People 4b) Fifteen People 4c) Twenty-four People	

Table 8.1: The different scenarios simulated to make comparisons on how the two PCMs perform with and without the HVAC system and with the presence of different internal loads.

The different combinations of cases that are listed in table 8.1 were simulated and the hourly results for the variable ‘Zone Mean Air Temperature’ were plotted for the different combinations. Figuratively, the difference in results between row 1 and row 2 would depict the difference in indoor air temperature with and without HVAC. Similarly the difference in results between row 1 and row 3 would represent the difference in indoor temperatures caused by the introduction of PCM into the indoor environment. Nevertheless, this combination i.e, the difference in row 1 and row 3 would include the HVAC system servicing the indoors as well. On the other hand, the difference in row 2 and row 4 would capture the difference caused by the PCM boards but without the HVAC system servicing the indoors. The plots for the variable 'Zone Mean Air Temperature' were analyzed on the month by month basis to understand the effects of PCM boards in an environment for the different combinations of internal loads. Since the PCM

melting at 25°C performed best when there were no internal loads (Zero people) and the PCM melting at 23°C performed best for the highest internal loads (24 people), the combination of the two scenarios were further analyzed (see table 8.1). The monthly loads for each of the cases were plotted to see how the performance of PCM boards differ with the introduction of different internal loads. Figure 7.6 depicts the monthly loads for the case, '23 Melt - 100 Ent - 0 People.' The top subplot corresponds to the monthly load when PCM boards are used. The middle subplot corresponds to the case without PCM and the bottom subplot displays the magnitude of energy saved, in mega joules.



Figure 8.6: Albuquerque - office HVAC – 23-100-PCM - 0 people - monthly loads. With PCM (top) without PCM (Middle), magnitude energy saved (bottom).

Figure 8.6 corresponds to the case 1a in table 8.1. The upper limit of the y-axis on the top two subplots was set at 2000 mega joules while the bottom subplot was set an upper limit of 600 mega joules. It was found that by using this particular PCM board, most energy was saved during the months of April, May, September and October. The maximum energy saved was during the month of October with approximately 300 mega joules but when the PCM melting temperature is changed to 25°C, there is a bigger difference in energy saved for that particular case. After all the

PCM melting at 25°C was found to work best when there are no internal loads. Figure 8.7 depicts the results for a 25-100-PCM.

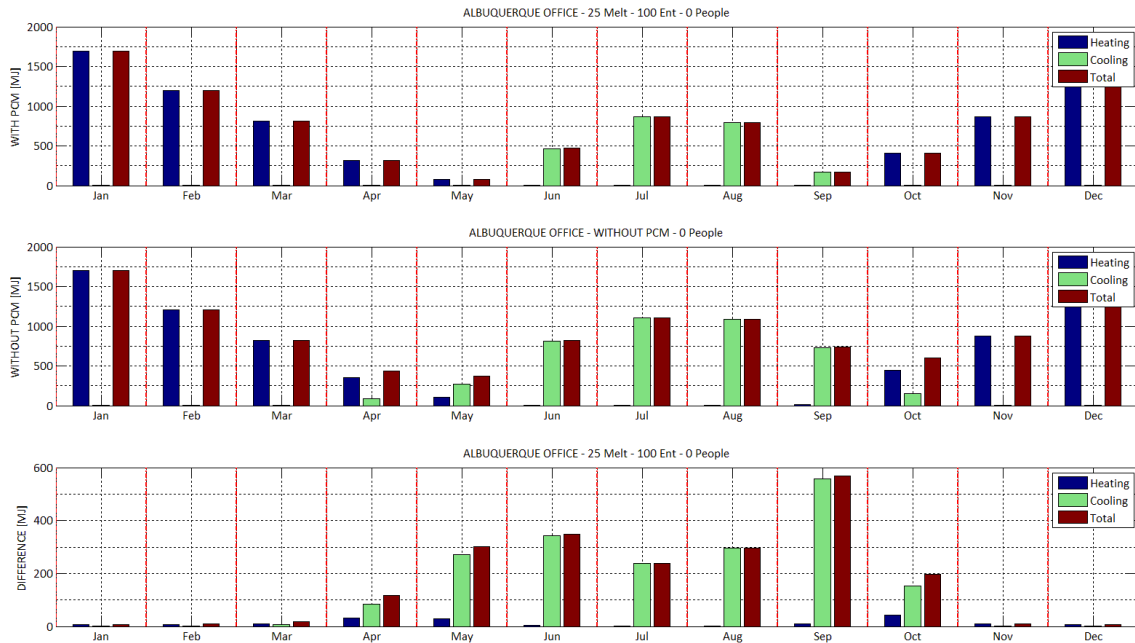


Figure 8.7: Albuquerque - office HVAC – 25-100-PCM - 0 people - monthly loads. With PCM (top) without PCM (Middle), magnitude energy saved (bottom).

In the case where a 25-100-PCM was used, the magnitude energy saved increased. The maximum amount of energy saved shifted to the month of September as opposed to October when PCM melting at 23°C was used. This is in accordance with the finding that as the melting temperature is increased the optimum months for when the PCM works shifts closer to the summer months. Comparing the two cases, Figure 8.6 (PCM melt 23°C) and 7.7 (PCM melt 25°C), it can be seen that for the month of April and October, the heating energy saved decreases for the case when PCM melting at 25°C is used. However, for the same scenario, the cooling energy saved increases drastically for the same months. By only changing the PCM melting temperature from 23°C to 25°C, there was a jump in cooling energy saved for the months of June, July, August and September. Due to the temporal and dynamic nature of heat transfer in buildings and the added complexity brought in by the HVAC and thermal storage systems, the exact reason

for this behavior cannot be specifically attributed to a particular variable. Figure 8.8 is analogous to Figure 8.6, only varying in the internal loads. Instead of 0 people occupying the indoors, Figure 8.8 represents the cases for 24 people.

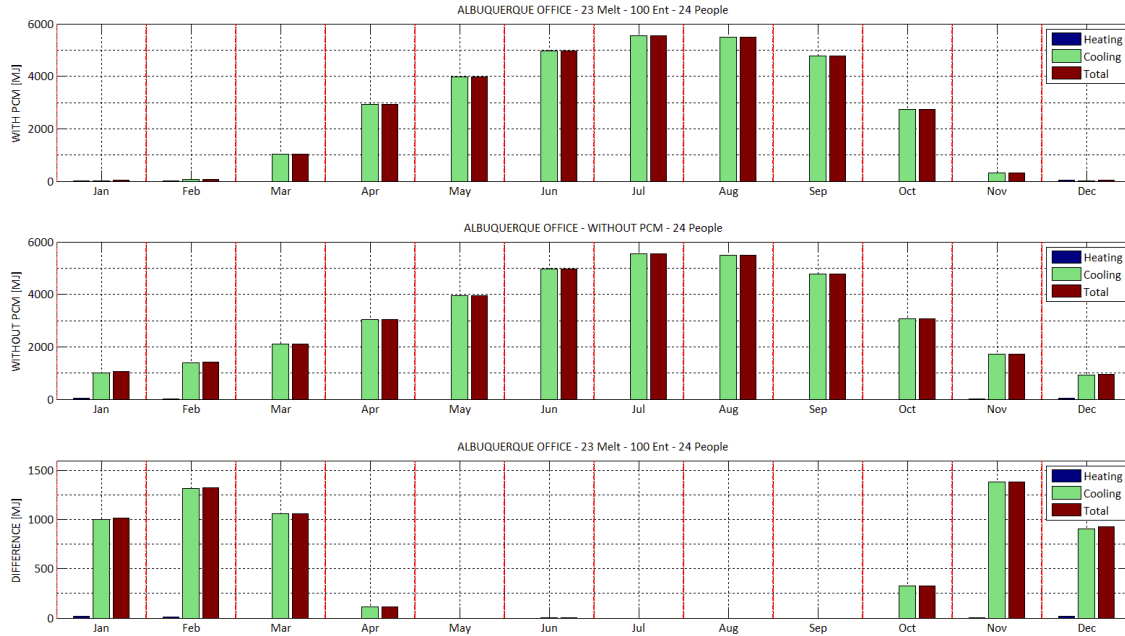


Figure 8.8: Albuquerque - office HVAC – 23-100-PCM - 24 people - monthly loads. With PCM (top), without PCM (Middle), magnitude energy saved (bottom).

Figure 8.8 is the case where the internal load is increased from 0 to 24 people. A number of changes are evident from when there was no internal load (Figure 8.6). First of all, comparing the middle subplot of both Figures (8.6 and 8.8), the case without PCM, it can be seen that the increase in internal loads from 0 to 24 people meant an increase in cooling loads and a drastic reduction of heating load for the cooling months. Suddenly the upper limit of the y-axis had to be increased to 6000 from 2000 mega joules. Now the optimum months where the PCM worked best shifted to the winter months. January, February, March, November and December were the months where PCM worked best. The internal loads in conjunction with the summer heat must have never allowed the PCM to discharge its stored heat during the months of May, June, July, August and September. If this were the case, obtaining the solidifying and melting profile of the PCM on each wall throughout the year would verify the non-participation of PCM during these

summer months. While this is investigated later in this section, the performance of a 25-100-PCM when the internal load is at 24 people is plotted in Figure 8.9.

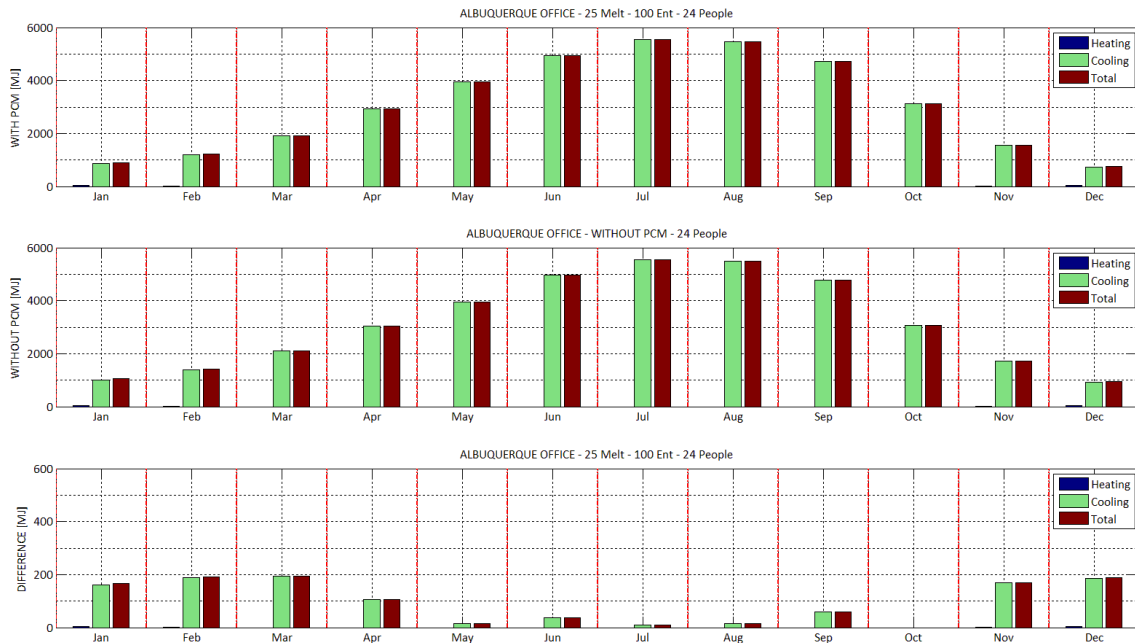


Figure 8.9: Albuquerque - office HVAC - 25-100-PCM - 24 people - monthly loads. With PCM (top), without PCM (Middle), magnitude energy saved (bottom).

The difference in Figure 8.8 and 8.9 is due to the fact that while every other parameter is kept constant, only the PCM melting temperature is changed from 23°C to 25°C. The months when the PCM boards performed best remained the same, while the only difference was that a much lower magnitude in energy savings could be observed. In retrospect, in Figure 8.6 and 8.7 (plots for no internal loads), the optimum months change when the melting temperature is changed. The cooling energy saved slightly increases during the months of June and September, by changing the PCM melting temperature from 23°C to 25°C. In the case of 24 people indoors (Figure 8.8 and 8.9); however, the change in melting temperature of PCM does not change the optimum months for when PCM performs best. The magnitude of energy saved however decreases drastically when a 'less than optimal' PCM melting temperature is chosen. This could be due to the fact that the HVAC system starts at a thermostat reading of 25°C indoors, and

therefore the purchased auxiliary air through the HVAC will condition the space before the PCM is able to absorb the energy indoors.

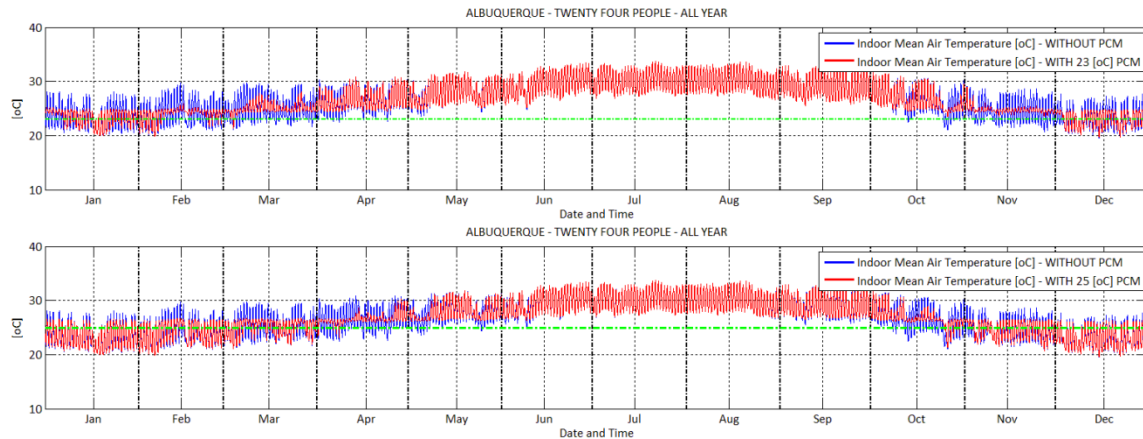


Figure 8.10:Albuquerque - office HVAC - 23°C and 25°C melt -100 enthalpy - 24 people - Indoor mean air temperature. 23°C PCM (top) - 25°C PCM (bottom) - WITHOUT HVAC.

In Figure 8.10 the top subplot corresponds to the use of PCM melting at 23°C and placed indoors without a HVAC system present. Therefore, any reduction in temperature in the indoors can be attributed to the application of PCM boards. Even though the PCM boards are placed on all the walls including the roof surface, the PCM reduces the indoor temperature to only 25°C. Similar to what can be seen in Figure 8.5, the higher the internal load, the PCM conditions the space to a temperature further away from its own melting temperature. For instance, looking back at the Figure 8.5, when the indoors is without any internal load, the PCM melting at 23°C is able to reduce the mean indoor temperature to 23°C. At an internal load of 15 people, the PCM melting at 23°C reduces the mean indoor temperature to 24°C. However as the internal load is increased to 24 people, the same PCM with a melting temperature of 23°C can only reduce the temperature to approximately 25°C. This seems to be the reason for which the PCM melting at 23°C performs better than the PCM melting at 25°C in the presence of higher internal loads. The PCM melting at 25°C can only reduce the mean indoor temperature to 27°C, evidenced in Figure 8.10.

An indoor temperature, with a thermostat set to a cooling set-point of 25°C will never allow the room to attain a temperature of 27°C. In other words the HVAC system will 'kick in' before the temperature indoors creeps above 25°C, thereby doing most of the work in place of the PCM boards. This is evident in Figure 8.11 in which the hourly cooling rate for the cases with PCM melting at 23°C (top) and 25°C (bottom) are plotted for an internal load of 24 people.

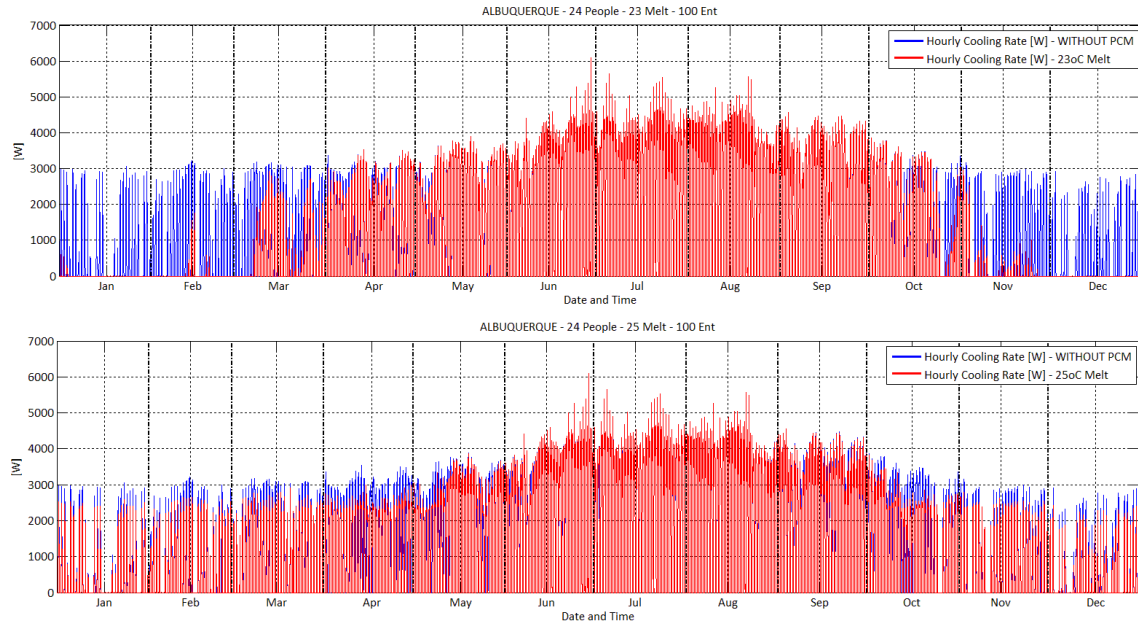


Figure 8.11: Albuquerque - office HVAC - 23°C and 25°C melt -100 enthalpy - 24 people - hourly cooling rate [W]. 23°C PCM (top) - 25°C PCM (bottom) - WITHOUT HVAC.

The difference in hourly cooling rate for when the two PCMs are used are easily distinguishable in front of the blue backdrop that represents the hourly cooling load for the same building and same internal load of 24 people, but without PCM. The PCM melting at 23°C curbs the cooling load for the colder months. The PCM melting at 25°C, on the other hand, does work for the same months but in a much lower magnitude.

The internal loads in a building therefore play an important role in determining the optimum months for when PCM work best. This in turn also dictates the choice of optimum PCM melting temperature to be selected. A distinct cause for why this is the case is still unsure. The temporal and dynamic aspect of heat flow and heat storage in conjunction with the non-

uniform external loads together makes it extremely complex to pinpoint the exact cause for the energy savings to fluctuate. Later in this chapter, the frequency of PCM melting and solidifying is also analyzed to help shed more light into why the magnitude of energy saved changes the way they do. As for now the monthly savings of PCM with every additional internal load is further analyzed.

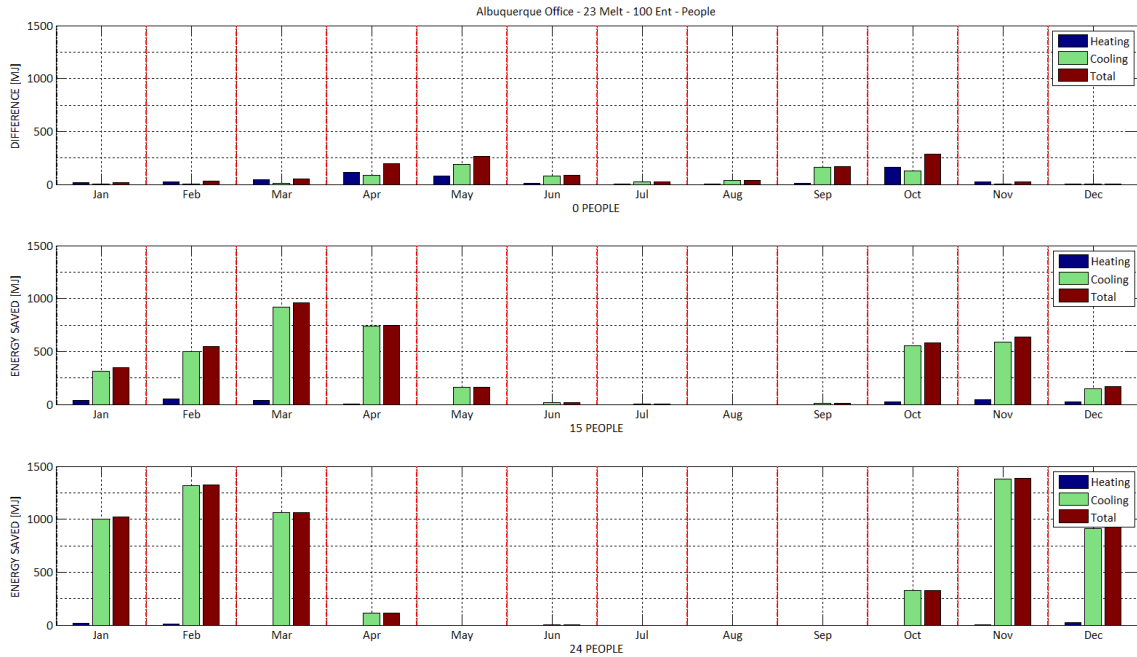


Figure 8.12: Albuquerque - office HVAC - 23 melt -100 enthalpy - energy saved with 0 people (top), energy saved with 15 people (middle), energy saved with 24 people (bottom).

In Figure 8.12 all the three cases of internal loads are plotted for the Albuquerque office HVAC building. The top subplot depicts the monthly energy saved with no internal loads (0 people). The middle and bottom subplot corresponds to 15 and 24 people respectively. A distinct trend can be seen for the three cases. As the internal load increases, the optimum months for when PCM boards perform best tend to move closer and closer to the cooler months. Initially, without any internal loads, the months of April, May, September and October boast the highest savings in energy. As soon as the internal load is increased to 15 people, the months where PCM performs optimally shifts towards early spring and late fall months. The increase in internal load

shifts the optimal performance of PCM to the swing months, which is in agreement with a recent study of PCMs (Cesar, 2012). In addition to this shifting in optimal months, the amount of energy saved also increases. When the internal load is further increased to 24 people, while everything else kept constant, the PCM offers absolutely no savings during the months of May, June, July, August and September. Instead the most savings are accrued for the months January, February, March, November and December. The magnitude of energy saved increased as well. Similar plots were generated for the building in San Francisco and the plots are placed in Appendix G. The optimum PCM melting temperature for San Francisco was found to be 21, 24 and 23°C for 0 people, 15 people and 24 people respectively. The maximum amount of energy saved was approximately 7.5 gigajoules (67% of 11.49 gigajoules) for PCM melting at 24°C in a 35'X35' building occupied by 15 people and the walls equipped with the prescribed minimum R-value of insulation. As soon as the internal loads were increased past 15 people the energy saving capacity of PCMs decreased, as evidenced in the Figure 8.13.

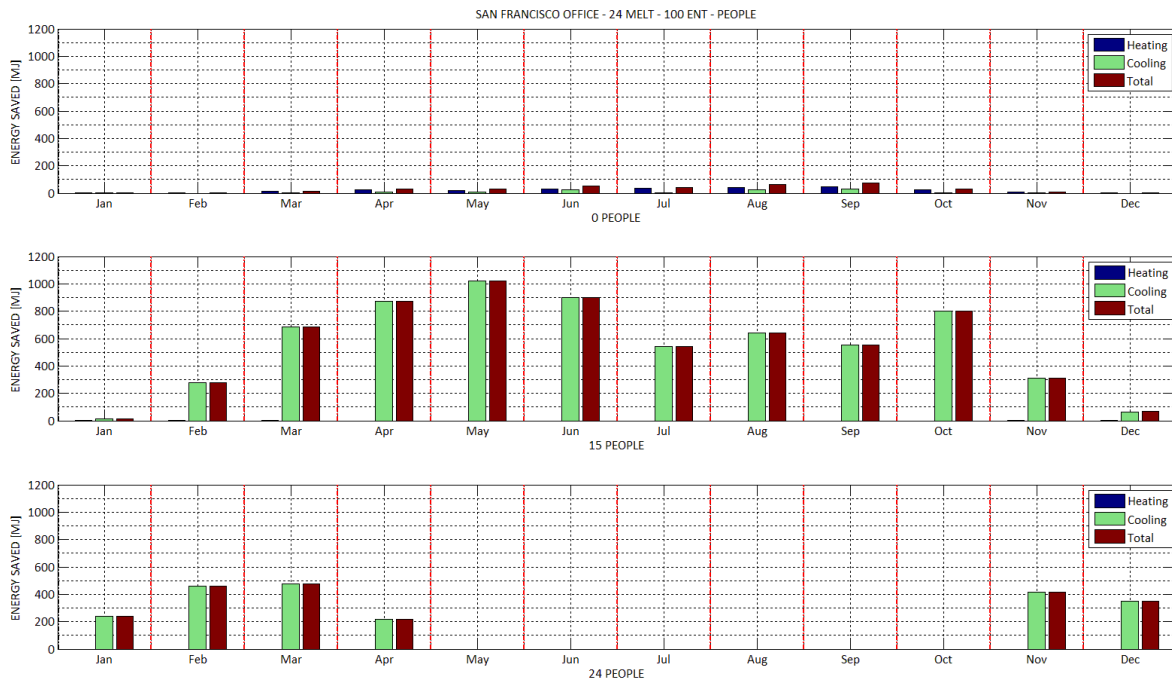


Figure 8.13: San Francisco - office HVAC - 24 melt -100 enthalpy - energy saved with 0 people (top), energy saved with 15 people (middle), energy saved with 24 people (bottom).

Nevertheless, it still holds true that any PCM that reduces the internal load to the cooling set-point temperature is the optimum melting temperature for the PCM. Figure 8.14 and 8.15 are the plots for 15 and 24 people indoors. While PCM melting at 24°C is the optimum melting temperature for 15 people occupying the indoors, PCM melting at 23°C is the optimum melting temperature for 24 people occupying the indoors.

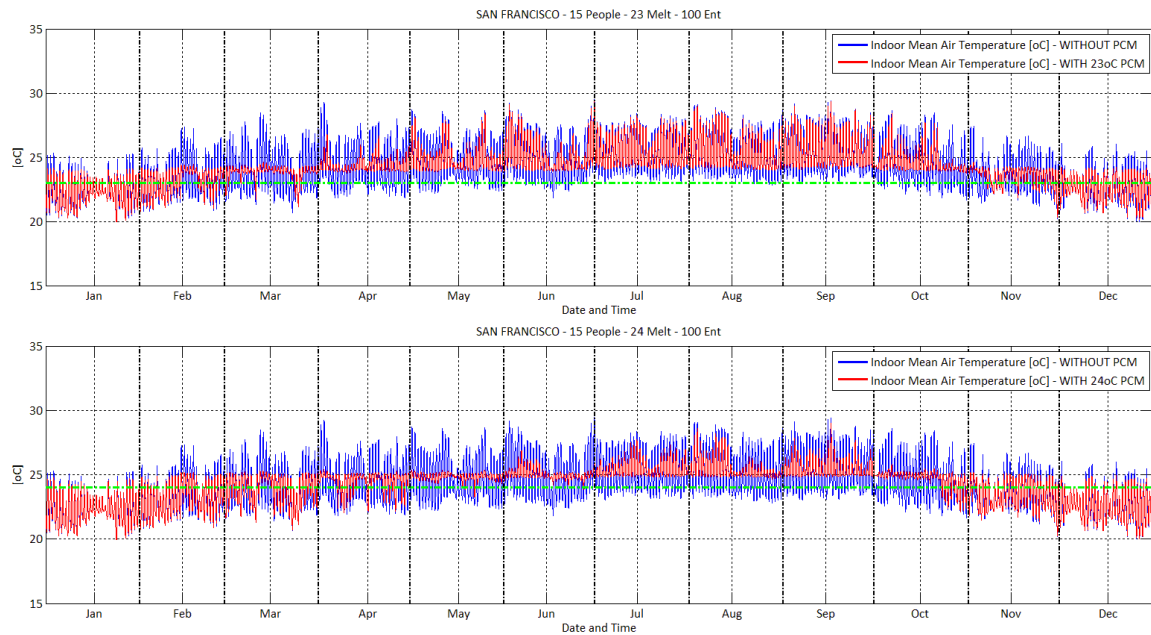


Figure 8.14: San Francisco - office HVAC - 23°C and 24°C melt -100 enthalpy - 15 people - indoor mean air temperature. 23°C PCM (top) - 24°C PCM (bottom) - WITHOUT HVAC.

For the building occupied by 15 people indoors and located in San Francisco, it was found that PCM melting at 24°C offered the most in energy savings. This is clearly evident in Figure 8.14. The PCM melting at 23°C does reduce the indoor mean air temperature to 24°C but the reductions in the mean air temperature occurs predominantly for the 'cooler' months where the need for purchased air cooling is not nearly of the same magnitude required during the 'warmer' months. On the other hand, the PCM melting at 24°C, works better because the mean indoor temperature is reduced to an optimum 25°C, when the HVAC system can actually 'kick in'. This is the 'sweet spot' where the PCM absorbs the majority of energy during the 'warmer' months and thus reducing the work required for the HVAC to condition the space to 25°C.

When the internal load is increased to 24 people, the PCM melting at 23°C performs better as opposed to the PCM melting at 24°C. The increase in internal loads to 24 people adds so much energy to the indoors that, for the months that the PCM works, the PCM melting at 24°C can only reduce the indoor temperature to 26°C. Reducing the indoor temperature to 26°C does not convert to high energy savings, due to the sheer fact that the cooling set-point is set to 25°C. Even though this reduction of mean indoor temperature occurs during the 'warmer' months, it is to no avail. The HVAC system does most of the work. Using PCM melting at 23°C however, reduces the mean indoor temperature to exactly 25°C during the 'cooler' months. This is the reason why, the largest savings in energy is seen for an internal load of 15 people in the San Francisco climate and not for the case with 24 people occupying the indoors.

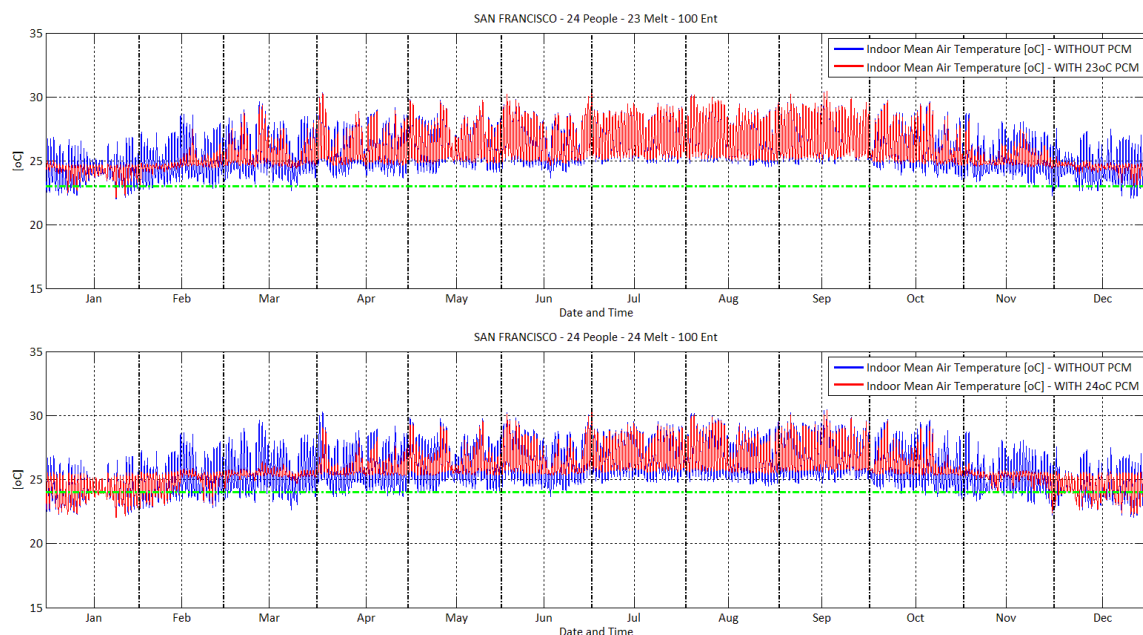


Figure 8.15: San Francisco - Office HVAC - 23°C and 24°C Melt -100 Enthalpy - 24 People - Indoor mean air temperature. 23°C PCM (top) - 24°C PCM (bottom) - WITHOUT HVAC.

Heating and cooling degree days (HDD & CDD)

The magnitude of energy saved increases with an increase in internal loads for Albuquerque, but for San Francisco the magnitude of energy saved decreases once the internal

load reaches a certain value (in this case, 15 people). As a hypothesis, San Francisco is considered a slightly warmer climate, during the cooler months, with less heating degree days and therefore the heat storage capacity of PCM is saturated quicker, with every increase in internal loads, than Albuquerque which is located in a climate slightly cooler thereby allowing more energy from indoors to be absorbed by the PCM. If the hypothesis were to hold true, all the climates with more heating degree days (towards the right of San Francisco in Figure 8.16) would have to have increased savings with every addition of internal loads. This was found not to be true. Seattle, Duluth and Fairbanks saw a decrease in magnitude of energy saved past a certain level of internal loads. Under the same token, if the hypothesis were to hold true, all the climates to the left of San Francisco would peak before reaching the 24 people mark. This too was found to be untrue. Apart from the climate of Miami climate, for all the other climates to the left of San Francisco, the highest magnitude of energy savings was observed for the highest internal loads setting.

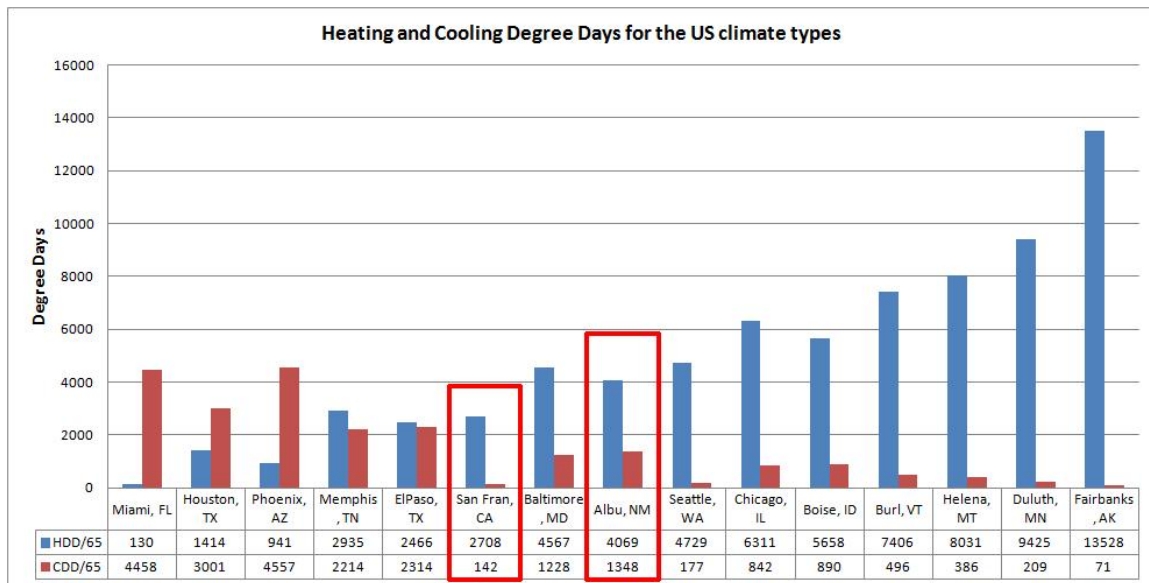


Figure 8.16: Heating and cooling degree days for the different climates using a base of 65°F (18°C). (Source: ASHRAE Handbook of Fundamentals 2009)

Although the heating and cooling degree days implicitly define the optimality of PCM choices, in the sense that the external environment is one of the biggest factors in determining the energy saved versus energy not saved, using the heating and cooling degree days by themselves alone, as an indicator to determine the optimum PCM is not a viable option. Even when only looking at the trend of optimum PCM and energy saved for each climate without any people occupying the indoors was found to be inconclusive. There was no distinguishable trend when going from climate 1 to climate 8 as shown in the table 8.2.

Climate	Representative City	Optimum PCM Melting Temperature [°C]	Maximum Energy Saved [GJ]
1A	Miami, FL	26	2.5
2A	Houston, TX	26	1.9
2B	Phoenix, AZ	26	2.0
3A	Memphis, TN	26	1.6
3B	El Paso, TX	26	2.2
3C	San Francisco, CA	21	1.8
4A	Baltimore, MD	26	2.0
4B	Albuquerque, NM	25	2.8
4C	Seattle, WA	25	1.9
5A	Chicago, IL	25	1.5
5B	Boise, ID	25	1.5
6A	Burlington, VT	25	0.9
6B	Helena, MT	25	0.8
7A	Duluth, MN	25	0.8
8A	Fairbanks, AK	22	0.4

Table 8.2: The optimum melting temperature of PCM and the corresponding energy saved observed for all climates with no internal loads in the buildings.

In table 8.2 the heating degree days increase and the cooling degree days decrease as the climate increases from 1 through 8. The results in column 4 of table 8.2 are only for the cases with no internal loads. For the most part, the HVAC and PCM boards work in conjunction to maintain the office HVAC set-point schedule by mitigating the effects of the external environment on the indoors. With the introduction of internal loads, the situation is further complicated. Therefore the fourth column *energy saved* is the amount of energy saved by using the particular PCM in the building with no internal loads. In essence the PCM and HVAC are

working to counter only the effects of the exterior environment. The heating and cooling degree days are measurements designed to reflect the demand of energy needed to heat and cool the building respectively. They serve as a rule-of-thumb representative of the climate. That being the case, as the heating degree days increase and in turn the cooling degree days decrease there seems to be no trend to suggest a correlation between PCM optimum melting temperature and energy saved with the representative climates.

The selection of heating and cooling degree days as an indicator of how well the PCM performs is therefore not viable. As of yet, it is uncertain as to why the optimality of PCM peaks at an internal load of 15 for San Francisco and at 24 (and possibly higher) for Albuquerque. This is because even though the increase in internal energy for every additional person can be calculated the magnitude of internal load that brings about a unit increase in indoor temperature cannot be calculated owing to the dynamic nature of heat gain and loss through the building. In order to assess the cause of PCM behavior, the hourly temperatures across the cross section of the wall needs to be studied. Also, the volumetric heat storage capacity of PCM the comparison between 40 kJ/kg and 100 kJ/kg still needs to be further analyzed.

Performance of two PCMs with different volumetric heat storage capacity

In chapter 7 it was seen that the addition of heat storage capacity of PCM past the 40 kJ/kg mark provided diminishing returns. Based on the size of a 35'X35' building, the heat storage capacity of the building for the different volumetric heat capacities of PCM is shown in table 8.3.

Surface With PCM	Area (ft ²)	Volume (ft ³)	Volume (m ³)	Density (kg/m ³)	Mass (kg)	Total Energy Storage MJ				
						20 kJ/kg	40 kJ/kg	60 kJ/kg	80 kJ/kg	100 kJ/kg
Walls	1220	50.834	1.439	784.9	1129.8	22.60	45.19	67.79	90.39	112.98
Roof	1225	51.042	1.445	784.9	1134.4	22.69	45.38	68.07	90.76	113.44
Total	2445	103	2.885	784.9	2264.3	45.29	90.57	135.86	181.14	226.43

Table 8.3: The total heat storage offered by the PCM with different volumetric heat storage capacities.

In table 8.3, it can be seen that, for the 35'X35' building equipped with PCM boards on the walls and roof, the PCM with a 100 kJ/kg enthalpy can absorb and dissipate 227 mega joules of energy in every melting/solidifying cycle. For instance, if the PCM is able to melt and solidify within a 24 hour period, the PCM with a heat storage capacity of 100 kJ/kg will have absorbed and later released 227 mega joules of energy that day. The PCM with a 40 kJ/kg on the other hand can only save 91 mega joules of energy for every melting/solidifying cycle. While the magnitude of energy absorbed/desorbed is considerably less for the 40 kJ/kg PCM than the 100 kJ/kg PCM, it is necessary to ascertain why or how the performances between the two vary by such a low margin. In Figure 8.17, the 40 kJ/kg plots with its corresponding internal loads are in the left column and the 100 kJ/kg plots are in the right.

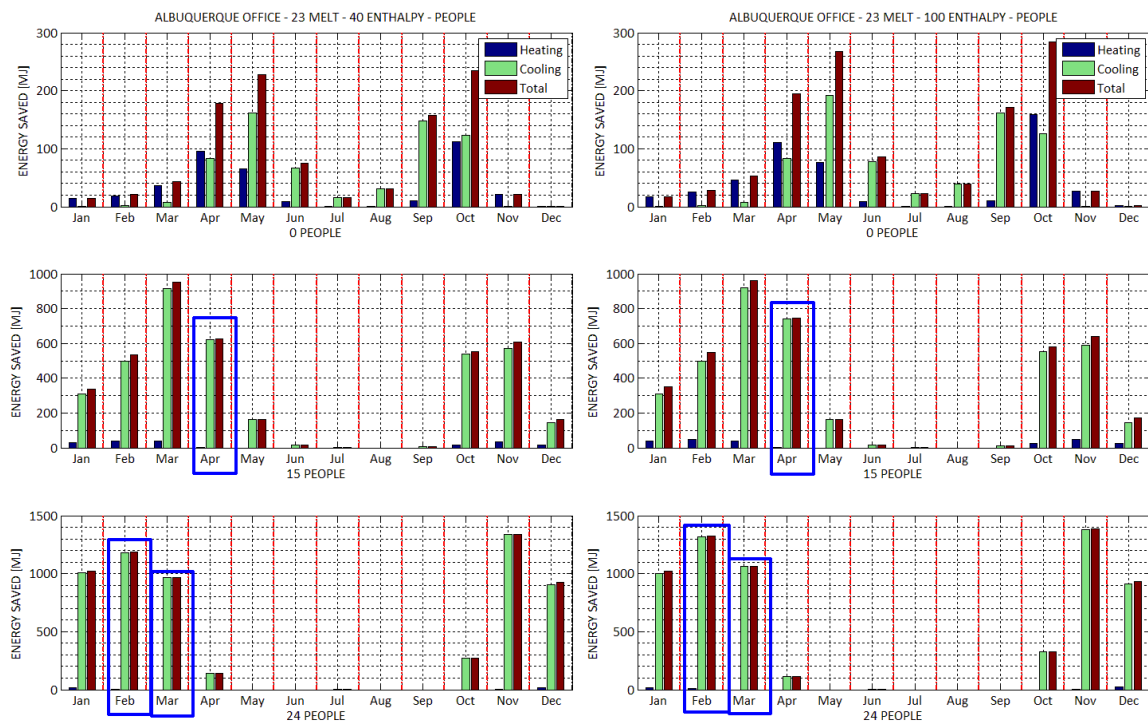


Figure 8.17: Comparison of monthly energy saved by using 40 kJ/kg PCM (left) versus 100 kJ/kg PCM (right). Rows correspond to the level of internal loads - 0, 15 and 24 people.

In Figure 8.17 the subplots in the left column correspond to the monthly energy saved when using PCM melting at 23°C with a heat storage capacity of 40 kJ/kg. In comparison, the

subplots in the right are for when the PCM of 100 kJ/kg enthalpy is used. The rows correspond to the internal loads of zero, fifteen and twenty-four people as internal loads. The first row corresponds to the zero people subplots and the majority of energy saved by switching between the two PCM heat storage capacities can be observed for the months May and October. The exact difference in magnitude of energy saved between the two PCMs is evident in Figure 8.18. In the Figure, the top subplot shows that for the month of May, using a 100 kJ/kg PCM versus a 40 kJ/kg PCM saves more of the cooling energy (approximately 25 mega joules) required to condition the building. While on the other hand, in the same subplot, for the month of October, the switch in PCM saves more of the heating energy (approximately 50 mega joules) required to condition the space.

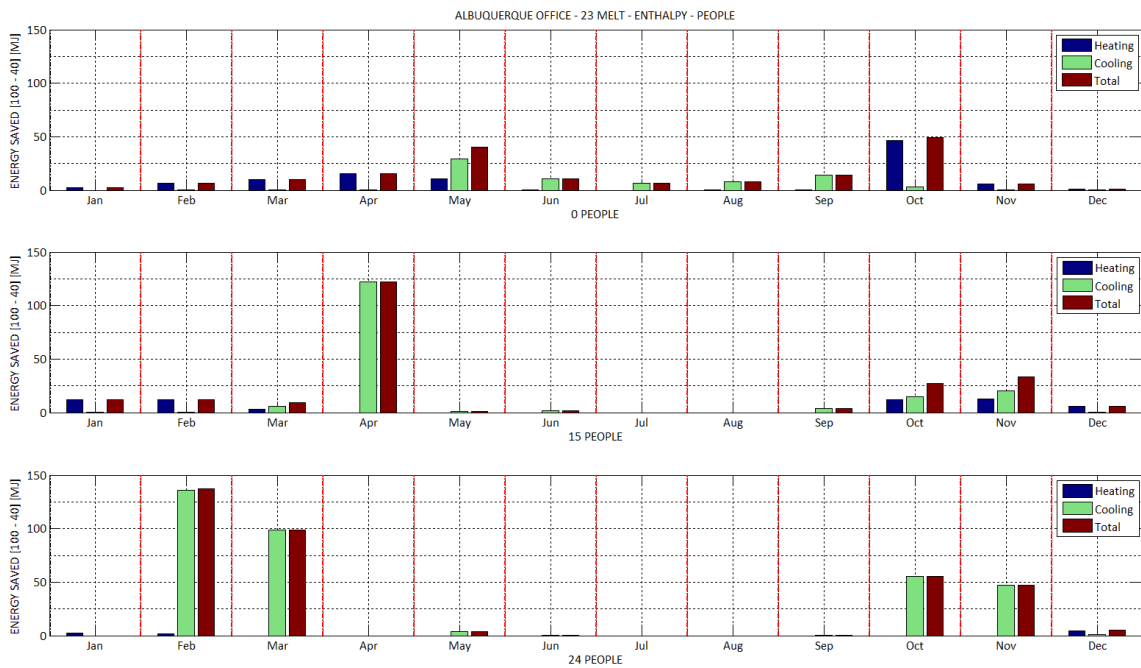


Figure 8.18: Monthly difference in energy saved between the two volumetric heat capacities (40 & 100 kJ/kg) - Top to bottom - 0 people, 15 people, 24 people.

As observed earlier, as the internal load is increased to 15 people, the optimum months for when PCM performs best start to shift closer to the months with higher cooling degree days. In Figure 8.18, in the second subplot it can be seen that for the month of April using a 100 kJ/kg

PCM saves approximately 125 mega joules more of the cooling energy than that for the 40 kJ/kg PCM. When compared to the subplot for no internal loads, it is can be seen that all the energy required to heat the building for the month of April is nonexistent for the case with an internal load of 15 people. It seems like the addition of 155.5 mega joules per day of energy indoors obviates the need for any heating during the month of April. With the addition of 4665.5 mega joules of energy per month by internal loads, the energy saving performance of the two PCMs (40 kJ/kg and 100 kJ/kg) is not too different at all. Except for the month of April, both of the PCMs perform the same. It is only for the month of April where the savings is 125 mega joules more than when using PCM with heat storage capacity of 40 kJ/kg. Similarly if the internal load is further increased from 15 to 24 people, the difference in performance between the two heat storage capacities is not very distinguishable. Now there are 7465 mega joules of energy released indoors on a monthly basis but still the only significant difference in energy saving potential between the two PCMs is evident for the months February and March. This non-uniform trend of monthly savings in energy leads to no conclusive answers as to why the PCMs with two different heat storage capacities perform the way they do. Also, it is still unclear as to why; the PCM with less than half the heat storage capacity performs nearly as well as the PCM with more than twice the capacity.

Internal loads	Watts	Joules/Day	MJ/Day	MJ/Month	MJ/year
15 People	1800	155520000	155.5	4665.6	56764.8
24 People	2880	248832000	248.8	7465.0	90823.7

Table 8.4: The energy dissipated indoors by the two levels of internal loads.

There are a couple of reasons that are linked to the melting and solidifying of PCM that could be responsible for the very small difference in energy savings between the two PCMs. They are as follows:

1. The PCM melting very fast, due to the high internal loads indoors, and not getting the opportunity to solidify again.

2. In addition to the previous point, the PCM is not going through the melting/solidifying cycles frequently enough.
3. The PCM is absorbing energy and melting too, but at a very slow rate thereby never reaching full saturation before the HVAC system comes into effect.

All of the aforementioned situations need to be addressed by looking closer at the hourly temperatures at the inside and outside surfaces of the PCM gypsum board.

Hourly melting/solidifying of PCM

EnergyPlus allows for the hourly reporting of results. Until now, the variables have only been reported in either annual or monthly formats. So far only the heating and cooling loads have been extracted as simulation results. In the case where the frequency of the melting/solidifying of PCM needs to be analyzed, hourly reporting of the results is required. Therefore the hourly results for 10 different variables were extracted from this set of simulations. The variables are listed in table 8.5.

Site Outdoor Dry Bulb Temperature [C]
Surface Inside Face Solar Radiation Heat Gain Rate per Area [W/m2]
Surface Outside Face Solar Radiation Heat Gain Rate per Area [W/m2]
CondFD Surface Nodal Temperature [C]
Zone Mean Air Temperature [C]
Zone Thermostat Heating Set-point Temperature [C]
Zone Thermostat Cooling Set-point Temperature [C]
Zone Ideal Loads Zone Total Heating Rate [W]
Zone Ideal Loads Zone Total Cooling Rate [W]

Table 8.5: Hourly reporting of the different variables from the simulations.

As for the hourly melting and solidifying of the PCM only Albuquerque cases will be analyzed in two directions namely the inclusion of internal loads and the change in enthalpy. These cases will be analyzed by outputting the hourly simulation data as opposed to the monthly or yearly outputs as done in the previous chapters.

EnergyPlus can simulate PCMs only with the conduction finite difference algorithm (CondFD). The introduction of the CondFD algorithm into recent versions of EnergyPlus was done in order to address the inability of the conduction transfer function (CTF) to simulate materials that changed thermo-physical properties with a change in temperature. The CTF algorithm is an efficient method to compute surface heat fluxes because they eliminate the need to know temperatures and fluxes within the surfaces (Energy, 2012). In addition, the CTF algorithm is a sensible heat only solution not taking in account moisture storage or diffusion in construction elements. However in the case of latent heat storage technologies such as PCMs the thermal properties are not constant and therefore require a different approach. For the PCM modeling, the CondFD algorithm is coupled with the enthalpy-temperature function that the user inputs to account for the enthalpy changes during phase change (Pederson, 2007). The enthalpy-temperature function is used to develop an equivalent specific heat at each time step. In the CondFD algorithm, all elements are divided or discretized automatically. Cesar (2012) have shown that leaving the default space discretization value of 3 in EnergyPlus and using a small time-step (i.e, 1 minute) maintained the accuracy of the results when modeling PCM in EnergyPlus. The dependence of the space discretization on the thermal diffusivity of a material, and time step has led to the roof having a total of 56 nodes while the wall only 17 nodes. The space discretization value used for the simulations has created two nodes on the inside and outside surface of the PCM gypsum board. Figure 7.19 details the construction of the roof and walls. The two nodes and its representative numeric values are highlighted on the inside and outside surface of the PCM boards. In the following analysis the hourly temperatures at these nodes are analyzed to:

1. Compute the number of times the PCM melts and solidifies.
2. Ascertain whether the PCM starts melting and/or solidifying from the indoors or the outdoors.

3. Comparing the melting and solidifying against any increase or decrease in exterior radiation, internal loads and HVAC heating and cooling.
4. Determine the particular months where the PCM works best to understand why the PCM worked better for those months.

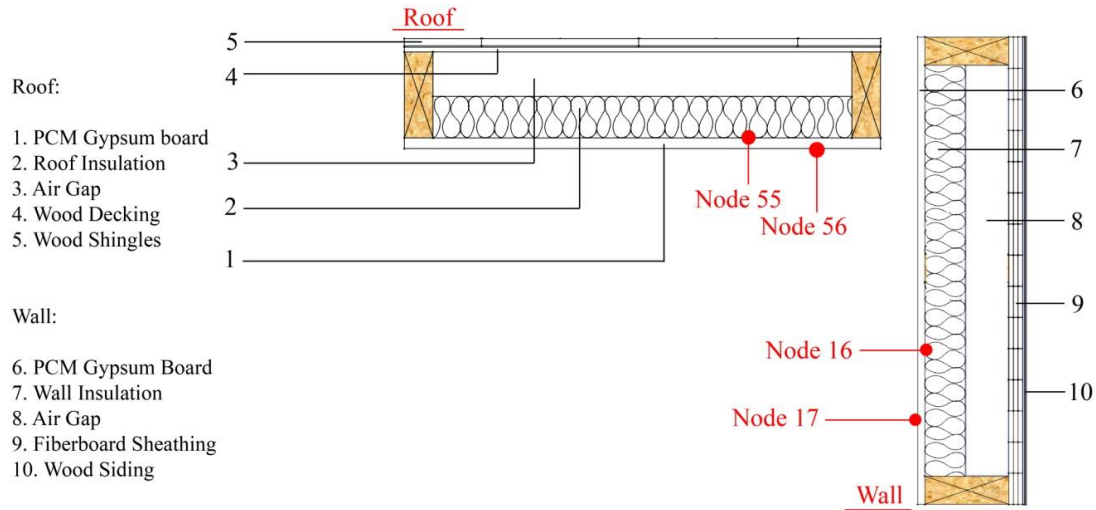


Figure 8.19: Construction details and the nodal placements for the Conduction finite difference algorithm.

In order to analyze the melting and solidifying trend of the PCM board, the hourly temperature of node 16 and 17 for the walls and node 55 and 56 for the roof were extracted. The PCM board, for the all cases analyzed for Albuquerque, completely melts at 23°C. At 23°C the PCM will have absorbed all the energy it can while transitioning from solid to liquid. However, the PCM enthalpy-temperature function defined within EnergyPlus was set up so that the melting range of the PCM was within 0.1°C. In other words, the PCM starts absorbing energy at 22.9°C and will have completely saturated at 23°C. The PCM board therefore absorbs all the energy it can, in that latent state, within that small 0.1°C range. For consistency and understanding, the temperature when the PCM starts melting, in this case 22.9°C, will be denoted as T_{Melting} (abbreviated to T_m). Similarly when the PCM is fully melted and starts cooling down, the PCM

will start solidifying at 23°C and will completely release all the energy until it reaches at 22.9°C. $T_{\text{Solidifying}}$ (abbreviated to T_s) will be used to denote the solidifying temperature, in this case 23°C.

The roof and walls have different node numbers denoting the inside and outside surface (55 & 56 for the roof and 16 & 17 for the walls) of the PCM board. While developing the logic for the melting/solidifying study, the node towards the indoors will be denoted node 1 and the one towards the exterior environment will be denoted as node 2. The outputs of the two nodal temperatures were obtained in two columns for each node. In order to identify when the PCM was melting and when it was solidifying, and for what direction various conditional statements written to identify the state of the PCM and corresponding values were assigned to each state.

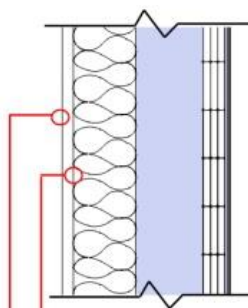
Condition to be fulfilled	Physical State	Wall Section
if Node1 & Node2 $\leq T_m$	Fully Solid	
if Node1 & Node2 $\geq T_s$	Fully Melted	
if $T_m \leq \text{Node2} \leq T_s$ & $\sim(T_m \leq \text{Node1} \leq T_s)$ then if Node2(t-1) < Node2(t)	Melting from the outside	
if $T_m \leq \text{Node2} \leq T_s$ & $\sim(T_m \leq \text{Node1} \leq T_s)$ then if Node2(t-1) > Node2(t)	Solidifying from the outside	
if $T_m \leq \text{Node1} \leq T_s$ & $\sim(T_m \leq \text{Node2} \leq T_s)$ then if Node1(t-1) < Node1(t)	Melting from the inside	
if $T_m \leq \text{Node1} \leq T_s$ & $\sim(T_m \leq \text{Node2} \leq T_s)$ then if Node1(t-1) > Node1(t)	Solidifying from the inside	
if $T_m \leq (\text{Node1} \& \text{Node2}) \leq T_s$ then if Node1(t-1) < Node1(t) & Node2(t-1) < Node2(t)	Melting	
if $T_m \leq (\text{Node1} \& \text{Node2}) \leq T_s$ then if Node1(t-1) > Node1(t) & Node2(t-1) > Node2(t)	Solidifying	
All Else	Changing Direction	

Table 8.6: The conditional statements that determine the physical state of the PCM.

The different conditions, seen in Table 8.6, were applied to the hourly temperatures for the two nodes. If the conditions were satisfied then the physical state of the PCM at that hour was determined. Once the data was broken down according to the physical state of the PCM, the frequency for the different cases of melting were added to obtain the number of hours the PCM was melting. Similarly the frequencies for the different cases of solidifying were added to obtain the number of hours the PCM was solidifying throughout the year. The terms that denote the PCM melting or solidifying from the inside or the outside were used to determine what the

underlying cause for the PCM to melt or solidify at that instance in time was. In other words, the melting and solidifying were compared against the temporal increase or decrease in internal loads, exterior radiation or the HVAC system's heating and cooling load. Finally, the number of cycles the PCM goes through, throughout the year, is collected by running a loop through the hourly temperature results for both of the nodal temperatures. The conditions for the loop are laid out in Table 8.7.

If this condition is satisfied	Then Do
Condition 1 $\text{if (Node1 \& Node2)} \geq T_s$	<ol style="list-style-type: none"> 1. Initialize counter, record Date & Time. 2. Iterate along the following time steps till condition 2 is satisfied.
Condition 2 $\text{if (Node1 \& Node2)} \leq T_m$	<ol style="list-style-type: none"> 3. Record Date & Time, +1 to the counter. 4. Initialize the loop to begin at this new recorded date and time. 5. Go back to running condition 1 again.

Table 8.7: The conditional statements that determine the number of cycles the PCM goes through.

Results

The hourly temperature profile for the mean temperature was generated for each case listed in table 8.1. The annual plots were generated comparing the cases with and without PCM. This was done in order to ascertain information on how the indoor temperature fluctuated with and without PCM applied to the walls. First the case with no internal loads is analyzed and progressively 15 and 24 people are added as internal loads. The number of cycles the PCM goes through and the melting and solidifying frequency for these different cases are analyzed.

Case 1: zero people - 40 kJ/kg - 100 kJ/kg – WITH/WITHOUT HVAC

For this case, the mean air temperature indoors for the case with no internal loads was evaluated first. This was obtained when the HVAC system was present and when there was no HVAC system to service the indoors. The main reason behind generating the data for the cases with and without HVAC was to understand how the PCM performed in a passive setting as opposed to an actively conditioned setting. In addition, the data was also plotted to compare in the

direction of volumetric heat storage capacity. The two enthalpies, 40 kJ/kg and 100 kJ/kg, were selected and plotted on top of each other in order to understand to what magnitude the two enthalpies contribute to reducing the indoor temperature.

Figure 8.19 depicts the case for no internal loads and the PCM melting at 23°C placed in the Albuquerque office HVAC setting. In Figure 8.20 the top subplot corresponds to the situation without an HVAC system conditioning the space. The green line going across the center depicts the temperature at which the PCM melts. The only difference that is visible when using PCM with 40 kJ/kg of heat storage capacity versus the PCM with a 100 kJ/kg is that when the blue curve (for 40 kJ/kg) protrudes out of the red curve (for 100 kJ/kg). The difference between the two PCMs is evident only in the months of May and October. The introduction of the HVAC does not seem to change the pattern on the difference between the two PCMs. It is, nevertheless, evident that placing PCM boards indoors mitigates the indoor temperature significantly for April, May and October.

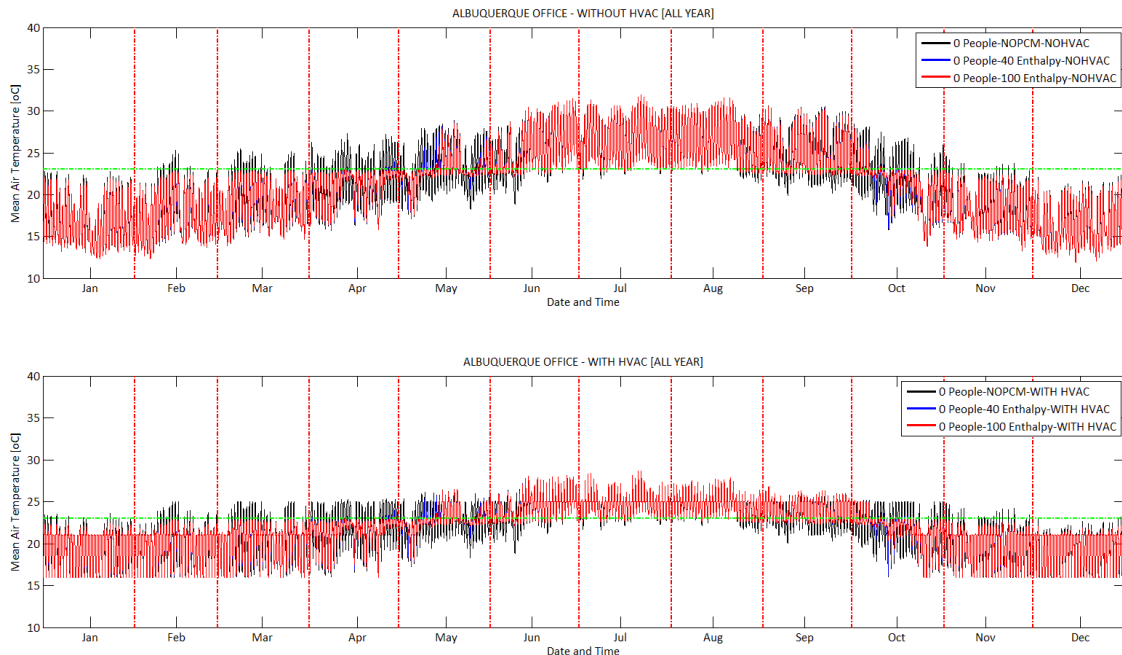


Figure 8.20: Hourly mean air temperature indoors for PCM melting at 23°C and 0 people. Without HVAC (top) and with HVAC (bottom).

In many cases the indoor mean air temperature was reduced by approximately 5°C. The plot in black represents the case without PCM and the ones in blue and red, with. As already seen in Figure 8.4, the summer months are where PCM does not perform well. For instance in Figure 8.20, the plot for the PCM, in red, completely overlaps the plot for without PCM, in black. Nevertheless, delving into the number of hours the PCM melts and solidifies can shed more light into this behavior. Table 8.8 lays out the percentage of hours the PCM cycles through the different physical states.

ZERO PEOPLE - 40 kJ/Kg											
Without HVAC	Melted (%)	Melting (%)	Solid (%)	Solidifying (%)	# of Cycles	With HVAC	Melted (%)	Melting (%)	Solid (%)	Solidifying (%)	# of Cycles
North	28.8	8.6	51.8	10.8	4	North	27.2	10.0	50.5	12.3	4
South	31.0	13.0	39.8	16.1	22	South	29.8	15.3	36.5	18.4	25
East	32.1	9.3	44.9	13.7	16	East	31.0	11.2	41.9	16.0	17
West	30.6	10.4	46.3	12.7	6	West	29.2	11.6	44.9	14.3	8
Roof	36.9	4.9	52.5	5.7	3	Roof	36.3	5.9	51.3	6.5	3
ZERO PEOPLE - 100 kJ/Kg											
Without HVAC	Melted (%)	Melting (%)	Solid (%)	Solidifying (%)	# of Cycles	With HVAC	Melted (%)	Melting (%)	Solid (%)	Solidifying (%)	# of Cycles
North	27.9	9.2	51.5	11.4	1	North	26.4	10.5	50.2	12.9	1
South	29.3	14.5	38.4	17.8	1	South	27.9	17.0	34.8	20.3	1
East	30.8	10.4	44.0	14.8	2	East	29.5	12.5	40.9	17.1	2
West	30.1	10.0	46.2	13.7	1	West	28.8	11.3	44.8	15.2	1
Roof	36.4	5.2	52.4	5.9	1	Roof	35.9	6.0	51.4	6.7	1

Table 8.8: The percentage of hours the PCM cycles through different physical states. 40 kJ/kg (top) and 100 kJ/kg (bottom). Without HVAC (Left) and with HVAC (Right).

The column labeled '# of Cycles' tracks how many times the PCM fully melts and fully solidifies throughout the year. In table 8.8. For instance, the surfaces that mostly participate in the PCM melting and solidifying process are usually the South, East and West surface. In the cases without HVAC, it makes sense that the *North surface*, is never really exposed to exterior direct solar radiation while the *Roof* on the other hand is the surface exposed to the bulk of the solar

radiation at all times. Therefore, the PCM placed on the north wall will comparatively participate less in the heat absorption and dissipation process than the other surfaces. The roof on the other hand will participate in the process but the PCM will saturate faster than when placed on any other surface, hence the high percentage of melted state than any other surface. This could be because, as soon as the PCM melts, it stays that way for long periods of time.

A significant observation is when the PCM's volumetric heat storage capacity is changed from 40 kJ/kg to 100 kJ/kg. The number of cycles the PCM goes through decreases drastically. In other words, the PCM with a 100 kJ/kg enthalpy rarely ever fully melts. And when it does full melt or saturate, it takes the PCM a really long time to fully solidify.

It can be seen in tables 8.9 and 8.10, that as soon as the PCM's heat storage capacity is changed from 40 kJ/kg to a 100 kJ/kg, the number of cycles the PCM goes through decreases drastically for both the surfaces. The 100 kJ/kg PCM takes a really long time to fully saturate (somewhere around early May), seen in table 8.9 and when it does fully saturate, it takes a long time for it to fully melt again (sometime around mid-October). In addition, when PCM with a heat storage capacity of 100 kJ/kg is used, the PCM fully melts and solidifies around the same time for all the surfaces regardless of whether the HVAC system is present or not. It should also be noted that the results in table 8.9 and table 8.10 correspond to a case with internal load of zero people. The PCM is therefore only responsible for mitigating any excessive load imparted by the environment.

ZERO PEOPLE - 100 kJ/kg											
	WITHOUT HVAC					WITH HVAC					
	North	South	East	West	Roof	North	South	East	West	Roof	
M	5/15/- 15:00	5/13- 19:00	4/28- 14:00	5/10- 18:00	5/14- 11:00	M	5/15/- 15:00	5/13- 19:00	4/28- 14:00	5/10- 18:00	5/14- 11:00
S	10/12/- 8:00	10/13- 4:00	5/4- 6:00	10/13- 4:00	10/13- 7:00	S	10/12/- 8:00	10/13- 4:00	5/4- 6:00	10/13- 4:00	10/13- 7:00
M			5/10- 14:00			M			5/10- 14:00		
S			10/13- 3:00			S			10/13- 3:00		
	1	1	2	1	1	#	1	1	2	1	1

Table 8.9: The exact date and time observed for when the PCM fully melts and proceeds to fully solidify. The number of cycles the PCM goes through, of full melting and then full solidifying, for a 100 kJ/kg PCM.

ZERO PEOPLE - 40 kJ/kg											
WITHOUT HVAC						WITH HVAC					
	North	South	East	West	Roof		North	South	East	West	Roof
M	5/9- 18:00	2/14- 18:00	4/1- 18:00	4/11- 20:00	4/29- 15:00	M	5/9- 18:00	2/13- 18:00	4/1- 17:00	4/1- 21:00	4/28- 17:00
S	5/12- 7:00	2/15- 2:00	4/2- 4:00	4/15- 12:00	5/4- 0:00	S	5/12- 7:00	2/14- 2:00	4/2- 5:00	4/2- 5:00	5/4- 0:00
M	5/12- 20:00	3/8- 18:00	4/11- 17:00	4/25- 20:00	5/9- 16:00	M	5/12- 20:00	2/14- 17:00	4/11- 16:00	4/11- 20:00	5/9- 15:00
S	5/25- 0:00	3/9- 3:00	4/12- 7:00	5/2- 5:00	5/25- 6:00	S	5/24- 23:00	2/15- 3:00	4/12- 8:00	4/15- 12:00	5/25- 6:00
M	5/27- 19:00	4/1- 18:00	4/12- 16:00	5/2- 21:00	5/27- 17:00	M	5/27- 19:00	3/7- 19:00	4/12- 16:00	4/25- 20:00	5/27- 18:00
S	6/9- 6:00	4/2- 5:00	4/15- 22:00	5/3- 22:00	10/9- 4:00	S	6/9- 5:00	3/8- 3:00	4/15- 22:00	5/2- 5:00	10/9- 3:00
M	6/10/- 17:00	4/11- 18:00	4/17- 19:00	5/8- 18:00		M	6/10/- 17:00	3/8- 18:00	4/17- 18:00	5/2- 21:00	
S	10/8/- 3:00	4/12- 7:00	4/18- 5:00	5/25- 0:00		S	10/8/- 3:00	3/9- 3:00	4/18- 5:00	5/3- 22:00	
M		4/12- 19:00	4/22- 18:00	5/26- 20:00		M		3/12- 18:00	4/22- 17:00	5/8- 18:00	
S		4/15- 14:00	4/23- 5:00	10/8- 4:00		S		3/13- 2:00	4/23- 5:00	5/25- 0:00	
M		4/25- 19:00	4/25- 17:00	10/10- 19:00		M		3/15- 19:00	4/25- 16:00	5/26- 20:00	
S		4/26- 8:00	5/2- 4:00	10/12- 7:00		S		3/16- 2:00	5/2- 4:00	6/9- 5:00	
M		4/26- 18:00	5/2- 17:00			M		4/1- 17:00	5/2- 17:00	6/9- 19:00	
S		5/2- 2:00	5/3- 23:00			S		4/2- 5:00	5/3- 23:00	10/8- 4:00	
M		5/8- 18:00	5/7- 17:00			M		4/11- 18:00	5/7- 17:00	10/10- 19:00	
S		5/24- 23:00	5/25- 3:00			S		4/12- 8:00	5/25- 3:00	10/12- 7:00	
M		5/27- 16:00	5/25- 16:00			M		4/12- 19:00	5/25- 16:00		
S		6/9- 8:00	5/26- 7:00			S		4/15- 14:00	5/26- 7:00		
M		6/10- 15:00	5/26- 14:00			M		4/25- 19:00	5/26- 14:00		
S		10/8- 5:00	6/9- 6:00			S		5/2- 2:00	6/9- 6:00		
M		10/8- 17:00	6/9- 16:00			M		5/8- 18:00	6/9- 16:00		
S		10/9- 5:00	10/8- 4:00			S		5/24- 23:00	10/8- 4:00		
M		10/9- 16:00	10/9- 18:00			M		5/27- 16:00	10/9- 18:00		
S		10/12- 7:00	10/10- 8:00			S		6/9- 7:00	10/10- 8:00		
M		10/14- 17:00	10/10- 16:00			M		6/10- 15:00	10/10- 16:00		
S		10/15- 3:00	10/12- 7:00			S		10/8- 5:00	10/12- 7:00		
M		10/15- 17:00	10/16- 18:00			M		10/8- 17:00	10/15- 18:00		
S		10/16- 5:00	10/17- 4:00			S		10/9- 5:00	10/16- 5:00		
M		10/16- 16:00	10/18- 18:00			M		10/9- 16:00	10/16- 18:00		
S		10/17- 5:00	10/19- 5:00			S		10/12- 7:00	10/17- 4:00		
M		10/17- 16:00	10/19- 17:00			M		10/14- 17:00	10/17- 18:00		
S		10/18- 5:00	10/20- 6:00			S		10/15- 3:00	10/18- 4:00		
M		10/18- 16:00				M		10/15- 16:00	10/18- 17:00		
S		10/19- 6:00				S		10/16- 6:00	10/19- 5:00		
M		10/19- 16:00				M		10/16- 16:00			
S		10/20- 7:00				S		10/17- 5:00			
M		10/21- 16:00				M		10/17- 16:00			
S		10/22- 4:00				S		10/18- 5:00			
M		10/28- 18:00				M		10/18- 16:00			
S		10/29- 2:00				S		10/19- 6:00			
M		10/30- 18:00				M		10/19- 16:00			
S		10/31- 2:00				S		10/20- 7:00			
M		10/31- 17:00				M		10/21- 16:00			
S		11/1- 4:00				S		10/22- 4:00			
M						M		10/28- 17:00			
S						S		10/29- 2:00			
M						M		10/30- 17:00			
S						S		10/31- 3:00			
M						M		10/31- 16:00			
S						S		11/1- 5:00			
	4	22	16	6	3		4	25	17	8	3

Table 8.10: The exact date and time observed for when the PCM fully melts and proceeds to fully solidify. The number of cycles the PCM goes through, of full melting and then full solidifying, for a 40 kJ/kg PCM.

Figure 8.21 and 8.22 are graphical representations of the full melting and solidifying of PCM placed on different surfaces within the building.

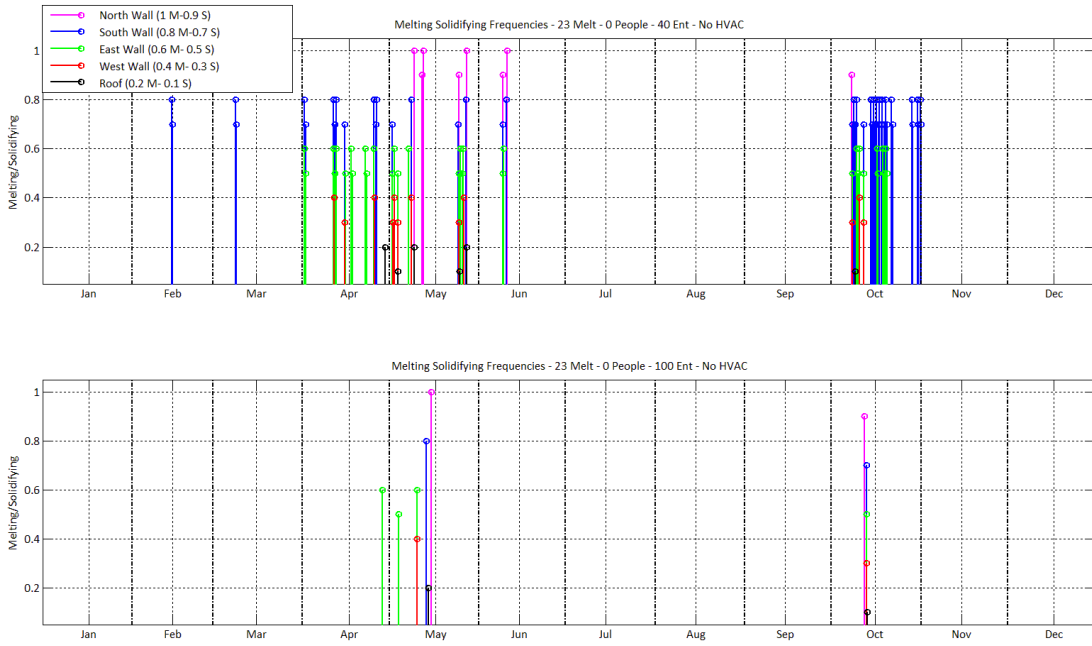


Figure 8.21: Graphical representation of melting/solidifying of the PCM in table 8.10 (top) & 8.9 (bottom) without HVAC

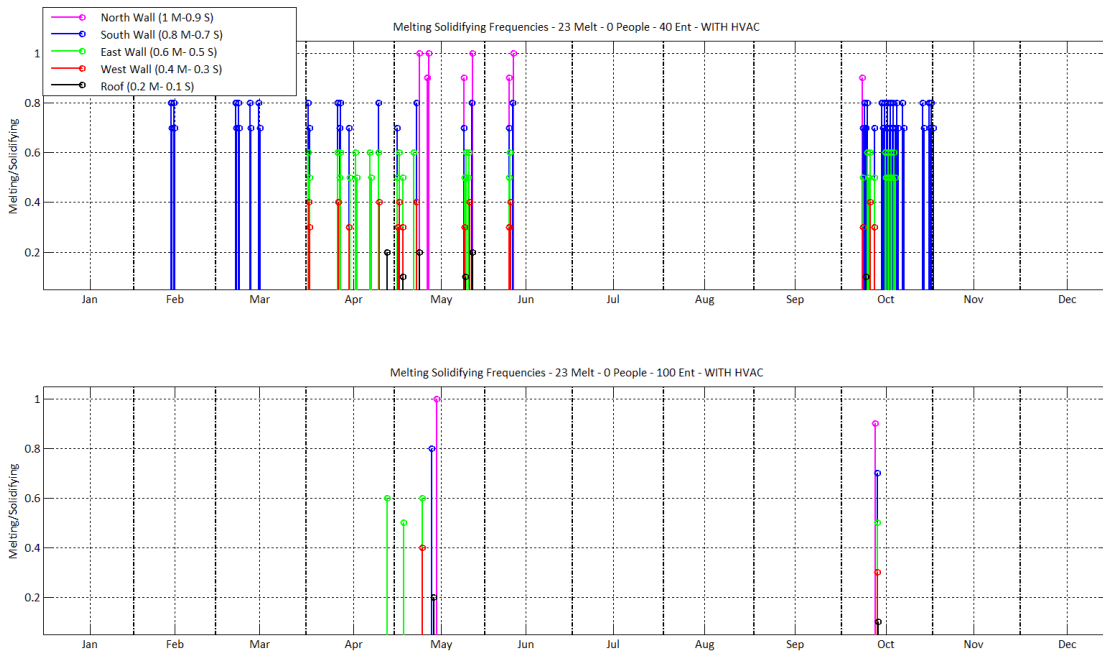


Figure 8.22: Graphical representation of melting/solidifying of the PCM in table 8.10 (top) & 8.9 (bottom) with HVAC.

In order to increase the ability to visualize the temporal aspect of the full melting and solidifying of PCM placed on different surfaces, numbers were assigned as placeholders for the different physical state the PCM was in. In Figure 8.21 and 8.2, if the PCM placed on the North wall was found completely melted, that specific date and time was denoted by the number 1. Similarly if the North wall was found to be completely solid, that specific date and time was then assigned the value 0.9. When the PCM on the South wall reached a state of complete saturation (fully melted) it was assigned a numerical value of 0.8 and when found completely solidified, the date and time was assigned a value of 0.7 and so forth for the remaining surfaces.

From Figure 8.20 it was evident that the difference in mean air temperature, when placing the PCMs with two different heat storage capacities, was observed for the months of May and October. Figure 8.21 depicts the melting and solidifying trends for a 23-40-PCM for all surfaces (top) and a 23-100-PCM for all surfaces (bottom) in the building without HVAC. The melting/solidifying trends for the PCMs with two enthalpies appear to differ during the months of May and October as well. However, the low number of melting/solidifying cycles in the bottom subplot should not be mistaken for the lesser performance of the two PCMs. It is actually the opposite. The bottom subplot corresponds to a 23-100-PCM and it actually performs better than the 23-40-PCM, albeit not by much. Therefore, the frequency of totally melted and totally solidified states does not necessarily translate to better performance of PCM. In addition, the introduction of air conditioning (Figure 8.22) does not drastically change the exact time the melting and solidifying occurs but rather increases the number of melting and solidifying hours. However it needs to be emphasized that for the case with no internal loads the optimum PCM melting temperature is 25°C and not 23°C, and this analysis of solidifying/melting cycle is performed on a PCM melting at 23°C. In order to understand the contribution in the directions of heat storage capacity and internal loads, it was important that the PCM melting temperature kept constant at 23°C.

A table was created for the number of hours when the PCM was melting, fully melted, solidifying, and fully solid for May and October, where the difference in performance between the two PCMs were noticed. Firstly the case without HVAC was run and analyzed. Table 8.11 represents the number of hours the state the PCM with a heat storage capacity of 40 and 100 kJ/kg takes throughout the month of May. Then table 8.12 represents the states for the month of October.

0 PEOPLE - NOHVAC					0 PEOPLE - NOHVAC				
MAY - 40 kJ/kg	Melted (hrs)	Melting (hrs)	Solid (hrs)	Solidifying (hrs)	MAY - 100 kJ/kg	Melted (hrs)	Melting (hrs)	Solid (hrs)	Solidifying (hrs)
North	166	163	139	212	North	103	209	130	226
South	194	146	105	232	South	133	174	66	258
East	262	121	62	253	East	209	158	38	288
West	200	147	88	221	West	156	145	58	242
Roof	300	96	87	166	Roof	231	120	68	149

Table 8.11: Number of hours that the PCM goes through each state during May. 40 kJ/kg & 100 kJ/kg

0 PEOPLE - NOHVAC					0 PEOPLE - NOHVAC				
OCT - 40 kJ/kg	Melted (hrs)	Melting (hrs)	Solid (hrs)	Solidifying (hrs)	OCT - 100 kJ/kg	Melted (hrs)	Melting (hrs)	Solid (hrs)	Solidifying (hrs)
North	46	136	373	147	North	42	145	336	171
South	126	143	243	218	South	76	172	175	280
East	83	155	280	207	East	66	170	236	243
West	60	155	316	178	West	54	122	268	197
Roof	78	104	411	117	Roof	75	86	360	155

Table 8.12: Number of hours that the PCM goes through each state during October. 40 kJ/kg & 100 kJ/kg.

Based on tables 8.11 and 8.12 the comparison between the two PCM heat storage capacities, shows that the PCM with an enthalpy of 100 kJ/kg is fully melted to a lesser extent

than the PCM with 40 kJ/kg enthalpy. The 23-100-PCM was therefore melting (absorbing heat) for longer hours than the 23-40-PCM. This is due to the fact that the 100 kJ/kg PCM takes much longer to saturate than the 40 kJ/kg PCM. The first column for the number of hours ‘melted’ show that, for both enthalpies during the month of May, the PCM on the *Roof* is fully melted the most. Similarly the second column shows the *Roof* as having the least number of hours ‘melting’, in comparison to other surfaces.

The tables also show that for the month of May, between the two PCMs, the PCM with the lower heat storage capacity stays in the *melting* and *solidifying* state a lot less number of hours than the PCM with the higher heat storage capacity. This suggests that the PCM with the higher volumetric heat capacity is in the melting state longer because it does not fully melt as soon as the other PCM with lower enthalpy does and thus is able to store more energy in the process. Similarly, the PCM with the higher heat storage capacity, once fully melted takes longer to dissipate the heat absorbed as evident in column *solidifying*. This opened up the possibility to test, but beyond the current scope, whether a decrease in surface thermal resistance of the PCM wallboard would facilitate a greater ability to exchange energy for the PCM boards with higher volumetric heat storage capacities. It has to be emphasized that in this case with no internal loads the optimum PCM melting temperature was found to be 25°C and not 23°C, as is analyzed in this solidifying/melting cycle. However, in order to understand the contribution in the directions of heat storage capacity and internal loads, it was important that the PCM melting temperature remain constant at 23°C.

Going back to table 8.8, the melting and solidifying percentage for the North wall and Roof are in agreement with the earlier hypothesis that the PCM on the roof melts faster predominantly because of the exterior radiation on its surface, while the North surface receives the least radiation therefore fully melts much less hours compared to other surfaces.

The outside face radiation heat gain rate per area (RHGRA) subplots in Figure 8.23 corresponds to the monthly gain for each surface. The centerlines in blue correspond to the monthly average RHGRA. It is evident from the second subplot, corresponding to the RHGRA for the Roof is where the highest volume of RHGRA is present. While the subplot for the Roof (2nd subplot) is highest in magnitude, the subplot for the North surface is the lowest in magnitude. The monthly average RHGRA subplots for the East wall and the West wall are identical. The South Wall receives, in average, a higher of the heat gain from radiation during the fall, spring and winter months and this could be attributed to the small angle of incidence of the solar rays on the surface during these months.

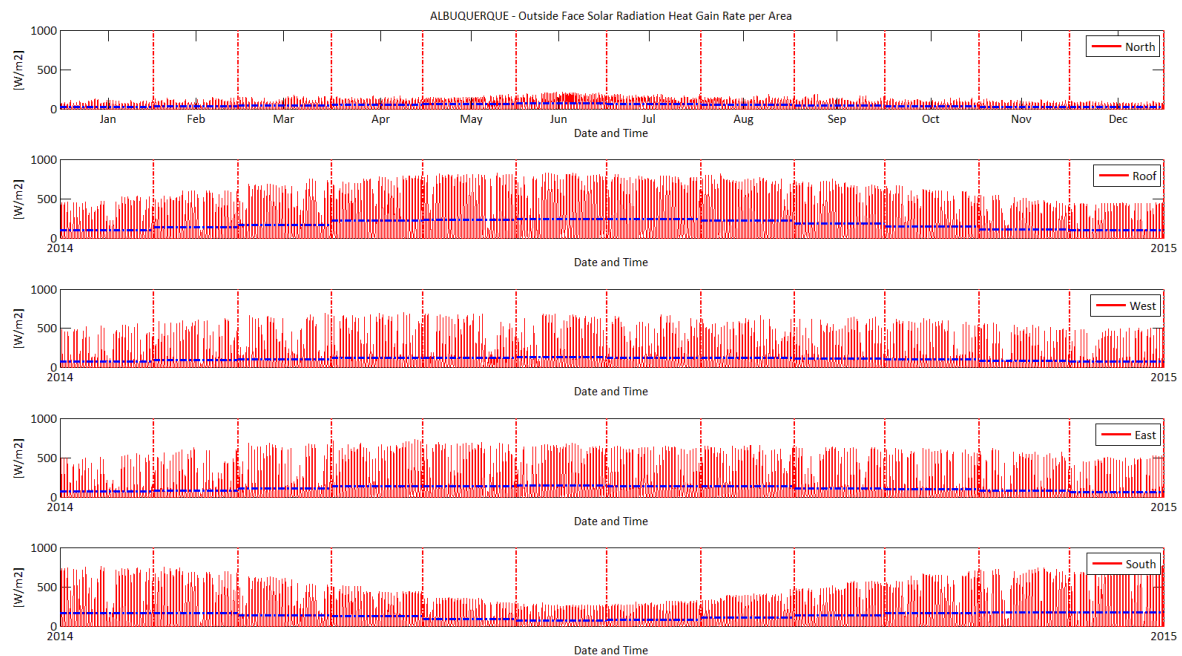


Figure 8.23: Outside face solar radiation heat gain rate per area [W/m²] for each surface.

It would make sense for the PCM on the Roof to stay melted the longest due to the high magnitude of radiation heat gain from the outside. However, the roof being melted from the outside is contradicted by the results in table 8.13.

ZERO PEOPLE - 40 kJ/kg - NO HVAC										
Without HVAC	Melted	M-Inside	M-Outside	M-ing	M-Total	Solid	S-Inside	S-Outside	S-ing	S-Total
North Wall (Hrs)	166	25	50	88	163	139	14	3	195	212
South Wall	194	20	40	86	146	105	10	12	210	232
East Wall	262	24	15	82	121	62	5	8	240	253
West Wall	200	32	52	63	147	88	17	18	186	221
Roof	300	52	12	32	96	87	126	20	20	166

Table 8.13: Number of hours that the PCM goes through each state during May. 0 People-23 Melt-40 Ent.

The number of hours the PCM melting from outside for the Roof during the month of May is only 12 while the number of hours for the Roof PCM melting from inside is 52. The solidifying trend however seems to align with the earlier hypothesis that since the Roof receives the most exterior solar radiation, the cooling process begins from the indoors and not the outdoors. Hence, the higher number of hours the PCM solidifies from the indoors. Nevertheless, the hypothesis is challenged by the fact that the North wall is melting more from the outdoors than the South wall, when it is clear that the magnitude of RHGRA is greater for the South wall, compared to the North wall. This indicates that there is a bigger contribution of the interior and exterior dry-bulb temperature both of which are symbiotically related to the exterior and interior radiation as well. Therefore, none of the environmental factors can be separated as individual elements to later superposition to explain the directional solidifying and melting of PCM indoors.

ZERO PEOPLE - 100 kJ/kg - NO HVAC										
Without HVAC	Melted	M-Inside	M-Outside	M-ing	M-Total	Solid	S-Inside	S-Outside	S-ing	S-Total
North Wall (Hrs)	103	34	44	131	209	130	14	3	209	226
South Wall	133	7	38	129	174	66	10	14	234	258
East Wall	209	31	9	118	158	38	10	14	264	288
West Wall	156	13	48	84	145	58	10	23	209	242
Roof	231	47	6	67	120	68	104	17	28	149

Table 8.14: Number of hours the PCM goes through each state during May. 0 people-23 melt-100 ent.

Similar results can be seen for the case with PCM volumetric heat capacity of 100 kJ/kg for the month of May from Table 8.14. The PCM on the roof surface still melts from the inside more so than from the outside. The melting of the PCM placed on the North wall is still

predominantly instigated from the outside and is greater in magnitude than the South surface. For the month of May however the melting hours from outside seem greater than melting from inside except for the Roof and East wall surface.

The melting and solidifying hours for the month of October are tabulated for each surface to see if there is any useful information that can be drawn as shown in Table 8.15.

ZERO PEOPLE - 40 kJ/kg - NO HVAC										
Without HVAC	Melted	M-Inside	M-Outside	M-ing	M-Total	Solid	S-Inside	S-Outside	S-ing	S-Total
North Wall (Hrs)	46	51	24	61	136	373	35	1	111	147
South Wall	126	46	32	65	143	243	16	38	164	218
East Wall	83	22	23	110	155	280	9	18	180	207
West Wall	60	43	44	68	155	316	15	51	112	178
Roof	78	86	1	17	104	411	89	13	15	117

Table 8.15: Number of hours the PCM goes through each state during October. 0 people-23 melt-40 ent.

While the trends are similar between 23-40-PCM (table 8.15) and 23-100-PCM (table 7.16), for the month of October, the symbolic difference from the month of May is that now the hours for melting from inside is greater than the hours for melting from outside. Both the tables show no type of uniform change with a change in only one variable, the volumetric heat storage capacity. Only the hours of ‘melting-total’ and ‘Solidifying-total’ seem to increase with the increase in volumetric heat capacity while everything else seems to decrease in the sense that when the volumetric heat capacity is increased the number of hours the PCM is absorbing energy increases. The number of hours the PCM stays melted is less for the 23-100-PCM as well as the number of hours the PCM stays solid is also less, compared to 23-40-PCM.

ZERO PEOPLE - 100 kJ/kg - NO HVAC										
Without HVAC	Melted	M-Inside	M-Outside	M-ing	M-Total	Solid	S-Inside	S-Outside	S-ing	S-Total
North Wall (Hrs)	42	60	21	64	145	336	52	2	117	171
South Wall	76	22	32	118	172	175	11	101	168	280
East Wall	66	12	21	137	170	236	8	23	212	243
West Wall	54	15	38	69	122	268	3	73	121	197
Roof	75	85	0	1	86	360	97	7	51	155

Table 8.16: Number of hours the PCM goes through each state during October. 0 people-23 melt-100 ent.

Another cause for concern is when the PCM placed on the North wall and the Roof fully melt and fully solidify around the same time (Table 8.09 and 8.10). If the Roof is receiving the bulk of the solar radiation and the North wall is receiving the least amount of radiation, why then does the PCM placed on the North wall fully melt and solidify around the same time as that of the PCM on the Roof.

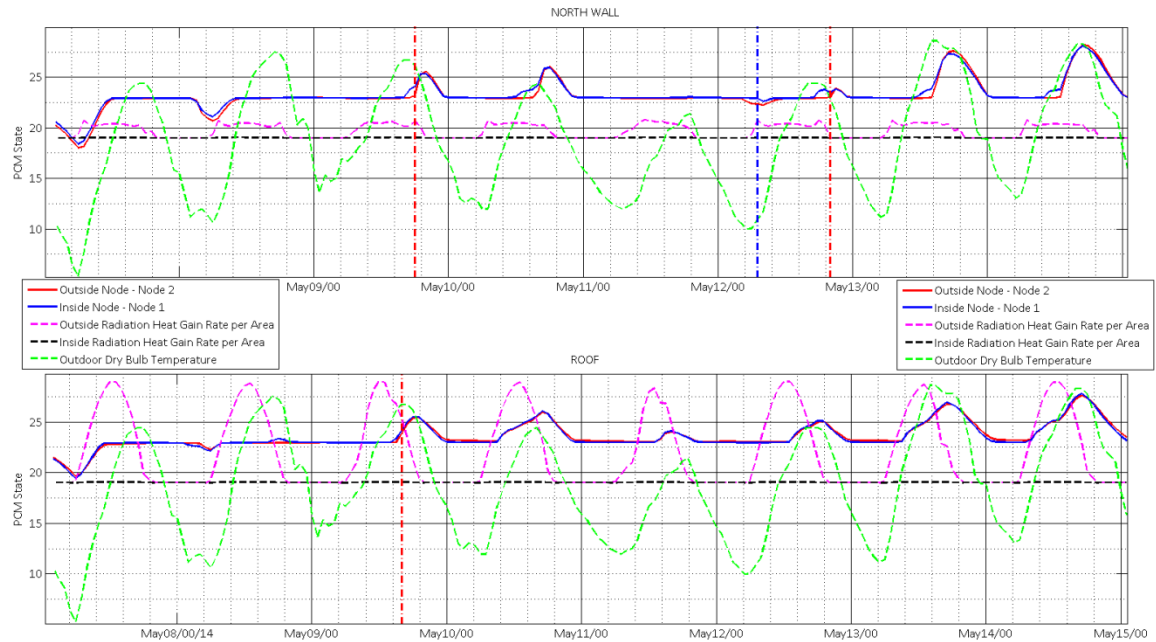


Figure 8.24: Nodal temperatures compared against outdoor dry bulb temperature and radiation heat gain for the week in May.

In Figure 8.24 and 8.25, the indoor and outdoor nodal temperatures for the North and Roof surfaces are plotted against the outdoor temperature and indoor temperatures respectively. The radiation heat gain per area on the inside surface and outside surface has been normalized to fall within the range of 18 and 29. The radiation heat gain rates per area in these plots are merely symbolic representations of their magnitudes. In both the Figures, the vertical lines in red correspond to the exact time when the PCM is fully melted and the vertical line in blue corresponds to the exact time when the PCM is fully solid. The nodal temperatures that correspond to the North wall and Roof, in both subplots, are the same nodal temperatures.

Figure 8.24 is zoomed out to incorporate the outdoor temperature in the plot space.

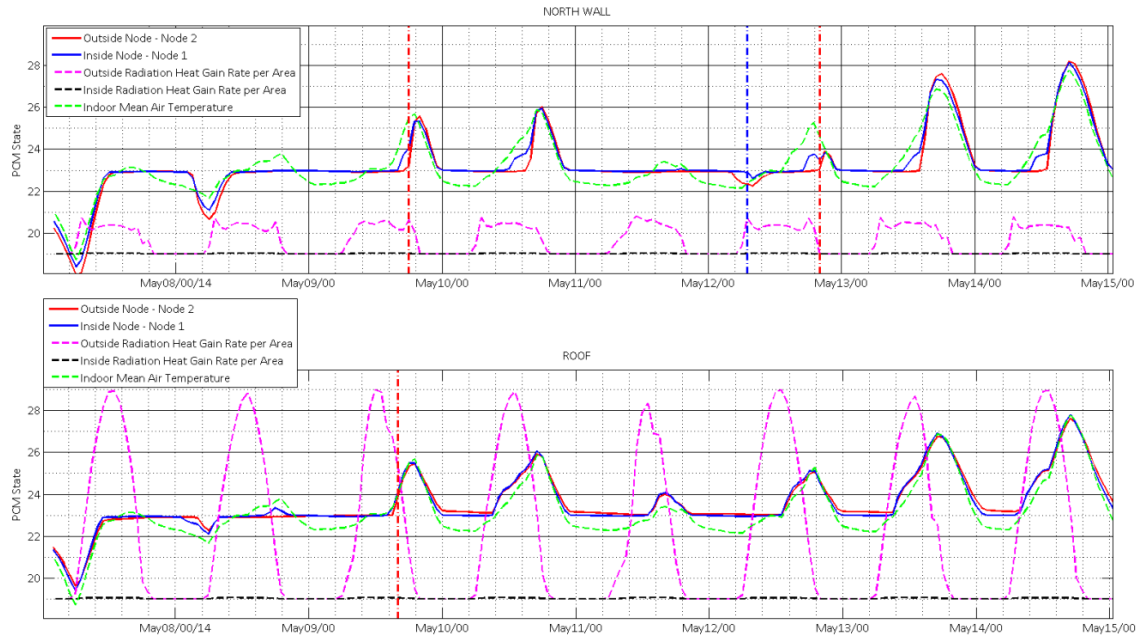


Figure 8.25: Nodal temperatures compared against indoor mean air temperature and radiation heat gain for the week in May.

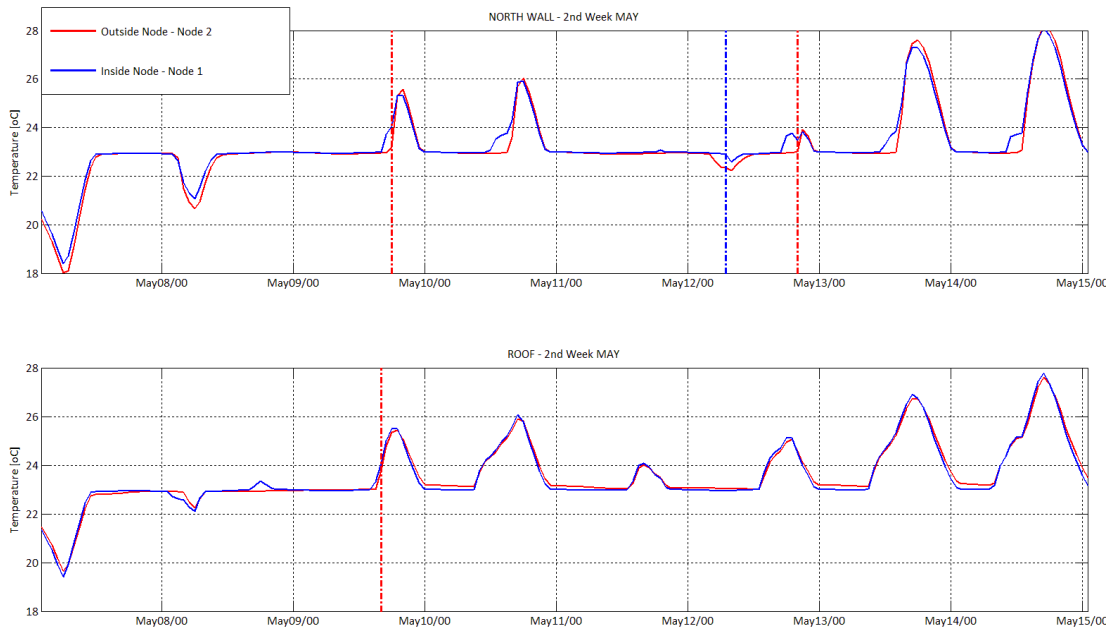


Figure 8.26: Nodal temperatures for the north wall (top) and roof (bottom) during the 2nd week in May.

So looking at Figure 8.25 and 8.26, the zoomed in plot for the week of May, it is clear that the solidifying of the PCM on the North Surface is always instigated from the outside since

the curve for the outside node always leads the way. On the other hand the melting process is always instigated from the inside where the blue curve leads the way. For the roof surface however it seems like both the melting and solidifying is instigated from the indoors because the inside nodal temperature constantly seems to lead the way. In addition, looking closer at the subplot for the Roof in Figure 8.25, the nodal temperature peaks prior to the indoor mean air temperature peaks, but it is the interior node that increases in temperature faster than the exterior node. Both these observations are contradictory to each other. The next time the Roof and North wall solidify together is the second week of October. The plots for October could shed better light on the melting/solidifying phenomena of PCM placed on these two surfaces. In Figure 8.27 the nodal temperatures for the inside surface and the outside surface of the PCM gypsum board is plotted for both the Roof surface and North wall.

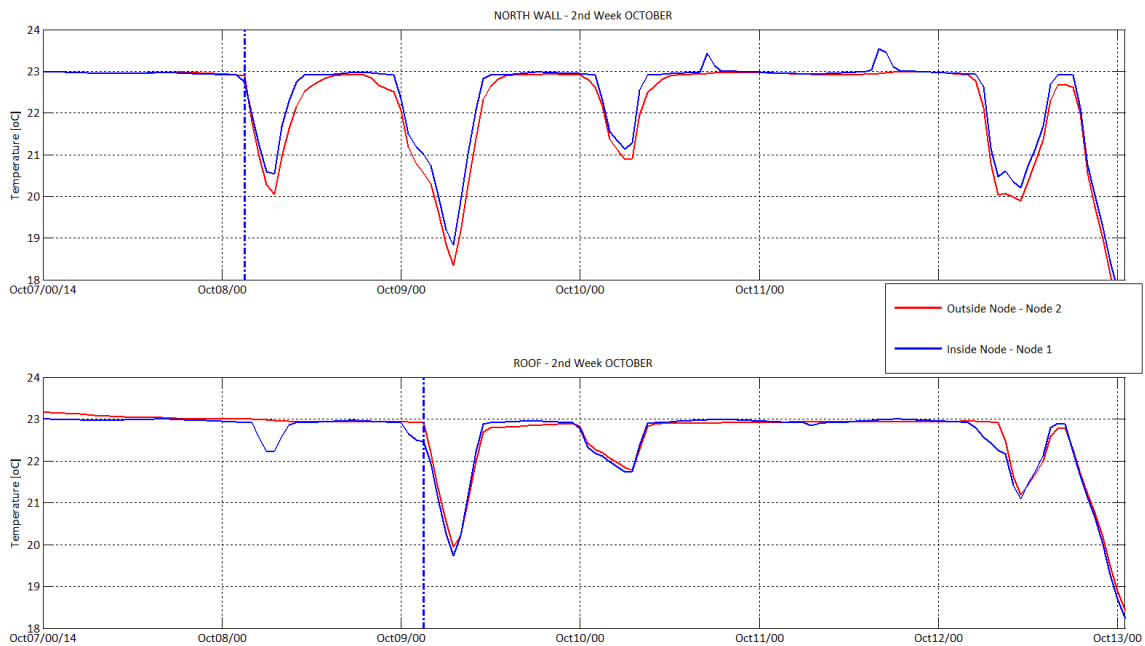


Figure 8.27: Nodal temperatures for the north wall (top) and roof (bottom) during the 2nd week in October.

In Figure 8.27, the nodal temperature for the PCM board placed on the Roof and North wall, during the month of October shows that the PCM board placed on the North wall again

starts solidifying from the outside where as it starts melting from the inside. The PCM board placed on the roof, however, starts solidifying from the inside and in addition starts to increase in temperature from the inside as well. This phenomenon needs further study to explain why , both the melting and solidifying of the PCM board placed on the Roof starts from the inside even though the roof is receiving the most solar radiation from the outside. This phenomenon can probably be isolated by allowing for each exterior environmental load to be incrementally added into the EnergyPlus weather file and gauge the behavior of PCM placed on all the surfaces accordingly, which at present out of the scope of this study.

Case 2: fifteen people - 40 kJ/kg - 100 kJ/kg – WITH-WITHOUT HVAC

The mean air temperature indoors for the case with 15 people occupying the indoors was obtained.

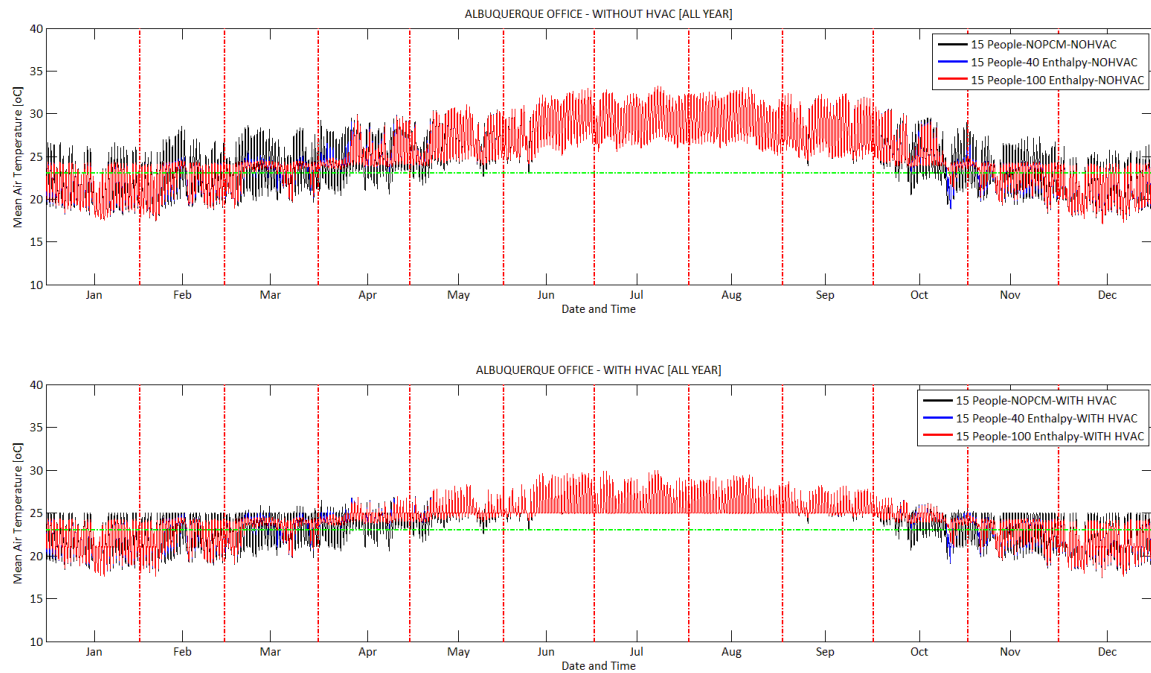


Figure 8.28: Hourly mean air temperature indoors for PCM melting at 23°C and 15 people. Without HVAC (top) and with HVAC (bottom).

Again, the temperatures were obtained for when the HVAC system was present (bottom subplot in Figure 8.28) and when there was no HVAC system to service the indoors (top subplot in Figure 8.28). In addition, the data was also plotted to compare in the direction of volumetric heat storage capacity. The two enthalpies, 40 kJ/kg (in blue) and 100 kJ/kg (in red), were selected and plotted on top of each other in order to understand to what magnitude the two enthalpies contribute to reducing the indoor temperature. In Figure 7.28 the indoor mean air temperature for the two PCMs with different enthalpies are almost identical. On the top subplot, the difference between the 23-40-PCM (blue) and the 23-100-PCM (in red) only seems to exist during the month of April. This was also evident in Figure 8.18. With 15 people occupying and dissipating heat indoors, it is expected that the PCM melts from the indoors more than it did with zero people indoors. In addition, it is expected that the PCM with stay melted a longer time due to the constant internal load. It is also expected that the increase in internal load push the optimum months for the use of PCM boards closer to the colder months.

FIFTEEN PEOPLE - 40 kJ/Kg											
Without HVAC	Melted (%)	Melting (%)	Solid (%)	Solidifying (%)	# of Cycles	With HVAC	Melted (%)	Melting (%)	Solid (%)	Solidifying (%)	# of Cycles
North	44.3	12.0	31.1	12.7	5	North	42.6	12.9	30.9	13.6	6
South	49.6	11.8	20.9	17.6	66	South	48.4	12.4	20.7	18.6	79
East	48.4	10.0	25.5	16.1	16	East	47.2	10.5	25.0	17.3	17
West	46.6	12.3	27.4	13.7	11	West	45.3	13.0	27.2	14.5	11
Roof	53.4	6.6	30.3	9.8	4	Roof	52.9	7.2	29.5	10.4	4
FIFTEEN PEOPLE - 100 kJ/Kg											
Without HVAC	Melted (%)	Melting (%)	Solid (%)	Solidifying (%)	# of Cycles	With HVAC	Melted (%)	Melting (%)	Solid (%)	Solidifying (%)	# of Cycles
North	43.5	12.6	30.9	13.1	1	North	41.8	13.5	30.5	14.2	1
South	46.4	14.6	18.3	20.7	4	South	44.9	15.4	18.0	21.8	4
East	46.9	11.2	24.3	17.7	1	East	45.9	11.6	23.7	18.8	1
West	45.8	12.7	27.0	14.5	1	West	44.5	13.2	26.7	15.6	1
Roof	53.2	7.1	30.0	9.7	1	Roof	52.8	7.7	29.2	10.3	1

Table 8.17: Percentage the PCM goes through each state. 15 people-23 melt- 40 and 100 ent.

A comparison of results in table 8.17 (15 people) and table 8.8 (0 people) shows an increase in percentage of hours the PCM is fully ‘melted’. This is expected, predominantly since the addition of 15 people indoors, dissipating 120 watts each, accrues 4667 mega joules per month of energy indoors. This increase in energy indoors is primarily the reason for the higher percentage of the PCM being fully melted. As a corollary, the percentage of hours the PCM stays fully ‘solid’ for all surfaces decreases when the internal load is increased to 15 people. Another observation is that the PCM placed on all the surfaces, except for a few instances on the South façade, is increased in percentage for the ‘melting’ and ‘solidifying’ state of PCM. The increase in internal load has therefore encouraged the PCM boards to be more ‘active’ in the absorption and release of energy. The number of cycles the 23-40-PCM goes through for the south wall tripled with the increase in internal load. While it was evident that the frequency of full melting and solidifying of PCM had increased, the months during which the melting/solidifying occurred had shifted more towards the cooler months. Figure 8.29 and 8.30 depict the dates and times the PCM board on each surface fully melts and fully solidifies throughout the year, without and with HVAC respectively.

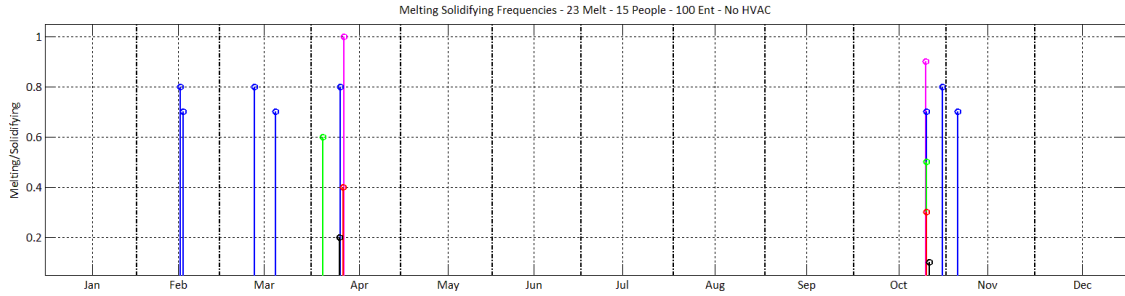
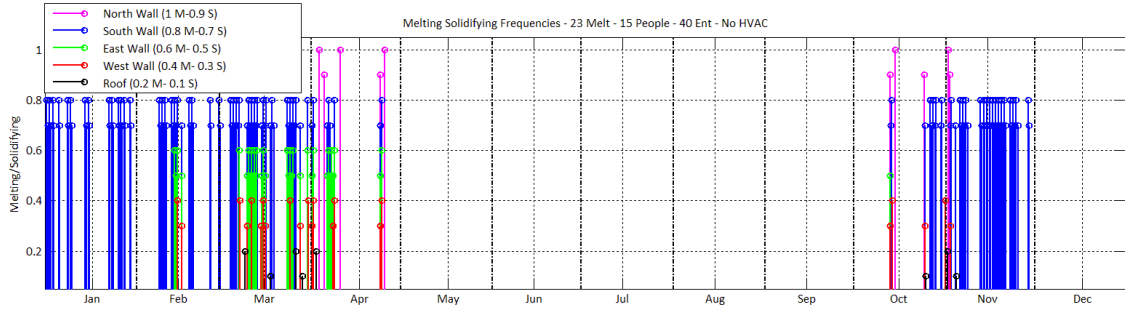


Figure 8.29: Graphical representation of melting/solidifying of the PCM in table 8.10 & 8.11 with HVAC.

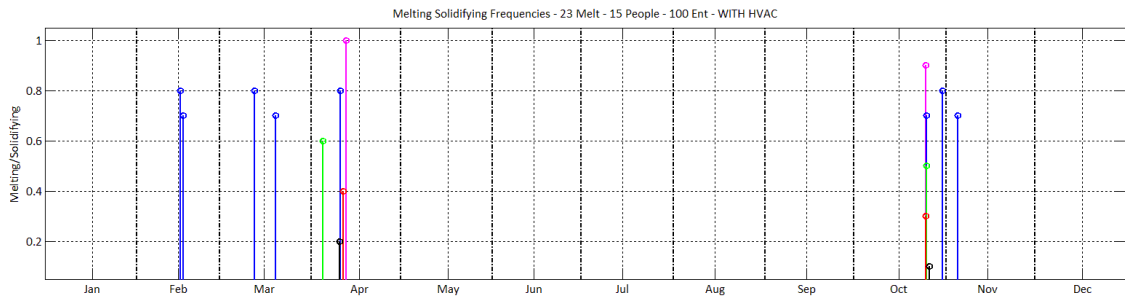
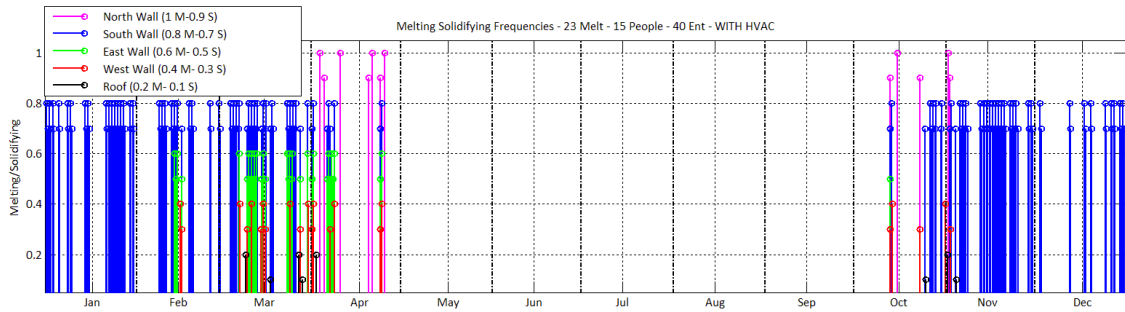


Figure 8.30: Graphical representation of melting/solidifying of the PCM in table 8.10 & 8.11 without HVAC.

Figure 8.29 and 8.30 are graphical representations of the full melting and solidifying of PCM placed on different surfaces within the building. In order to increase the ability to visualize

the temporal aspect of the full melting and solidifying of PCM placed on different surfaces, numbers were assigned as placeholders for the different physical state the PCM was in. For instance, if the PCM placed on the North wall was found completely melted, that specific date and time was denoted by the number 1. Similarly if the North wall was found to be completely solid, that specific date and time was then assigned the value 0.9. When the PCM on the South wall reached a state of complete saturation (fully melted) it was assigned a numerical value of 0.8. And when found completely solidified, the date and time was assigned a value of 0.7 and so forth for the remainder of surfaces.

It can be seen in Figure 8.30 that the 23-40-PCM fully melts and solidifies many times than the 23-100-PCM. Predominantly the PCM board placed on the South wall undergoes many melting and solidifying cycles. Even though the 23-40-PCM goes through the complete cycle many times for the months of January, February, March, October, November and December, as compared to 23-100-PCM, there is no significant difference in energy saved between the two PCMs for these months. The majority of difference in savings between these two PCMs was found during the month of April, this was seen in Figure 8.18 as well. The melting and solidifying trend for the month of April is tabulated to understand the trend for the two different enthalpies.

15 PEOPLE - NOHVAC					15 PEOPLE - NOHVAC				
APR - 40 kJ/kg	Melted (hrs)	Melting (hrs)	Solid (hrs)	Solidifying (hrs)	APR - 100 kJ/kg	Melted (hrs)	Melting (hrs)	Solid (hrs)	Solidifying (hrs)
North	210	197	52	252	North	176	215	63	246
South	283	132	24	268	South	224	169	4	273
East	338	100	16	258	East	271	151	0	273
West	275	167	14	248	West	221	197	2	256
Roof	451	42	0	173	Roof	385	79	0	136

Table 8.18: Number of hours the PCM goes through each state during April. 40 kJ/kg & 100 kJ/kg - NO HVAC.

Table 8.18 depicts the number of hours the 23-40-PCM and 23-100-PCM go through each physical state during the month of April. The two cases are for when the HVAC is not used.

Unless there is much difference in trend for the two PCMs, when HVAC is used, then it can be seen that the difference in energy saved for the month of April between the two PCMs comes predominantly from the fact that 23-100-PCM is not completely solid or completely melted nearly as much as the 23-40-PCM. Therefore the 23-100-PCM participates in the energy absorption/release far many hours than the 23-40-PCM.

15 PEOPLE - WITHHVAC					15 PEOPLE - WITHHVAC				
APR - 40 kJ/kg	Melted (hrs)	Melting (hrs)	Solid (hrs)	Solidifying (hrs)	APR - 100 kJ/kg	Melted (hrs)	Melting (hrs)	Solid (hrs)	Solidifying (hrs)
North	179	213	60	259	North	137	239	61	264
South	265	137	25	277	South	202	180	3	282
East	323	105	17	267	East	261	153	0	282
West	254	179	19	251	West	201	204	0	273
Roof	438	46	0	179	Roof	376	81	0	138

Table 8.19: Number of hours the PCM goes through each state during April. 40 kJ/kg & 100 kJ/kg - WITH HVAC.

When the HVAC was turned on for the two cases, the 23-40-PCM stayed melted approximately 50 hours longer than the 23-100-PCM for all the surfaces during the month of April, thereby not participating in the heat absorption, that the 23-100-PCM otherwise did.

FIFTEEN PEOPLE - 40 kJ/kg - NO HVAC										
Without HVAC	Melted	M-Inside	M-Outside	M-ing	M-Total	Solid	S-Inside	S-Outside	S-ing	S-Total
North Wall (Hrs)	210	73	111	13	197	52	68	72	112	252
South Wall	283	25	60	47	132	24	59	72	137	268
East Wall	338	12	38	50	100	16	50	62	146	258
West Wall	275	53	92	22	167	14	49	66	133	248
Roof	451	15	24	3	42	0	84	8	81	173

Table 8.20: Number of hours the PCM goes through each state during April. 15 people-23 melt-40 ent.

FIFTEEN PEOPLE - 100 kJ/kg - NO HVAC										
Without HVAC	Melted	M-Inside	M-Outside	M-ing	M-Total	Solid	S-Inside	S-Outside	S-ing	S-Total
North Wall (Hrs)	176	66	108	41	215	63	69	69	108	246
South Wall	224	6	114	49	169	4	10	79	184	273
East Wall	271	1	88	62	151	0	9	59	205	273
West Wall	221	43	120	34	197	2	16	78	162	256
Roof	385	22	40	17	79	0	74	6	56	136

Table 8.21: Number of hours the PCM goes through each state during April. 15 people-23 melt-100 ent.

No specific trend can be discerned from the two tables 8.20 and 8.21 that depict the number of hours and the direction from which the PCM boards melt. One counter intuitive observation is that, with this increase in internal loads from zero to fifteen people, there was more number of hours during April where the melting of the PCM is initiated from the outside and not the inside. However, looking back at the cases for zero people in tables 8.13, 8.14, 8.15 and 8.16 there is nothing to suggest that because there are no internal loads, that the majority of melting is instigated from the outside and not the inside either.

Case 3: twenty four people - 40 kJ/kg - 100 kJ/kg – WITH/WITHOUT HVAC

The internal load was increased to 24 people and the mean air temperatures were obtained for when the HVAC system was present (bottom subplot in Figure 8.31) and when there was no HVAC system to service the indoors (top subplot). In addition, the data was also plotted to compare in the direction of volumetric heat storage capacity.

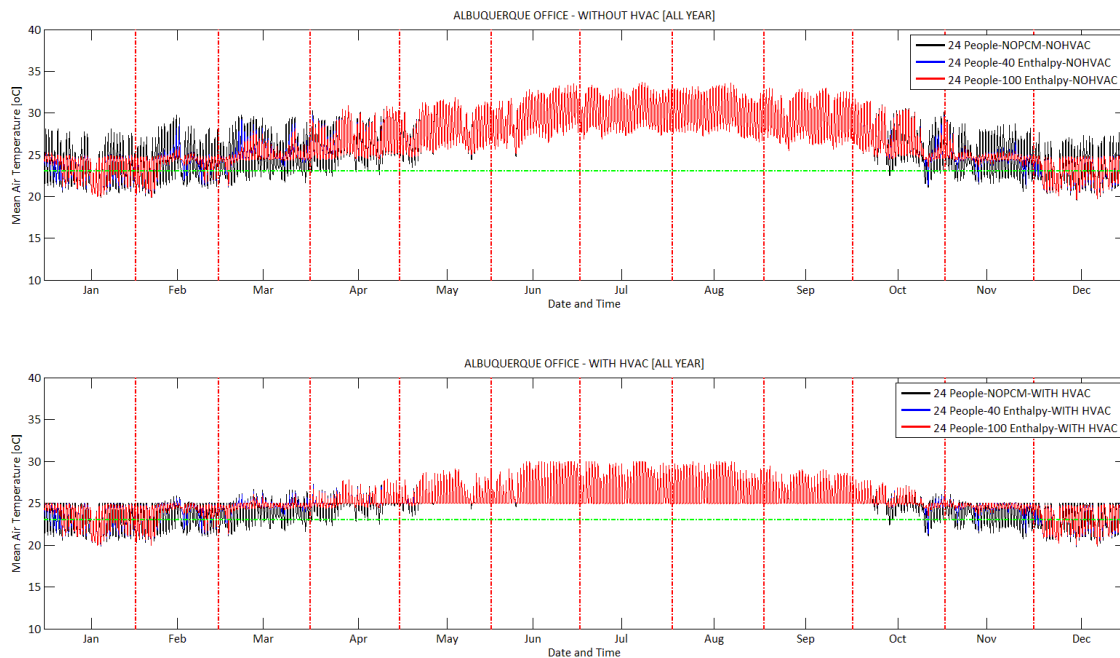


Figure 8.31: Hourly mean air temperature indoors for PCM melting at 23°C and 24 people. Without HVAC (top) and with HVAC (bottom).

The two enthalpies, 40 kJ/kg (in blue) and 100 kJ/kg (in red), were selected and plotted on top of each other in order to understand how the magnitude the two enthalpies contribute towards reducing the indoor temperature.

The optimum months to place PCM boards have shifted further to the winter months with this change in internal loads from 15 people to 24 people. This is clearly evident in the frequency plot, Figure 8.32, and for total melting and solidifying of PCM for the different internal loads as well.

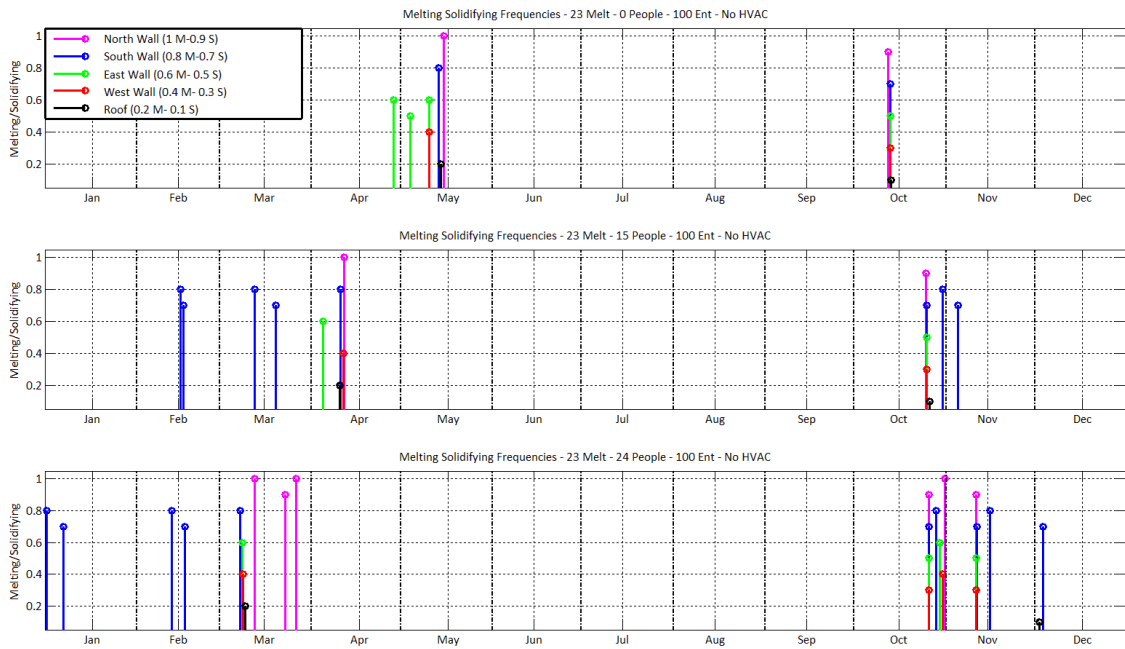


Figure 8.32: Graphical representation of the melting/solidifying frequency shifts for the 23-100-PCM - change in internal loads from 0 people (top) to 15 people (middle) to 24 people (bottom) - without HVAC.

The trend of the PCM melting frequency shifting closer and closer to the winter months with every addition in internal loads is expected, since it was found early on in this chapter that every increase in internal load pushes the optimal months towards the colder months while the increase in melting temperature pushes the optimal months closer to the warmer months.

Nonetheless, in the presence of an HVAC thermostat, the perfect balance between the PCM

melting temperature and internal loads is what determines the optimality of the PCM. While there is still no conclusive way right now to correlate the number of hours the PCM on each surface is melting, melted, solidifying or solid to the amount of energy stored or released for each of the cases, this methodology employed that calculates the exact number of hours the PCM goes through each stage and the directional indicator can be used in a future study to pinpoint the behavior of PCM in a dynamic setting.

The plots in Figure 8.33 align with what is already known about the melting/solidifying frequency of the 23-40-PCM and 23-100-PCM that the PCM with the lower enthalpy will go through more full cycles of melting and solidifying as opposed to the PCM with a higher enthalpy.

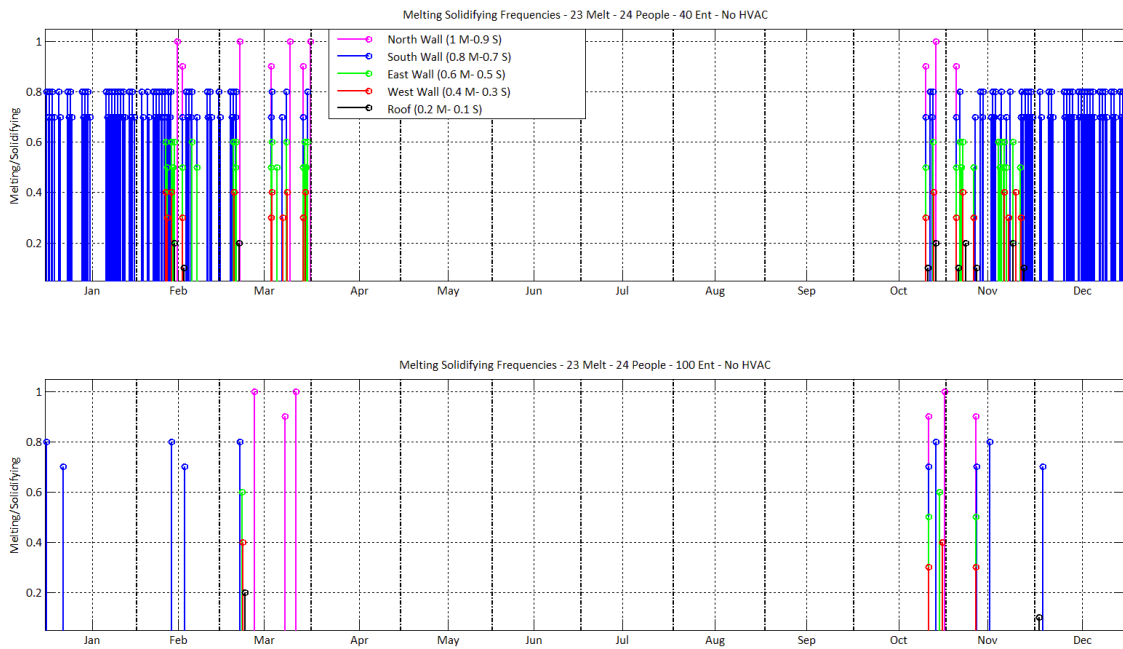


Figure 8.33: Graphical representation of melting/solidifying of the 23-40-PCM and 23-100-PCM on each surface for the case with 24 people occupying the indoors - without HVAC.

TWENTY FOUR PEOPLE - 40 kJ/Kg

Without HVAC	Melted (%)	Melting (%)	Solid (%)	Solidifying (%)	# of Cycles	With HVAC	Melted (%)	Melting (%)	Solid (%)	Solidifying (%)	# of Cycles
North	52.5	12.2	19.8	15.5	5	North	49.6	13.8	20.1	16.5	6
South	58.7	10.1	12.4	18.9	72	South	56.9	10.7	12.5	19.9	73
East	55.3	10.2	15.8	18.7	17	East	53.5	10.8	16.0	19.7	14
West	55.0	13.6	17.2	14.1	10	West	53.0	14.8	17.5	14.7	9
Roof	63.4	8.4	13.8	14.4	5	Roof	62.1	8.7	13.9	15.3	5

Table 8.22: Percentage of hours the PCM goes through each state throughout the year and the number of cycles the PCM goes through total melting and total solidifying. 24 people - 23-40-PCM.

An observation from table 8.22 is that the PCM increased in percentage for the ‘melting’, ‘melted’ and ‘solidifying’ state for all the surfaces except for the South wall which saw a decrease in the percentage of hours of ‘melting’ state. The increase in internal load to 24 people indoors has therefore encouraged the PCM boards to be more ‘active’ in the absorption and release of energy. The number of cycles the 23-40-PCM goes through for the south wall increased with the increase in internal load from 15 to 24 people.

TWENTY FOUR PEOPLE - 100 kJ/Kg

Without HVAC	Melted (%)	Melting (%)	Solid (%)	Solidifying (%)	# of Cycles	With HVAC	Melted (%)	Melting (%)	Solid (%)	Solidifying (%)	# of Cycles
North	50.8	13.7	17.8	17.6	3	North	47.8	15.5	18.3	18.5	2
South	55.6	14.4	8.5	21.4	5	South	53.7	15.2	8.6	22.4	5
East	55.3	10.9	13.6	20.2	2	East	53.3	11.6	13.8	21.3	3
West	54.0	15.7	15.3	15.1	2	West	51.6	17.0	15.5	15.9	2
Roof	63.0	8.4	12.2	16.4	1	Roof	61.9	8.8	12.3	17.1	1

Table 8.23: Percentage of hours the PCM goes through each state throughout the year and the number of cycles the PCM goes through total melting and total solidifying. 24 people - 23-100-PCM.

While it still holds true that the PCM with higher enthalpy stays ‘melted’ or ‘solid’ less than the PCM with a lower enthalpy, the frequency of melting and solidifying of the PCM on each surface, whether it be from the indoors or outdoors cannot help determine the main cause for the melting and solidifying. This phenomenon can be better understood by allowing for each

exterior environmental load for the Albuquerque weather file to be incrementally added into the EnergyPlus weather file and gauge the behavior of PCM placed on all the surfaces accordingly.

Chapter Nine

Conclusion

Given that the building sector in the United States alone accounts for 40% of primary energy use, and increasing the thermal mass of a building is able to achieve indoor temperature management and energy efficiency, the use of Phase Change Materials in buildings to increase its thermal mass represents an excellent opportunity for the reduction in energy usage and indoor temperature management.

This thesis discusses the viability of using PCM boards in lightweight buildings located in 8 different climate types within the United States as defined by the Department of Energy. The buildings in each climate were carefully designed in accordance to the requirements laid out in the ASHRAE 90.1 standard for a baseline building. The window-to-wall ratios of all surfaces were kept at a constant 14%. The R-value of the insulation and the solar heat gain coefficient (SHGC) of the windows were designed to meet the minimum requirements of each climate. A full factorial experimental design was chosen to study the effect of different levels of each independent variable on the energy consumption of the building.

Contribution and discussion

The major elements of this research were the development of climate maps and the corresponding regression models, payback period analysis for the PCM boards in comparison to the cost per kWh of electricity at different locations, the effect of each independent variable on the performance of PCM in the building and the development of the melting/solidifying method to understand the temporal and directional aspect of PCM solidifying and melting within the building.

- Climate Maps: In the initial study the PCM boards were studied in two directions, the melting temperature and enthalpy. While every other variable identified in the research design were kept constant, only the melting temperature and enthalpy were parametrically studied for each climate type. From the study it was concluded that the PCM boards performed optimally in hot, dry and marine climates. As such, San Francisco and Albuquerque were identified as the two optimal climate types for the placement of PCM boards. The diurnal fluctuation of ambient temperature in the hot and dry climates as well as the mild marine climates could be attributed for the better performance of PCMs. The PCM boards did not perform optimally in cold and humid or the hot and humid climates. The reason for the poor performance of PCM boards in humid climates can also be attributed to the fact that the PCM boards need to work harder to extract energy from humid air and therefore the HVAC system is employed longer to meet the humidity set point indoors.

The 'pseudo' payback period of the use of PCM boards were comparatively very high. For the PCM boards to be economically viable, considering \$0.07/kWh of electricity, the cost of PCM boards would have to cost around \$1/kg. The effect of the time value of money, the savings accrued due to the downsizing of HVAC equipment, reduction in construction costs, and the lower interest rates provided by the energy efficient mortgage (EEM) and other federal subsidies for the investment in energy efficient homes could reduce the number of years on the return on investment (ROI).

The sensitivity study showed that the optimum temperature was an important factor in determining the energy saving potential of the PCM board. A slight divergence from the optimum temperatures for each climate reduced the energy saving potential by 5-10 percent.

The climate maps were generated to visually demonstrate the optimum PCM, magnitude of energy saved and payback period of the PCM in each climate. The climate maps help to convey a large number of numerical data pertaining to the use of PCM boards in an efficient color coded format. The climate maps therefore serve as a tool for architects and engineers to determine the applicability of PCMs in each climate in a visual and efficient way.

The empirical models and climate maps developed are by no means exhaustive of all the design parameters and the design possibilities for the PCM buildings. Other empirical models that can be developed should focus on buildings with different construction and with different levels of independent variables. For instance the window to wall ratio of a building determines the amount of incident solar radiation indoors, and since the internal loads were determined to be an important variable, the effect of added incident solar radiation as a variable is important for the development of an all encompassing empirical model.

- *Location of PCM and HVAC set-point schedule*: This study was performed in 3 directions i.e., PCM melting temperature, placement of PCMs on different facades, and the three different HVAC set-point schedules for the building located in Albuquerque. The heat storage capacities (enthalpy) of the PCM boards were normalized on the basis of the surface area to which it was appended. It was found that there was not much variability in the amount of energy saved in the direction of the placement of PCM on the walls. The variation was comparatively large in the direction of the PCM melting temperature.

Additionally, it was also found that the office HVAC set-point schedule with a night time setback was more conducive to the performance of PCM boards. The PCM boards placed on the same building with a residential HVAC set-point schedule showed the least savings in energy with the application of PCMs. In addition to the HVAC

schedules, it is also important for the simulations to include different night time ventilation strategies (i.e., a more active HVAC control schedule) that can purge the absorbed heat from the PCM boards in question. Since the PCM boards in most of the climates did not follow a daily melting/solidifying trend, it is important to include HVAC control strategies that can foster a diurnal melting/solidifying cycle of the PCM boards.

In terms of the location of PCM on the different surfaces, for the seven cases, internal loads and HVAC schedules it was observed that the placement of optimum PCM on the larger surface area was invariably better than placing it on a smaller area, even though the surfaces exhibited the same amount of latent heat storage capacity. It was found that the surface area of the placement of PCM dictated the magnitude of energy savings. It was best to cover more surface area with a lesser latent heat storage capacity than to concentrate large latent heat storage one surface area of the building. Spreading the PCM on a larger area, as opposed to concentrating it on a small area, seemed more conducive because of the smaller 'thermal bridge' that the larger surface area provided. The building as a 'system' was therefore without a thermal bridge when the PCM was spread equally through the surface area. The PCM spread out at a larger area also provided more surface contact with the indoors to participate in the energy absorption/release cycle. Therefore the increase in PCM surface area in a building saved more energy than just concentrating it in a smaller area.

- Regression Models: This research aimed to be one of the first comprehensive studies on the effect of 6 independent variables on the performance of PCM placed in buildings. The data obtained from the full factorial design simulations were arranged on a climatological basis. A set of regression models were also developed for the cases with PCM in each climate location for each HVAC type. The *data-split* at the 25°C melting temperature mark was optimal in defining the behaviour of PCM boards in the lightweight building

with the different levels of independent variables. Similarly regression models were developed for the control group. Once the models for the two cases (with PCM and without PCM) were developed, they were combined in order to predict the magnitude and percent energy savings in each climate.

The global test for the regression models (except for San Francisco and Seattle) at a significance level of α (Alpha) = 0.05 was found significant in predicting the annual load with and without PCM. The predicted values were within 5% of the actual data for all the models developed. Therefore, the regression models when connected with the climate maps developed in Chapter 4, as well as the cost of energy in each city, was developed to assist architects, engineers and researchers to effectively visualize the magnitude of energy saved and payback period of using PCM boards in the specific climates.

The regression models developed are again, by no means exhaustive of all the design parameters and the design possibilities for the PCM buildings. Other independent variables, listed in the future study, needs to be included when developing regression models for the rest of the climates.

- *Payback period*: A payback period analysis was performed on each climate for the actual data obtained from the full factorial design simulations. The payback period was calculated for all the climates using the average retail price of electricity that is based on the end use sector, commercial or residential. Similarly, for the payback period analysis, the cost of PCM boards was allowed to take on the actual current price of \$6/ft² and checked to see if placing PCM boards in any climate offered a payback period less than 75 years. After filtering the optimum climates to a select few, the PCM boards were allowed to take on a much cheaper price than what was communicated by a manufacturer here in the U.S (\$6/ft²). The PCMs boards were allowed to take on a price of \$0.50/ft²,

which is \$0.20/ft² more expensive than ordinary gypsum boards (\$0.30/ft²). This was done in order to ascertain the payback period for PCM boards if it were to cost comparatively similar yet gradually expensive than ordinary gypsum boards.

It was found that, for the assumed cost of PCM boards, only the PCM boards placed in buildings with the office HVAC settings for the climate types represented by Albuquerque and San Francisco was below the 15 year payback period mark. While placing PCM boards in the same building located in Seattle showed considerable savings in energy, the cheap cost of electricity for Seattle pushed the payback period over the 15 year mark. Until and unless the cost of energy increases or the cost of PCM boards decreases from the current levels, the viability of PCM boards in other climates besides the ones represented by Albuquerque and San Francisco seems unpromising.

The payback period analysis was performed on the basis of initial investment versus the energy saved in monetary terms. The time value of money, the reduction in size of the HVAC equipment and the federal subsidies available for energy efficient buildings are a few parameters that were not included in the payback period analysis. In addition the cost of electricity around the United States varies depending on the state, location within the state, and by local electric distribution companies. While there may not be a large variance in price within the locations of an individual climate zone, that discrepancy in cost per kWh of electricity still exists. Furthermore, the cost of electricity at a location is also adjusted for peak demand tariff and declining block tariffs. Therefore the simple payback period analysis in this study only serves as an initial review of the return on investment for using PCM boards in buildings. A more detailed approach will have to include the aforementioned variables as well as the cost of other energy forms that will service the building indoors.

- Internal Loads: Occupant behaviour is arguably the single greatest challenge to building energy researchers and analysts (O'Brien, 2011). While mathematical and physical models continue to increase to high levels of accuracy, there is still a lot of uncertainty on how building occupants behave to affect building energy use. In addition, lighting and plug loads are beginning to dominate over envelope based loads. This research identified the importance of occupant based loads on the proper selection of PCM melting temperature.

It was found that the optimum melting temperature of PCM boards changed with the increase or decrease in internal loads. While the external environment does play a role in determining the viability of Phase Change Materials, the optimal melting temperature of PCM boards is determined by and large by the change in internal loads in the building. In this study, as the internal loads were increased by increasing the occupancy indoors, the optimum melting temperature shifted to 23°C for most of the climates. The PCM melting at 23°C therefore reduced the mean indoor air temperature to exactly 25°C which incidentally was the cooling set-point temperature. Because of the fact that the majority of savings were accrued for the cooling load, the PCM melting temperature that reduced the mean indoor air temperature to the cooling set-point temperature was the PCM that performed the best. The internal load, therefore, when increased or decreased, requires a PCM that will reduce the indoor temperature to exactly the cooling set-point temperature. The optimum melting temperature of the PCM was therefore greatly dependent on the internal loads.

In this research while the occupancy based loads were allowed to take on 7 different values, the occupancy schedule was kept constant. This deliberation was made in order to first understand the performance of PCM boards under different levels of internal loads that were constant in time. However the occupancy behavior and the

impact of internal loads in an actual building is far from constant or consistent for that matter. In general the measured energy use of buildings exhibit large discrepancies even between buildings with the same function and located in similar climates (Hong, 2013). Occupancy behavior is the driving factor contributing to such discrepancies. How occupants set the comfort criteria (including thermal, visual, and acoustic), interact with building energy and services systems, and response to environmental discomfort directly affect the operation of buildings and thus their energy use. Various behavioral traits of the occupants affects the building energy use either directly or indirectly. The energy use is affected by opening/closing windows, dimming lights, turning on/off office equipment, turning on/off HVAC systems, and setting indoor thermal, acoustic, and visual comfort criteria. The behavioral combinations are infinite. Thus these variables need to be included in a more detailed study to better understand the performance of PCM boards under different internal loads.

- *R-value of insulation*: It was found that for lightweight buildings lined with PCM boards on all walls and roof, the increase in R-value of the insulation was counter-productive and therefore not suitable for simultaneous operation with PCM boards. For most climates it was evident that increasing the insulation R-value by a factor of 1.25 could perform just as well, if not better than, placing PCM boards in the building.

In order to absorb energy on its next cycle, the PCM board needs to first release the energy absorbed in the preceding cycle. Ideally, in situations where the indoors needs to be cooled, the energy absorbed by the PCM should be released outdoors. The greater the indoors is insulated from the outside, the PCM will therefore not get the proper opportunity to release the absorbed energy to the outdoors. For this very reason any increase in R-value after the prescriptive minimum prohibits the optimal functioning of PCM boards. The PCM boards, on the other hand, performed better with increased R-

value in the colder climates because the stored energy in the PCM boards were released indoors due to the higher level of insulation on the walls preventing the stored energy from being released outdoors. This process therefore compensated for some of the heating load required during the months that required heating.

- *Volumetric heat storage capacity (Enthalpy)*: The PCM boards were appended with 5 different levels of heat storage capacity. It was found that, for all the cases, the energy savings increased at a decreasing rate after any increase in PCM heat storage capacity of 40 kJ/kg. Every 20 kJ/kg increase in heat storage capacity for the PCM yielded fewer and fewer monetary savings annually. The increase in enthalpy for the PCM boards did not yield a one-to-one increase in energy savings. These findings were very counter intuitive since it is logical to expect an increase in energy savings with every increase in heat storage capacity. However that was not the case. The melting and solidifying trend for the different PCM enthalpies showed that the PCM with the largest volumetric heat storage capacity did not fully melt/solidify nearly as much as the PCM with the lower volumetric heat storage capacity. While that was the case, the PCM with a higher enthalpy still saved a larger amount of energy, it only did not keep up with the increase in its energy storage capacity. So if the PCM with the largest enthalpy did not fully melt/solidify nearly as much as the PCM with the smallest enthalpy, then it is probably beneficial to decrease the surface resistance of the PCM board to foster heat transfer to and from the indoor environment. Could it be that the surface resistance of the PCM boards is what is preventing the PCM with larger enthalpy not work to its full potential? In other words, it is still uncertain as to whether it is a property of the PCM board that is preventing it from absorbing the maximum energy or if it is a factor of the indoor environment such as releasing the indoor energy through the windows faster than allowing the PCM board to absorb it.

- Melting/Solidifying study: The current work examined the concept of melting/solidifying hours, for different cases, more deeply than any literature on the topic that was found. This research developed a procedure to study the temporal and directional melting of the PCM. The melting and solidifying of the PCM was studied for all the surfaces in the building. The study was undertaken in two directions: internal loads and volumetric heat storage capacity (enthalpy). This study confirmed earlier results that showed that the increase in internal load shifts the optimum months (for the application of PCM) towards the winter. The study also verified the hypothesis that the PCM with high volumetric heat storage capacity exhibited a higher thermal inertia, hence lower rate of fully melting and solidifying, than the PCM with low enthalpy. The difference in performance between the two PCMs (with different enthalpy) however was not significant and therefore opened up the possibility of studying the effect of surface thermal resistance of the PCM boards to enhance the energy storing and releasing capacity of the PCM.

Future work

During this research, a number of topics for future work were identified as being valuable, but beyond the current scope. They are listed as follows:

- New variables: As mentioned earlier, occupant behaviour is arguably the single greatest challenge to building energy researchers and modellers. In this study while the occupancy was altered independently, they were kept constant throughout the year once one occupancy level was selected. The infiltration of air into the building was also left constant. The reason for allowing a constant internal load and infiltration was prompted primarily because any additional modeling of occupancy behaviour or infiltration added to the simulation run time and therefore prohibited such a large factorial design to be

completed on a timely fashion. Now that the climates and levels of variables have been considerably filtered down, the occupancy, plug load schedules and infiltration schedules can be altered to study the behaviour of PCM for different occupancy and infiltration loads. The next and important variable to study is the window-to-wall ratio. In this research, the buildings were modeled with a constant window-to-wall ratio of 14%. Windows were placed on each of the vertical surfaces. The effect of the combinations of different window-to-wall ratios and window placements needs to be studied to further understand the behaviour of PCM boards in the climates. The surface thermal resistance is also another variable that was identified as a possible factor in enhancing the heat storage and release of energy for PCM boards with a higher heat storage capacity.

- Connecting the regression models to the climate maps: The climate maps were generated to assist architects and engineers quickly visualize the benefits of placing PCM in their designs. The regression models developed in this study, along with others developed in a future study; need to be connected to the climate maps so that a quick input of independent variable (within the design space) will generate climate maps for the magnitude of energy savings, payback period and optimum PCM for the specific application.
- Melting/Solidifying study: The melting/solidifying study was performed on the Albuquerque climate data and on the PCM placed on each individual surface working together to mitigate the indoor temperature. This added a lot of complexity towards understanding and distinguishing the major causes for the performance of PCM. In a future study, the weather files that are input in EnergyPlus need to be customised. By gradually adding one environmental load at a time, the behaviour of PCM in each climate can be studied properly. In addition, the melting/solidifying study needs to be performed on PCM enhanced wall with adiabatic heat transfer surfaces surrounding it. These are a

- few recommendations so that the frequency and directional melting/solidifying of the PCM can be understood better to really identify the optimal PCM for a variety of settings.
- *Exterior surface radiation*: An important consideration is also the surrounding buildings that may or may not shade the building with PCM. A future study needs to place the building in a realistic setting to understand how the present of neighbouring buildings affect the performance of PCM.
 - *Building form*: This research focused on a 1225 ft² rectangular building. This research needs to be extended to buildings with different forms and shapes to either solidify the findings or add to the findings presented by this research.
 - *Cascade storage*: A recommended addition to the future study would be to include the cascading of PCMs in buildings. It was found that for most climates the PCM melting at 21°C showed savings during the winter period for heating. However since the majority of savings were accrued for cooling energy, the PCM melting at 23°C performed optimally in most cases and overshadowed the performance of other melting temperatures. Cascading is the use of several different PCMs with different melting temperatures within the same building structure. The idea is to absorb energy at different indoor temperature variations. For example, if the PCM melting at 21°C works well towards mitigating the heating energy indoors and the 23°C PCM works optimally for the cooling load reduction, these two PCMs can be placed indoors to work during heating and cooling dominant months. This study can therefore enhance the energy performance of PCM indoors.

APPENDICES

Appendix A

PCM versus R-values and the payback period

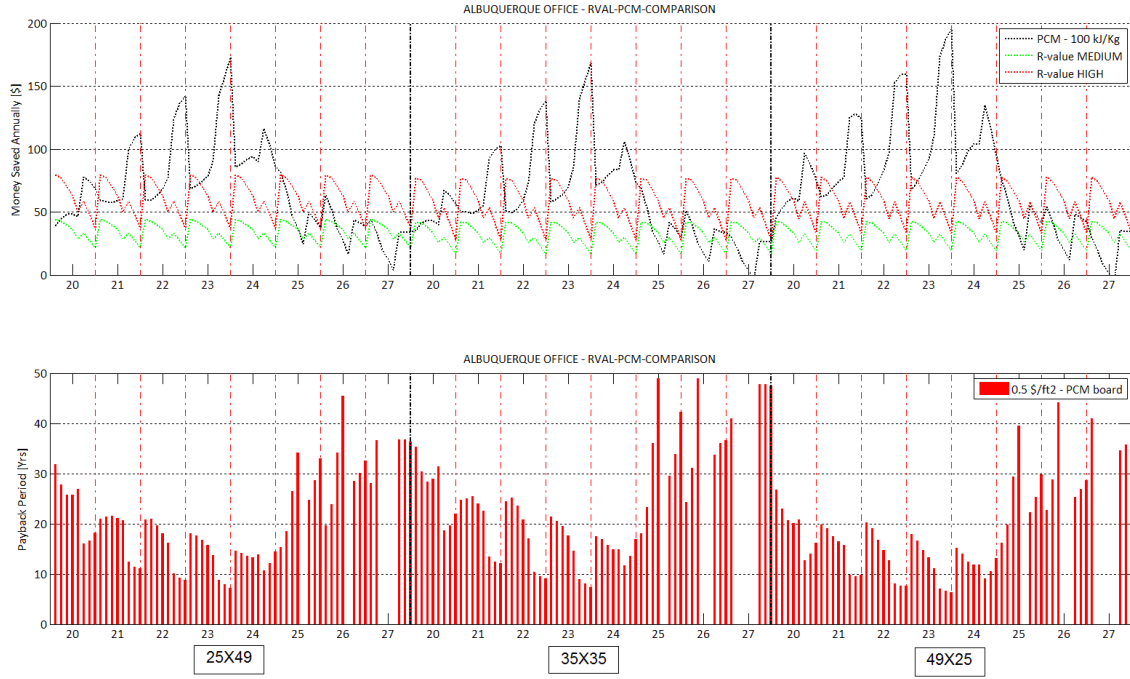


Figure A.1: Albuquerque office R-value, PCM comparison (top), payback period (bottom)

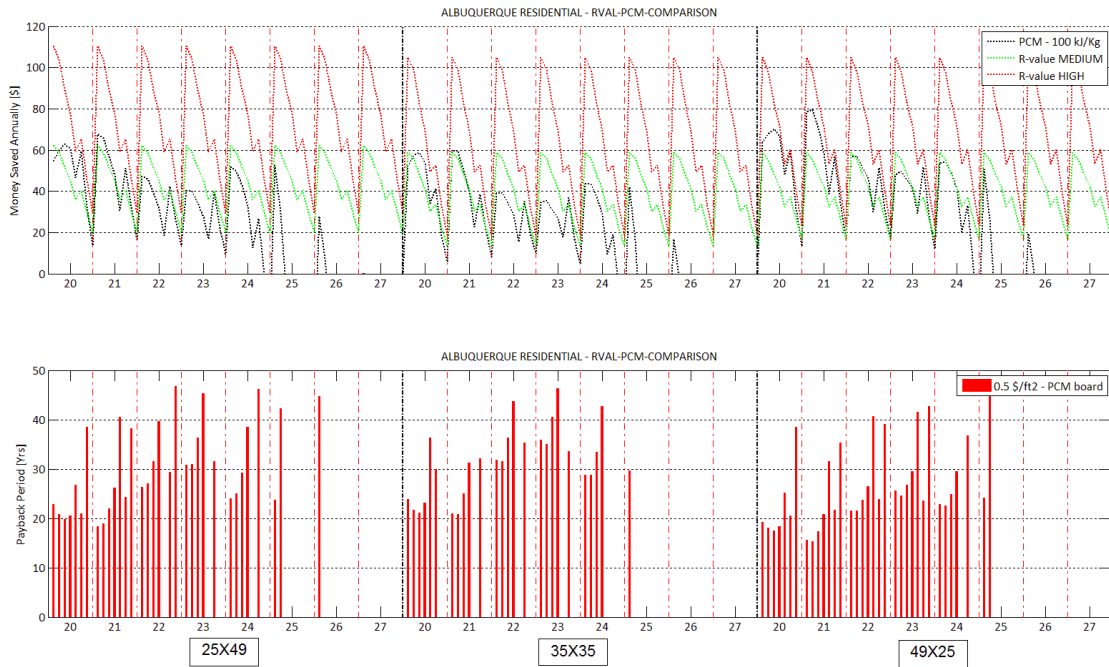


Figure A.2: Albuquerque residential R-value, PCM comparison (top), payback period (bottom)

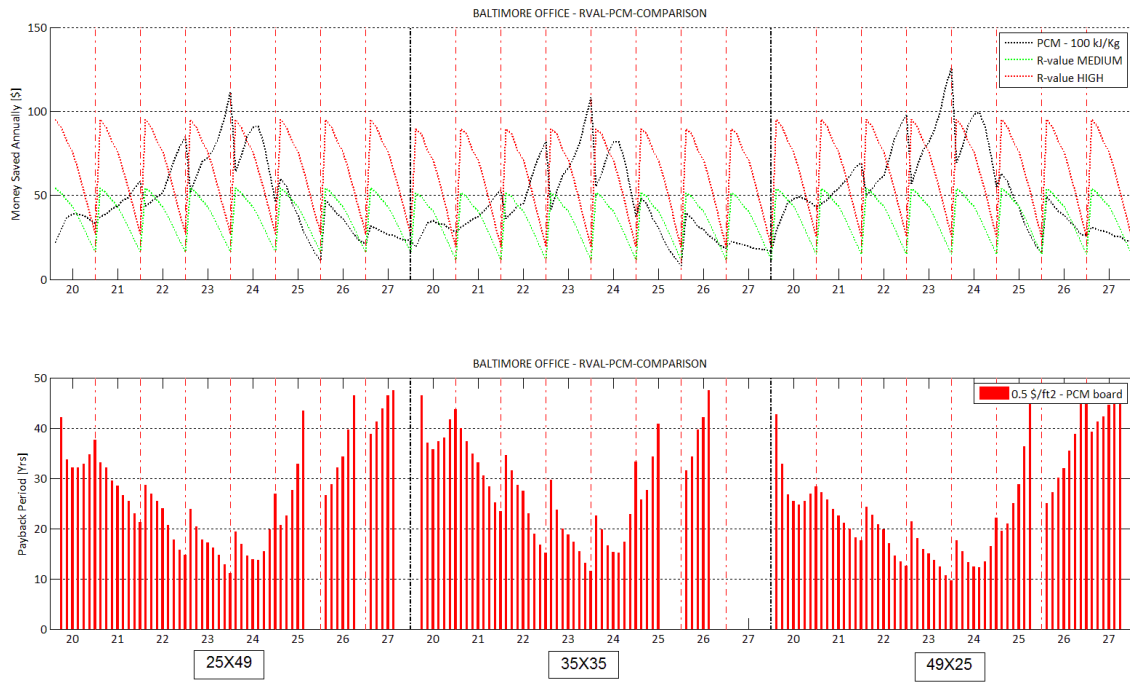


Figure A.3: Baltimore office R-value, PCM comparison (top), payback period (bottom)

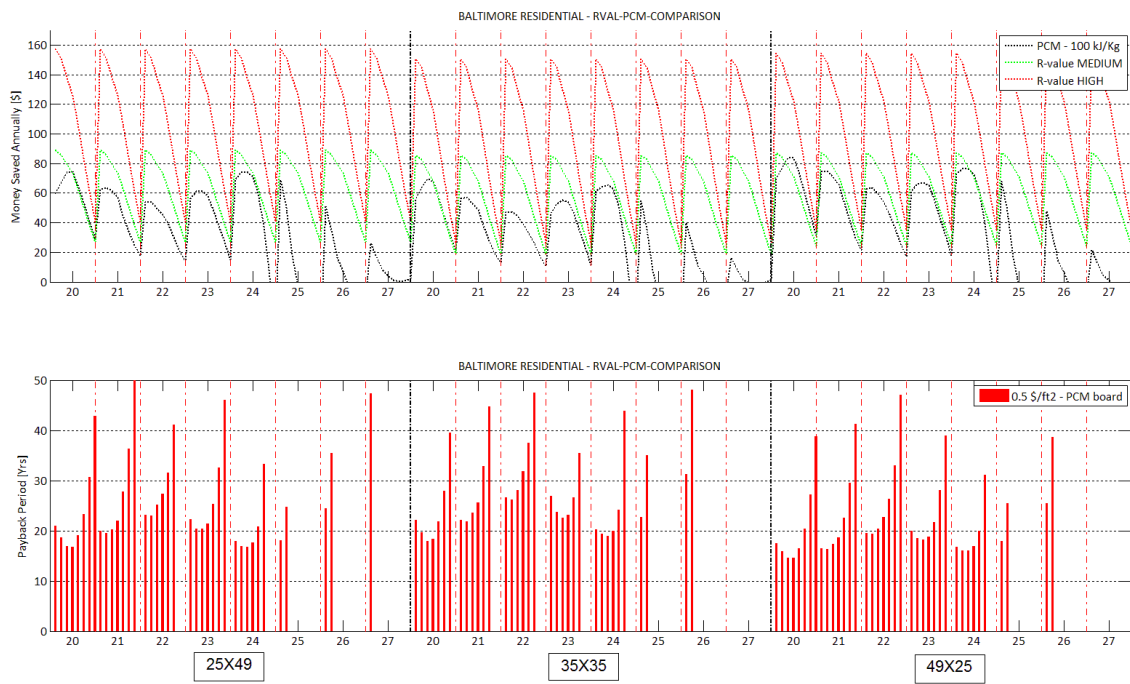


Figure A.4: Baltimore residential R-value, PCM comparison (top), payback period (bottom)

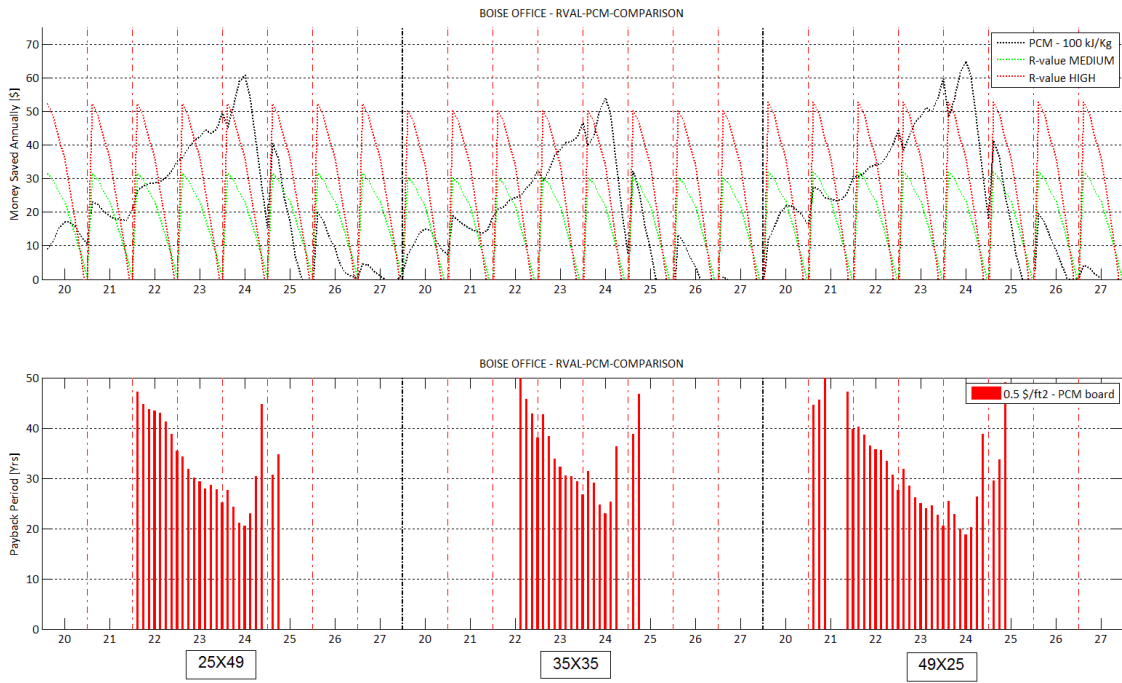


Figure A.5: Boise office R-value, PCM comparison (top), payback period (bottom)

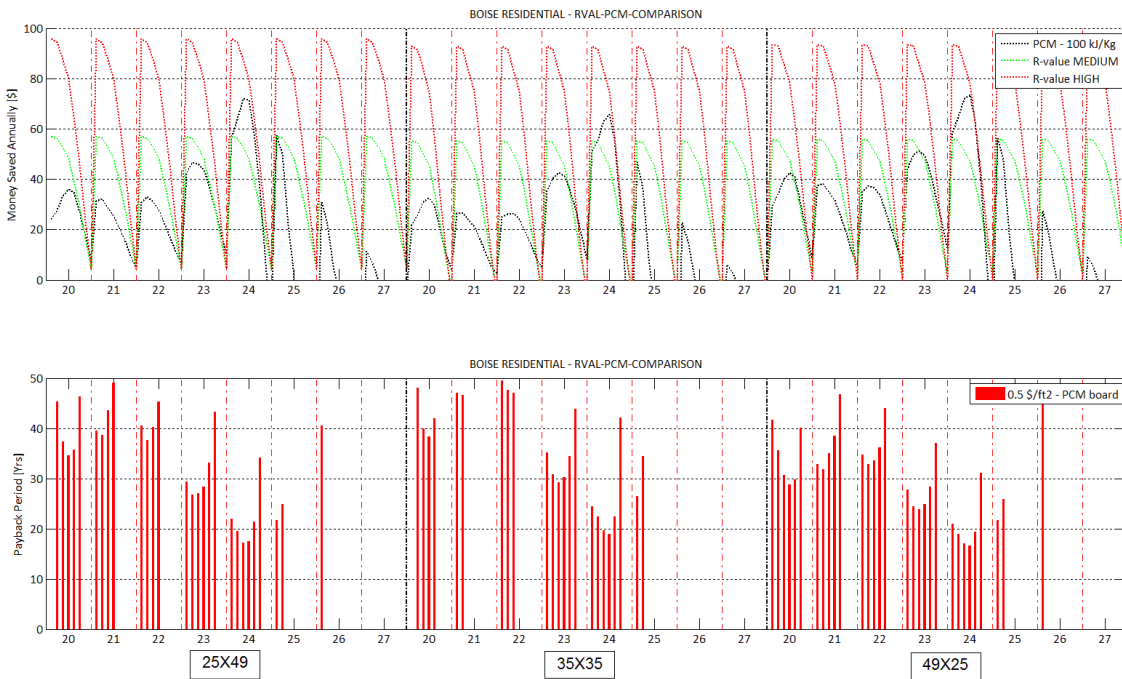


Figure A.6: Boise residential R-value, PCM comparison (top), payback period (bottom)

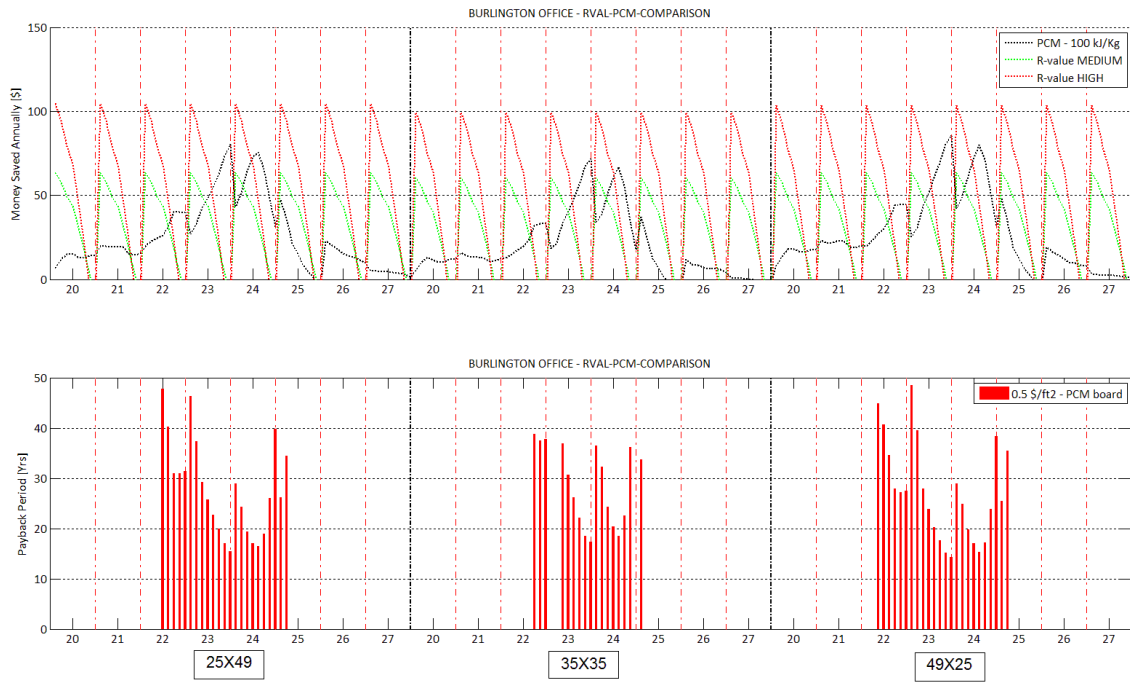


Figure A.7: Burlington office R-value, PCM comparison (top), payback period (bottom)

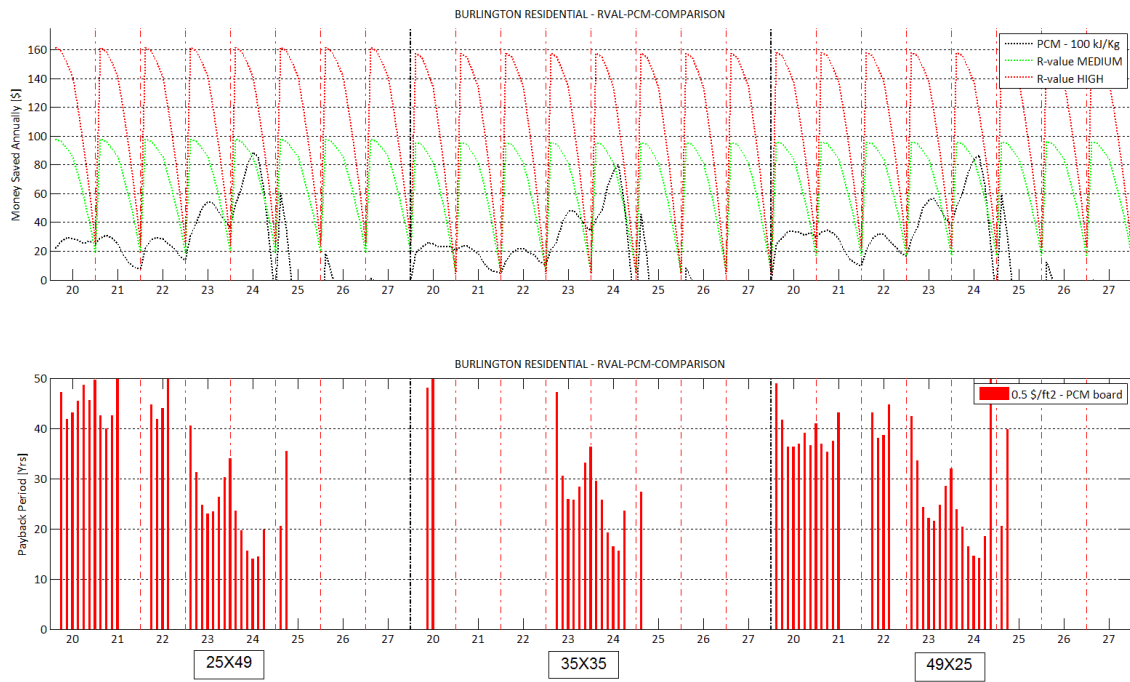


Figure A.8: Burlington residential R-value, PCM comparison (top), payback period (bottom)

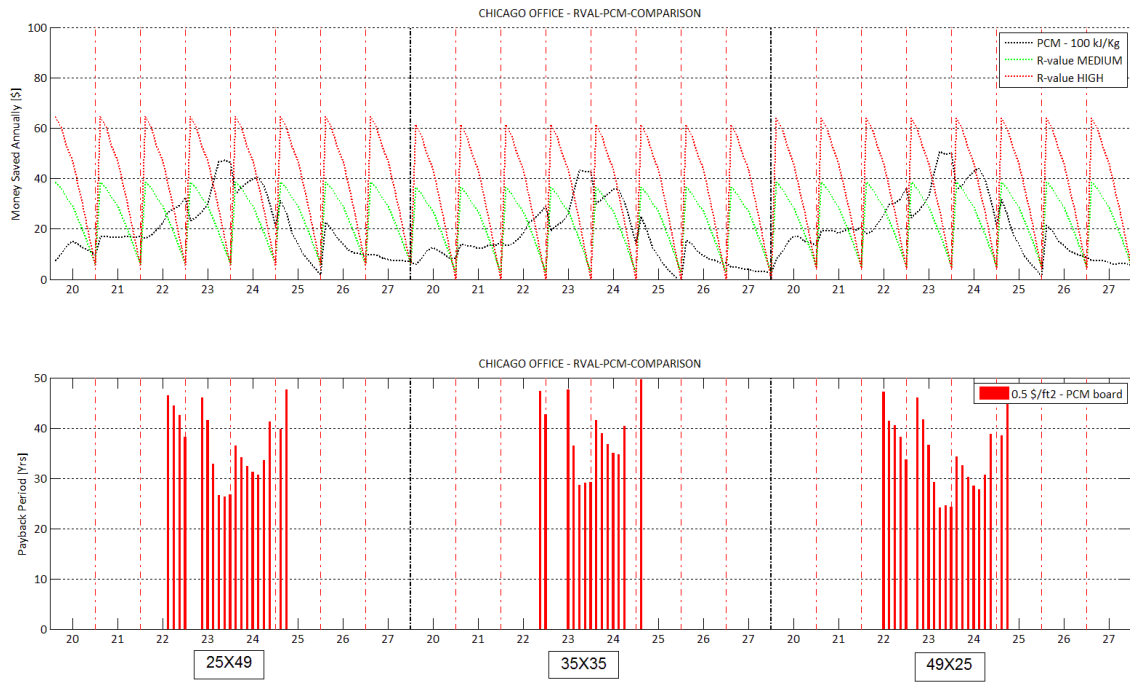


Figure A.9: Chicago office R-value, PCM comparison (top), payback period (bottom)

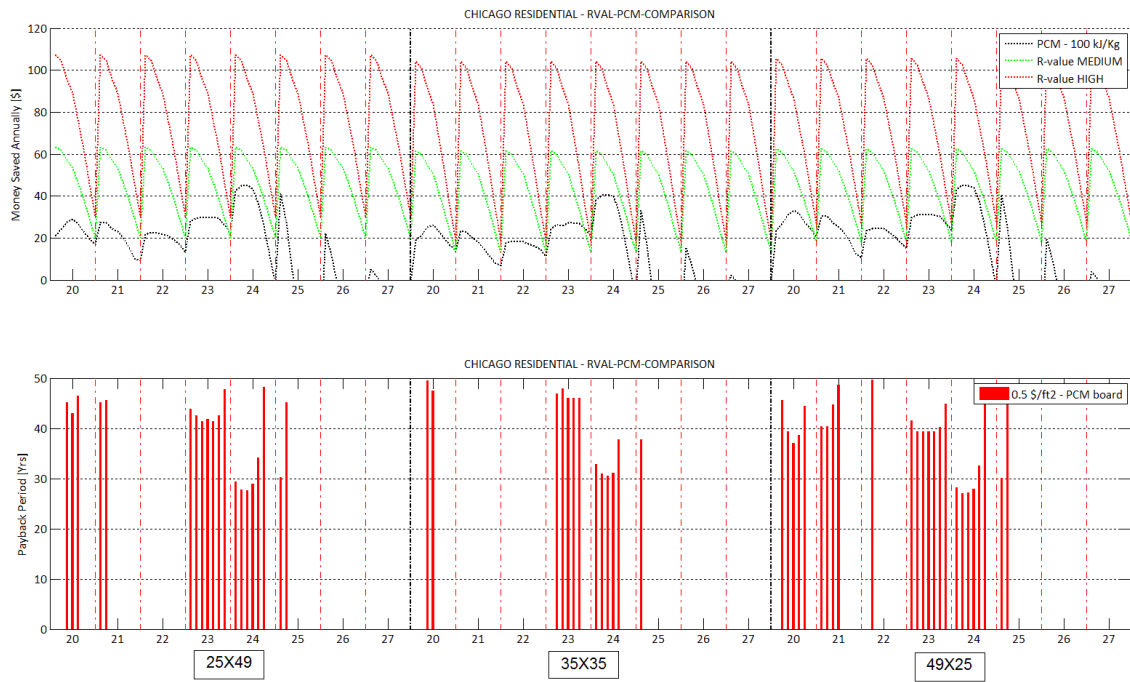


Figure A.10: Chicago residential R-value, PCM comparison (top), payback period (bottom)

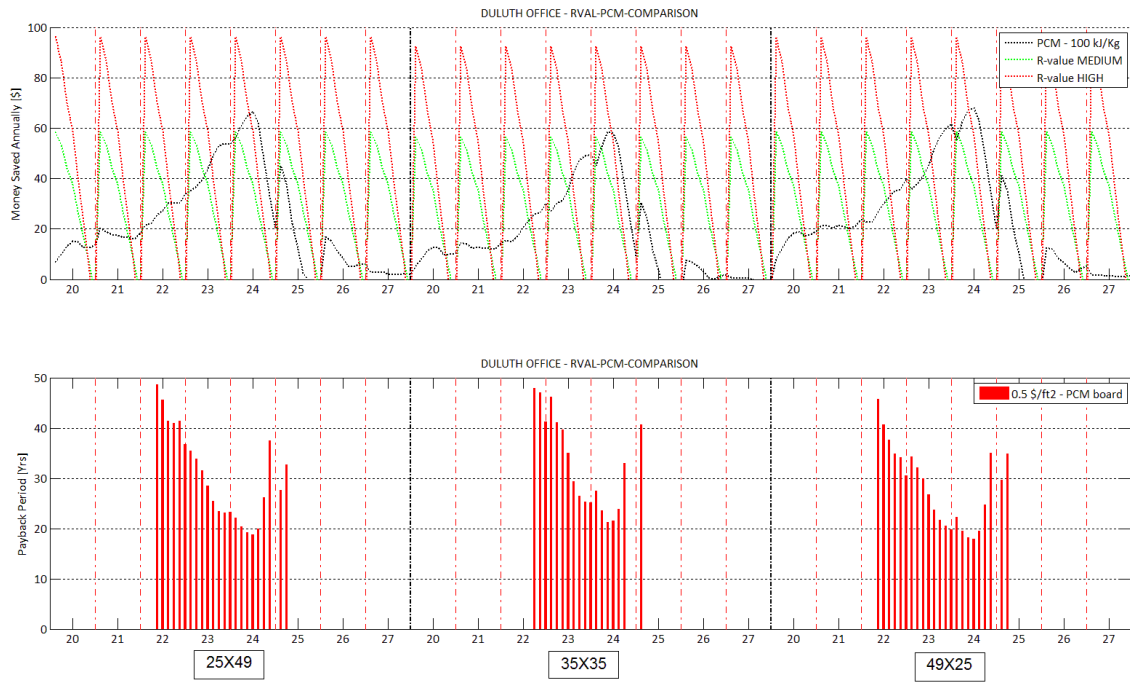


Figure A.11: Duluth office R-value, PCM comparison (top), payback period (bottom)

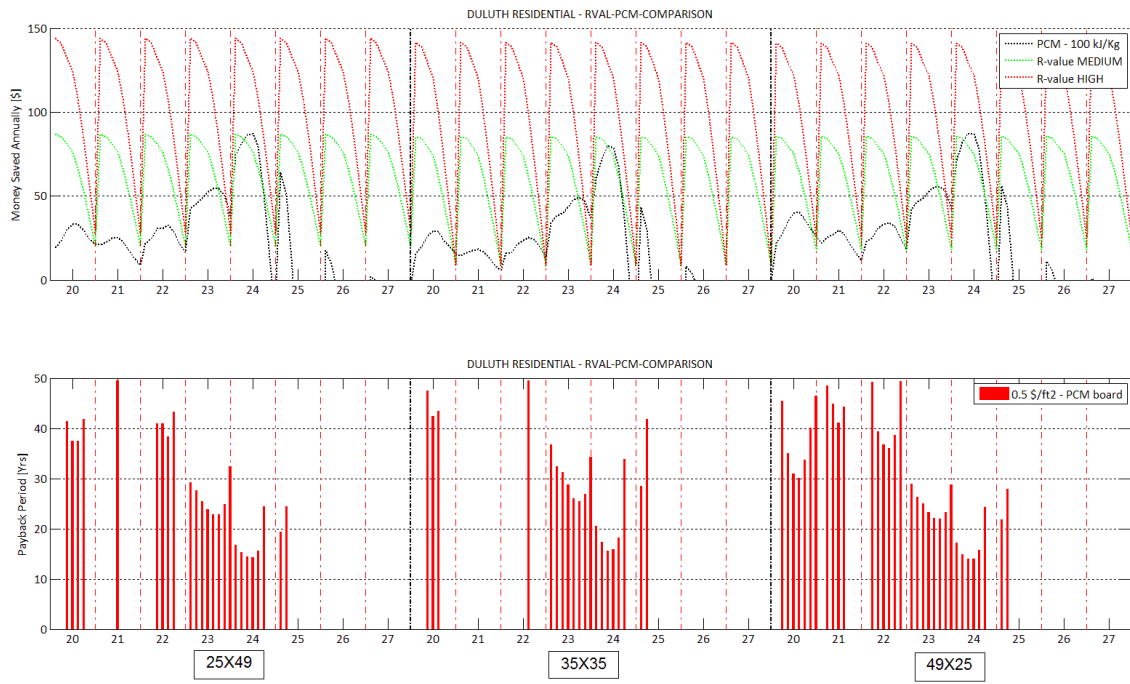


Figure A.12: Duluth residential R-value, PCM comparison (top), payback period (bottom)

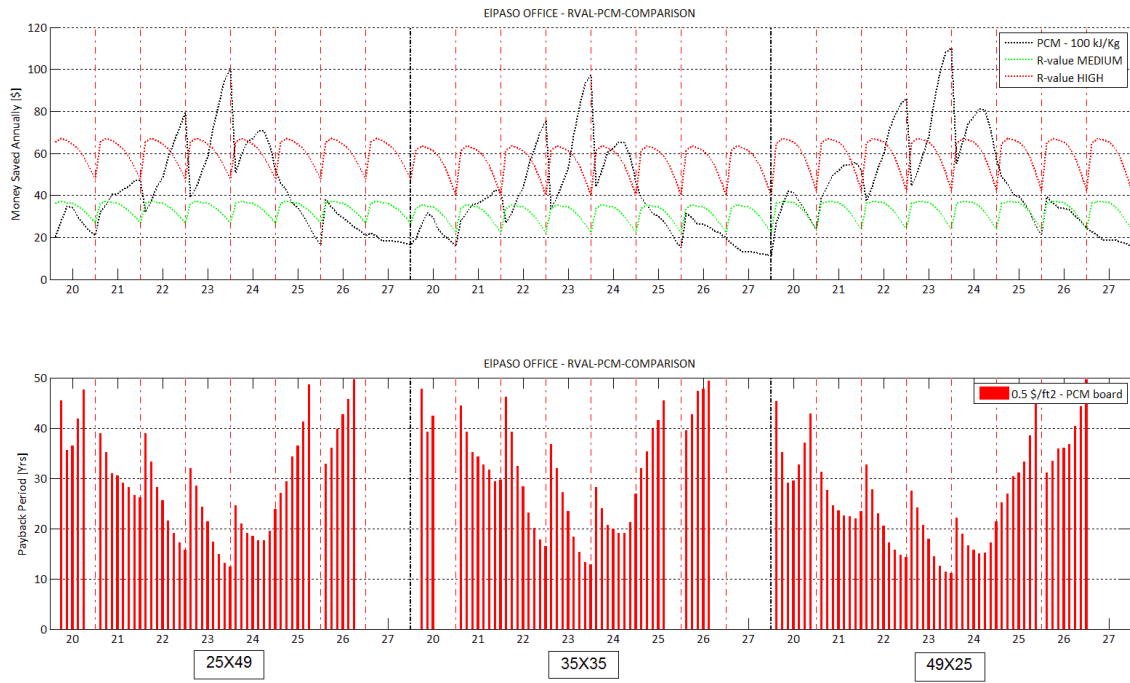


Figure A.13: El Paso office R-value, PCM comparison (top), payback period (bottom)

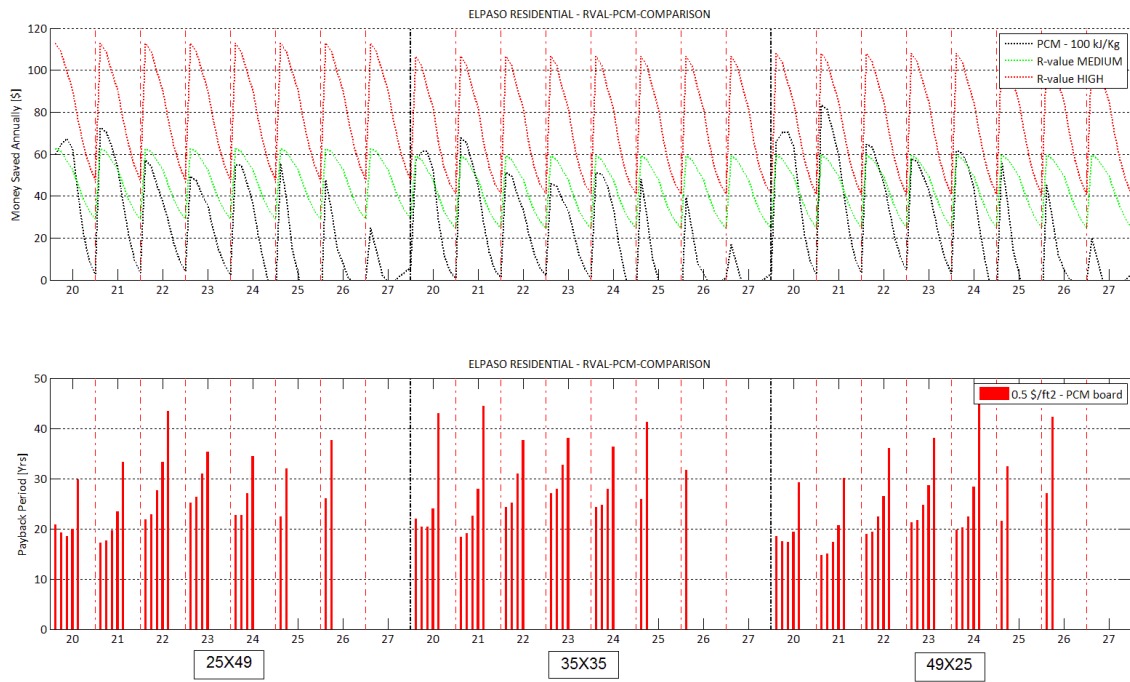


Figure A.14: El Paso residential R-value, PCM comparison (top), payback period (bottom)

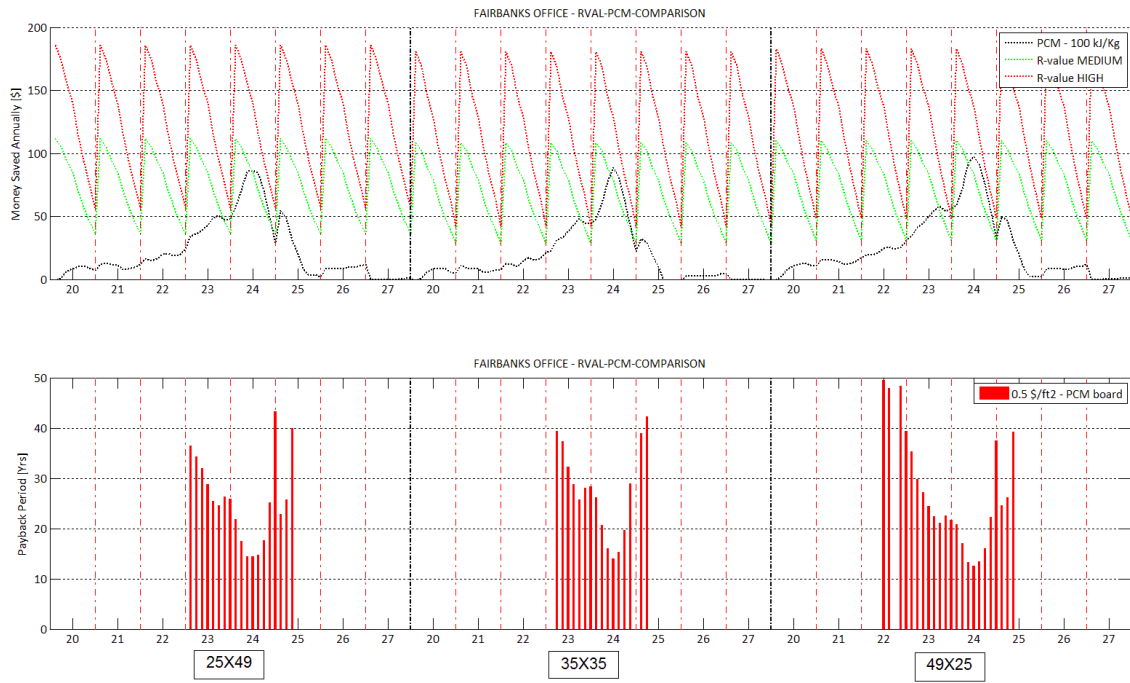


Figure A.15: Fairbanks office R-value, PCM comparison (top), payback period (bottom)

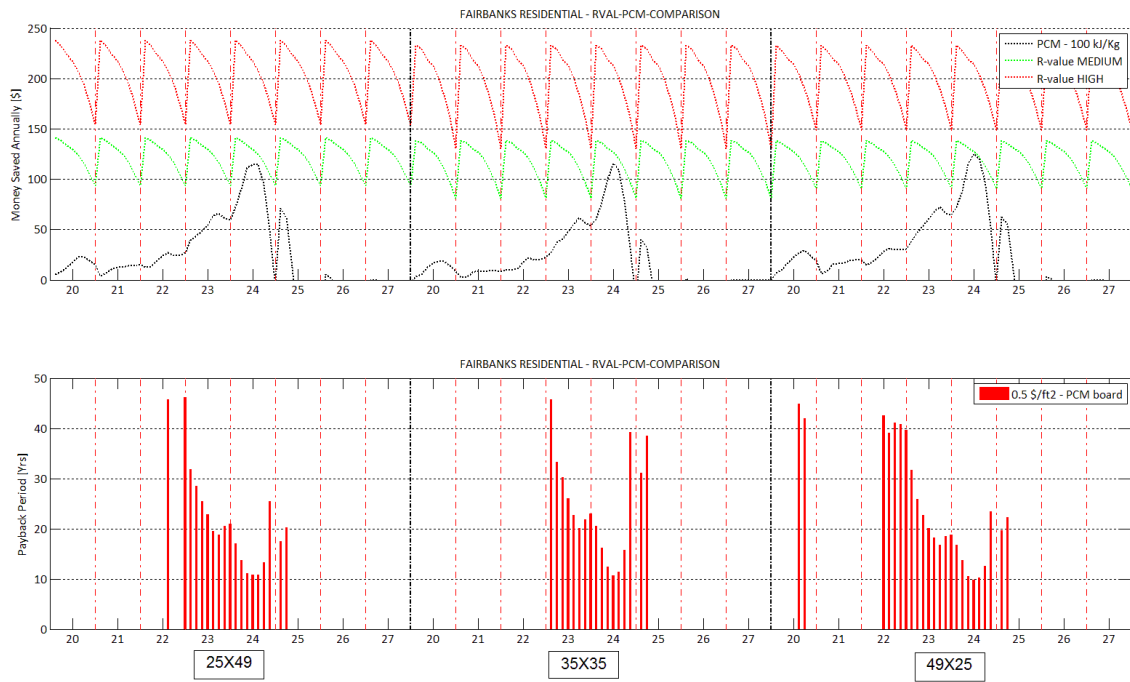


Figure A.16: Fairbanks residential R-value, PCM comparison (top), payback period (bottom)

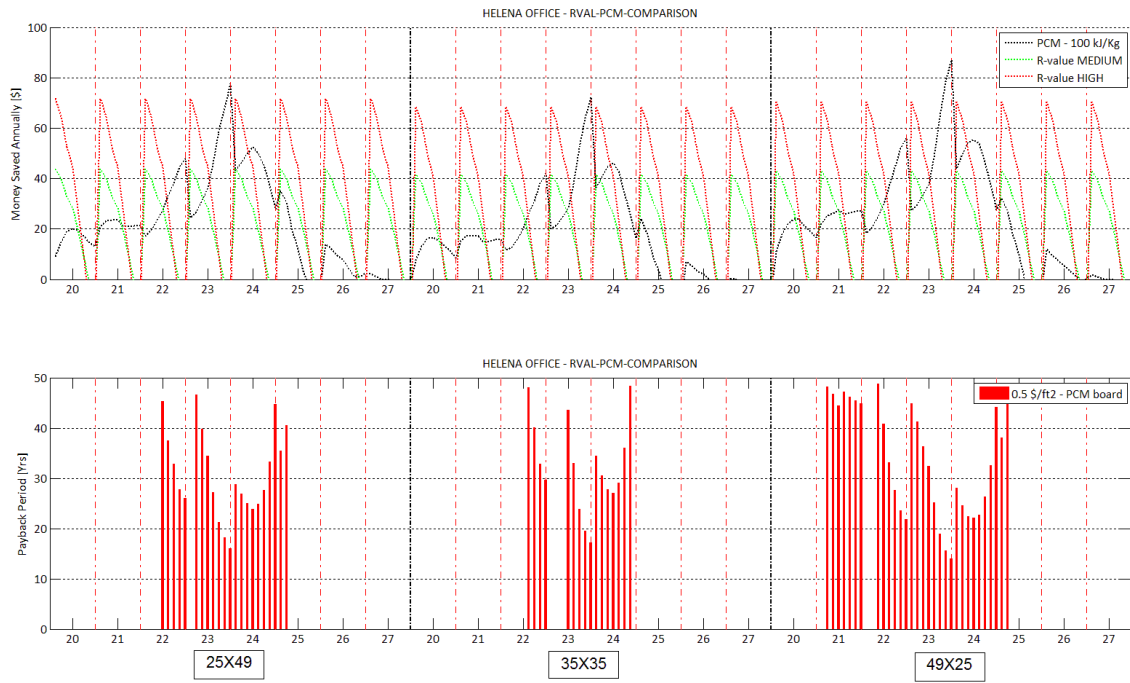


Figure A.17: Helena office R-value, PCM comparison (top), payback period (bottom)

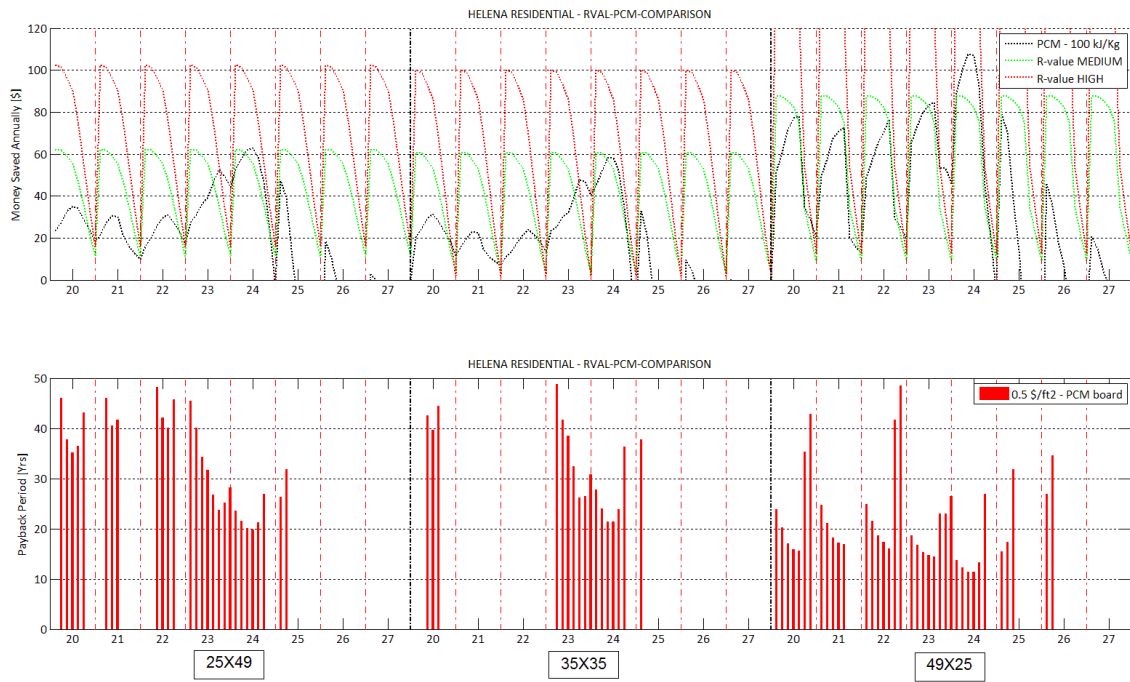


Figure A.18: Helena residential R-value, PCM comparison (top), payback period (bottom)

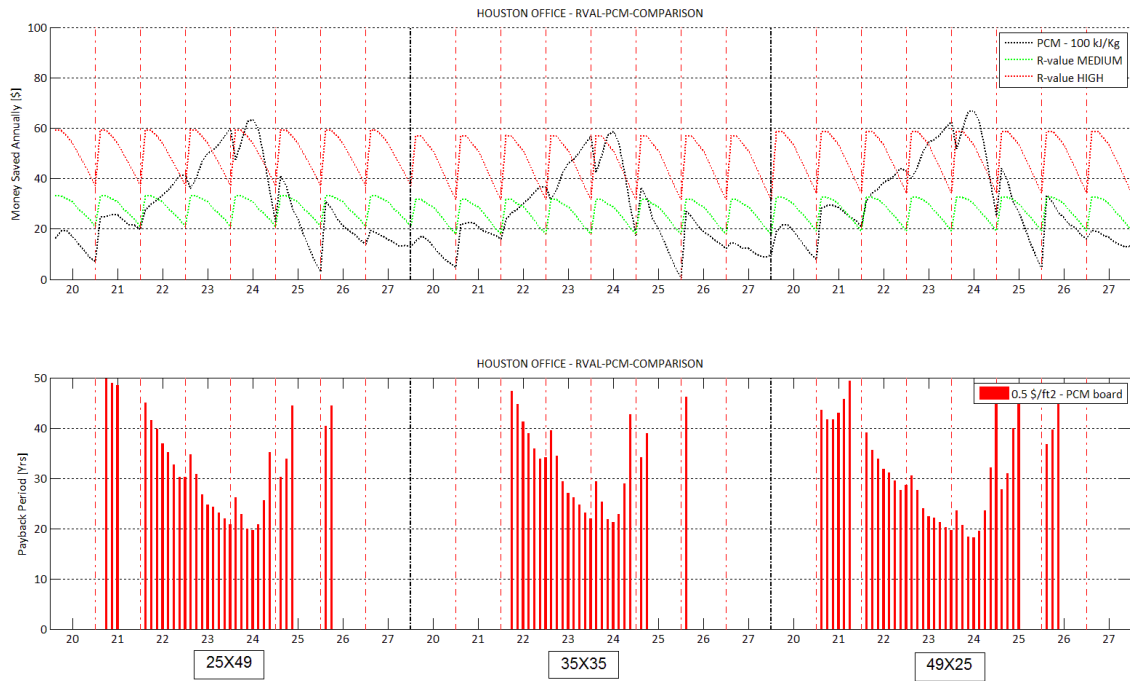


Figure A.19: Houston office R-value, PCM comparison (top), payback period (bottom)

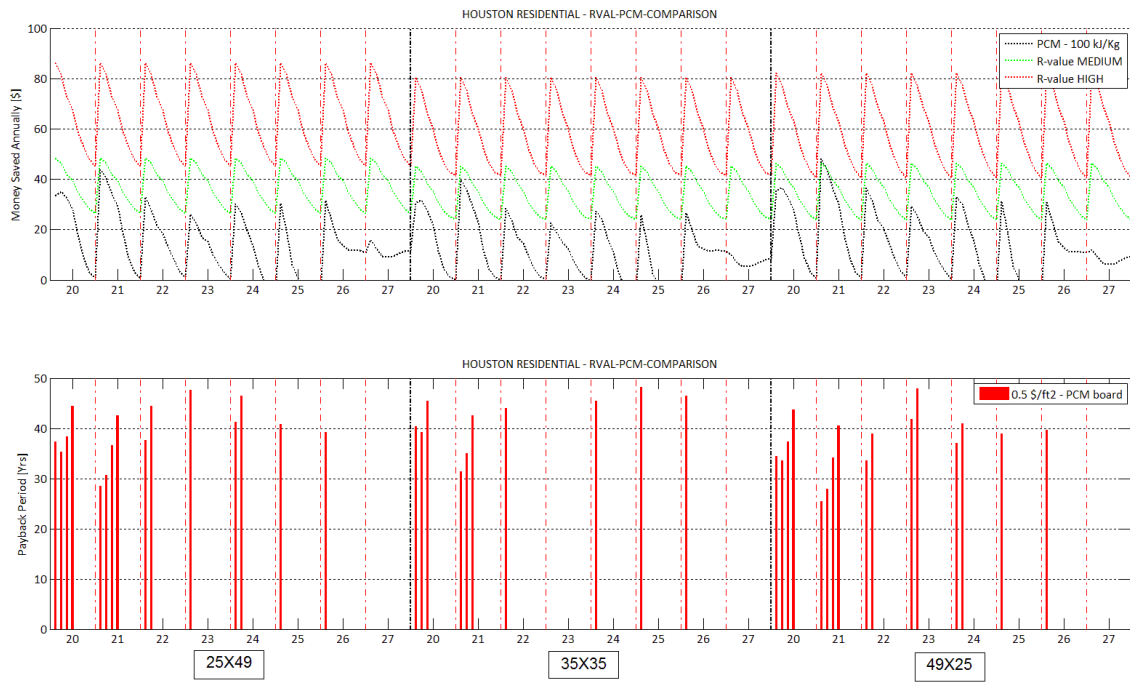


Figure A.20: Houston residential R-value, PCM comparison(top), payback period (bottom)

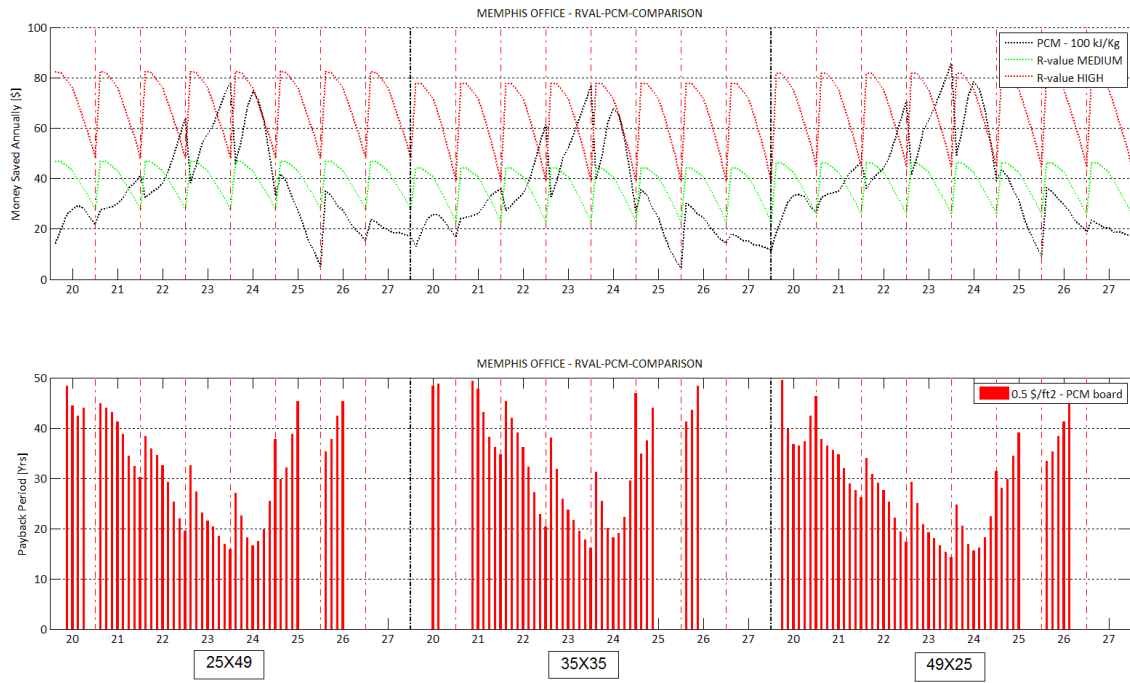


Figure A.21: Memphis office R-value, PCM comparison (top), payback period (bottom)

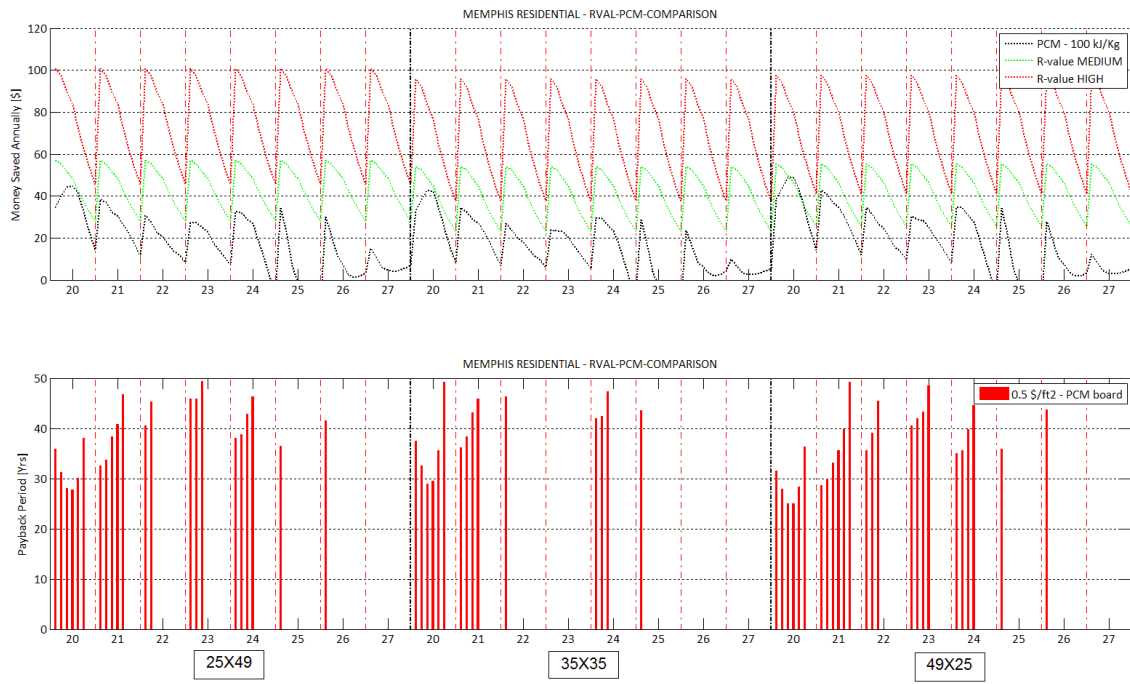


Figure A.22: Memphis residential R-value, PCM comparison (top), payback period (bottom)

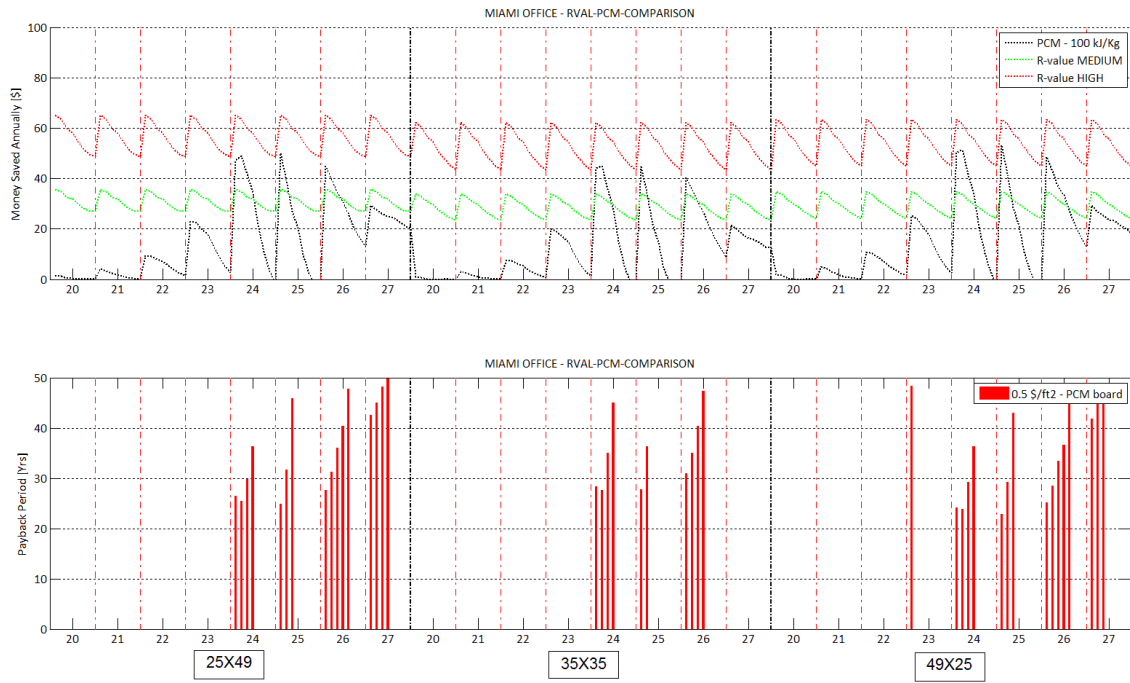


Figure A.23: Miami office R-value, PCM comparison (top), payback period (bottom)

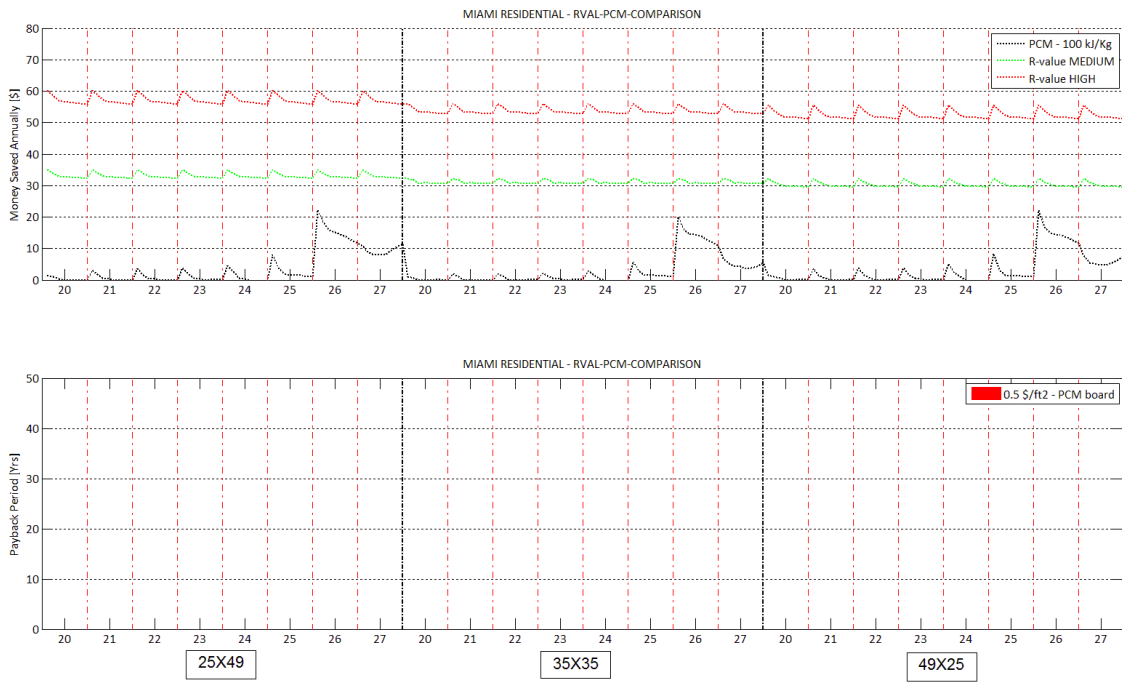


Figure A.24: Miami residential R-value, PCM comparison (top), payback period (bottom)

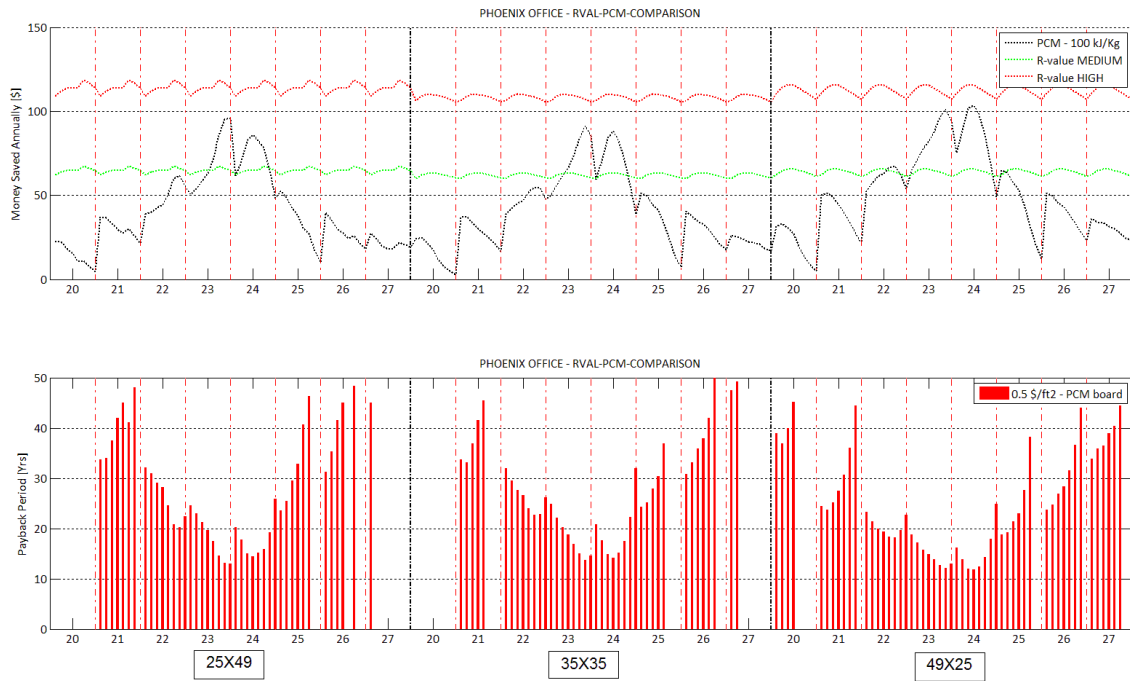


Figure A.25: Phoenix office R-value, PCM comparison (top), payback period (bottom)

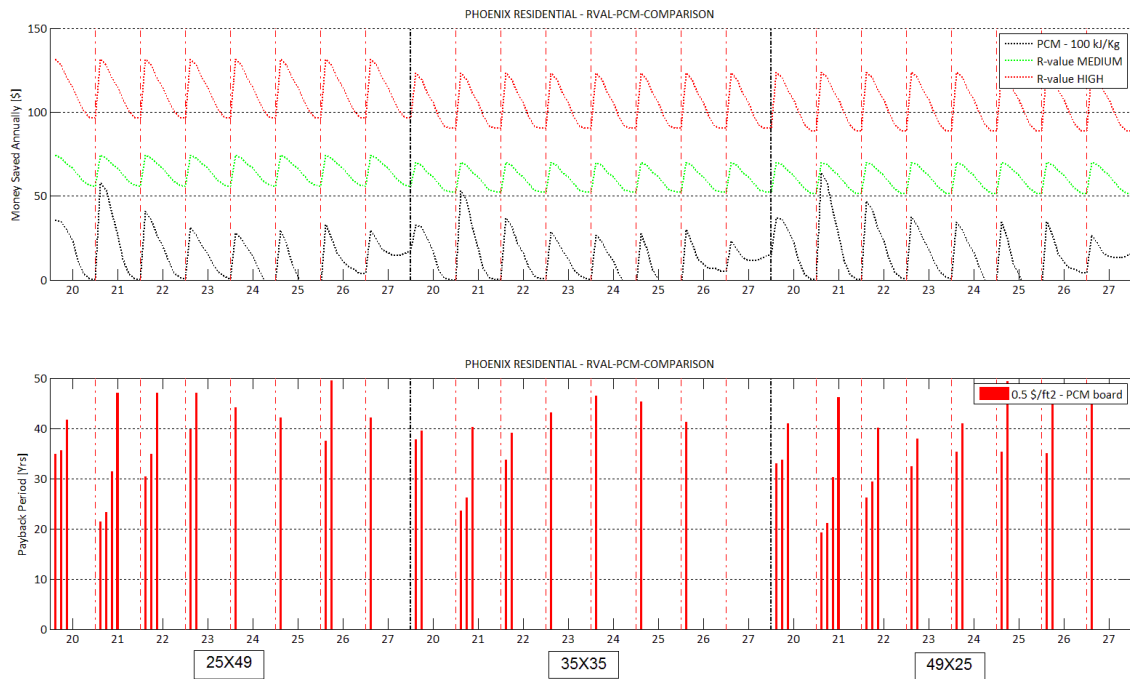


Figure A.26: Phoenix residential R-value, PCM comparison (top), payback period (bottom)

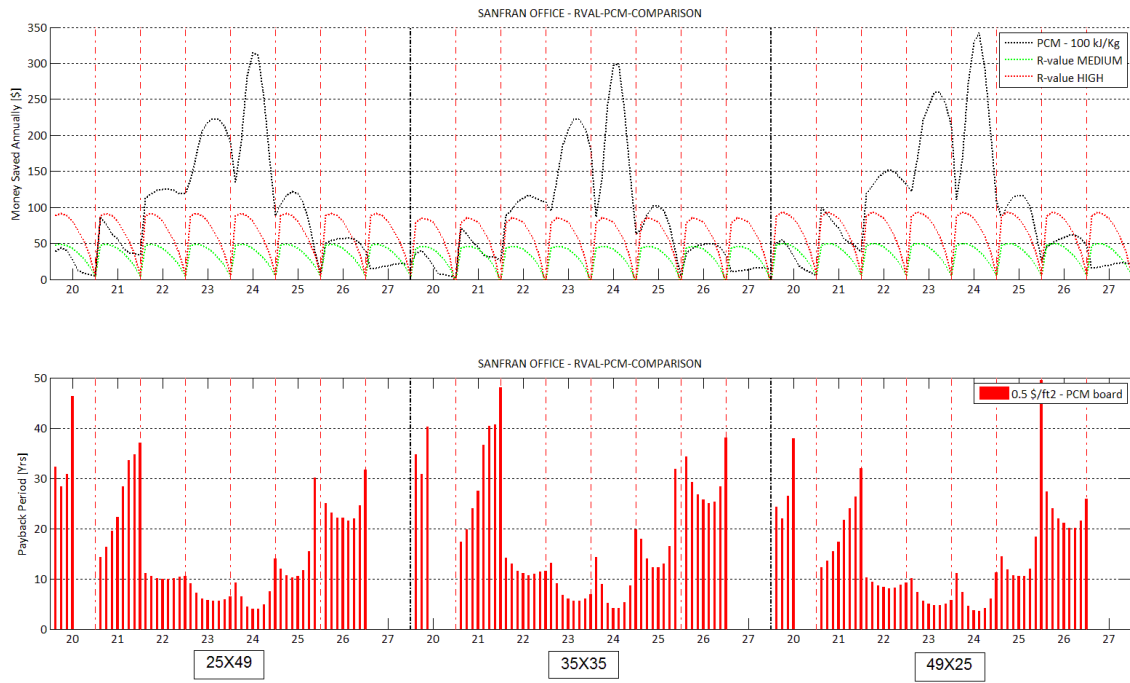


Figure A.28: San Francisco office R-value, PCM comparison (top), payback period (bottom)

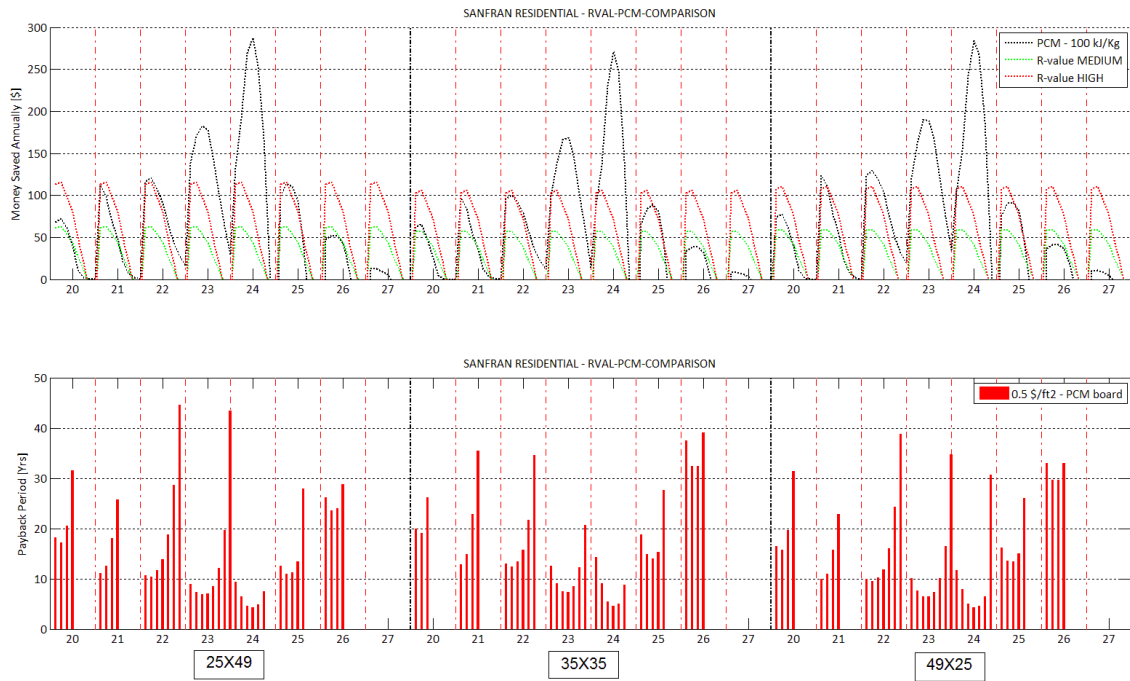


Figure A.28: San Francisco residential R-value, PCM comparison (top), payback period (bottom)

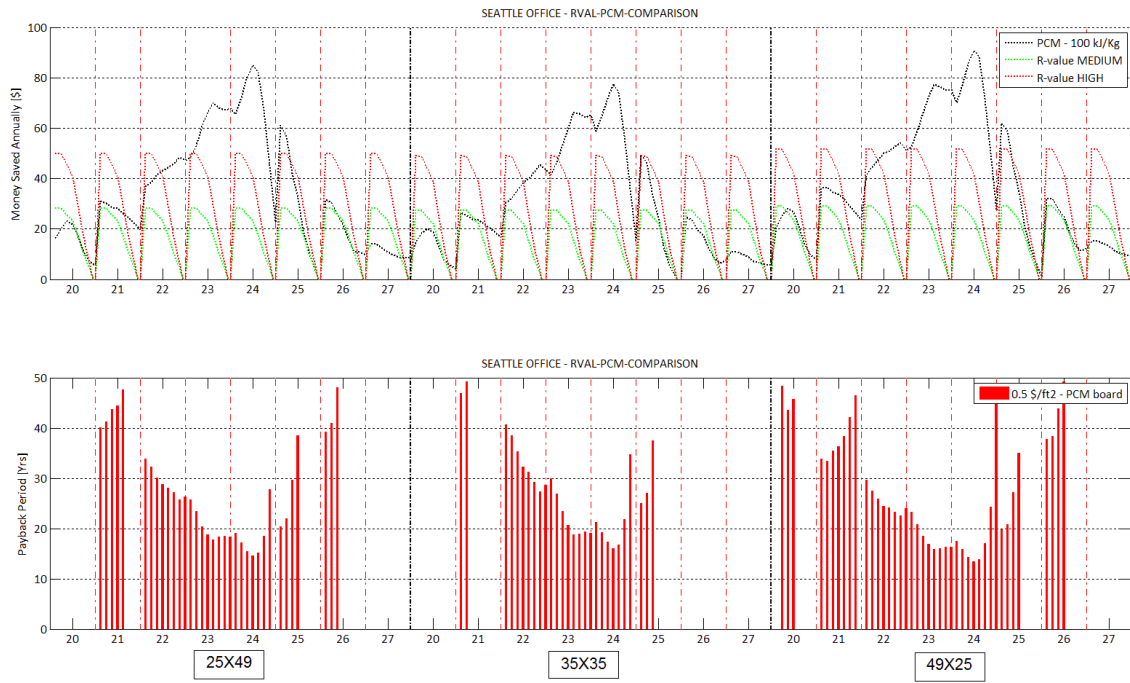


Figure A.29: Seattle office R-value, PCM comparison (top), payback period (bottom)

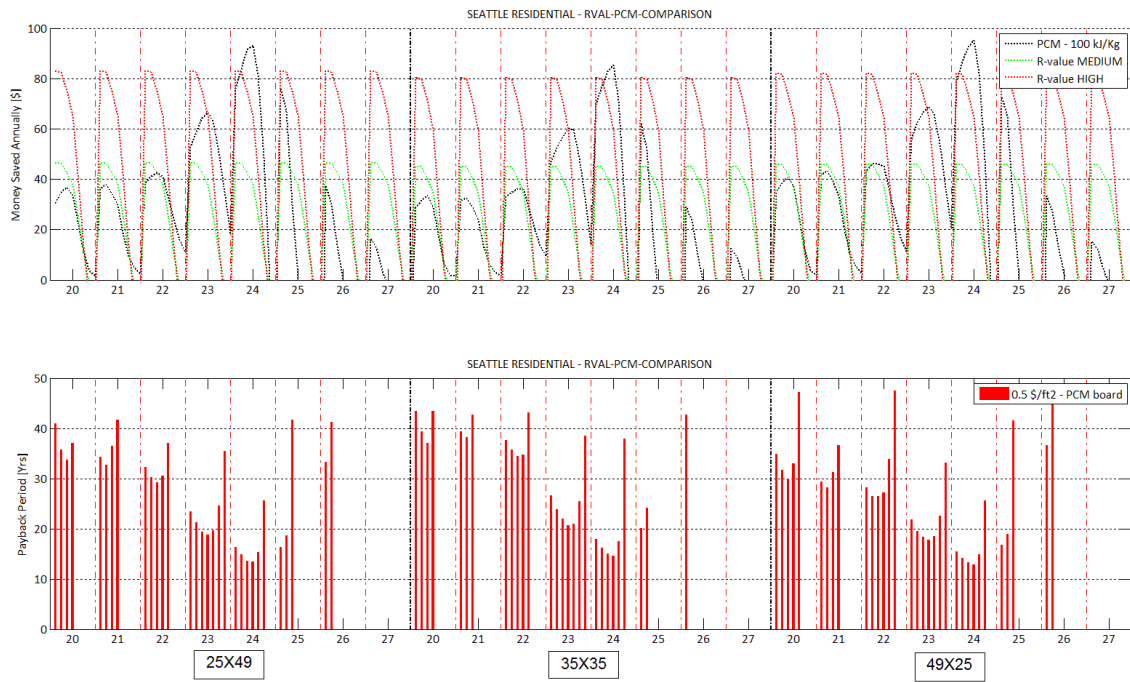


Figure A.30: Seattle residential R-value, PCM comparison (top), payback period (bottom)

Appendix B

Comparison of PCM versus the different insulation R-values

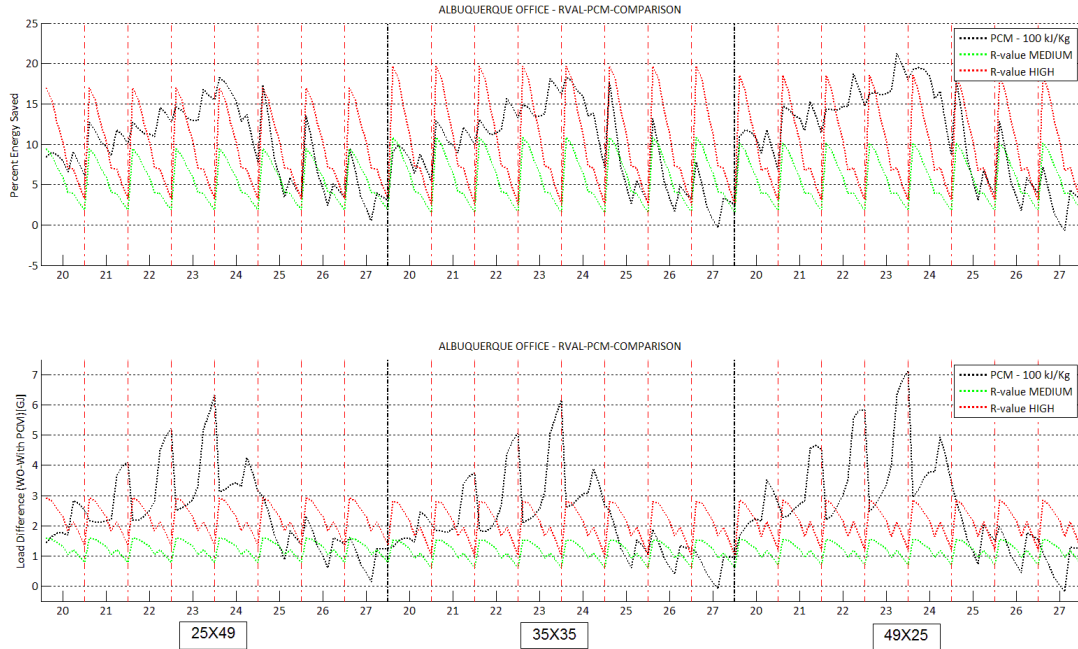


Figure B.1: Albuquerque office R-value, PCM comparison. percent (top) magnitude (bottom)

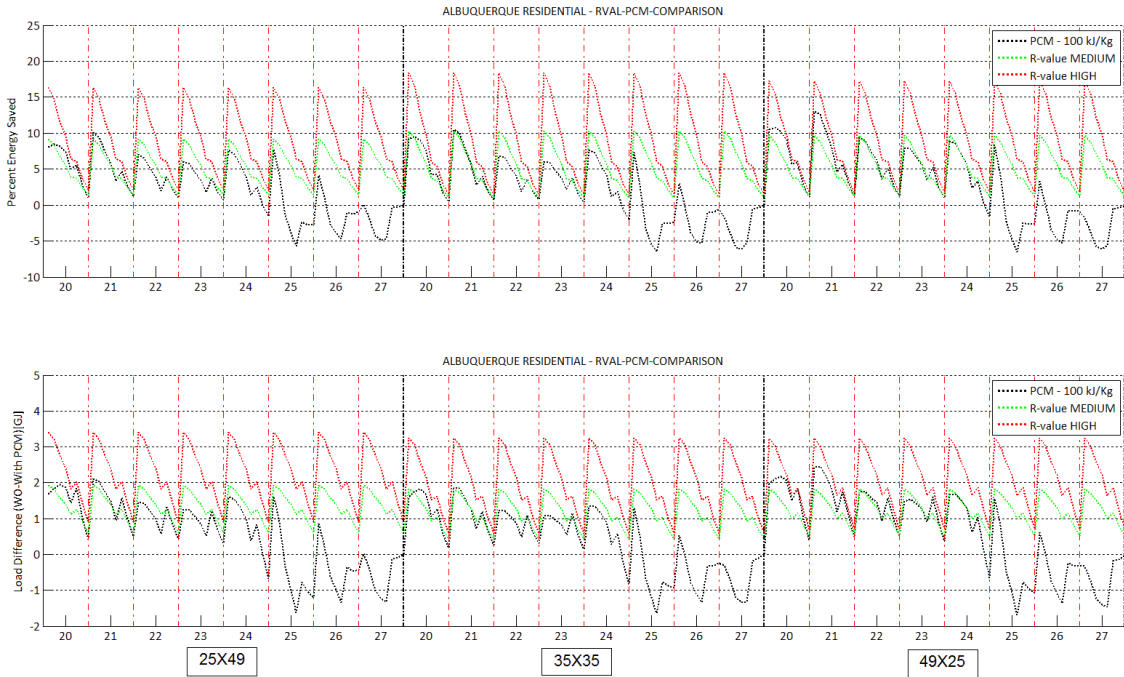


Figure B.2: Albuquerque residential R-value, PCM comparison. percent (top) magnitude (bottom)

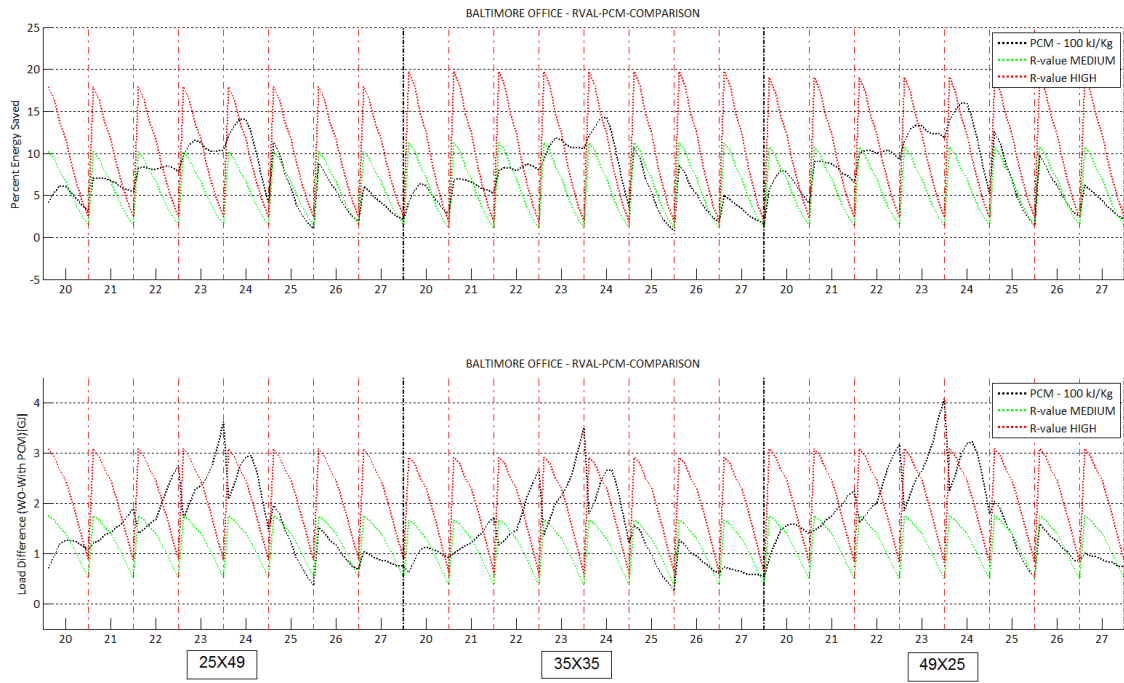


Figure B.3: Baltimore office R-value, PCM comparison. percent (top) magnitude (bottom)

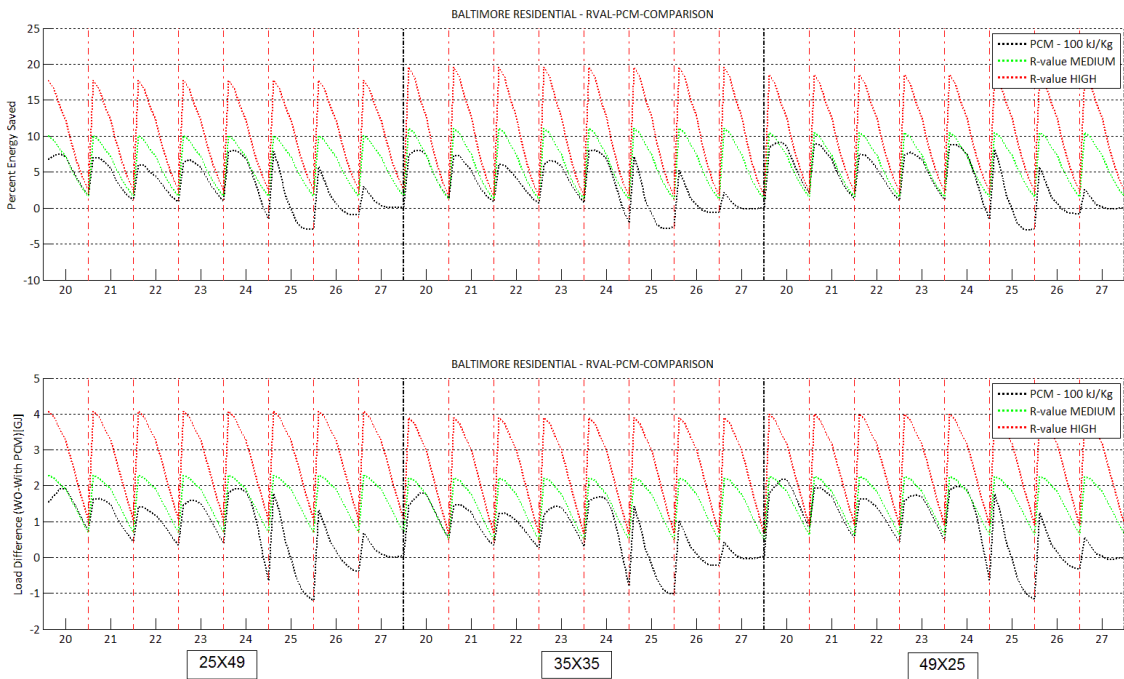


Figure B.4: Baltimore residential R-value, PCM comparison. percent (top) magnitude (bottom)

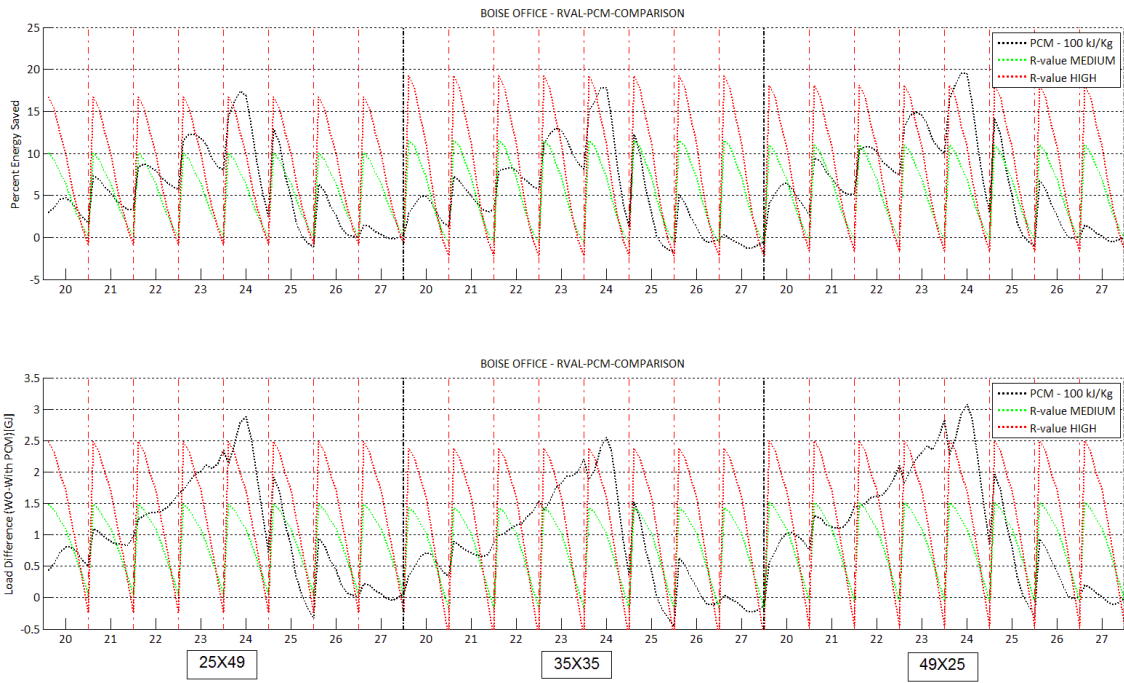


Figure B.5: Boise office R-value, PCM comparison. percent (top) magnitude (bottom)

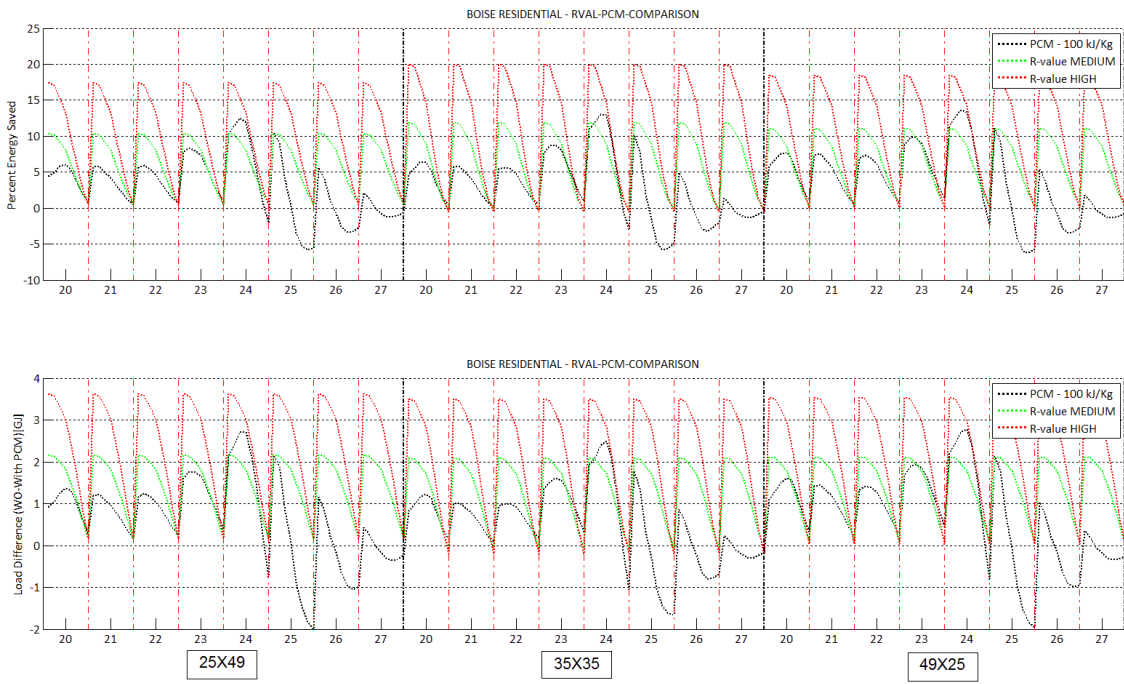


Figure B.6: Boise residential R-value, PCM comparison. percent (top) magnitude (bottom)

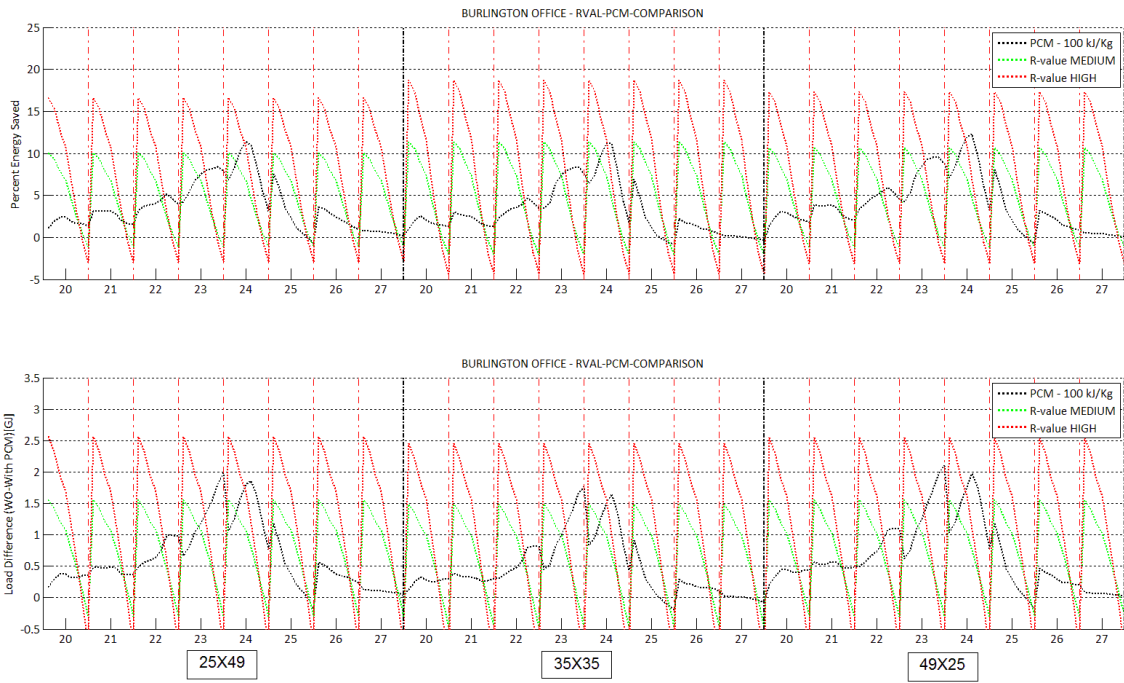


Figure B.6: Burlington office R-value, PCM comparison. percent (top) magnitude (bottom)

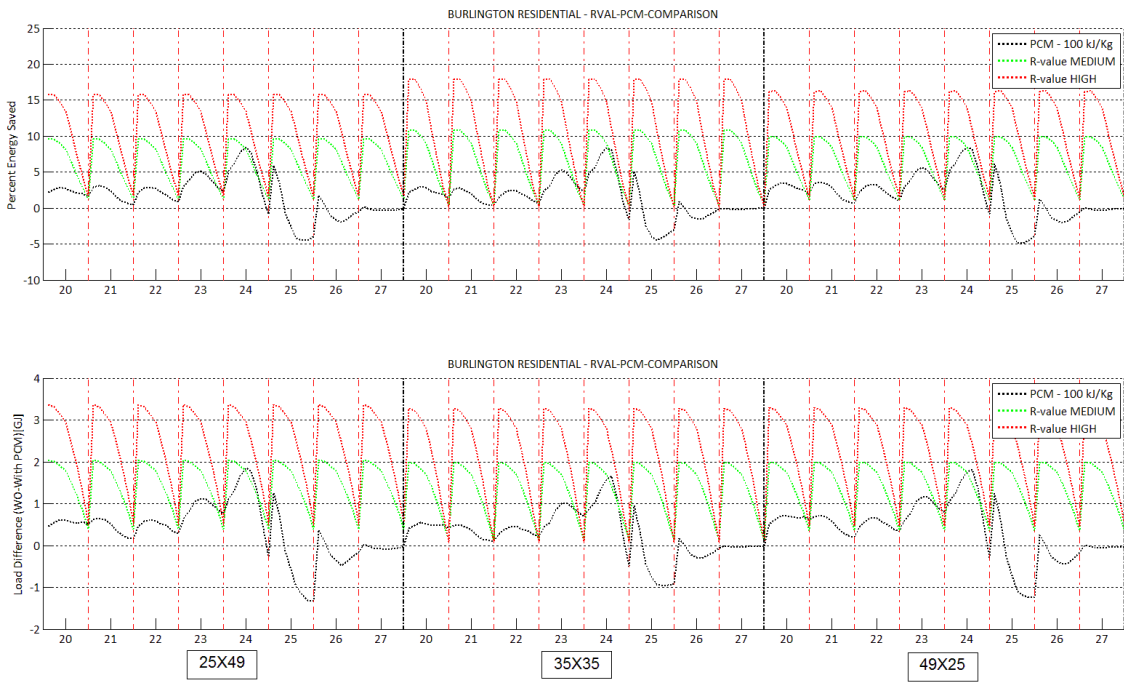


Figure B.7: Burlington residential R-value, PCM comparison. percent (top) magnitude (bottom)

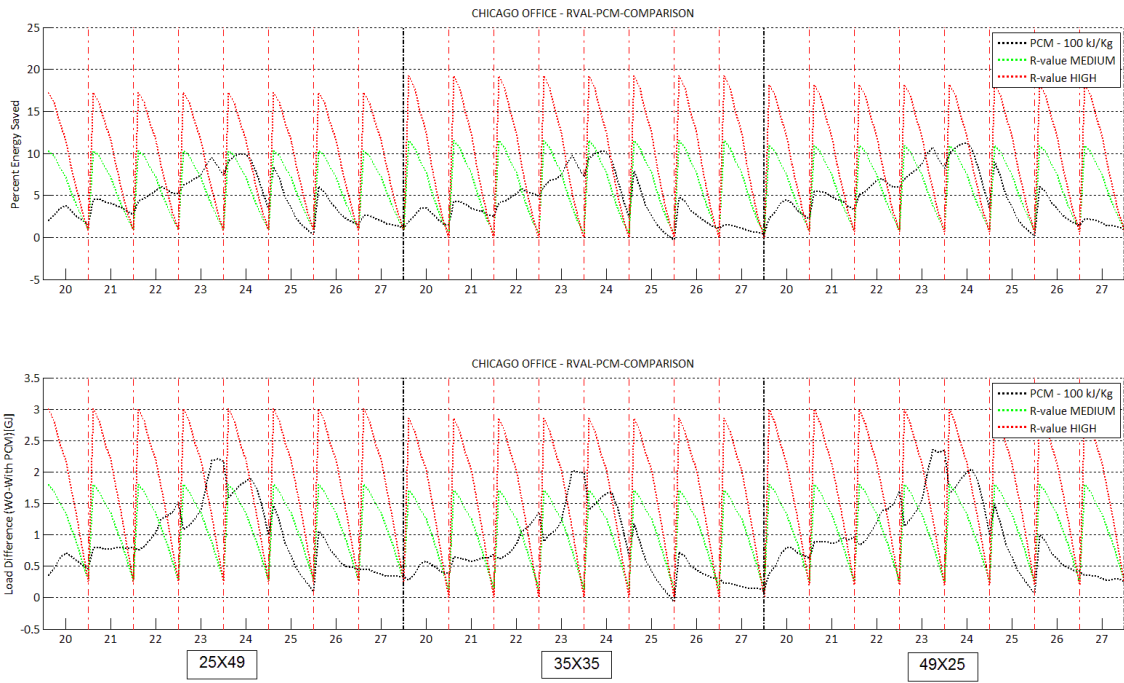


Figure B.9: Chicago office R-value, PCM comparison. percent (top) magnitude (bottom)

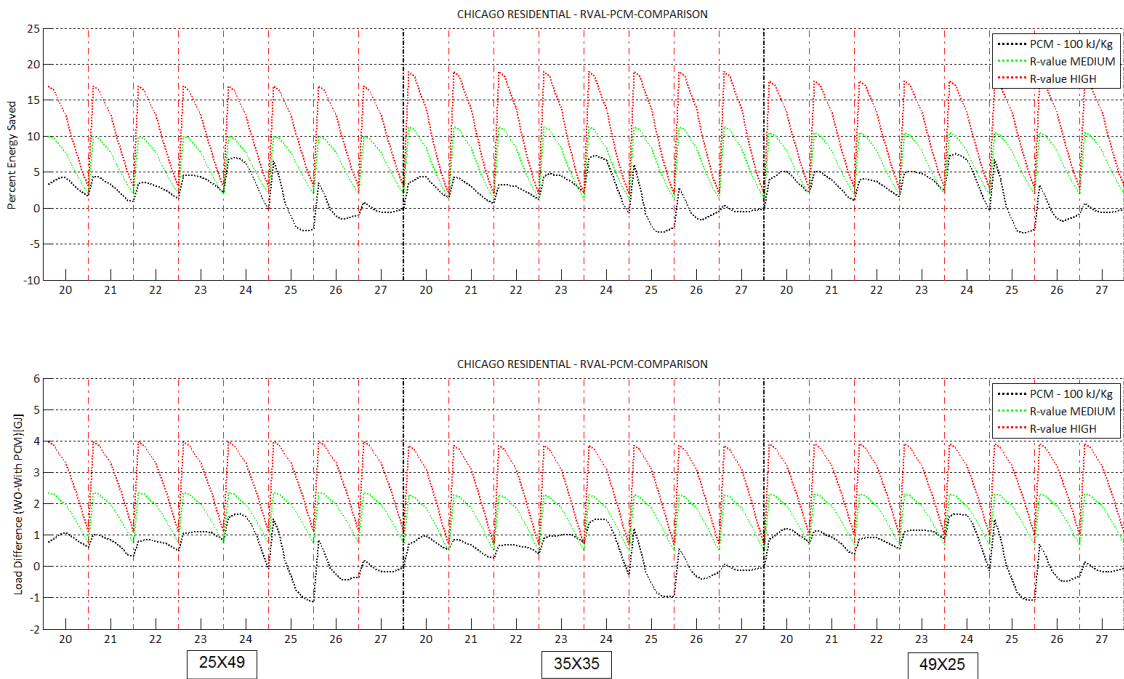


Figure B.10: Chicago residential R-value, PCM comparison. percent (top) magnitude (bottom)

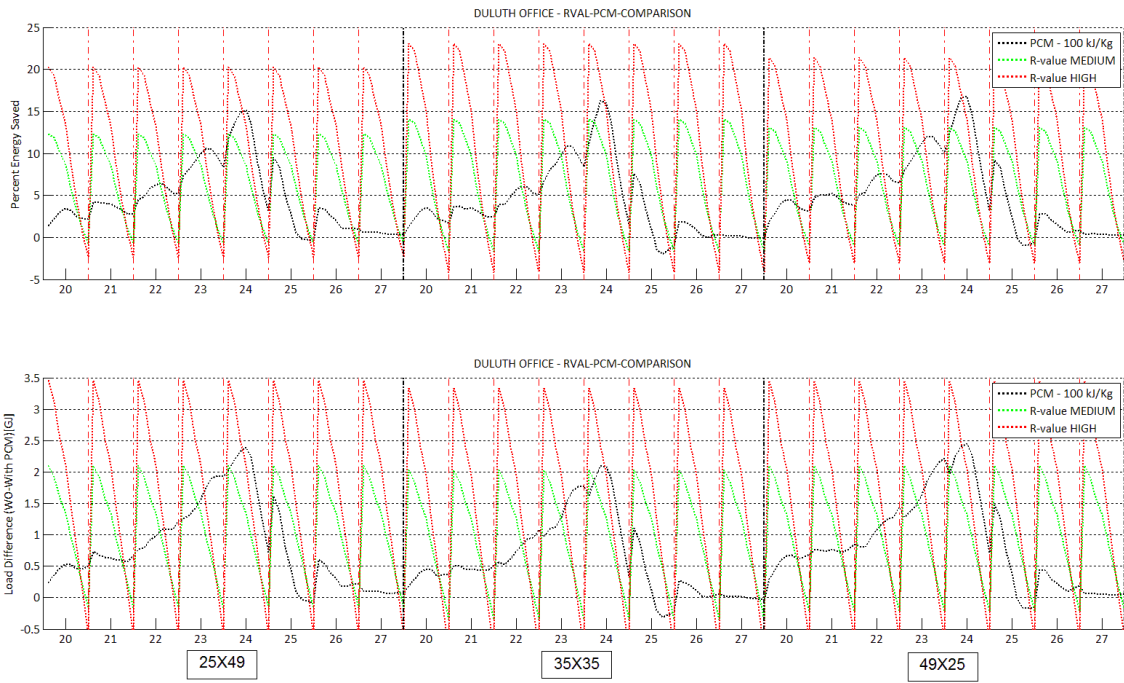


Figure B.11: Duluth office R-value, PCM comparison. percent (top) magnitude (bottom)

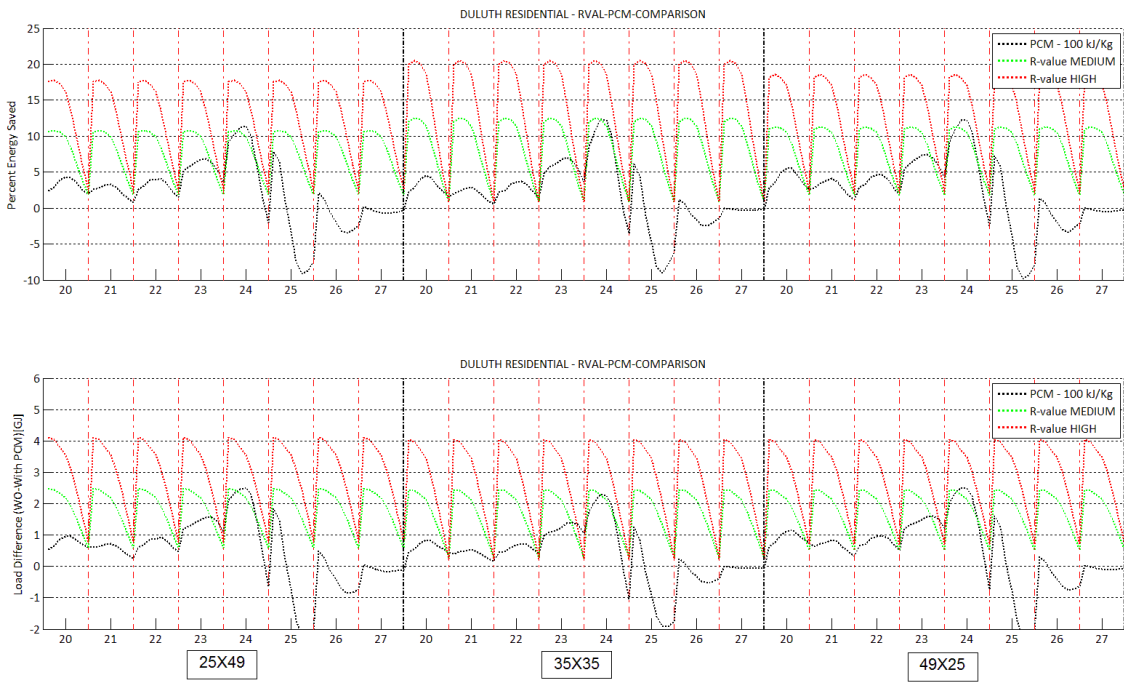


Figure B.12: Duluth residential R-value, PCM comparison. percent (top) magnitude (bottom)

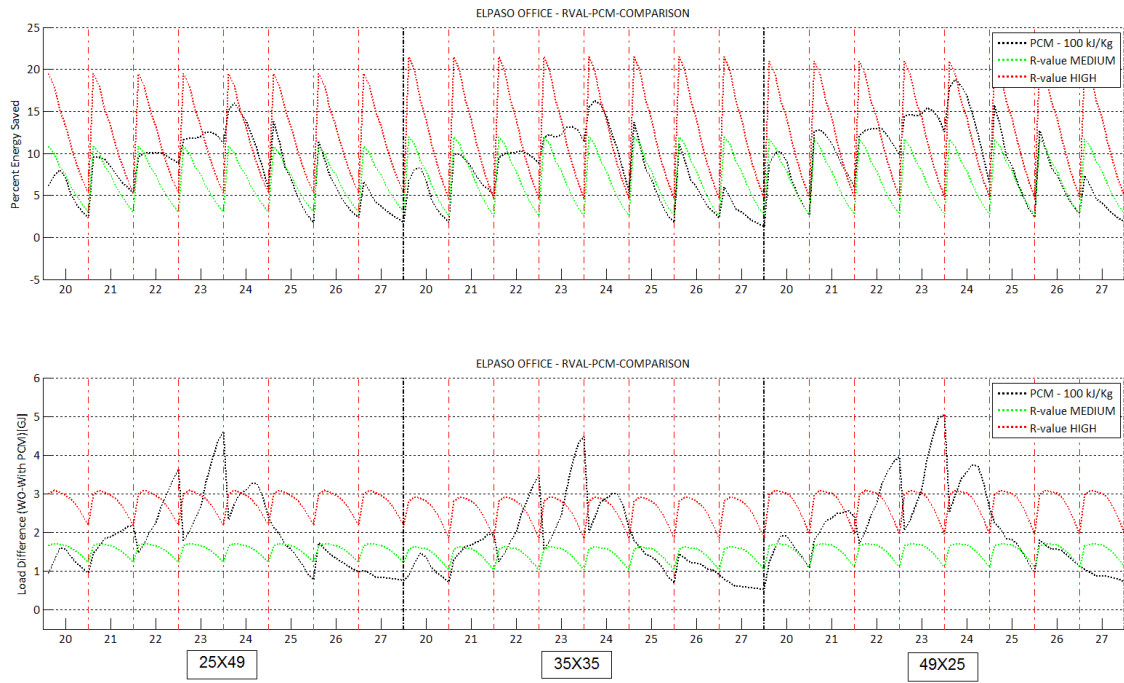


Figure B.13: El Paso office R-value, PCM comparison. percent (top) magnitude (bottom)

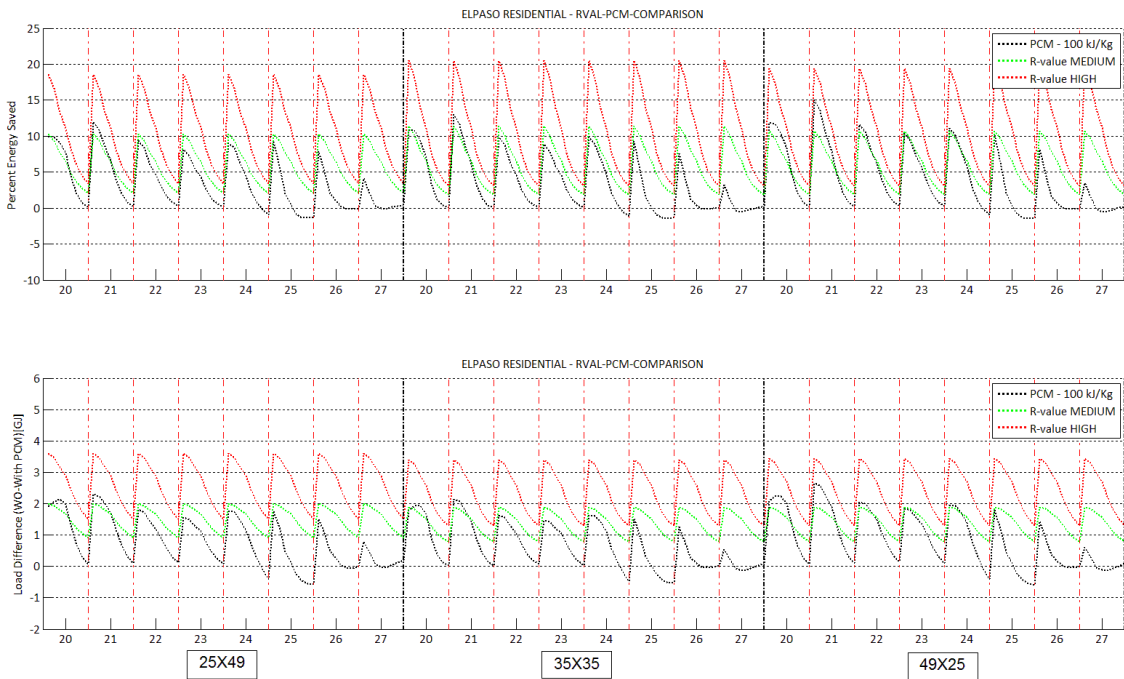


Figure B.14: El Paso residential R-value, PCM comparison. percent (top) magnitude (bottom)

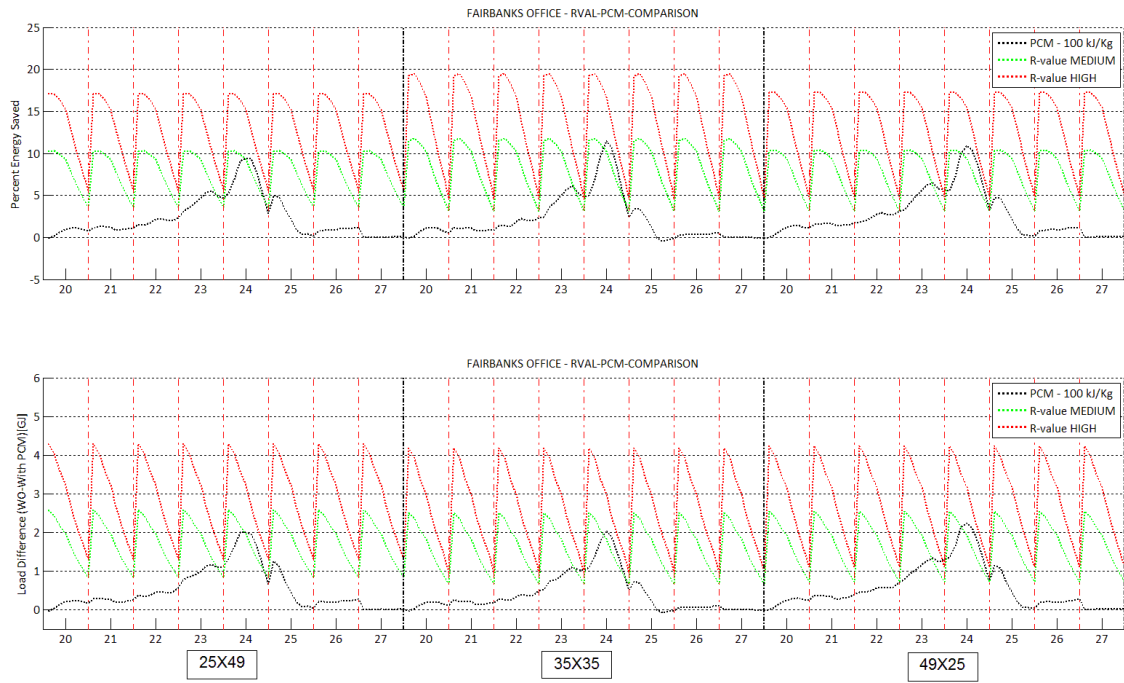


Figure B.15: Fairbanks office R-value, PCM comparison. percent (top) magnitude (bottom)

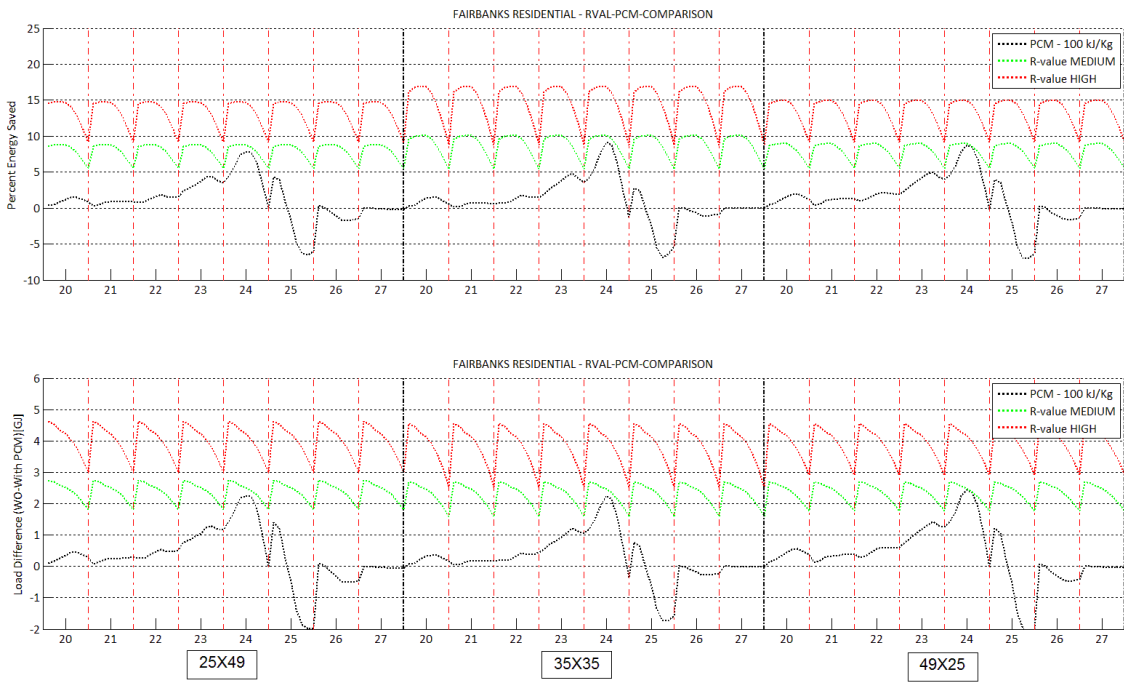


Figure B.16: Fairbanks residential R-value, PCM comparison. percent (top) magnitude (bottom)

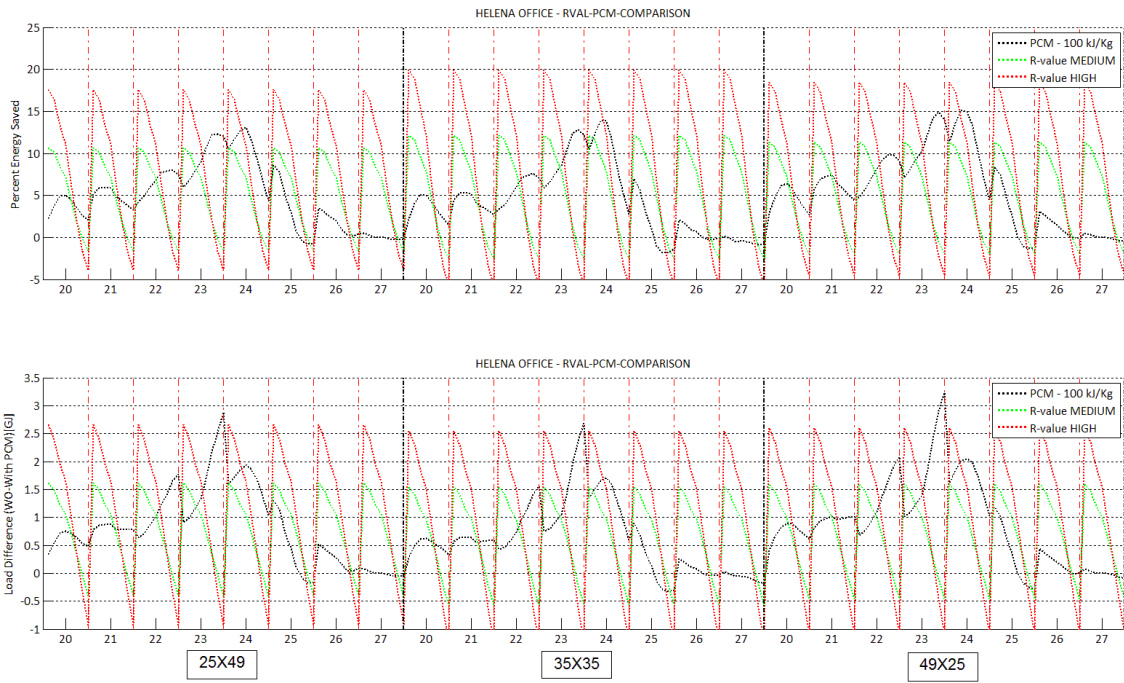


Figure B.17: Helena office R-value, PCM comparison. percent (top) magnitude (bottom)

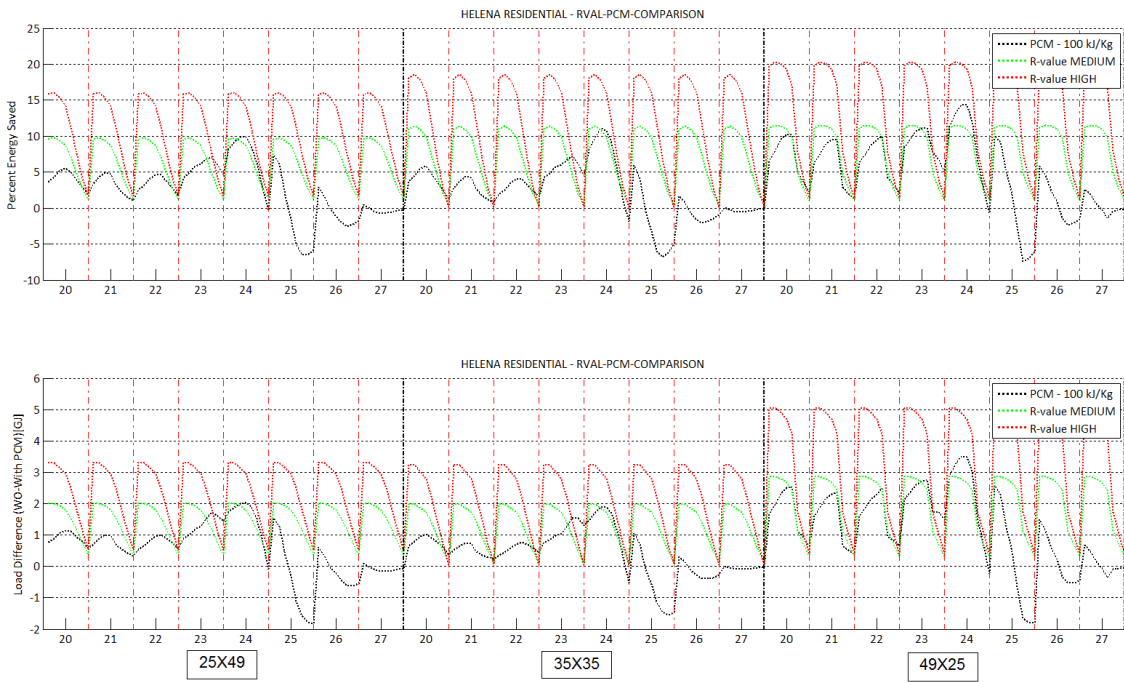


Figure B.18: Helena residential R-value, PCM comparison. percent (top) magnitude (bottom)

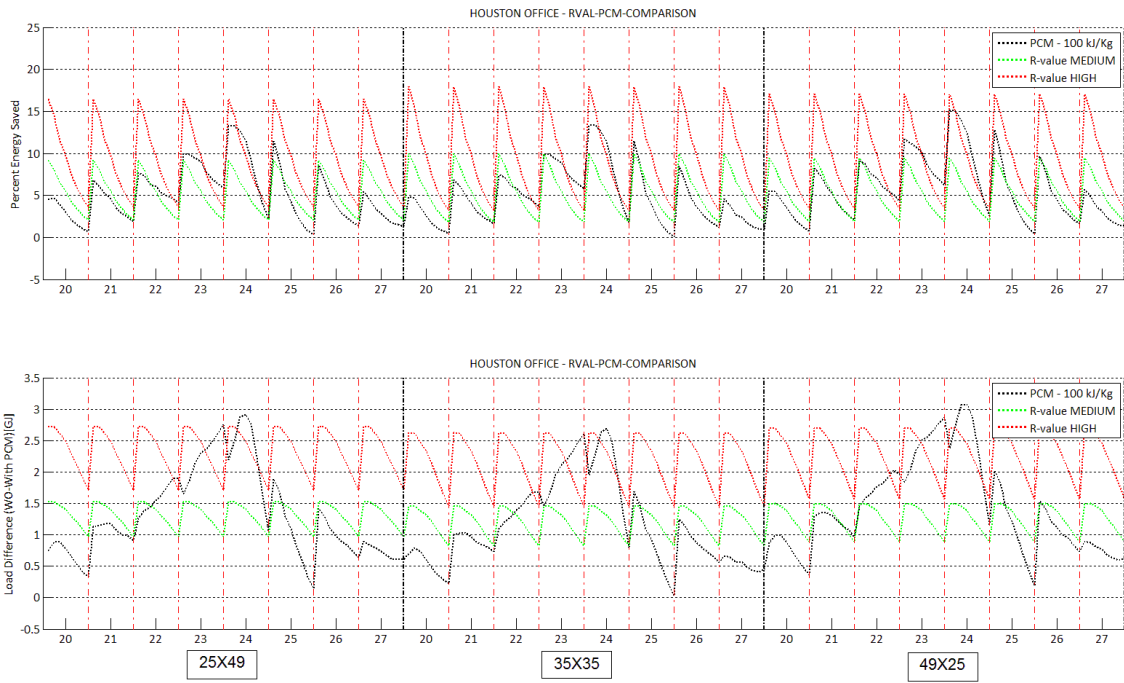


Figure B.19: Houston office R-value, PCM comparison. percent (top) magnitude (bottom)

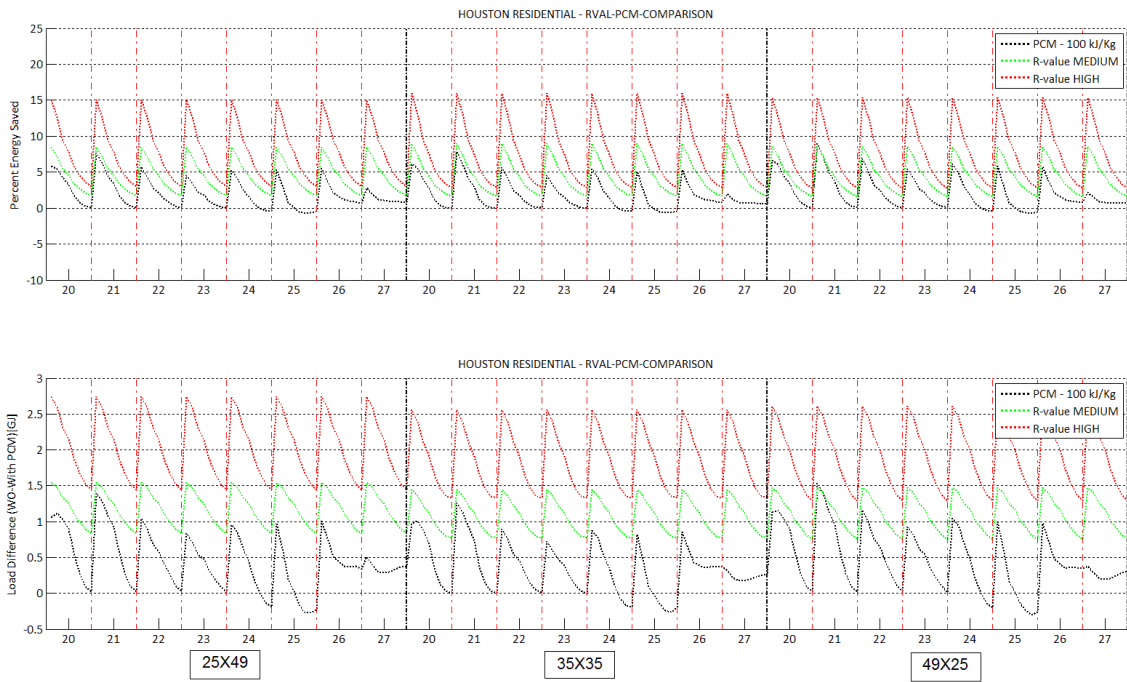


Figure B.20: Houston residential R-value, PCM comparison. percent (top) magnitude (bottom)

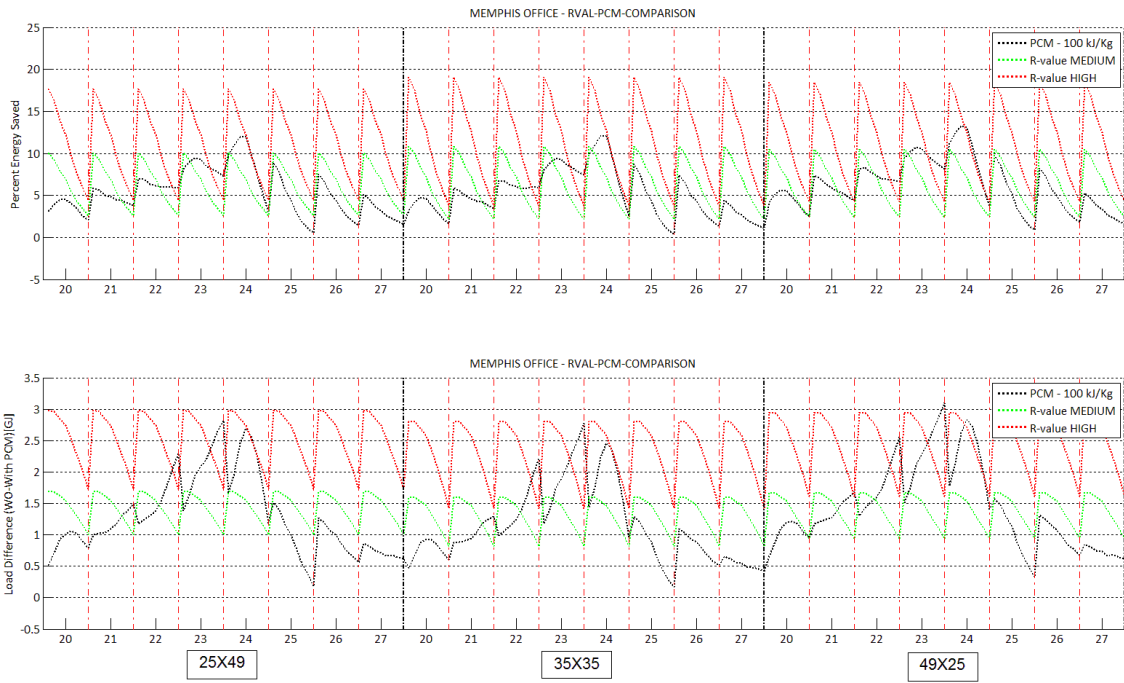


Figure B.21: Memphis office R-value, PCM comparison. percent (top) magnitude (bottom)

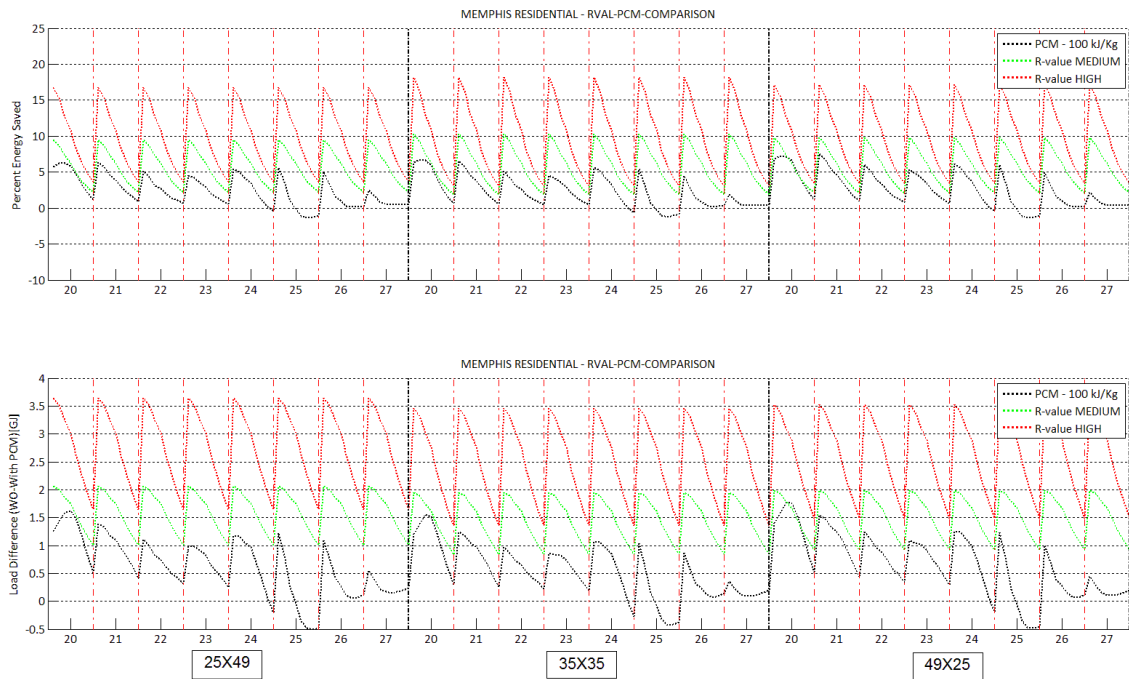


Figure B.22: Memphis residential R-value, PCM comparison. percent (top) magnitude (bottom)

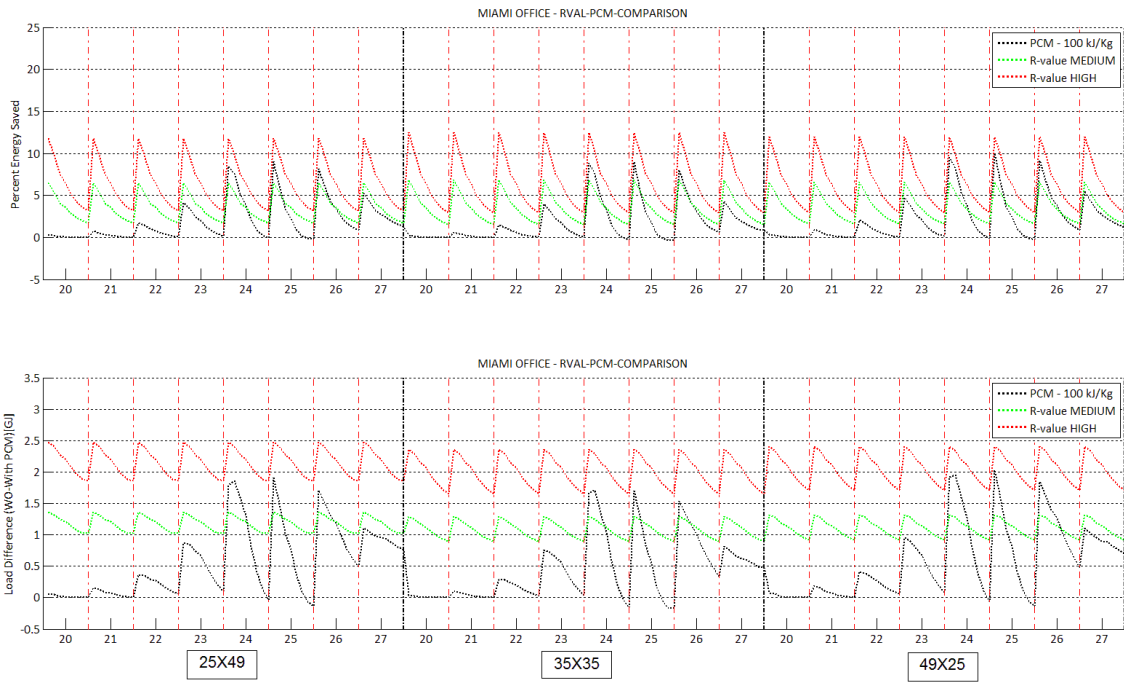


Figure B.23: Miami office R-value, PCM comparison. percent (top) magnitude (bottom)

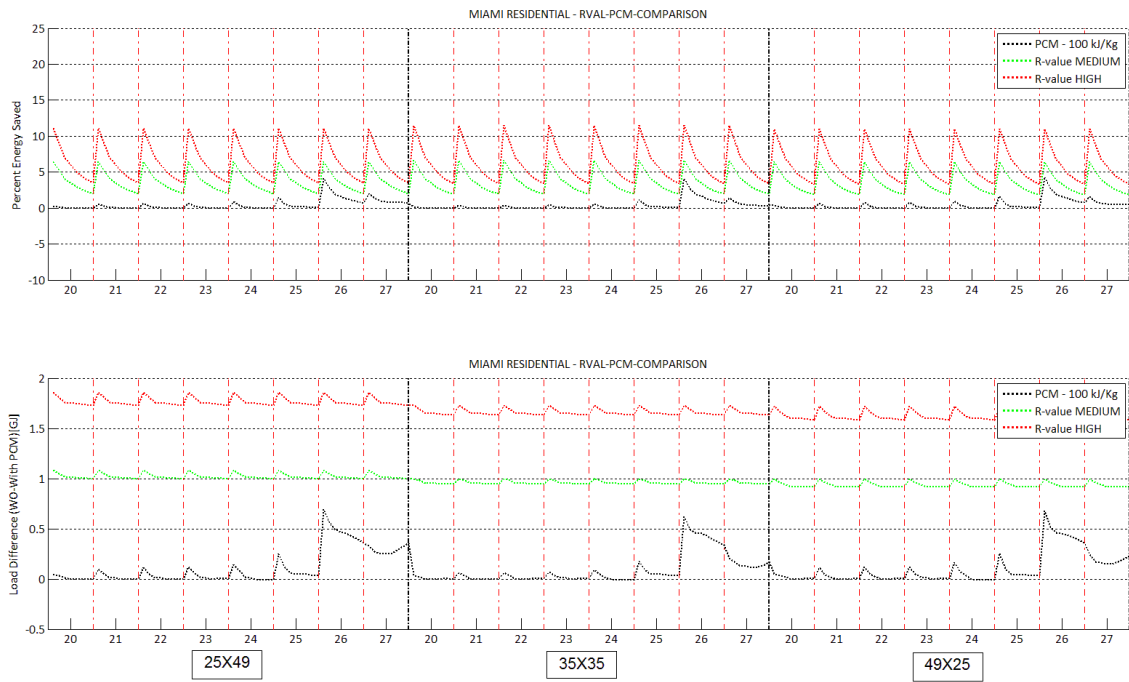


Figure B.24: Miami residential R-value, PCM comparison. percent (top) magnitude (bottom)

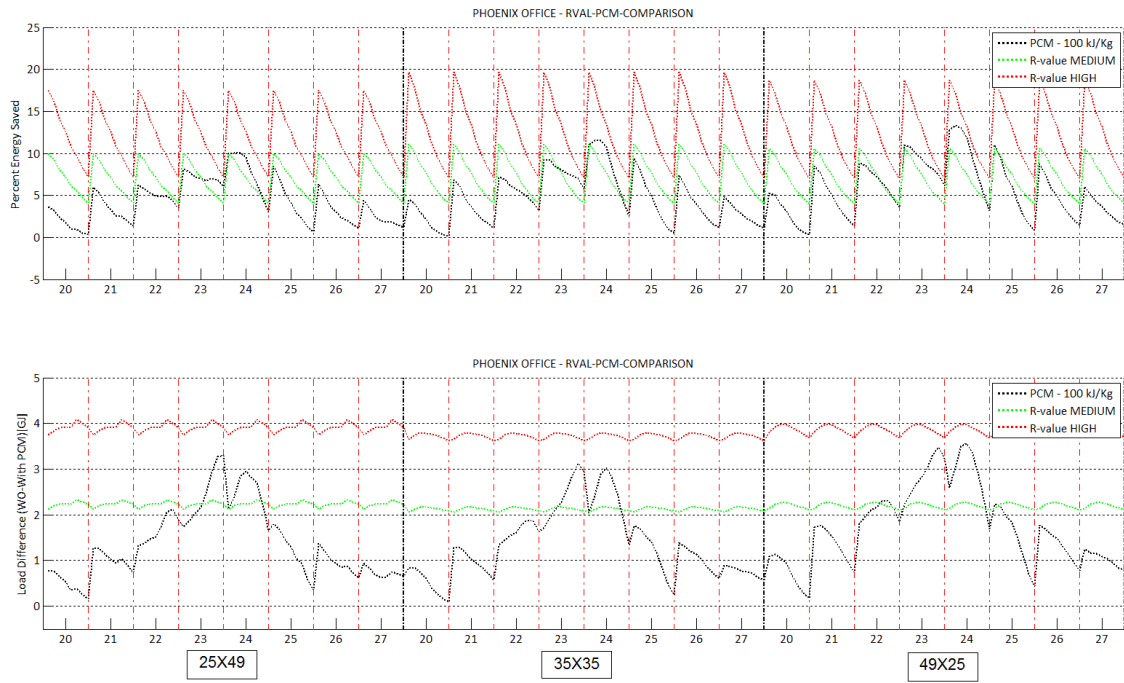


Figure B.25: Phoenix office R-value, PCM comparison. percent (top) magnitude (bottom)

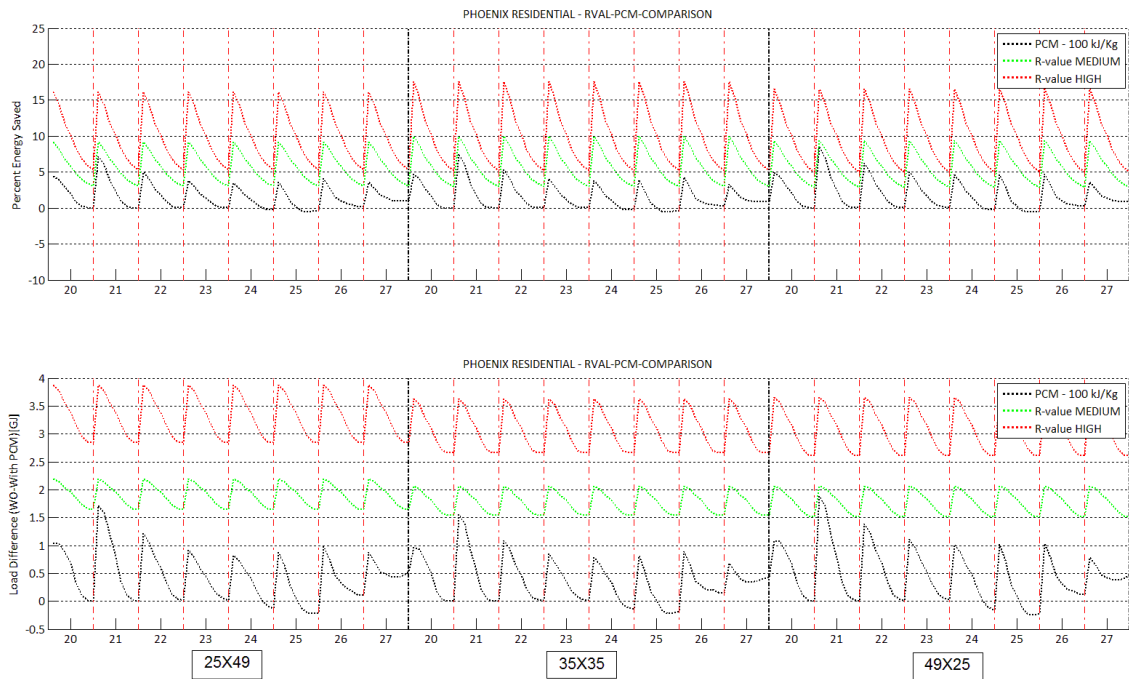


Figure B.26: Phoenix residential R-value, PCM comparison. percent (top) magnitude (bottom)

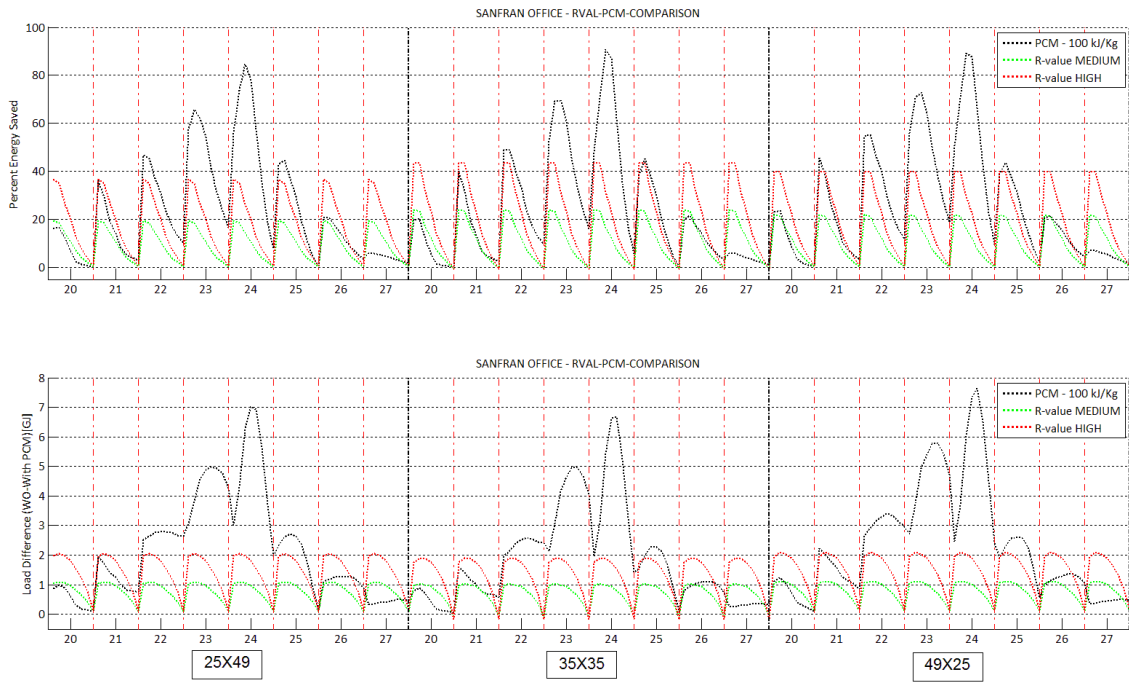


Figure B.28: San Francisco office R-value, PCM comparison. percent (top) magnitude (bottom)

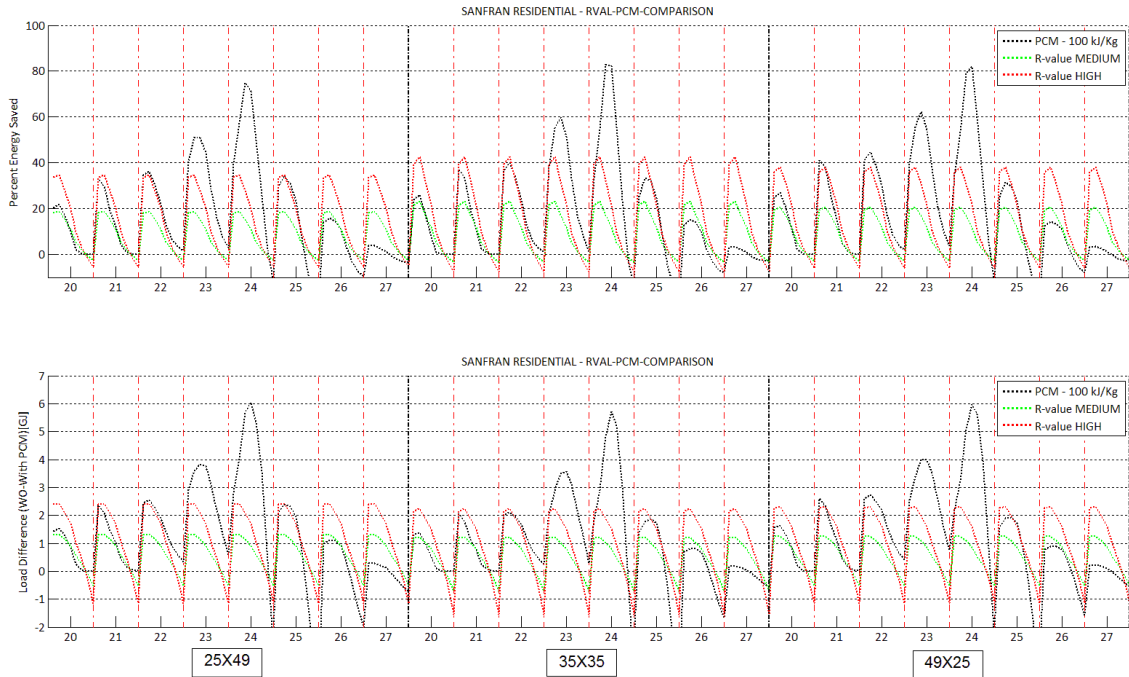


Figure B.28: San Francisco residential R-value, PCM comparison. percent (top) magnitude (bottom)

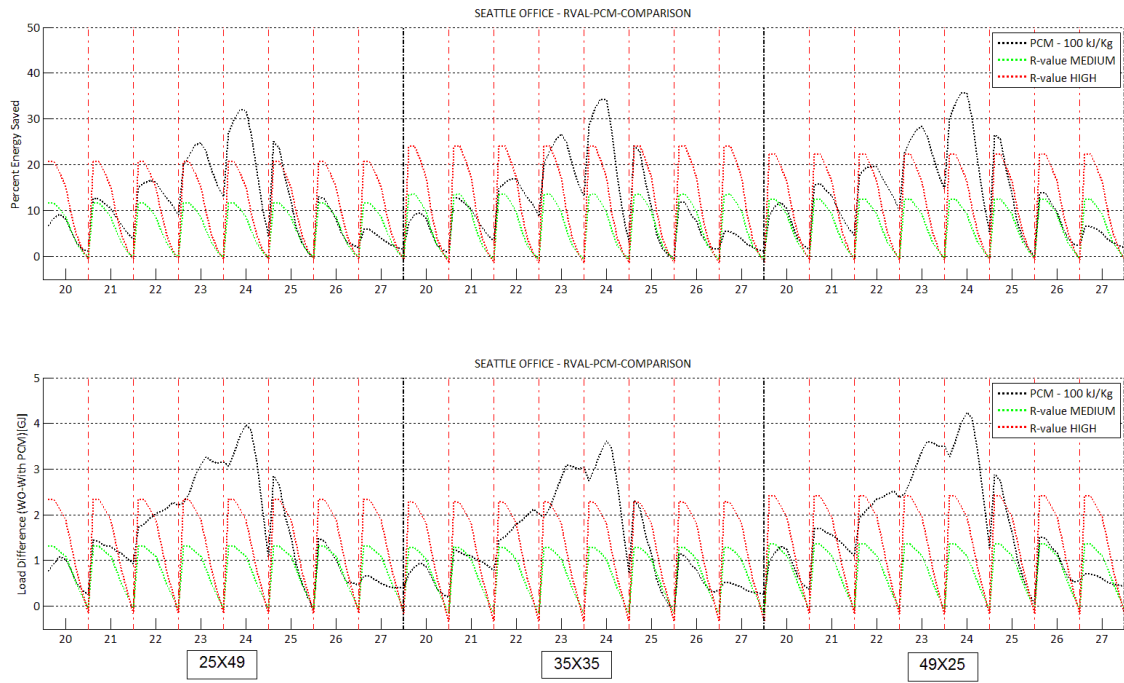


Figure B.29: Seattle office R-value, PCM comparison. percent (top) magnitude (bottom)

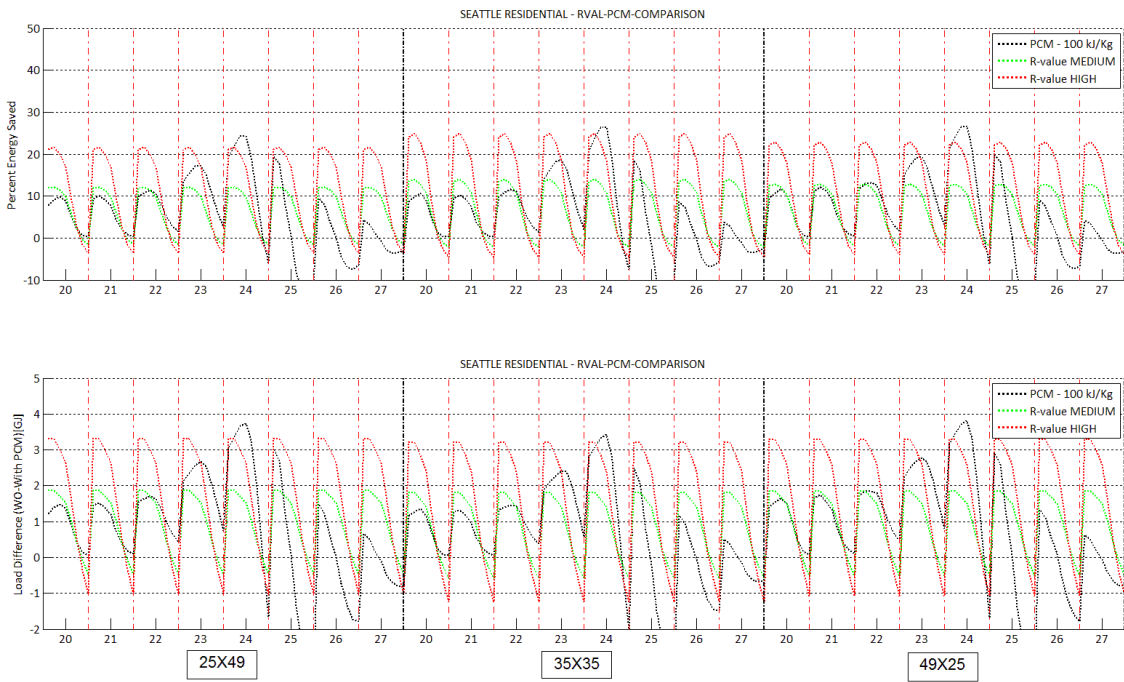


Figure B.30: Seattle residential R-value, PCM comparison. percent (top) magnitude (bottom)

Appendix C

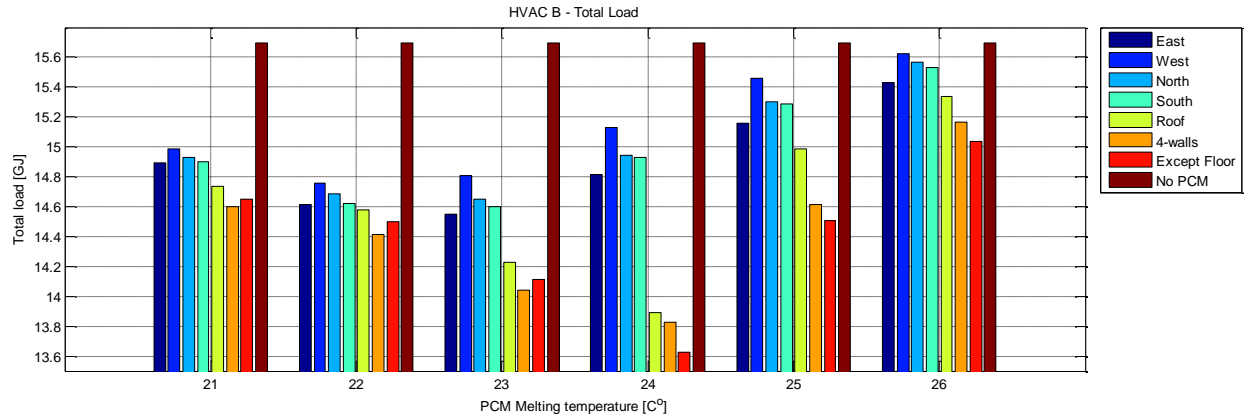


Figure C.1. HVAC B: Total load chart for PCM with different melting temperatures placed on different surfaces.

The scenario for the monthly heating loads follows a similar trend as to the results from HVAC A as can be seen in Table C.1. The magnitude of the monthly heating loads however is half of what was seen for each corresponding month in HVAC A. While there is no heating required for the months April, May, June, July, August and September, the heating loads for the remaining months do not vary among the seven different cases either when PCM melting at 24°C is used.

Months	Jan	Feb	Mar	Apr	May	Jun	Jul	Aug	Sep	Oct	Nov	Dec
Surface	[MJ]	[MJ]	[MJ]	[MJ]	[MJ]	[MJ]	[MJ]	[MJ]	[MJ]	[MJ]	[MJ]	[MJ]
East	332	200	57	1	0	0	0	0	0	22	92	344
West	335	204	61	1	0	0	0	0	0	23	97	346
North	333	202	62	1	0	0	0	0	0	23	94	344
South	330	198	57	1	0	0	0	0	0	22	91	342
Roof	332	196	53	0	0	0	0	0	0	22	90	345
4 Walls	328	191	50	0	0	0	0	0	0	22	85	342
Except Floor	329	192	50	0	0	0	0	0	0	22	86	343
Mean	331	197	56	1	0	0	0	0	0	22	91	344
Std Dev	2	5	5	1	0	0	0	0	0	1	4	1
No PCM	338	210	74	5	0	0	0	0	0	28	101	347

Table C.1: HVAC B: Monthly heating load [MJ] for PCM melting at 24°C appended to the seven different scenarios.

Months	Jan	Feb	Mar	Apr	May	Jun	Jul	Aug	Sep	Oct	Nov	Dec
Surface	[MJ]	[MJ]	[MJ]	[MJ]	[MJ]	[MJ]	[MJ]	[MJ]	[MJ]	[MJ]	[MJ]	[MJ]
East	33	134	351	922	1463	2281	2677	2650	2098	999	156	6
West	75	178	408	953	1473	2280	2677	2650	2097	1031	221	22
North	40	144	395	946	1470	2281	2677	2650	2097	1005	170	8
South	44	148	378	938	1470	2280	2677	2650	2098	1016	177	10
Roof	1	38	133	720	1390	2272	2677	2650	2095	834	41	0
4 Walls	0	25	117	723	1386	2271	2677	2650	2093	838	28	0
Except Floor	0	11	68	664	1369	2269	2677	2650	2093	785	16	0
Mean	28	97	264	838	1432	2276	2677	2650	2096	930	116	7
Std Dev	29	69	150	129	47	5	0	0	2	105	84	8
No PCM	104	231	512	1074	1519	2287	2677	2650	2104	1113	290	35

Table C.2: HVAC B: Monthly cooling load [MJ] for PCM melting at 24°C appended to the seven different scenarios.

Table C.2: depicts the monthly cooling load in mega joules. PCM does not perform well for the months June, July, August, and September. In fact there is almost no variability in the seven cases and additionally every case exhibits the same annual load as the case when no PCM is used. Once again it can be seen that the PCM does not perform optimally during the summer months in Albuquerque under the HVAC B schedule.

Appendix D

Regression model plots for each climate

Climate 1 - Hot/Humid

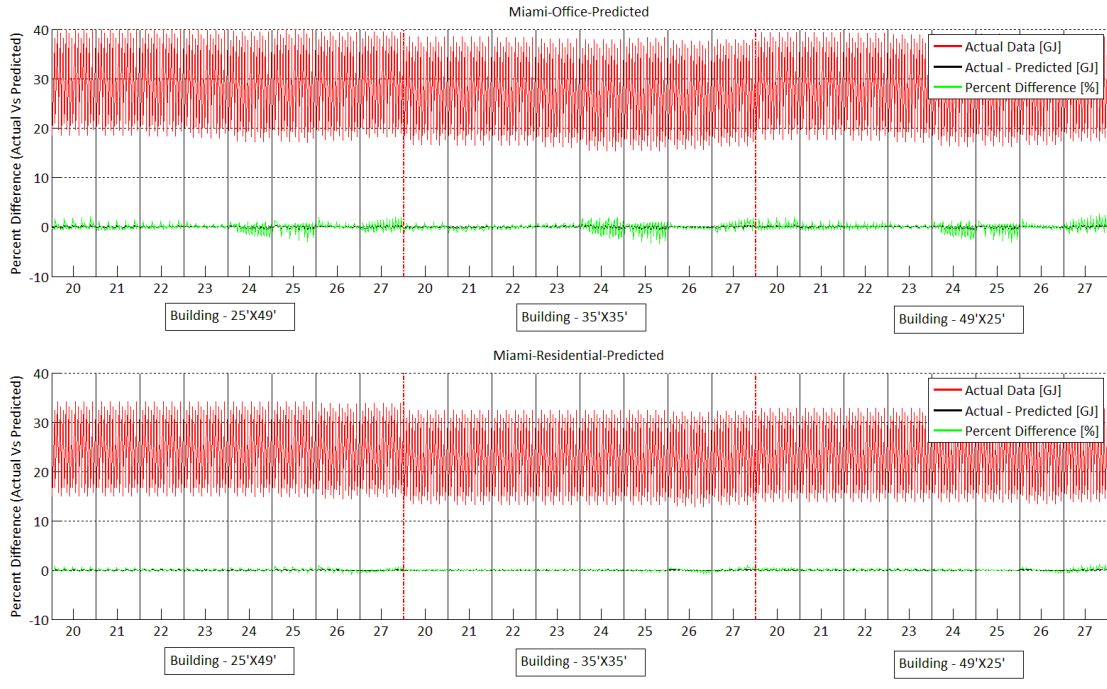


Figure D.1: Difference between the actual and predicted data for climate 1, Miami.

Climate 2

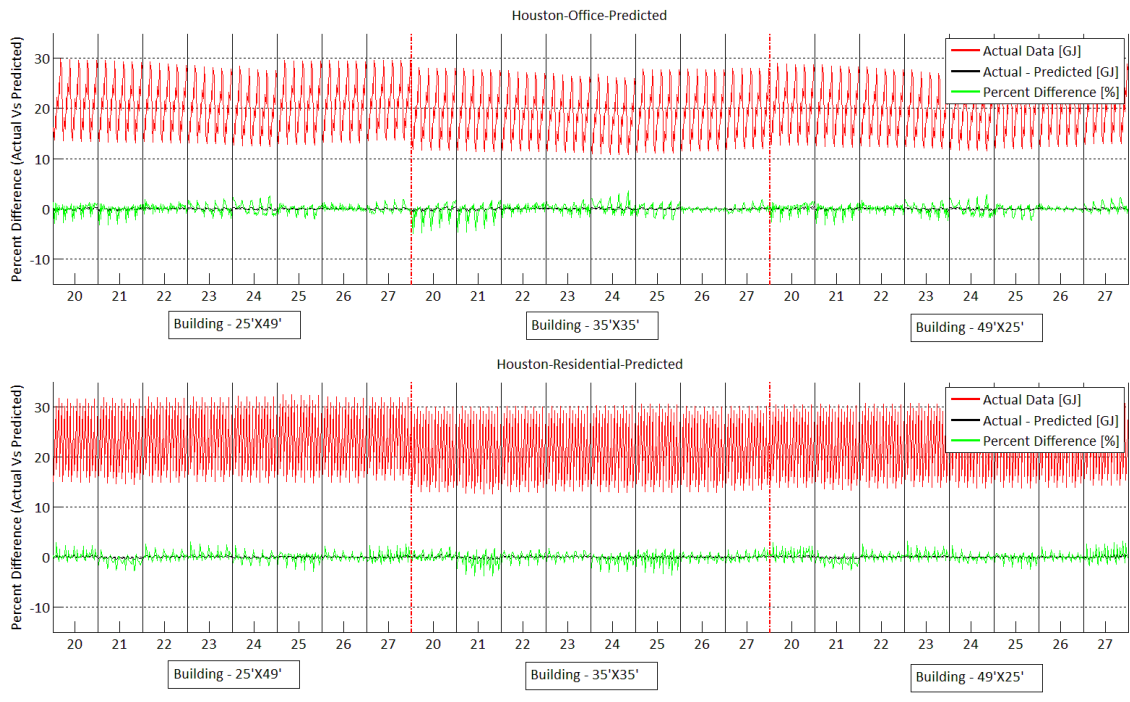
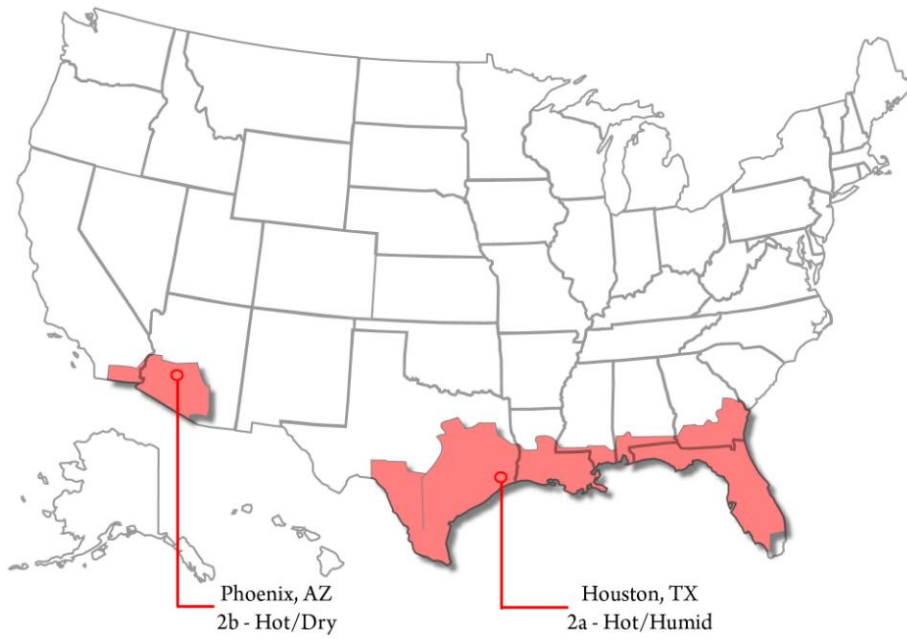


Figure D.2: Difference between the actual and predicted data for climate 2a, Houston.

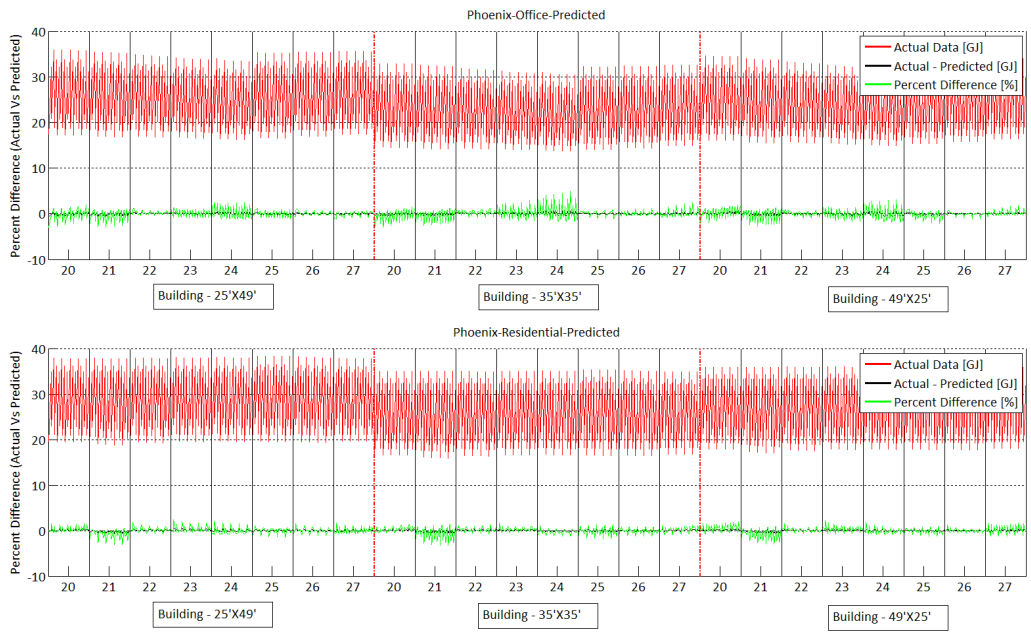
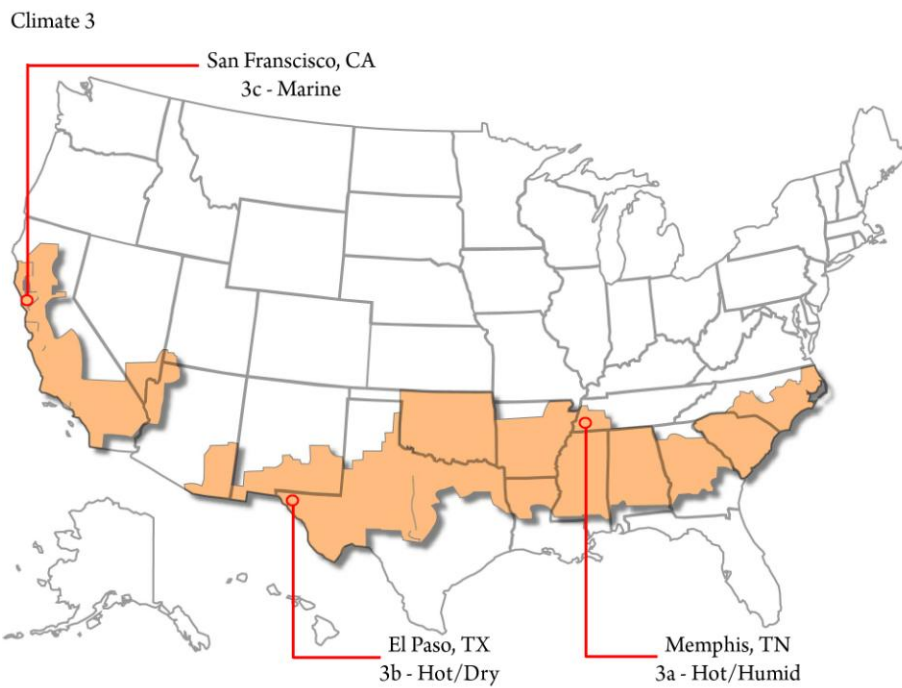


Figure D.3: Difference between the actual and predicted data for climate 2b, Phoenix.



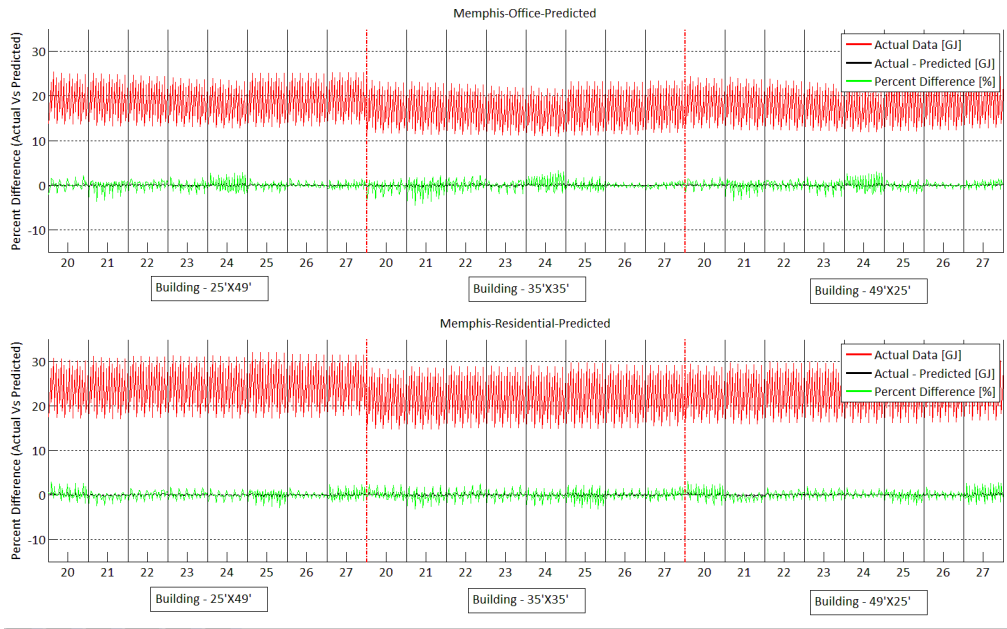


Figure D.4: Difference between the actual and predicted data for climate 3a, Memphis.

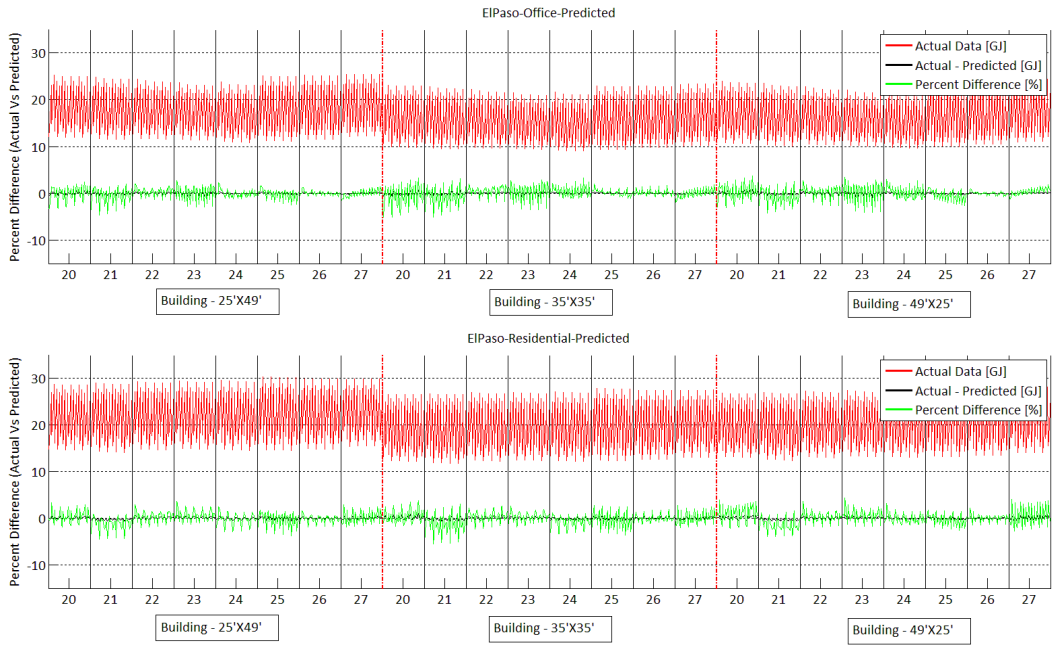


Figure D.5: Difference between the actual and predicted data for climate 3b, El Paso.

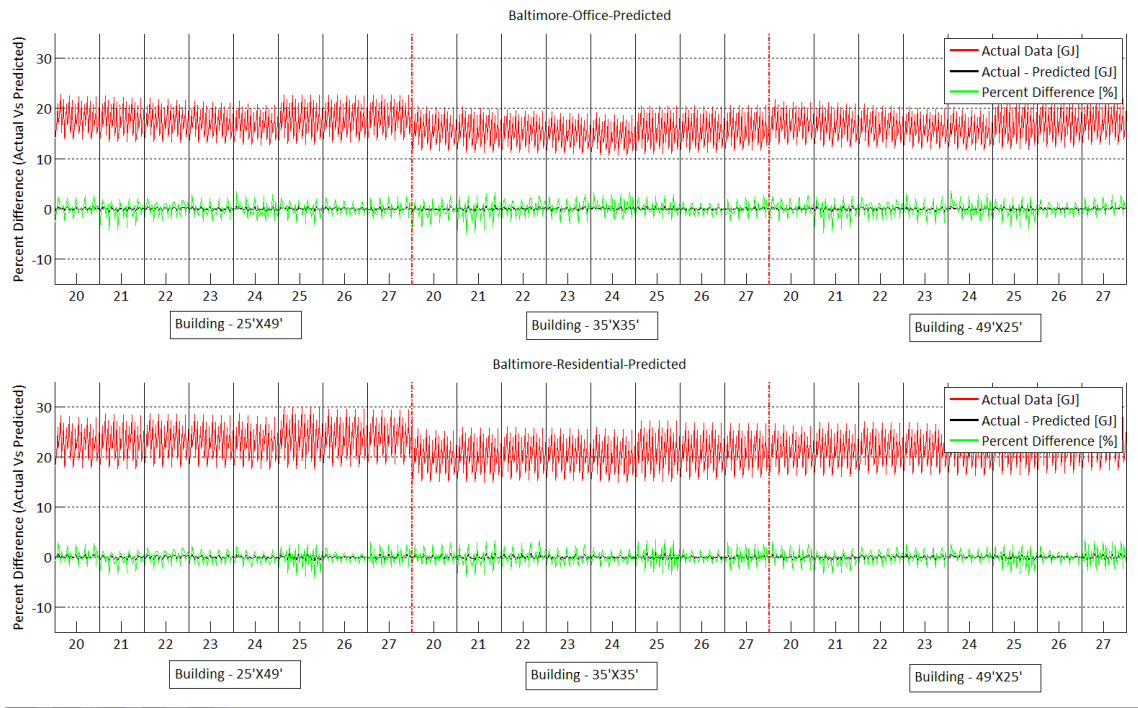
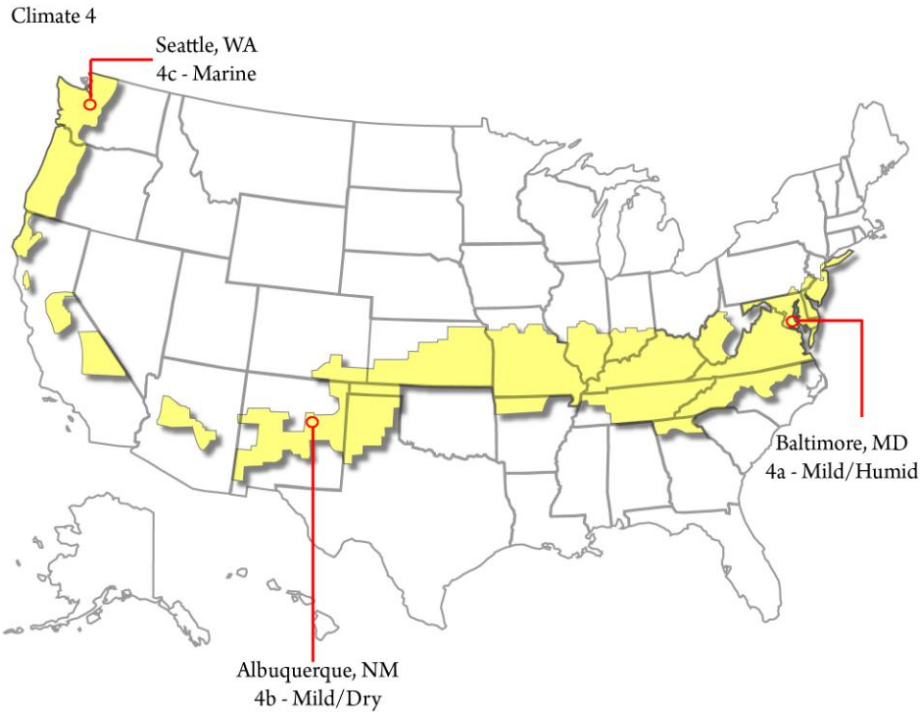


Figure D.6: Difference between the actual and predicted data for climate 4a, Baltimore.

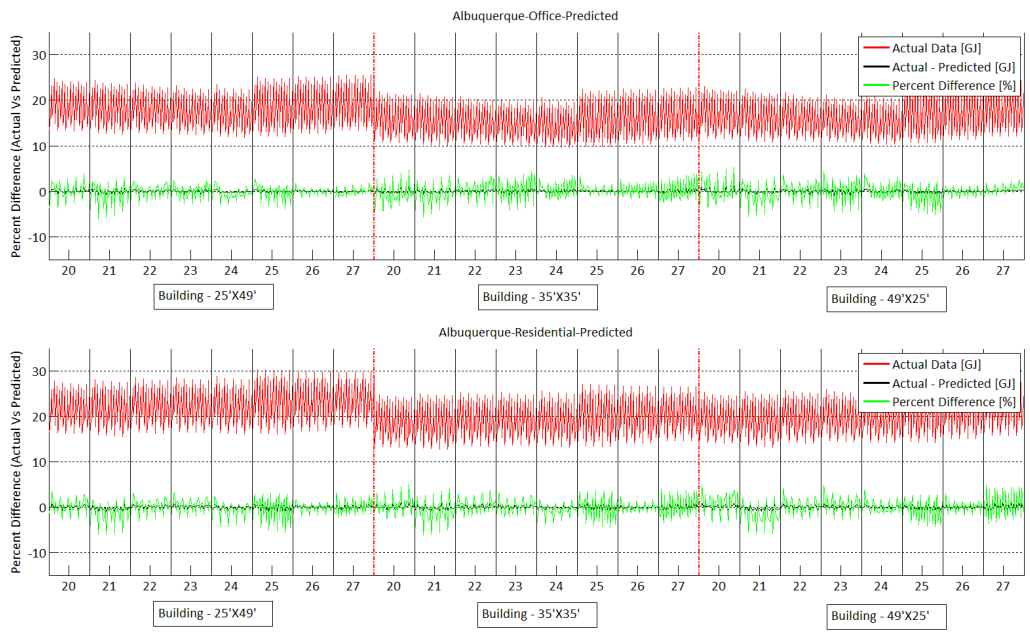


Figure D.7: Difference between the actual and predicted data for climate 4b, Albuquerque.

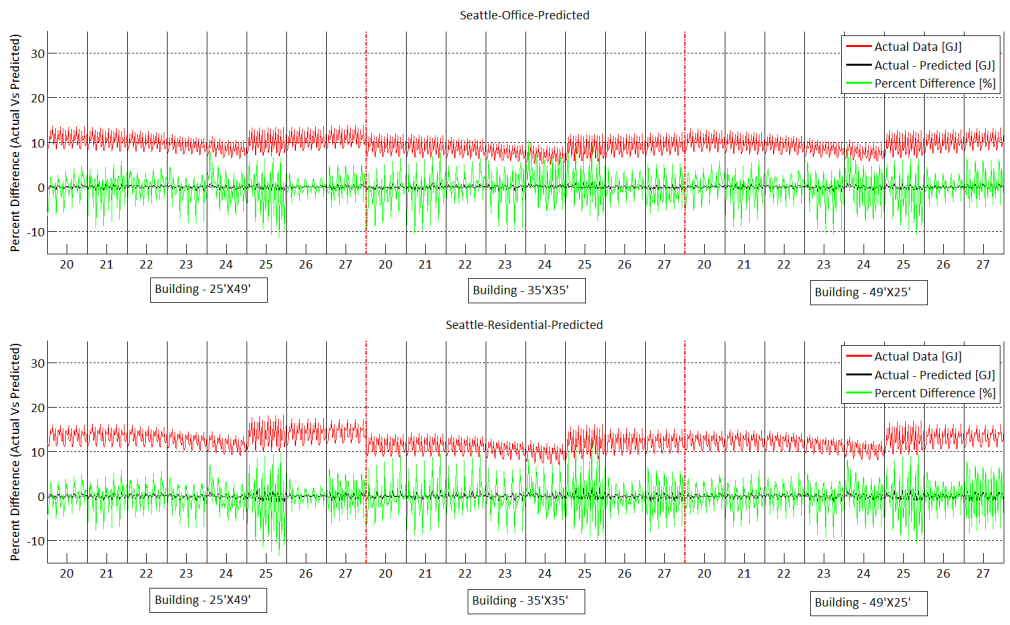


Figure D.8: Difference between the actual and predicted data for climate 4c, Seattle.

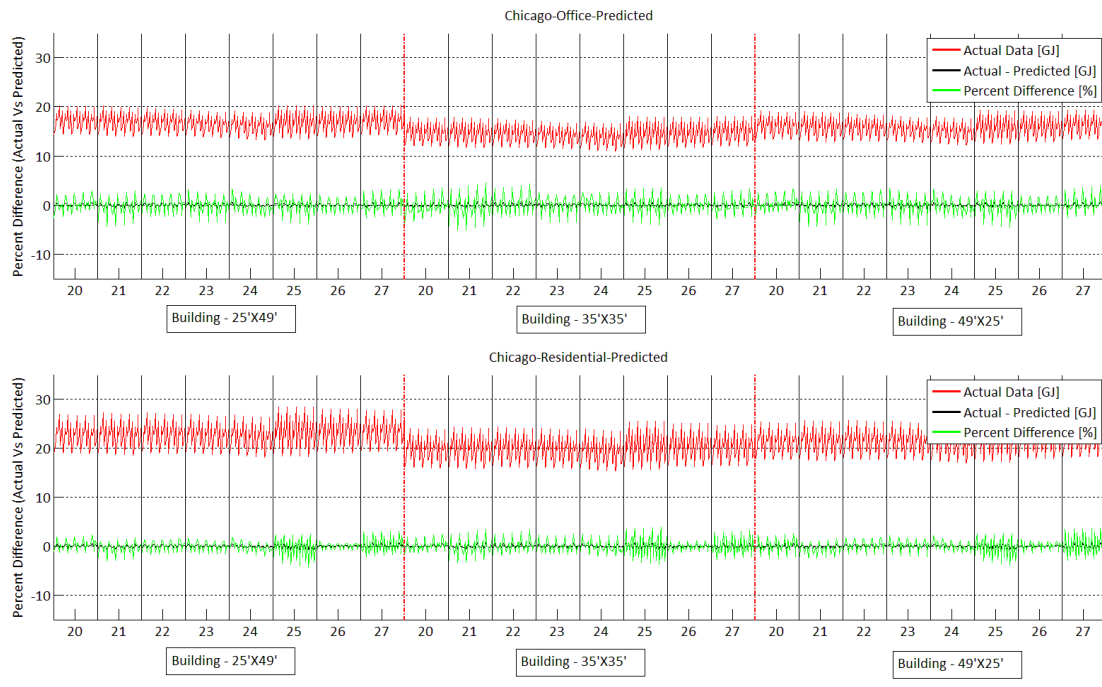
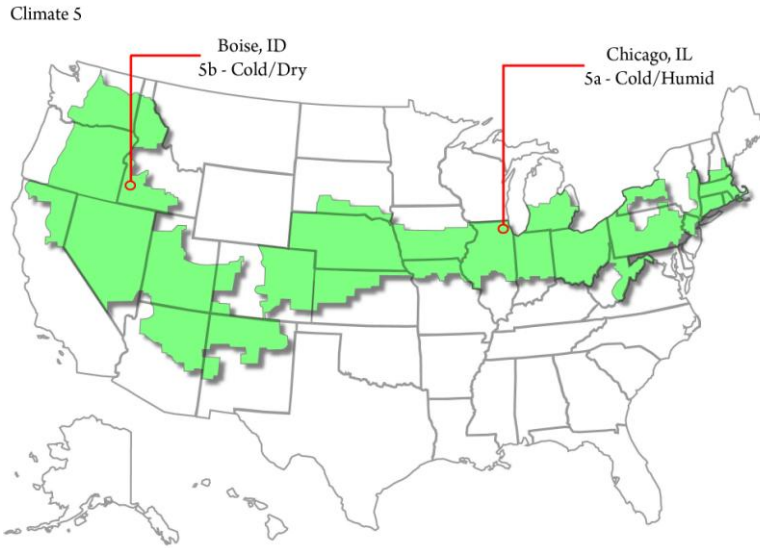


Figure D.9: Difference between the actual and predicted data for climate 5a, Chicago.

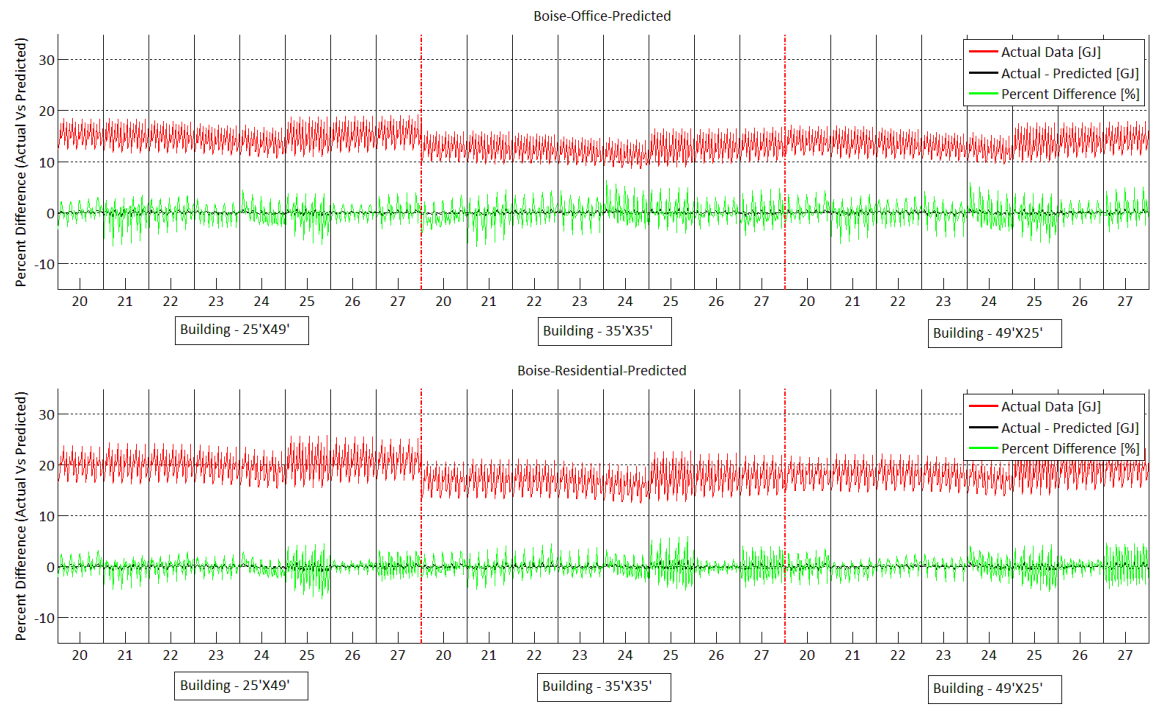
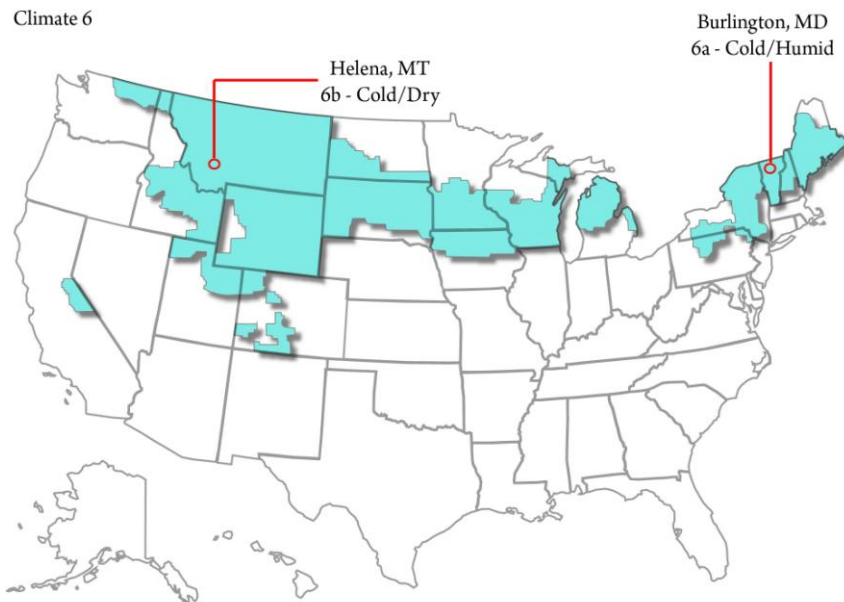


Figure D.10: Difference between the actual and predicted data for climate 5b, Boise.



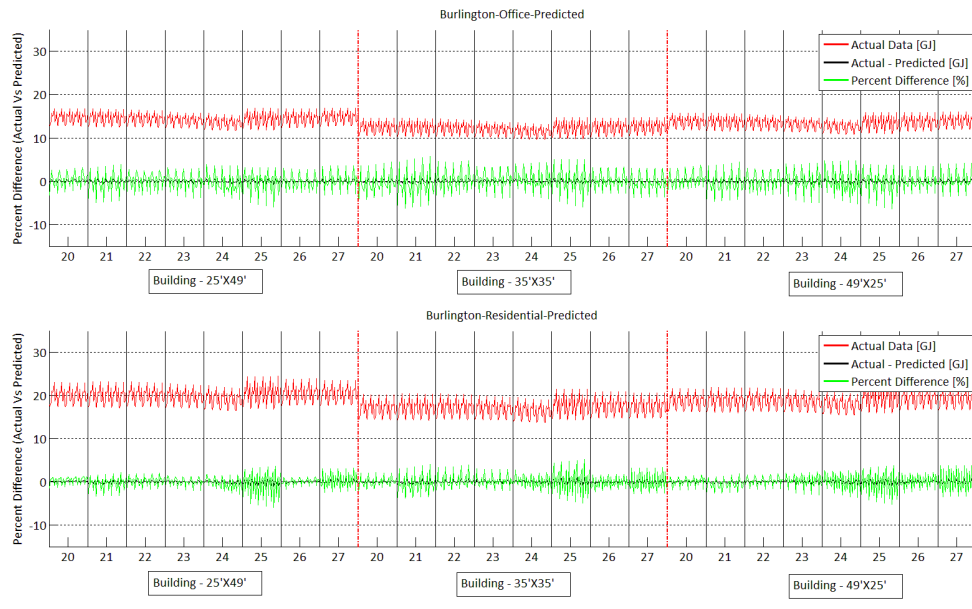


Figure D.11: Difference between the actual and predicted data for climate 6a, Burlington.

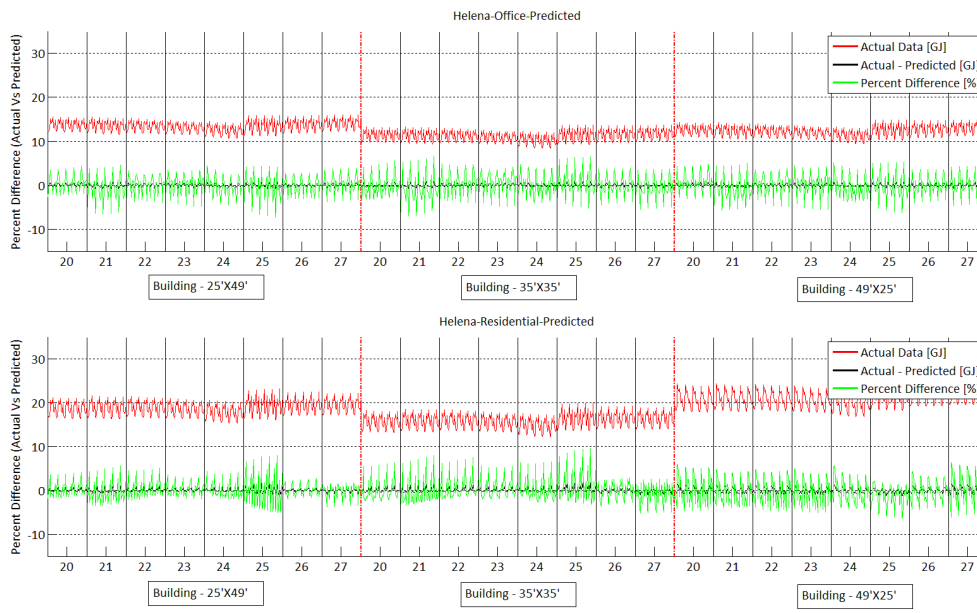


Figure D.12: Difference between the actual and predicted data for climate 6b, Helena.

Climate 7 - Very Cold

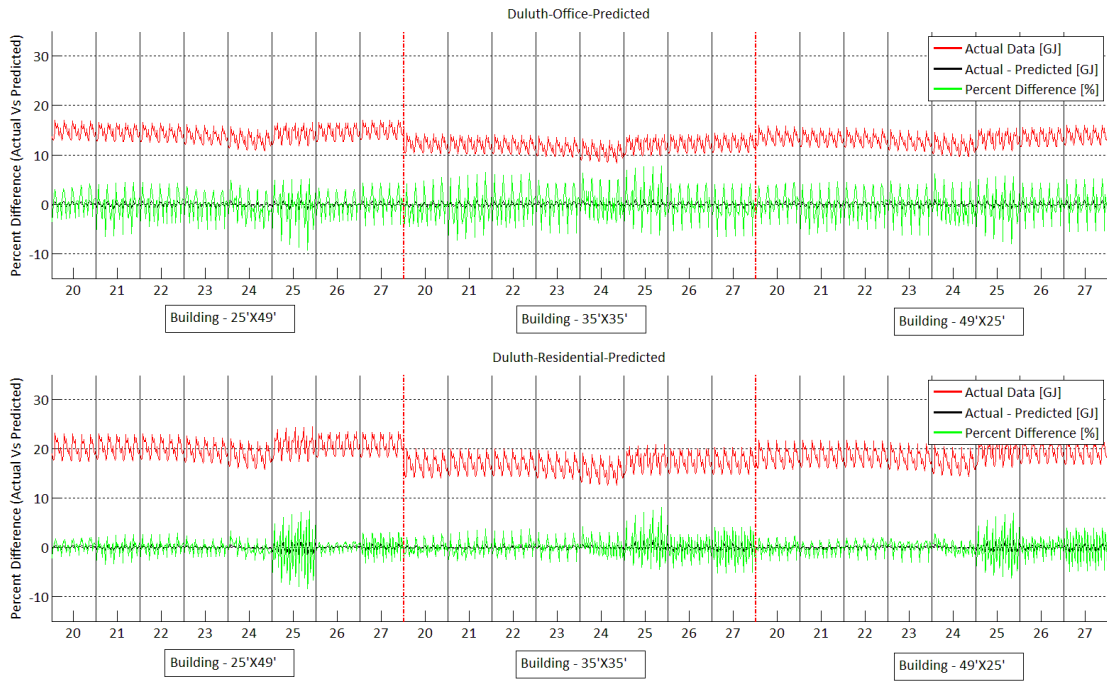
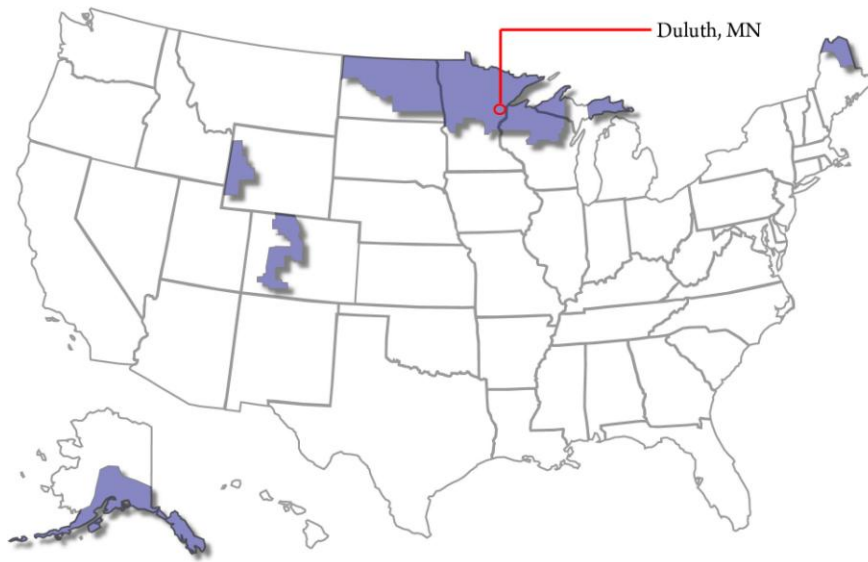


Figure D.13: Difference between the actual and predicted data for climate 7, Duluth.

Climate 8 - Extreme Cold

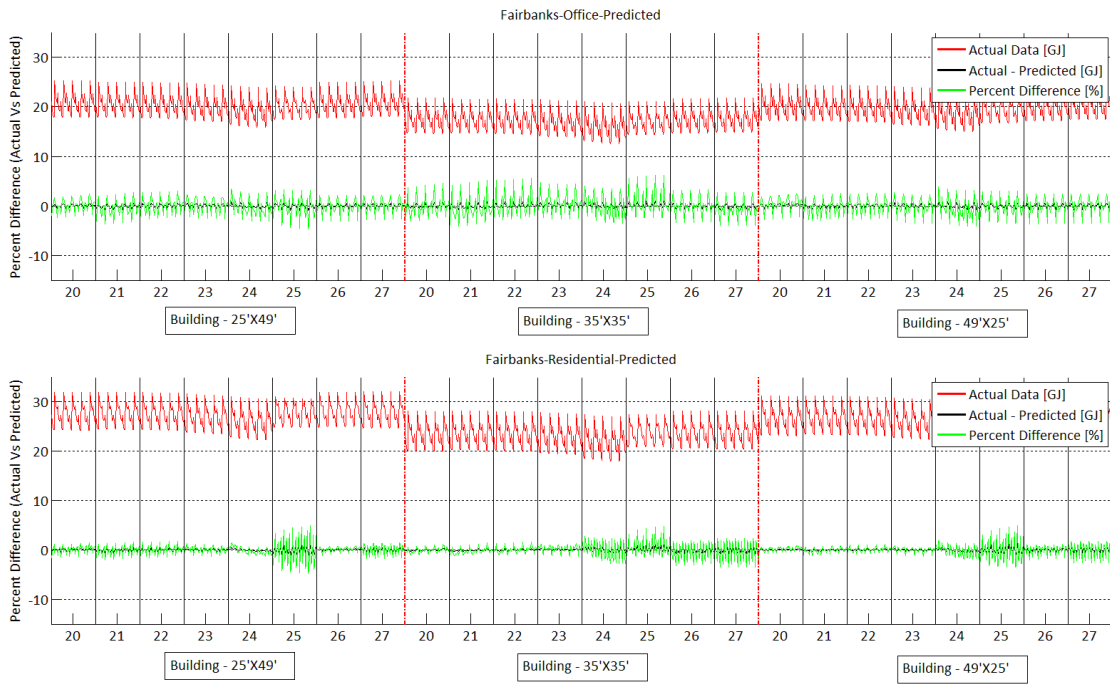
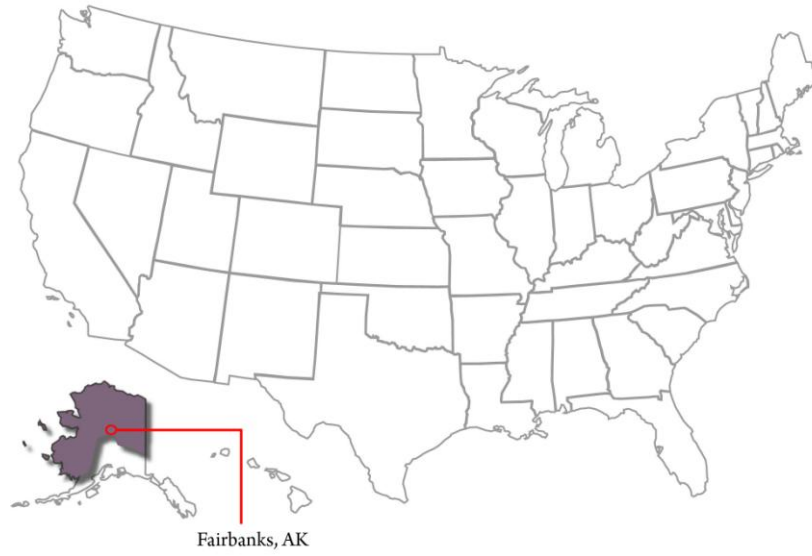


Figure D.14: Difference between the actual and predicted data for climate 8, Fairbanks.

Appendix E

Magnitude of energy saved for each additional level of internal load

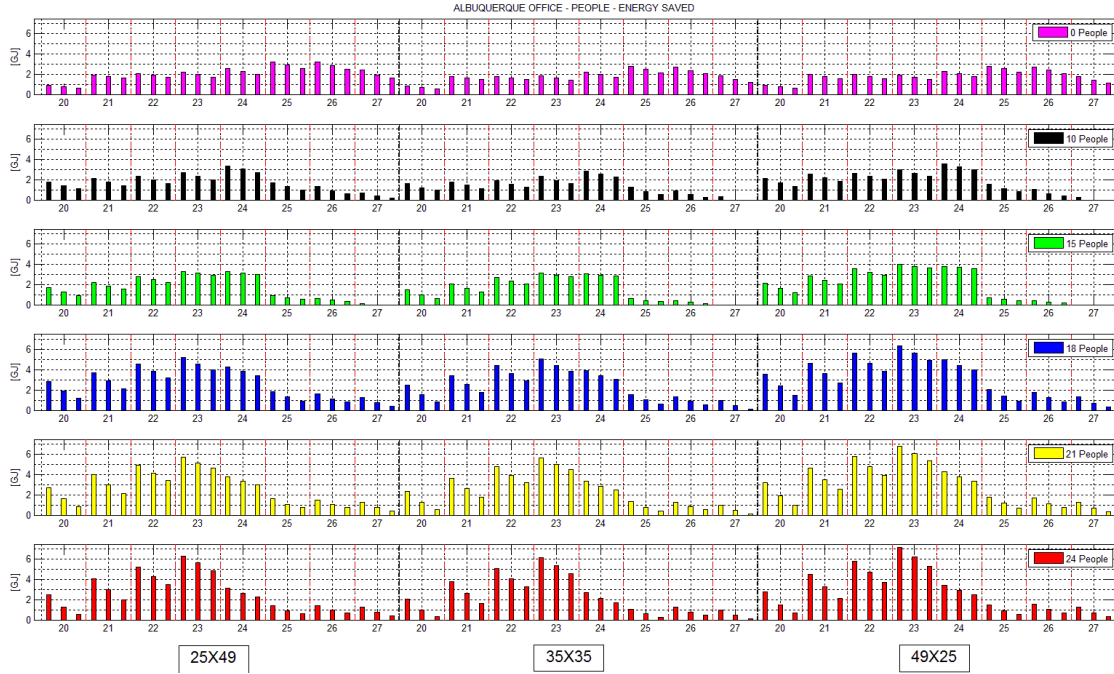


Figure E.1: Albuquerque office, energy saved – different levels of internal load.

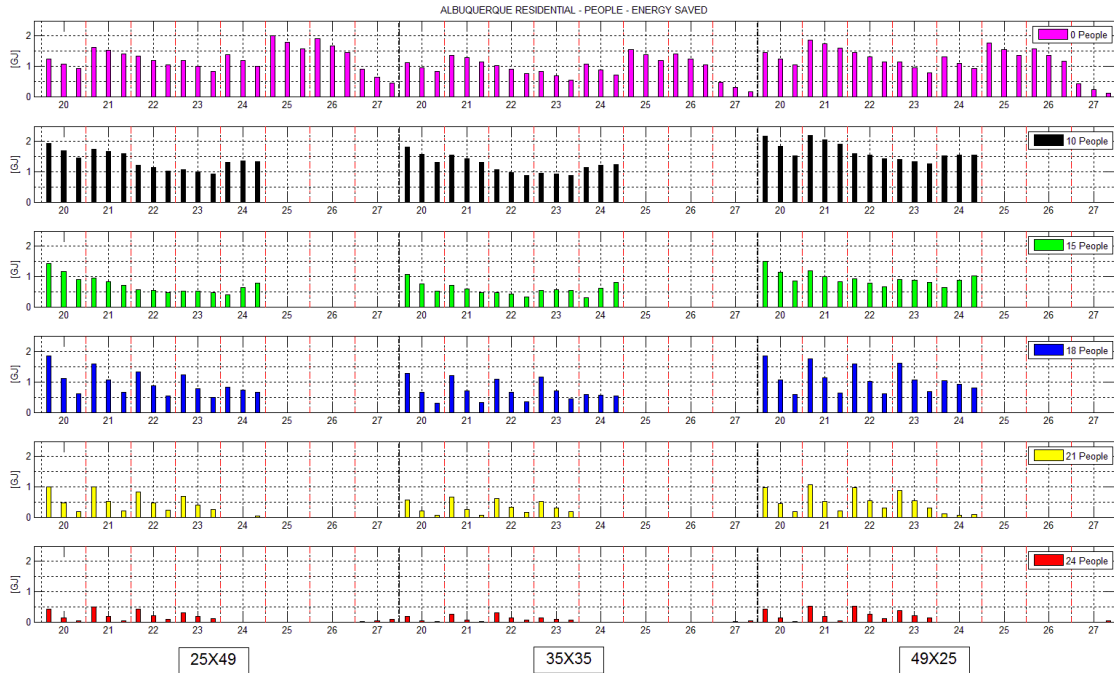


Figure E.2: Albuquerque residential, energy saved – different levels of internal load.

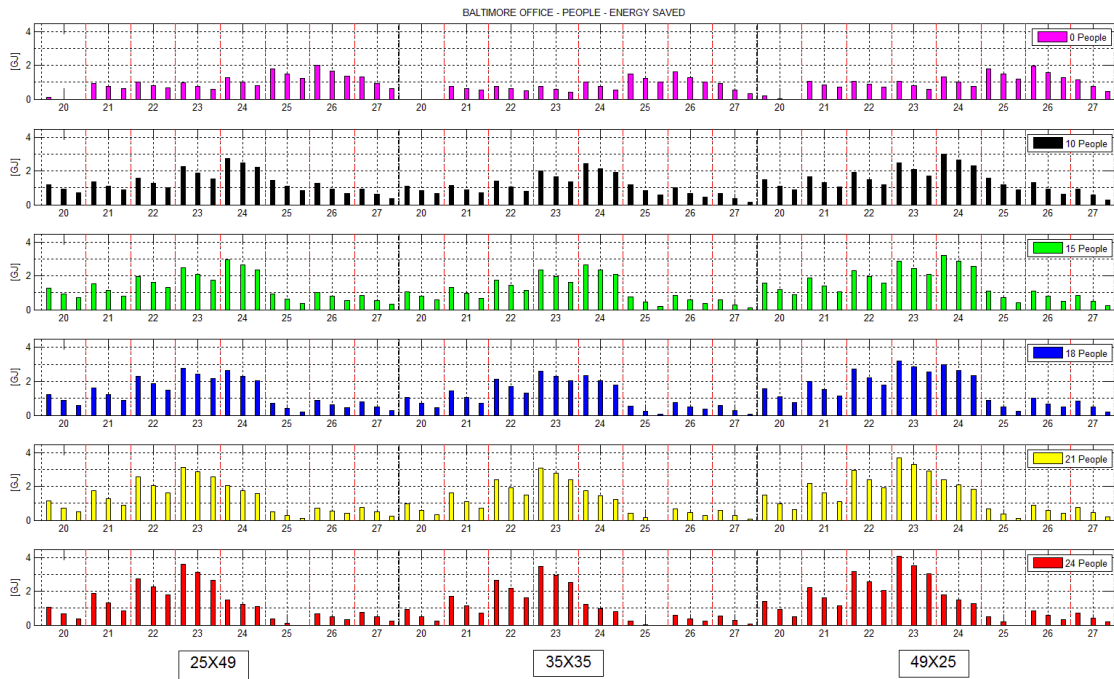


Figure E.3: Baltimore office, energy saved – different levels of internal load.

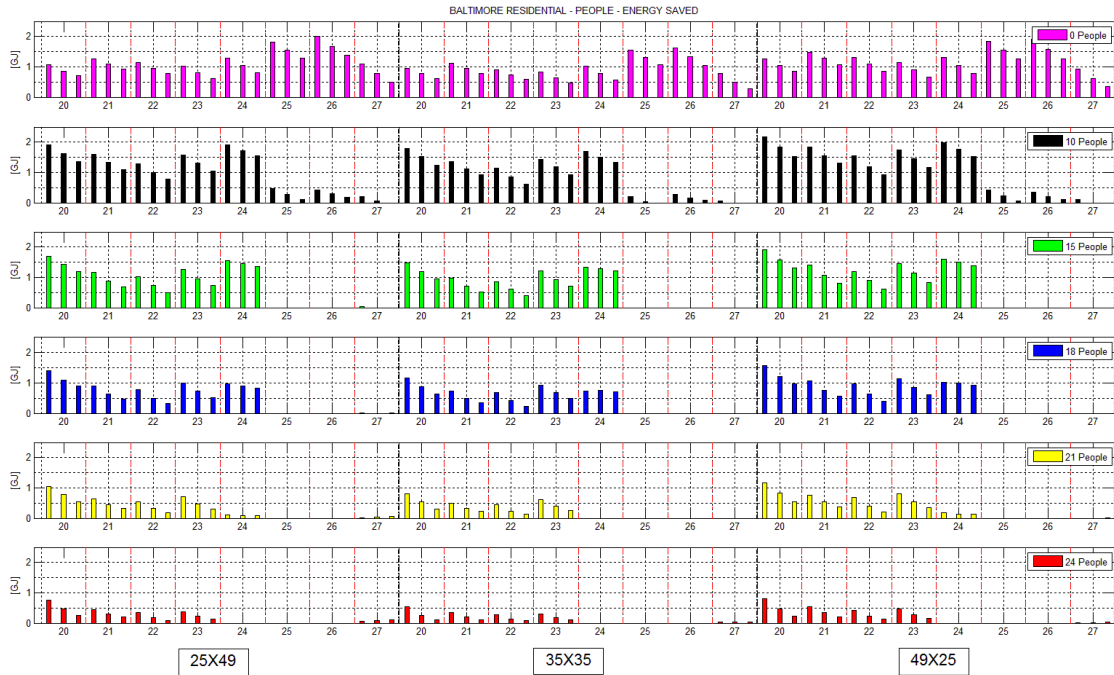


Figure E.4: Baltimore residential, energy saved – different levels of internal load.

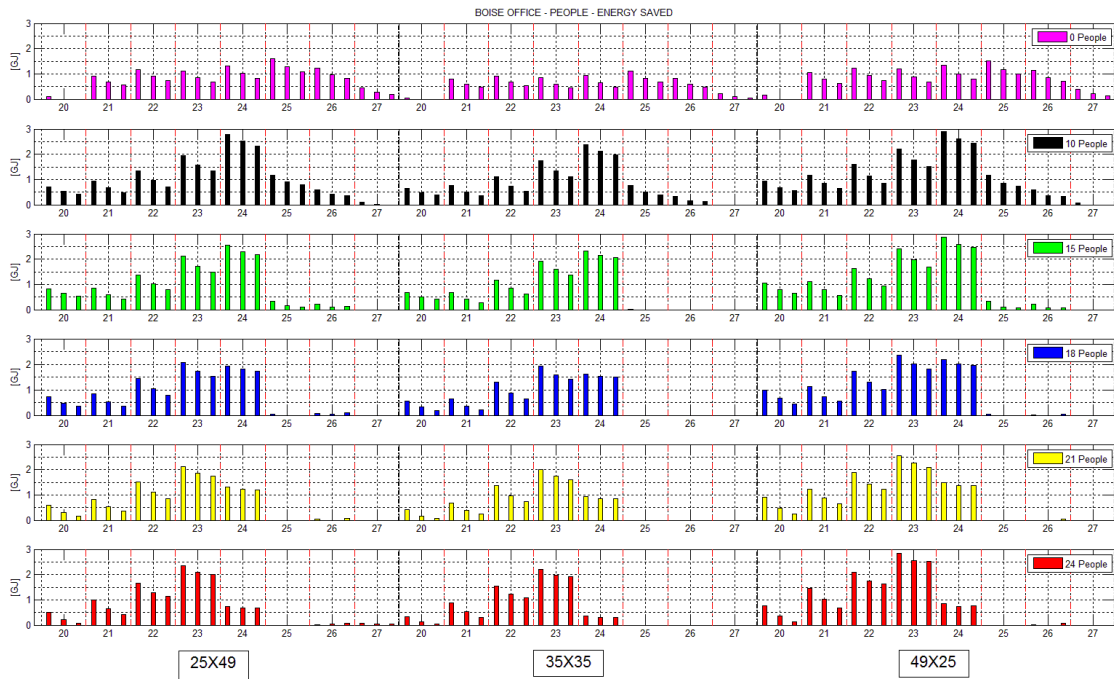


Figure E.5: Boise office, energy saved – different levels of internal load.

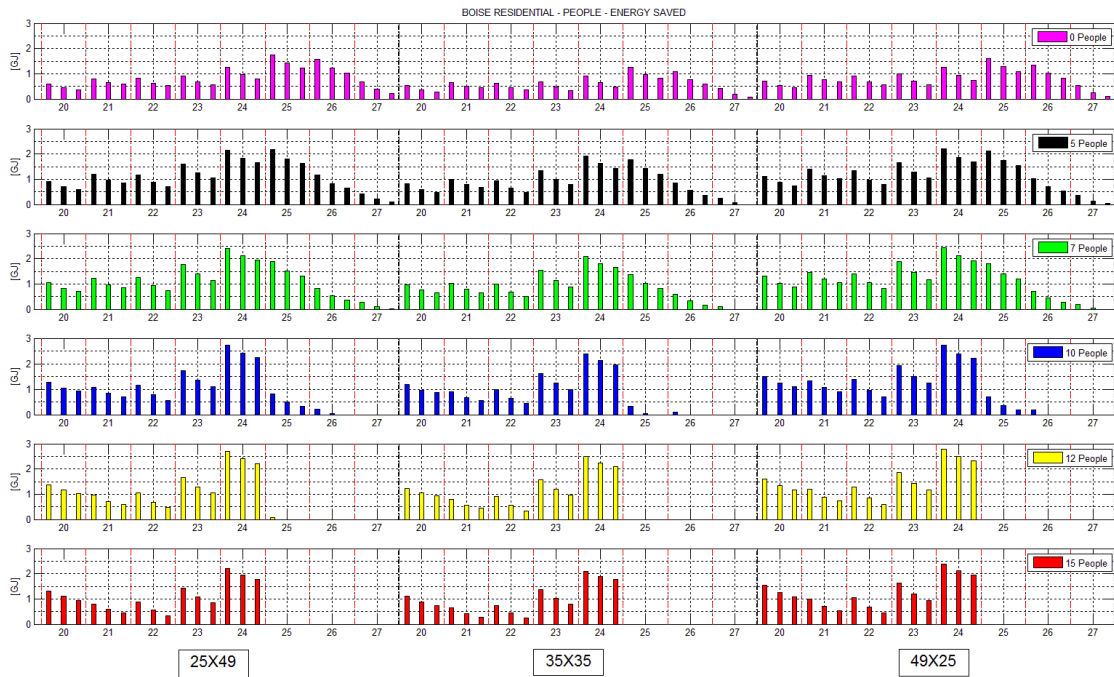


Figure E.6: Boise residential, energy saved – different levels of internal load.

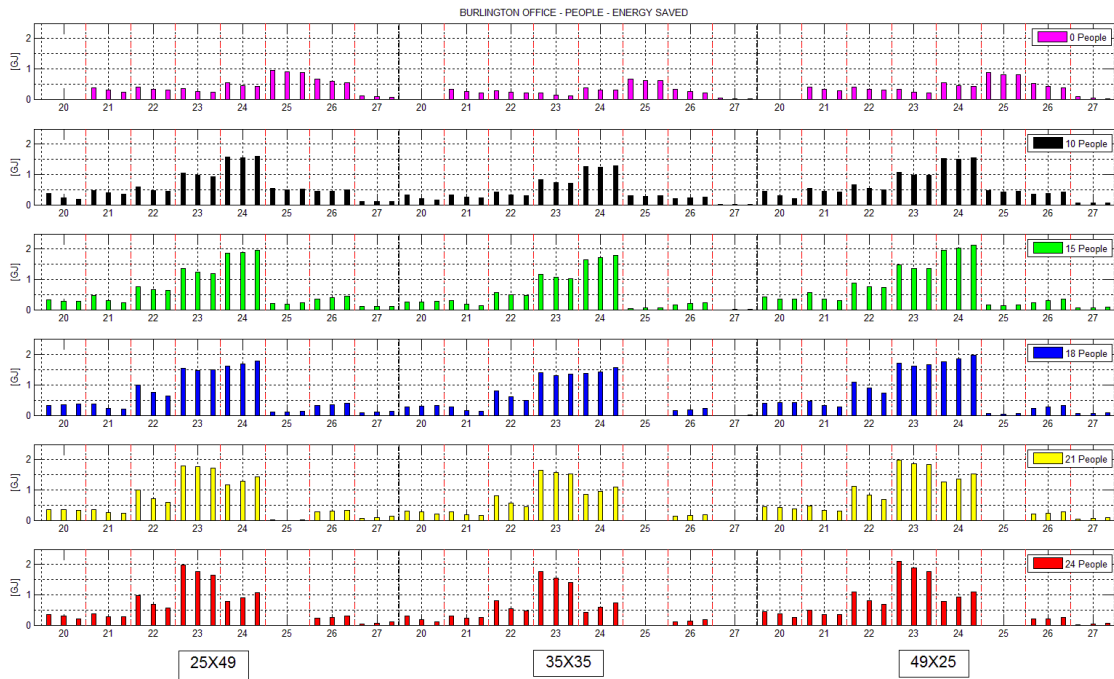


Figure E.7: Burlington office, energy saved – different levels of internal load.

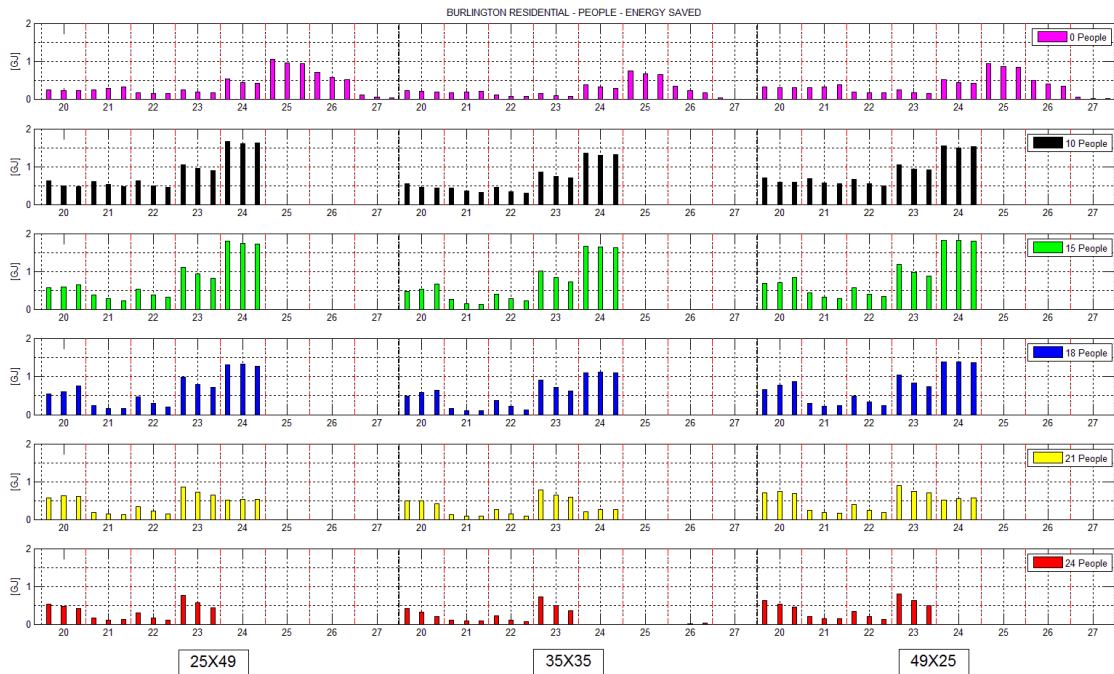


Figure E.8: Burlington residential, energy saved – different levels of internal load.

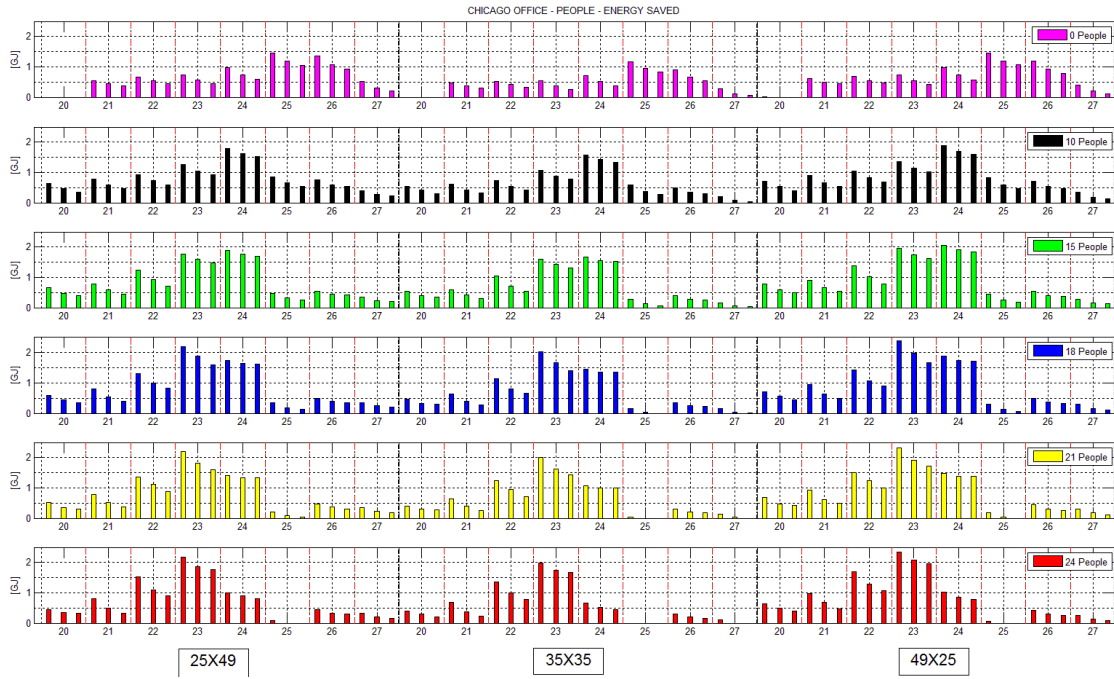


Figure E.9: Chicago office, energy saved – different levels of internal load.

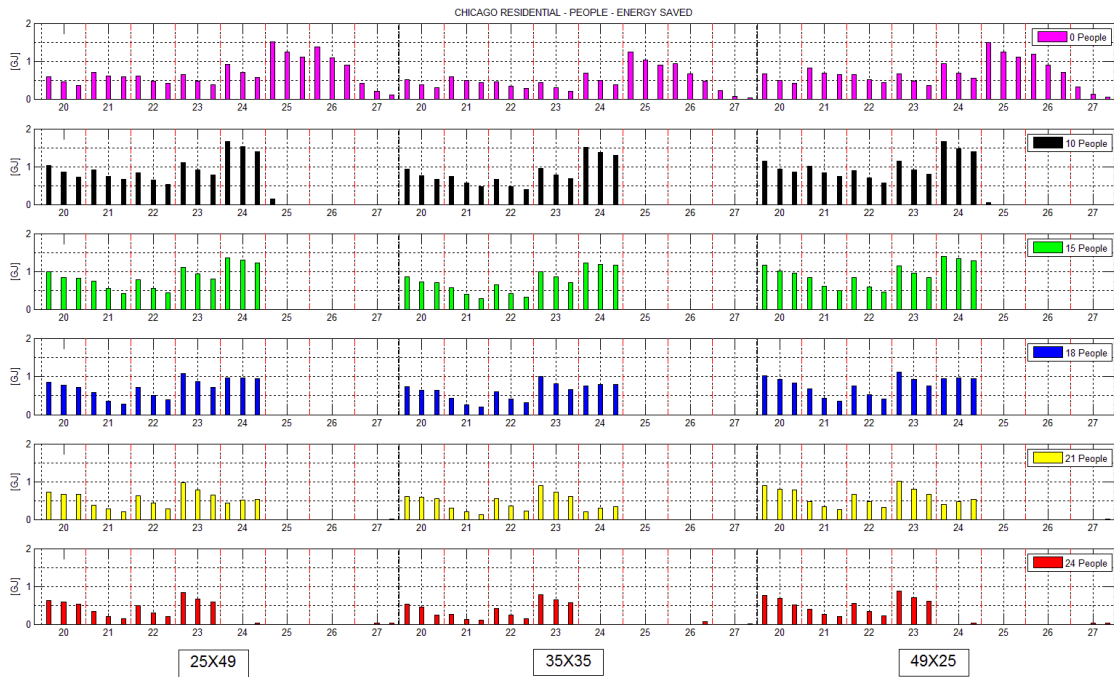


Figure E.10: Chicago residential, energy saved – different levels of internal load.

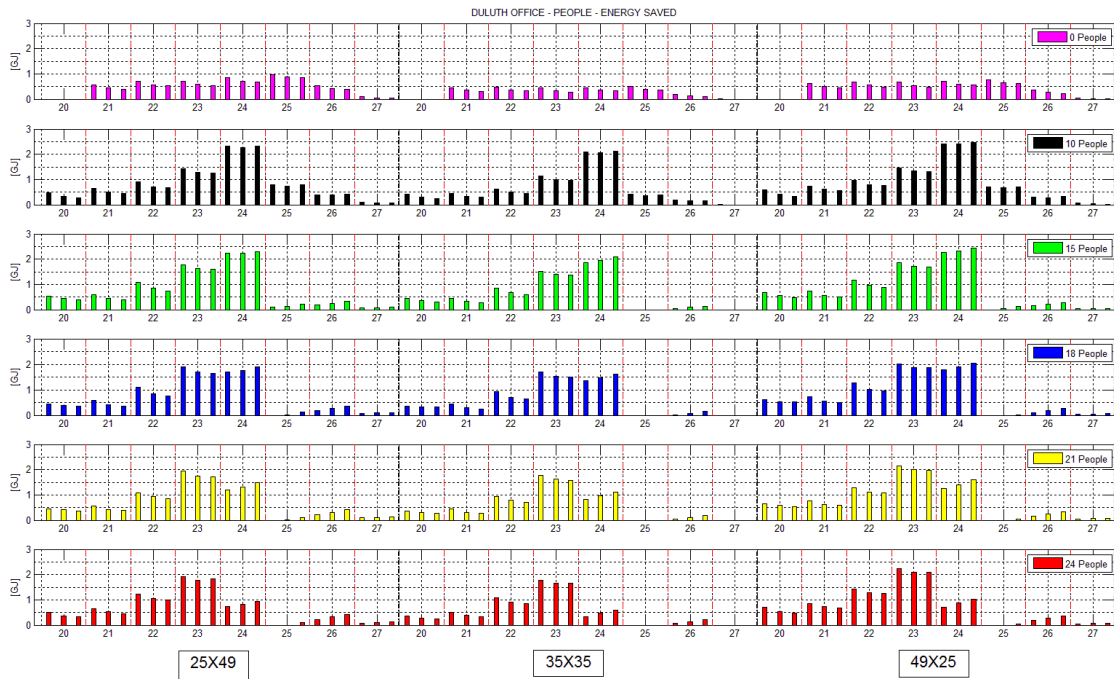


Figure E.11: Duluth office, energy saved – different levels of internal load.

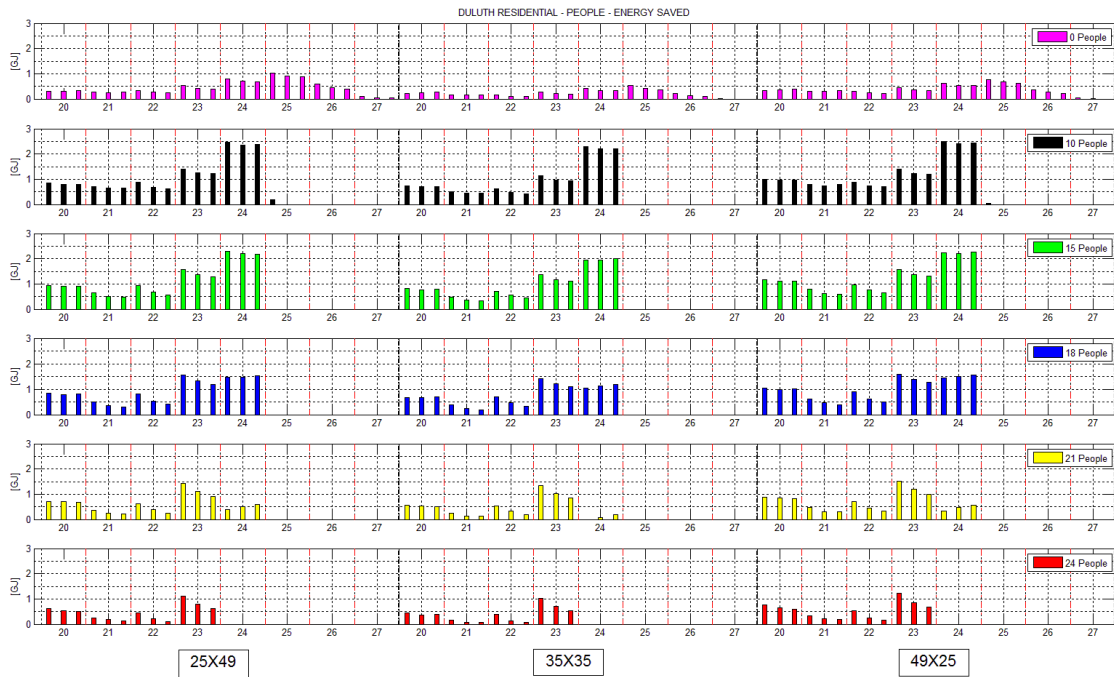


Figure E.12: Duluth residential, energy saved – different levels of internal load.

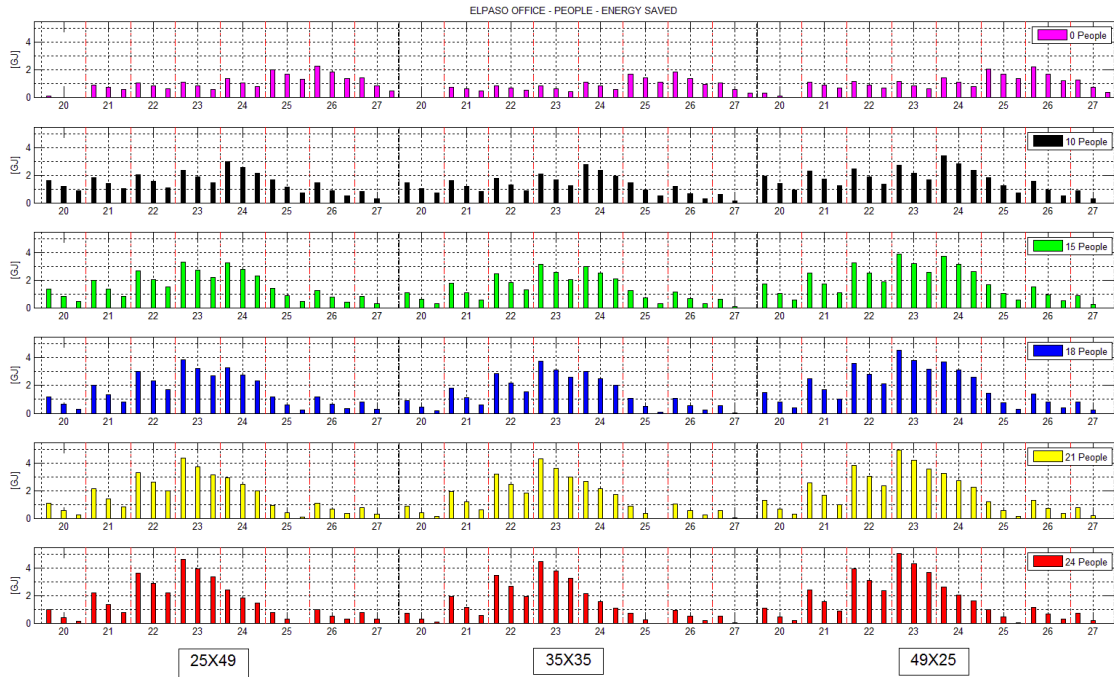


Figure E.13: El Paso office, energy saved – different levels of internal load.

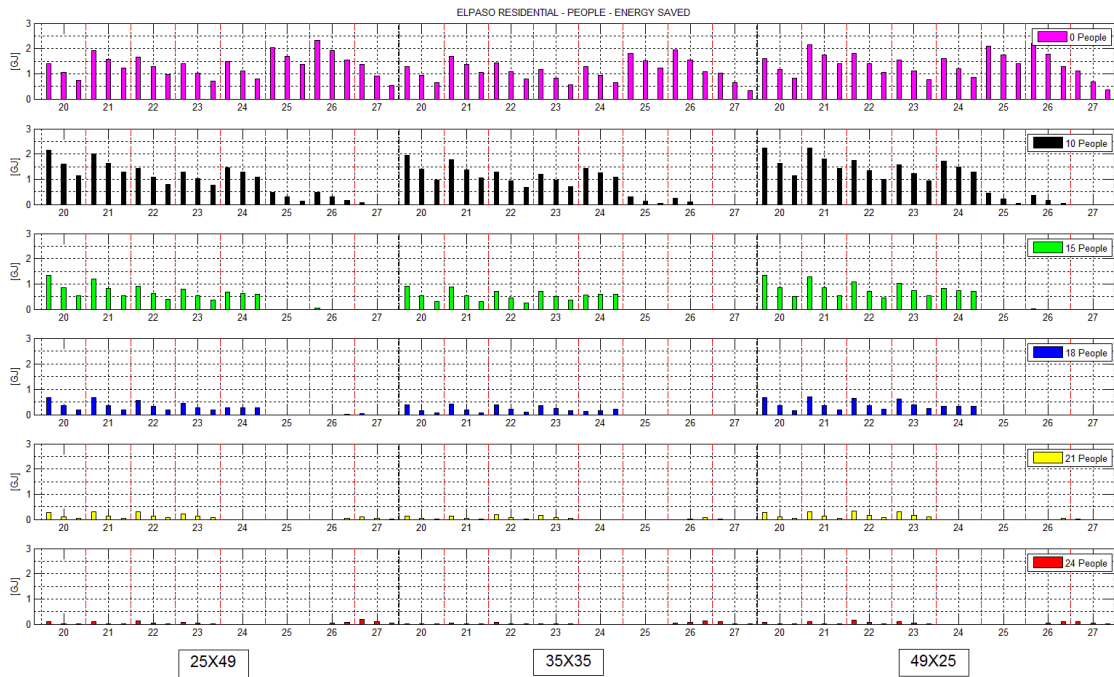


Figure E.14: El Paso residential, energy saved – different levels of internal load.

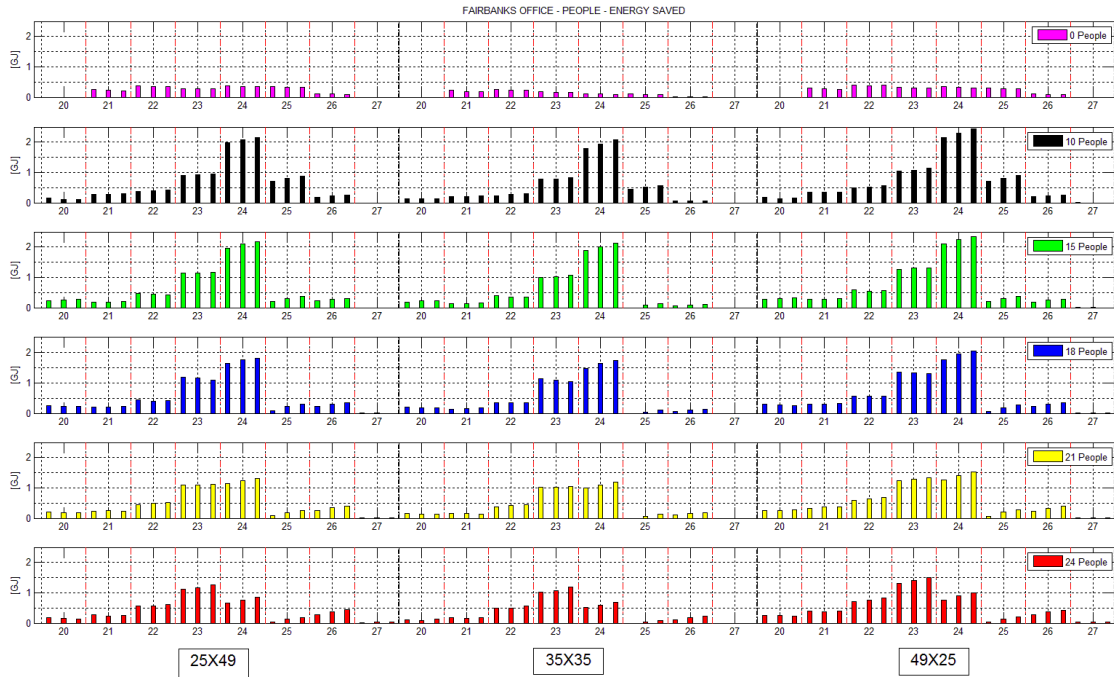


Figure E.15: Fairbanks office, energy saved – different levels of internal load.

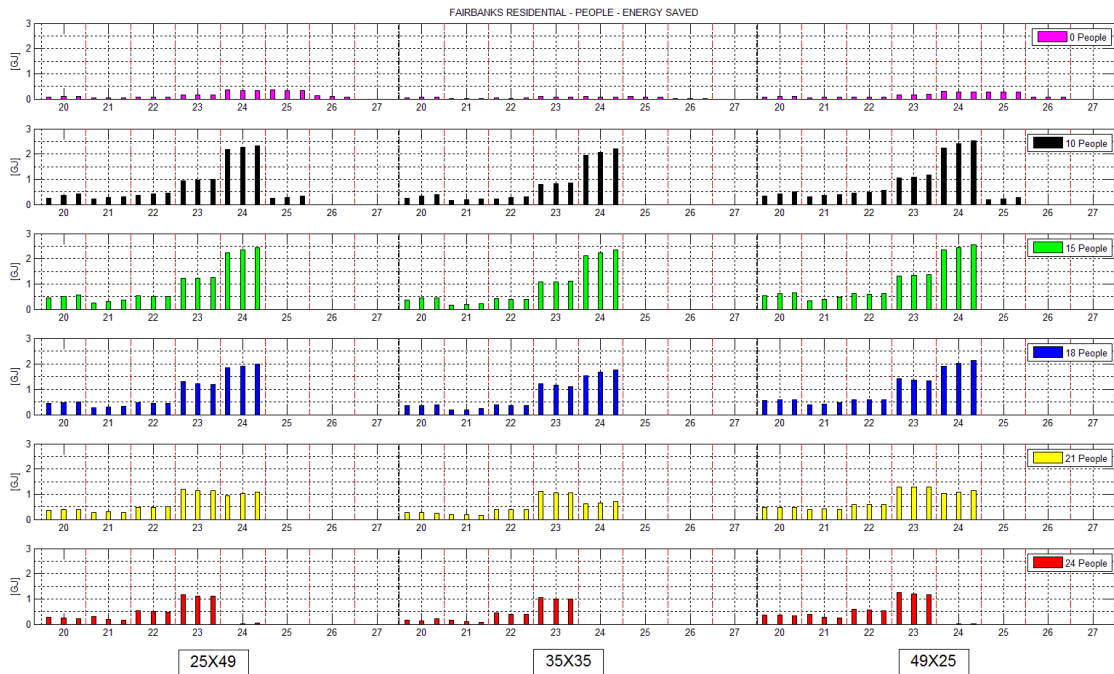


Figure E.16: Fairbanks residential, energy saved – different levels of internal load.

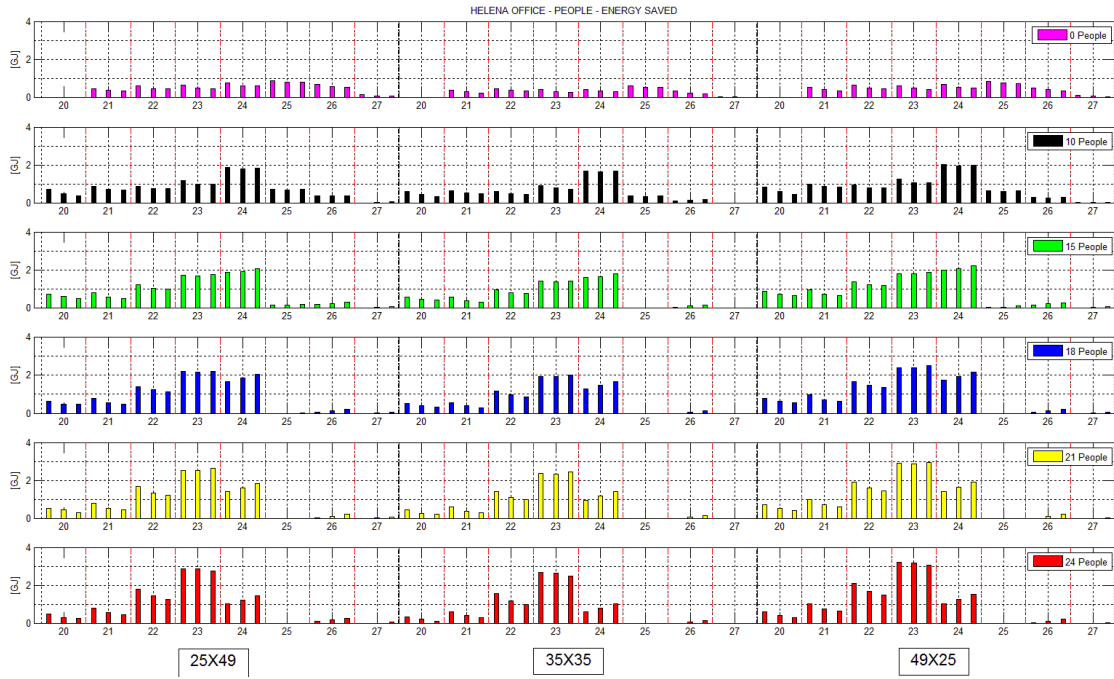


Figure E.17: Helena office, energy saved – different levels of internal load.

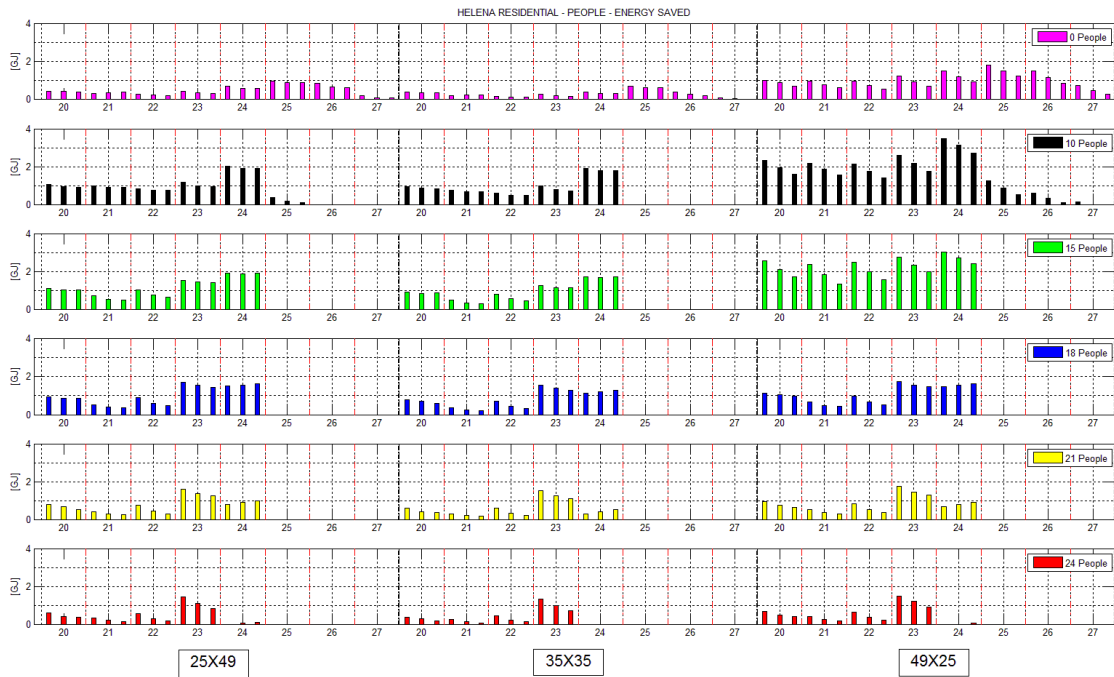


Figure E.18: Helena residential, energy saved – different levels of internal load.

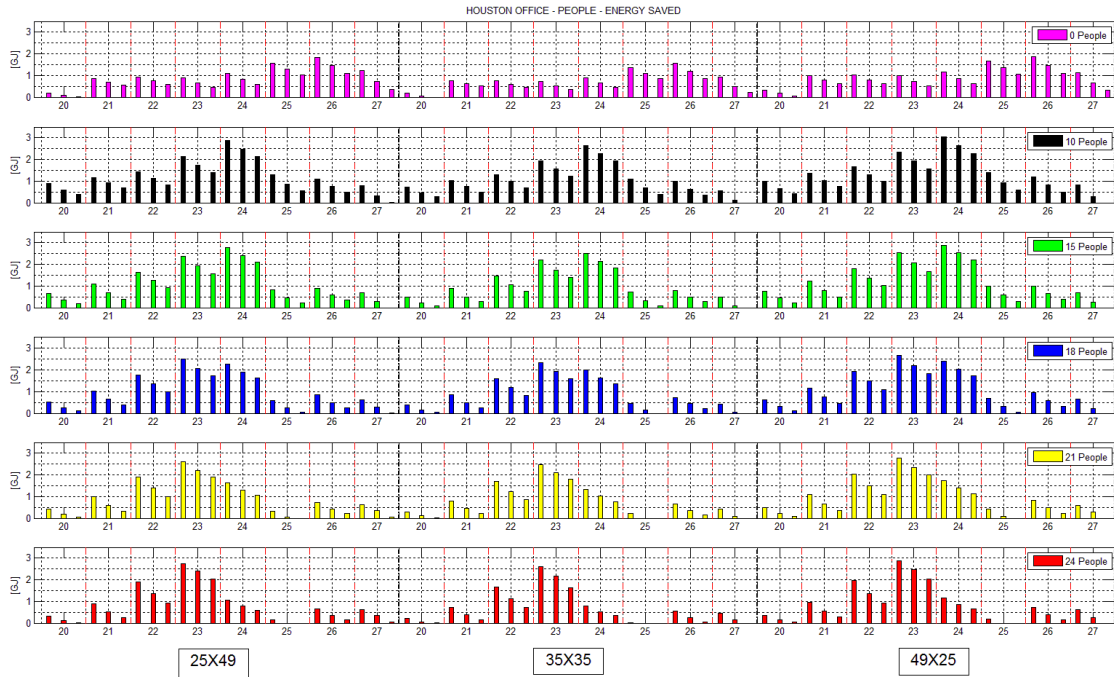


Figure E.19: Houston office, energy saved – different levels of internal load.

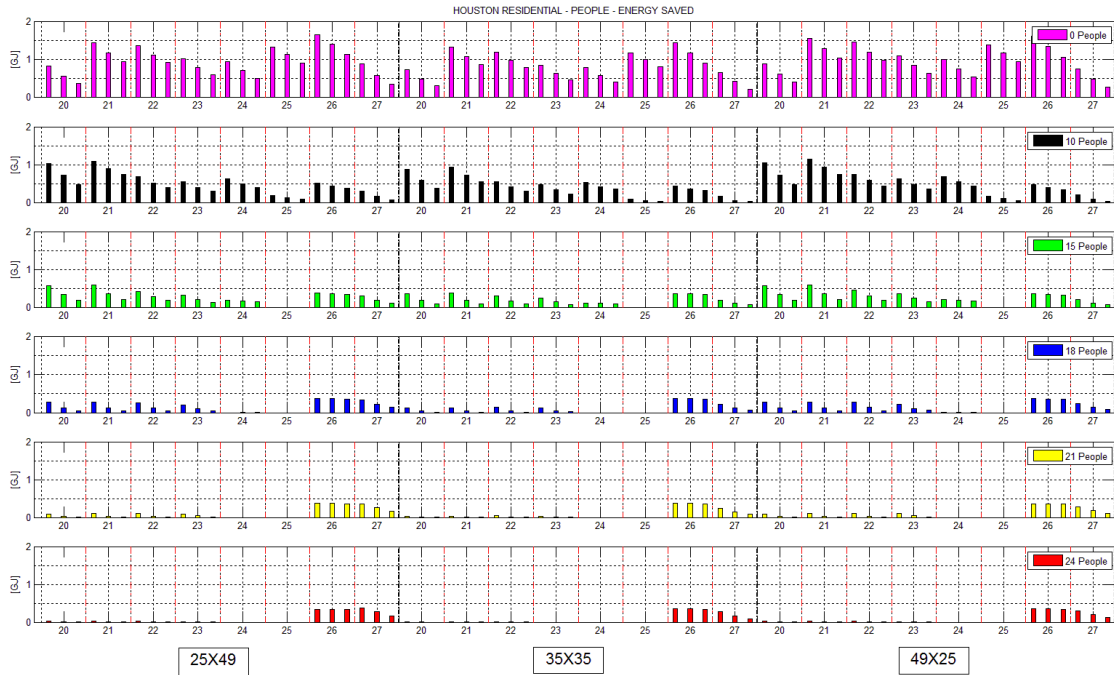


Figure E.20: Houston residential, energy saved – different levels of internal load.

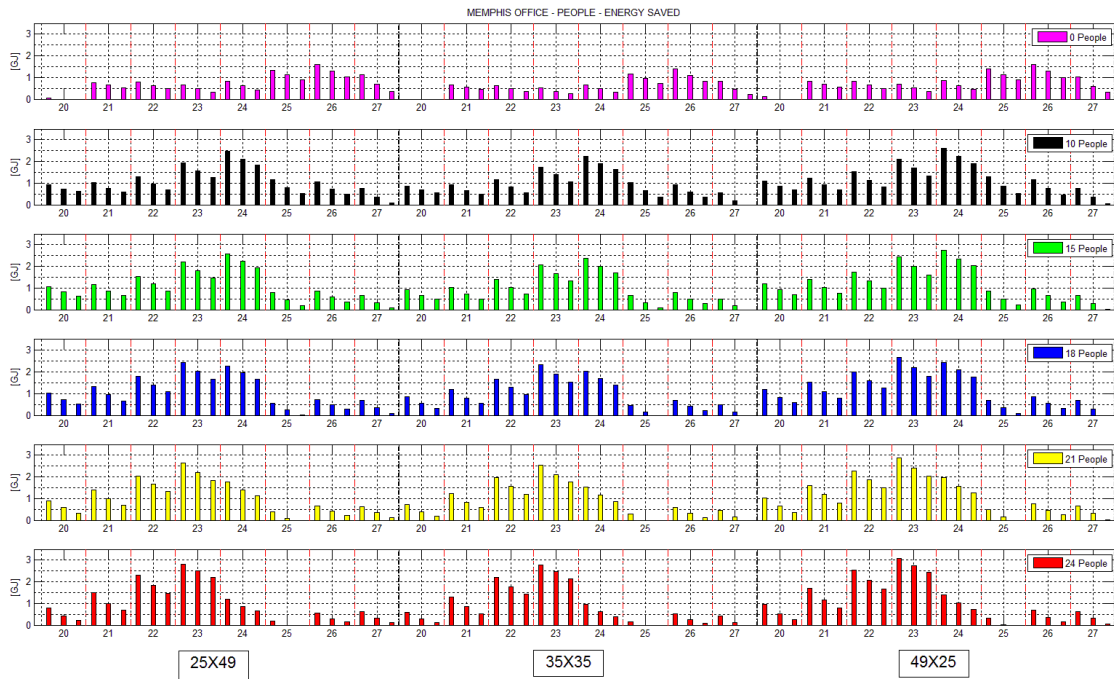


Figure E.21: Memphis office, energy saved – different levels of internal load.

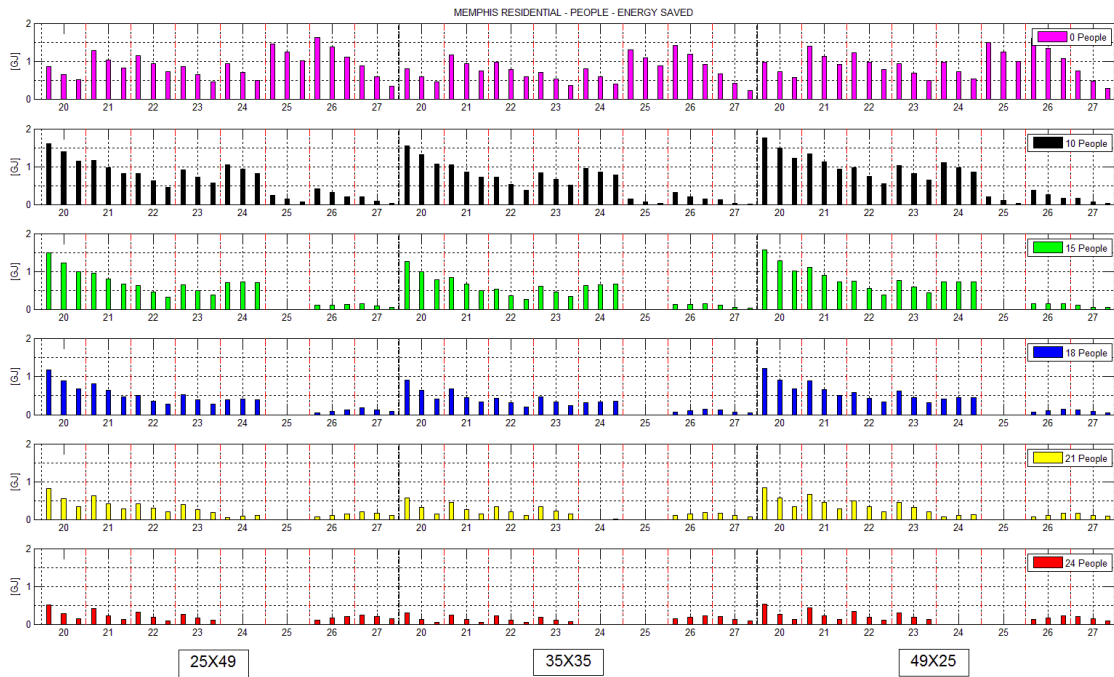


Figure E.22: Memphis residential, energy saved – different levels of internal load.

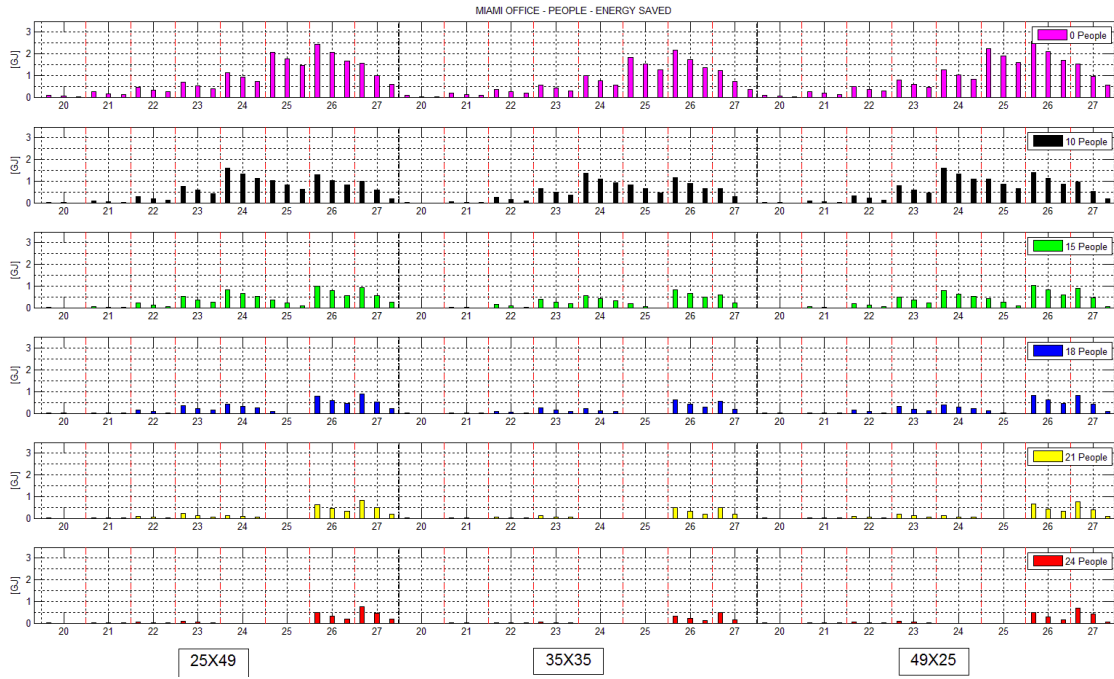


Figure E.23: Miami office, energy saved – different levels of internal load.

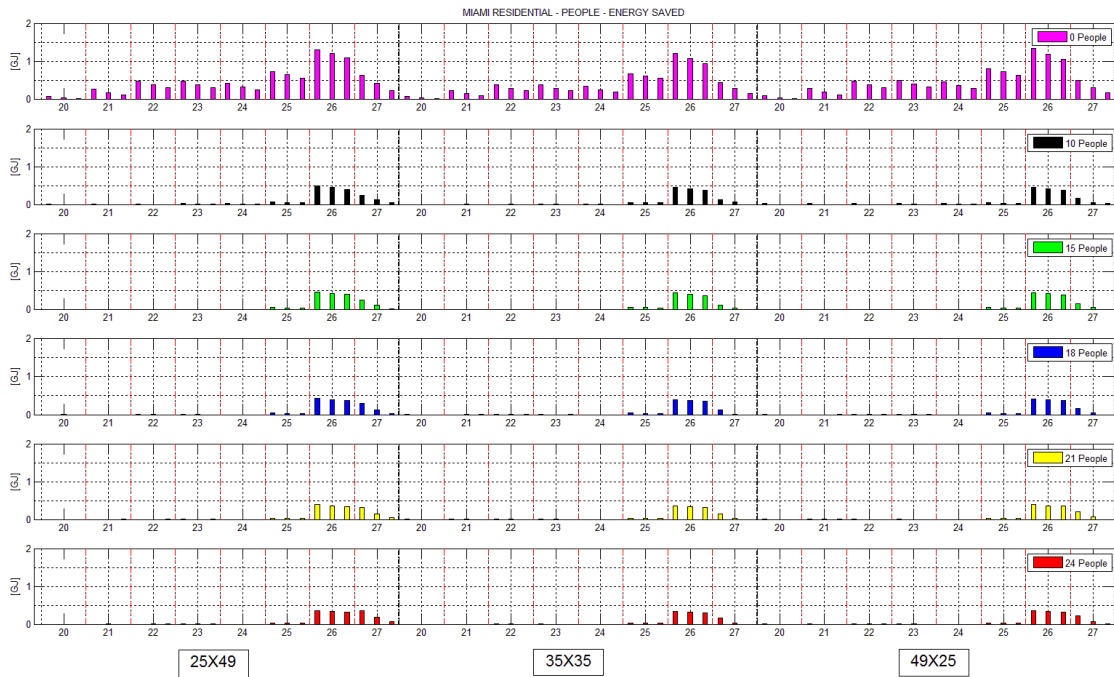


Figure E.24: Miami residential, energy saved – different levels of internal load.

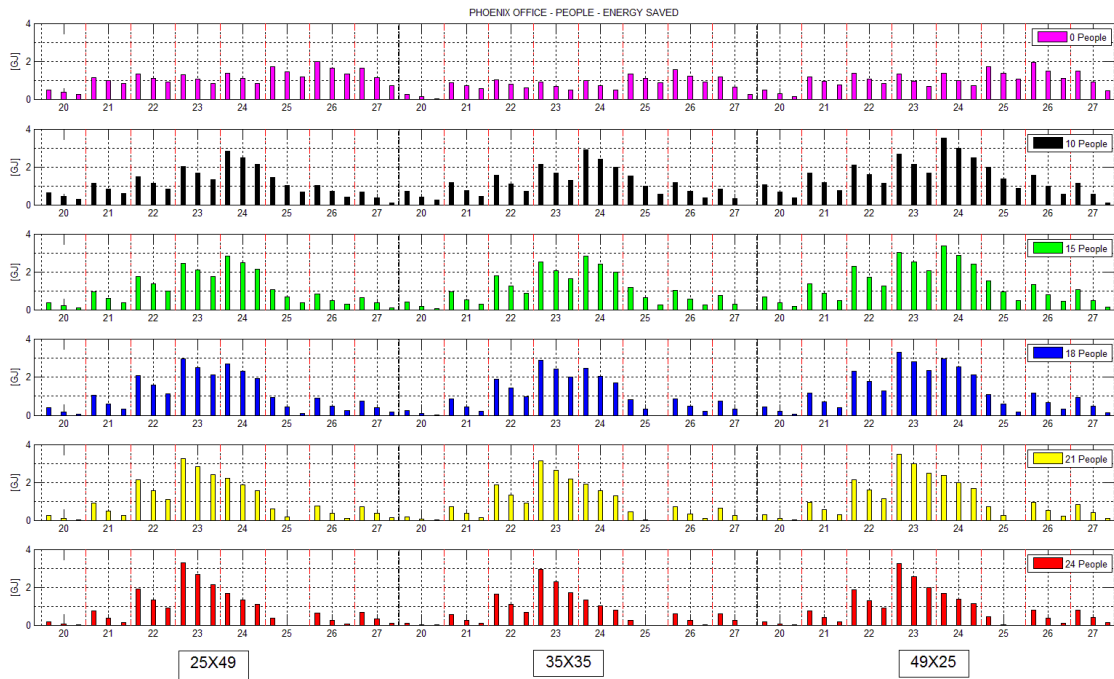


Figure E.25: Phoenix office, energy saved – different levels of internal load.

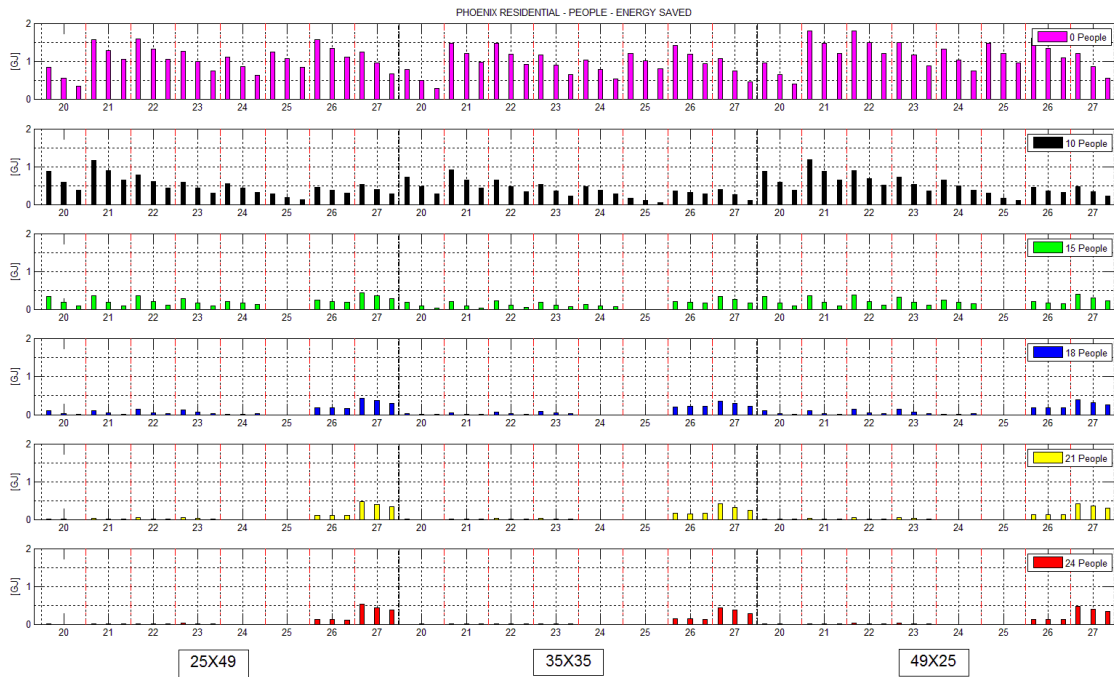


Figure E.26: Phoenix residential, energy saved – different levels of internal load.

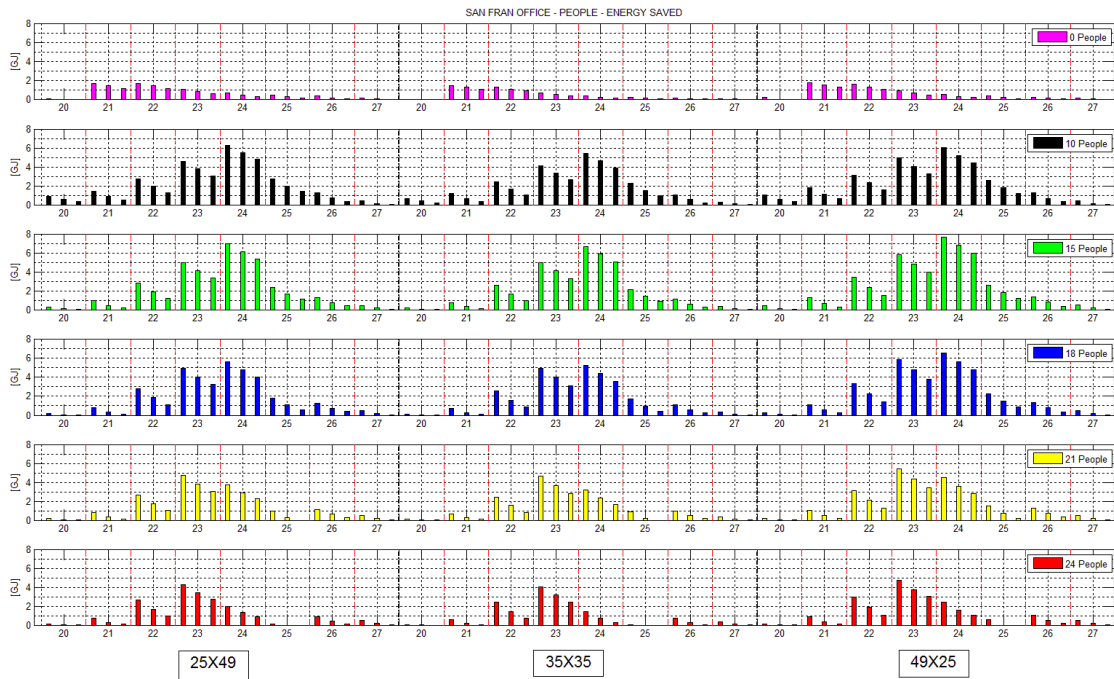


Figure E.28: San Francisco office, energy saved – different levels of internal load.

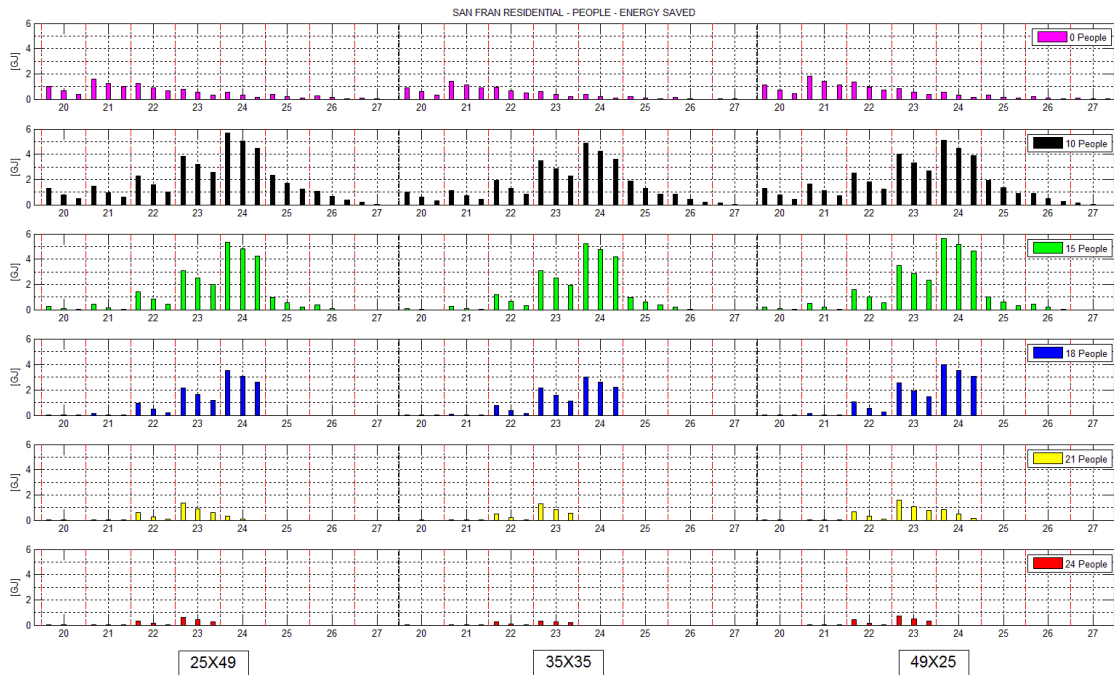


Figure E.28: San Francisco residential, energy saved – different levels of internal load.

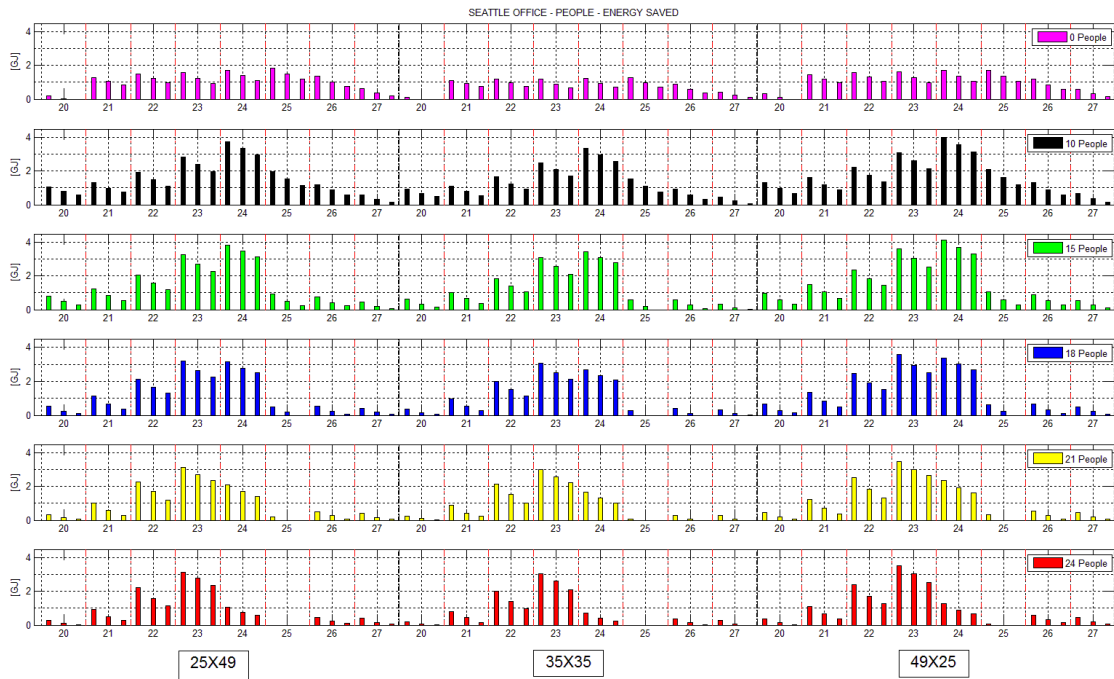


Figure E.29: Seattle office, energy saved – different levels of internal load.

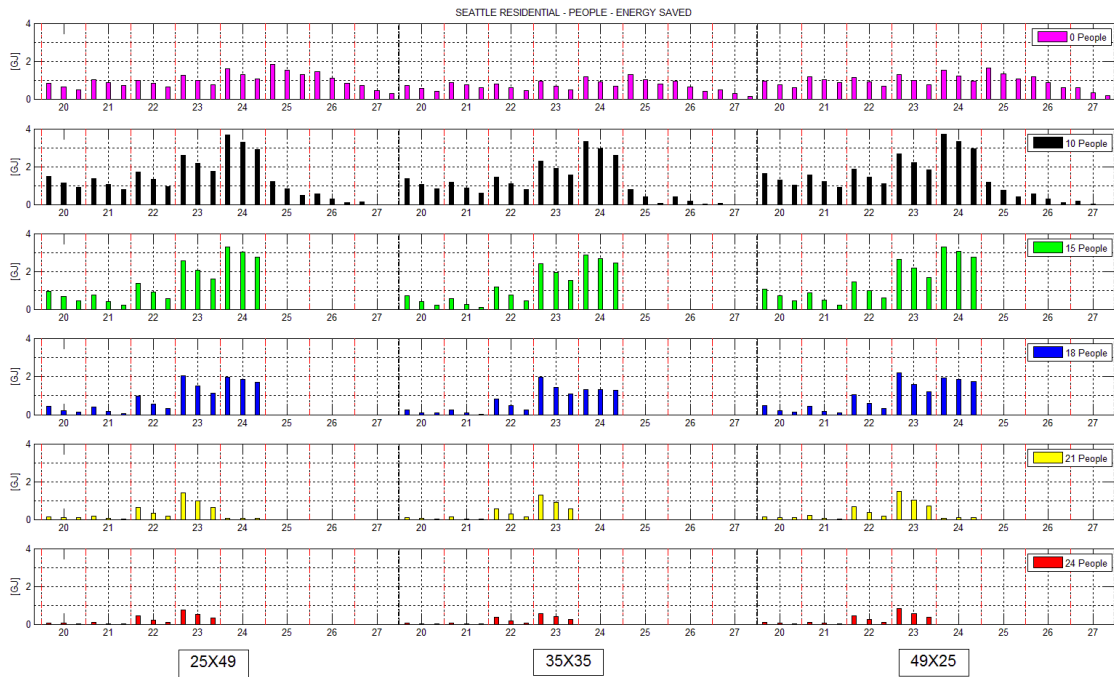


Figure E.30: Seattle residential, energy saved – different levels of internal load.

Appendix F

Monetary savings for each additional level of Enthalpy

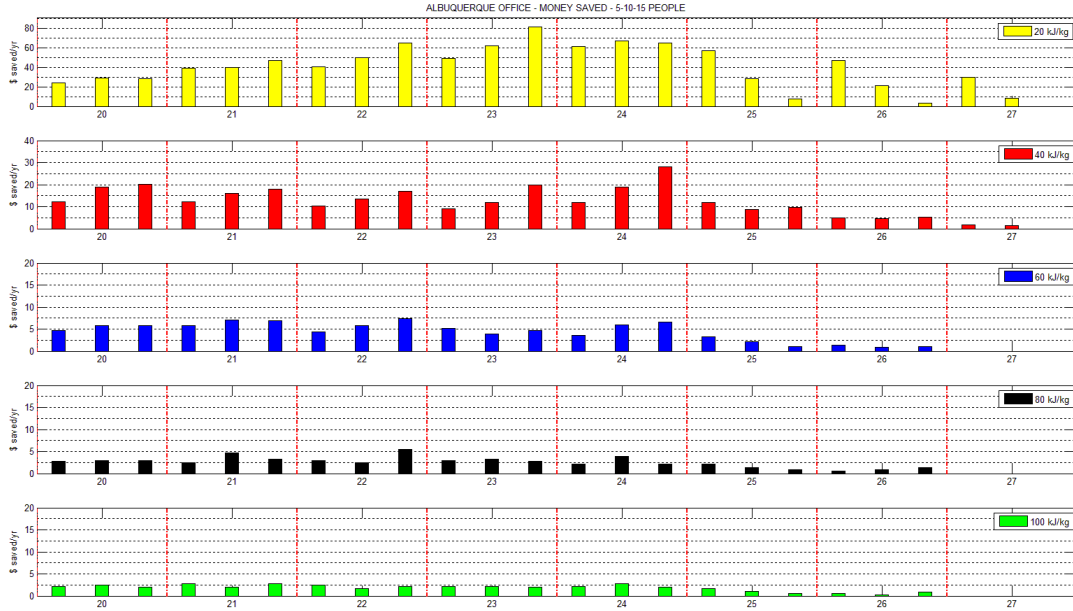


Figure F.1: Albuquerque office, additional money saved – different levels of enthalpy.

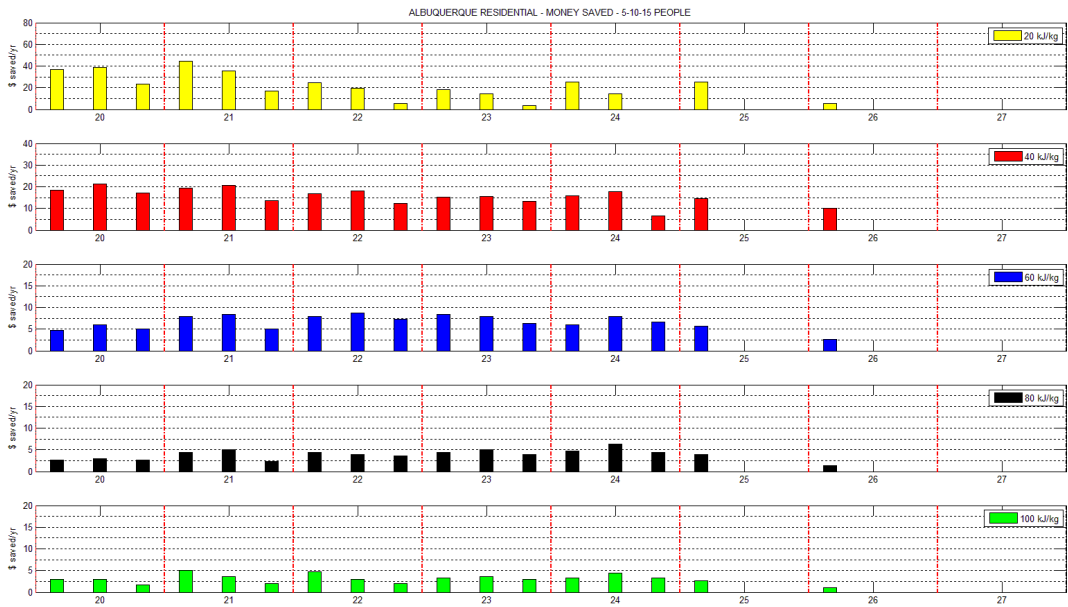


Figure F.2: Albuquerque residential, additional money saved – different levels of enthalpy.

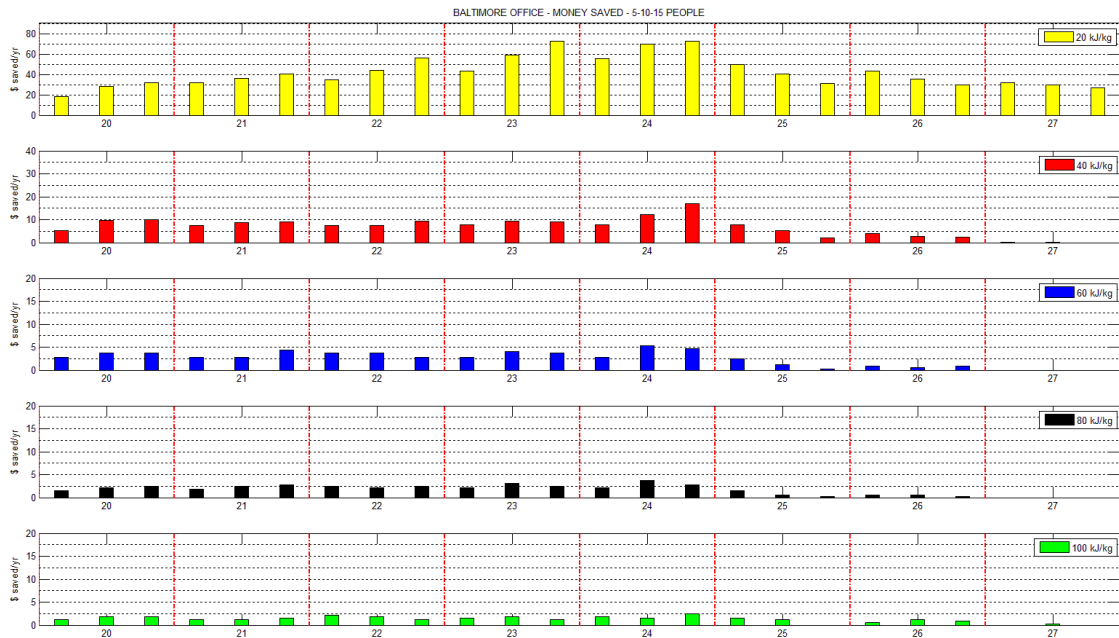


Figure F.3: Baltimore office, additional money saved – different levels of enthalpy.

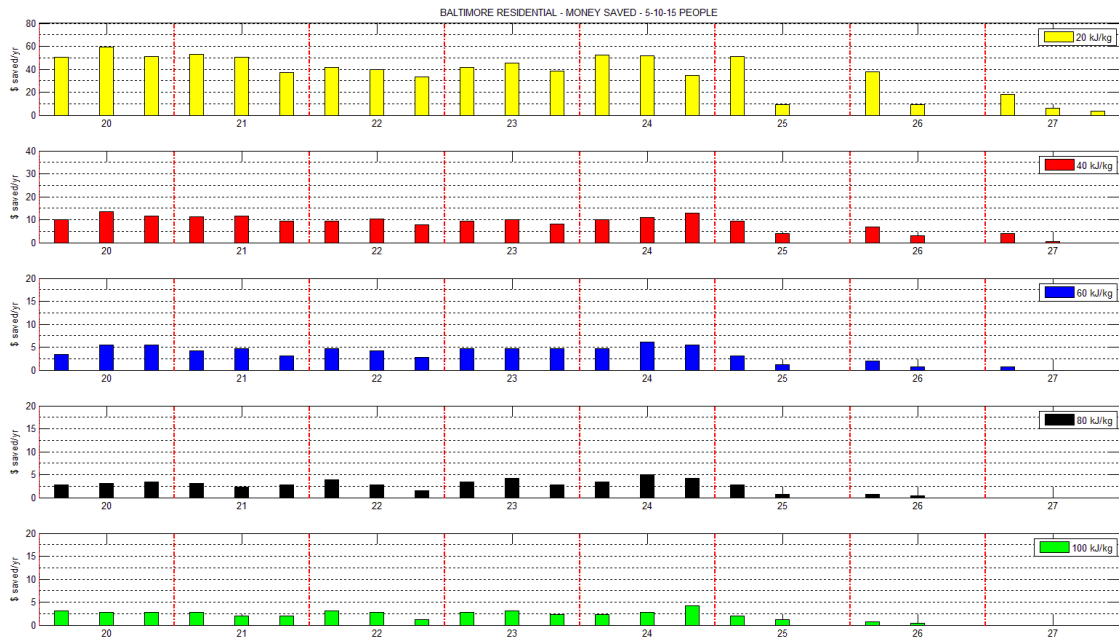


Figure F.4: Baltimore residential, additional money saved – different levels of enthalpy.

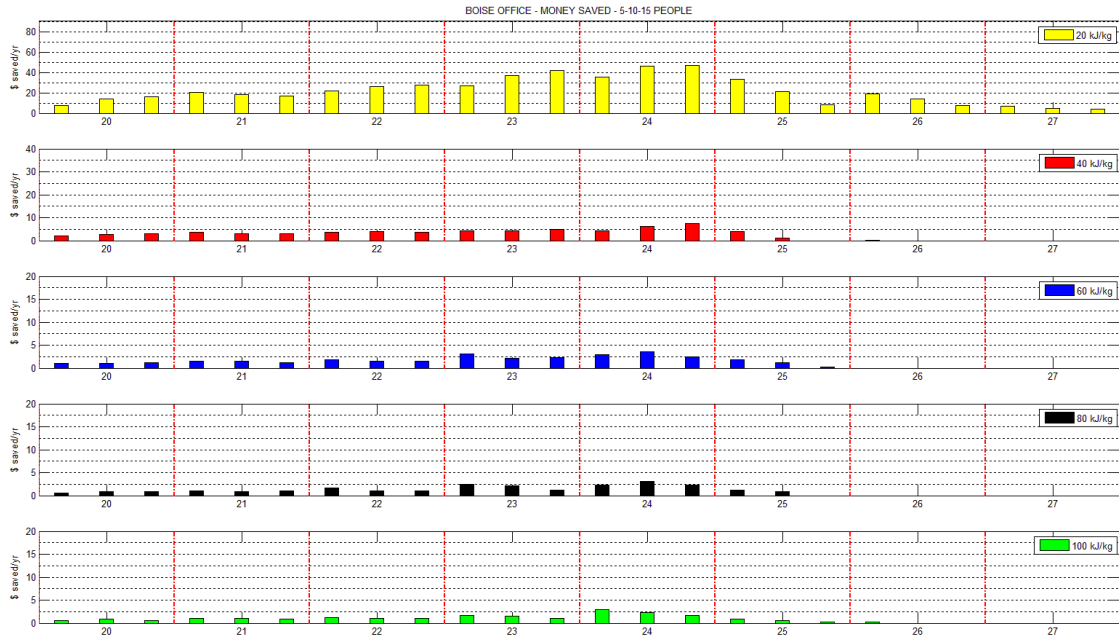


Figure F.5: Boise office, additional money saved – different levels of enthalpy.

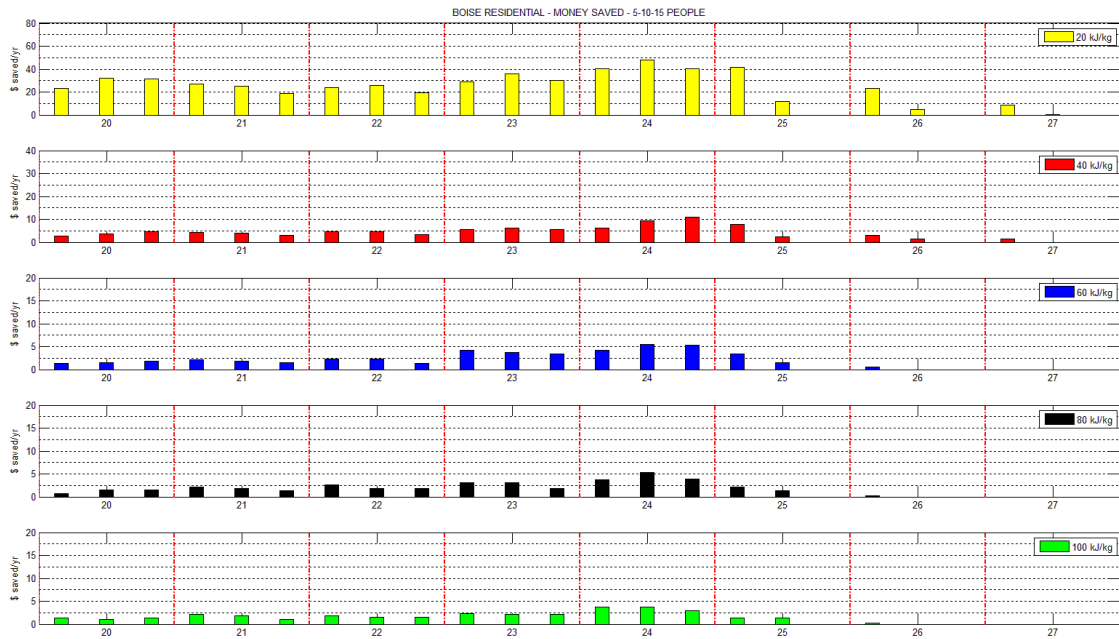


Figure F.6: Boise residential, additional money saved – different levels of enthalpy.

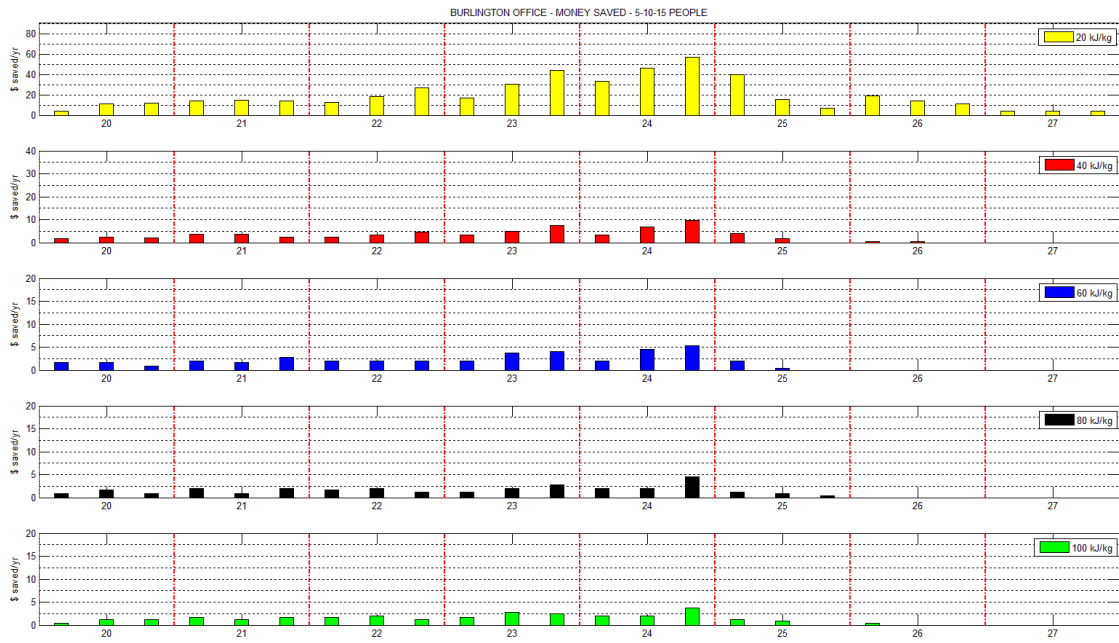


Figure F.7: Burlington office, additional money saved – different levels of enthalpy.

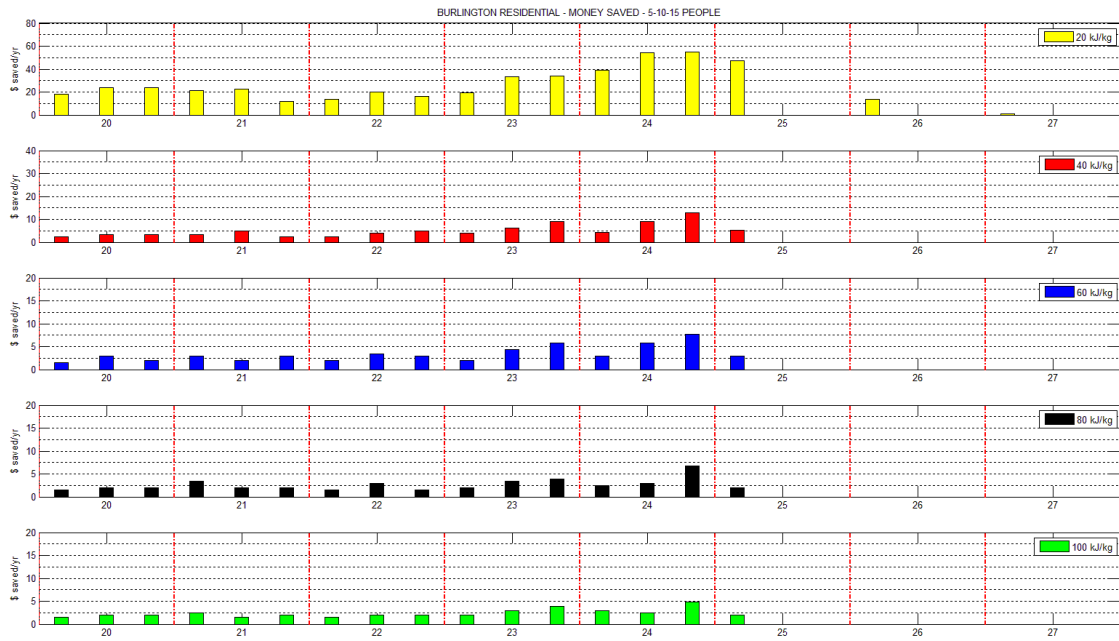


Figure F.8: Burlington residential, additional money saved – different levels of enthalpy.

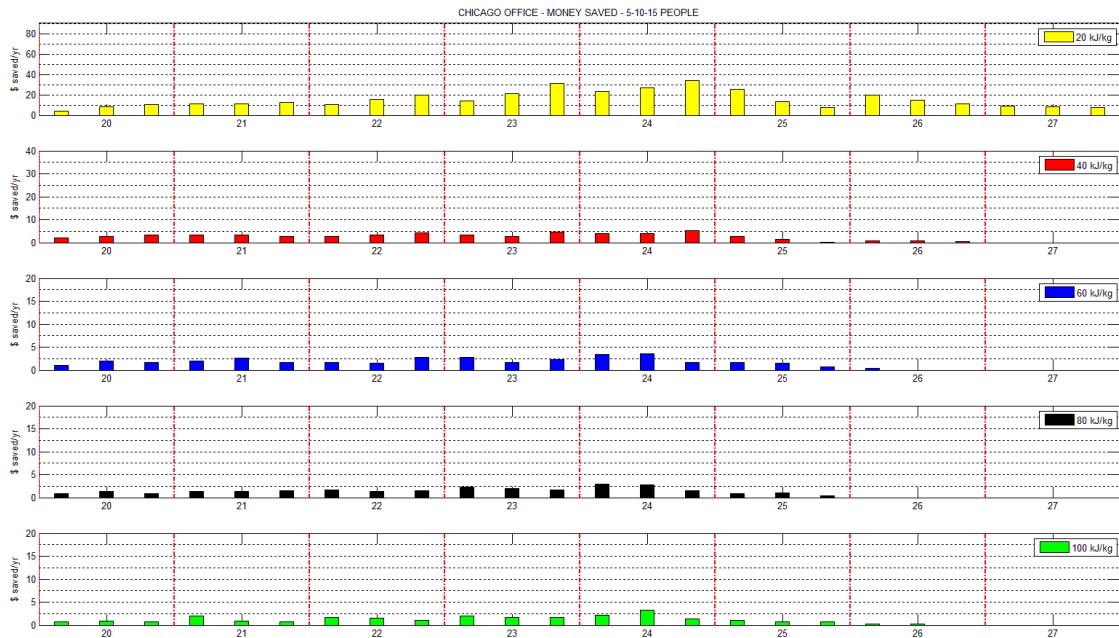


Figure F.9: Chicago office, additional money saved – different levels of enthalpy

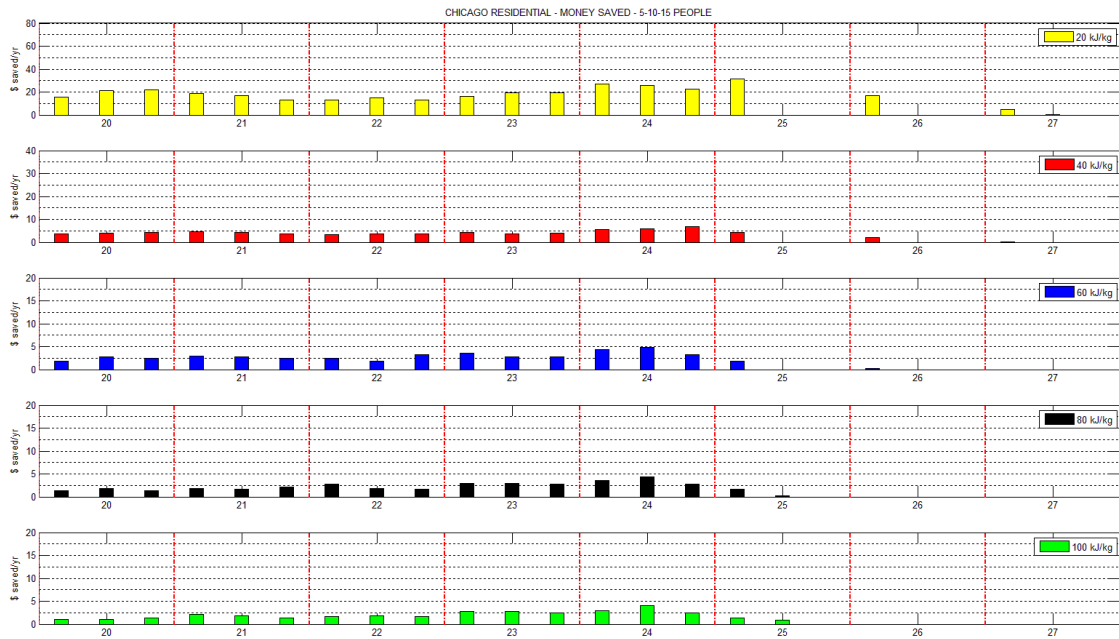


Figure F.10: Chicago residential, additional money saved – different levels of enthalpy.

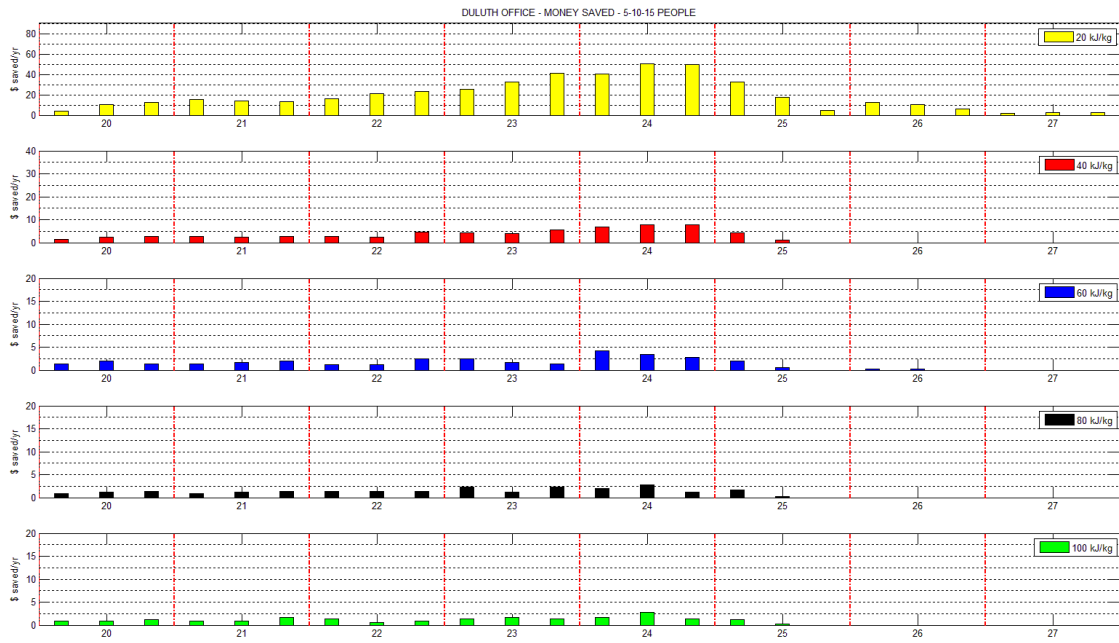


Figure F.11: Duluth office, additional money saved – different levels of enthalpy.

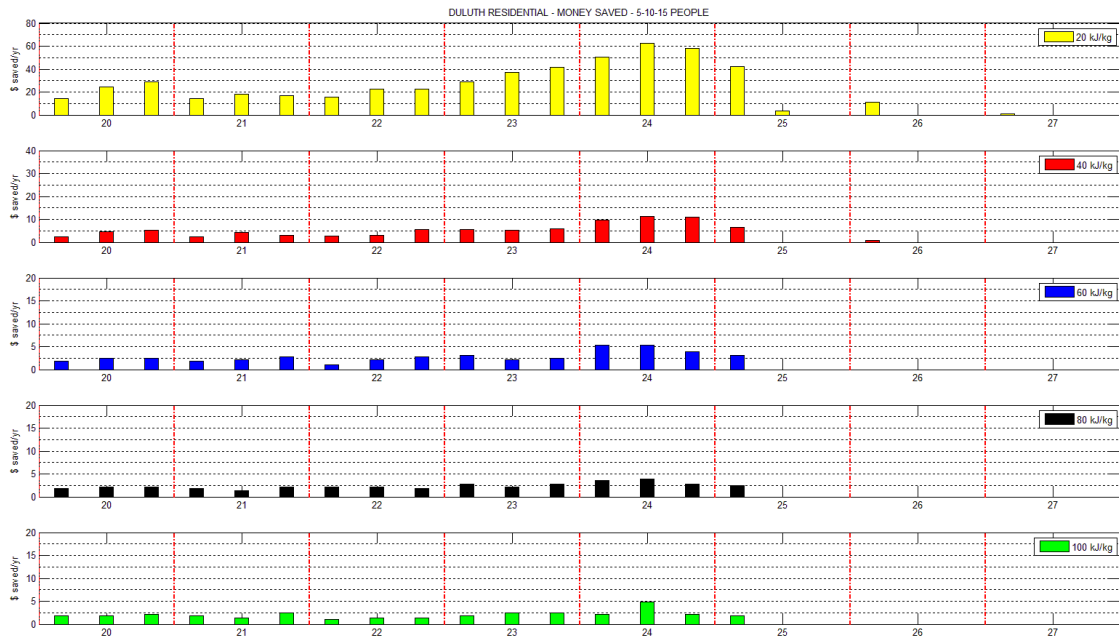


Figure F.12: Duluth residential, additional money saved – different levels of enthalpy.

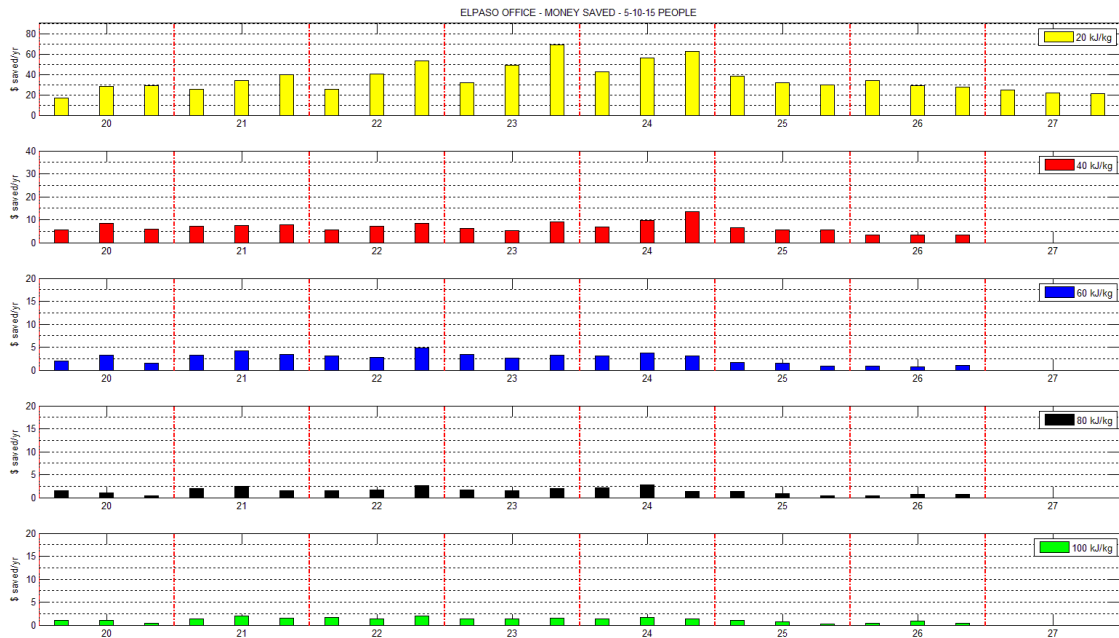


Figure F.13: El Paso office, additional money saved – different levels of enthalpy.

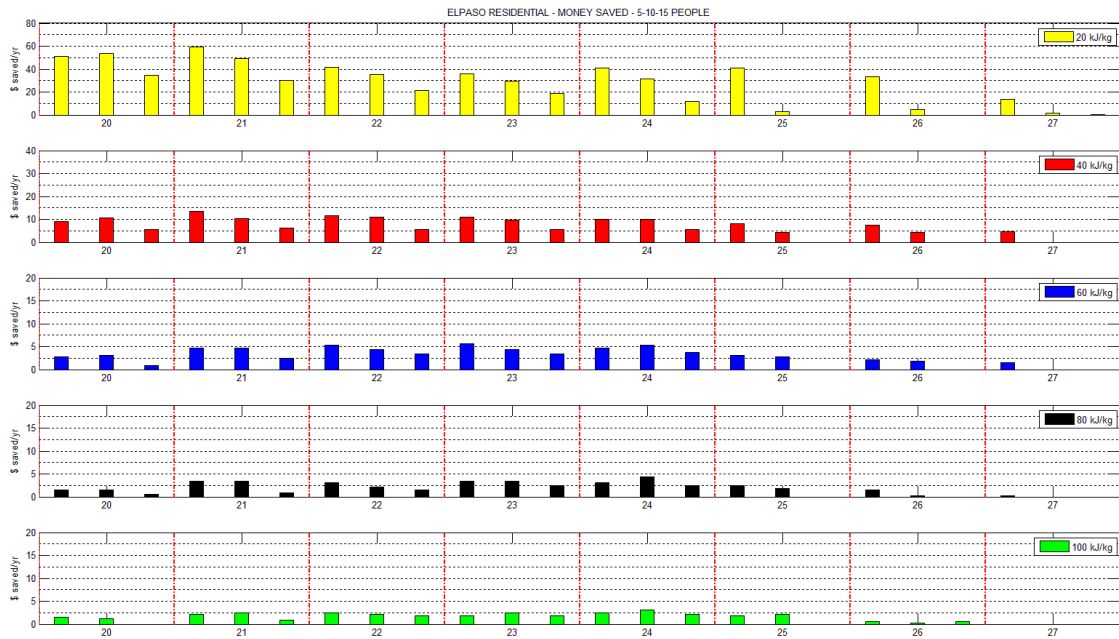


Figure F.14: El Paso residential, additional money saved – different levels of enthalpy.

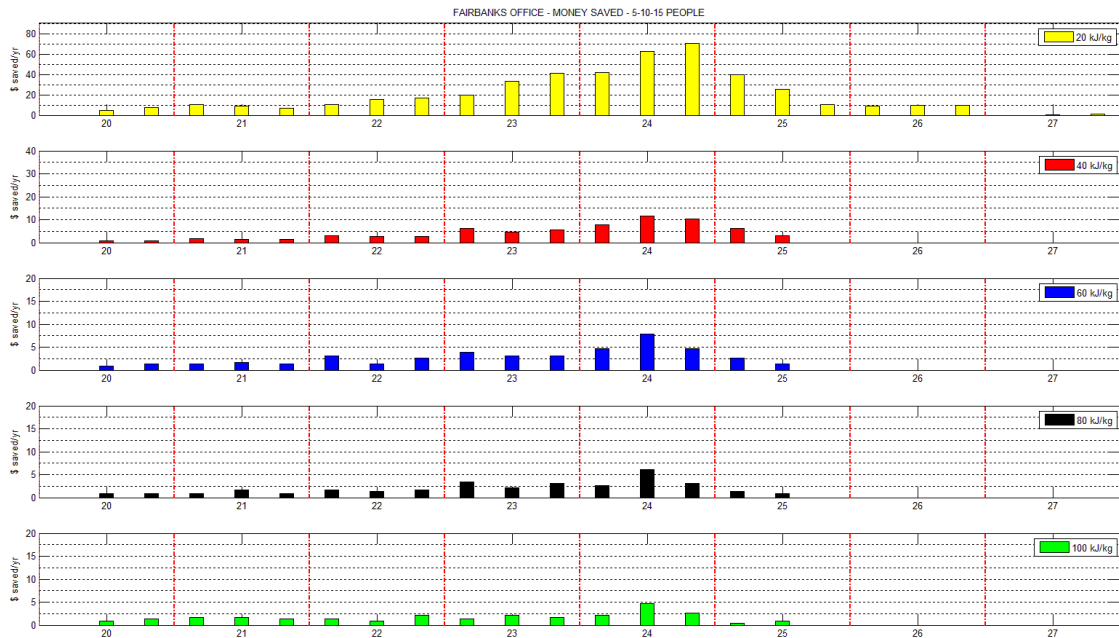


Figure F.15: Fairbanks office, additional money saved – different levels of enthalpy.

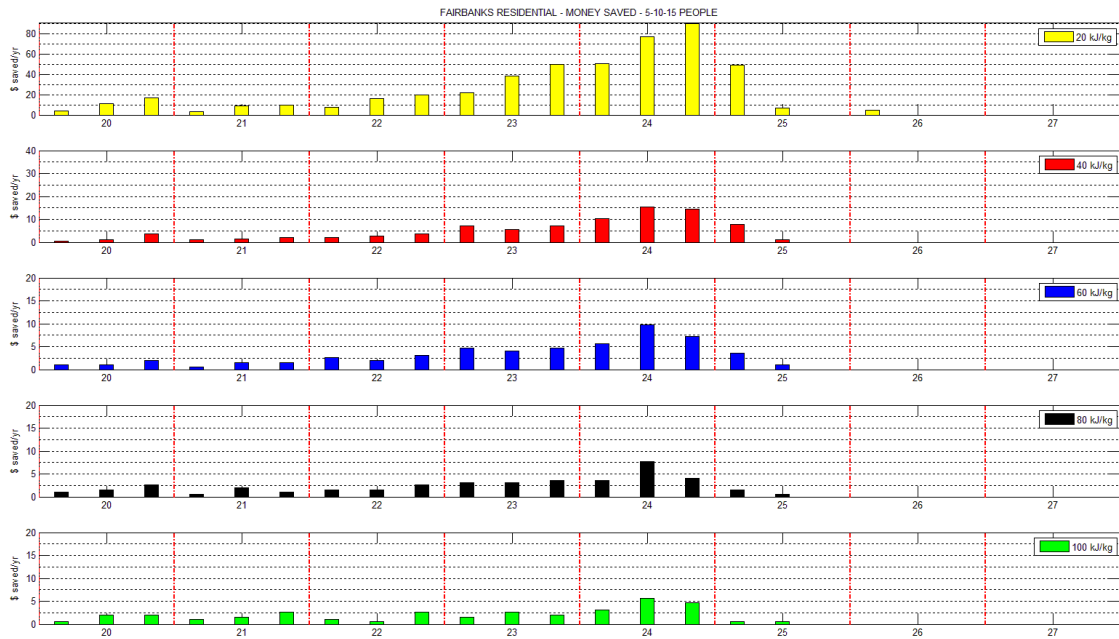


Figure F.16: Fairbanks residential, additional money saved – different levels of enthalpy.

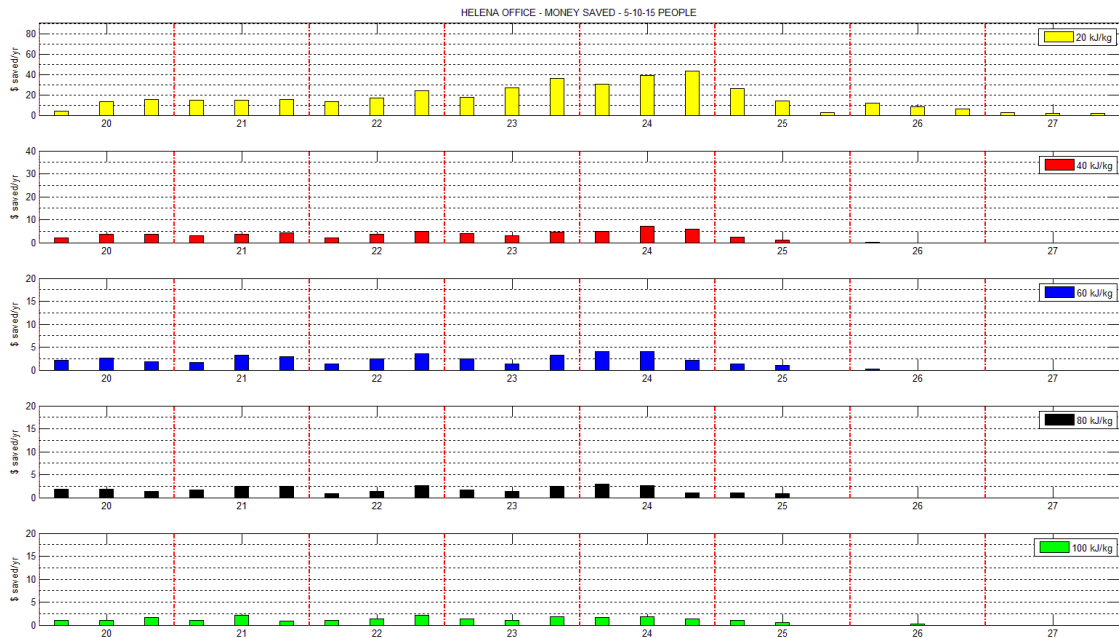


Figure F.17: Helena office, additional money saved – different levels of enthalpy.

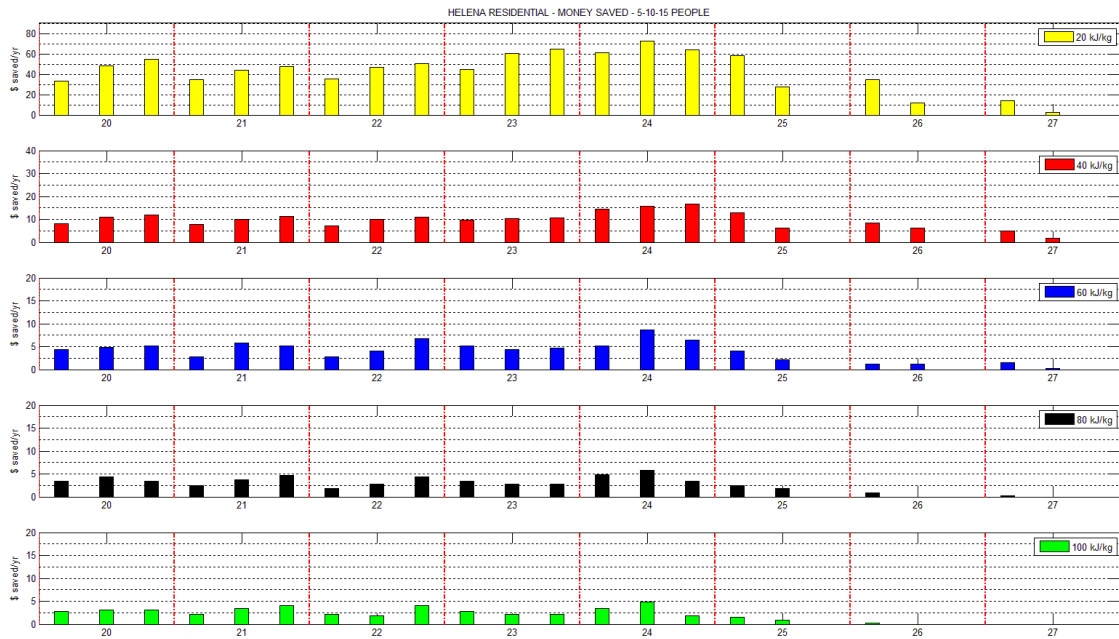


Figure F.18: Helena residential, additional money saved – different levels of enthalpy.

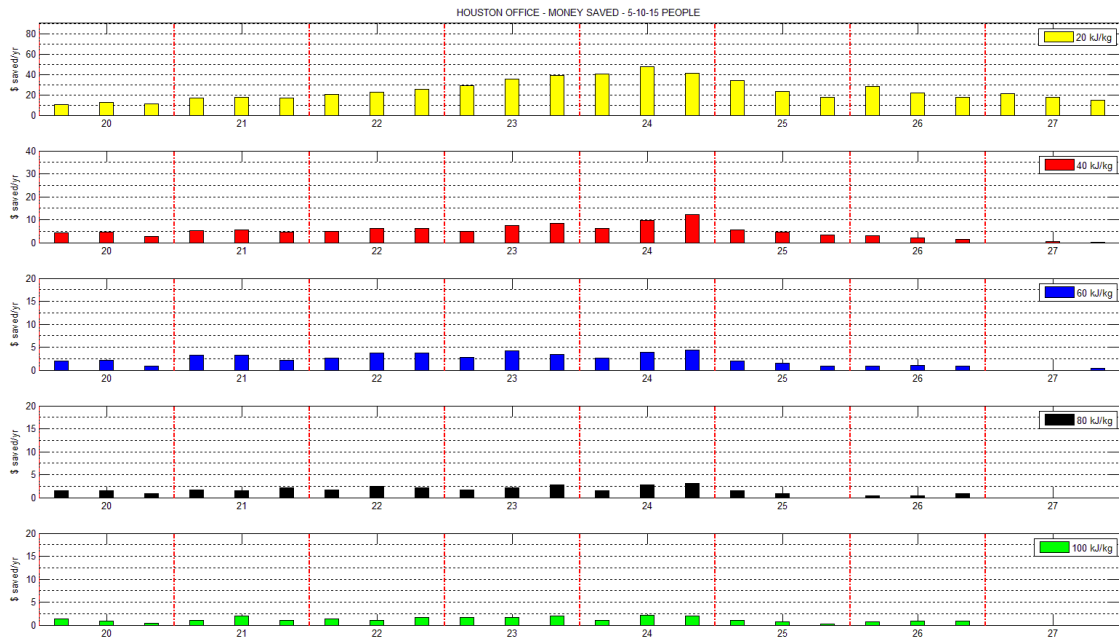


Figure F.19: Houston office, additional money saved – different levels of enthalpy.

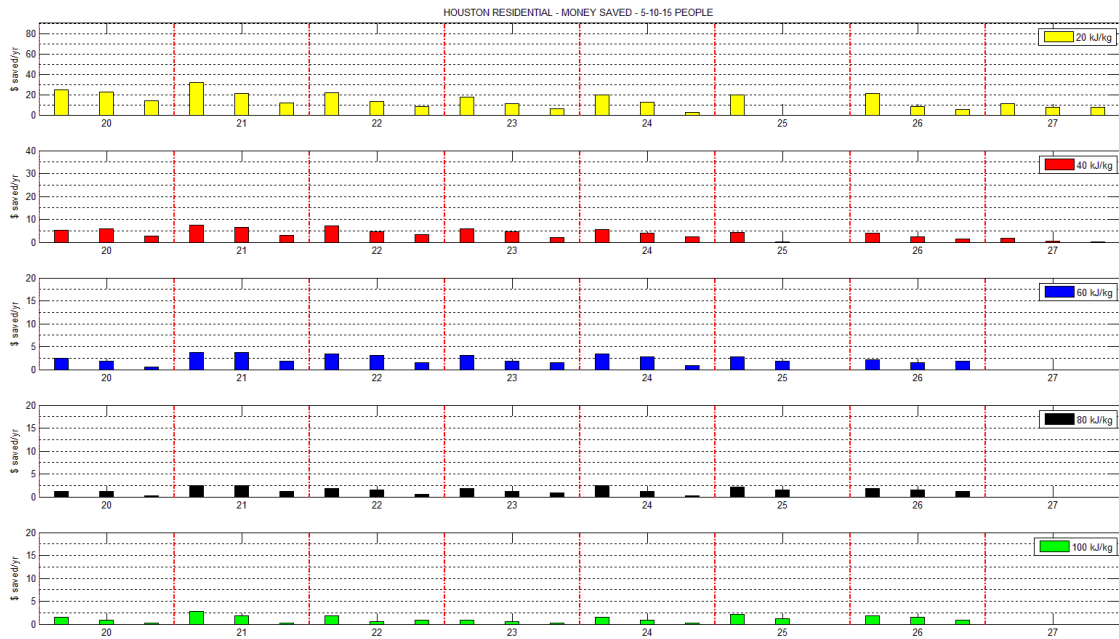


Figure F.20: Houston residential, additional money saved – different levels of enthalpy.

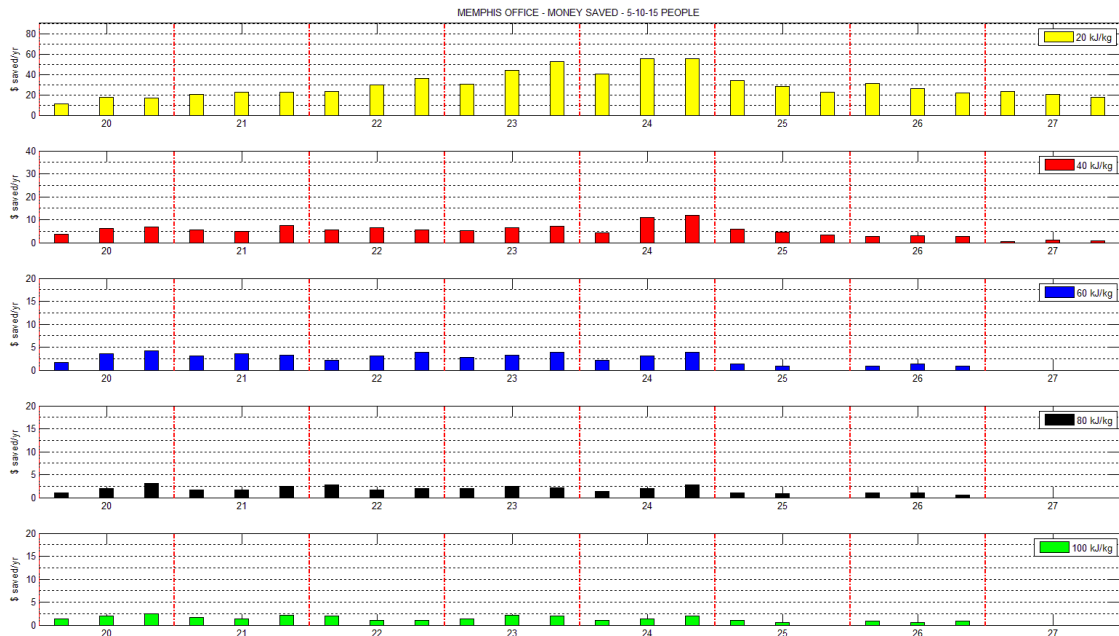


Figure F.21: Memphis office, additional money saved – different levels of enthalpy.

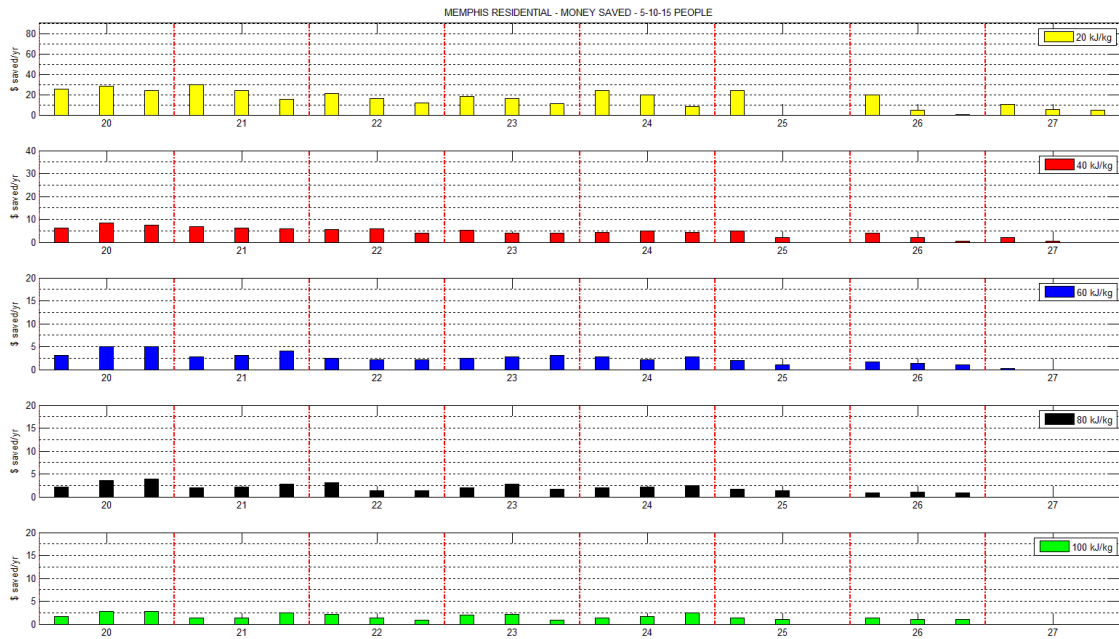


Figure F.22: Memphis residential, additional money saved – different levels of enthalpy.

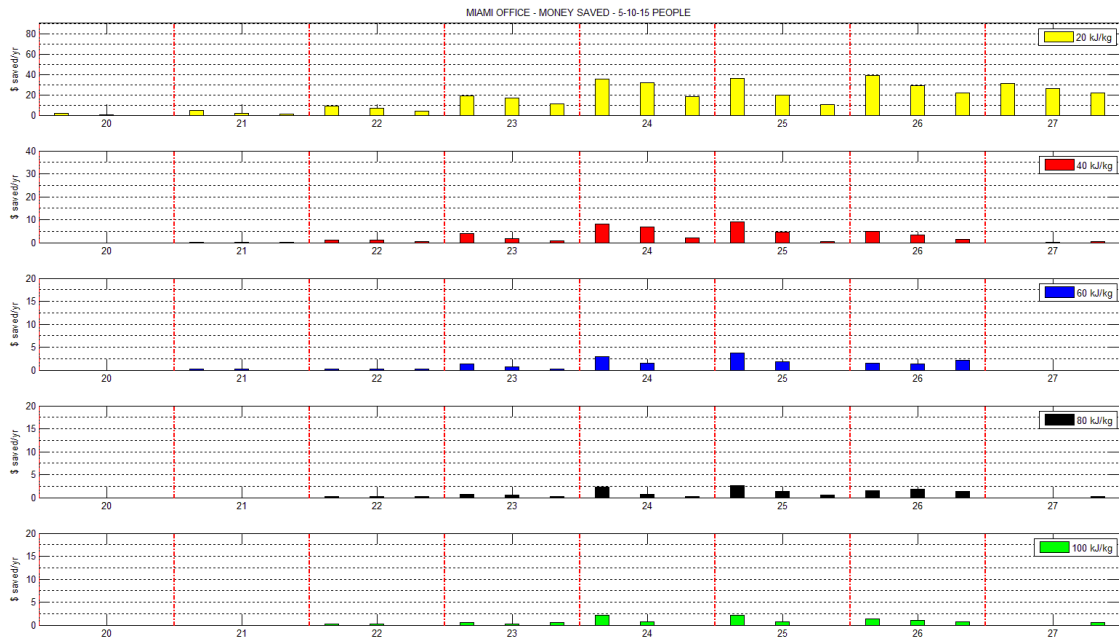


Figure F.23: Miami office, additional money saved – different levels of enthalpy.



Figure F.24: Miami residential, additional money saved – different levels of enthalpy.

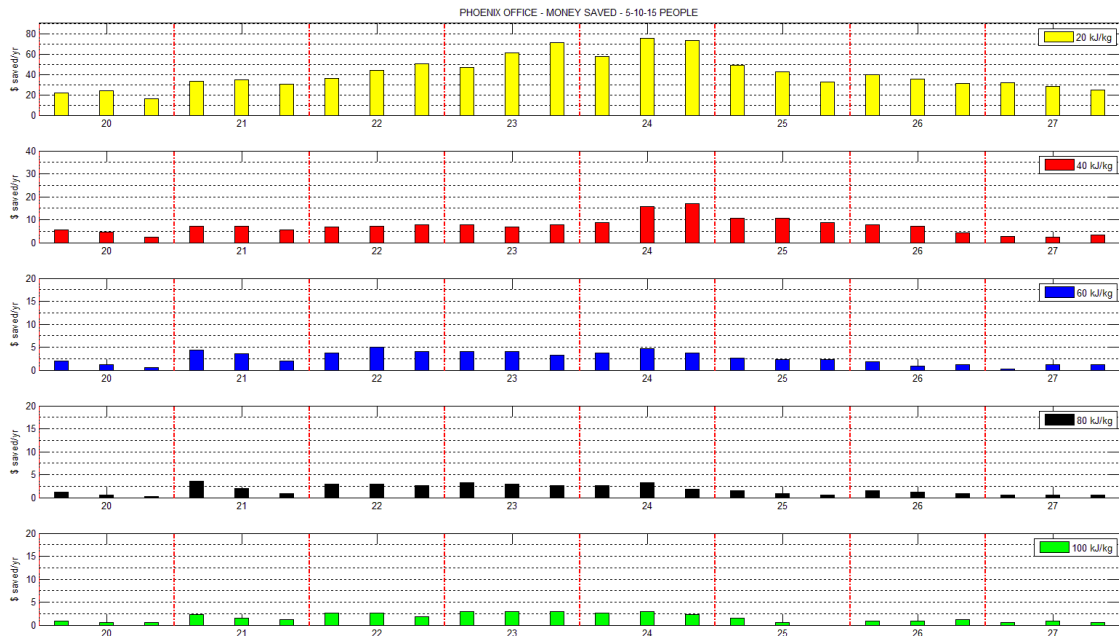


Figure F.25: Phoenix office, additional money saved – different levels of enthalpy.

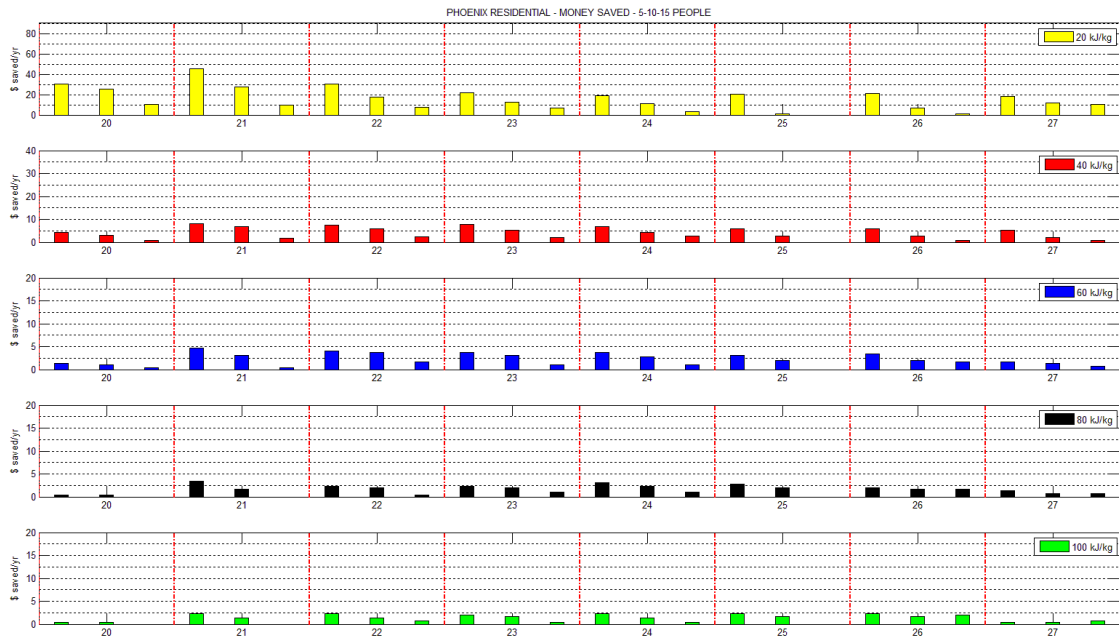


Figure F.26: Phoenix residential, additional money saved – different levels of enthalpy.

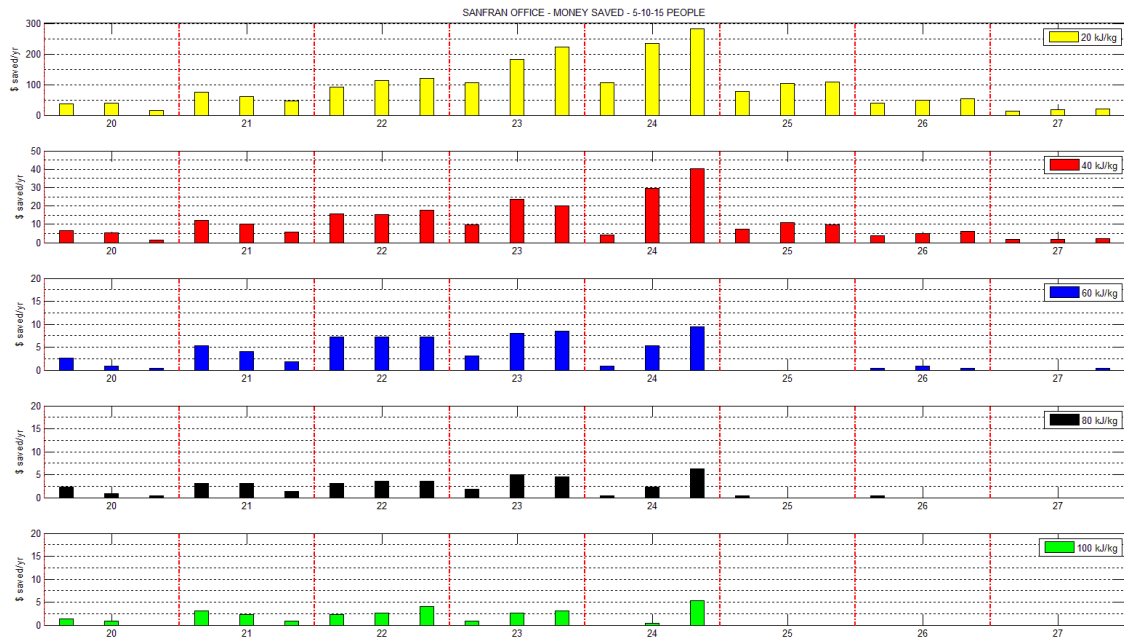


Figure F.28: San Francisco office, additional money saved – different levels of enthalpy.

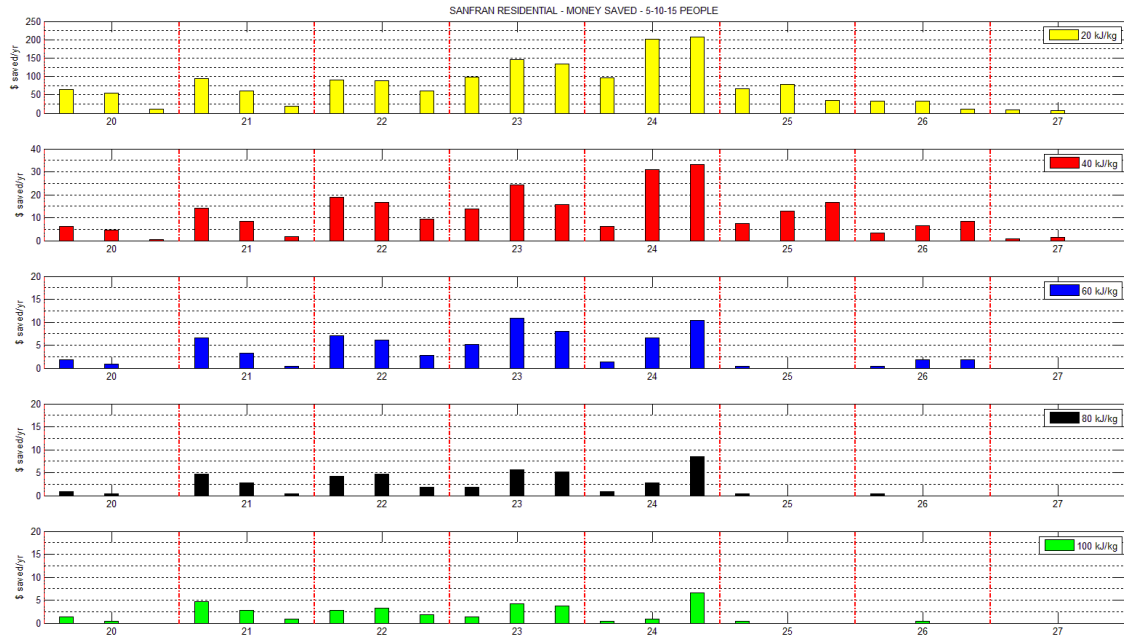


Figure F.28: San Francisco residential, additional money saved – different levels of enthalpy.

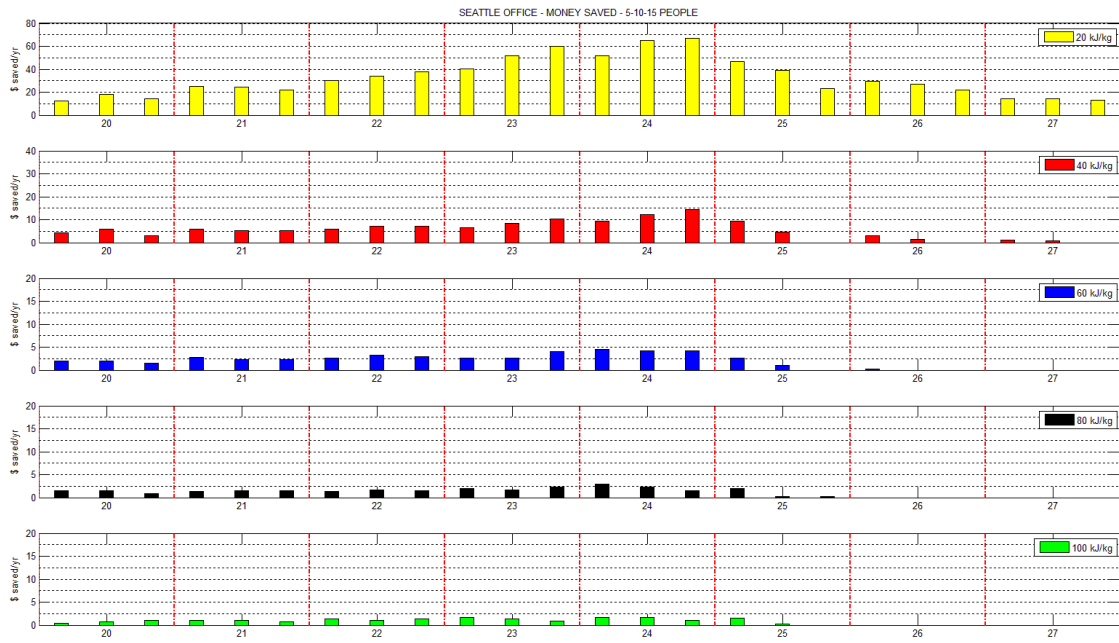


Figure F.29: Seattle office, additional money saved – different levels of enthalpy.

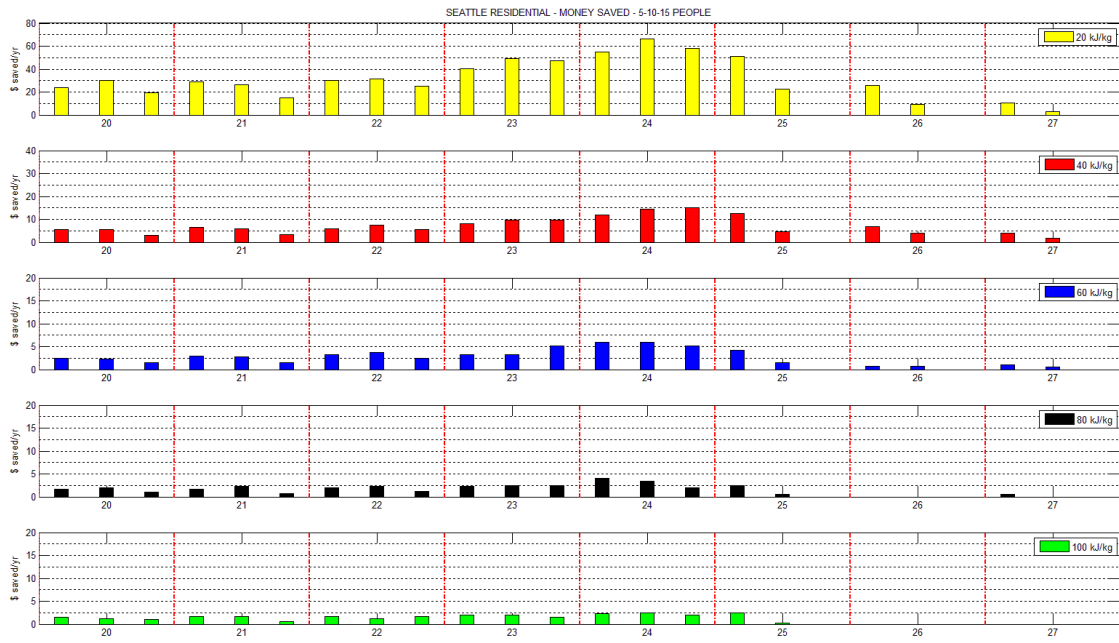


Figure F.30: Seattle residential, additional money saved – different levels of enthalpy.

Appendix G

Indoor Mean Air Temperature plots for San Francisco

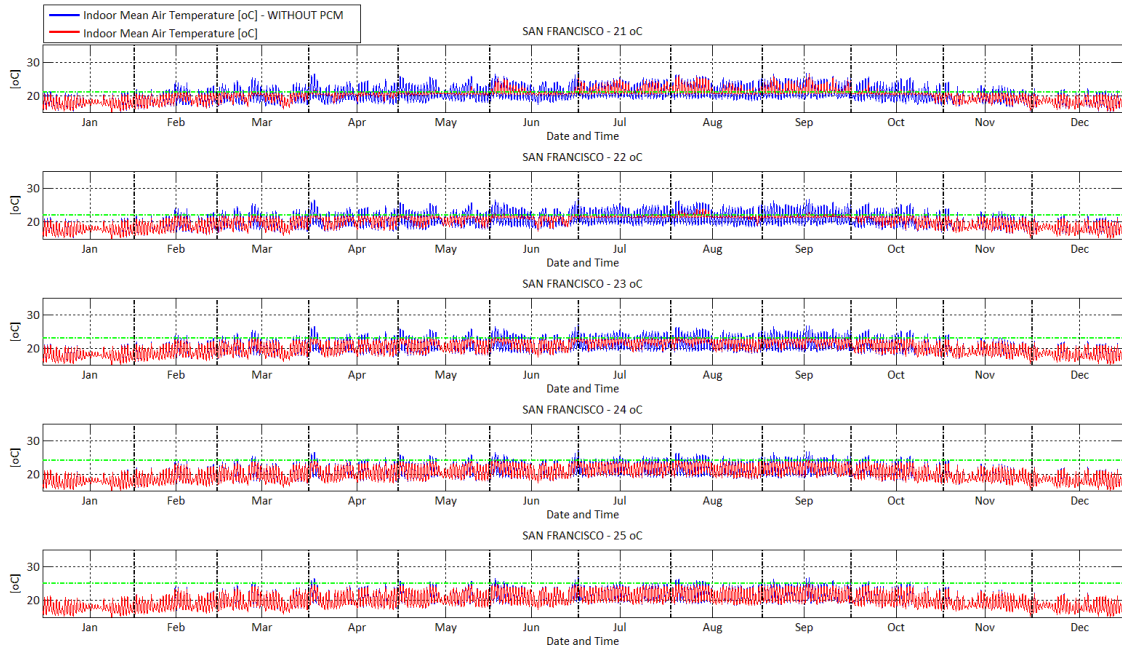


Figure G.1: San Fran: indoor temperature for PCM with different melting temperatures. 0 – people

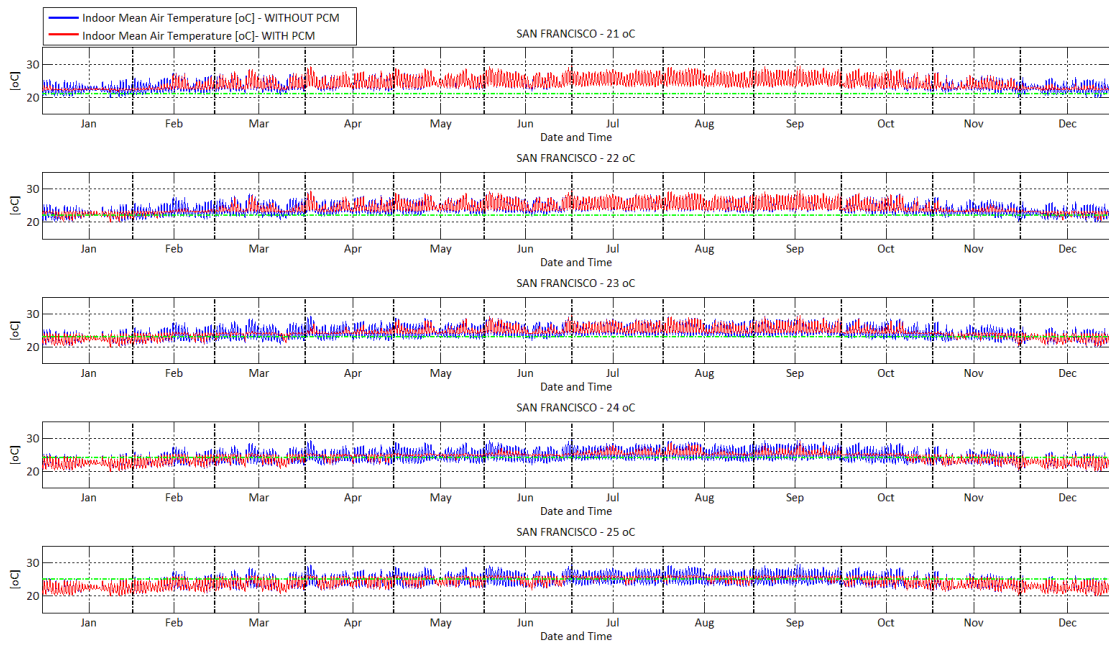


Figure G.2: San Fran: indoor temperature for PCM with different melting temperatures. 15 – People

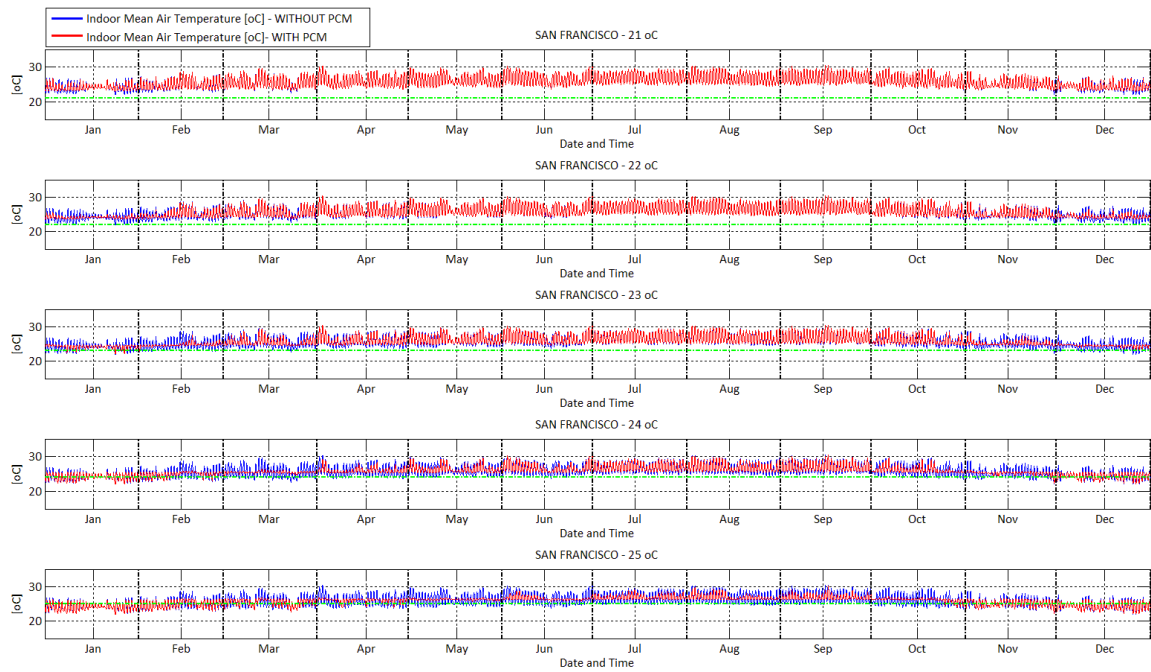


Figure G.3: San Fran: indoor temperature for PCM with different melting temperatures. 24 – People

REFERENCE LIST

- Addington, M., & Schodek, D. (2004). *Smart Materials and Technologies: For the Architecture and Design Professions* (p. 241). Routledge.
- Agyenim, F., Hewitt, N., Eames, P., & Smyth, M. (2010). A review of materials, heat transfer and phase change problem formulation for latent heat thermal energy storage systems (LHTESS). *Renewable and Sustainable Energy Reviews*, 14(2), 615–628. doi:10.1016/j.rser.2009.10.015
- Ahmad, M., Bontemps, A., Sallée, H., & Quenard, D. (2006). Experimental investigation and computer simulation of thermal behaviour of wallboards containing a phase change material. *Energy and Buildings*, 38(4), 357–366. doi:10.1016/j.enbuild.2005.07.008
- Alawadhi, E. M. (2008). Thermal analysis of a building brick containing phase change material. *Energy and Buildings*, 40(3), 351–357. doi:10.1016/j.enbuild.2007.03.001
- ASHRAE. (2007). *ANSI/ASHRAE Standard 62.1 Ventilation for Acceptable Indoor Air Quality*.
- ASHRAE. (2009). *2009 ASHRAE Handbook -- Fundamentals (SI)*. Retrieved from http://www.techstreet.com/ashrae/products/1858361?ashrae_auth_token=
- ASHRAE. (2010). *ANSI/ASHRAE/IES Standard 90.1-2013 - Energy Standard for Buildings Except Low-Rise Residential Buildings*.
- Athienitis, A. K., Liu, C., Hawes, D., Banu, D., & Feldman, D. (1997). Investigation of the thermal performance of a passive solar test-room with wall latent heat storage. *Building and Environment*, 32(5), 405–410. doi:10.1016/S0360-1323(97)00009-7
- Balaras, C. A. (1996). The role of thermal mass on the cooling load of buildings. An overview of computational methods. *Energy and Buildings*, 24(1), 1–10. doi:10.1016/0378-7788(95)00956-6
- Banu, D., Feldman, D., & Hawes, D. (1998). Evaluation of thermal storage as latent heat in phase change material wallboard by differential scanning calorimetry and large scale thermal testing. *Thermochimica Acta*, 317(1), 39–45. doi:10.1016/S0040-6031(98)00368-2
- Bessant, J., & Rush, H. (1995). Building bridges for innovation: the role of consultants in technology transfer. *Research Policy*, 24(1), 97–114. doi:10.1016/0048-7333(93)00751-E

- Borreguero, A. M., Luz Sánchez, M., Valverde, J. L., Carmona, M., & Rodríguez, J. F. (2011). Thermal testing and numerical simulation of gypsum wallboards incorporated with different PCMs content. *Applied Energy*, 88(3), 930–937. doi:10.1016/j.apenergy.2010.08.014
- Campbell, K. R. (2011). *Phase Change Material as a Thermal Storage Device for Passive Houses*. Portland State University, *Dissertations and Theses*. Portland State University. Retrieved from <http://www.amazon.com/Material-Thermal-Storage-Passive-Houses/dp/1249846145>
- Carbonari, A., De Grassi, M., Di Perna, C., & Principi, P. (2006). Numerical and experimental analyses of PCM containing sandwich panels for prefabricated walls. *Energy and Buildings*, 38(5), 472–483. doi:10.1016/j.enbuild.2005.08.007
- Castell, A., Menoufi, K., de Gracia, A., Rincón, L., Boer, D., & Cabeza, L. F. (2013). Life Cycle Assessment of alveolar brick construction system incorporating phase change materials (PCMs). *Applied Energy*, 101, 600–608. doi:10.1016/j.apenergy.2012.06.066
- Chan, A. L. S. (2011). Energy and environmental performance of building façades integrated with phase change material in subtropical Hong Kong. *Energy and Buildings*, 43(10), 2947–2955. doi:10.1016/j.enbuild.2011.07.021
- Chen, C., Guo, H., Liu, Y., Yue, H., & Wang, C. (2008). A new kind of phase change material (PCM) for energy-storing wallboard. *Energy and Buildings*, 40(5), 882–890. doi:10.1016/j.enbuild.2007.07.002
- Cooke, R., Cripps, A., Irwin, A., & Kolokotroni, M. (2007). Alternative energy technologies in buildings: Stakeholder perceptions. *Renewable Energy*, 32(14), 2320–2333. doi:10.1016/j.renene.2006.12.004
- Darkwa, K., & O’Callaghan, P. W. (2006). Simulation of phase change drywalls in a passive solar building. *Applied Thermal Engineering*, 26(8-9), 853–858. doi:10.1016/j.applthermaleng.2005.10.007
- Darkwa, K., O’Callaghan, P. W., & Tetlow, D. (2006). Phase-change drywalls in a passive-solar building. *Applied Energy*, 83(5), 425–435. doi:10.1016/j.apenergy.2005.05.001
- Dincer, I., & Dost, S. (1996). A perspective on thermal energy storage systems for solar energy applications. *International Journal of Energy Research*, 20(6), 547–557. doi:10.1002/(SICI)1099-114X(199606)20:6<547::AID-ER173>3.0.CO;2-S

- Dincer, I., Dost, S., & Li, X. (1997). Thermal energy storage applications from an energy saving perspective. *International Journal of Global Energy Issues : IJGEI*, 9(4), p. 351–364.
- Dincer, I., & Rosen, M. (2002). *Thermal Energy Storage: Systems and Applications* (p. 596). John Wiley & Sons.
- Dincer, I., & Rosen, M. (2010). *Thermal Energy Storage: Systems and Applications* (p. 620). Wiley; 2 edition.
- Energy Information Administration. (2011). *International Energy Outlook 2011 - Energy Information Administration*. Retrieved from <http://www.eia.gov/forecasts/ieo/>
- Energy, U. S. D. of. (2012). *Engineering reference – The Encyclopedic Reference to EnergyPlus V 8.1*.
- Farid, M. M., Khudhair, A. M., Razack, S. A. K., & Al-Hallaj, S. (2004). A review on phase change energy storage: materials and applications. *Energy Conversion and Management*, 45(9-10), 1597–1615. doi:10.1016/j.enconman.2003.09.015
- Fernandez, J. (2005). *Material Architecture* (p. 344). Routledge.
- Gracia, A., Rincón, L., Castell, A., Jiménez, M., Boer, D., Medrano, M., & Cabeza, L. F. (2010). Life Cycle Assessment of the inclusion of phase change materials (PCM) in experimental buildings. *Energy and Buildings*, 42(9), 1517–1523. doi:10.1016/j.enbuild.2010.03.022
- Halford, C. K., & Boehm, R. F. (2007). Modeling of phase change material peak load shifting. *Energy and Buildings*, 39(3), 298–305. doi:10.1016/j.enbuild.2006.07.005
- Heim, D. (2010). Isothermal storage of solar energy in building construction. *Renewable Energy*, 35(4), 788–796. doi:10.1016/j.renene.2009.09.005
- Heim, D., & Clarke, J. A. (2004). Numerical modelling and thermal simulation of PCM–gypsum composites with ESP-r. *Energy and Buildings*, 36(8), 795–805. doi:10.1016/j.enbuild.2004.01.004
- Huang, M., Eames, P., & Hewitt, N. (2006). The application of a validated numerical model to predict the energy conservation potential of using phase change materials in the fabric of a building. *Solar Energy Materials and Solar Cells*, 90(13), 1951–1960. doi:10.1016/j.solmat.2006.02.002
- Hyde, R. (2008). *Bioclimatic Housing: Innovative Designs for Warm Climates*: (R. Hyde, Ed.). London: Earthscan. Retrieved from <http://www.amazon.com/Bioclimatic-Housing-Innovative-Designs-Climates/dp/1844072843>

- Ibáñez, M., Lázaro, A., Zalba, B., & Cabeza, L. F. (2005). An approach to the simulation of PCMs in building applications using TRNSYS. *Applied Thermal Engineering*, 25(11-12), 1796–1807. doi:10.1016/j.applthermaleng.2004.11.001
- Khudhair, A. M., & Farid, M. M. (2004). A review on energy conservation in building applications with thermal storage by latent heat using phase change materials. *Energy Conversion and Management*, 45(2), 263–275. doi:10.1016/S0196-8904(03)00131-6
- Kim, J., & Moon, J. W. (2009). IMPACT OF INSULATION ON BUILDING ENERGY CONSUMPTION. *Building Simulation 2009*, 674–680.
- Kosny, J., Kossecka, E., Brzezinski, A., Tleoubaev, A., & Yarbrough, D. (2012). Dynamic thermal performance analysis of fiber insulations containing bio-based phase change materials (PCMs). *Energy and Buildings*, 52, 122–131. doi:10.1016/j.enbuild.2012.05.021
- Kosny, J., Shukla, N., & Fallahi, A. (2012). *Cost Analysis of Simple Phase Change Material-Enhanced Building Envelopes in Southern U.S. Climates*.
- Kosny, J., Yarbrough, D. W., Miller, W. A., Wilkes, K. E., & Lee, E. S. (2009). Analysis of the dynamic thermal performance of berous insulations containing phase change materials. In *11th International Conference on Thermal Energy Storage*.
- Kuznik, F., David, D., Johannes, K., & Roux, J.-J. (2011). A review on phase change materials integrated in building walls. *Renewable and Sustainable Energy Reviews*, 15(1), 379–391. doi:10.1016/j.rser.2010.08.019
- Kuznik, F., Virgone, J., & Johannes, K. (2010). Development and validation of a new TRNSYS type for the simulation of external building walls containing PCM. *Energy and Buildings*, 42(7), 1004–1009. doi:10.1016/j.enbuild.2010.01.012
- Kuznik, F., Virgone, J., & Noel, J. (2008). Optimization of a phase change material wallboard for building use. *Applied Thermal Engineering*, 28(11-12), 1291–1298. doi:10.1016/j.applthermaleng.2007.10.012
- Lane, G. A. (1983). *Solar Heat Storage: Latent Heat Materials, Volume 1* (p. 238). CRC Press. Retrieved from <http://www.amazon.com/Solar-Heat-Storage-Background-Scientific/dp/0849365856>
- Liang, J., Li, B., Wu, Y., & Yao, R. (2007). An investigation of the existing situation and trends in building energy efficiency management in China. *Energy and Buildings*, 39(10), 1098–1106. doi:10.1016/j.enbuild.2006.12.002

- Mehling, H., & Cabeza, L. F. (2008). *Heat and cold storage with PCM: An up to date introduction into basics and applications* (p. 324). Springer.
- Mendenhall, W., & Sincich, T. (2003). *A Second Course in Statistics: Regression Analysis* (6th ed., p. 816). Pearson; 6 edition.
- Michels, H., & Pitz-Paal, R. (2007). Cascaded latent heat storage for parabolic trough solar power plants. *Solar Energy*, 81(6), 829–837. doi:10.1016/j.solener.2006.09.008
- Moheisem, R., Kozlowski, K., Shaaban, A., Rasmussen, C., Yacout, A., & Keith, M. (2011). *Utilization of Phase Change Materials to Reduce Energy Consumption in Buildings*. Retrieved from <http://www.dtic.mil/dtic/tr/fulltext/u2/a554348.pdf>
- Neeper, D. A. (2000). Thermal dynamics of wallboard with latent heat storage. *Solar Energy*, 68(5), 393–403. doi:10.1016/S0038-092X(00)00012-8
- O'Brien, W. (2011). *Development of a Solar House Design Methodology and its Implementation into a Design Tool*. Concordia University.
- Ogoli, D. M. (2003). Predicting indoor temperatures in closed buildings with high thermal mass. *Energy and Buildings*, 35(9), 851–862. doi:10.1016/S0378-7788(02)00246-3
- Pasupathy, A., Athanasius, L., Velraj, R., & Seeniraj, R. V. (2008). Experimental investigation and numerical simulation analysis on the thermal performance of a building roof incorporating phase change material (PCM) for thermal management. *Applied Thermal Engineering*, 28(5-6), 556–565. doi:10.1016/j.applthermaleng.2007.04.016
- Pasupathy, A., Velraj, R., & Seeniraj, R. V. (2008). Phase change material-based building architecture for thermal management in residential and commercial establishments. *Renewable and Sustainable Energy Reviews*, 12(1), 39–64. doi:10.1016/j.rser.2006.05.010
- Pedersen, C. (2007). Advanced Zone Simulation in EnergyPlus: Incorporation of Variable Properties and Phase Change Material (PCM) Capability. *Building Simulation*, 1341–1345.
- Peippo, K., Kauranen, P., & Lund, P. D. (1991). A multicomponent PCM wall optimized for passive solar heating. *Energy and Buildings*, 17(4), 259–270. doi:10.1016/0378-7788(91)90009-R

- Poudel, N., & Blouin, V. (2013). US map visualization of optimal properties of phase change materials for building efficiency. In *The visibility of research in Architecture*. Charlotte, North Carolina.
- Ren, H., Zhou, W., Gao, W., & Wu, Q. (2010). Life System Modeling and Intelligent Computing. *Life System Modeling and Intelligent Computing*, 6328, 361–371. doi:10.1007/978-3-642-15621-2_40
- Ryghaug, M., & Sørensen, K. H. (2009). How energy efficiency fails in the building industry. *Energy Policy*, 37(3), 984–991. doi:10.1016/j.enpol.2008.11.001
- Schittich, C. (Ed.). (2003). *In Detail: Solar Architecture* (p. 176). Birkhäuser Architecture; 1 edition.
- Sharma, A., Tyagi, V. V., Chen, C. R., & Buddhi, D. (2009). Review on thermal energy storage with phase change materials and applications. *Renewable and Sustainable Energy Reviews*, 13(2), 318–345. doi:10.1016/j.rser.2007.10.005
- Shove, E. (1998). Gaps, barriers and conceptual chasms: theories of technology transfer and energy in buildings. *Energy Policy*, 26(15), 1105–1112. doi:10.1016/S0301-4215(98)00065-2
- Shrestha, S. S., Miller, W. A., Stovall, T., Desjarlais, A., Childs, K., Porter, W., & Bhandari, M. (2011). Modeling PCM-Enhanced Insulation System and Benchmarking EnergyPlus against Controlled Field Data. In *Proceedings of Building Simulation 2011: 12th Conference of International Building Performance Simulation Association* (pp. 14–16).
- Som S Shrestha, W. A. M. (2011). Modeling PCM-Enhanced Insulation System and Benchmarking EnergyPlus against Controlled Field Data.
- Stovall, T. K., & Tomlinson, J. J. (1995). What are the Potential Benefits of Including Latent Storage in Common Wallboard? *Journal of Solar Energy Engineering*, 117(4), 318. doi:10.1115/1.2847868
- Thomas, K. L. (2006). *Material Matters: Architecture and Material Practice* (p. 272). Taylor & Francis.
- Tsoutsos, T. D., & Stamboulis, Y. A. (2005). The sustainable diffusion of renewable energy technologies as an example of an innovation-focused policy. *Technovation*, 25(7), 753–761. doi:10.1016/j.technovation.2003.12.003
- Tyagi, V. V., & Buddhi, D. (2007). PCM thermal storage in buildings: A state of art. *Renewable and Sustainable Energy Reviews*, 11(6), 1146–1166. doi:10.1016/j.rser.2005.10.002

- Tyagi, V. V., Kaushik, S. C., Tyagi, S. K., & Akiyama, T. (2011). Development of phase change materials based microencapsulated technology for buildings: A review. *Renewable and Sustainable Energy Reviews*, 15(2), 1373–1391. doi:10.1016/j.rser.2010.10.006
- Underwood, C., & Yik, F. (2004). *Modelling Methods for Energy in Buildings*. (C. P. Underwood & F. W. H. Yik, Eds.). Oxford, UK: Blackwell Publishing Ltd. doi:10.1002/9780470758533
- Velasco, P. C., Christensen, C., & Bianchi, M. (2012). Verification and validation of EnergyPlus phase change material model for opaque wall assemblies. *Building and Environment*, 54, 186–196. doi:10.1016/j.buildenv.2012.02.019
- Zalba, B., Marín, J. M., Cabeza, L. F., & Mehling, H. (2003). Review on thermal energy storage with phase change: materials, heat transfer analysis and applications. *Applied Thermal Engineering*, 23(3), 251–283. doi:10.1016/S1359-4311(02)00192-8
- Zhang, Y. (2009). Parallel EnergyPlus and the development of a parametric analysis tool. In *Building Simulation - Eleventh International IBPSA Conference*. Retrieved from <https://www.dora.dmu.ac.uk/xmlui/handle/2086/3588>
- Zhang, Y., Lin, K., Jiang, Y., & Zhou, G. (2008). Thermal storage and nonlinear heat-transfer characteristics of PCM wallboard. *Energy and Buildings*, 40(9), 1771–1779. doi:10.1016/j.enbuild.2008.03.005
- Zhang, Y. P., Lin, K. P., Yang, R., Di, H. F., & Jiang, Y. (2006). Preparation, thermal performance and application of shape-stabilized PCM in energy efficient buildings. *Energy and Buildings*, 38(10), 1262–1269. doi:10.1016/j.enbuild.2006.02.009
- Zhang, Y., Zhou, G., Lin, K., Zhang, Q., & Di, H. (2007). Application of latent heat thermal energy storage in buildings: State-of-the-art and outlook. *Building and Environment*, 42(6), 2197–2209. doi:10.1016/j.buildenv.2006.07.023
- Zhou, D., Zhao, C. Y., & Tian, Y. (2012). Review on thermal energy storage with phase change materials (PCMs) in building applications. *Applied Energy*, 92, 593–605. doi:10.1016/j.apenergy.2011.08.025
- Zhou, G., Zhang, Y., Wang, X., Lin, K., & Xiao, W. (2007). An assessment of mixed type PCM-gypsum and shape-stabilized PCM plates in a building for passive solar heating. *Solar Energy*, 81(11), 1351–1360. doi:10.1016/j.solener.2007.01.014
- Zhu, N., Ma, Z., & Wang, S. (2009). Dynamic characteristics and energy performance of buildings using phase change materials: A review. *Energy Conversion and Management*, 50(12), 3169–3181. doi:10.1016/j.enconman.2009.08.019

Zhuang, C.-L., Deng, A.-Z., Chen, Y., Li, S.-B., Zhang, H.-Y., & Fan, G.-Z. (2010). Validation of veracity on simulating the indoor temperature in PCM light weight building by energyplus, 486–496.